

https://dspace.org/

A simplified model for spontaneous combustion in coal stockpiles

Brooks, Kevin Seth

2009-11-09T12:12:19Z
http://hdl.handle.net/10539/7424

Downloaded from a DSpace repository. https://dspace.org/

A SIMPLIFIED MODEL FOR SPONTANEOUS COMBUSTION IN COAL STOCKPILES

Kevin Seth Brooks

A thesis submitted to the Faculty of Engineering, University of the Witwatersrand, Johannesburg, in fulfilment of the requirements for the degree of Doctor of Philosophy.

July 1985

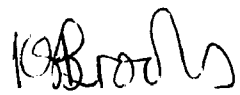
Johannesburg

NK 6717/1

DECLARATION

The work described in this thesis was carried out in the Department of Chemical Engineering of the University of the Witwatersrand, Johannesburg, and is the original and independent work of the author except where specifically acknowledged in the text.

No part of the thesis has previously been submitted for a degree in the University of the Witwatersrand, or is being submitted to any other University.



K S BROOKS

July 1985

ABSTRACT

Based on a study of the fundamental processes of heat,mass and momentum transfer, a one-dimensional model to predict the behaviour of coal dumps with respect to spontaneous combustion is presented.

Heat transfer within the dump is modelled using an effective thermal conductivity. This quantity has been measured for a typical coal sample using a guarded hot ring apparatus. Mass transfer is considered to occur by natural convection and wind pressure. Diffusion is shown to be unimportant except for very fine material.

A shrinking-core model for the low temperature oxidation of coal is proposed; the model explains the fact that the coal reactivity decreases with time. The effects of moisture on the coal reactivity are neglected due to lack of data.

Estimates of the parameters required for the model have been obtained experimentally. The equations are solved analytically in both the steady and unsteady-state under the assumption of unchanging rate constant. A numerical method has been used to solve the equations without this assumption.

It has been shown that coal dumps may be classified as either safe, unsafe or conditionally safe. Safe coal dumps are either oxygen limited or heat transfer limited. The former is the case for fine reactive coal; the high reactivity of the coal means that all the oxygen reacts close to the surface where the heat produced can easily be dissipated. The latter is the case for for coarse, unreactive material; although the oxygen is freely available throughout the dump, the reactivity per unit volume of the coal is sufficiently low such that heat produced can be dissipated without the temperature rising significantly.

It is shown that the important parameters in predicting the behaviour of a coal bed are the particle size distribution of the coal, the bed voidage and the reaction rate parameters. The effect on the temperature in a coal bed of changing each of parameter is presented graphically. The unsteady-state behaviour of the model shows that the time taken to reach a certain critical temperature may be the best way of arriving at a safe stockpiling time.

For my wife, Ilana:

A good typist and an even better cook

ACKNOWLEDGEMENTS

I should like to express my gratitude to my supervisor, Professor David Glasser, for his help, interest and encouragement during the course of this work.

As well as being a good friend, Mr (now Dr) Michael Itay performed the experimental work described in Chapter 2.

Mr L Schwartz and Mr A C Harris were of great assistance in the building of experimental apparatus.

The work described in this thesis was made possible by the financial assistance of the Iron and Steel Corporation of South Africa.

CONTENTS

	Page
DECLARATION	ii
ABSTRACT	iii
DEDICATION	iv
ACKNOWLEDGEMENTS	v
CONTENTS	vi
LIST OF FIGURES	x
LIST OF TABLES	xii
LIST OF SYMBOLS	xiii
1. AN OVERVIEW OF SPONTANEOUS COMBUSTION	1
1.1 Introduction	1
1.2 Previous Investigations into Spontaneous Combustion	3
1.3 Transport in a Coal Dump	6
1.4 The Chemical Reactivity of Coal	6
1.4.1 Reaction between Coal and Water	7
1.4.2 Low Temperature Oxidation of Coal	8
1.5 Heat Transfer within a Coal Dump	12
1.6 A Mathematical Model for Spontaneous Combustion	12
1.7 Experimental Investigation	13
1.8 Results and Conclusions	13
2. ANALYSIS OF SUGGESTED MECHANISMS FOR INGRESS OF REACTANTS	14
2.1 Introduction	14
2.2 Natural Convection and Wind Pressure	14
2.3 Analysis of Molecular Diffusion	18
2.4 Barometric Breathing	21
2.5 Thermal Breathing	22
2.6 Conclusions	23
3. THEORETICAL MODELS FOR HEAT TRANSFER IN PACKED BEDS	25
3.1 Introduction	25
3.2 Mechanisms of Energy Transfer in Packed Beds	25
3.3 Describing the Overall Energy Transfer in a Packed Bed	26

3.4 Models for Energy Transfer in which only conduction is considered 26

3.5 Models for Energy Transfer in which conduction and radiation are considered 31

3.5.1 Conditions under which radiation in a packed bed is likely to be significant 33

3.6 Theoretical Studies of Natural Convection 34

3.7 The Effect of flow on Energy Transfer in a Packed Bed 37

3.8 Conclusions 37

4. MEASUREMENT OF THE EFFECTIVE THERMAL CONDUCTIVITY OF A PACKED BED OF COAL 39

4.1 Introduction 39

4.2 Theory of the Measurement of Thermal Conductivity 39

4.3 Steady-state Methods for Measuring Thermal Conductivity 40

4.3.1 Measurements in the rectangular system 41

4.3.2 Measurements in the cylindrical system 43

4.3.3 Measurements in the spherical system 44

4.4 Unsteady-state or Dynamic Methods 44

4.5 Choice of Measurement Method for Packed Bed of Coal 45

4.6 Design and Construction of Guarded Hot Ring Apparatus 46

4.6.1 General Design Considerations 46

4.6.2 Heat Sinks 46

4.6.3 Heating Elements 48

4.6.4 Outer Containing Vessel 48

4.6.5 Water supply to heat sinks 50

4.6.6 Measurement Techniques 50

4.7 Experimental Procedure 51

4.8 Results and Discussion 52

5. MATHEMATICAL MODELLING OF A ONE-DIMENSIONAL ANALOGUE OF A COAL DUMP 54

5.1 Introduction 54

5.2 Literature survey of mathematical models 54

5.3 A One-dimensional Analogue of a Coal Dump 61

5.4 Model Equations 63

5.5 Discussion of the Model Equations 65

5.6 Boundary and Initial Conditions 66

6. SIMPLIFICATION OF THE MODEL EQUATIONS AND THEIR SOLUTION 67

6.1 Introduction 67
6.2 The Steady-State form of the Equations 69
6.3 The Solution of the Unsteady-State Equations with a constant rate 71
6.4 A Numerical Method for Solving the Unsteady-State Equations 72

7. EXPERIMENTAL INVESTIGATION OF THE BEHAVIOUR OF A ONE-DIMENSIONAL ANALOGUE OF A COAL DUMP 75

7.1 Introduction 75
7.2 Experimental 75
7.3 Results 78
7.4 Discussion 81

8. RESULTS OF SOLVING THE MODEL EQUATIONS 82

8.1 Introduction 82
8.2 Steady-State Solution for constant r 82
8.2.1 The Character of the Solutions 83
8.2.2 Effect of varying the voidage 90
8.2.3 Effect of varying the pre-exponential Factor 92
8.2.4 Effect of varying the activation energy 94
8.2.5 Effect of different assumptions about the reactive surface area of coal 94
8.2.6 The Meaning of Particle Size 95
8.2.7 Effect of wind on maximum Temperature 98
8.2.8 Effect of Thermal Conductivity on maximum Temperature 98
8.2.9 Effect of Changing the Bed Length 98
8.3 Unsteady-State solutions for r constant 101
8.3.1 Introduction 101
8.3.2 The Character of the Solutions 101
8.3.3 Discussion 107
8.4 Results of solving the equations numerically 107
8.4.1 Introduction 107
8.4.2 Comparison Between the Numerical Method and the Analytical Method 108
8.5 Conclusions 110

9. CONCLUSIONS 111

Appendix 1 Derivation of a rate equation for the low temperature oxidation of coal 116

Appendix 2 Tabulation of measured thermal conductivities 120

Appendix 3 Derivation of model equations 122

Appendix 4 The continuum and pseudo steady-state assumptions 130

Appendix 5 The inclusion of a radial heat loss term in equation 6.1.4 132

Appendix 6 Explanation for the Instability of the Runge-Kutta algorithm 135

Appendix 7 Solution of equation 6.2.2 with r constant 136

Appendix 8 Solution of equation 6.1.5 with r constant 137

Appendix 9 Application of the method of lines to the solution of equation 6.1.5 140

Appendix 10 Results of chimney experiment 142

Appendix 11 Model Parameters used as base case 165

Appendix 12 Listing of computer programs 166

REFERENCES 194

LIST OF FIGURES

Figure		Page
1.1	Temperature, Oxygen and Carbon Dioxide Versus Time	9
3.1	Geometrical Conduction Models (Beveridge & Haughey, 1971)	28
4.1	Guarded hot ring apparatus - Heat sink	47
4.2	Guarded hot ring apparatus - Assembled apparatus	49
5.1	Streamlines in a packed bed containing a line source	62
7.1	Chimney experiment - Apparatus	76
7.2	Chimney experiment - Fitting heat transfer coefficients	79
7.3	Chimney experiment - Fitting ageing run 1	79
7.4	Chimney experiment - Fitting ageing run 2	80
7.5	Chimney experiment - Fitting ignition runs	80
8.1	LHS and RHS of equation 8.2 as a function of θ	86
8.2	Locus of solutions to equation 8.2	86
8.3	Stable and unstable solutions for the base-case	91
8.4	Effect of varying voidage on the maximum temperature	91
8.5	Effect of varying the pre-exponential factor on the maximum temperature	93
8.6	Effect of varying the activation energy on the maximum temperature	93
8.7	Pre-exponential factor versus particle size for the two cases considered	96
8.8	Effect of different assumptions about surface area on the maximum temperature	96
8.9	Effect of wind on the maximum temperature	99
8.10	Effect of varying bed thermal conductivity on the maximum temperature	99
8.11	Effect of varying bed length on the maximum temperature	100
8.12	Temperature-time curves in the centre of a coal bed for different initial temperatures	102
8.13	Temperature profiles in a coal bed Particle size 10 mm - Analytical solution	102
8.14	Temperature-time behaviour at bed centre Particle size 6 mm - Analytical solution	106
8.15	Temperature profiles in a coal bed Particle size 10 mm - Numerical Method	106

Figure		Page
8.16	Temperature profiles with ignition Particle size 2 mm - 5 m/s wind - Numerical method	109
8.17	Cross plot of Figure 8.16 at bed centre	109
A1.1	Simplified coal particle geometry	116
A2.1	Measured thermal conductivities versus difference between guard and main heater temperatures	121
A3.1	Differential element of a coal bed	122
A5.1	Differential element in the form of a ring	132

LIST OF TABLES

Table		Page
2.1	Molar Flowrates for Various Particle Sizes	17
2.2	Comparison of Molecular Diffusion and Convection	21
5.1	Values of ΔT L Required for Ra = 4 π^2	59
5.2	Unknowns in the model equations	65
8.1	Particle Size Distribution for a typical sample	97
8.2	Model Parameters for Figure 8.12	101
8.3	The Quantity 'a' For Various Particle Sizes	105
A2.1	Measured Thermal Conductivities	120

LIST OF SYMBOLS

a: Dimensionless quantity in equation 6.1.4

a': Fitting constant in equation 5.2.1

a_{ij}: Weighting coefficients for first derivatives

A: Area

A': Fitting constant in equation 5.2.1

A^*: Arrhenius pre-exponential factor

$\underline{A}$: Matrix of coefficeints a_{ij}

A_o: Pre-exponential factor in equation 5.2.8

b: Dimensionless quantity in equation 6.1.4

b_{ij}: Weighting coefficients for second derivatives

B: Elovich constant

$\underline{B}$: Matrix of coefficients b_{ij}

Bi_o: Biot number at $X = 0$

Bi_1: Biot number at $X = 1$

Bi_2: $Bi_o + a/2$

Bi_3: $Bi_1 + a/2$

c: Heat loss coefficient

$\bar{c}$: Heat capacity per unit mass

$\bar{c}_s$: Heat capacity per unit mass of solid

$\bar{c}_w$: Heat capacity per unit mass of liquid water

$\bar{c}_j$: Heat capacity per unit mass of component j in the solid

$\bar{c}_b$: Heat capacity per unit mass of bed

$\hat{c}$: Molar heat capacity of the gas

$\hat{c}_i$: Molar heat capacity of component i in the gas

C_p: Specific heat capacity

C: Oxygen concentration

C_s: Oxygen concentration at reaction surface

C_1: Integration constant

C_2: Integration constant

C_3: Integration constant

D: Molecular diffusion coefficient

D_e: Effective diffusivity of oxycoal

D_p: Particle diameter

E: Activation energy

f: d'Arcy's law constant

f_j: Mass fraction of component j in the solid

g: Acceleration due to gravity

$g(X)$: Auxilary temperature function

G: Molar flowrate per unit area

h_o, h_1: Heat transfer coefficients

h_R: Heat transfer coefficient on radial surface

$\hat{H}$: molar enthalpy of gas

$\hat{H}_i$: molar enthalpy of component i in the gas

$\bar{H}$: Solid enthalpy per unit mass

$\bar{H}_j$: Enthalpy per unit mass of component j in solid

I_m: Main heater current

J_i: ith order Bessel function of the first kind

k: Thermal Conductivity

k_g: Gas thermal conductivity

k_s: Solid thermal conductivity

k_b: Bed thermal conductivity

$k_{b,x}$: Bed thermal conductivity in axial direction

$k_{b,R}$: Bed thermal conductivity in radial direction

k_o: Pre-exponential factor

k_r: $k_o \exp(-E/(RT))$

l: sample thickness

l_1, l_2: Distances between heater and sinks (equation 4.6.2)

L: Bed length or height

L_e: Effective particle length

m: Moles of oxygen per moles of nitrogen in the gas

m: Water flowrate

M: number of components in the solid phase

M_c: Mass of coal

M_w: Mass of absorbed water in the coal

M_p: Percent moisture in the coal

M_n: n th root of the equation $J_o(M_n)=0$

M': Dimensionless quantity defined by equation 5.2.3

n: Order of the Legendre polynomial P_n

N: Number of components in the gas phase

N': Dimensionless quantity defined by equation 5.2.4

p_j: Rate of Formation per unit bed volume of component j in the solid

P: Pressure

P_∞: ambient pressure

$\hat{P}$: $P - P_\infty$

$P_n(X)$: n th order Legendre polynomial

$P_n^*(X)$: n th order shifted Legendre polynomial

q: Amount of O_2 taken up per unit mass of coal

q_g: Flux in gas

q_s: Flux in solid

q': Source term in Diffusion Equation

Q': Rate of energy transfer by Conduction

Q_c: Rate of Convection from Solid to Gas

Q: Rate of energy input

Q_q: Rate of Energy absorption

Q_R: Radial Flux

Q_x: Axial Flux

r_i: Rate of formation per unit bed volume of i in the gas phase

r_o: Rate of oxidation at T_∞ for fresh coal

r: Rate of oxygen adsorption per unit bed volume for unity mole fraction oxygen

R: Gas constant

r: Radial co-ordinate (Chapter 4)

R: Spherical co-ordinate (Chapter 4)

R: Radial Distance (Appendix 5)

R_o: Bed Radius (Appendix 5)

S_t: Total reactive surface per particle volume

S: Total external surface per particle volume

S_m: External surface area per unit mass

S': Total surface area for reaction

t: Time

T: Temperature

T_∞: Ambient Temperature

T_g: Gas Temperature

T_s: Solid temperature

T': Temperature averaged radially

T_∞: Ambient Temperature

T_{av}: Average temperature = $L/\int_0^L T^{-1}dx$

$T_o(X)$: Initial temperature profile

U: Flow velocity

U_g: Gas internal energy

U_s: Solid internal energy

$\hat{U}$: Molar internal energy of the gas

$\bar{U}_s$: Internal energy of the solid per unit mass

$u(X,\tau)$: Auxilary temperature function (equation A8.2)

V: Wind velocity

v: Temperature above ambient

$v(X,\tau)$: Auxilary temperature function (equation 6.3.2)

V_b: Bed volume

V_p: Particle volume

V_m: Main heater voltage
x: Distance along bed
X: Dimensionless distance = x/L
y: Rectangular co-ordinate (Chapter 4)
y_i: Mole fraction of i in the gas phase
y_o: Mole fraction of oxygen at X=0
y: Mole fraction oxygen in the gas phase
z: Rectangular co-ordinate (Chapter 4)
z: Thickness of oxycoal layer
Z: Fractional conversion of coal
$Z_n(X)$: See equaiton 6.3.3

Greek Symbols

α: Fitting constant in equation 5.2.1
β: Roots of equation 6.3.4
γ_1,γ_2: $((a\pm(a^2+4C))^{1/2})/2$
γ_3: $-rL/G$
ΔH_w: Latent heat + heat of wetting
ΔH_r^i: Enthalpy of reaction
ΔH_r: Enthalpy of reaction for oxygen adsorption
ΔT: Temperature rise or temperature difference
ϵ: Voidage
η: Tortuosity factor
θ: Dimensionless temperature
$\theta_o(X)$: Initial dimensionless temperature profile
$\theta_{ss}(X)$: Steady-state dimensionless temperature profile
κ: Thermal diffusivity
μ: Gas viscosity
ν: D P/(R T)
ξ: $1/\tau'$
ρ: Density
ρ_s: Solid density
ρ_b: Bed density
ρ_g: Molar density of gas
ρ_∞: Density of gas at T_∞,P_∞
ρ_m: Molar density of oxycoal
σ: Stefan-Boltzmann constant
τ: Dimensionless time
τ_o: Period of oscillation
τ': Time constant for heat loss (Equation 5.2.5)
$\phi(X)$: Auxilary temperature function (equation A8.2)
ϕ_1,ϕ_2: Fitting constants in equation 8.1
τ_d: Time constant for equilibration of gas and solid

temperatures

τ_c: Time constant for conduction

τ_f: Time constant for flow

τ_p: Time constant for pressure change

1. AN OVERVIEW OF SPONTANEOUS COMBUSTION OF COAL

1.1 Introduction

The need to stockpile coal arises in many situations, most importantly in the following fields:

a) The generation of electricity

b) The coal mining industry

c) Coal transport

d) Steel making

It is well known that certain types of coal, when stockpiled, are liable to spontaneous combustion. Coal may undergo spontaneos combustion in many storage situations, among them:

a) In coal dumps

b) Underground

c) In the holds of ships

d) In storage silos or bunkers

The work described in this thesis concerns mainly spontaneous combustion as it relates to coal dumps. However, many of the conclusions reached are of significance, to a greater or lesser extent, in all of the storage situations mentioned above.

Spontaneous combustion of coal may lead to some or all of the following problems:

a) Loss of all or part of the coal dump. If the coal dump is a large one, as is the case at many mines and power stations, the economic effects of spontaneous combustion may well be disastrous.

b) Pollution. A burning coal dump presents a very real environmental problem, with noxious gases and particulate matter

being introduced into the atmosphere. This can present serious problems to communities in the vicinity of the burning dump.

c) Danger to human lives. Burning coal dumps can give rise to a dangerously high level of carbon monoxide, which may affect people working in the vicinity. Similarly, fires in ship's holds or underground can be extremely dangerous as well as costly.

Methods have been suggested, and are in use, for making coal dumps less liable to spontaneous combustion. These methods include compacting the dump, covering the dump with tar or sand, or spraying a cement-like substance on the surface of the dump. In addition much discussion has revolved around the monitoring of coal dumps, in order to obtain early warning of potential problems. Temperature monitoring by means of thermocouples, the taking of infra-red photographs and gas sampling have all been suggested and used as means of monitoring coal dumps.

One of the problems with the methods discussed above is that they tend to be costly, and the economic justification for their use is often not immediately obvious. The reason for this is that the knowledge that has been obtained in the field of spontaneous combustion is largely empirical, being based on experience gained by people working in the field. Although this knowledge is exteremely valuable, it is not always of great use when new stockpiling situations arise, or when a new mine is opened and the newly mined coal's liability to spontaneous combustion is an unknown quantity.

It seems clear that what is required is a sound scientific analysis of spontaneous combustion, on which decisions as to stockpiling practice can be based. The aim of this thesis is to provide this analysis, by analyzing the fundamental processes occuring in a coal dump, and synthesizing their effects in a mathematical model. The model can then be used as a basis on which predicitions about the behaviour of a certain coal in a certain stockpiling situation can be made. Hopefully this will lead to the construction of stockpiles in which the chances of spontaneous combustion occuring are minimized.

1.2 Previous Investigations into Spontaneous Combustion

A comprehensive reviews of spontaneous combustion of coal has been presented by Itay (1984). The aim of this section is to provide a critical review in which the important facts that have emerged are summarised. These facts will then be further discussed.

Many workers have concerned themselves with oxidation of coal (Van Krevelen,1981) and the literature on the subject has been reviewed by Guney (1968). The main conclusions reached are

a) The oxidation of coal appears to be a chemisorption reaction at temperatures under 70 ^{o}C; oxygen is taken up without water or carbon dioxide being formed.

b) The enthalpy of reaction is of the order of 300 kJ per mole of oxygen adsorbed (Edwards, 1983 and Sondreal & Ellman, 1974). This may be compared with an enthalpy of reaction of 390 kJ/mole for the reaction

$$C(graphite) + O_2(g) = CO_2(g).$$

c) The rate of oxidation decreases with time i.e. the coal ages.

d) The reaction rate appears to be of order ½ to 1 with respect to the oxygen concentration.

A series of investigators have reported different activation energies for the oxidation; these discrepancies appear to be due to the various ranges of temperature covered.

Van Krevelen (1981) believed that the primary reaction of chemisorption of oxygen has a relatively low activation energy of approximately 3 - 4 Kcal/mole.

Above a temperature of 70 ^{o}C decomposition of the adsorption complex may occur, with an activation energy of approximatley 6.5 Kcal/mole. However, chemisoption of oxygen occurs up to a temperature of 350 ^{o}C.

Many other investigators, notably Guney (1972) and Bhattacharyya

(1970) have investigated the effect ot moisture in the coal and reacting gas. The absorption of water is, not surprisingly, associated with a large enthalpy of reaction. In addition it appears that the absorbed moisture in the coal plays a part in the oxidation reaction, for dry coal oxidises at a far lower rate than moist coal. However, the effect of moisture on self heating of coal is still a subject of intense debate, mainly because different investigators have reported different results. This appears to be due to different apparatus and analysis methods being used, as well as different sample preparation techniques (e.g. vacuum drying, oil drying and air drying all at room temperature or elevated temperatures).

One important point has emerged from the studies performed by Murtagh (1966) who used a computer simulation technique. His main conclusion is that at low temperature moisture transfer is the dominant heat transfer mechanism in a dump, but that spontaneous ignition does not occur when only moisture is considered. His explanation for this is that at about 100 ^{o}C inherent moisture is driven from the coal, causing a cooling. Since there can be no further absorption of water, the maximum temperature that can occur is approximately 100 ^{o}C. It should be pointed out that should a coal dump reach a temperature of 100 ^{o}C, then it might be well on the way to combustion, since the rate of oxidation could be very high at this temperature.

It thus appears from the literature that moisture effects, especially the absorption of water by dry coal, can lead to an increase in the temperature of a coal dump to the point where the rate of oxidation becomes appreciable. In this situation the coal dump could be at risk.

This conclusion has a important consequence when one considers spontaneous combustion underground as opposed to spontaneous combustion above ground. In the underground situation the coal is likely to be dry, especially if it is newly mined. In addition the humidity of the air in the mine is high. Thus underground spontaneous combustion could be largely triggered by moisture absorption. However, when considering coal stockpiles, it should be remembered that these are normally laid down with water to facilitate compaction. In addition the coal that is stockpiled has generally come from a washing plant, and is thus wet. Thus the effect of moisture on a newly laid down coal dump is likely

(1970) have investigated the effect ot moisture in the coal and reacting gas. The absorption of water is, not surprisingly, associated with a large enthalpy of reaction. In addition it appears that the absorbed moisture in the coal plays a part in the oxidation reaction, for dry coal oxidises at a far lower rate than moist coal. However, the effect of moisture on self heating of coal is still a subject of intense debate, mainly because different investigators have reported different results. This appears to be due to different apparatus and analysis methods being used, as well as different sample preparation techniques (e.g. vacuum drying, oil drying and air drying all at room temperature or elevated temperatures).

One important point has emerged from the studies performed by Murtagh (1966) who used a computer simulation technique. His main conclusion is that at low temperature moisture transfer is the dominant heat transfer mechanism in a dump, but that spontaneous ignition does not occur when only moisture is considered. His explanation for this is that at about 100 ^{o}C inherent moisture is driven from the coal, causing a cooling. Since there can be no further absorption of water, the maximum temperature that can occur is approximately 100 ^{o}C. It should be pointed out that should a coal dump reach a temperature of 100 ^{o}C, then it might be well on the way to combustion, since the rate of oxidation could be very high at this temperature.

It thus appears from the literature that moisture effects, especially the absorption of water by dry coal, can lead to an increase in the temperature of a coal dump to the point where the rate of oxidation becomes appreciable. In this situation the coal dump could be at risk.

This conclusion has a important consequence when one considers spontaneous combustion underground as opposed to spontaneous combustion above ground. In the underground situation the coal is likely to be dry, especially if it is newly mined. In addition the humidity of the air in the mine is high. Thus underground spontaneous combustion could be largely triggered by moisture absorption. However, when considering coal stockpiles, it should be remembered that these are normally laid down with water to facilitate compaction. In addition the coal that is stockpiled has generally come from a washing plant, and is thus wet. Thus the effect of moisture on a newly laid down coal dump is likely

to be a beneficial one i.e. the evaporation of water will cause cooling. However, should there be very dry conditions causing drying out of the coal, followed by humid conditions, moisture absorption may well occur.

It is neccessary to look at the other factors involved in spontaneous combustion. These have been shown by many investigators (Sondreal & Ellman, 1974, Nordon, 1979) to be:

a) Transport into the dump and
b) Heat transfer within the dump.

As many investigators have pointed out, the importance of these two effects should not be underestimated. No matter how reactive a given coal is it will not undergo spontaneous combustion if

a) The reactants cannot get to it or
b) The heat generated by reaction can be readily transferred out of the dump.

Investigators have previously used mathematical models, based on energy balances for a reacting bed of coal, to try and predict the onset of spontaneous combustion. Notable among these investigators are Van Doornum (1954), Murtagh (1966), Sondreal & Ellman (1974) and Nordon (1979). The work of Murtagh (1966) has been discussed, and the work of the other three investigators will be further discussed in section 5.2. It is shown that the models used by these investigators suffer from the shortcoming that the effect of natural convection is ignored. The justification for ignoring this effect has been based on conclusions drawn by these researchers from the work of Lapwood (1948). The validity of these conclusions will be discussed in section 5.2.

Having reviewed the literature on the subject of spontaneous combustion of coal, it is felt that three main areas of importance in predicting the behaviour of a coal dump have been identified.

They are:

a) Mechanisms whereby reactants such as oxygen and water are transported into a dump.

b) The chemical reactions that occur betwen coal and these reactants, in particular the thermal effects of these reactions.

c) Heat transfer within the dump.

These three areas will now be discussed separately.

1.3 Transport in a Coal Dump

Five mechanisms whereby reactants may be transported into a coal dump have been identified. They are:

a) Natural convection caused by self heating of the dump.

b) Wind pressure on the inclined surfaces of the dump which causes flow.

c) Molecular diffusion caused by concentration gradients.

d) Barometric breathing caused by changes in barometric pressure.

e) Thermal breathing caused by the daily variation in temperature.

In order to decide which, if any, of these mechanisms is the most important source of reactants to a coal dump it was felt necessary to derive simple models to describe each mechanism. These models give an idea of the order of magnitude of each of the effects and lead to important conclusions regarding which mechanisms may be neglected and which may not. A full discussion of these models is given in Chapter 2.

1.4 The Chemical Reactivity of Coal

Spontaneous combustion of coal occurs due to reaction between atmospheric gases and coal. The gases that are of importance are water vapour and oxygen. A discussion of the reactivity of coal towards these reactants follows.

1.4.1 Reaction between Coal and Water

Much experimental effort has been devoted to the elucidation of the effect of moisture on spontaneous combustion of coal. Nordon, Young & Bainbridge (1979) have pointed out that the effect of moisture on the self heating of coal is two-fold. Firstly absorbed water exerts a catalytic effect on the oxidation rate, and secondly there is a transient effect which occurs as moisture is absorbed or desorbed. This partly explains why so many apparently contradictory results in connection with the effect of gas and coal moisture on self heating of coal have been obtained, since confusion arises due to the different ways in which the coal is dried, and the coal and atmospheric moisture contents are reported.

The catalytic effect of coal moisture content on the oxidation rate is well documented in the literature. Sondreal & Ellman (1974) report oxidation rates of lignite as being proportional to

$$1 + 0.674\ M_p - 0.01634\ M_p^2$$

where M_p is the moisture content expressed in percent. This expression implies that the rate of oxidation is a maximum when M_p is equal to twenty percent. This value is close to the equilibrium moisture content of coal.

The second effect mentioned is the transient absorption and desorption of moisture. The heat effect associated with the absorption of moisture is the latent heat of vaporization plus the heat of wetting. The former has a value of 500 cal/g at 25 °C and the latter has been reported by Sondreal & Ellman (1974) to be of the order of 24 cal/g. A simple energy balance may be written to calculate the temperature rise due to absorption of moisture by dry coal.

1.4.1

$$M_c\ \bar{c}_b\ \Delta T = M_w\ \Delta H_w$$

where M_c = mass of coal
$\bar{c}_b$ = specific heat capacity of coal
ΔT = temperature rise
M_w = mass of water absorbed
ΔH_w = latent heat + heat of wetting

Therefore $\Delta T = \frac{M_w \Delta H_w}{M_c \bar{c}_b}$ 1.4.2

Assume $M_w/M_c = 0,05$ i.e the coal absorbs five percent of its mass of moisture. The specific heat of a typical coal is 0,25 cal/g/K. By equation 1.4.2

$$\Delta T = \frac{0,05 \times 524}{0,25} = 104,8 \text{ K}$$

This is a substantial temperature rise, which will never be achieved in practise since as the coal absorbs moisture and the temperature increases the vapour pressure of the water above the coal increases and the reaction rapidly comes to equilibrium.

As has been pointed out by Kibria (1972) heating due to moisture absorption may bring coal to a temperature where oxidation occurs at a dangerous rate. This point is extremely important; water absorption may well be a starting mechanism whereby the tempe- rature inside a coal pile which is at risk starts rising leading to the onset of a large amount of oxidation and eventual com- bustion. The opposite is also true; if a coal dump is inherently safe no amount of water absorption will start it burning; com- bustion occurs due to oxidation, and not due to moisture effects.

1.4.2 Low Temperature Oxidation of Coal

The amount of literature on the chemical reactivity of coal, and in particular its low temperature oxidation, is vast. However, for the reason that every coal is likely to have a different reactivity, it was felt that a new study had to be undertaken. This work was performed by M. Itay, at the department of Chemical Engineering at the University of the Witwatersrand. A summary of the conclusions reached by Itay (1984) is presented in this section.

The experimental apparatus used to conduct these studies was a nearly adiabatic reaction vessel into which coal is packed and oxygen introduced. The temperature-time history of the reaction is recorded, and gas samples are taken periodically and analyzed for O_2, N_2, CO, CO_2, and H_2O. The measured temperature time

curve is used to back calculate the adiabatic temperature time curve, and this curve is used to obtain information on the rate of reaction and on the thermal effects associated with the reaction.

The data obtained thus far points very strongly to the conclusion that the chemical reactivity of the coal falls off with the degree of oxidation of the sample. This effect is well known and has been much reported in the literature (see for example Van Krevelen, 1981). However few plausible explanations for the effect have been given.

Another important conclusion is that the disappearance of oxygen is not neccessarily accompanied by the appearance of reaction products e.g. CO_2. It appears that at a low temperature coal adsorbs O_2 strongly and desorbs CO_2 at a far lower rate. This has also been noted in the literature, and the increase in density of reacting coal samples strongly supports this fact (Van Krevelen, 1981). In addition the desorption of the CO_2 appears to have a small enthalpy of reaction. This behaviour is shown graphically in Figure 1.1.

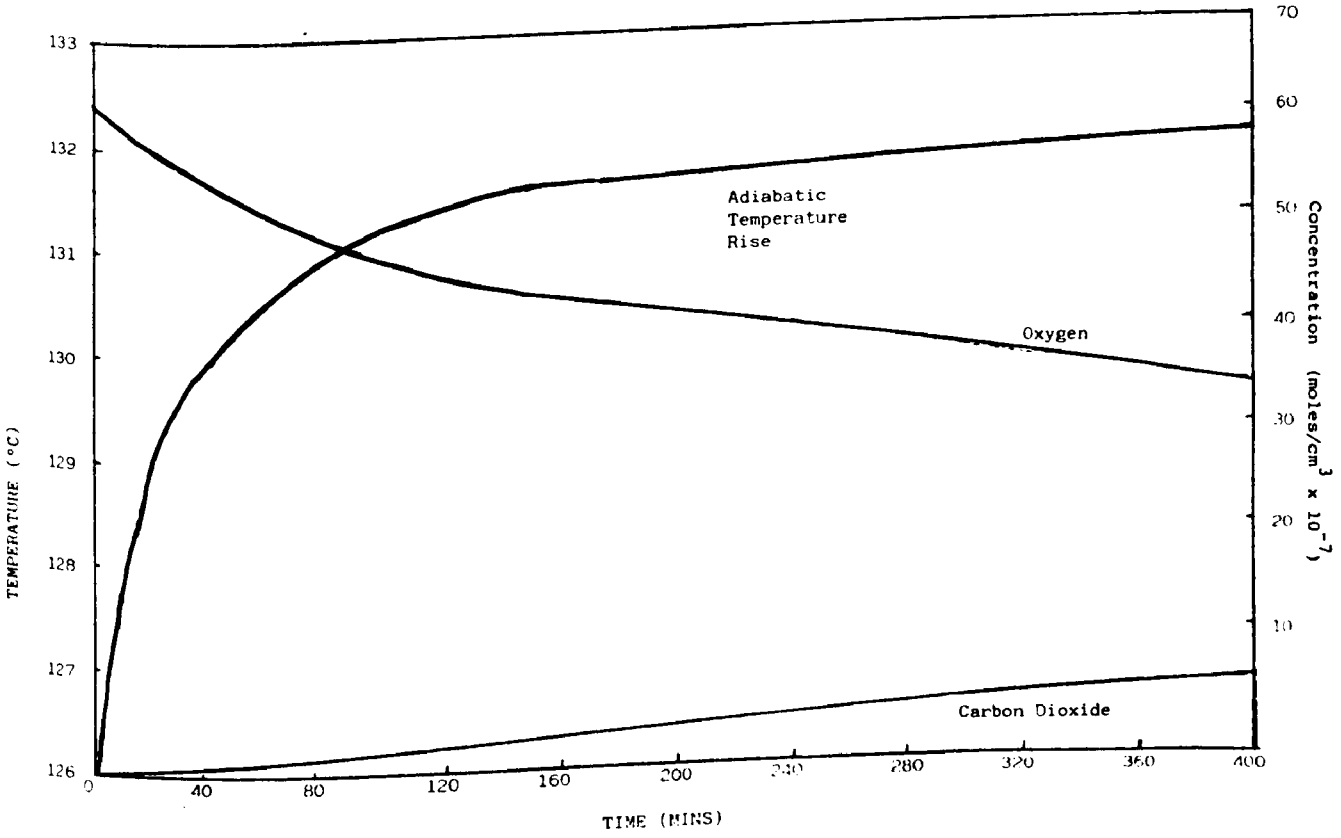


Figure 1.1 Temperature, Oxygen and Carbon Dioxide Versus Time

(After Itay, 1984)

In order to explain these effects a model for the reaction of coal with oxygen has been jointly derived by this researcher and Itay . The model is based on the hypothesis that coal absorbs oxygen to form a complex, which may be called oxycoal, without the formation of any gaseous products. The formation of an oxycoal layer on the surface of the coal has been demonstrated in the literature, and photographs showing this effect have been published by Van Krevelen (1981). As the oxycoal layer builds up the reaction rate slows down due to the fact that oxygen now has to diffuse through the oxycoal to react with the coal. This reaction model is an example of the so called shrinking core model, which is thoroughly discussed by Levenspiel (1962).

The derivation of the rate equation that follows from these assumptions is given in Appendix 1. The equations take the form:

Rate of adsorption of oxygen / unit volume of bed =

$$r = \frac{S_t\ (1-\epsilon)\ C}{1/k_r + Z/(S_t\ D_e)} \qquad 1.4.3$$

$$\frac{dZ}{dt} = \frac{S_t\ C}{\rho_m\ (1/k_r + Z/(S_t\ D_e))} \qquad 1.4.4$$

Where $S_t = \dfrac{\text{total surface area of particle}}{\text{volume of particle}}$

ϵ = bed voidage

C = O_2 concentration

k_r = surface rate constant

Z = fractional conversion of coal

D_e = effective diffusivity of oxycoal layer

ρ_m = molar density of coal

The temperature dependence of the reaction is given by the usual Arrhenius relationship i.e.

$$k_r = k_o \exp(-E/(R\,T)) \qquad 1.4.5$$

k_o = pre-exponential factor
E = activation energy
R = gas constant
T = temperature

In order to better understand the behaviour of this reaction model, the equations were solved under the assumptions of constant O_2 concentration and a constant value of k_r, the surface rate constant.

Under this assumption equation 1.4.4 gives

$$Z/(S_t\,D_e) = -1/k_r^2 + (1/k_r^2 + 2Ct/(\rho_m\,D_e))^{1/2} \qquad 1.4.6$$

Back substitution in equation 1.4.5 gives

$$r = S_t\,(1-\epsilon)\,C\,/(1/k_r^2 + 2Ct/(\rho_m\,D_e))^{1/2} \qquad 1.4.7$$

Two limiting cases were considered. In the early stages of reaction the oxycoal layer has not built up and the rate of the chemical reaction is limiting. In this case

$$1/k_r^2 \gg 2Ct/(\rho_m\,D_e)$$

$$\text{and } r = k_r S_t (1-\epsilon) C \qquad 1.4.8$$

i.e. in the early stages of reaction the rate is first order with respect to the O_2 concentration and is time independent.

However when more reaction has taken place it is reasonable to assume that the diffusion through the oxycoal layer is limiting. In this case

$$1/k_r^2 \ll 2Ct/(\rho_m\,D_e)$$

$$\text{and} \qquad r = ((\rho_m\,D_e\,C/(2t))^{1/2}\,S_t\,(1-\epsilon) \qquad 1.4.9$$

In the later stages of the reaction the rate is half order with respect to the O_2 concentration and exhibits a $1/t^{1/2}$ dependence on time.

This model therefore is in agreement with the observed behaviour of coal reactivity i.e. that the reactivity shows a definite falling off with time, which is in fact a falling off with degree of oxidation, and that the reaction order with respect to oxygen varies between one and a half . Fractional reaction orders have been reported by Sondreal & Ellman (1974).

It is therefore felt that a reaction model has been derived which is consistent with the available evidence. The problem that remains is to use the available experimental data to derive the model constants, in order that the model may be checked and used with confidence.

1.5 Heat Transfer within a coal dump

The safety or otherwise of a coal dump is likely to depend upon the balance between the rate of temperature rise due to reaction and the rate at which this energy is transferred away from the hot zone. It is known that coal is a fairly good insulator, but little data is available on the physical characteristics of heat transfer in coal beds. In addition these characteristics are likely to be dependent on both the voidage and particle size of the coal bed. For these reasons a literature survey was performed on the subject of heat transfer in packed beds; the results of this survey are presented in Chapter 3.

Following from this work, it was felt worth while to design and construct an apparatus to measure the so called effective thermal conductivity of a packed bed of coal. This aspect of the work is also discussed in Chapter 4 together with the results obtained.

1.6 A Mathematical Model For Spontaneous Combustion

In Chapter 5 a literature survey of existing mathematical models for spontaneous combustion of coal is presented. It is shown that all of these models suffer from one or more shortcomings. A set of equations, describing the behaviour of a so-called one-dimensional analogue of a coal dump is thus derived and discussed. In Chapter 6 certain simplifications to the model are discussed and justified. The methods used to solve this simplified set of equations are discussed.

1.7 Experimental Investigation

In Chapter 7 an experiment used to test the model as well as to obtain parameters for the model is discussed. The conclusion is reached that the model accurately describes the behaviour of a one-dimensional analogue of a coal dump.

1.8 Results and Conclusions

The large majority of Chapter 8 is devoted to a parameter study on the effect of on the model of changing certain parameters. The results obtained are discussed and the implications for the practising engineer pointed out. A simplified analysis is performed in order to deduce the temperature-time behaviour of the model, and the practical implications discussed. Shortcomings of the model are also discussed, together with suggestions for further research. Finally, in Chapter 9, the important conclusions reached in the thesis are summarised.

2. ANALYSIS OF SUGGESTED MECHANISMS FOR INGRESS OF REACTANTS

2.1 Introduction

The various mechanisms suggested for transport into a coal dump have been mentioned in section 1.2. They are repeated here for convenience.

a) Natural convection caused by self heating of the dump.

b) Flow caused by differential pressure between inclined and flat surfaces of the dump.

c) Molecular diffusion caused by concentration gradients.

d) Barometric breathing caused by changes in barometric pressure.

e) Thermal breathing caused by the daily variation in temperature.

In order to decide which of these mechanisms are important simple models were used to obtain order of magnitude estimates of their effect. It proves convenient to analyze mechanisms a) and b) together.

2.2 Natural Convection and Wind Pressure

In Chapter 5 a so-called one-dimensional model of the processes occuring in a coal dump is discussed. In Appendix 3 it is shown that the following momentum balance, for a vertically aligned bed open at both ends, may be written:

$$\frac{d\hat{P}}{dx} = -f\,U + \rho_\infty\, g\,(1 - T_\infty/T) \qquad 2.2.1$$

$\hat{P}$ = Pressure - ambient pressure
f = D'Arcy's law constant for the packed bed.
U = Superficial flow velocity
ρ_∞ = density of ambient air
g = acceleration due to gravity
T_∞ = ambient air temperature
T = bed temperature

Bird, Stuart & Lightfoot (1960) have discussed equations that attempt to correlate the factor f. One such equation is the Ergun equation which is

$$f = \frac{150\ (1-\epsilon)^2\ \mu\ S^2}{36\ \epsilon^3} + \frac{10.5\ (1-\epsilon)\ \rho\ U\ S}{\epsilon^3} \qquad 2.2.2$$

ϵ = bed voidage
μ = gas viscosity
ρ = gas density
$S = \frac{\text{total particle external surface area}}{\text{volume of particle}}$

It has been shown that for small flowrates the second term on the R.H.S. is negligible giving:

$$f = \frac{150\ (1-\epsilon)^2\ \mu\ S^2}{36\ \epsilon^3} \qquad 2.2.3$$

Note that no assumption need be made on the geometry of the particles or the bed packing. A mean particle diameter may be defined to be

$$D_p = 6/S \qquad 2.2.4$$

Under still air conditions the following boundary conditions are used for equation 2.2.1:

$$\hat{P}\ (x=0) = 0 \qquad 2.2.5$$

$$\hat{P}\ (x=L) = 0 \qquad 2.2.6$$

These boundary conditions merely reflect the fact that the ends of the bed are at atmospheric pressure.

In an attempt to compare the magnitude of natural convection induced flows with those of flows due to pressure differences, it is assumed that the stagnation pressure of a wind flow of velocity U may be use as an upper bound on the pressure difference that can arise between any two points on the surface of a coal dump. It is thus assumed that an estimate of the flows due to wind pressure may be obtained by assuming that the pressure at the bottom of the bed is increased by the stagnation pressure of the wind of velocity U.

Therefore

$$P(x=0) = P_\infty + \rho_\infty U^2/2 \qquad 2.2.7$$

and

$$\hat{P}(x=0) = \rho_\infty U^2/2 \qquad 2.2.8$$

Therefore the effect of wind is to change the boundary condition at $x = 0$ to

$$\hat{P} = \rho_\infty U^2/2 \qquad 2.2.9$$

Assuming U constant for small variations in temperature, equation 2.2.1 may be integrated to give:

$$\hat{P}(x=L)-\hat{P}(x=0) = -f\ U\ L + \rho_\infty\ g\ (L - \int_0^L (T_\infty/T\ dx)) \qquad 2.2.10$$

or

$$-\rho_\infty U^2/2 = -f\ U\ L + \rho_\infty\ g\ L\ (1 - (T_\infty/T_{aU})) \qquad 2.2.11$$

where

$$1/T_{aU} = 1/L \int_0^L T^{-1}\ dx \qquad 2.2.12$$

Therefore

$$U = \frac{\rho_\infty U^2}{2\ f\ L} + \frac{\rho_\infty g}{f}\ (1-T_\infty/T_{aU}) \qquad 2.2.13$$

or $$U = U(\text{Wind pressure}) + U(\text{Natural convection}) \quad 2.2.14$$

therefore

$$\frac{U(\text{Wind})}{U(\text{convection})} = \frac{v^2}{2\,L\,g\,(1-T_\infty/T_{av})} \quad 2.2.15$$

To illustrate the use of this equation, it will be used to calculate the wind velocity required to cause the same flow through a 10 m bed as a temperature rise of 20 ^{o}C.

i.e. $$1 = \frac{v^2}{2 \times 10 \times 9.8 \times (1-300/320)} \quad 2.2.16$$

or $$v = 3.5 \text{ m/s} = 12.6 \text{ km/hr}$$

This implies that for a windspeed of 12.6 km/hr natural convection will supply as much oxygen to the dump as will the differential wind pressure effect.

In order to compare these effects with the effects of molecular diffusion it is neccesary to calculate the molar flow rate per unit area for various average particle sizes. The relationships used are

$$G = \frac{P\,U}{R\,T} \quad 2.2.17$$

together with equations 2.2.2 and 2.2.15.

This calculation has been performed for L = 10 m, T_{av} = 320 K and ϵ = 0.3. The results are presented in Table 2.1.

TABLE 2.1 MOLAR FLOWRATES FOR VARIOUS PARTICLE SIZES

D_p (mm)	f (kg/m^2/s)	G (kmol/m^2/s)
1	5.6×10^{4}	5.1×10^{-7}
2	1.4×10^{4}	2.0×10^{-6}
5	2.2×10^{3}	1.3×10^{-4}

2.3 Analysis of Molecular Diffusion

In order to analyze the importance of diffusion as a mechanism for oxygen ingress a simplified analysis was performed. Considering diffusion as the only transport mechanism for oxygen into the dump the following energy and mass balances may be written:

Energy balance: $$K_b \frac{\partial^2 T}{\partial x^2} - r \Delta H = 0 \qquad 2.3.1$$

Mass balance: $$D\epsilon \frac{\partial^2 C}{\partial x^2} - r = 0 \qquad 2.3.2$$

The boundary conditions are:

$$\text{At } x=0 \quad T = T_\infty \quad C = C_\infty$$

$$\text{At } x=L \quad \frac{\partial T}{\partial x} = 0 \quad \frac{\partial C}{\partial x} = 0$$

These correspond to ambient conditions on the top surface of the dump, and a bottom surface that is perfectly insulating and impervious. These conditions will lead to a maximum temperature rise. Although this geometry is somewhat different to the geometry used in section 2.2, and thus the results obtained will not be directly comparable, it should be stressed that all that is required is an upper bound for comparison purposes; the geometry is unlikely to make a large difference on the bound.

Multiplying 2.3.2 by ΔH and subtracting the result from 2.3.1 gives:

$$K_b \frac{\partial^2 T}{\partial x^2} - D\epsilon\Delta H \frac{\partial^2 C}{\partial x^2} = 0 \qquad 2.3.3$$

or $$\frac{\partial^2}{\partial x^2}\left(T - \frac{D\epsilon\Delta H}{K_b} C\right) = 0 \qquad 2.3.4$$

This equation may be integrated to give:

$$T - \frac{D\epsilon\Delta H}{K_b} C = Ax + B \qquad 2.3.5$$

A and B may be determined from the boundary conditions as

follows:

At $x=0$ $T=T_\infty$ $C=C_\infty$

Therefore $$T_\infty - \frac{D\epsilon\Delta H}{k_b} C_\infty = B$$

and $$T - T_\infty - \frac{D\epsilon\Delta H}{k_b} (C - C_\infty) = Ax \qquad 2.3.6$$

Differentiating 2.3.5 wrt x gives:

$$\frac{\partial T}{\partial x} - \frac{D\epsilon\Delta H}{k_b} \frac{\partial C}{\partial x} = A \qquad 2.3.7$$

but at $x=L$ both derivatives in 2.3.7 are 0, therefore $A=0$.

Therefore $$T - T_\infty = \frac{D\epsilon\Delta H}{k_b} (C_\infty - C) \qquad 2.3.8$$

From 2.3.8 the maximum temperature rise with diffusion as the only transport mechanism may be calculated. This maximum temperature rise will occur at a point where $C=0$. Then:

$$T - T_\infty = \frac{D\epsilon\Delta H C_\infty}{k_b} \qquad 2.3.9$$

Typical values for the quantites in this equation are:

$$D = 2 \times 10^{-5} \text{ m}^2/\text{s}$$
$$\epsilon = 0.3$$
$$\Delta H = 3 \times 10^{8} \text{ J/kmol}$$
$$C_\infty = 8 \times 10^{-3} \text{ kmol/m}^3$$
$$k_b = 0.2 \text{ W/m/K}$$

Therefore

$$T - T_\infty = \frac{2\times10^{-5}\times0.3\times3\times10^{8}\times8\times10^{-3}}{0.2}$$

$$= 72 \text{ K}$$

This temperature rise, though appreciable, is not sufficient to explain the high temperatures observed in burning coal dumps. It is thus suggested that, in the same way that moisture absorption can act as a trigger for the oxidation reaction, diffusion can act as a trigger whereby the temperature in a coal dump starts rising, eventually giving rise to stable natural convection flows. These flows supply more oxygen to the dump than diffusion can, and eventually lead to spontaneous combustion.

Having concluded that diffusion can not explain spontaneous combustion, it is felt important to attempt to calculate the flowrates that diffusion causes. This facilitates the comparison of the magnitude of the flowrate caused by diffusion with the flowrates already calculated for wind and natural convection. To model molecular diffusion the coal is considered to adsorb oxygen, as discussed in section 1.3, and the isothermal steady state material balance for oxygen is

$$0 = \frac{D\ P}{R\ T}\frac{d^2y}{dx^2} - G\frac{dy}{dx} - r\ y \qquad 2.3.10$$

D = molecular diffusion coefficient
y = mole fraction oxygen
r = reaction rate per unit bed volume

The boundary conditions for equation 2.3.1 are:

$$y(x = 0) = .21 \qquad 2.3.11$$

and $$y(x \to \infty) = 0 \qquad 2.3.12$$

The solution is:

$$y = .21\ \exp((G - (G^2 + 4\ r\ \nu)^{1/2})\ x/\nu) \qquad 2.3.13$$

where $$\nu = D\ P/(R\ T)$$

The oxygen flux at x = 0 is

$$\frac{D\ P}{R\ T}\frac{dy}{dx} = .21\ ((G^2/4 + r\ \nu)^{1/2} - G/2) \qquad 2.3.14$$

Using the simplified equation

$$r = k_o\ S_t\ (1-\epsilon)\ \exp(-E/(R\ T))\ P/(R\ T) \qquad 2.3.15$$

with the values

k_o = 10 m/s
E/R = 7000 K
S_t = $6/D_p$
ϵ = 0.3

$$D = 1.8 \times 10^{-8} \ m^2/s$$

and the data from Table 2.1 the entries in Table 2.2 have been calculated.

TABLE 2.2 COMPARISON OF MOLECULAR DIFFUSION AND CONVECTION

D_D (mm)	r (kmol/m^3/s)	Diffusional O_2 Flux (kmol/m^2/s)	Convective O_2 Flux (kmol/m^2/s)
1	1.2×10^{-7}	2.8×10^{-8}	1.0×10^{-7}
2	6.2×10^{-8}	4.4×10^{-9}	4.0×10^{-6}
5	2.5×10^{-8}	2.8×10^{-10}	2.6×10^{-5}

It can be seen from Table 2.2 that the effect of molecular diffusion is very much less pronounced for larger particles. For a particle size of 1 mm molecular diffusion supplies approximately 1/4 as much O_2 as a natural convection flow driven by a 20 ^oC temperature rise. In addition the molecular diffusion flux decreases with increasing particle size, while the convective flux increases. Although the analysis presented above may be criticized on the grounds that the transport equations have been decoupled, it can be seen that, except for the smallest particle sizes, the convective flux is orders of magnitude larger than the diffusional flux. This result justifies the use of the decoupled analysis to obtain order of magnitude estimates.

In the absence of wind or any temperature rise molecular diffusion may well be the only mechanism for O_2 transport into the dump. However it can be seen that as soon as there is any temperature rise in the dump natural convection will take over as the mechanism of O_2 transport.

2.4 Barometric Breathing

Barometric breathing occurs when the barometric pressure changes, causing a change in the volume of air that was in the dump. If the barometric pressure increases, this will cause a flow of air into the dump.

Consider a dump of 100 m x 50 m x 20 m high. Assume the barometric pressure increases from 620 mm Hg to 630 mm Hg in a time period of 24 hrs.

The air in the dump has a volume

$$100 \times 20 \times 50 \times 0.3 = 3 \times 10^4 \text{ m}^3$$

assuming $\epsilon = 0.3$.

This amount of air would shrink to a volume of

$3 \times 10^4 \times 620/630 \text{ m}^3 = 2.95 \times 10^4 \text{ m}^3$

and thus $4{,}76 \times 10^2 \text{ m}^3$ of air will flow in.

This flow will occur through the sides and the top of the dump i.e. a surface area of

$100 \times 50 + 2 \times 20 \times 50 + 2 \times 100 \times 20 = 11\,000 \text{ m}^2$

Thus the flowrate of air into the dump will be

$$\frac{4.76 \times 10^2}{11\,000 \times 24 \times 3600} = 5 \times 10^{-7} \text{ m/s}$$

This corresponds to a flux of 2×10^{-8} kmol/m^2/s which is an extremely small flux, and can safely be ignored.

Under certain weather conditions the barometric pressure may change far more rapidly than 10 mm Hg over a 24 hr period. This is the case for instance after a thunderstorm. These rapid changes may supply the dump with an appreciable amount of gas over a short period of time. The effect of this may well be to increase local temperatures in the dump and lead to the onset of natural convection flows. Thus rapid changes in barometric pressure may be a starting mechanism for the onset of spontaneous combustion in a dump that is in an unsafe condition.

2.5 Thermal Breathing

It has been hypothesized that the daily variation in temperature may lead to breathing of the dump i.e. hot air may leave the dump at night and be replaced by cold air thus supplying the dump with fresh reactants.

Measurements made at Grootegeluk coal mine indicate that surface temperature variations extend into the dump only a short distance; typically 325 mm.

A theoretical analysis of a problem of a semi-infinite solid with the surface temperature varying sinusoidally with time is discussed by Eckert & Drake (1972) who draw the conclusion that the oscillations are unimportant when

$$\frac{x}{2\,(\pi K \tau_o)^{1/2}} > 0.8 \qquad 2.5.1$$

Where K = thermal diffusivity of medium
τ_o = period of oscillation
x = distance into medium

For the case of daily fluctuations τ_o = 24 hrs. A typical value for the diffusivity of a coal bed is 8×10^{-4} m^2 / hr.

Therefore equation 2.5.1 gives

$$x > 2 \times 0.8 \times (\pi \times 8 \times 10^{-4} \times 24)^{1/2}$$

or $$x = 0.37 \text{ m}$$

This value agrees well with the measurements made on coal dumps discussed above.

It can be seen that thermal breathing will only supply reactants to the surface of the dump. Since any temperature rise near the surface of the dump is likely to be dissipated to the surface, it is unlikely that thermal breathing need be considered as an important reactant transport mechanism.

2.6 Conclusions

It may be concluded from the admittedly simplified analyses presented above that both wind pressure and natural convection must be considered as important mechanisms of O_2 transport into a coal dump. Molecular diffusion and barometric breathing may well be starting mechanisms, whereby the temperature begins rising in a coal dump. Natural convection soon becomes the dominant mech-

anism supplying O_2. This process may lead to eventual spontaneous combustion of a coal dump that is in an unsafe situation.

3. THEORETICAL MODELS FOR HEAT TRANSFER IN PACKED BEDS

3.1 Introduction

Thermal transfer of energy in packed beds is a field in which much work has been performed. The main reason for this is the importance of heat transfer in the design of packed bed catalytic chemical reactors. Other fields in which this knowledge is required include drying, nuclear reaction engineering and powder technology.

The literature survey that follows is very general, with no specific reference to coal beds. This is because the processes occuring in a packed bed of coal are no different to those occuring in packed beds of other materials.

3.2 Mechanisms of Energy Transfer in Packed Beds

In general energy transfer in a packed bed containing stagnant or moving fluid occurs by conduction, convection and radiation. The following potential mechanisms can be identified in the general case (Beveridge & Haughey, 1971).

Conductions Mechanisms

1. Conduction through the solid particles
2. Conduction across the gas in the voids
3. Conduction across the stagnant gas surrounding the points of contact between particles.
4. Conduction through the points of contact between particles

Radiation Mechanisms

5. Radiation between adjacent particle surfaces
6. Radiation between particle surfaces seen through more than one void space
7. Radiation absorption by the gas

Convection Mechanisms

8. Natural convection in the gas
9. Forced convection solid-gas transfer
10. Forced convection due to bulk flow, turbulent diffusion or mixing of the gas.

Of these mechanisms, mechanisms 1,2,4,5,6 and 7 are independent of fluid flow, while the other mechanisms depend to a greater or lesser extent on fluid flow, especially at low Reynolds numbers (Yagi & Kunii, 1957).

In general, thermal transfer of energy will take place by various combinations of series and parallel paths of these mechanisms.

3.3 Describing the overall energy transfer in a packed bed

The most common way of describing the overall transfer in a packed bed is by means of the so called effective thermal conductivity of the bed (Beveridge & Haughey, 1971). This quantity has also been called the thermal dispersion coefficient in the literature (Gunn & Khaled, 1975).

This formulation treats the system as homogeneous allowing the Fourier equation for the flux per unit area Q to be written

$$Q' = -k_b \frac{\partial T}{\partial X}$$

where $\partial T/\partial X$ is the temperature gradient in the required direction (axial or radial).

It can be seen from the discussion in 3.2 that k_b, the effective thermal conductivity, is in fact a function of many parameters including gas velocity, gas and solid temperatures, relative directions of gas and energy flow, fluid and solid properties as well as bed voidage and structural characteristics. It is the elucidation of this functional relationship that has been the goal of much of the work, both theoretical and experimental, that has been done in this field.

3.4 Models for energy transfer in which only conduction is considered

Many researchers have used as their starting point a model of a packed bed in which only conduction is considered. Models so derived should give good results provided the following conditions are met:

1. There is no gas flow
2. The particles are sufficiently small, and the temperature

sufficiently low, so that natural convection and radiation may be ignored.

Exactly what is meant by sufficiently small and sufficiently low will be discussed in greater detail later. Suffice it to say that if these conditions are met then the effective thermal conductivity, k_b, will be primarily a function of the thermal conductivities of the solid particle and stagnant gas. k_s and k_g respectively, and the structure of the bed.

Many models have been published to account for the four conduction mechanisms discussed in section 2, most of which describe the system in terms of its fluid and solid phase elements arranged in some regular array.

These models have been summarized by Beveridge & Haughey (1971), and their geometric significance is shown in figure 3.1

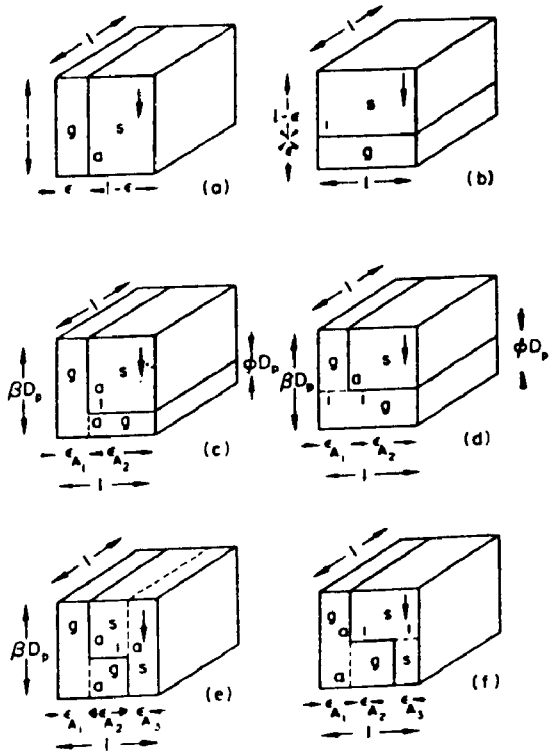


FIGURE 3.1 GEOMETRICAL CONDUCTION MODELS

a. adiabatic plane

i. isothermal plane

g. gas phase

s. solid phase

→ direction of energy transfer

(Beveridge & Haughey, 1971)

The simplest model is that represented by Fig 3.1a which postulates that conduction through the solid (mechanism 1) acts over a solid volume $1-\epsilon$, and the conduction across the gas in the voids and the stagnant gas round the points of contact (mechanisms 2 and 3) act over a gas volume ϵ. An arithmetic mean corresponding to a parallel arrangement of the two phases gives

$$\frac{k_b}{k_g} = \epsilon + (1 - \epsilon) \frac{k_s}{k_g} \qquad 3.4.1$$

The harmonic mean which corresponds to a series arrangement of the phases (Fig 3.1b) yields

$$\frac{k_b}{k_g} = \frac{k_s}{\epsilon\, k_s + (1 - \epsilon)\, k_g} \qquad 3.4.2$$

In attempting the formulation of more realistic models the concept of the unit cell is introduced, i.e. a representative element which is repeated throughout the packing. The basic geometric cell is that of Fig 3.1c with a cell of unit area perpendicular to the energy flow and height equal to the particle layer thickness $\beta' D_p$ where D_p = average diameter of particles.

Energy flow is one dimensional in parallel paths which are insulated from each other, and the distribution on the two phases is handled only by a two dimensional variation. This system then gives (see Fig 3.1c)

$$k_b = k_g\, \epsilon_{a1} + \frac{(1 - \epsilon_{a1})\, k_s}{\alpha' X + 1 - \alpha'} \qquad 3.4.3$$

where $\alpha' = \frac{\phi}{\beta'}$

and $\epsilon_{a1} = \frac{\epsilon - \alpha'}{1 - \alpha'}$

Modifications include that shown in Fig 3.1d which gives

$$k_b = \left[\alpha' k_g + \frac{1 - \alpha'}{k_g\, \epsilon_{a1} + k_s\, (1 - \epsilon_{a1})} \right]^{-1} \qquad 3.4.4$$

However, none of these models take into account the point to point

contact resistance (mechanism 4). One approach to this problem is that one used by Kunii & Smith (1960) who define a "heat" transfer coefficient h_p, accounting for an energy transfer contact resistance in parallel with the gas phase portion of the gas-solid series mechanism yielding:

$$\frac{k_b}{k_g} = \epsilon_{a1} + \frac{(1 - \epsilon_{a1})\, k_s/k_g}{(1 - \alpha) + \dfrac{\alpha\, k_s/k_g}{1 + \dfrac{h_p\, D_p}{k_g}}} \qquad 3.4.5$$

The quantity h_p has not been well correlated in the literature.

A more logical approach is the inclusion of the contact resistance in the idealized cell model as a solid energy flux path (represented by an area fraction ϵ_{a3}) arranged parallel to the gas path (Fig 3.1e) giving:

$$k_b = \epsilon_{a1}\, k_g + \frac{\epsilon_{a2}\, k_s}{\alpha' \dfrac{k_s}{k_g} + 1 - \alpha'} + \epsilon_{a3}\, k_s \qquad 3.4.6$$

A further extension to this approach is the one presented by Beveridge & Haughey (1971) in which the adiabatic boundary between the two parallel paths is replaced by an isothermal boundary (Fig 3.1f). This yields

$$\frac{k_b}{k_g} = \epsilon_{a1} + \left[\frac{1 - \alpha'}{\dfrac{k_s}{k_g}(1 - \epsilon_{a1})} + \frac{\alpha'}{\epsilon_{a2} + \epsilon_{a3}}\right]^{-1} \qquad 3.4.7$$

This approach has the advantage of allowing flux line bending in the solid phase.

It is shown by Beveridge & Haughey (1971) that k_b is a function of k_s/k_g, ϵ and ϵ_{a3} only. While k_s/k_g and ϵ are definable physical properties the parameter ϵ_{a3} must be determined experimentally for a given set of particles, since it will be affected by the particle loading and deformation as well as the surface

characteristics of the solid. It is also important to note that the effect of pressure on the thermal conductivity of the gas, k_g, must be properly taken into account.

3.5 Models for energy transfer in which conduction and radiation are considered.

Although radiant energy transfer will occur only through the voids of a packed bed of opaque solid pseudo-homogenous models have beem proposed which consider the solid and the gas as a single homogenous medium. The solution of the resultant integro-differential equations for conduction and radiation in absorbing and scattering models has been examined, most notably by Chan & Churchill (1963). They found that in an optically thick bed that the so called radiant conductivity $k_{b,r}$ could be written as

$$k_{b,r} = \frac{8 \sigma T^3}{a' + 2b'} \qquad 3.5.1$$

where σ = Stephan - Boltzmann constant
T = average bed temperature
a' = absorption cross section per unit volume of packing
b' = back scattering cross seciton per unit volume of packing

Note that the radiant conductivity is defined as the radiant energy flux density divided by the temperature gradient.

The radiant contribution has also been calculated by Bosworth (1952) from a random walk model giving

$$k_{b,r} = \frac{4 D_p T^3}{3}$$

The simplest radiation geometric model is that with two radiating plane surfaces at temperature T_1 and T_2, the radiant energy flux Q_r' being given by

$$Q'_r = \chi \sigma (T_1^4 - T_2^4) \qquad 3.5.3$$

where χ = view factor and emmisivity function

The elucidation of the function χ is difficult both theoretically and experimentally.

The energy flux Q'_r can be related to a radiation thermal conductivity $k_{b,r}$, and to a radiation coefficient $h_{b,r}$, by

$$Q'_r = -k_{b,r} \frac{\partial T}{\partial x} = h_{b,r} (T_1 - T_2) \qquad 3.5.4$$

When $T_1 - T_2$ is small compared to the absolute value of $T = T_1$ then:

$$\frac{k_{b,r}}{\beta D_p} = h_{b,r} = 4 \chi \sigma T^3 \qquad 3.5.5$$

The parameters in these models have a highly complex interaction with the structural and physical properties of the bed, and for this reason Beveridge & Haughey (1971) feel that there is little justification in representing the radiation mechanism other than by adding suitable terms to the simplest model such as the geometrical conduction models of Fig 1. Schotte (1960) used an analysis similar to that of Argo & Smith (1953) accounting for both the radiation between adjacent particle surfaces (mechanism 5) and the radiation between particle surfaces seen through more than one void space (mechanism 6) giving

$$Y_r = \epsilon X_{r,g} + \frac{1 - \epsilon}{\frac{k_g}{k_s} + \frac{1}{X_{r,s}}} \qquad 3.5.6$$

where $Y_r = \frac{k_{b,r}}{k_g}$

$$X_{r,g} = X_{r,s} = \frac{h_r D_p}{k_g} = \frac{4 D_p \chi \sigma T^3}{k_g} \qquad 3.5.7$$

The thermal conductivity of the bed is then given by

$$Y_t = Y_c + Y_r$$

In fact there is an interaction between the radiation and other energy transfer mechanisms and the contribution Yr cannot be added simply to the conduction terms. It is more satisfactory to utilize h_r within the conduction type model (Fig 3.1e). This was done by Yagi & Kunii (1957) who obtained

$$y_t = \epsilon_{a1}\,(1+ X_{r,g}) + \frac{\epsilon_{a2}}{\frac{\alpha'}{1 + \alpha' X_{r,s}} + \frac{1-\alpha'}{X}} + \epsilon_{a3} X \qquad 3.5.9$$

Normally no distinction is made between the Nusselt Numbers $X_{r,s}$ and $X_{r,g}$, although Yagi and Kunii (1957) used

$$X_{r,s} = \frac{4D_p}{k_g}\left[\frac{e}{2-\epsilon}\right] T^3 \qquad 3.5.10$$

$$X_{r,g} = \frac{4D_p}{k_g}\left[1 + \frac{\epsilon(1-e)}{2(1-\epsilon)e}\right]^{-1} \qquad 3.5.11$$

The model used by Beveridge and Haughey (1971) results in the expression

$$Y = \epsilon_{a1}(1+H_r) + \left[\frac{1-\alpha'}{X(1-\epsilon_{a1})} + \frac{\alpha'}{\epsilon_{a2}(1+H_r) + X\epsilon_{a3}}\right]^{-1}$$

$$H_r = \frac{\beta h_r D_p}{k_g} = \frac{4\beta D_p X \sigma T^3}{k_g} \qquad 3.5.12$$

Beveridge & Haughey (1971) treated X as an unknown function of temperature, and deduced the functional form experimentally.

3.5.1 Conditions under which radiation in a packed bed is likely to be significant

Young (1975) has performed calculations of the radiation contribution to the effective thermal conductivity of packed beds. The calculations were based on the radiation model of Schotte (1960) in conjunction with the correlation of Deissler and Eian (1952). The calculations show that radiation will become important for 1 mm particles about 400 °C and for 0,1 mm particles above 1500 °C. For

5 mm particles at an average bed temperature of 400 ^{o}C radiation will account for approximately 20 % of the total energy transfer.

3.6 A Theoretical Study of Natural Convection.

The first theoretical study of natural convection in packed beds is that of Lapwood (1948). This author formulated the equations describing natural convection in a porous medium with an imposed vertical temperature gradient as follows:

Equation of motion:

$$\rho \frac{D}{Dt}(U,V,W) = -\left[\frac{\partial}{\partial x},\frac{\partial}{\partial y},\frac{\partial}{\partial z}\right] P - \frac{\rho g}{K'}(U,V,W) - (0,0,\rho g) \qquad 3.6.1$$

Equation of continuity:

$$\frac{1}{\rho}\frac{D\rho}{Dt} = \frac{\partial U}{\partial x} + \frac{\partial V}{\partial y} + \frac{\partial W}{\partial z} \qquad 3.6.2$$

Conservation of energy:

$$\frac{DT}{Dt} = \kappa \nabla^2 T \qquad 3.6.3$$

Equation of state:

$$\rho = \rho_{\infty}[1 - \alpha(T-T_{\infty})] \qquad 3.6.4$$

(U,V,W) = the macroscopic velocity components of an element of fluid at (x,y,z)

P = pressure at (x,y,z).

T = temperature at (x,y,z)

ρ = gas density at (x,y,z)

g = acceleration due to gravity

κ = thermal diffusivity = $k_b/(\rho\, c_g)$

k_b = effective thermal conductivity of medium

c_g = specific heat capacity of gas

α = coefficient of thermal expansion of fluid

K' = coefficient of permeability of medium for fluid concerned
= Kg/ν

ρ_{∞} = density at ambient temperature

ν = kinematic viscosity of fluid

K = permeability of medium

Note that Darcy's law has been used in the equation of motion in place of the usual viscosity term.

In order to reduce these equations to a more manageable form Lapwood (1948) makes the following assumptions:

1) All velocities, and departures of temperature, density, and pressure from the equilibrium state, are small enough to neglect second order terms and to formulate a useful first order theory.

2) Variations of density can be neglected, except in so far as they modify the action of gravity (the Boussinesq assumption).

These assumptions mean that D/Dt can be replaced everywhere except in the energy equation to give

Equation of motion:

$$\rho \frac{\partial}{\partial t}(U,V,W) = -\left(\frac{\partial}{\partial x},\frac{\partial}{\partial y},\frac{\partial}{\partial z}\right) P - \frac{\rho g}{K'}(U,V,W) - (0,0,\rho g)$$

Equation of continuity:

$$\frac{\partial U}{\partial x} + \frac{\partial V}{\partial y} + \frac{\partial W}{\partial z} = 0$$

Conservation of energy:

$$\frac{DT}{Dt} = \kappa \nabla^2 T$$

Equation of state:

$$\rho = \rho_\infty [1 - \alpha(T-T_\infty)] = \rho_\infty \frac{T}{T_\infty} \quad \text{for an ideal gas}$$

Lapwood (1948) reworks this set of equations for small disturbances from equilibrium, and obtains the 4th order differential equation

$$\left(\frac{\partial}{\partial t} + \frac{Q}{K}\right)\left(\frac{\partial}{\partial t} - K'^2\right)\nabla^2\theta = g\frac{\Delta T}{L}\nabla^2\theta$$

where $\theta = T-T_0$, $T_0 = -\Delta T(z/L)$

The equation is solved for the following boundary conditions:

$$T, \quad \frac{\partial^2 T}{\partial z^2} = 0 \qquad \text{at } z=0 \text{ and } z=L$$

It is shown that the solution obtained leads to exponential decay for

$$Ra = \frac{\Delta T \ \rho_0 K \ L \ g}{\kappa \ \mu \ T_\infty} < 4\pi^2 \qquad 3.6.5$$

where Ra = Rayleigh Number

Lapwood (1948) thus states that $Ra = 4\pi^2$ is the criterion for convective flow; if Ra is less than this value the disturbance dies away, but if it reaches this value steady convection becomes possible.

These results also show that the temperature depth relationship is, except in the vicinity of the boundaries,

$$T = T_0 - \frac{\Delta T}{L} z + A \sin\left(\frac{\pi z}{L}\right) \sin(lx) \sin(my) \qquad 3.6.6$$

Where A,l,m are constants.

This equation shows that in the presence of convection the temperature is no longer a linear function of z.

3.7 The Effect of Flow on Energy Transfer in Packed Beds

When there is bulk flow of gas through a packed bed, the thermal transfer of energy becomes many times more complicated. It has been mentioned in section 2 that of the 10 proposed mechanisms of energy transfer, only 6 are completely independent of fluid flow. Briefly the mechanisms which are believed to be dependent on the fluid flow are:

1) Conduction across the stagnant gas surrounding the contact points. (This is likely to be a weak function of fluid flow).
2) Natural convection in the gas.
3) Forced convection in the gas.
4) Forced convection due to bulk flow, turbulent diffusion or mixing of the gas.

Mechanisms 3 and 4 are unlikely to be of importance for a coal bed, since forced convection is not being considered except for the case of wind. The flowrates through packed beds of coal are in any case very small. The flow velocity may be calculated from the entries in Table 2.1. For a particle size of 5 mm the velocity is of the order of 10 m/hr.

It may thus be concluded that the effects of flow on heat transfer in packed beds of coal is likely to be negligible.

3.8 Conclusions

A variety of theoretical models have been presented in this chapter. In order to apply the results of this literature survey to reacting coal beds, the following should be borm in mind:

a) The temperature range considered to be important is 100 ^{o}C and below. From practical experience as well as from considerations of the oxidation rate once a coal bed reaches 100 ^{o}C it is well on its way to combustion, and the model developed in this work no longer describes the situation accurately.

b) The flowrate through a bed of coal is sufficiently small (as shown above) that the effect of flow on the effective thermal conductivity is likely to be negligible.

The first point means that radiation can for all practical purposes be ignored as a significant mechanism for heat transfer in coal beds. The second point suggests that the effects of flow on the effective thermal conductivity can be ignored.

The conclusion is that only conduction type models need be considered for describing the effective thermal conductivity. Thus an equation like 3.4.5 could be rewritten

$$k_b = \epsilon k_g + (1-\epsilon)\ \eta k_s \qquad 3.8.1$$

where η = tortuosity factor

and η can be determined experimentally, with the expectation that η will not be a strong function of temperature.

Having reached this conclusion it was decided to measure k_b for a packed bed of coal. This is the subject of the next chapter.

4. MEASUREMENT OF THE EFFECTIVE THERMAL CONDUCTIVITY OF A PACKED BED OF COAL

4.1 Introduction

Very broadly speaking, methods for measuring thermal conductivities fall into one of two categories, i.e. steady-state or unsteady-state methods. The vast majority of unsteady-state methods do not measure the thermal conductivity directly, but instead measure the thermal diffusivity, κ, where:

$$\kappa = \frac{k}{\rho C_p} \qquad 4.1.1$$

k = thermal conductivity
ρ = density
C_p = specific heat capacity

One exception to this is the hot wire method which measures both the thermal conductivity and the thermal diffusivity. Steady state methods, on the other hand, measure the thermal conductivity directly.

4.2 Theory of the Measurement of Thermal Conductivity

Thermal conductivity is defined by Fourier's law:

$$Q' = -kA \frac{dT}{dx} \qquad 4.2.1$$

Q' is the rate of energy transfer by conduction

A is the area at right angles to the direction of transfer

$\frac{dT}{dx}$ is the temperature gradient in the direction of transfer

This equation may be combined with an energy balance for a solid or static fluid to give:

$$\rho C_p \frac{\partial T}{\partial t} = \frac{\partial}{\partial x}\left[k \frac{\partial T}{\partial x}\right] + \frac{\partial}{\partial y}\left[k \frac{\partial T}{\partial y}\right] + \frac{\partial}{\partial z}\left[k \frac{\partial T}{\partial z}\right] + q' \qquad 4.2.2$$

T is the temperature
q' is a source term, which may be due to chemical or nuclear reaction or the passage of a current.

In general in the measurment of thermal conductivities an attempt is made to ensure that only one dimensional conduction takes place. In this case equation 4.2.2 becomes:

$$\rho C_p \frac{\partial T}{\partial t} = k \frac{\partial^2 T}{\partial x^2} + q' \qquad 4.2.3$$

This equation may be written for cylindrical or spherical coordinate systems giving:

Cylindrical co-ordinates: $$\rho C_p \frac{\partial T}{\partial t} = \frac{k}{r} \frac{\partial}{\partial r}\left[r \frac{\partial T}{\partial r}\right] + q' \qquad 4.2.4$$

Spherical co-ordinates: $$\rho C_p \frac{\partial T}{\partial t} = \frac{k}{R^2} \frac{\partial}{\partial R}\left[R^2 \frac{\partial T}{\partial R}\right] + q' \qquad 4.2.5$$

4.3 Steady-State Methods for Measuring Thermal Conductivity

The second order differential equations 4.2.3 - 4.2.5 may be solved in the steady-state to give:

Rectangular co-ordinates: $$T = \frac{-q'x^2}{2k} + C_1 x + C_2 \qquad 4.3.1$$

Cylindrical co-ordinates: $$T = \frac{-q'r^2}{4k} + C_1 \ln(r) + C_2 \qquad 4.3.2$$

Spherical co-ordinates: $$T = \frac{-q'R^2}{6k} - \frac{C_1}{R} + C_2 \qquad 4.3.3$$

The constants of integration are found from known boundary conditions. In writing the above equations k has been assumed to be independent of temperature. In general in attempting to

measure thermal conductivity one would avoid introducing sources into the sample i.e. q′ would be zero in the above equations.

4.3.1 Measurements in the Rectangular System

The temperature-position equation in the rectangular system with q′=0 is:

$$T = C_1 x + C_2 \qquad 4.3.4$$

This equation implies a linear temperature profile.

In order to use equation 4.3.4 to measure thermal conductivity a heater is used to provide a known energy input Q. The boundary condition at x=0 is therefore:

$$Q = -kA \left.\frac{dT}{dx}\right]_{x=0} \qquad 4.3.5$$

The sample is cooled at the end. The boundary condition at x = L is therefore:

$$T = T_o \qquad 4.3.6$$

Solving for the integration constants C_1 and C_2:

$$C_1 = \frac{Q}{-kA} \qquad 4.3.7$$

$$C_2 = T_o + \frac{QL}{kA} \qquad 4.3.8$$

Therefore $$T = T_o + \frac{Q}{kA}(L - x) \qquad 4.3.9$$

Suppose that the measured temperature at x = 0 is T_1. Then:

$$T_1 = T_o + \frac{QL}{kA} \qquad 4.3.10$$

$$K = \frac{QL}{A(T_1 - T_0)} \qquad 4.3.11$$

This formula is the basis for measurements of the thermal conductivity of a material in rod or slab form. It requires measurement of five quantities i.e

The power input	Q
The sample length	L
The sample area	A
The temperature	T_0
The temperature	T_1

An improved version of the apparatus is one in which two identical samples, heated in the middle are used. The apparatus has the advantage that no energy loss can occur through the ends provided $T_0 = T_\infty$.

The equation used to calculate the thermal conductivity is now:

$$K = \frac{QL}{2A\ (T_1 - T_0)} \qquad 4.3.12$$

Despite the advantages of this apparatus energy loss may still occur along the sides. For this reason the so called guarded hot ring method has been developed. In this apparatus a circular electrical heating element is used and it is surrounded by a heating element in the form of a ring. During the experiment the power input to this guard ring is adjusted so that the temperature measured on the ring is the same as that measured on the main heater. This implies that any energy losses are supplied by the guard heater, and that all the energy supplied by the main heater passes through the sample.

The design of guarded hot plate apparatus has been the subject of much study, and is covered in ASTM C177 (1963) and BS 874 (1956). This method has been used by many investigators in the field of thermal conductivity of packed beds; notably Beveridge & Haughey (1971).

4.3.2 Measurements in the Cylindrical System.

In radial flow methods use is made of equation 4.3.2 with $q' = 0$:

$$T = C_1 \ln (r) + C_2 \qquad 4.3.13$$

With boundary conditions:

$$Q = -2\pi r_1 l \, k \left.\frac{dT}{dr}\right]_{r_1} \quad \text{at } r = r_1 \qquad 4.3.14$$

$$T = T_2 \quad \text{at } r = r_2 \qquad 4.3.15$$

Solving equation 4.3.14 for the constants and rewriting in terms of k gives:

$$k = \frac{Q}{2\pi l \, (T_1 - T_2)} \ln \left[\frac{r_1}{r_2}\right] \qquad 4.3.16$$

Two different experimental apparatus may be designed in order to make use of equation 4.3.16. In the first type of apparatus the specimen is placed between an outer shell which is kept at temperature T_2, and is heated centrally. In the second type of apparatus the sample is heated on the outside surface, and the energy is removed at the centre of the sample.

In order to ensure that energy transfer is occuring only in the radial direction it is neccesary either to use a large sample length to thickness ratio, or to make use of end guard heaters. If guard heaters are used a fairly complicated experimental apparatus is neccesary, involving movable thermocouples in order to measure axial temperature gradients. This aspect of the design of such equipment is covered by Tye (1969).

Examples of the use of such methods for measurements of thermal conductivity of packed beds are Yagi & Kunii (1957) who used a centrally heated specimen, and Young (1975) who used a centrally cooled specimen.

4.3.3 Measurements in the Spherical System

Equation 4.3.3 may be solved to give:

$$k = \frac{Q\ (1/r_1 - 1/r_2)}{4\pi(T_2 - T_1)} \qquad 4.3.17$$

The spherical system has the advantage that all the energy supplied by a central heater passes through the specimen. The disadvantages of the method include the difficulty of fabricating a uniform heater and specimen, and the fact that the thermo-couples used for temperature measurement cannot lie along isotherms.These disadvantages mean that the spherical system has not been used for the measurement of thermal conductivity of packed beds.

4.4 Unsteady-State or Dynamic Methods

In general dynamic methods involve the measurement of the thermal diffusivity. The experiment consists of measuring the temperature history of a heated sample of known geometry, and then using this data and the appropriate integrated form of equation 4.2.2 to solve for the thermal diffusivity.

These methods have the advantage that no measurement of power input need be made. The disadvantages include the fact that many temperature measurements must be made, and that solving for the diffusivity may require complex numerical techniques.

An example of the use of a dynamic method to measure the thermal conductivity of a coal bed is the investigation by Brooks & Woods (1980). These investigators used a cylindrical vessel of diameter 500 mm and height 1600 mm. The vessel was heated on the outside surface by steam and radial temperature profiles were measured as a function of time. These measurements were made every 15 minutes for periods of up to 8 hrs.

It can be shown that under the above experimental conditions equation 4.2.4 may be solved to give

$$\frac{T - T_s}{T_o - T_s} = 2 \sum_{n=1}^{\infty} \frac{\exp \frac{-M_n^2 K t}{R^2} \; J_o \frac{M_n r}{R}}{M_n \; J_1(M_n)} \qquad 4.4.1$$

where T = temperature at radial position r

T_s = surface temperature

T_o = initial bed temperature

R = radius of cylinder

r = radius measured from axis of cylinder

t = time

J_i = i th order Bessel function of the first kind

M_n = n th root of the equation $Jo(M_n) = 0$

A computer program was used to minimize the sum of squared errors between the measured and predicted temperatures by choice of K. It can be appreciated that this process is far more complicated than the direct application of an equation such as 4.3.12.

Although only one dynamic method has been discussed it should be appreciated that all such methods involve the same sort of experiment and analysis, and differ only in the sample geometry chosen. One of the problems with applying these methods to coal beds is the small value of K of such beds which leads to long experiments.

4.5 Choice of Measurement Method for a Packed Bed of Coal

From experience gained by Brooks & Woods (1980) in trying to measure this quantity by use of an unsteady-state method, it was felt that a steady-state method would be better. The reason for this is that it is far easier to analyze the effect of a temperature dependent thermal conductivity in the case of a simple equation such as 4.3.12, whereas this task may be extremely difficult in the case of an equation such as 4.4.1. Put another way, it was felt that a thermal conductivity calculated by equation 4.3.12 is far better defined than one calculated from equation 4.4.1.

Having decided on a steady-state method the choice had to be made between axial or radial energy transfer. Again experience gained

in a previous study led to the choice of axial energy transfer. The reason for this was that the previous study indicated that convection may be a significant mechanism of energy transfer. If this is the case the axial method would lead to the determination of the "correct" thermal conductivity i.e the one in which the energy transfer by conduction and convection are in the same direction (This of course assumes that the apparatus has the heater horizontal).

It was also felt that, by designing the equipment in such a way that the energy absorbed at the two sinks could be measured, the presence or absence of convection could be detected, and its effect measured. To do this would be much more difficult in a radial type of apparatus.

4.6 Design and Construction of Guarded Hot Ring Apparatus

4.6.1 General Design Considerations

Although standards exist for the design of guarded hot ring apparatus, it was felt in the present case that accuracy of measurement could be sacrificed for ease of experimental design and construction, and for versatility of the apparatus. It was felt that due to the inhomogeneous nature of coal and variations in packing geometry, accurate and repeatable values for the thermal conductivity would not in any case be achieved.

In order to make measurements on coal up to 20 mm in size it was decided to make the test section of the apparatus of diameter 200 mm and length 200 mm. These dimensions should be sufficient to make end and edge effects negligible. However it was noted that the recommended D/L ratio is three or more, and that using a smaller ratio would lead to a loss in accuracy (Tye ,1969).

4.6.2 Heat Sinks

As mentioned before the sinks are designed in such a way that the energy absorbed by the sinks can be measured. This is achieved by placing thermistors in the inlet and outlet streams from the sinks, in order to measure the temperature difference in the water flowing through the sinks. The rate of energy absorption

is calculated as

$$Q = m\ \bar{c}\ \Delta T_w \qquad 4.6.1$$

Q = rate of energy absorption
m = water flowrate
$\bar{c}$ = specific heat capacity of water
ΔT_w = temperature difference of water

The sinks are provided with spiral baffles in order to ensure good mixing of the cooling fluid, which was in all cases water. The sinks are surrounded by guard sinks in order to prevent radial energy losses.

A sketch of one heat sink is shown in Figure 4.1.

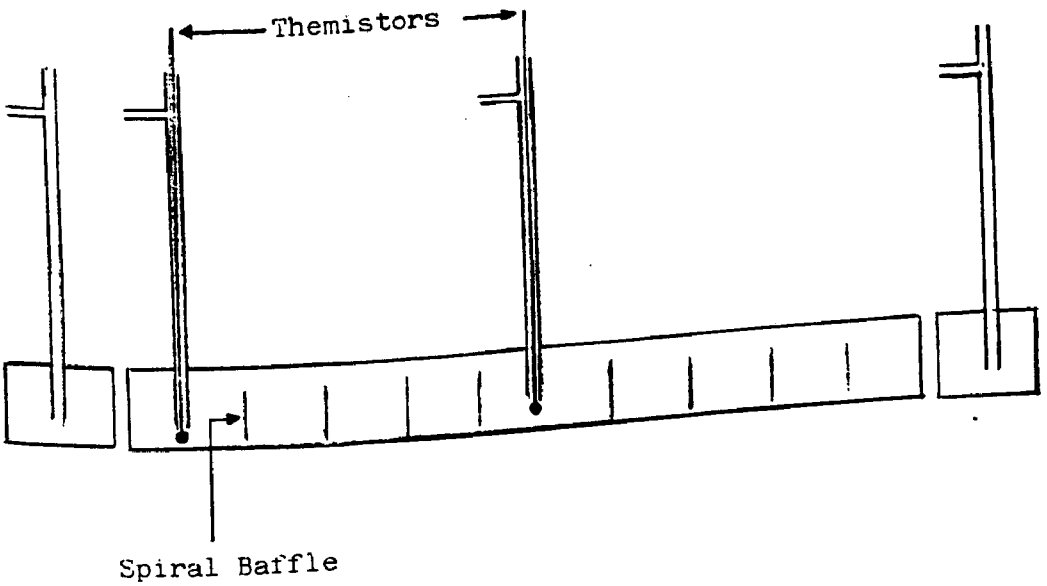


Figure 4.1 Guarded hot ring apparatus - Heat sink

4.6.3 Heating Elements

The heating elements were fabricated commercially, and consist of Nichrome wire ribbon wrapped around mica formers, which assembly is then sandwiched between more mica. The heaters are clad in light aluminium, and the whole assembly then sandwiched between 2 mm steel plates which are bolted together. The steel plates are used to prevent buckling.

The central heater has a diameter of 145 mm and the guard ring has an internal diameter of 150 mm and an external diameter of 200 mm. There is thus a 2.5 mm gap between the main and guard heaters.

4.6.4 Outer containing Vessel

The vessel has a diameter of 600 mm and a length of 600 mm. It is constructed from 6 mm mild steel. The ends of the vessel have 10 mm mild steel flanges in order to support the 10 mm MS end plates. The flanges are fitted with 5 mm rubber ring gaskets, and the endplates are held on with 18 bolts.

In order to facilitate electrical connections to the heaters as well as the placement of the thermocouples, six bushes have been placed on the midline of the apparatus. The bushes are shown in figure 4.2 and have proved satisfactory in sealing.

The end plates are provided with four similar bushes in order that the cooling sink pipes may pass through them. In addition the bottom end plate has an additional bush for connection of a vacuum pump or gas cylinder.

A sketch of the assembled apparatus is shown in Figure 4.2.

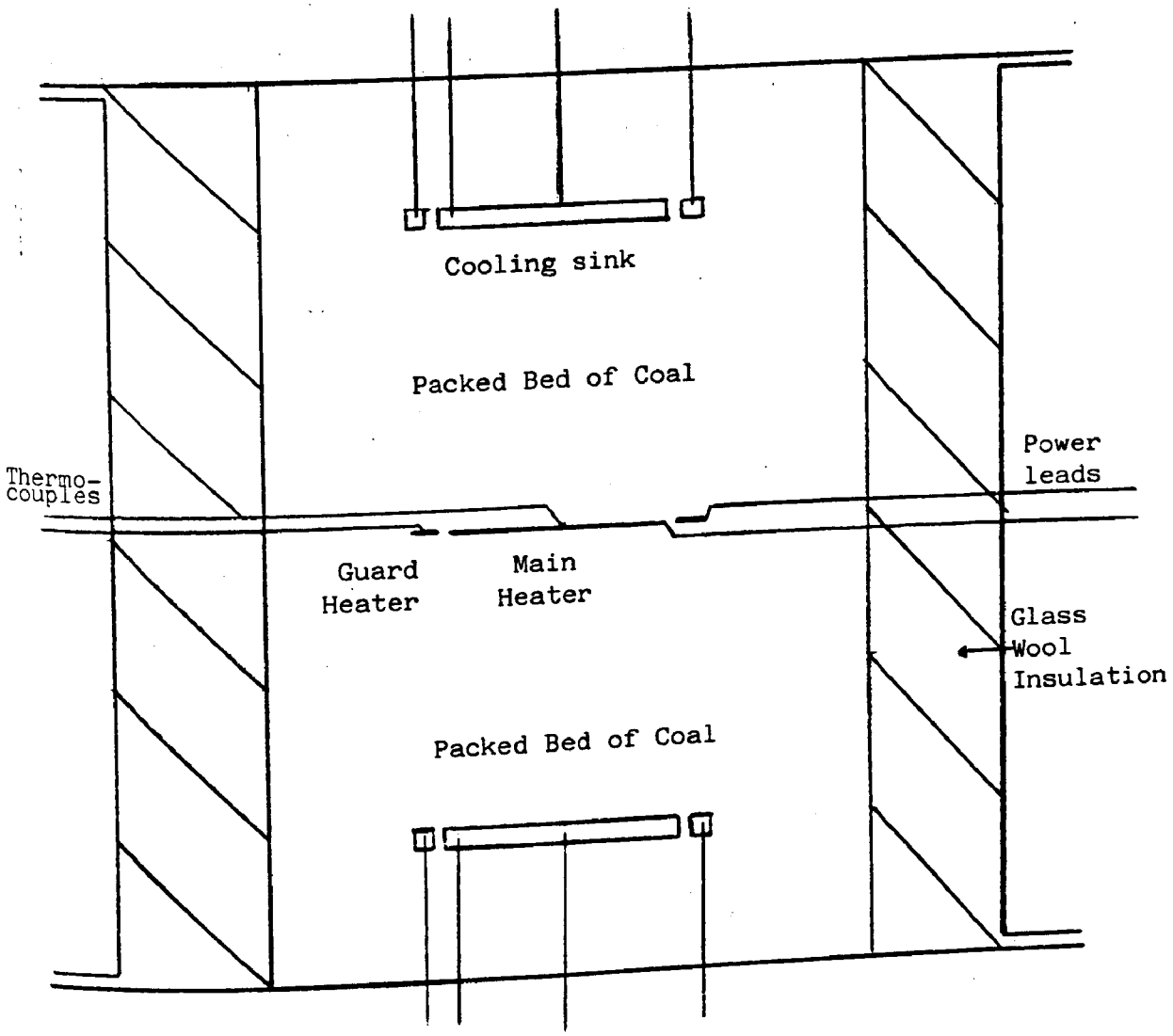


Figure 4.2 Guarded hot ring apparatus - Assembled apparatus

4.6.5 Water Supply to Heat Sinks

The apparatus is designed so that the temperature rise of the water flowing through the sinks is approximately 1 ^{o}C. A larger temperature rise is not used as this would upset the accuracy of the measurement of the temperature difference between the hot and cold faces. In order to measure this 1 ^{o}C temperature rise accurately it is neccessary to control the temperature of the water entering the sinks to at least 0.05 ^{o}C and preferably to 0.01 ^{o}C. To achieve this the following system is used:

Water flows from a constant head tank through a coil which is immersed in a constant termperature bath. The bath is controlled with a proportional controller. After leaving the bath the water flows through a jacketed copper pipe and hence to the heat sink. The jacketed pipe has water flowing in the jacket countercurrent to the flow to the sink. The water in the jacket is pumped from the constant temperature bath.

4.6.6 Measurement Techniques

The temperature of the main heater and guard heater are measured with chromel-alumel thermocouples. The cold junctions of the thermocouples are placed in glass tubes filled with glycerine, which are then placed in a "Thermos" flask filled with ice. The thermocouple voltage is measured using a Cambridge Slide Wire Potentiometer, i.e the voltage is measured at zero current.

The current supplied to the main heater is measured by a Fluke digital multimeter which is continuously in the circuit. This prevents the neccessity of correcting for the internal resistance of the meter. The voltage across the heaters is measured when required by another Fluke multimeter.

The resistances of the thermistors in the cooling sinks are measured in a Wheatstone bridge circuit, using a Kipp and Zonen recorder to measure the off balance voltage from the bridge.

The other values required to solve equation 4.3.12 for K are the heater area A and the length l. A is measured by measuring the diameter of the heater, and l is measured at the time of packing

the equipment with coal.

In fact the heater is not exactly betwen the two sinks, and thus l must be averaged. The correct average is

$$l = \frac{2\, l_1\, l_2}{l_1 + l_2} \qquad 4.6.2$$

where l_1, l_2 are the distances from the bottom and top sinks to the heater respectively.

4.7 Experimental Procedure

The experimental procedure is to switch on the main and guard heaters, setting the voltages so that there is no temperature difference between the guard and main heaters. The equipment takes approximately one week to reach steady-state, and each subsequent adjustment of the guard heater voltage requires further time for steady-state to be reached.

At the time of taking measurements the following are measured:

1) The voltage across the main heater and the guard heater.
2) The current through the main heater.
3) The thermocouple voltages on the main and guard heaters.
4) The resistance of the thermistors in the cooling sinks.

Once the thermocouple voltages and thermistor resistances have been converted to temperatures using calibration tables, the thermal conductivity is calculated from

$$k = \frac{V_m\, I_m\, l}{2\, A\, \Delta T} \qquad 4.6.3$$

V_m = main heater voltage
I_m = main heater current
ΔT = temperature difference between heater and sink

4.8 Results and Discussion

The results of the series of runs performed over the period March 1982 to August 1982 are tabulated in Appendix 2.

Although the resistances of the thermistors in the heat sinks were measured, it was not possible to calculate the energy absorbed at one heat sink. This was due to the fact that the thermistors are not identical i.e. they have slightly different resistances at the same temperature. An attempt was made to calibrate the thermistor pairs, but this was not succesful due to the fact that the calibration drifts with time. In addition problems were experienced with thermistors leaking and giving erratic readings. This facet of the experiment was consequently abandoned.

As can be seen from these results the thermal conductivity of the coal does not vary significantly in the temperature range considered. The mean value is 0.22 W/m/K.

It should be noted that for the largest tempeature difference used in the apparatus, the Rayleigh number as calculatedfrom equation 3.6.5 is 1.9. Therefore it may be safely assumed that only heat transfer by conduction was measured in this series of experiments, since this Rayleigh number is below the value required for the onset of natural convection.

The original intention of this experiment was to obtain experimental values for the so-called effective thermal conductivity of a coal bed, and deduce its functional relationship with particle size and voidage. However during the early stages of the mathematical modelling performed as part of this investigation, it was found that the thermal conductivity did not play as crucial a role in the equations as first believed. For this reason the experimental work was considered complete once a value of the thermal conductivity had been obtained for a typical sample of coal.

It is felt that a simple relationship for relating the thermal conductivity of the bed to that of the coal and the gas is all that is required. The relationship

$$k_b = \epsilon\, k_g + (1-\epsilon)\, \eta\, k_s \qquad 3.8.1$$

k_g = gas thermal conductivity
k_s = solid thermal conductivity
ϵ = voidage
η = tortuosity factor

which was presented and discussed in chapter 3 is probably satisfactory for a study of this type.

Using the values

k_g = 0.026 W/m/K (Perry & Chilton, 1973)
k_s = 0.28 W/m/K (Badzioch, Gregory & Field, 1964)
k_b = 0.22 W/m/K
ϵ = 0.38 (Appendix 2)

gives a value for η of 1.2.

5. MATHEMATICAL MODELLING OF A ONE-DIMENSIONAL ANALOGUE OF A COAL DUMP

5.1 Introduction

In any attempt to understand a natural phenomenon a model for the phenomenon is invaluable. In the case of a coal dump a mathematical model is required which has the ability to show the behaviour of a real coal dump, while still being simple enough to be solved. The full three dimensional equations for the transport processes occuring in a coal dump would be extremely complicated, and may indeed be impossible to solve without a tremendous amount of computation. A simpler model is required which may be solved without the excessive use of computation, but which nevertheless within its limits of applicability has the ability to predict whether a given coal dump may be considered to be safe or unsafe, and if unsafe what measures may be taken to render it safe. A model which is fundamentally based may be used to extrapolate measured data, which is not the case with models that are mainly empirical in nature. In addition the mathematical model points to the best experiments to measure the parameters required. It is believed that the mathematical model presented here has many of these desirable characteristics.

Mathematical models for coal dumps have been presented before, and in order to understand the reason for deriving a new one, a brief survey of these models and their shortcomings follows.

5.2 Literature survey of mathematical models for coal dumps

Much experimental effort has been devoted to measurement of physiochemical properties of coal over the last century. Less attention has been given to the development of a method to predict self heating.

An early model that attempts to predict safe conditions of storage of coal is that of Van Doornum (1954). The essential assumption of this model is that the coal may be considered to be a source of energy given by:

$$q' = A' \exp (a'v - \alpha t) \qquad 5.2.1$$

where q' = rate of generation
A' = fitting constant
a' = fitting constant
v = temperature above ambient
α = fitting constant
t = time

It should be noted that the form of equation 5.2.1 is in disagreement with the usual Arrhenius type temperature dependence of chemical reactions.

Van Doornum (1954) solves the conduction equation:

$$\rho_b \bar{c}_b \frac{\partial v}{\partial t} = \nabla^2(kv) + q' \qquad 5.2.2$$

where ρ_b = density of pile
$\bar{c}_b$ = specific heat capacity of coal
k = thermal conductivity
q' = source given by 5.2.1

for various geometries. From an analysis of the stability of the solutions the following is made that the safety or otherwise of a coal pile may be characterized by two dimensionless numbers M' and N' given by:

$$M' = \frac{A'a'}{\alpha \rho_b \bar{c}_b} \qquad 5.2.3$$

$$N' = \alpha \tau' \qquad 5.2.4$$

τ' = time constant for heat loss

τ' depends on the storage situation. For heat loss by conduction

$$\tau' = \frac{k \pi^2}{4 L^2 \rho_b \bar{c}_b} \qquad 5.2.5$$

L = height of pile

The criterion derived is as follows:

For $M' < 0.63$: a coal is unconditionally safe
$M' > 1.2$: the occurence of spontaneous combustion is very likely.

For the region $0.63 < M' < 1.2$ the situation, depending on the value of N', is normally manageable if care is taken.

This work has been adopted by the National Institute for Coal Research of South Africa as a test on the exportability of coal. The numbers M' and N' are found experimentally from a non-linear regression of the temperature-time curve at the centre of a 15 ton sample of coal which is aerated in a test bunker.

The chief disadvantage of this model is that no specific account is taken of the effect of oxygen depletion on the safety of a dump. In addition the constants in equation 5.2.1 have to be measured experimentally for every different coal; for instance, it is not possible to extrapolate measured data for one size grading of coal to a different size grading of the same coal.

Sondreal & Ellman (1974) performed exhaustive tests on North Dakota lignite, which data was used to perform computer simulations of spontaneous heating. The quantities measured by these investigators were the following:

a) The rate of oxidation of lignite, and the heat of reaction.
b) The specific heat of lignite.
c) The heat of wetting.
d) Airflow through a bed of compacted lignite.
e) The thermal conductivity of solid lignite.

In all case the quantities were measured at various moisture contents and bulk densities. The authors have used least squares techniques to fit the data to equations which are largely empirical in nature. These empirical equations have been used in computer simulations of spontaneous heating, using finite difference forms of the differential equation 5.2.2 together with a material balance equation for oxygen.

The authors present a large number of graphs showing the temperature rise in lignite under various assumptions. The cases

considered include the effects of prior oxidation, pressure gradients due to wind, porosity and moisutre content of the coal.

Although these investigators were most thorough in their approach, the chief disadvantage of this study is that it is highly specific to the particular lignite used. The authors state that the range of validity of their empirical correlations is limited to the range studied, and that extrapolations should only be made with caution. In addition Sondreal & Ellman (1974) take no account of airflow due to natural convection.

Nordon (1979) has presented a model for the self heating reactions of coal or char. The reactants considered are oxygen and water vapour, which are transported into the pile by molecular diffusion and forced convection due to differential wind pressure. A one-dimensional model is used in which the differential equations describing heat and mass transfer are:

$$(1-\epsilon)\,\rho_b\,\bar{c}_b\,\frac{\partial T}{\partial t} = \frac{(1-\epsilon)}{K}\,\frac{\partial^2 T}{\partial x^2} - \epsilon\,U\,\rho_g\,\hat{c}\,\frac{\partial T}{\partial x} - r\,\Delta H_r \qquad 5.2.6$$

where
K = thermal diffusivity
x = length along bed
U = flow velocity
ρ_g = density of gas
$\hat{c}$ = specific heat capacity of gas
r = reaction rate per volume of coal
ΔH_r = enthalpy of reaction

$$0 = \epsilon\,\frac{\partial m}{\partial t} + U\,\frac{\partial m}{\partial x} - D\,\frac{\partial^2 m}{\partial x^2} + \rho_g\,r \qquad 5.2.7$$

m = moles of oxygen per moles of nitrogen in gas
D = diffusion coefficient

These equations are solved using a finite difference method. No account is taken of natural convection flow. The reaction rate of the oxidation reaction is modelled using the so-called Elovich equation:

considered include the effects of prior oxidation, pressure gradients due to wind, porosity and moisutre content of the coal.

Although these investigators were most thorough in their approach, the chief disadvantage of this study is that it is highly specific to the particular lignite used. The authors state that the range of validity of their empirical correlations is limited to the range studied, and that extrapolations should only be made with caution. In addition Sondreal & Ellman (1974) take no account of airflow due to natural convection.

Nordon (1979) has presented a model for the self heating reactions of coal or char. The reactants considered are oxygen and water vapour, which are transported into the pile by molecular diffusion and forced convection due to differential wind pressure. A one-dimensional model is used in which the differential equations describing heat and mass transfer are:

$$(1-\epsilon)\,\rho_b\,\bar{c}_b\,\frac{\partial T}{\partial t} = \frac{(1-\epsilon)}{\kappa}\,\frac{\partial^2 T}{\partial x^2} - \epsilon\,U\,\rho_g\,\hat{c}\,\frac{\partial T}{\partial x} - r\,\Delta H_r \qquad 5.2.6$$

where
κ = thermal diffusivity
x = length along bed
U = flow velocity
ρ_g = density of gas
$\hat{c}$ = specific heat capacity of gas
r = reaction rate per volume of coal
ΔH_r = enthalpy of reaction

$$0 = \epsilon\,\frac{\partial m}{\partial t} + U\,\frac{\partial m}{\partial x} - D\,\frac{\partial^2 m}{\partial x^2} + \rho_g\,r \qquad 5.2.7$$

m = moles of oxygen per moles of nitrogen in gas
D = diffusion coefficient

These equations are solved using a finite difference method. No account is taken of natural convection flow. The reaction rate of the oxidation reaction is modelled using the so-called Elovich equation:

$$\frac{dq}{dt} = r_o A' \exp(-(E + Bq)/RT) \qquad 5.2.8$$

where q = amount of O_2 taken up per unit weight of char.
r_o = rate of oxidation at $T_\infty = 20^oC$ when q = 0.
A' = Arrhenius pre-exponential factor = $\exp(E/RT_\infty)$.
E = activation energy.
B = Elovich constant.

In the results by Nordon (1979) no account has been taken of the presence of moisture. As in the case of Sondreal & Ellman (1974) this author presents graphs showing the effect of various parameters on the temperature rise in char beds. The cases considered are:

a) Self heating for various bed lengths where diffusion is the only transport process.

b) Dependence of steady state temperature on critical bed size for various activation energies.

c) Self heating where diffusion and convection processes are present.

d) The moderating influence of Elovich kinetics.

The author concludes that there is a critical bed length above which spontaneous combustion will occur. He states that for bed lengths smaller that this critical value the steady state temperature rise is small and is limited by heat transfer. The high temperature steady state is caused by the reaction being limited by the rate of oxygen diffusion. With forced convection present this oxygen limitation may be removed; however when the forced convection becomes large loss of heat through flow will limit the reaction, leading to a low temperature steady state. Note however that the air flow required for this to occur is of the order of 10^{-4} m/s which is a fairly large flowrate for the fine (-3,35 mm) material considered in this study.

This study then is theoretically sound, and the author presents a

good discussion of the nature of self-heating. The main drawback of the model is the failure to take account of natural convection flows.

The omission by these researchers of natural convection deserves some explanation. It has been suggested by some researchers that the work of Lapwood (1948), as discussed in section 3.6, shows that natural convection is unimportant in coal dumps. The argument used is that Lapwood (1948) states that a Rayleigh number of $4\pi^2$ is a criterion for the onset of stable convection flows. This would seem to imply that the temperature rise required for natural convection flows to take place in a coal dump can be calculated using equation 3.6.5. The equation is

$$Ra = \frac{\Delta T \; \rho_g^2 \; L \; g \; c_g}{k_b \; f \; T_\infty}$$

where the identities $f = \mu/K$ and $\alpha = 1/T_\infty$ for an ideal gas have been used.

Setting the Rayleigh number equal to $4\pi^2$ in the above equation, the quantity $\Delta T \; L$ may be solved for. The results of doing this calculation are summarised in Table 5.1 below.

TABLE 5.1 VALUES OF $\Delta T \; L$ REQUIRED FOR $Ra = 4\pi^2$

D_p (mm)	f ($kg/m^3/s$)	$\Delta T \; L$ (K m)
1	5.6×10^4	9500
2	1.4×10^4	2375
5	2.2×10^3	380
20	1.4×10^2	24

These results have been taken by other researchers to indicate that for a 2 metre bed of 20 mm particles a 12 K temperature rise is necessary for the onset of natural convection flows, and that for 1 mm particles natural convection flows are very unlikely to occur.

There is however a fallacy in this argument. Lapwood investigated natural convection flows for the case of an imposed temperature gradient in the vertical direction, and with impermeable

horizontal faces. The problem is thus constrained to a one-dimensional temperature gradient. The boundary conditions that are implied are not appropriate for the case of a coal dump. A coal dump has no impermeable sides and has each of its surfaces at nearly ambient temperature, and experiences a three-dimensional temperature field.

Young (1985) has reworked this problem for the case of a coal bed open on the top surface, with impermeable sides and a two-dimensional temperature field. For this case it can be shown that the equation governing the stream function of the flow in the bed is:

$$\frac{\partial^2 \psi}{\partial X^2} + \frac{\partial^2 \psi}{\partial Y^2} = \frac{\partial \theta}{\partial X}$$

The right hand side of this equation represents the horizontal temperature gradient. If this quantity is 0 and the boundary conditions are such that ψ is zero everywhere, then this equation can be satisfied by the case of no flow. However, when the temperature gradient in the horizontal direction is non-zero, convection can be expected under all conditions.

Young (1985) has also shown experimentally that for his case as soon as there is any temperature rise in such a bed, natural convection will occur. There is thus no obvious critical Rayleigh number for this case.

Weber (1974) has studied theoretically a similar situation to Lapwood, but with a small horizontal temperature gradient. It appears from this work that there exists no critical Rayleigh number below which there is no flow, but rather that there is a critical Rayleigh number above which there is a fairly rapid increase in flow. The application of this work to coal beds is not completely obvious, because the infinite region considered requires infinite temperatures at the ends; hence only horizontal flows occcur at Rayleigh numbers below a certain critical value.

Bejan (1978) has studied convection in an infinite porous medium with a concentrated heat source; for this case there is no critical Rayleigh nmuber for the onset of convection. The steady-state flow pattern shows an upward flow that becomes very intense near the source. The upward flow extends throughout the medium, and as the Rayleigh number increases, the warmer region

moves upwards. It is felt that this case is likely to be more similar to the situation in a coal dump, than the situation modelled by Lapwood (1948) and Weber (1974).

In conclusion, having reviewed the available models for self-heating it is felt that a model similar to that used by Nordon (1979), but taking into account natural convection flows and neglecting diffusion, (as discussed in Chapter 2), should be developed in order to make predictions about the behaviour of stockpiled coal.

5.3 A one-dimensional analogue of a coal dump

In order to derive a mathematical model of a coal dump which will yield results fairly simply, certain simplifying assumptions have to be made. The main assumption in the model presented here is that the processes of heat, mass and momentum transfer occur in one direction only. Although this is known not to be true in a real coal dump, it does represent a limiting case which in many respects is the worst case. It can be seen that considering heat transfer in one direction only is likely to be the worst case, since the heat loss is limited to one direction only. Similarly considering flow in only one direction is the worst case, since reactant depletion is likely to be less in a one dimensional model than in one in which reactant flows from many directions.

In many important respects the one-dimensional model is accurate. A one-dimensional model is likely to be accurate for the case of coal stored in a silo, if proper allowance is made for radial heat losses that can occur. In the middle of a very large dump of coal heat transfer to the sides is unlikely to be significant because of the large distances involved; significant heat transfer will occur only to the surface of the dump. In addition should a "hot-spot" occur in a dump the flow due to natural convection will be in the same direction as the heat transfer. The existence of hot spots in coal dumps is well known; spontaneous combustion in its early stages is localized, as has been shown by infra-red photography. The reasons for the existence of hot-spots in coal dumps may include inhomogeneity of the bed in respect of degree of compaction, coal reactivity or moisture content. Experimental work by Young (1985), on natural convection in a porous bed containing a line source, shows

clearly that there is a region close to the source through which most of the flow passes. This is shown diagramatically in Figure 5.1, in which model streamlines are plotted for one half of a symmetrical bed, of infinite length in the Z direction, containing a line source located at X=0, Y=0.6. Note that the reason that no flow occurs through the side X=1 is that in solving the model equations Young assumed that this surface was impermeable. This assumption should not drastically effect the behaviour of the streamlines near the source. Although the situation modelled by Young (1985) is not identical to that in a coal bed, it is felt that the flow patterns near a hot-spot are unlikely to be very different to the flow patterns found near a line source.

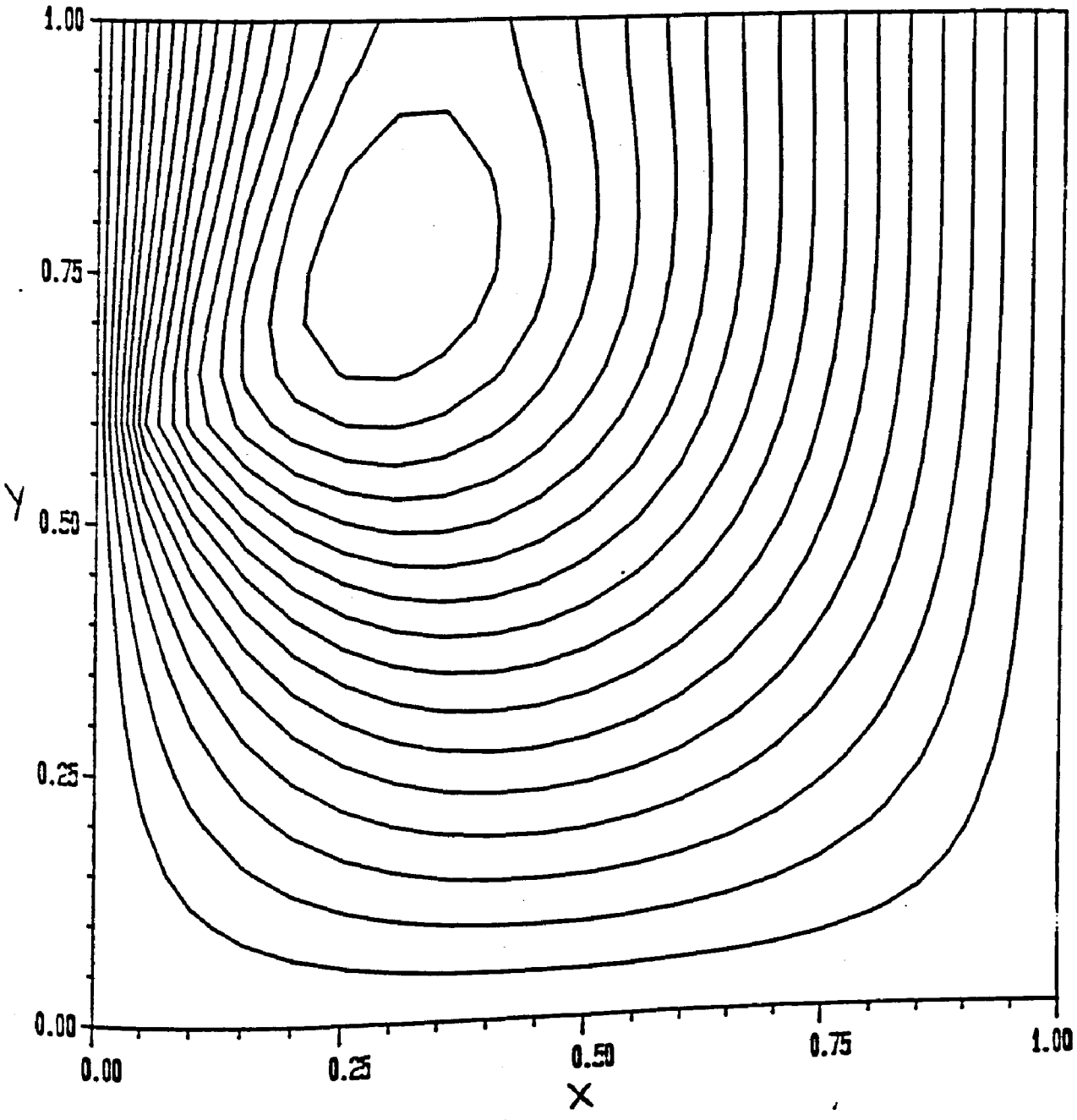


Figure 5.1 Streamlines in a Packed Bed Containing a Line Source (From Young, 1985)

Assuming that a hot spot arises in a coal dump for some reason, it can be reasoned that a chimney effect will take place. Air will flow up the chimney, and be replaced by air flowing in from the sides and top of the dump. If the behaviour of this chimney inside the coal dump can be modelled, then valuable insight into the nature of spontaneous combustion can be obtained. This is the physical basis for the model presented here.

To model the chimney inside the coal bed would be difficult. To make the model simpler the chimney is considered to be perfectly insulating radially. All the flow is considered to occur through the bottom of the bed, with no flow occurring through the sides. The bottom of the bed is considered to be open to atmosphere. These assumptions mean that the chimney can be modelled separately from the rest of the coal dump.

The disadvantages of this model are the following:

a) No simple relationship has been found relating the length of the chimney in the model to the size of the coal dump. Since the bed length is an important model parameter, this limits the applicability of the results obtained. This point will be further discussed in chapter 8.

b) It is assumed that the bottom of the chimney is open and thus loses heat to the atmosphere. In a real dump the bottom of the chimney loses heat to the surrounding coal. It is difficult to gauge how dissimilar these heat loss mechanisms are, and in what way this assumption will affect the results.

Despite these disadvantages the chimney or one-dimensional model may be considered to be a model that has a sound physical basis. The behaviour of the chimney should be similar to the behaviour of a coal dump in many important respects. The shortcomings of the the model are appreciated, but are not expected to invalidate the results obtained, provided these results are not taken to be directly applicable in a quantitative sense.

The great advantage of the model is that the equations derived may be solved fairly easily. A study of the parameters that are important in the prediction of spontaneous combustion may thus be performed without excessive computation.

The main assumptions in the mathematical model used in this study are therefore:

a) Flow and heat transfer occur in the same direction, and since the gas is assumed to flow in plug flow there are no radial gradients in the bed.

b) The reactions considered are

$$n\,C(s) + O_2(g) \rightarrow C_nO_2(s)$$
$$C_nO_2 \rightarrow CO_2 + (n-1)\,C(s)$$
$$\tfrac{1}{2}\,C_nO_2 \rightarrow CO(g) + (\tfrac{1}{2}n-1)\,C(s)$$
$$H_2O(g) \rightleftarrows H_2O(abs)$$

This reaction scheme is in agreement with the observed behaviour of the low temperature reactions of coal, as discussed in Chapter 1. C_nO_2 is oxycoal but note that no specific hypothesis about its structure needs to be made. The fourth reaction is water absorption, which has been reported to be of importance in spontaneous combustion of coal dumps, as has been discussed in chapter 2.

c) Flow is considered to be caused by natural convection and by differential pressure. Molecular diffusion is neglected as discussed in Chapter 2. Natural convection flows occur as soon as there is any temperature rise in the bed, since the bed is considered to be vertically aligned and open top and bottom.

Under these assumptions and some other minor assumptions which arise in the derivation of the equations a mathematical model has been derived. The full derivation is given in Appendix 3.

5.4 Model Equations

The model equations are:

5.4.1 Component mass balances (Gas phase)

$$G\frac{\partial y_i}{\partial x} + \frac{P\,\epsilon}{R\,T_g}\frac{\partial y_i}{\partial t} = r_i - y_i \sum r_j \qquad (i = 1 \text{ to } N)$$

G = molar flowrate per unit area

y_i = mole fraction of i in the gas phase

x = distance along bed

P = pressure

R = gas constant

ϵ = bed voidage

T_g = gas temperature

t = time

r_j = rate of formation of j in the gas phase per unit bed volume

N = number of components in gas phase

5.4.2 Overall gas mass balance

$$\frac{\partial G}{\partial x} + \frac{\epsilon}{R}\frac{\partial (P/T)}{\partial t} = \sum_{j=1}^{N} r_j$$

5.4.3 Component mass balances (Solid phase)

$$(1-\epsilon)\frac{\partial (\rho_s f_j)}{\partial t} = p_j \qquad (j = 1 \text{ to } M)$$

ρ_s = density of solid

f_j = mass fraction of j in the solid

p_j = rate of formation of j in the solid

M = number of components in solid phase

5.4.4 Overall solid mass balance

$$(1-\epsilon)\frac{\partial \rho_s}{\partial t} = \sum_{j=1}^{M} p_j$$

5.4.5 Gas phase energy balance

$$\frac{P\epsilon}{RT_g}\hat{c}\frac{\partial T_g}{\partial t} - \epsilon\frac{\partial P}{\partial t} = -G\hat{c}\frac{\partial T_g}{\partial x} + \epsilon K_g\frac{\partial^2 T_g}{\partial x^2} + Q_c$$

$\hat{c}$ = molar specific heat capacity of gas

K_g = thermal conductivity of gas

Q_c = rate of convection from solid to gas

5.4.6 Solid phase energy balance

$$(1-\epsilon)\,\rho_s\,\bar{c}_s\,\frac{\partial T_s}{\partial t} - (1-\epsilon)\,\frac{\partial P}{\partial t} = (1-\epsilon)\,\eta\,k_s\,\frac{\partial^2 T_s}{\partial x^2} - Q_c - \Sigma\,(r_i \Delta H_r^i)$$

T_s = solid temperature
η = tortuosity factor
k_s = thermal conductivity of solid
ΔH_r^i = enthalpy of reaction for formation of i

5.4.7 Momentum balance

$$\rho\,\frac{\partial U}{\partial t} = -f\,U + g\,\rho_\infty(1-T_\infty/T) - \frac{\partial(P-P_\infty)}{\partial x}$$

U = flow velocity
f = D'Arcy's law constant
ρ_∞ = density of ambient air
P_∞ = ambient air pressure

5.5 Discussion of the model equations

This is a set of M + N + 5 differential equations. The unknowns are tabulated in Table 5.2.

TABLE 5.2 UNKNOWNS IN THE MODEL EQUATIONS

UNKNOWN	DESCRIPTION	NUMBER
y_i	Gas mole fractions	N
G	Molar flowrate/area	1
f_i	Solid mass fractions	M
ρ_s	Solid density	1
T_g	Gas temperature	1
T_s	Solid temperature	1
P	Gas pressure	1

Although the equations have been derived for any number of gas and solid components, in the discussions that follow the gases considered are O_2, N_2, CO_2, CO and H_2O. The solid is considered to be composed of four fractions i.e. carbon, oxycoal, absorbed water and inert material.

5.6 Boundary and Initial Conditions

The following are the boundary conditions used: (x=0 refers to the bottom of the bed and x=L refers to the top).

$$y_i(0,t) = \text{Mole fraction of i in ambient air}$$

The pressure boundary conditions have been discussed in section 2.2 and are:

$$P(0,t) = P_\infty + \rho_\infty V^2/2$$

$$P(L,t) = P_\infty$$

$$V = \text{wind velocity}$$

For the gas phase energy balance

$$\epsilon k_g \frac{\partial T_g(0,t)}{\partial x} = G \hat{c} (T(0,t) - T_\infty)$$

$$\frac{\partial T_g(L,t)}{\partial x} = 0$$

The first boundary condition reflect the fact that the gas entering the bed is heated to the gas temperature. At the end of the bed it is assumed that there is no heat loss due to flow; the gas is assumed to leave the bed in plug-flow, implying that the temperature just outside the bed is equal to the temperature just inside the bed.

For the solid phase energy balance

$$(1-\epsilon) \eta k_s \frac{\partial T_s(0,t)}{\partial x} = h_1 (T_s(0,t) - T_\infty)$$

$$(1-\epsilon) \eta k_s \frac{\partial T_s(L,t)}{\partial x} = -h_2 (T_s(L,t) - T_\infty)$$

These are convective boundary conditions, but h_1 and h_2 may be interpreted as radiation heat transfer coefficients. Initial conditions for the equations involve assigning values to each of the variables at time zero for all x. In most cases ambient values would be used.

6. SIMPLIFICATON OF THE MODEL EQUATIONS AND THEIR SOLUTION

6.1 Introduction

Although a one-dimensional formulation has been used to simplify the equations and reduce their number, the equations remain complicated. In order to simplify them further to perform computation the following assumptions (which are discussed more fully in Appendix 4) were made:

a) The gas and solid temperatures are unlikely to be very different; therefore equations 5.4.5 and 5.4.6 may be combined to give one equation in temperature, ie a continuum assumption is made. The reason for deriving the gas and solid phase energy balances separately is that the boundary conditions for use in the continuum model are not clear; deriving the balances separately and then combining them allows the correct boundary conditions to be deduced mathematically.

b) Since the heat transfer is by far the slowest transfer process occuring in the bed, the other transfer processes may be considered to be at steady state i.e. a pseudo steady state formulation is used.

In order to simplify still further it is convenient to define a rate (ry) which is the rate at which oxygen disappears. Similarly an enthalpy of reaction ΔH_r is defined; this may be considered to be the enthalpy of reaction associated with the disappearance of oxygen. The reaction involving water is ignored for the following reasons:

a) It is likely to be only a starting mechanism whereby the temperature in a coal bed is raised to the point where natural convection flows and oxidation become the mechanisms whereby the dump combusts.

b) As yet no reliable data for this reaction is available, and it is in any case believed that the reaction is likely to be close to equilibrium in most cases.

It would appear from equation 5.4.2 that the change in flowrate due to reaction has to be considered. However, if air is the reactant then even if all the oxygen in the flow is removed the flowrate will only change by twenty percent. It is therefore

6. SIMPLIFICATON OF THE MODEL EQUATIONS AND THEIR SOLUTION

6.1 Introduction

Although a one-dimensional formulation has been used to simplify the equations and reduce their number, the equations remain complicated. In order to simplify them further to perform computation the following assumptions (which are discussed more fully in Appendix 4) were made:

a) The gas and solid temperatures are unlikely to be very different; therefore equations 5.4.5 and 5.4.6 may be combined to give one equation in temperature, ie a continuum assumption is made. The reason for deriving the gas and solid phase energy balances separately is that the boundary conditions for use in the continuum model are not clear; deriving the balances separately and then combining them allows the correct boundary conditions to be deduced mathematically.

b) Since the heat transfer is by far the slowest transfer process occuring in the bed, the other transfer processes may be considered to be at steady state i.e. a pseudo steady state formulation is used.

In order to simplify still further it is convenient to define a rate (ry) which is the rate at which oxygen disappears. Similarly an enthalpy of reaction ΔH_r is defined; this may be considered to be the enthalpy of reaction associated with the disappearance of oxygen. The reaction involving water is ignored for the following reasons:

a) It is likely to be only a starting mechanism whereby the temperature in a coal bed is raised to the point where natural convection flows and oxidation become the mechanisms whereby the dump combusts.

b) As yet no reliable data for this reaction is available, and it is in any case believed that the reaction is likely to be close to equilibrium in most cases.

It would appear from equation 5.4.2 that the change in flowrate due to reaction has to be considered. However, if air is the reactant then even if all the oxygen in the flow is removed the

6. SIMPLIFICATON OF THE MODEL EQUATIONS AND THEIR SOLUTION

6.1 Introduction

Although a one-dimensional formulation has been used to simplify the equations and reduce their number, the equations remain complicated. In order to simplify them further to perform computation the following assumptions (which are discussed more fully in Appendix 4) were made:

a) The gas and solid temperatures are unlikely to be very different; therefore equations 5.4.5 and 5.4.6 may be combined to give one equation in temperature, ie a continuum assumption is made. The reason for deriving the gas and solid phase energy balances separately is that the boundary conditions for use in the continuum model are not clear; deriving the balances separately and then combining them allows the correct boundary conditions to be deduced mathematically.

b) Since the heat transfer is by far the slowest transfer process occuring in the bed, the other transfer processes may be considered to be at steady state i.e. a pseudo steady state formulation is used.

In order to simplify still further it is convenient to define a rate (ry) which is the rate at which oxygen disappears. Similarly an enthalpy of reaction ΔH_r is defined; this may be considered to be the enthalpy of reaction associated with the disappearance of oxygen. The reaction involving water is ignored for the following reasons:

a) It is likely to be only a starting mechanism whereby the temperature in a coal bed is raised to the point where natural convection flows and oxidation become the mechanisms whereby the dump combusts.

b) As yet no reliable data for this reaction is available, and it is in any case believed that the reaction is likely to be close to equilibrium in most cases.

It would appear from equation 5.4.2 that the change in flowrate due to reaction has to be considered. However, if air is the reactant then even if all the oxygen in the flow is removed the flowrate will only change by twenty percent. It is therefore considered adequate to regard the flowrate as a constant to be considered adequate to regard the flowrate as a constant to be calculated from equation 5.4.7.

Under these assumptions the number of equations to be solved is reduced to three i.e. a temperature equation, an oxygen equation and a flowrate equation. These equations are given below.

Temperature: $$\rho C_b \frac{\partial T}{\partial t} = k_b \frac{\partial^2 T}{\partial x^2} - G \hat{c} \frac{\partial T}{\partial x} + r\, y\, \Delta H_r \qquad 6.1.1$$

ρ_b = density of bed
C_b = specific heat capacity of bed
k_b = thermal conductivity of bed
y = mole fraction oxygen
ΔH_r = enthalpy of reaction for oxygen disappearance

Oxygen: $$G \frac{dy}{dx} = -r\, y \qquad 6.1.2$$

Flowrate: $$\frac{d(P-P_\infty)}{dx} = -f\, G\, R\, T/P + g(\rho_\infty - \rho) \qquad 6.1.3$$

One possible functional form for the rate of reaction r has been discussed in Section 1.3, but should a superior rate expression for the oxidation be proposed it would be a simple matter to use this expression in the model.

The boundary conditions on the equations are:

$$k_b \frac{\partial T(0,t)}{\partial x} = (h_0 + G \hat{c})\,(T(0,t)-T_\infty)$$

$$k_b \frac{\partial T(L,t)}{\partial x} = -h_1\,(T(L,t)-T_\infty)$$

$y(x=0)$ = mole fraction of oxygen in air

$P(x=0) = P_\infty + \rho_\infty V^2/2$

$P(x=L) = P_\infty$

The initial condition for equation 6.1.1 is a given temperature profile e.g. $T(x,0) = T_0(x)$.

It is convenient in what follows to make equation 6.1.1 dimen-

sionless. To do this the following substitutions are made:

$$\theta = T/T_\infty$$
$$X = x/L$$
$$\tau = \kappa t/L^2$$
$$a = G\,\hat{c}\,L/k_b$$
$$b = L^2\,r\,(-\Delta H_r)/(T_\infty\,k_b)$$
$$\gamma_s = -r/G$$
$$Bi_0 = h_0\,L/k_b$$
$$Bi_1 = h_1\,L/k_b$$

Equation 6.1.1 becomes:

$$\frac{\partial\theta}{\partial\tau} = \frac{\partial^2\theta}{\partial X^2} - a\,\frac{\partial\theta}{\partial X} - b\,\gamma \qquad 6.1.4$$

with boundary conditions

at X=0 $$\frac{\partial\theta}{\partial X} = (Bi_0+a)(\theta-1)$$

at X=1 $$\frac{\partial\theta}{\partial X} = -Bi_1(\theta-1)$$

The initial condition is $\theta(X,0) = \theta_0(X)$

This equation may be improved by including a heat loss term. This heat loss term takes into account radial heat losses that are not taken into account in the original model. The term, as is shown in Appendix 5, may be written as $C(\theta - 1)$. In a sense C is a free parameter. It does however have real meaning in simulating a coal dump as will be seen in Chapter 7. Equation 6.1.4 becomes:

$$\frac{\partial\theta}{\partial\tau} = \frac{\partial^2\theta}{\partial X^2} - a\,\frac{\partial\theta}{\partial X} - b\,\gamma - C\,(\theta - 1) \qquad 6.1.5$$

with boundary and initial conditions as above.

6.2 The Steady-State form of the Equations

It may be argued that the set of equations does not have a steady-state solution since the reaction rate r is a function of the amount of oxidation and therefore of time. If the reaction rate is constantly falling off with time, i.e. the coal is

ageing, then there is no steady state. However it is convenient to study the behaviour of the equations in the limit of steady state, and for this purpose the ageing of the coal is ignored, and the so-called reaction rate of fresh coal is used. This is in a sense the worst case since the fresh coal has the highest reaction rate.

The temperature equation then becomes

$$0 = \frac{d^2\theta}{dX^2} - a\frac{d\theta}{dX} - b\,y - C\,(\theta - 1) \qquad 6.2.1$$

First attempts to solve equation 6.2.1 with equation 6.1.2 and 6.1.3 involved the use of a Runge - Kutta algorithm. The method used was a shooting one i.e. a temperature at X = 0 and flowrate were guessed, and the equations integrated forward to try and meet the boundary conditions at X = 1. This method met with no success at all, since the calculated temperature was very sensitive to the assumed value of the inlet temperature. Changing the value of this temperature led either to the temperature increasing without bound or becoming negative. An explanation for this behaviour is given in Appendix 6.

An alternative method of solving equation 6.2.1 involves making the assumption that the reaction rate r may be considered constant throughout the bed. This is a very large assumption since the form of r involves an exponential of the temperature, and thus r cannot in fact be constant unless the bed temperature is constant. However over a fairly small range of temperature the assumption of an average rate in the bed is acceptable, even though the answers it gives will not be quite correct. A further justification for making this assumption is that an analytic form for the temperature profile in the coal bed may be obtained, and thus the characteristics of the solution may be quickly investigated.

The details of the solution are given in Appendix 7, and the temperature equation has the form:

$$\theta_{ss}(X) = 1 + C_1\exp(\gamma_1 X) + C_2\exp(\gamma_2 X) + C_3\exp(\gamma_3 X) \qquad 6.2.2$$

The coefficients γ_1, γ_2, C_1, C_2, and C_3 are given functions of the known parameters.

The solution of the equation set is in fact iterative, since some average temperature is assumed and the flowrate and average reaction rate calculated. This in turn leads to a new temperature profile, flowrate, and average reaction rate and so on till the process converges. The computer code to perform this calculation is given in Appendix 12.

The character of the solutions so obtained and their significance is discussed in Chapter 8.

6.3 The Solution of the Unsteady-State Equations with a Constant Rate

The unsteady state behaviour of the equation set is of great practical importance. If a coal dump is going to be reclaimed in a relatively short time, then its long time or steady-state behaviour is of little importance in predicting the safety or otherwise of the dump. In addition it is only possible to decide whether a given dump will achieve a safe or unsafe steady-state by considering the behaviour of the temperature with time.

As a continuation of the work in which the equation set is solved using a constant rate, a solution was sought for the unsteady state behaviour under the same assumption.

The equation to be solved is equation 6.1.5 and the details of the solution are given in Appendix 8. The solution is:

$$\theta(X,\tau) = \theta_{ss}(X) + v(X,\tau)\exp(-\tau(a^2/4-C) + aX/2) \qquad 6.3.1$$

where $$v(X,\tau) = \Sigma \{Z_n(X)\exp(-\beta_n^2\tau)\ Z_n(X')\ g(X')\ dX'\} \qquad 6.3.2$$

$$Z_n(X) = \frac{2(\beta_n^2+Bi_3^2)(\beta_n\cos(\beta_n X)+Bi_2\sin(\beta_n X))}{((\beta_n^2+Bi_2^2)(\beta_n^2+Bi_3^2+Bi_3)+Bi_2(\beta_n^2+Bi_3^2))}$$

$$g(X) = (\theta_o(X) - \phi_{ss}(X))\exp(-aX/2) \qquad 6.3.3$$

$$Bi_2 = Bi_0 + a/2$$

$$Bi_3 = Bi_1 + a/2$$

and the β_n are the positive roots of

$$\tan(\beta) = \frac{\beta(Bi_3 + Bi_2)}{(Bi_2\, Bi_3 + \beta^2)} \qquad 6.3.4$$

Obtaining the final solution (equation 6.3.1) at a given X and τ is a stepwise process, since starting with the initial condition $\theta_0(X)$ the coefficients a, b, and γ_3 are calculated. A time step is then taken and the temperature profile calculated. This in turn gives new values of a, b, and γ_3 and the process continued.

The solution has been programmed in BASIC on a HP 9835 computer, and the code is given in Appendix 12. In practice it has been found that only twenty terms of the series need be taken. Nevertheless obtaining the solution is a fairly lengthy process, since for each time step $Z_n(X)$ and the integral in equation 6.3.2 must be calculated for a number of X values.

The character of the solutions obtained by this method is discussed in Chapter 8.

6.4 A Numerical Method for Solving the Unsteady State Equations

A numerical method for solving the equation set has the following advantages:

a) The variation of the reaction rate with temperature and amount of oxidation of coal can be taken into account.

b) The model can be used to fit data obtained from experiments such as the one described in Chapter 7. This data can then be used to make predictions about the behaviour of a given coal in a given stockpiling situation.

The disadvantage of a numerical method is that no general observations can be made about the form of the solution, as is possible with an analytic solution. Also the amount of computation may become prohibitive.

The method chosen for solving the equations in this case is one first presented by Bellman, Kashef & Casti (1972), which has been

termed the method of lines. The technique involves the use of a Legendre polynomial to fit the temperature profile at any given time t. This has the effect of reducing the partial differential equation to a set of ordinary differential equations, which may then be solved by one of many available methods e.g. Runge-Kutta or Adams-Moulton.

The advantage of this method over the more normally used finite difference approach is that the finite difference methods require calcualtion at a large number of points in order to obtain accurate results at the points of interest. Consequently both the computing time and storage required are large. In contrast, the approach of doing the calculation at the nodes of the shifted Legendre polynomial offers a moderately accurate solution at a few points, and the solution may be calculated rapidly.

The essence of the method rests in writing

$$\frac{\partial\theta(X_j,\tau)}{\partial X} = \Sigma(a_{ij}\ \theta(X_j,\tau)) \qquad \text{for } i=1 \text{ to } n \qquad 6.4.1$$

The X_j are chosen to be the nodes of the shifted Legendre polynomial

$$P_n^*(X) = P_n(1-2X) \qquad 6.4.2$$

and the matrix a_{ij} of weighting factors may be calculated once and for all.

The details of the application of the technique to the particular set of equations under consideration are given in Appendix 9. In many respects the solution procedure is similar to that discussd in Section 6.3, since the coefficients a, b, and γ_3 are recalculated at each time step.

This solution method has also been programmed in BASIC on an HP 9816 computer, and the code is given in Appendix 12. The choice of the length of the time step chosen is critical to the stability of the method, but apart from this the method is very effective. Calculational time is in fact shorter than that required to obtain the solution 6.3.1 and it has been found that using a ninth order Legendre Polynomial is entirely adequate.

Further discussion of the method and the results obtained is given in Chapter 8.

7. EXPERIMENTAL INVESTIGATION OF THE BEHAVIOUR OF A ONE DIMENSIONAL ANALOGUE OF A COAL DUMP

7.1 Introduction

In order to attempt to validate the equations derived in the previous sections, as well as to obtain data to use in a parameter study, it was decided to build a coal chimney. The apparatus used and results obtained are discussed in this chapter.

7.2 Experimental

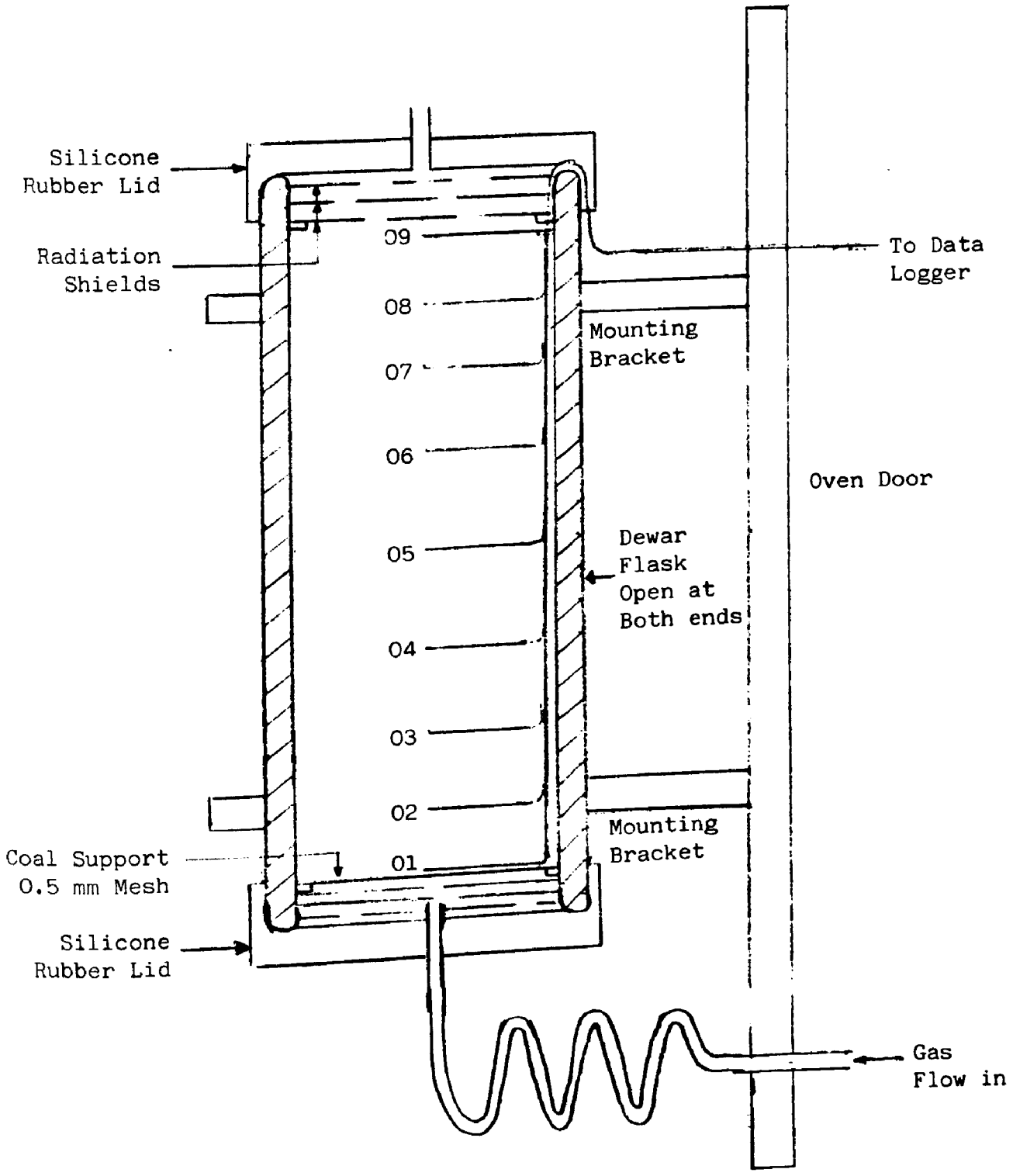
A skethch of the apparatus used is shown in figure 7.1. The coal chimney is constructed from an open ended Dewar Flask of 78 mm internal diameter and 240 mm height. Dimples of glass 20 mm from the bottom of the apparatus provide support for a piece of thin mesh, which in turn supports the coal. The chimney is provided with removable silicone rubber lids above and below. Both lids have 6 mm copper tubing moulded in, to provide for flow of gas in and out.

To minimize heat losses radiation shields manufactured from aluminium foil covered balsa wood discs are used. 10 mm Holes are punched in these discs in such a way that if three discs are assembled 5 mm apart, no direct rays of radiation can escape.

Thermocouples are manufactured by sparking together 20 SWG fabric coverd copper and constantan. The thermocouples are tested at 0°C and at the boiling point of water.

At the time of packing the bed with coal, the thermocouples are placed with their exposed ends on the centre line of the apparatus. Nine thermocouples are placed in the apparatus at positions corresponding to the nodes of the ninth order Legendre polynomial used in the solution method discussed in section 6.4.

In order to record the temperature-time behaviour of the chimney, these nine thermocouples, together with a tenth thermocouple placed in the oven containing the apparatus, are connected to a HP 3054 Data Aquisition Unit controlled by an HP 85 computer. A program



01 - 09: Copper Constantan Theromcouples

Figure 7.1 Chimney Experiment - Apparatus

supplied by Hewlett Packard is used to record the temperatures at a suitable time interval, as well as to print the temperatures and record them on tape. The program converts thermocouple voltages to temperatures using a fourth order polynomial; a silicon device built in to the data logger provides the cold junction reference temperature.

The apparatus is contained within a thermostatically controlled oven. Considerable care is taken to ensure that the temperature variations within the oven are small. The temperature in the oven is continually recorded using an eleventh thermocouple and a recorder. The temperature control of the oven is better than one degree centigrade.

The bed is supplied with gas (either nitrogen and oxygen) from cylinders. A series of valves are used to drop the pressure from the cylinder to the inlet of the bed, and to provide control over the flowrate of gas into the bed. This flowrate is measured usng a Tri Flat Variable Area Floe Meter. The manufacturer's curves are used to convert a reading on the meter to a volumetric flowrate. The barometric pressure is recorded in order that the volumetric flowrate can be converted to a molar flowrate. In order to ensure that the gas entering the bed is at oven temperature, a coil of length 0.5 m of 6 mm copper pipe is provided within the oven. enables the temperature time and temperature distance profiles to be automatically logged at any suitable time interval.

Experimental procedure consists of setting the oven temperature to the desired level, and placing the apparatus in the oven with a flow of nitrogen through the bed. Temperatures are recorded until they are considered to be steady. The flow is then switched to oxygen, and the temperature-time data recorded. For each run fresh coal that has been stored under water is used, in order to minimize the amount of prior oxidation of the coal. The coal is allowed to dry in a thin layer overnight at ambient temperature.

The experimental data obtained is tabulated in Appendix 10.

7.3 Experimental Results

The accuracy of results obtained from this experiment is limited by the accuracy to which the heat transfer characteristics of the apparatus are known. In order to calculate the numbers Bi_o, Bi_1, and C required for the model the bed was heated under nitrogen and then removed from the oven while continuing the nitrogen flow. The temperature time curve was then recorded, and a trial and error method used to calculate the values of the coefficients which best fit the data. The results of this fitting procedure are shown in Figure 7.2.

It can be seen that the experimental data is fitted very well at the centre of the bed but rather poorly at the ends of the bed. This indicates that the heat transfer mechanism at the ends of the bed is not well modelled by a heat transfer coefficient. However it was felt that if the rest of the fitting was done with temperature time curves at the centre of the bed the results would at least yield suitable values to use in a parameter study.

Two different sorts of behaviour have been observed during the experiments in which oxygen is flowed through a preheated coal bed. The different sorts of behaviour depend on the particle size of the coal used and the oven temperature.

The first type of behaviour which is observed is a fairly gentle rise of the temperature in the bed, with some maximum temperature being reached, after which the temperature begins to fall off again. This behaviour can only occur if the reactivity of the coal is falling off with time; this implies that the coal is ageing. This behaviour, observed for the larger particle sizes at oven temperatures of approximately 90 ^{o}C, has been used to calculate the various constants in the shrinking core model discussed in Section 1.3; these fits are shown in Figures 7.3 and 7.4.

The second type of behaviour observed is a fairly rapid temperature increase in the coal bed with the rate of temperature rise increasing with time. This behaviour may be considered to be combustion. When this occurs the coal bed has to be cooled down by taking the apparatus out of the oven and restoring the

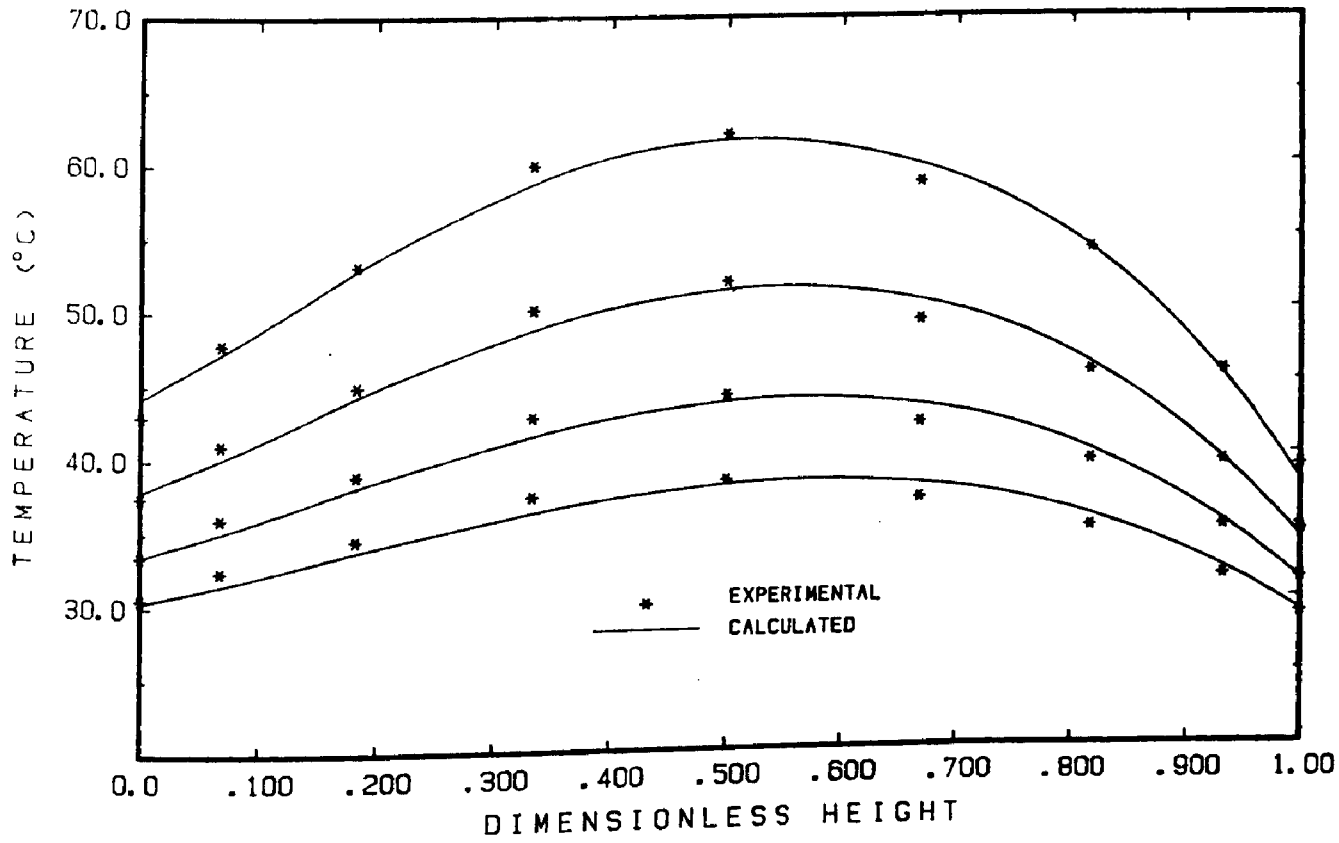


Figure 7.2 Chimney experiment - Fitting heat transfer coefficients

Profiles plotted every 30 minutes

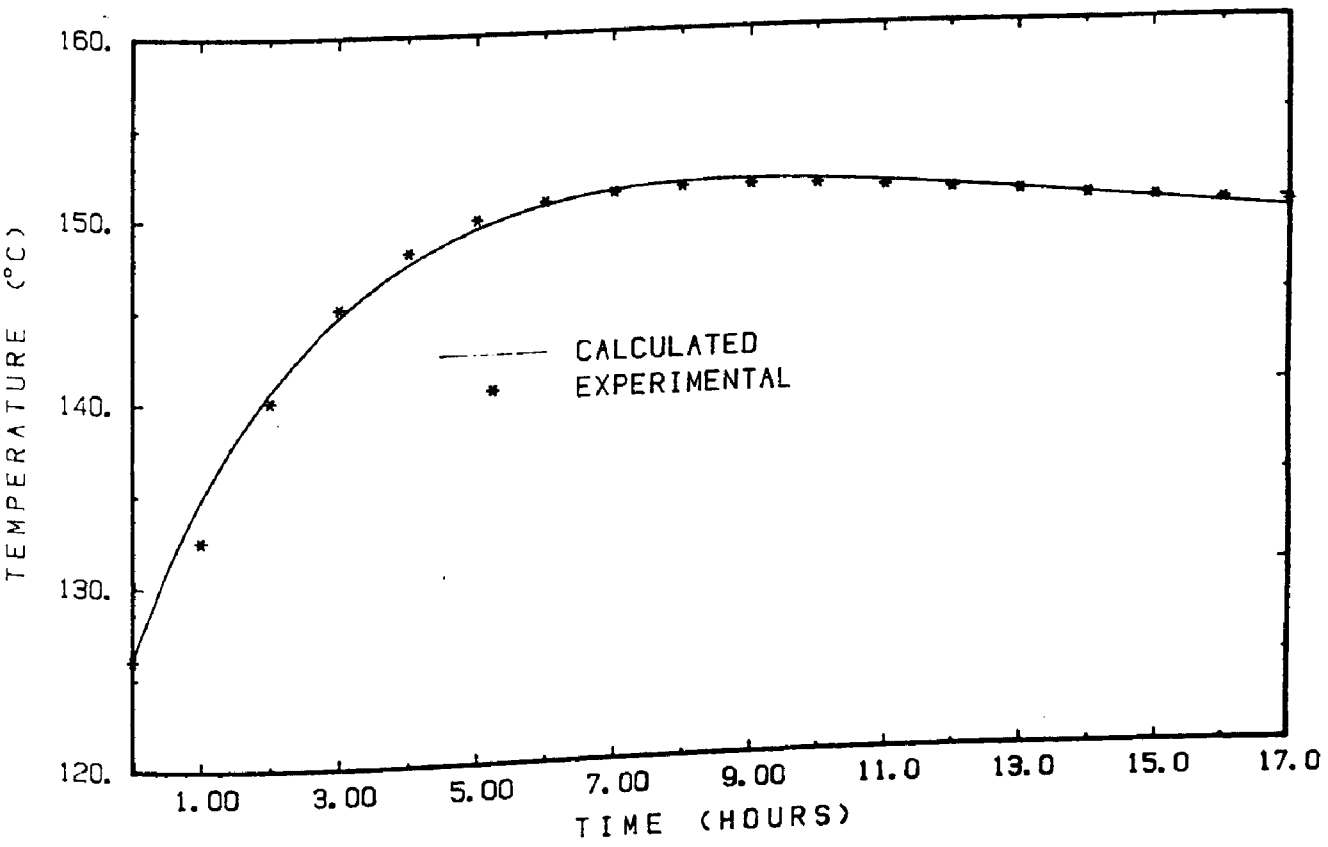


Figure 7.3 Chimney experiment - Fitting ageing run 1

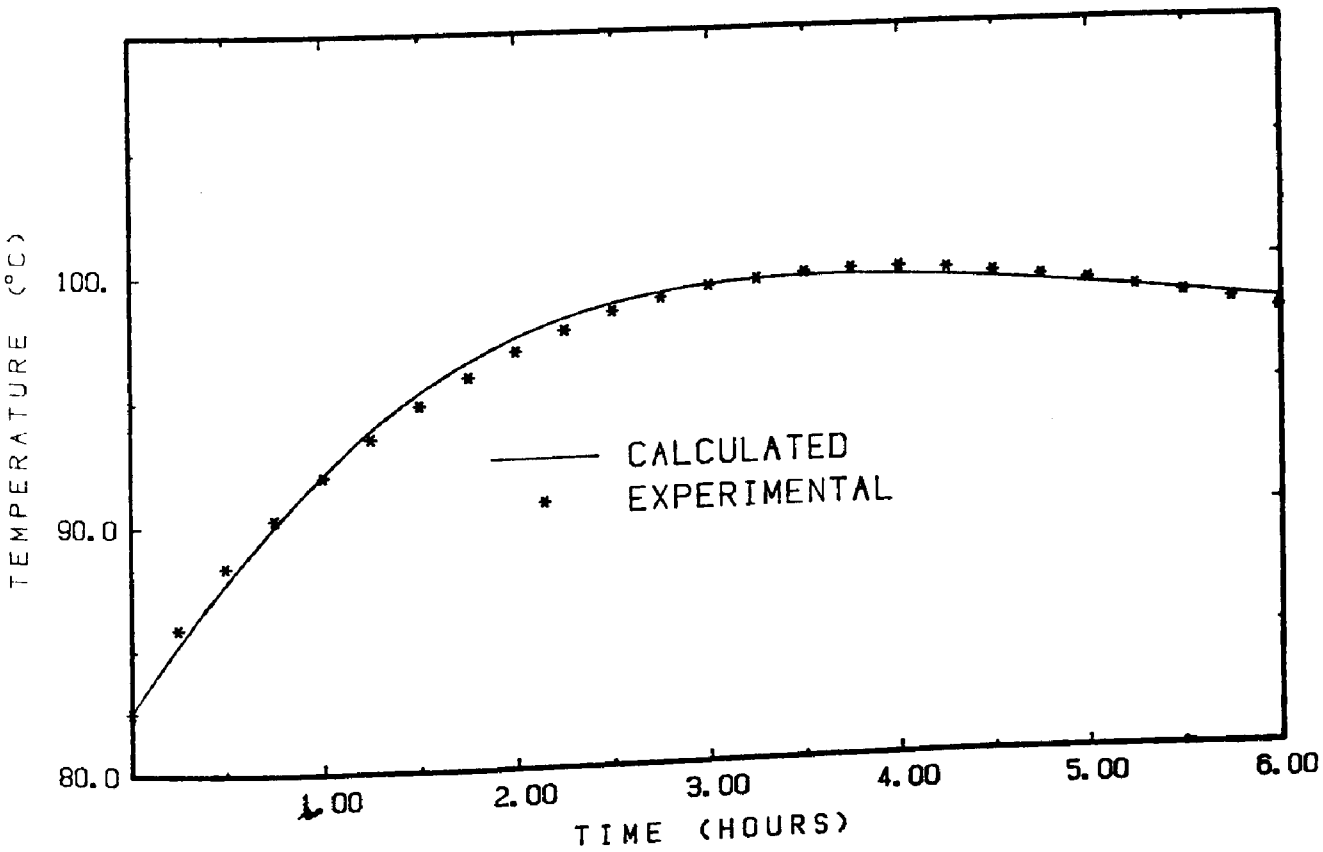


Figure 7.4 Chimney experiment - Fitting ageing run 2

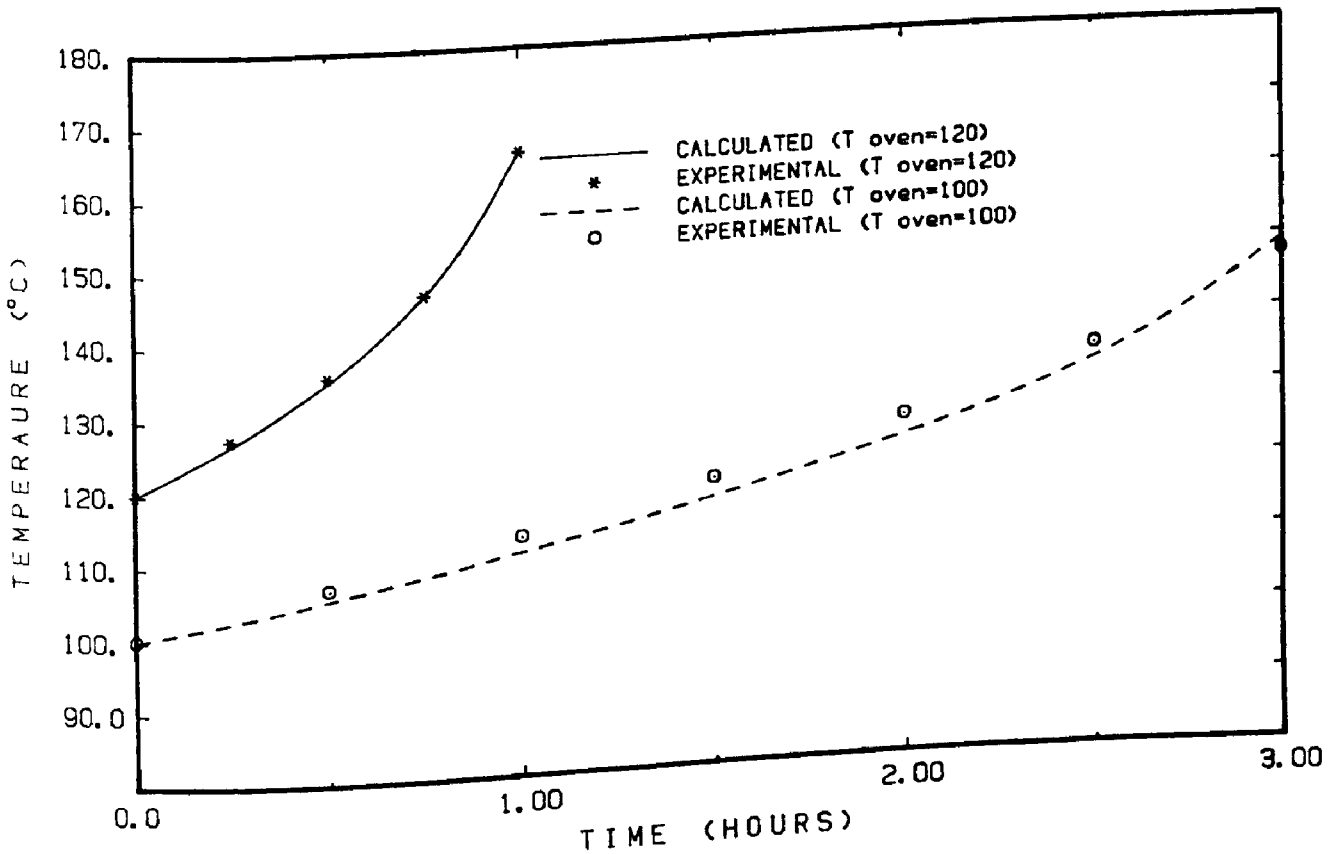


Figure 7.5 Chimney experiment - Fitting ignition runs

nitrogen flow.

These ignition runs yield very valuable information since it proves simpler to deduce the kinetic data from these runs then from the runs in which there is a gentle temperature rise. The reasons for this are that the temperature rises are much larger, meaning that ageing is a smaller effect. An example of the fitting of this data is shown in Figure 7.5 where two different experimental runs are fitted with the same data. The fit is fair but tends to be poorer as the temperature increases more rapidly. The reason for this is that at these higher temperature some of the model assumptions breakdown.

The values of the parameters used to obtain the fits shown in figures 7.2 to 7.5 are tabulated in Appendix 10. It must be stressed that these parameters, in particular the reaction rate values, are likely to be very different for different coals.

7.4 Discussion

The experiment used to derive the results in this section is not a good experiment from the point of view of analyzing the results to obtain the parameters required. This is partly because many of the parameters required in the model need to be estimated, and there may be a high cross correlation between the estimated parameters, and those found by curve fitting. However it is felt that the parameters calculated are accurate enough to give starting values for the parameter analysis discussed in the next chapter.

The analysis of the experiment may be improved in many respects e.g. by the use of a minimization routine to calculate the parameters. This was not felt neccessary in the present study.

8. RESULTS OF SOLVING THE MODEL EQUATIONS

8.1 Introduction

In this chapter the results of solving the model equations are presented. The three cases considered are:

a) Solving the steady-state equations with constant r.
b) Solving the unsteady-state equations with constant r.
c) Solving the equations with no assumptions, using a numerical method.

8.2 Steady-State Solution for constant r

Since an analytic solution exists for the temperature profile in this case, it has been used to perform a parameter study of the effect that changing the model parameters has on the calculated temperature profiles. In order to perform this parameter study a base set of parameter values had to be chosen, and certain assumptions made. The values of the parameters for this base case are given in Appendix 11. The assumptions made were the following:

a) The coal may be characterized by a single particle diameter, D_p, where

$$D_p = 6/S$$

S = external surface area per particle volume

b) The surface area for reaction, S_t, is set equal to the external surface area, S. However, the effect of changing this assumption has been investigated.

c) The wind velocity is set to zero, as is the heat loss coefficient, C.

d) Radiation heat transfer coefficients are used for h_1 and h_2; these could easily be replaced by natural convection heat transfer coefficients, if these were found to be more appropriate.

8.2.1 The Character of the Solutions

In order to investigate the character of the solutions, the following analysis was used:

Equaton 6.1.5 with C set equal to zero (i.e. no radial heat loss) is :

$$\frac{\partial\theta}{\partial\tau} = \frac{\partial^2\theta}{\partial X^2} - a\frac{\partial\theta}{\partial X} - by$$

Integrating from X = 0 to X = 1 gives

$$\int_0^1 \frac{\partial\theta}{\partial\tau}\,dX = \int_0^1 \frac{\partial^2\theta}{\partial X^2}\,dX - \int_0^1 a\frac{\partial\theta}{\partial X} - \int_0^1 by\,dX \qquad 8.1$$

Now, as shown in Appendix 4, $y = y_o \exp(\gamma_3 X)$. In addition a and b are not functions of X since they are calculated at an average temperature.

Thus equation 8.1 becomes

$$\frac{\partial\bar{\theta}}{\partial\tau} = \frac{\partial\theta}{\partial X}\Big]_1 - \frac{\partial\theta}{\partial X}\Big]_0 - a\,[\theta_1 - \theta_0] - \frac{by_o}{\gamma_3}[\exp(\gamma_3) - 1]$$

$$\frac{\partial\bar{\theta}}{\partial\tau} = -Bi_1(\theta_1 - 1) - (Bi_o + a)(\theta_0 - 1) - \frac{by_o}{\gamma_3}[\exp(\gamma_3) - 1]$$

$$\frac{1}{a}\frac{\partial\bar{\theta}}{\partial\tau} = -\frac{Bi_1}{a}(\theta_1 - 1) - \left(\frac{Bi_o}{a} + 1\right)(\theta_0 - 1) + \frac{by_o}{a\gamma_3}[1-\exp(\gamma_3)]$$

This equation may be written as

$$\frac{1}{a}\frac{\partial\bar{\theta}}{\partial\tau} = RHS - LHS \qquad 8.2$$

where

$$LHS = \frac{Bi_1}{a}(\theta_1 - 1) + \left(\frac{Bi_o}{a} + 1\right)(\theta_0 - 1)$$

$$RHS = \frac{by_o}{a\gamma_3}[1-\exp(\gamma_3)]$$

Equation 8.2 is the overall energy balance for the bed.

The quantity $by_o/(a\gamma_3)$ may be evaluated by substituting for a,b and γ_3 to give $(-\Delta H_r y_0) / (\hat{c}T_\infty)$. This quantity is the dimensionless adiabatic temperature rise i.e. the temperature rise that would occur if there was total conversion and no heat loss.

The steady-state solutions to equation 8.2 may be found by plotting LHS and RHS against θ , and observing where the two curves cross, since where the two curves cross

$$\frac{\partial\theta}{\partial\tau} = 0$$

The advantage of this procedure over solving the equation directly is that both stable and unstable steady-state solutions may be easily found.

A problem that occurs in using equation 8.2 is that , in the absence of wind, $T = T_\infty$ is always a solution of the equation. This is not a realistic solution, and arises from the assumpton in the model that natural convection is the only flow mechanism. In reality some diffusion will occur, and in this case this solution will vanish. In order to avoid numerical difficulties that arise, and also to make the solutions more realistic, in what follows it is assumed that the flowrate G may be written as

$$G = G_0 + G_{convection} \qquad 8.3$$

where G_0 is small but non-zero.

In the programs used to generate the figures in this section G_0 is assumed to caused by a 0.1 m/s wind. Equation 2.2.13 can be used to show that for a 5m long bed, this wind velocity causes the same flow as a temperature rise of 10^{-4} K, which is of course entirely negligible.

Several general points may be deduced from the definitions of RHS and LHS. In particular it is instructive to take limits of both the RHS and LHS as θ tends to 1 and to infinity.

When θ tends to 1, r tends to a finite quantity and G tends

to G_o by equation 8.3. (When $\theta = 1$ $G_{convection} = 0$). However since G_o can be chosen arbitrarily small the quantity exp(-rL/G) tends to 0. No other quantities in equation 8.2 are functions of θ , therefore

$$\lim_{\theta \to 0} (RHS) = - \frac{\Delta H_r y_o}{\hat{c}\, T_\infty}$$

For the values tabulated in Appendix 11 this quantity, which is the dimensionless adiabatic temperature rise, evaluates to 7.

When θ tends to 1 the LHS tends to zero by equation 8.2 , since both θ_o and θ_1 and tend to 1 as θ tends to 1.

When θ tends to infinity, the RHS tends to 0. This may be seen by considering the behaviour of rL/G for this case.

When θ tends to inifinity the LHS is not bounded, since both θ_o and θ_1 tend to infinity.

This suggests that the behaviour of the graph of RHS and LHS versus θ is as sketched in Figure 8.1.

From figure 8.1 it is clear that there must be an odd number of solutions to equation 8.2, and that the curves intersect at least once.

A further analysis of equation 8.2 leads to the ability to predict whether a cetain solution is an unstable or stable solution. Referring to equation 8.2 it may be seen that if LHS < RHS then $\partial\theta/\partial\tau > 0$ i.e. the bed tempeature is increasing. Referring to figure 8.1, and in particular to point B, it can be seen that at a temperature just above the temperature at which LHS and RHS intesect RHS is greater then LHS i.e. the derivative is positive. This implies that should the bed be at point B and the temperature rise, it will carry on rising since the derivative remains positive. Only at point C when this derivative is again 0 will the temperature stop rising. This implies that point B represents an unstable steady-state. A similar analysis can be performed to show that points A and C are stable steady-states.

The general conclusion from this analysis is:

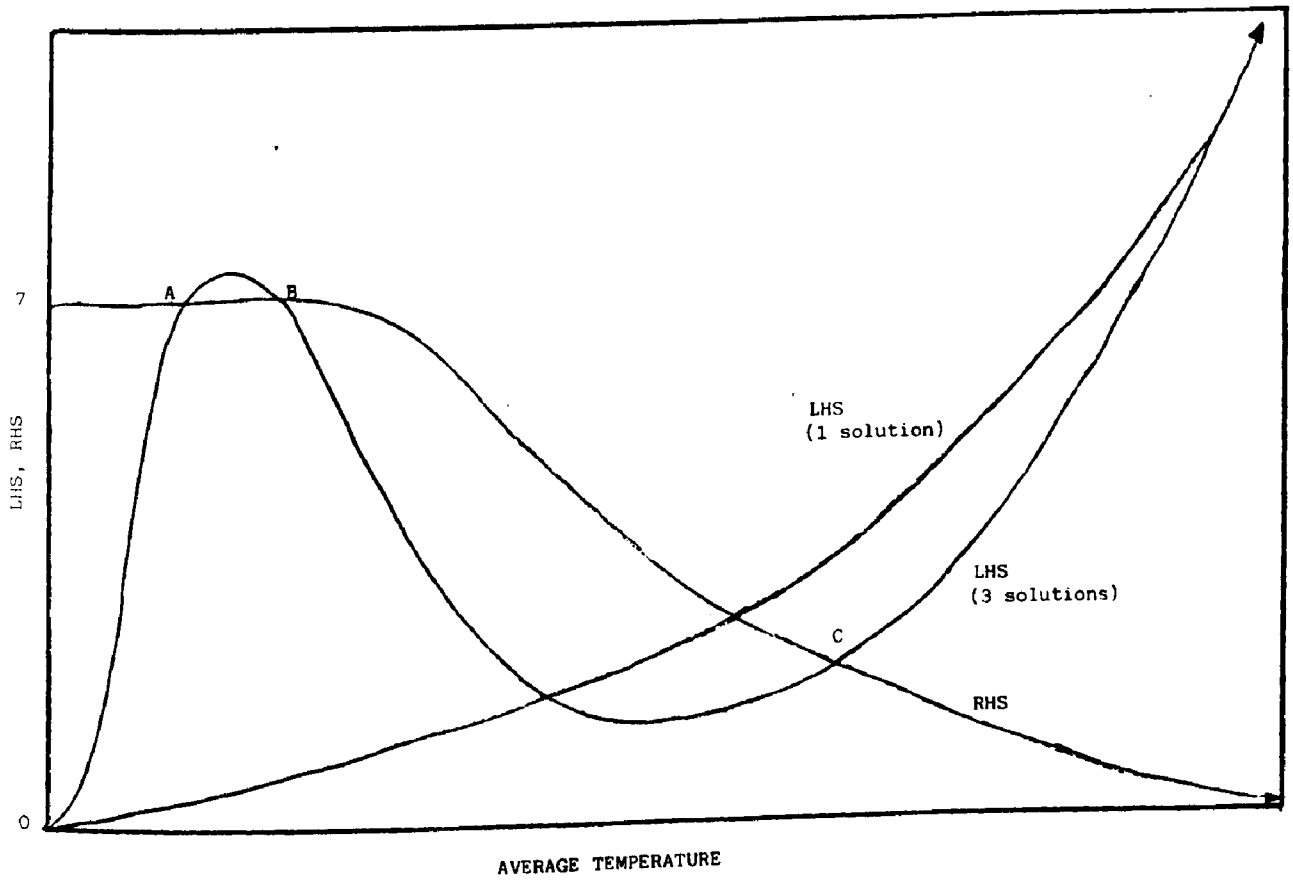


Figure 8.1 LHS and RHS of equation 8.2 as a function of θ

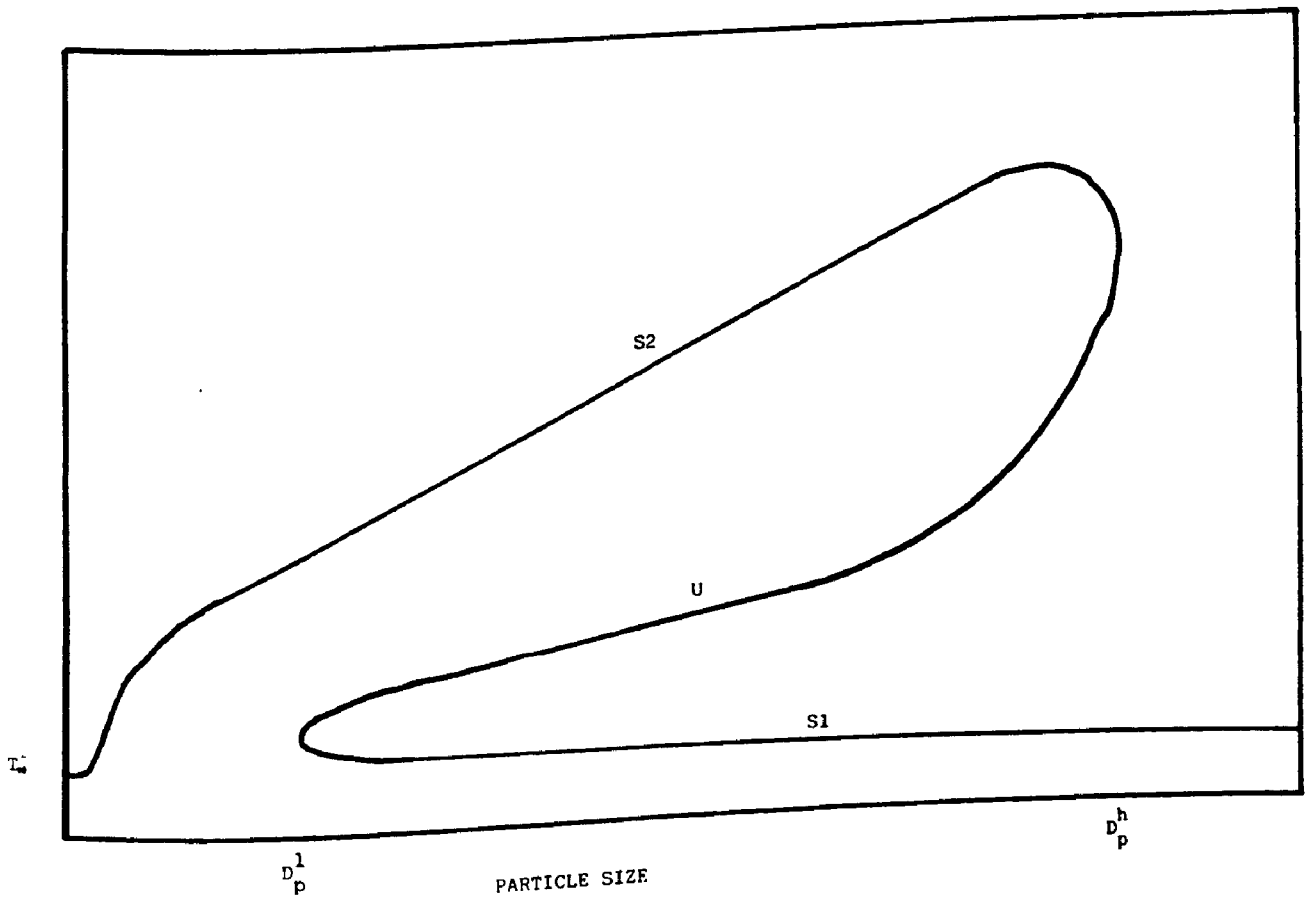


Figure 8.2 Locus of solutions to equation 8.2

For a stable solution at crossing θ_c the following condition must be true:

$$\left.\frac{d\ RHS}{d\bar{\theta}}\right]_{\theta_c} < \left.\frac{d\ LHS}{d\bar{\theta}}\right]_{\theta_c}$$

and conversely for an unstable solution:

Referring to figure 8.1 it is clear that the solutions A and C are stable solutions, while B is an unstable solution. In general the first and last solutions must be stable, and in between the solutions occur as unstable-stable-unstable etc. If there is only one solution it is stable.

This discussion serves to relate the behaviour of coal beds, as deduced in this study, to the behaviour of autothermal chemical reactors, and is extremaly valuable in understanding the nature of the solutions. A further discussion of the behaviour of autothermal reactors is given by Kramers & Westerterp (1963). In the beds investigated in this study, only beds with 1 or 3 solutions have been found. This does not mean that it is not possible that a certain coal bed may have more solutions; indeed this may be possible depending on the parameters in the model.

The procedure of plotting LHS and RHS versus θ has been performed for the base case, for different particle sizes. The graphs obtained are summarized in figure 8.2, in which is sketched the locus of solutions to equation 8.2, with particle size along the x-axis and average temperature on the y-axis.

The following conclusions may be drawn from figure 8.2:

a) Below a certain particle size, which may be called D_p^l, there exists only only 1 solution to equation 8.2.

b) Above D_p^l, but below a certain particle size D_p^h, there exist 3 solutions to equation 8.2.

c) Above D_p^h there exists only one solution to the equation.

Referring to figure 8.2 it can be seen that two different types of stable solution exist, labelled S1 and S2 respectively. The branch labelled S1 is characterized by a temperature rise of less than 30 ^{o}C. This implies that the assumption of a constant rate is a good one in this region. This solution is associated with little use up of oxygen. Beds in this region may be considered to be heat-transfer limited, i.e. they do not experience a large temperature rise because the heat transfer is high enough to remove most of the sensible heat of reaction. This solution ceases to exist below D_p^l since the heat transfer is no longer high enough to remove the sensible heat.

The branch labelled S2 is characterized by total consumption of oxygen. It should be noted that the values of the temperature on this branch are likely to be quite wrong, since the assumption of a constant rate used to calculate these values is a poor one. This is not of great practical importance since these beds may be considered to be burning, and the temperature at which the burning occurs is not of great importance. What is of importance is that for small temperature rises, ie safe beds, the model is accurate, and it is safe beds that are of interest. This high temperature solution ceases to exist above D_p^h since the surface area available for reaction becomes too small to support combustion. It should be pointed out that the values of D_p^h obtained in this study are in the region of 100 mm, which is above the particle size at which coal is normally stockpiled. A further point to note is that the details of the kinetics on branch S2 are also not of great importance. The reason for this is that when there is total consumption of oxygen the energy balance no longer contains any kinetic parameters ie the RHS of the energy balances reduces to the dimensionless adiabatic temperature rise.

Of great practical importance is the behaviour of branch S2 for small particle sizes. Below a certain particle size, which for the base-case parameters is of the order of 1 mm, the average temperature rise falls to less than 70 ^{o}C. Practical experience has shown that these beds, although experiencing a substantial temperature rise, are safe. In many practical cases, the effective particle size of a sample of coal will be below this value, and the bed will be safe. The meaning of particle size, as used in this study, is further discussed in section 8.2.6.,

It should be pointed out that neglecting molecular diffusion as a transport mechanism for oxygen is not a good assumption for particles in the sub 1mm range. Thus the temperatures the model predicts for these particle sizes in likely to be in error. However as has been shown in Chapter 2, the maximum temperature rise due to diffusion is of the order of 70 K. This temperature rise will not occur in practice due to the fact that that heat losses will occur. It is important to realise that even if there is a 70 K rise, the natural convection flows will be extremely small for these fine particles, implying that the beds will remain safe.

It can be seen from figure 8.2 that between D_p^1 and some small particle size the only solution to equation 8.2 is one in which the average temperature in the bed is dangerously high. Thus the model agrees with the often noted fact that certain coals cannot be safely stockpiled, and will, given enough time, spontaneously combust.

Also of practical importance is the branch labelled u in Figure 8.2. This is the locus of the unstable solutions, and serves to separate the stable solutions. The implication of this curve is that should a bed reach an average temperature above the average temperature given by the curve u, then the bed will combust. On the other hand, should the average temperature stay below u, then the temperature of the bed cannot reach the value given by the branch S2.

The possibility of multiple steady-states occurring in fixed bed chemical reactors has been noted in the literature. Luss (1968) and Luss & Amundson (1967) have used bifurcation theory to derive sufficient conditions for the existence of a unique steady-state in a fixed bed chemical reactor. This knowledge would be very valuable in the present study. The problem solved by Luss (1968) is similar, but not identical, to the problem studied in the present work. Unfortunately, the results obtained are not directly applicable to the model presented here, due to the differing mechanisms for reactant transport. This factor makes the application of the method presented by Luss (1968) to the present problem somewhat less than straightforward.

It would indeed be very useful to predict parameter values for which there are a given number of solutions to equation 8.2.

Balakotaiah & Luss (1984) have presented methods for determining the regions of parameters for which a given number of steady-state solutions exist in reacting systems. This work hhas been applied to the problem of predicting multiple steady-states in continuous stirred tank chemical reactors. In these cases the systems are described by algebraic rather than differential equations. The extension of the methods presented by Balakotaiah & Luss (1984) to differential equations is in principle simple; in practice the mathematics soon become intractable.

For the purposes of this study a less mathematically involved, albeit simple minded, approach has been used to determine how many steady-states exist for a given set of parameter values. The approach taken is to calculate the low temperature solution for particle size 20 mm. The particle size is then reduced by 1 mm and the calculation repeated. Eventually no low temperature solution to the equation can be found; thus the particle size at which the low temperature solution ceases to exist is found to an accuracy of 1 mm. The high temperature solution to the equation is then calculated. Although it is known that the model is poor for high temperatures, it is nevertheless important to calculate along this branch since, for sufficiently small particle sizes, the calculated temperatures are below 340 K. These beds may be considered to be safe. It should be noted that if a calculational scheme had been adopted whereby only the number of solutions to equation 8.2 was calculated, then these safe oxygen limited dumps would not have been identified.

The computational effort in performing the calculation described above is minor, even for a large range of parameter values. A computer program to perform the calculation is listed in Appendix 12. In figure 8.3 the results of calculating the locus of solutions to equation 8.2 for the parameter values given in Appendix 11, is presented. The results have been calculated in steps of 1 mm up to particle size 20 mm. Figure 8.3 is the base case, and is used in what follows as a means of comparing the effects of changing the parameters in the model.

The results presented in this section are critical to understanding the behaviour of coal dumps, and will therefore now be summarised:

a) Coal dumps may be classified as either safe, unsafe or con-

ditionally safe.

b) Dumps that are safe are composed of either fine reactive material in which case they are oxygen limited, or coarse unreactive material, in which case they are heat transfer limited.

c) Dumps which are conditionally safe may burn if the temperature of the dump rises above a certain critical temperature. If the temperature of the dump stays below this critical value, the dump remains safe.

d) There are cases in which the dump will, given enough time, undergo spontaneous combustion.

In this study particle size has been chosen as the independent variable for the purposes of presenting in a graphical form the results of solving the model equations. The reason for this is that by varying the particle size, the behaviour of different coal dumps may be observed. However, the other physical parameters of the bed are of extreme importance. For this reason the effect of changing one parameter in the model at a time was investigated. The results are presented graphically in figures 8.3 - 8.11 , and discussed in depth below.

It will be noted that the different branches on the curves are labelled 'small temperature rise' and 'combustion'. It may seem contradictory that for fine material the temperatures on the combustion curve are relatively low. However, combustion may be regarded as a situation in which the large majority of available oxygen is reacting, and in this sense the label combustion is accurate for these curves.

In the discussions below 340 K is used as a dividing value between safe and unsafe coal beds. This value must not be taken too literally, since it has been arbitarily chosen. Its use merley proves convenient in comparing the results obtained for different parameter values.

8.2.2 Effect of varying the voidage

Voidage is a parameter which may be varied in practice by means of compaction. The effect of this is shown in Figure 8.4, from which the following conclusions may be drawn:

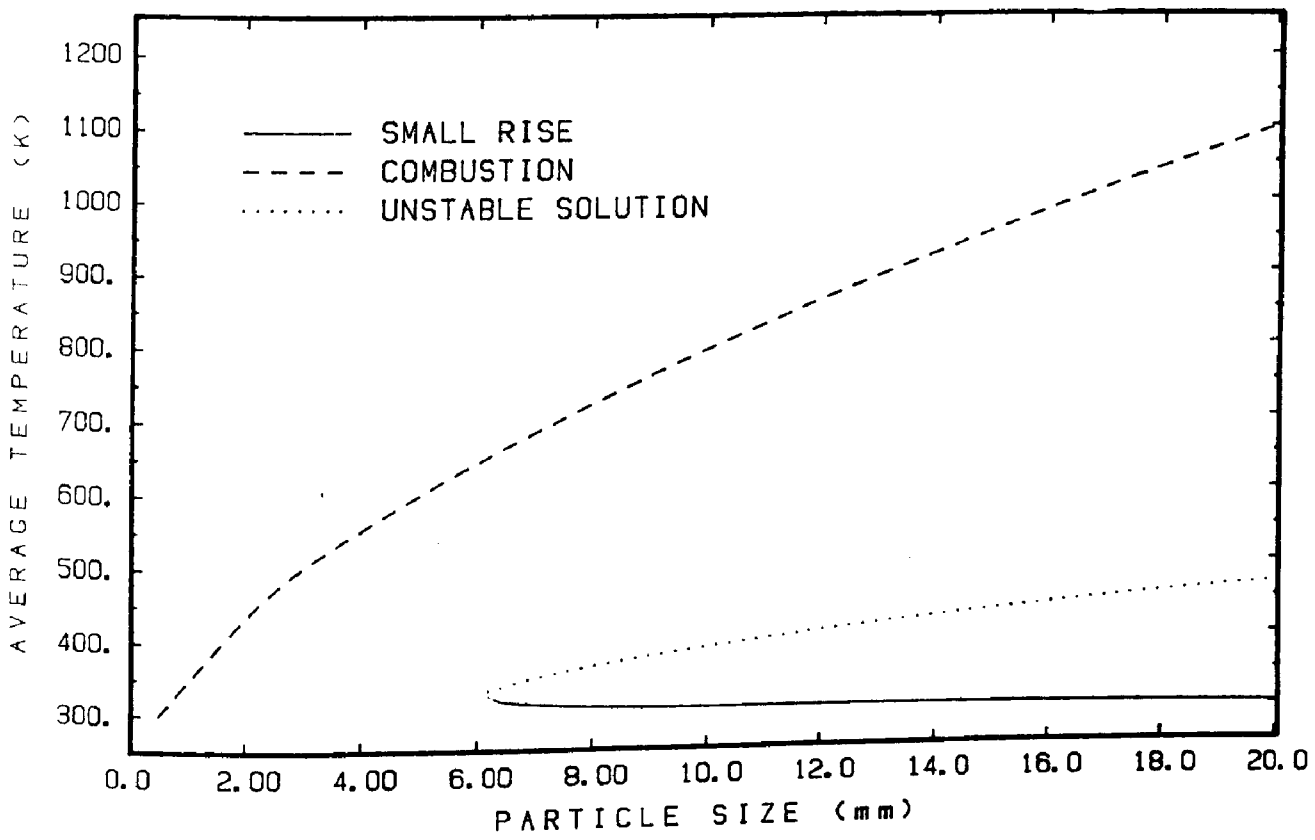


Figure 8.3 Stable and unstable solutions for the base-case

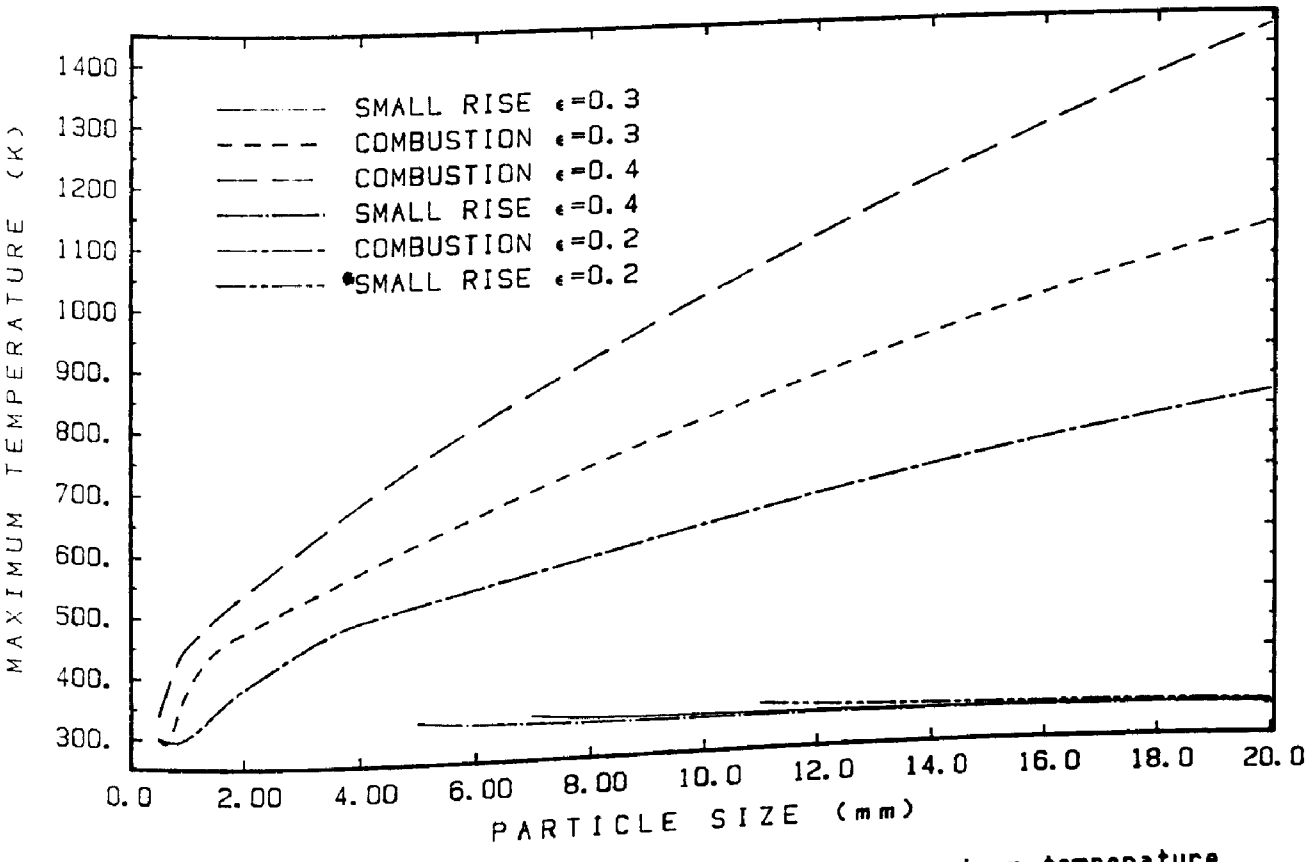


Figure 8.4 Effect of varying voidage on the maximum temperature

a) For fine material, compacting the bed will help make it safer. This can be seen from the fact that the combustion or oxygen limited curve is lower in temperature for lower voidages. Put another way, a fine coal may be safely stockpiled uncompacted, whereas a slightly coarser coal may have to be compacted when stockpiled in order for it to be safe. Using the rough criterion of 340 K then for this particular case material of voidage 0.2 is safe up to particle size 1.8 mm, while for voidage 0.3 the material is safe only up to particle size 0.8 mm.

b) Compacting coarse material may be detrimental. This is shown by the fact that the small temperature rise solution ceases to exist at $D_p = 11$ for $\epsilon = 0.2$, $D_p = 8$ for $\epsilon = 0.3$ and at $D_p = 5$ for $\epsilon = 0.4$.

The last conclusion may seen odd, and deserves some explanation. By compacting the bed the surface area per unit volume of the bed is increased. This in turn has two effects:

a) The resistance to flow is greater and
b) The mass of reactive material per unit bed volume is greater.

For the heat-transfer limited beds, i.e. the ones that experience a small temperature rise, the second result of more reactive material per bed volume more than outweighs the first of reducing oxygen ingress, since the bed was not in any case oxygen limited. (In fact, the reduction in flow also causes a rise in temperature since the heat loss due to flow is decreased). However for the case of oxygen limited beds compaction makes them safer by increasing the rate at which oxygen is scavenged from the air by reaction, as well as increasing the resistance to flow and therefore reducing the flowrate.

8.2.3 Effect of varying the pre-exponential factor

The purpose of varying the pre-exponential factor K_o is to try and simulate the fact that different coals will have different reactivities. Figure 8.5 indicates very clearly that for heat transfer limited beds, the larger K_o, the less safe the bed is. However, the opposite is true for oxygen limited beds. This surprising result can be understood in terms of the fact that

a) For fine material, compacting the bed will help make it safer. This can be seen from the fact that the combustion or oxygen limited curve is lower in temperature for lower voidages. Put another way, a fine coal may be safely stockpiled uncompacted, whereas a slightly coarser coal may have to be compacted when stockpiled in order for it to be safe. Using the rough criterion of 340 K then for this particular case material of voidage 0.2 is safe up to particle size 1.8 mm, while for voidage 0.3 the material is safe only up to particle size 0.8 mm.

b) Compacting coarse material may be detrimental. This is shown by the fact that the small temperature rise solution ceases to exist at $D_p = 11$ for $\epsilon = 0.2$, $D_p = 8$ for $\epsilon = 0.3$ and at $D_p = 5$ for $\epsilon = 0.4$.

The last conclusion may seen odd, and deserves some explanation. By compacting the bed the surface area per unit volume of the bed is increased. This in turn has two effects:

a) The resistance to flow is greater and
b) The mass of reactive material per unit bed volume is greater.

For the heat-transfer limited beds, i.e. the ones that experience a small temperature rise, the second result of more reactive material per bed volume more than outweighs the first of reducing oxygen ingress, since the bed was not in any case oxygen limited. (In fact, the reduction in flow also causes a rise in temperature since the heat loss due to flow is decreased). However for the case of oxygen limited beds compaction makes them safer by increasing the rate at which oxygen is scavenged from the air by reaction, as well as increasing the resistance to flow and therefore reducing the flowrate.

8.2.3 Effect of varying the pre-exponential factor

The purpose of varying the pre-exponential factor k_o is to try and simulate the fact that different coals will have different reactivities. Figure 8.5 indicates very clearly that for heat transfer limited beds, the larger k_o, the less safe the bed is. However, the opposite is true for oxygen limited beds. This surprising result can be understood in terms of the fact that

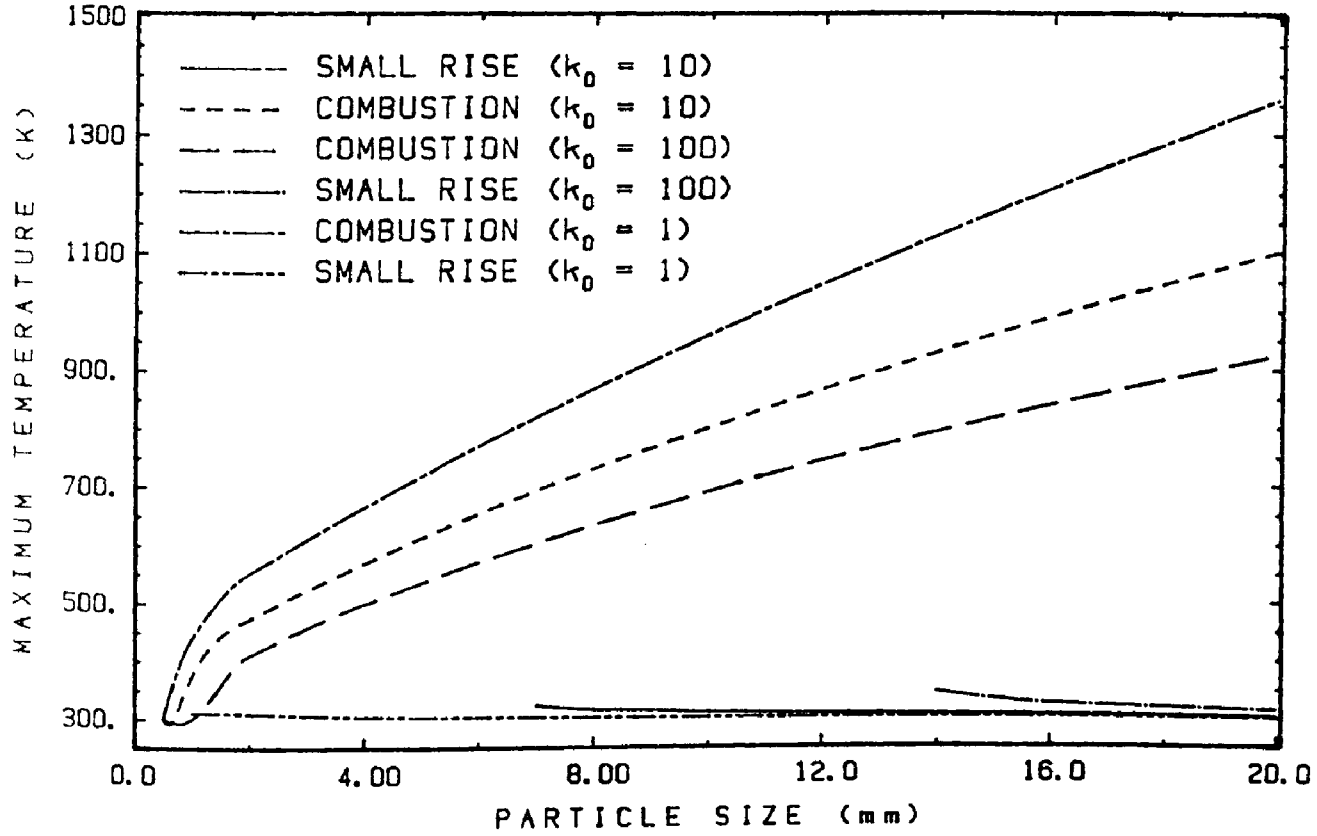


Figure 8.5 Effect of varying the pre-exponential factor on the maximum temperature

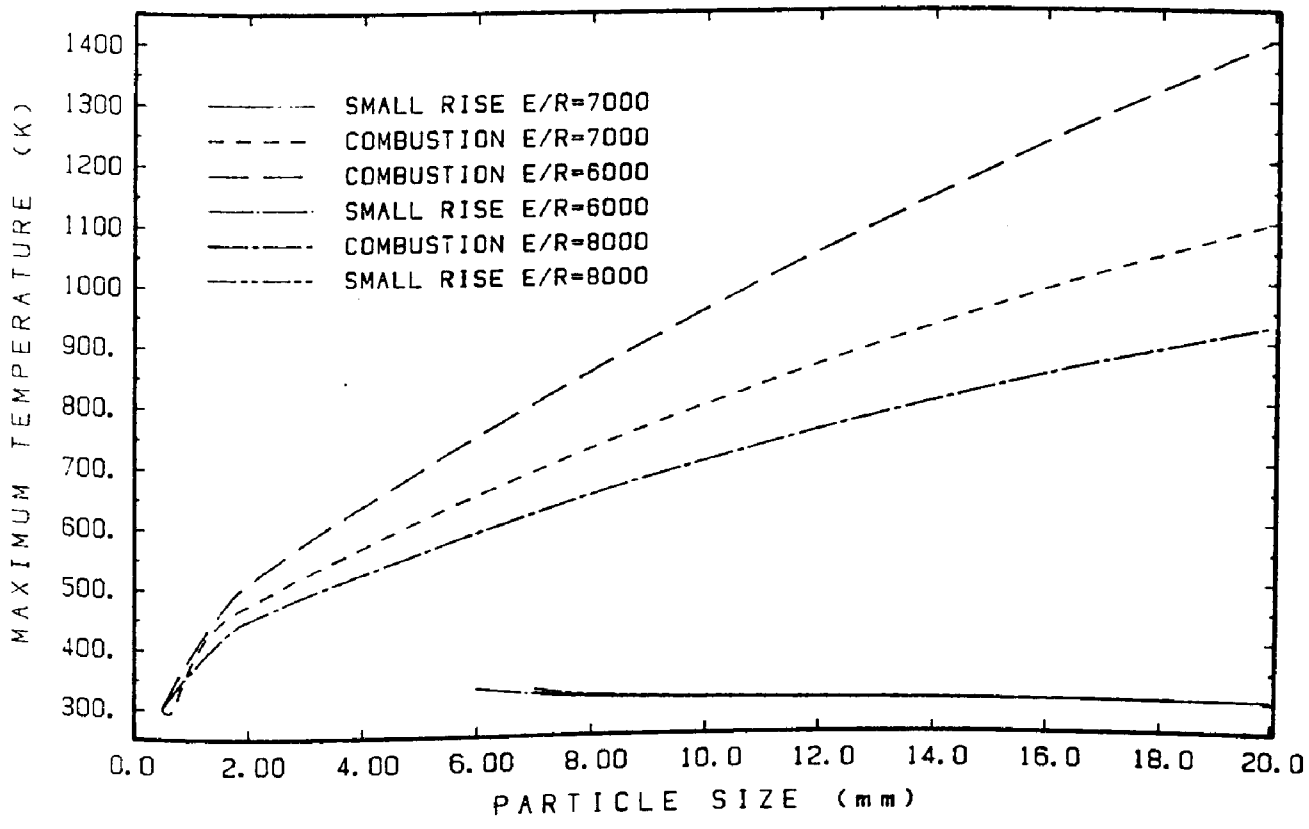


Figure 8.6 Effect of varying the activation energy on the maximum temperature

the oxygen depletion is less when k_o is lower, implying that the oxygen in the bed can penetrate further, leading to a larger temperature rise. When k_o is very large, all the oxygen is consumed close to the surface, where the sensible heat of reaction is easily conducted away.

Using the criterion of 340 K then for k_o = 1 m/s beds are safe below approximately 0.5 mm particle size, whhile for k_o = 100 m/s beds are safe below 1.5 mm particle size. This shows that for these small particle sizes, the more reactive the coal, the safer it is to stockpile.

Also of interest in Figure 8.5 is the fact that that for k_o=1 there is only a small range of particle sizes for which the bed is unsafe. This is a logical conclusion since it is to be expected that very unreactive material will not combust spontaneously.

Figure 8.5 indicates very clearly that k_o is a critical model parameter, and as such needs to be accurately measured.

8.2.4 Effect of varying the activation energy

To study the effect of changing the activation energy, it is necessary at the same time to vary k_o, so that the reactivity is the same at some base temperature. In this case a base temperature of 300 K was chosen. Figure 8.6 thus shows the behaviour of three different coals with the same room temperature reactivity but different activation energies. It can be seen from Figure 8.5 that there is little effect on both the curves. This then indicates that the activation energy is not a critical parameter for coals which have the same room temperature reactivity. However, two coals which have both different activation energies and different room temperature reactivities will have different liabilities toward self heating. The activation energy must thus be measured, and used in conjuction with k_o as a measure of the reactivity of the coal.

8.2.5 Effect of different assumptions about the reactive surface area of coal

The relationship between the particle size of coal and its reactive surface area has been discussed by Sondreal & Ellman (1974). They state that low-temperature oxidation rates have reported to

the oxygen depletion is less when k_o is lower, implying that the oxygen in the bed can penetrate further, leading to a larger temperature rise. When k_o is very large, all the oxygen is consumed close to the surface, where the sensible heat of reaction is easily conducted away.

Using the criterion of 340 K then for k_o = 1 m/s beds are safe below approximately 0.5 mm particle size, whhile for k_o = 100 m/s beds are safe below 1.5 mm particle size. This shows that for these small particle sizes, the more reactive the coal, the safer it is to stockpile.

Also of interest in Figure 8.5 is the fact that that for k_o=1 there is only a small range of particle sizes for which the bed is unsafe. This is a logical conclusion since it is to be expected that very unreactive material will not combust spontaneously.

Figure 8.5 indicates very clearly that k_o is a critical model parameter, and as such needs to be accurately measured.

8.2.4 Effect of varying the activation energy

To study the effect of changing the activation energy, it is necessary at the same time to vary k_o, so that the reactivity is the same at some base temperature. In this case a base temperature of 300 K was chosen. Figure 8.6 thus shows the behaviour of three different coals with the same room temperature reactivity but different activation energies. It can be seen from Figure 8.5 that there is little effect on both the curves. This then indicates that the activation energy is not a critical parameter for coals which have the same room temperature reactivity. However, two coals which have both different activation energies and different room temperature reactivities will have different liabilities toward self heating. The activation energy must thus be measured, and used in conjuction with k_o as a measure of the reactivity of the coal.

8.2.5 Effect of different assumptions about the reactive surface area of coal

The relationship between the particle size of coal and its reactive surface area has been discussed by Sondreal & Ellman (1974). They state that low-temperature oxidation rates have reported to

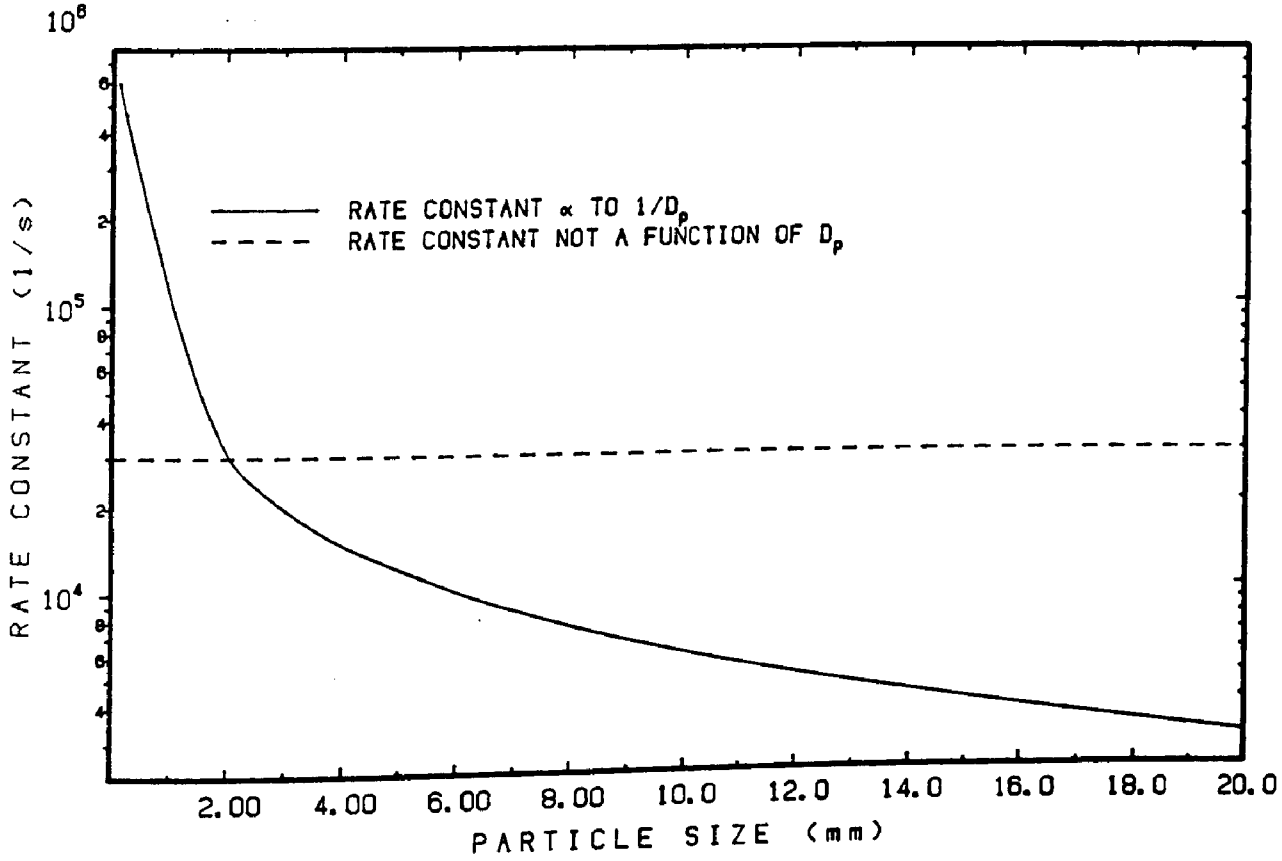


Figure 8.7 Pre-exponential factor versus particle size for the two cases considerd

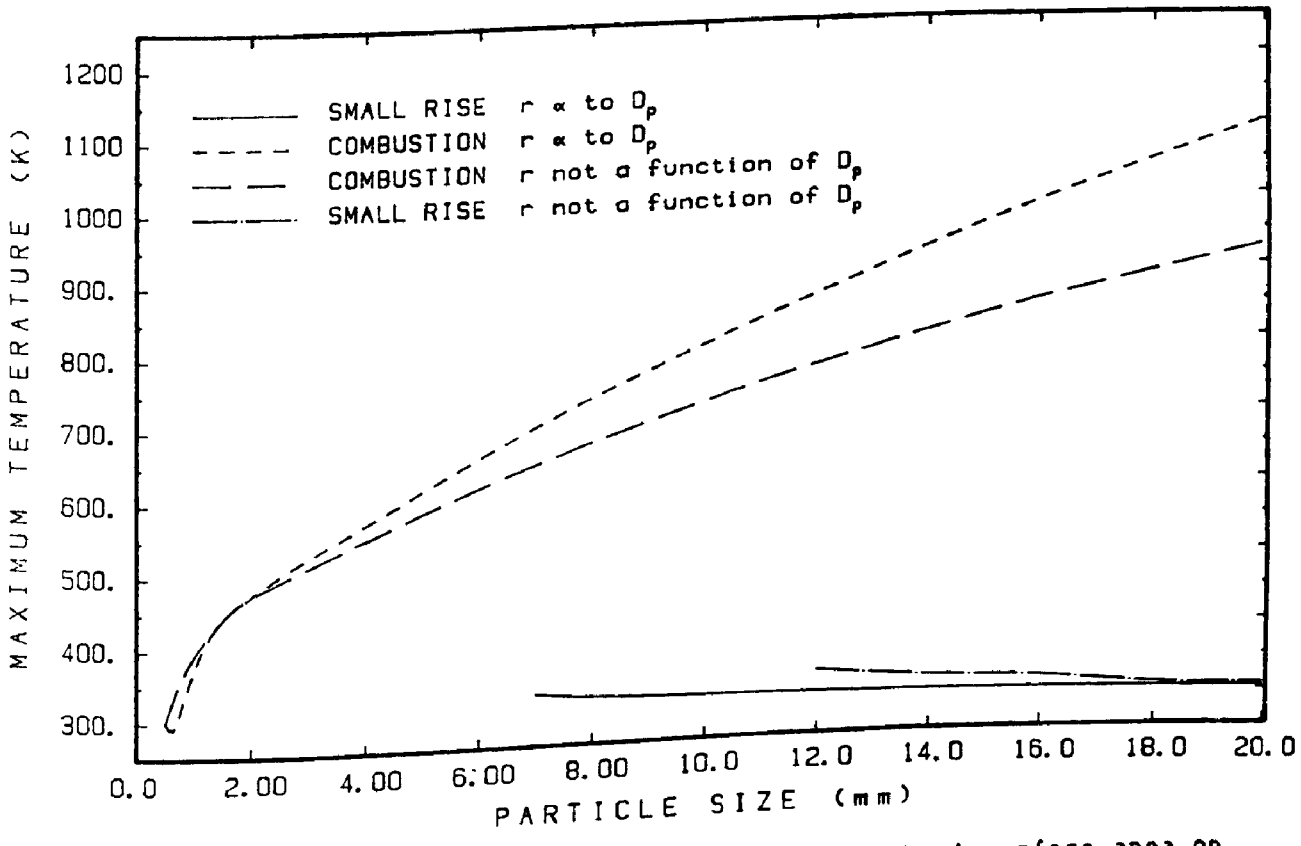


Figure 8.8 Effect of different assumptions about surface area on the maximum temperature

8.2.6 The Meaning of Particle Size

It should be noted that the particle size as used in the graphs presented in this section is defined by:

$$D_p = 6/S_t \qquad 8.5$$

and that this is of great importance when calculating the particle size of a coal sample with a particle size distribution. The correct particle size to use is the one defined by

$$S_t = 6 \sum_{i=1}^{N} \frac{m_i}{D_{p_i}} \qquad 8.6$$

together with equation 8.5

where D_{p_i} = average particle size of class i

m_i = mass fraction of coal in class i

N = number of classes

$$D_p = \sum_{i=1}^{N} D_{p_i} m_i \qquad 8.7$$

is not the correct average for this case.

Should a full particle size distribution be available, the summation in the above equations may be replaced by integrals.

To demonstrate the importance of the above discussion consider a coal with the size distribution given in Table 8.1.

TABLE 8.1 PARTICLE SIZE DISTRIBUTION FOR A TYPICAL SAMPLE

PARTICLE SIZE IN mm		MASS %
	+6.68	26,9
-6.68	+4.70	12.3
-4.70	+2.36	20.2
-2.36	+1.20	12.9
-1.20	+0.59	10.1
-0.59	+0.10	15.7
-.10		1.9

Calculating Dp by equation 8.7 gives a value of 4.5 mm while using equations 8.5 and 8.6 gives 0.9 mm. It can be seen that even a relatively small amount of fine material has the effect of drastically changing the effective particle size of the coal. This is of great importance when considering the liability towards spontaneous combustion of so-called segregated coal

8.2.7 Effect of Wind on Maximum Temperature

The effect of wind on the maximum temperature in the coal bed is shown in Figure 8.9. It appears from this figure that the presence or absence of wind has little effect on the calculated temperatures. However the curve plotted in Figure 8.9 assumes the wind blows constantly until steady-state is reached. This is highly unlikely to occur in practice. The more likely case is a wind which blows for a while, and then dies away. This is obviously on unsteady-state phenomenon, and as such will be discussed in section 8.3.

8.2.8 Effect of Thermal Conductivity on Maximum Temperature

Although the effective thermal conductivity of a packed bed of coal has been measured, it was felt worthwhile to investigate the effect of changing this parameter. It can be seen from Figure 8.10 that both halving and doubling this parameter have little effect on the calculated curves. It thus appears satisfactory to use the measured value of the effective thermal conductivity in all calculations.

8.2.9 Effect of Changing the Bed Length

The bed length is the most difficult model parameter to relate to a real coal dump. It is incorrect to assume that this bed length bears a fixed relationship to the physical size of a coal dump, e.g. its height or width. The bed length in the one-dimensional model in fact corresponds to the path length for flow in the real situation. This path length in general will not be known, although the physical size of the dump sets an upper bound on this quantity.

For the purposes of this study three bed lengths were chosen, in order to see the effect of changing this quantity. From Figure 8.11 it can be seen that the effect of bed length is very pro-

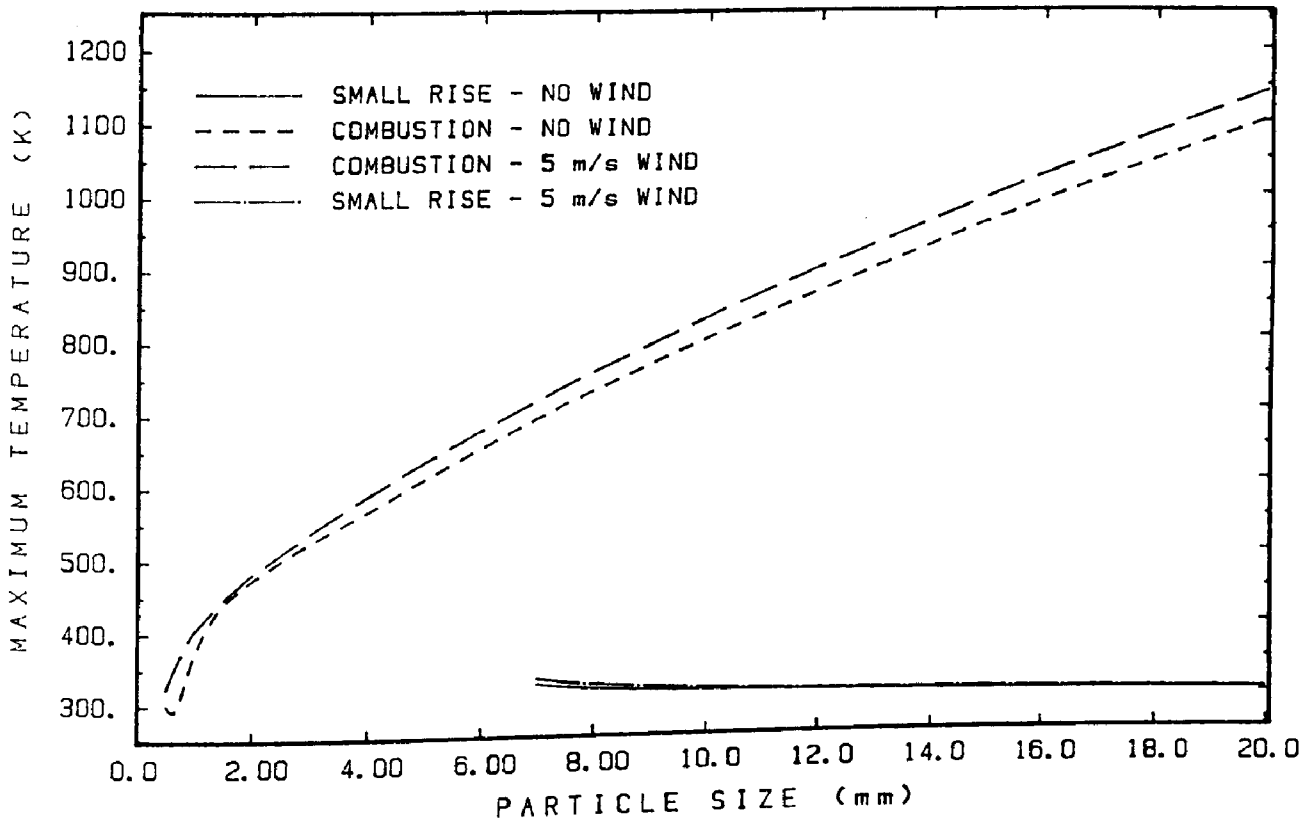


Figure 8.9 Effect of wind on the maximum temperature

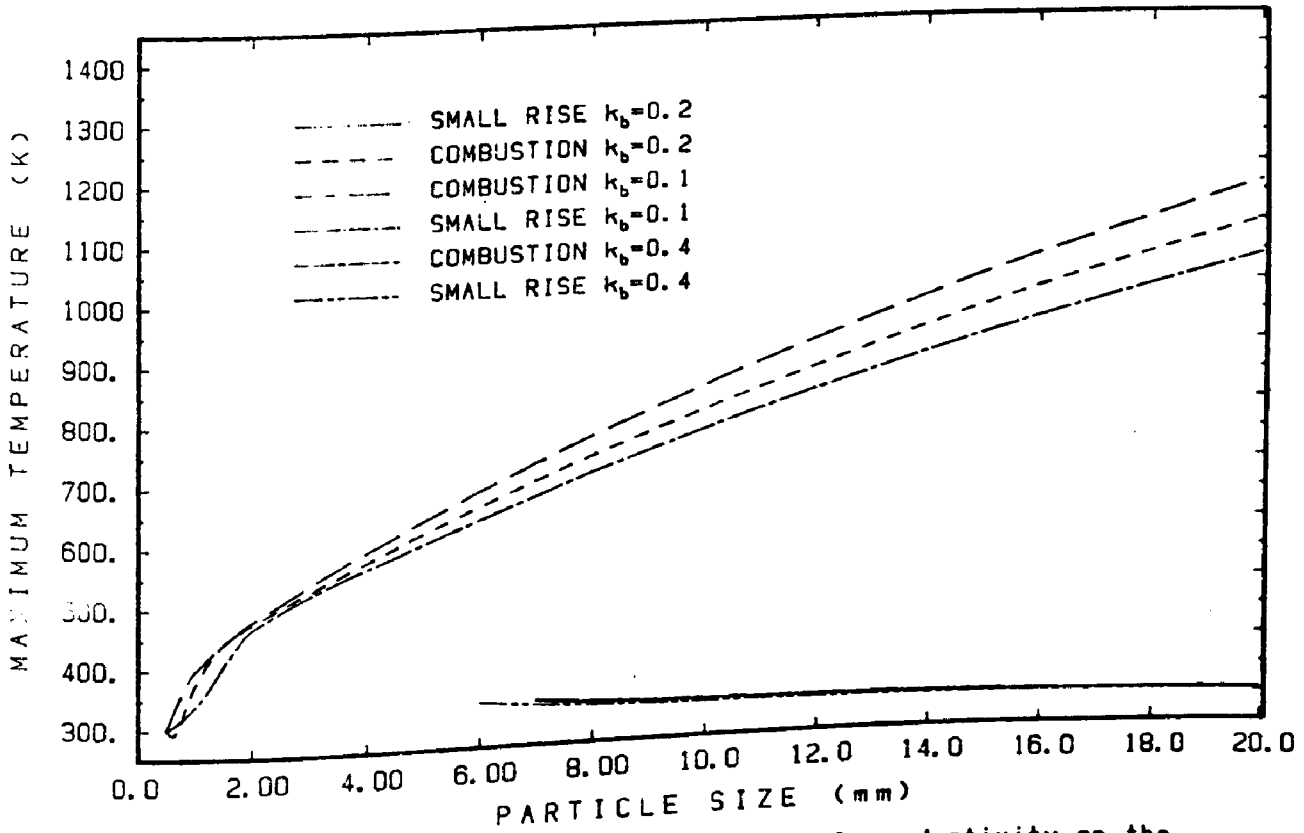


Figure 8.10 Effect of varying bed thermal conductivity on the maximum temperature

nounced on the low temperature solution curves. For the oxygen limited beds, there is little difference between the curves for bed length 5 and 10 m. The curve for bed length 1 m has a somewhat different shape, and for particle sizes less than 1 mm the temperature rise is negligible. In addition the range of particle sizes for which the bed can be considered to be unsafe is between approximately 1.5 and 2 mm.

The fact that the curves for 5 m and 10 m are so similar can be explained as follows: For an oxygen limited bed the oxygen in the flow is used up very close to the inlet to the bed. From that point in the bed where there is to all intents and purposes no oxygen, no more reaction can occur. The temperature profile in the rest of the bed is thus governed by conduction, especially for the beds of finer particles for which the flowrates are low. This implies that making the bed longer will have little effect on the maximum temperature in the bed, since all the temperature rise occurs very close to the inlet.

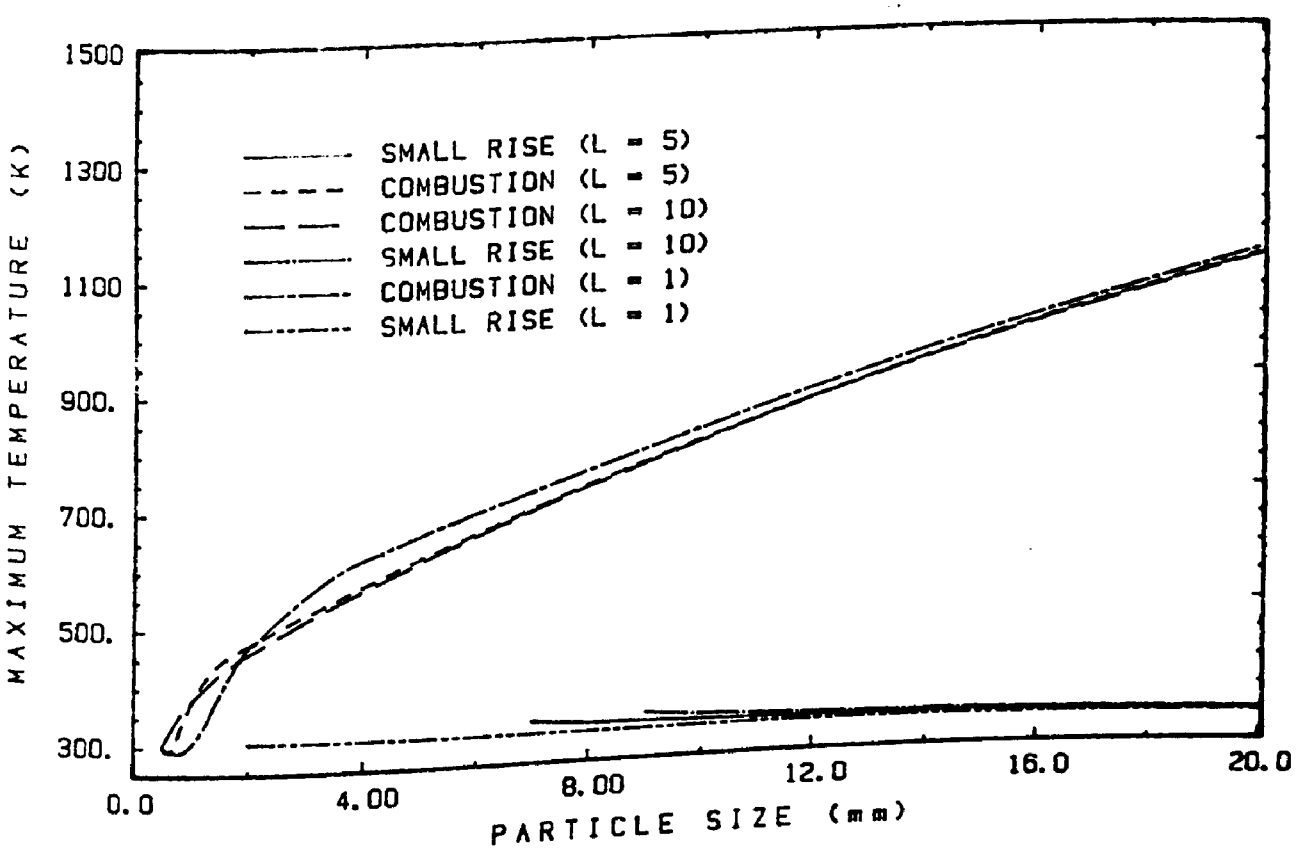


Figure 8.11 Effect of varying bed length on the maximum temperature

8.3 Unsteady-State Solutions for r constant

8.3.1 Introduction

The unsteady-state solution for r constant has been discussed in section 6.3. The resulting solution has been programmed in BASIC on an HP 9835 computer, and a lsiting of the program is given in Appendix 12.

It has been found that obtaining the solution to the analytical equation is in fact slower than obtaining the solution using the numerical method discussed in section 6.4. The aim of what follows is thus to point out the pertinent facts that emerge from solving the equation, without presenting an extensive array of graphs.

8.3.2 The Character of the Solutions

It is already known from calculations in the previous section what the steady-state temperature profiles for a given bed will look like. The advantage of the unsteady-state method thus lies in the fact that should the bed be conditionally safe, the unsteady-state solution will be able to predict from the initial condition what the final steady-state will be.

The temperature time curves in the centre of a coal bed using three different initial conditions are plotted in figure 8.12. The initial condition used is the somewhat artificial one of a coal bed with an initial uniform temperature.

The model parameters used to obtain the curves shown in Figure 8.12 are given in Table 8.2.

TABLE 8.2 MODEL PARAMETERS FOR FIGURE 8.12

Particle Size	5 mm
Voidage	0.4
Bed Length	1 m
K_o	0.7 m/hr
E/R	2889 K

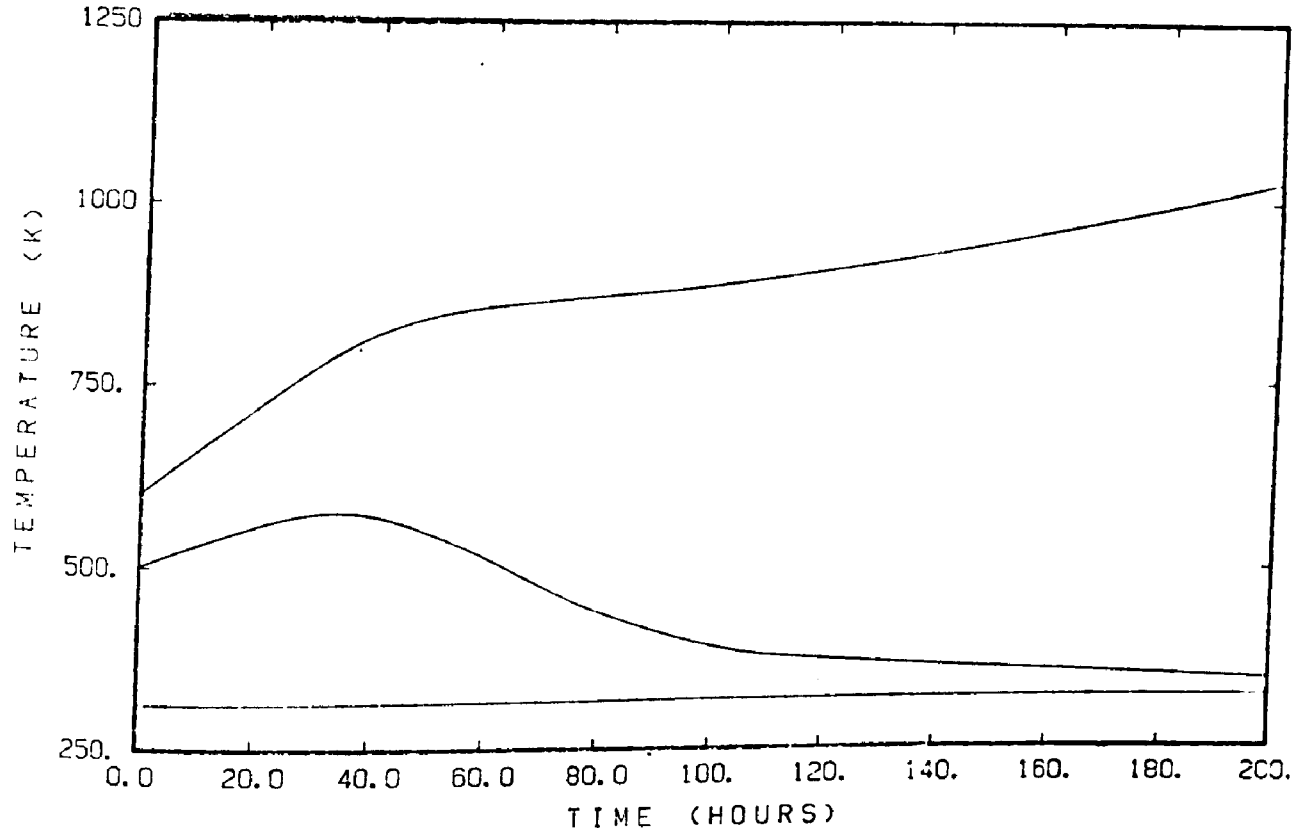


Figure 8.12 Temperature-time curves in the centre of a coal bed for different initial temperatures

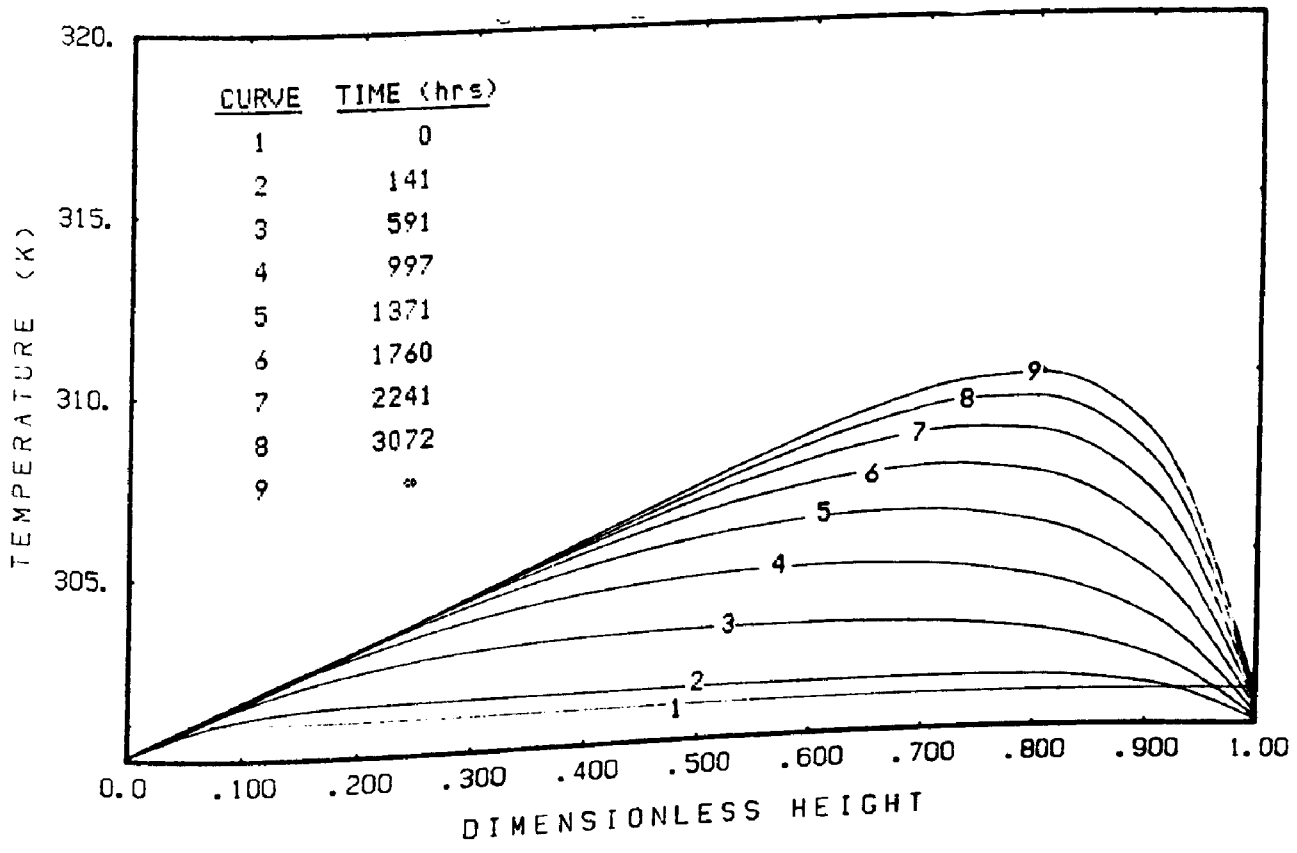


Figure [illegible] Temperature profiles in a coal bed

It can be observed from figure 8.12 that starting with an initial temperature of 301 K the temperature in the bed gradually rises to eventually reach a stable low temperature steady-state. Starting with a bed temperature of 500 K the temperature initially increases but then decreases to eventually again reach the low temperature stable steady-state. However starting at 600 K the temperature increases monotonically, leading to combustion. Thus for this particular bed the critical temperature appears to be between 500 & 600 K. This temperature would in fact correspond to the unstable solution temperature discussed in section 8.2.

Temperature profiles for a coal bed with parameters as given in Appendix 11, for a particle size of 10 mm and length of 5 m are shown in figure 8.13. Referring to figure 8.3 it can be seen that such a bed has a stable steady-state at a maximum temperature of 310 K. In figure 8.13 it can be observed that starting with a temperature of 301 K the bed gradually heats up to its final steady-state temperature. Although in theory the bed reaches steady-state after only an infinite time, it can be seen that after 3568 hrs or nearly 150 days, the bed is to all intents and purposes at steady-state.

It is tempting to try and define a time constant for a coal bed, in order that predictions may be made on safe stockpiling times. In order to do this one would hypothesize that the temperature in a coal bed could be described by an equation of the form

$$\frac{\theta(X,\tau) - \theta_{ss}(X)}{\theta(X,0) - \theta_{ss}(X)} = \exp(-\frac{\tau}{\tau_c}) = \exp(-\frac{t}{t_c}) \qquad 8.3.1$$

where τ_c is a dimensionless time constant, and t_c is a time constant.

In fact using equation 6.3.2, and assuming that only the first term in the series $V(X,\tau)$ need be considered it can be shown that

$$\tau_c = (\beta_1^2 + a^2/4)^{-1} \qquad 8.3.2$$

It is thus immediately obvious that τ_c is not constant, but in fact a function of time, since the quantity, a, which is proportional to the flowrate, is a function of time.

For cases when $\beta_1^2 \gg a^2/4$, the use of a time constant is justified. It can be shown that $\beta_1 \approx \pi$, therefore $a/2 \ll \pi$ is the criterion for using a time constant.

Converting τ_c to time units using the relationship

$$\tau_c = \frac{\kappa t_c}{L^2} \qquad 8.3.3$$

In the case when $a/2 \ll \pi$

$$\tau_c = \frac{1}{\beta_1^2} = \frac{1}{\pi^2}$$

$$t_c = \frac{L^2}{\pi^2 \kappa} \qquad 8.3.4$$

The time constant in this case is governed by the thermal diffusivity of the bed, which implies that the heat transfer in the bed is mainly by conduction.

Then

$$t_c = \frac{L^2}{\pi^2 \times 8 \times 10^{-4}} = 126L^2 \text{ hrs} \approx 5L^2 \text{ days}$$

This implies that for cases where the heat transfer in the bed is governed by conduction, the bed will be 37 % away from its steady-state temperature after $5L^2$ days and 14 % after $10L^2$ days.

A similar calculation for the case $a/2 \gg \pi$ is not justifiable, since a is a function of time. However, using the definition of of the quantity a

$$a = \frac{\hat{G}cL}{k_b}$$

and using the simplified formula for the flowrate G

$$G = \frac{q}{fM_w}\left[\frac{\theta-1}{\bar{\theta}^2}\right]$$

Is is possible to calculate the quantity a, and compare it to 2π to deduce whether the dominant transfer mechanism is conduction or flow.

Using values from Table 2.1 and Appendix 11, and assuming an average dimensionless temperature of 1,1 ie an average temperature of 330 K the values in Table 8.3 have been calculated

TABLE 8.3 THE QUANTITY 'a' FOR VARIOUS PARTICLE SIZES

Particle Size (mm)	a
1	0.1L
2	0.4L
5	2.5L
20	40L

It thus appears that for a 5 m bed of 5 mm particles at an average temperature of 330 K that flow is a more important heat transfer mechanism than conduction. For finer particles in shorter beds conduction will dominate, and then equation 8.3.1 together with 8.3.4 may be used to calculate the time varying behaviour of the coal bed.

Plotted in figure 8.14 is the temperature-time behaviour at the centre of a bed composed of 6 mm particle and 5 m in length. All the other model parameters are base case values. Referring to Figure 8.3 it can be seen that for this coal bed there is no low temperature solution. This conclusion is confirmed by the unsteady-state calculation.

It can be seen that the temperature rise in the centre of this bed is gradual with a value of 0.24 K/day until approximately 80 days. At this time the temperature increases dramatically

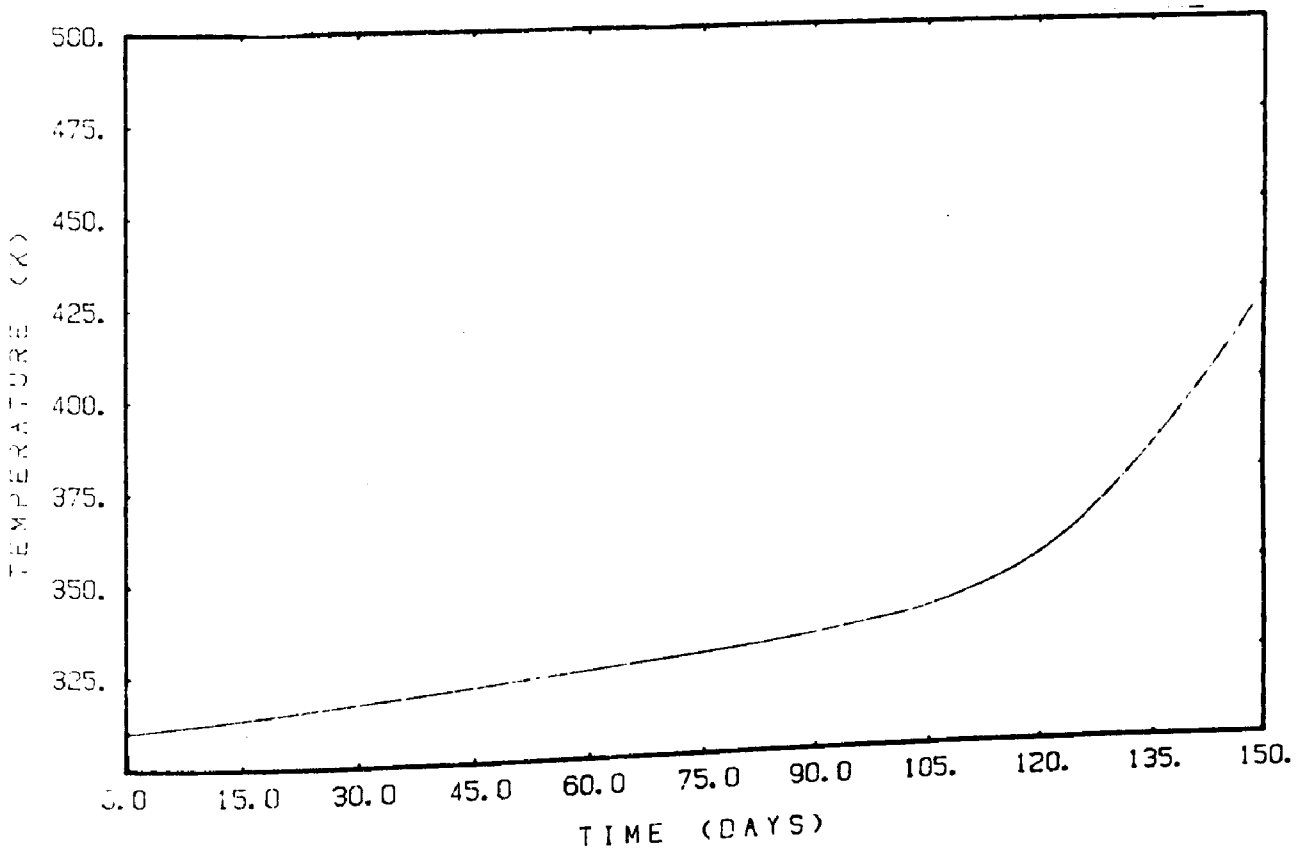


Figure 8.14 Temperature-time behaviour at bed centre
Particle size 6 mm - Analytical solution

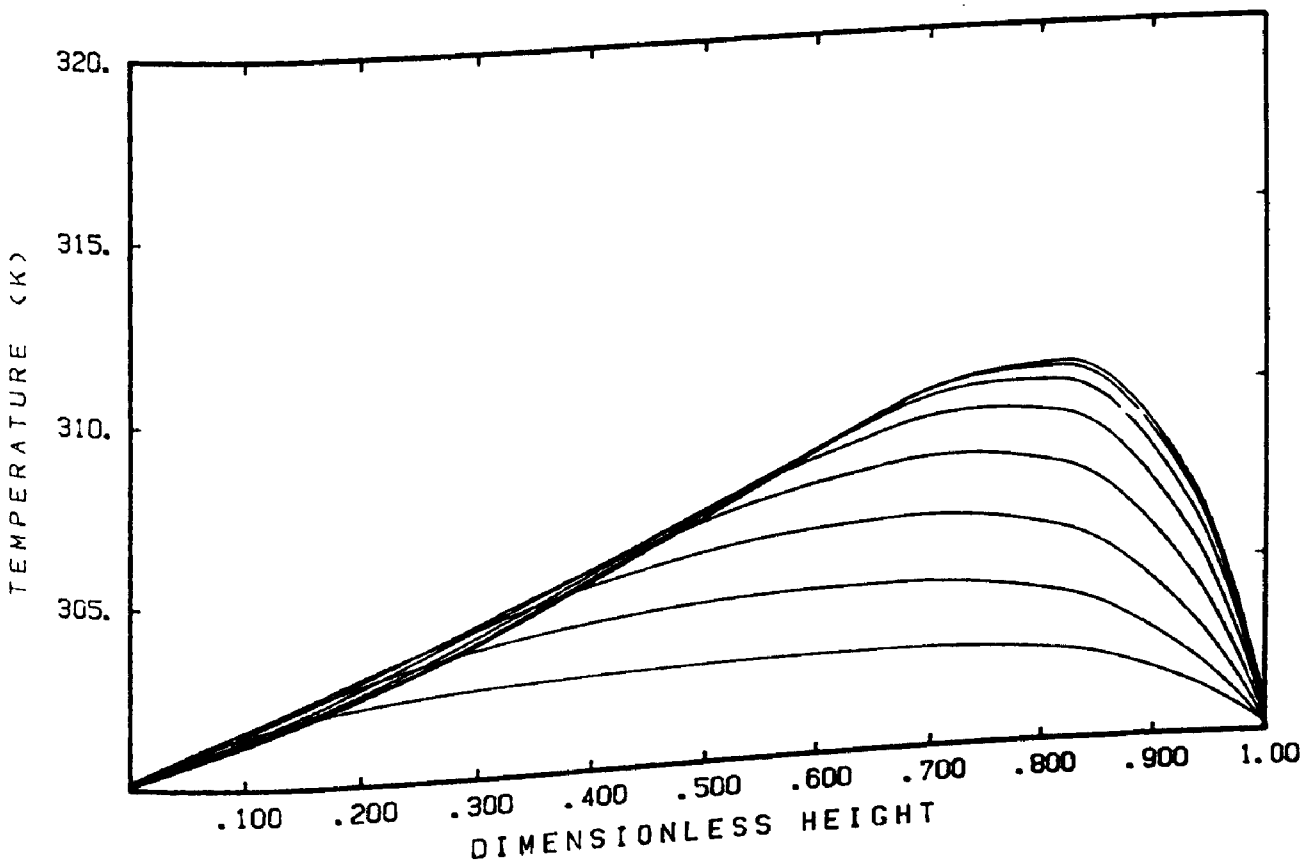


Figure 8.15 Temperature profiles in a coal bed
size 10 mm - Numerical Method

leading to eventual combustion. From this plot 60 ^{o}C appears to be a critical temperature. It is interesting to note that from Table 8.3, at 57 ^{o}C flow is already dominating conduction as the significant heat transfer mechanism, since the value of the quantity 'a' is 3.6L or 18 which is significantly greater than 2π.

8.3.3 Discussion

The results presented in this section confirm the validity of the plots presented in section 8.2. The following are the important conclusions from the section.

a) Depending on the initial condition, a coal bed may either attain a low or high temperature steady state.

b) For coal beds in which conduction is the dominating heat transfer mechanism, a simple formula may be used to calculate the temperature of a coal bed as a function of time.

c) A method has been presented whereby it may be calculated whether conduction or flow is the dominant heat transfer mechanism in a coal bed. In general conduction will only be dominant for short coal beds of fine particles, in which the temperature rise remains small.

d) Results have been presented showing the temperature time behaviour of a coal bed on its way to spontaneous combustion. The bed is characterized by a gradual temperature rise until 60 ^{o}C at which point the temperature rise becomes more dramatic. It has been pointed out that at 60 ^{o}C flow is the dominant heat transfer mechanism in the bed.

8.4 Results of Solving the Equations Numerically

8.4.1 Introduction

As has been discussed, the numerical method for solving the equations involves no assumptions about the reaction rate being constant, and allows for the effect of prior oxidation on the reaction rate. The solutions can be found quickly, even using a fairly unsophisticated microcomputer, and if programmed on a more powerful mainframe computer, the computer time involved would be small.

8.4.2 Comparison Beteewn the Numerical Method and the Analytical Method

The results presented in Figures 8.13 were recalculated using the numerical method. In figure 8.15 the results for the case D_p = 10 mm are presented. It can be seen that for this low temperature case the results obtained are very similar. This is to be expected since the temperature variation in the bed is only of the order of 10 K, and therefore the assumption of a constant rate constant is fairly good.

In figure 8.16 temperature profiles through a reacting bed of coal of size 2 mm with a wind velocity of 5 m/s. A glance at Figure 8.9 will show that for this range of the parameters the bed is unsafe, with a final predicted maximum temperature of 450 K. In fact, as can be seem from figure 8.16 the maximum temperature reached is approximately 1100 K, indicating that the assumption of constant rate constant used to generate the curves in Figure 8.9 is a poor one for this case.

A point of interest in Figure 8.16 is the way in which ignition appears to occur. Between day 40 and day 45 a hump appears in the temperature profile, subsequently the maximim temperature in the bed moves toward the entrance of the bed. This effect is due to the fact that as the temperature increases so does the rate of reaction, leading to the oxygen being depleted near the entrance of the bed. The curves between day 55 and day 80 show some evidence that the numerical method does not cope very well with the ingition, which is in fact a shock phemomenon. In particular the curve for day 55, which exhibits two maxima is unrealistic, Nevertheless the temperature profile after 80 days appears to be in agreement with what one would expect, except for a slightly concave shape.

In Figure 8.17 is shown a cross plot of the results in Figure 8.16 at the bed centre. This curve shows a dramatic increase in temperature between 40 and 45 days of 130 K. The critical temperature from this plot appears to be in the region of 75 ^{o}C.

This bed appears to "take-off" after 40 days whereas the results shown in Figure 8.14 appears to become dangerous after 80 days. The difference between these two cases is the particle sizes of the coal and the fact that that for the results shown in Figure

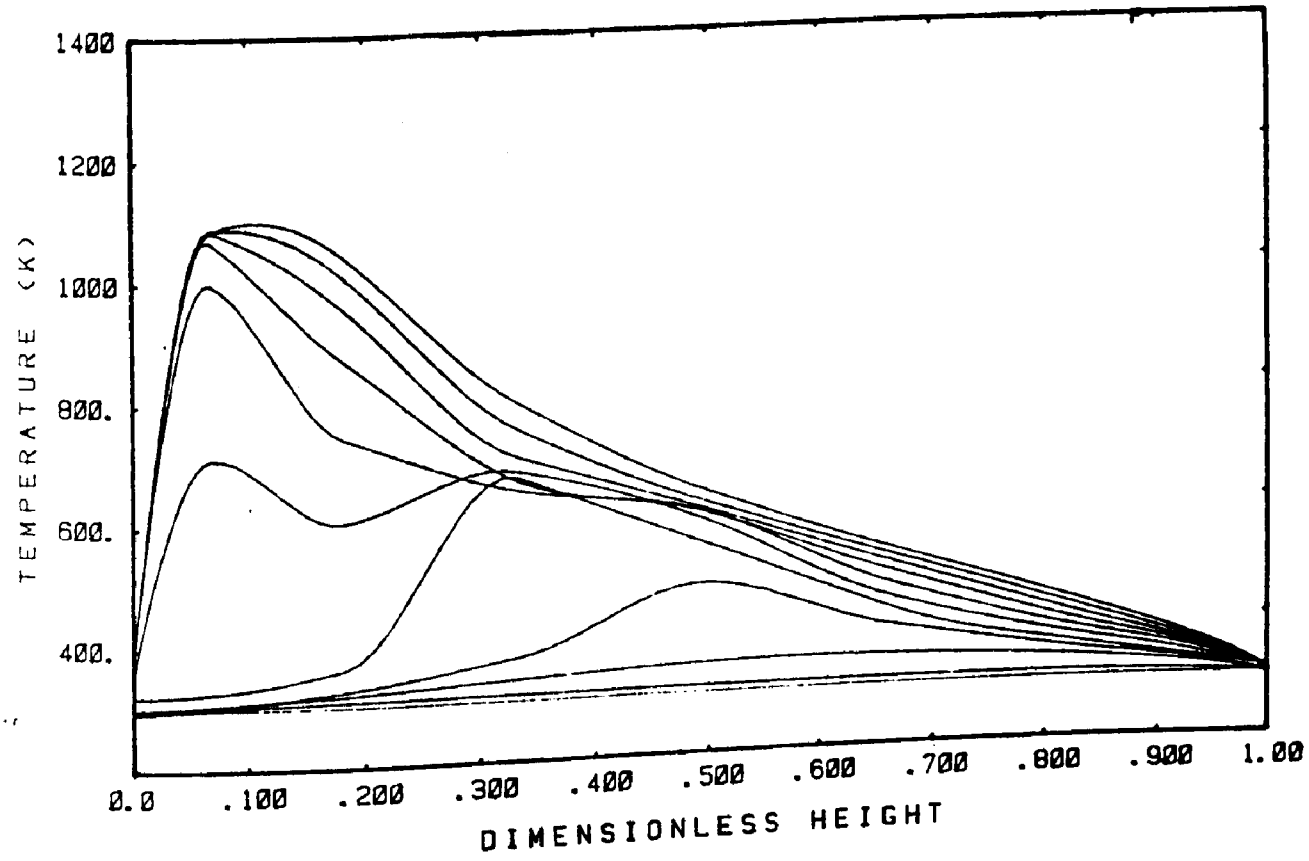
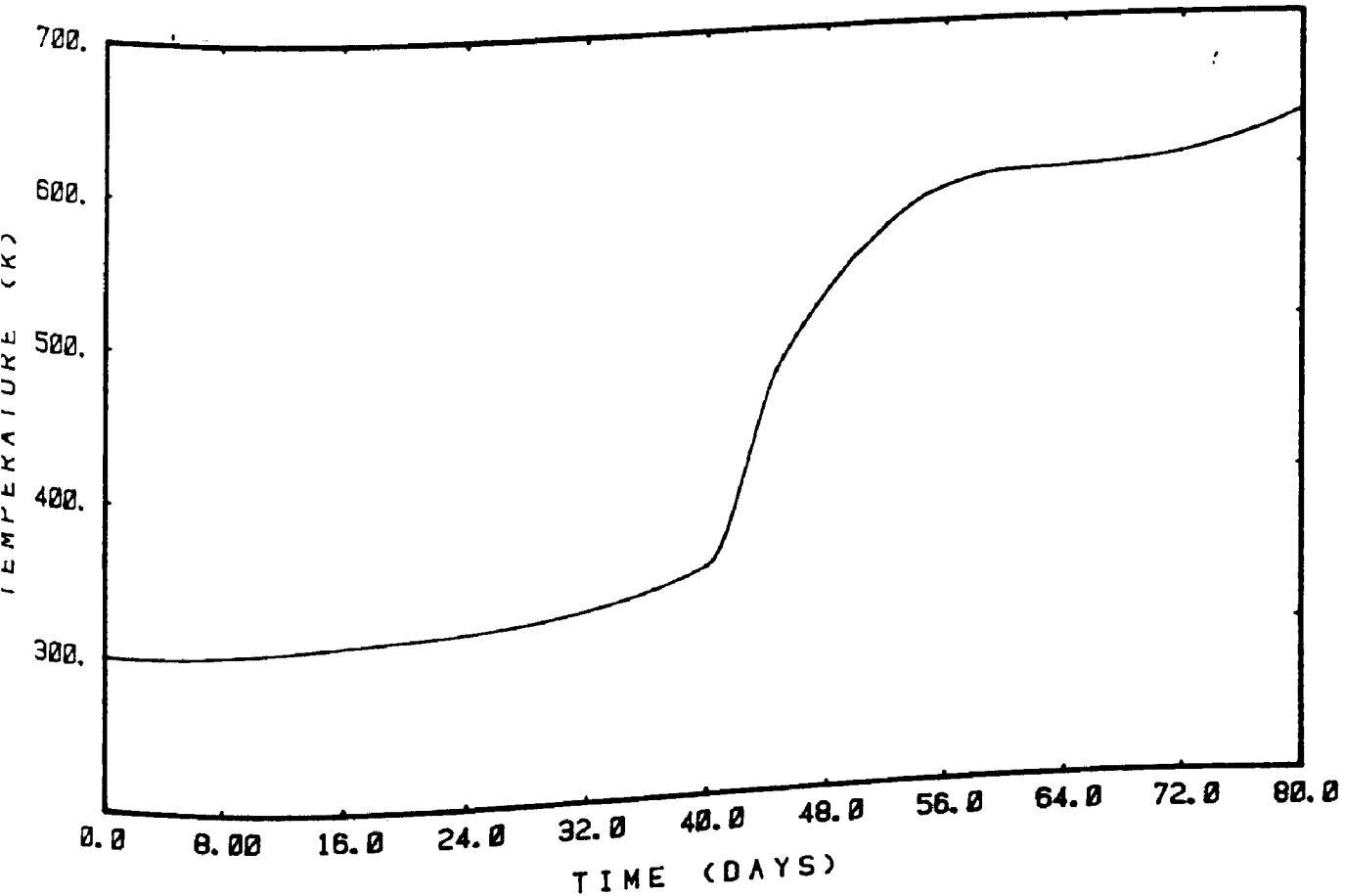


Figure 8.16 Temperature profiles with ignition
Particle size 2 mm - 5 m/s wind - Numerical method
First three curves 20 days apart
Subsequent curves 5 days apart



8.16 a 5 m/s wind has been assumed to blow constantly. It would be expected that the finer, more reactive coal would combust in a shorter time provided is is supplied with enough oxygen, as is the case here with the wind blowing.

8.6 Conclusions

The results presented in this chapter represent the results of solving the model equations for various values of the model parameters. It is felt that the parameters used are realistic, and therefore that the results obtained can be regarded as at the worst semi-quantitative.

The results of solving the equations for both the steady and unsteady-states have been presented. The results are consistent with practical experience. It has been shown that the assumption of a constant rate constant is a good one for beds in which the temperature remains less than approximately 350 K. The results of solving the unsteady-state equations numerically show that the model can predict the onset of spontaneous combustion, although numerical difficulties occur when the temperature gradients become large.

9. CONCLUSIONS

The important physical processes occuring in coal dumps have been identified and modelled. They are:

a. The ingress of reactants into the dump

b. The reaction between these reactants and coal

c. Heat transfer in the coal dump

It has been shown that natural convection and wind pressure are the most imprtant mechanisms whereby reactants are transported into a coal dump, with molecular diffusion only being of importance for fine material.

A shrinking-core model for the oxidation of coal at low temperatures has been proposed. This model explains the well known but little understood fact that the reactivity of the coal falls off with time.

It has been shown that heat transfer in a coal dump may be modelled using an effective thermal conductivity; the effective thermal conductivity of a typical coal bed has been measured.

All these effects have been incorporated into a one-dimensional model, with the aim of studying their combined effect on spontaneous combustion of coal. The model has been shown to have the correct characteristics in the prediction of the onset of spontaneous combustion. The model equations exhibit multiple solutions for certain values of the model parameters; it is concluded that stockpiles may be classified as safe, unsafe or conditionally safe.

Safe coal dumps have been shown to be either oxygen limited or heat transfer limited. In both cases the dump is safe because the sensible heat of reaction can be dissipated at temperatures near ambient. For oxygen limited beds the high reactivity of the coal toward oxygen causes oxygen to be consumed and thus the sensible heat to be produced close to the surface of the dump, where it is easily dissipated. For heat transfer limited beds, oxygen is readily available throughout the bed, but the reactivi-

ty per unit bed volume of the coal is sufficiently low that the sensible heat of reaction may be dissipated even from deep within the dump at near ambient temperatures.

The important parameters that must be known in order to make qualitative predictions about the safety of coal dumps have been shown to be:

a. The particle size distribution of the coal.

b. The voidage of the bed.

c. The pre-exponential factor and activation energy for the oxidation of the coal.

The model presented here may be used to qualitatively determine the effect of changing certain parameters which are under the control of the persons responsible for coal plant operation and particular dumping practise. In particular the effects of particle size distribution and compaction have been clearly pointed out. Compaction makes oxygen limited dumps safer, but appears to be ineffective in improving the safety of heat transfer limited dumps.

The efect of particle size distribution on the safety of dumps may be summarized as follows:

If the dump is oxygen limited adding fines may help make the dump safer, both by reducing the voidage and increasing the rate of oxygen depletion. If the dump is heat transfer limited then removing fine material may help make it safer.

An important practical implication of this work is that there is a dump size for an oxygen limited coal dump, above which the dump is effectively no more liable to spontaneous combustion. For very reactive coals this is a comforting result, since it implies that very reactive coals may be safely stockpiled on very large dumps, with obvious economic advantages. Caution must be exercised to ensure that the dump is oxygen limited, and that the oxygen levels below a certain depth remain negligible. At this stage the quantification of what this depth is, is not possible, but it appears from practical experience that 2 metres is a sensible upper limit on the depth at which the percentage oxygen in a safe

coal dump should be negligible.

Safe stockpiling times are not available from the model, and there is reason to believe that the concept of a safe stockpiling time can be misleading. It has been shown, both in practise and from the model, that a slow rise in temperature may suddenly become a rapid rise in temperature. The critical temperature appears to be in the region of 60 to 100 ^{o}C. The time taken to reach this critical temperature might be a better way of arriving at a safe stockpiling time.

The concepts presented in this thesis may also help to answer questions about stockpiling practise. In particular the following points are of practical importance:

Segregated coal dumps i.e. dumps in which particle size segregation occurs due to stacking methods employed, are potentially dangerous. It can clearly be seen from the results presented in this thesis that such dumps are dangerous because air can penetrate the dump through the coarse material, and react deep in the dump with finer material, that is inherently more reactive, thus leading to a temperature rise deep within the dump where the energy cannot easily be dissipated.

Covering dumps of coal has been suggested as a means of preventing spontaneous combustion. Broadly speaking a dump may be covered with either an inert or reactive material. An inert covering may be permeable or impermeable. In the case of an inert permeable covering such as sand, the fact that there is a balance between oxygen ingress and heat loss must always be borne in mind. Enough sand must be put down to substantially reduce the amount of oxygen ingress, recognising that the dump is being insulated at the same time. If an attempt is made to cover the dump with an impermeable layer of a material such as tar, it must be recognized that cracks in the covering may lead to large localized flows of oxygen into the dump, possibly giving rise to a hot spot.

Schmidt (1945) states that covering a coal dump with a layer of very fine coal and then with a layer of coarser coal provides an efficient coating. The coarse coal is packed on top of the fine coal to prevent wind and water erosion. In the light of the results presented in this chapter, this is an eminently

reasonable suggestion provided all the oxygen can be removed close to the surface.

In the case of dumps that are safe due to the fact that they are oxygen limited, the danger exists that with time the outer layer of coal will become unreactive due to the ageing effect, and that oxygen will penetrate deeper into the dump where any reaction that occurs may lead to a dangerous temperature rise. One of the practical conclusions that arises out of this analysis is that analysing for oxygen at various depths in a coal dump is an excellent way of monitoring the dump. It has been found in practise that in oxygen limited type of dump, the gas in the dump will contain virtually no oxygen at a depth of 2m. It has therefore been suggested that should appreciable oxygen be found at this depth an attempt be made to recompact the dump. Should this fail to rectify the situation the next logical step is the laying down of fresh coal on the dump. This would have the effect of limiting the amount of oxygen that is able to penetrate to appreciable depths. In the light of the model presented here, these suggestions seem sensible as well as practical.

A limitation of the model presented here is the inability at this stage to easily translate the size of a coal dump to the parameter of bed length used in the model. It can be demonstrated that there is a worst depth associated with natural convection, and a worst path length associated with wind driven flows. However at this stage it has not been possible to calculate these distances. A full three- dimensional analysis of the situation could give an idea of the magnitude of these distances; these could then be used in the simpler one-dimensional model for predictive purposes.

The omission of moisture effects in the model is simply rectified as has been demonstrated by Murtagh (1966). It must be borne in mind that in addition to the heat transfer mechanism of condensation and vaporization, moisture appears to exert a catalytic effect on the oxidation reaction. Schmidt (1945) discusses moisture effects in some detail; the ommision of these effects in the model presented here is mainly due to lack of data. There is thus scope for further work in determining the effects of both atmospheric and coal moisture content on the rate of oxidation.

One of the main areas of uncertainty in the field of spontaneous combustion of coal is the functional relationship between rates of oxidation and coal particle size. Much conflicting data has been published in ths regard (Schmidt, 1945, Sondreal & Ellman, 1974). It is felt that there is much need for further study in this regard.

APPENDIX 1 DERIVATION OF A RATE EQUATION FOR THE LOW TEMPERATURE OXIDATION OF COAL

The reaction mechanism considered here is one of diffusion of O_2 through an inert layer of oxycoal followed by reaction between the O_2 and the coal. No reaction products are formed and reaction at the reaction zone is considered to first order with respect to the O_2 concentration

In order to account for the fact that coal has both internal and external surface, the simplification is made that this surface area S′ may be considered to behave as if it was all external i.e. pore diffusion is neglected. This is a good assumption provided the particle size is not too large, as has been mentioned by Gijbels & Bruining (1982).

The coal particle is thus considered to have the geometry shown in Figure A1.1.

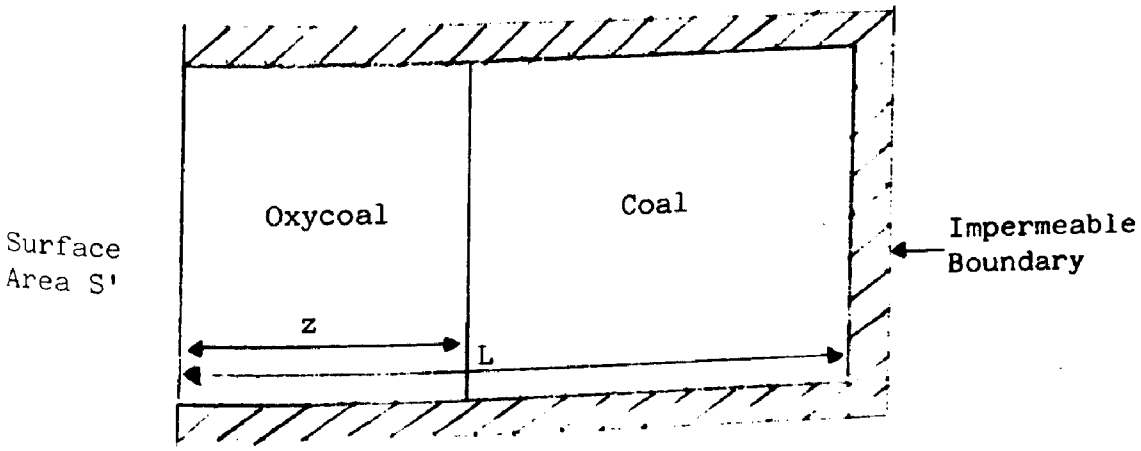


Figure A1.1 Simplified coal particle geometry

A particle length L is defined such that

$$S'L = V_p \qquad \text{A1.1}$$

where V_p = particle volume

At a time when the oxycoal layer has a thickness x the following equations may be written:

$$\text{Rate of diffuson of } O_2 \text{ through oxycoal} = S'D_e\,(C-C_s)/x \qquad \text{A1.2}$$

Rate of reaction of O_2 at reaction front = $S' k_s C_s$ A1.3

where D_e = effective diffusivity of oxycoal layer
C = free stream oxygen concentration
C_s = oxygen concentration at reaction boundary
k_r = surface rate constant

Under the pseudo steady state assumption that there is no accumulation of O_2 in the oxycoal these two rates must be equal i.e.

$$D_e (C - C_s)/x = k_r C_s \qquad \text{A1.4}$$

and solving for C_s gives

$$C_s = \frac{C}{1 + k_r x/D_e} \qquad \text{A1.5}$$

Back substitution in equation A1.2 gives

Rate of adsorption of O_2 by one particle $= \dfrac{S' k_r c}{1 + k_r x/D_e}$ A1.6

Now in a time Δt let the reaction front move a distance Δx.

Volume of coal reacted $= S' \Delta x$ A1.7

Moles of coal reacted $= \rho_m S' \Delta x$ A1.8

where ρ_m = molar density of reactive unit.

However the moles of coal reacted must equal the rate of adsorption times the time interval i.e.

$$\rho_m S' \Delta x = \frac{k_r C S' \Delta t}{1 + k_r x/D_e} \qquad \text{A1.9}$$

letting Δt, Δx tend to zero gives

$$\rho_m \frac{dx}{dt} = \frac{k_r C}{1 + k_r x/D_e} \qquad \text{A1.10}$$

In order to write the equations in terms of fractional

conversion of the coal, rather than the thickness of the oxycoal layer, it is noted that the volume of reacted material is S′x and the total volume is S′L.

Therefore the fractional conversion X is $S'x/(S'L) = x/L$

However L as defined by equation A1.1 is equal to V_p/S'.

Therefore $L = V_p/S' = 1/S_t$ A1.11

where S_t is now the total particle surface area per unit volume of particle.

Therefore, fractional conversion $X = xS_t$ A1.12

and substituting in equation A1.10 gives

Rate of adsorption of O_2 by one particle $= \dfrac{S_t\ V_p\ k_r\ C}{1 + k_r\ X/(S_t\ D_e)}$ A1.13

$$\rho_m\ S'\ \frac{dX}{dt} = \frac{k_r\ C\ S_t}{1 + k_r\ X/(S_t\ D_e)} \qquad \text{A1.14}$$

The rate that is required is however the rate per unit bed volume.

Rate / unit bed volume = Rate per particle x $\dfrac{\text{no of particles}}{\text{unit bed volume}}$

A volume V of the bed contains a volume $V(1-\epsilon)$ of coal where ϵ is the bed voidage.

The number of particles in the volume is therefore

$$V(1 - \epsilon)/V_p$$

and the number of particles per unit volume is

$$(1 - \epsilon)/V_p$$

Therefore the rate per unit bed volume is

$$r = \frac{S_t\, k_r\, C\, (1-\epsilon)}{1 + k_r\, X/(S_t\, D_e)} \qquad \text{A1.15}$$

APPENDIX 2 TABULATION OF MEASURED THERMAL CONDUCTIVITIES

A2.1 Details of Coal Used

Particle size range: -6.32 + 3.4 mm

Mass of coal: 67 Kg

Density of coal (measured): 1.36 g/cm^3

Volume of apparatus: .08 m^3

Voidage of bed: 0.38

A2.2 Measured Values

The values measured during 1982 are given in Table A2.1.

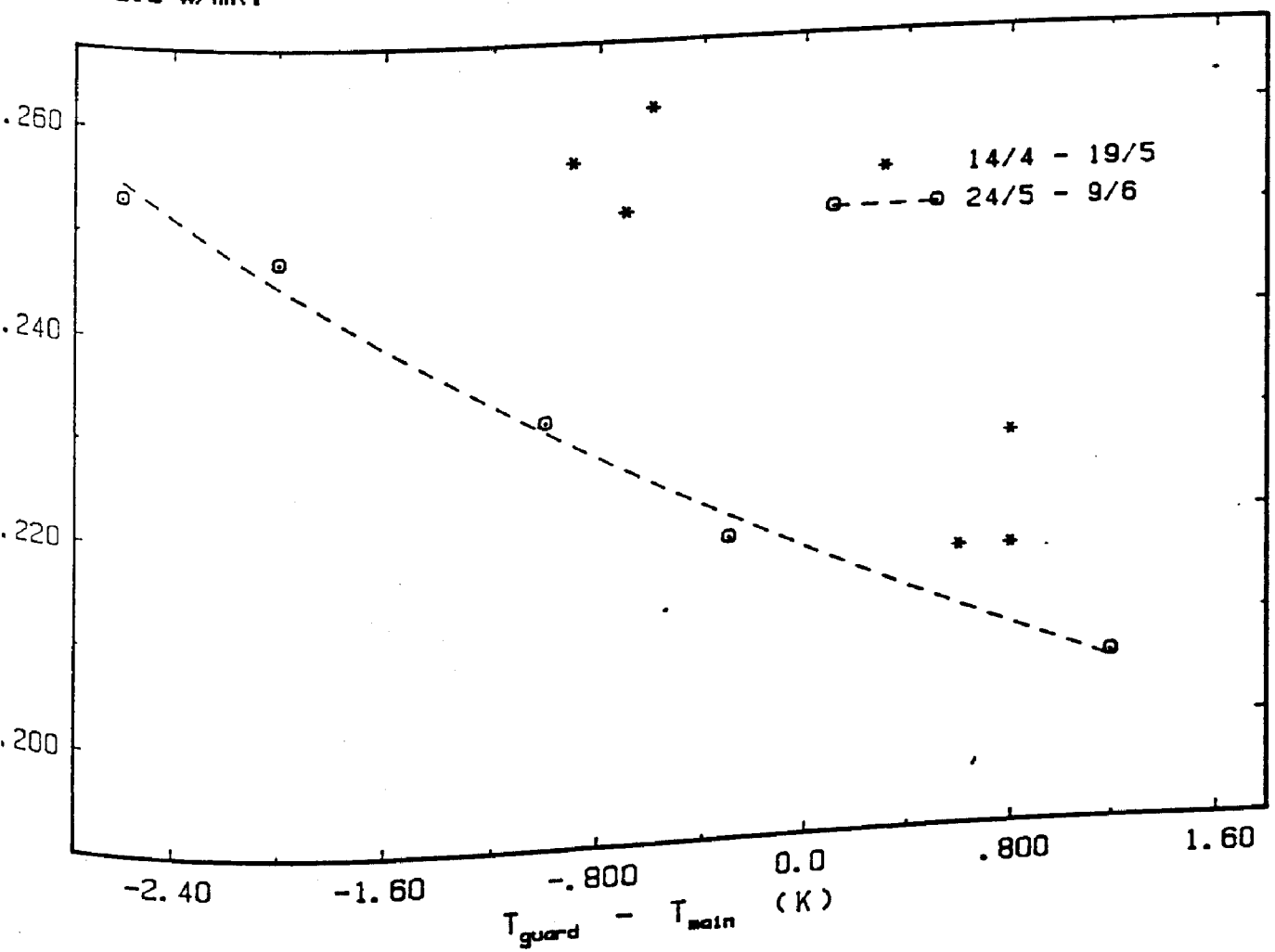
TABLE A2.1 MEASURED THERMAL CONDUCTIVITIES

DATE	MAIN TEMP(^{o}C)	GUARD TEMP(^{o}C)	MAIN VOLTAGE(V)	MAIN CURRENT(mA)	WATER TEMP(^{o}C)	k_b(W/mK)
14/4	67.8	68.6	11.66	139.8	23.0	0.217
16/4	68.7	69.5	11.66	139.8	24.0	0.228
6/5	57.8	58.4	11.64	139.5	24.0	0.286
10/5	62.2	61.6	11.64	139.7	25.0	0.261
18/5	60.2	59.5	11.69	140.2	22.0	0.251
19/5	60.0	59.1	11.69	140.2	22.5	0.256
24/5	98.2	95.6	16.46	196.7	23.0	0.253
27/5	99.7	97.7	16.45	196.7	23.0	0.247
28/5	104.9	103.9	16.46	196.6	23.0	0.231
4/6	109.2	108.9	16.45	196.4	23.0	0.219
9/6	114.8	116.0	16.45	196.5	23.0	0.206
25/6	86.8	88.6	13.94	166.6	23.0	0.213
23/7	91.3	91.1	14.00	167.2	23.0	0.201

The thermal conductivities measured between 14/4 and 9/6 are graphed against the temperature difference between the main and guard heaters on Figure A2.1. The reason for this choice

of plot is that in theory the guarded hot ring apparatus should be operated with the guard ring and main heater temperatures equal. Since this is impossible to achieve in practice, and since the calculated thermal conductivity is sensitive to differences between the main and guard heater temperatures, some form of interpolation must be used in calculating the thermal conductivty for the case of equal guard and main heater temperatures.

In figure A2.1 the data is plotted for the two different power inputs used. As can be seen, the data for the period 14/4 to 19/5, at the lower power input, shows considerable scatter. This could be due to a number of factors including failure to allow the apparatus to come to steady-state, as well as the variations in the cooling water temperature which are evident from Table A2.1. Due to the scatter in the data no attempt has been made to interpolate to $T_{guard} = T_{main}$. The data for the period 24/5 - 9/6 shows far more consistency. A quadratic least squares curve fits this data well, as can be seen from the graph. The interpolated value for $T_{guard} = T_{main}$ is 0.216 W/mK. The value obtained by linear interpolation between the values measured on 25/6 and 23/7 (which are not shown on the graph) is 0.202 W/mK.



APPENDIX 3 DERIVATION OF MODEL EQUATIONS

A3.1 Mass Balances

A3.1.1 Gas Phase Mass Balances

Consider the element of a bed of coal shown in Figure A3.1. The element has cross sectional area A and height Δx. The volume of gas in the element is $A \Delta x \epsilon$. The molar flowrate per unit area of the gas through the voids is G .

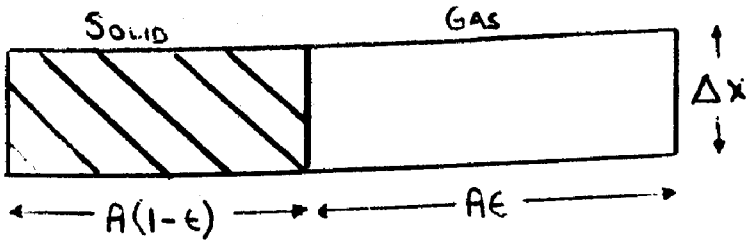


Figure A3.1 Differential element of a coal bed

The mass balance for component i in the gas phase is:

$$(\text{Moles of i in gas})\big|_{t+\Delta t} - (\text{Moles of i in gas})\big|_{t}$$

$$= (\text{Moles in})\big|_{x} - (\text{Moles in})\big|_{x+\Delta x} + \text{Moles produced in time } \Delta t$$

or

$$\left(\frac{P \epsilon}{R T_g} A \Delta x \, y_i\right)\Big|_{t+\Delta t} - \left(\frac{P \epsilon}{R T_g} A \Delta x \, y_i\right)\Big|_{t}$$

$$= (A G y_i \Delta t)\big|_{x} - (A G y_i \Delta t)\big|_{x+\Delta x} + r_i A \Delta x \Delta t$$

where
- G = molar flowrate per unit area
- y_i = mole fraction of i in the gas phase
- x = distance along bed
- P = pressure
- R = gas constant
- ϵ = bed voidage
- T_g = gas temperature
- t = time
- r_i = rate of formation of i per unit bed volume

Dividing by A Δx Δt and letting Δx and Δt tend to zero gives:

$$\frac{\partial}{\partial t}\left(\frac{P \epsilon}{R T_g} y_i\right) + \frac{\partial}{\partial x}(G y_i) = r_i \qquad \text{A3.1.1}$$

Equation A3.1.1 may be summed over all i to give:

$$\frac{\partial G}{\partial x} + \frac{\epsilon}{R} \frac{\partial}{\partial t} \frac{P}{T_g} = \sum_{i=1}^{N} r_i \qquad \text{A3.1.2}$$

where N = number of components in gas phase

Substitution of equation A3.1.1 in A3.1.2 gives:

$$G \frac{\partial y_i}{\partial x} + \frac{P \epsilon}{R T_g} \frac{\partial y_i}{\partial t} = r_i - y_i \sum_{j=1}^{N} r_j \qquad (i = 1 \text{ to } N) \qquad \text{A3.1.3}$$

A3.2 Solid Phase Mass Balances

Let the mass fraction of component j in the solid phase be f_j, and the rate of formation of j per bed volume be p_j.

The mass balance for the solid phase is:

Increase of mass of j in time Δt
= rate of formation of j x bed volume x Δt

or: $(A \Delta x \rho (1-\epsilon) f_j)_{t+\Delta t} - (A \Delta x \rho (1-\epsilon) f_j)_t = p_j \Delta t A \Delta x$

Dividing by A Δx Δt and letting Δt tend to zero gives:

$$(1-\epsilon) \frac{\partial (\rho f_j)}{\partial t} = p_j \qquad (j = 1 \text{ to } M) \qquad \text{A3.1.4}$$

ρ = density of solid
f_j = mass fraction of j in the solid
p_j = rate of formation of j in the solid
M = number of components in solid phase

where it has been assumed that the voidage of the bed does not change with time.

Summing over all j gives:

$$(1-\epsilon)\frac{\partial \rho}{\partial t} = \sum_{j=1}^{M} p_j \qquad \text{A3.1.5}$$

A3.2 Energy Balances

The general energy balance used in this section is:

Rate of change of internal energy of the volume =

Internal energy in - Internal energy out +

energy transferred thermally + energy transferred mechanically

In the derivations that follow changes in kinetic and potential energy have been neglected.

A3.2.1 Gas Phase Energy Balance

Application of the above formula to the gas in the volume shown in Figure A3.1 gives:

$\frac{\partial U_g}{\partial t}$ Rate of change of internal energy

$= (A\ \epsilon\ q_g)_{/x} - (A\ \epsilon\ q_g)_{/x+\Delta x}$ conduction/radiation

$+ (A\ G\ \hat{H})_{/x} - (A\ G\ \hat{H})_{/x+\Delta x}$ flow

$+ A\ \Delta x \sum_{i=1}^{N} r_i\ \hat{H}_i$ Reaction

$+ Q_c\ A\ \Delta x$ Convection from solid to gas

where U_g = Internal energy of gas in volume

q_g = flux due to conduction and radiation in gas

$\hat{H}$ = molar enthalpy of flowing gas

$\hat{H}_i$ = molar enthalpy of gas leaving or entering by reaction

Q_c = rate of convection from gas to solid

It should be noted that the flow and reaction terms involve enthalpies and not internal energies. This is because the process is to all intents and purposes constant pressure and reversible, and therefore the mechanical work term may be combined with the flow and reaction terms which then may be written as enthalpies.

Now:

$$U_g = A\,\Delta x\,\epsilon\,\rho_g\,\hat{U} = A\,\Delta x\,\epsilon\,P\,\hat{U}/(R\,T_g)$$

where the ideal gas law

$$\rho_g = P/(R\,T_g)$$

has been used.

Substituting this in the above energy balance, dividing by $A\,\Delta x$ and letting Δx tend to zero gives:

$$\epsilon\,\frac{\partial}{\partial t}\,\frac{P\,\hat{U}}{R\,T_g} = -\,\epsilon\,\frac{\partial q_g}{\partial x} - \frac{\partial}{\partial x}\,(G\,\hat{H}) + \sum_{i=1}^{N} r_i\,\hat{H}_i + Q_c \qquad \text{A3.2.1}$$

But

$$\hat{U} = \hat{H} - R\,T_g$$

since the ideal gas assumption has been made. Substituting this in Equation A3.2.1 gives:

$$\epsilon\,\frac{\partial}{\partial t}\,\frac{P\,\hat{H}}{R\,T_g} - \epsilon\,\frac{\partial P}{\partial x} = -\,\epsilon\,\frac{\partial q_g}{\partial x} - \frac{\partial}{\partial x}\,(G\,\hat{H}) + \sum_{i=1}^{N} r_i\,\hat{H}_i + Q_c \qquad \text{A3.2.2}$$

For an ideal gas

$$\hat{H} = \sum_{i=1}^{N} y_i\,\hat{H}_i$$

and

$$d\hat{H} = \sum_{i=1}^{N} (y_i\,d\hat{H}_i + \hat{H}_i\,dy_i)$$

Therefore

$$\epsilon \frac{\partial}{\partial t}\frac{P\hat{H}}{R T_g} + \frac{\partial}{\partial x}(G\hat{H}) = \frac{\epsilon P}{R T_g}\frac{\partial \hat{H}}{\partial t} + G\frac{\partial \hat{H}}{\partial x} + \epsilon \hat{H}\frac{\partial}{\partial t}\frac{P}{R T_g} + \hat{H}\frac{\partial G}{\partial x}$$

$$= \frac{P\epsilon}{R T_g}\sum_{i=1}^{N}\left(y_i\frac{\partial \hat{H}_i}{\partial t} + \hat{H}_i\frac{\partial y_i}{\partial t}\right) + G\sum_{i=1}^{N}\left(y_i\frac{\partial \hat{H}_i}{\partial x} + \hat{H}_i\frac{\partial y_i}{\partial x}\right) + \hat{H}\left(\epsilon\frac{\partial}{\partial t}\frac{P}{R T_g} + \frac{\partial G}{\partial x}\right)$$

Combining terms and using the gas phase mass balance (equation A3.1.3) the right hand side of the above equation may be written as

$$\sum_{i=1}^{N}\left(\hat{H}_i\left(r_i - y_i\sum_{j=1}^{N} r_j\right)\right) + \frac{P\epsilon}{R T_g}\sum_{i=1}^{N}\left(y_i\frac{\partial \hat{H}_i}{\partial T}\frac{\partial T}{\partial t}\right)$$

$$+ G\sum_{i=1}^{N}\left(y_i\frac{\partial \hat{H}_i}{\partial T}\frac{\partial T}{\partial t}\right) + \hat{H}\sum_{i=1}^{N} r_i$$

For an ideal gas $\frac{\partial \hat{H}_i}{\partial T} = \hat{c}_i$ by definition

and $$\sum_{i=1}^{N} y_i\,\hat{c}_i = \hat{c}$$

Substituting in the above expression gives:

$$RHS = \sum_{j=1}^{N}\hat{H}_i\,r_i + \frac{P\epsilon}{RT_g}\hat{c}\frac{\partial T_g}{\partial t} + G\,\hat{c}\frac{\partial T_g}{\partial x}$$

Finally, back substitution in A3.2.2 gives the gas phase energy balance:

$$\frac{P\epsilon}{RT_g}\hat{c}\frac{\partial T_g}{\partial t} - \epsilon\frac{\partial P}{\partial t} = -G\,\hat{c}\frac{\partial T_g}{\partial x} + \epsilon k_g\frac{\partial^2 T_g}{\partial x^2} + Q_c$$

where use has been made of Fourier's law in writing

$$\frac{\partial q_g}{\partial x} = -k_g\frac{\partial^2 T_g}{\partial x^2}$$

A3.2.2 Solid Phase Energy Balance

The approach taken is to write an energy balance for the whole system, and then to subtract the gas phase energy balance to leave the solid phase energy balance.

Thus, using equation A3.2.1

$$(U_s + U_g)/_{t+\Delta t} - (U_s + U_g)/_t$$

$$= [A\epsilon q^g_{cr}/_x - A\epsilon q^g_{cr}/_{x+\Delta x}]\Delta t \qquad \text{(Conduction and radiation in gas)}$$

$$+ [A(1-\epsilon)q^s_c/_x - A(1-\epsilon)q^s_c/_{x+\Delta x}]\Delta t \qquad \text{(Conduction in solid)}$$

$$+ [A\hat{G}\hat{H}/_x - A\hat{G}\hat{H}/_{x+\Delta x}]\Delta t \qquad \text{(Bulk Flow)} \quad \text{A3.2.6}$$

Note that there are no reaction or convection terms since these terms are associated with transport between the phases.

Subtracting the appropriate gas-phase energy balance leaves:

$$U_s/_{t+\Delta t} - U_s/_t$$

$$= [A(1-\epsilon)q^s_c/_x - A(1-\epsilon)q^s_c/_{x+\Delta x}]\Delta t$$

$$- Q_c A\Delta x\Delta t \qquad \text{A3.2.7}$$

Now $U_s = \rho A\Delta x(1-\epsilon)\bar{U}_s$ since $A\Delta x(1-\epsilon)$ is the volume of the solid phase and $\bar{U}_s$ is the specific mass internal energy of the solid.

Substituting this in equation A3.2.7, dividing by $A\Delta x\Delta t$ and letting Δx and Δt tend to zero gives:

$$\frac{\partial}{\partial t}(\rho\bar{U}_s) = -(1-\epsilon)\frac{\partial q^s_c}{\partial x} - Q_c \qquad \text{A3.2.8}$$

Now

$$\bar{U}_s = \bar{H}_s - \frac{P}{\rho} \qquad \text{A3.2.9}$$

Therefore

$$\frac{\partial}{\partial t}(\rho\bar{U_s}) = \frac{\partial}{\partial t}(\rho\bar{H_s}) - \frac{\partial P}{\partial t} \qquad \text{A3.2.10}$$

$$= \bar{H}_s\frac{\partial\rho}{\partial t} + \rho\frac{\partial\bar{H}}{\partial t}s - \frac{\partial P}{\partial t} \qquad \text{A3.2.11}$$

Assuming $\bar{H}_s$ may be written as the sum of pure component enthalpies ie:

$$\bar{H}_s = \sum_{j=1}^{N} f_j\bar{H}_j \qquad \text{A3.2.12}$$

Therefore

$$\frac{\partial\bar{H}}{\partial t}s = \sum_{j=1}^{N}\frac{\partial}{\partial t}(f_j\bar{H}_j) = \sum_{j=1}^{N}(\bar{H}_j\frac{\partial f}{\partial t}j + f_j\frac{\partial\bar{H}}{\partial t}j) \qquad \text{A3.2.13}$$

Now, using equation A3.2.13 and the solid phase mass balance A3.1.5 it may be shown that:

$$(1-\epsilon)\frac{\partial}{\partial t}(\rho\bar{H}_s) = \sum_{j=1}^{N}\bar{H}_j\rho_j + (1-\epsilon)\rho\sum_{j=1}^{N}f_j\frac{\partial\bar{H}}{\partial t}j \qquad \text{A3.2.14}$$

Now

$$\frac{\partial\bar{H}}{\partial t}j = \left(\frac{\partial\bar{H}}{\partial T}j\right)_p\frac{\partial T}{\partial t}s + \left(\frac{\partial\bar{H}}{\partial P}j\right)_{T_s}\frac{\partial P}{\partial t} \qquad \text{A3.2.15}$$

$$= \bar{c}_j\frac{\partial T}{\partial t}s + \left(\frac{\partial H}{\partial P}j\right)_{T_s}\frac{\partial P}{\partial t} \qquad \text{A3.2.16}$$

Therefore

$$\sum_{j=1}^{N}f_j\frac{\partial\bar{H}}{\partial t}j = \sum_{j=1}^{N}\left(f_j\bar{c}_j\frac{\partial T}{\partial t}s + f_j\left(\frac{\partial\bar{H}}{\partial t}j\right)_{T_s}\frac{\partial P}{\partial t}\right) \qquad \text{A3.2.17}$$

$$= \bar{c}_s\frac{\partial T}{\partial t}s + \frac{\partial P}{\partial t}\sum_{j=1}^{N}f_j\left(\frac{\partial\bar{H}}{\partial P}j\right)_{T_s} \qquad \text{A3.2.18}$$

At this point the assumption is made that the solid enthalpy is not a function of pressure. Thus the last term of equation

A3.2.18 can be dropped. Substitution of the above results in equation A3.2.18 yields:

$$(1-\epsilon)\rho_s \bar{c}_s \frac{\partial T_s}{\partial t} - (1-\epsilon)\frac{\partial P}{\partial t} = (1-\epsilon)\frac{\partial q^s_c}{\partial x} - Q_c - \sum_{j=1}^{N} p_j H_j$$

Finally, use is made of Fourier's Law in writing

$$\frac{\partial q^s_c}{\partial x} = \eta k_s \frac{\partial^2 T_s}{\partial x^2}$$

where η is a tortuosity factor allowing for the fact that the conduction in the solid does not occur in a straight line.

A3.3 Momentum Balance

The equation of motion for the one-dimensional flow of a Newtonian fluid is given by Bird, Stewart & Lightfoot (1960) to be:

$$\rho \frac{\partial U}{\partial t} = -\rho U \frac{\partial U}{\partial x} + \mu \frac{\partial^2 U}{\partial x^2} - \rho g - \frac{\partial P}{\partial x} \qquad \text{A3.3.1}$$

Bird et al (1960) state that for flow through packed beds the steady-state equation of motion may be simplified to:

$$0 = -fU - \rho g - \frac{\partial P}{\partial x} \qquad \text{A3.3.2}$$

This implies that the unsteady-state equation of motion in the case of a packed bed is:

$$\rho \frac{\partial U}{\partial t} = -fU - \rho g - \frac{\partial P}{\partial x} \qquad \text{A3.3.3}$$

The equation of motion for the air far from the bed is:

$$0 = -\rho_\infty g - \frac{\partial P_\infty}{\partial x} \qquad \text{A3.3.4}$$

Subtracting A3.3.4 from A3.3.3 gives:

$$\rho \frac{\partial U}{\partial t} = -fU + g(\rho_\infty - \rho) - \frac{\partial}{\partial x}(P - P_\infty) \qquad \text{A3.3.5}$$

If the gas is assumed to behave ideally, and its molecular weight is constant then

$$\frac{\rho}{\rho_\infty} = \frac{T_\infty}{T}$$

Substituting this in equation A3.3.5 gives, for the steady-state:

$$\frac{\partial}{\partial x}(P-P_\infty) = -fU + g\,\rho_\infty\left(1 - \frac{T}{T_\infty}\right) \qquad 2.2.1$$

APPENDIX 4 THE CONTINUUM AND PSEUDO STEADY-STATE ASSUMPTIONS

The continuum assumption for a packed bed may be made when the solid and gas temperatures are not very different. In this case equations 5.4.5 and 5.6.4 may be added to give equation 6.1.1.

Edwards (1983) has discussed the conditions under which the particle and gas temperatures tend to equilibrate, and has shown that this will occur within a time τ_d given by:

$$\tau_d = \frac{\rho_s \, C_s \, D_p^2}{4 \, k_s} \qquad \text{A4.1}$$

This author's calculations indicate that the particle surface and air temperatures are nearly in equlibrium. This can be understood if τ_d is evaluated for the following values:

$$\rho_s = 1200 \text{ kg/m}^3$$
$$C_s = 1000 \text{ J/kg/K}$$
$$k_s = 0.4 \text{ W/m/K}$$

Then $\tau_d = 750 \times 10^3 \, D_p^2$

For $D_p = 1$ mm $\qquad \tau_d = 750 \times 10^{-3}$ s

For $D_p = 20$ mm $\qquad \tau_d = 300$ s

Both of these times are small in comparison to the residence time of the gas in the bed, and therefore thermal equilibrium between gas and solid should be reached.

The pseudo-steady state assumption may be made when the time constant for one process is very much larger than the time constant for the other process. In the case of a coal bed the time constant for conduction is given by

$$\tau_c = \frac{4L^2 \, \rho_b \, C_b}{\pi^2 \, k_b} = \frac{4 \, L^2}{\pi^2 \, \kappa}$$

Using a typical value for κ of 8×10^{-4} m^2/hr gives

$$\tau_c = \frac{4 \, L^2}{\pi^2 \, 8 \times 10^{-4}} = 500 \, L^2 \text{ hours}$$

The time constant for gas flow and gas composition is the residence time of the gas i.e.

$$\tau_f = \frac{L}{U} = \frac{P\,L}{G\,R\,T}$$

Using values from Table 2.1 for D_p = 5 mm gives

$$\tau_f = \frac{8.3 \times 10^3 \times 320 \times 1.3 \times 10^{-4}\,L}{1 \times 10^5} = 0.08\,L \text{ hours}$$

The time constant associated with the momentum balance is

$$\tau_p = \frac{\rho_g L}{f} = \frac{1.173\,L}{2.2 \times 10^3} = 5.3 \times 10^{-4}\,L \text{ seconds}$$

It can be seen that the time constants for gas flow and composition and for pressure changes are very much smaller than that for conduction. Furthermore the time constant for conduction depends on L^2 while the other time constants depend on L. For these reasons the pseudo-steady state assumption on the gas mass balances and the momentum balance is a good one.

APPENDIX 5 THE INCLUSION OF A RADIAL HEAT LOSS TERM IN EQUATION 6.1.4

In order to include radial heat losses in equation 6.1.4, an alternative derivation of the temperature equation is used.

Consider an element in the form of a ring, as shown in Figure A5.1:

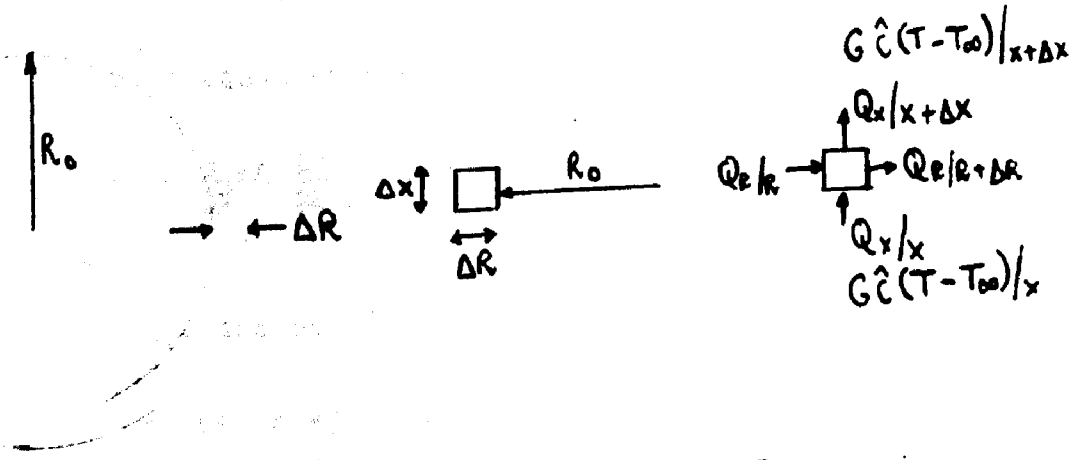


FIGURE A5.1 ELEMENT IN THE FORM OF A RING

The following energy balance may be written:

Rate of accumulation of energy in the volume =

Rate of energy transfer into volume +

Rate of generation in volume -

Rate of energy transfer out of volume

or

$$\rho C_p \frac{\partial}{\partial t}(T\ 2\pi R\ \Delta R\ \Delta x)$$

$$= (Q_R\ 2\pi R\ \Delta x)|_R + (Q_x\ 2\pi R\ \Delta R)|_x + G\hat{c}\ 2\pi R\ \Delta R\ (T-T_\infty)|_x$$

$$+ r_x(-\Delta H_r)\ 2\pi R\ \Delta R\ \Delta x$$

$$- (Q_R\ 2\pi R\ \Delta x)|_{R+\Delta R} - (Q_x\ 2\pi R\ \Delta R)|_{x+\Delta x} - G\hat{c}\ 2\pi R\ \Delta R\ (T-T_\infty)|_{x+\Delta x}$$

Dividing by $\Delta R\ \Delta x$ and letting them tend to zero gives:

$$\rho\ C_p\ 2\pi R\ \frac{\partial T}{\partial t} = -\frac{\partial}{\partial R}(Q_R\ 2\pi R) - \frac{\partial}{\partial x}(Q_x\ 2\pi R) - G\ \hat{c}\ 2\pi R\ \frac{\partial T}{\partial x} + ry(-\Delta H_r)2\pi R$$

Using Fourier's law $\quad Q_R = -k_{b,R}\ \frac{\partial T}{\partial R}$

and $\quad Q_x = -k_{b,x}\ \frac{\partial T}{\partial x}$

Substituting in above equation gives:

$$\rho\ C_p\ 2\pi R\ \frac{\partial T}{\partial t} = 2\pi\ k_{b,R}\ \frac{\partial}{\partial R}(R\ \frac{\partial T}{\partial R}) + 2\pi R\ k_{b,x}\ \frac{\partial^2 T}{\partial^2 x} - G\ \hat{c}\ 2\pi R\ \frac{\partial T}{\partial x} + ry(-\Delta H_r)2\pi R$$

assuming $k_{b,R}$ and $k_{b,x}$ are not functions of R and x respectively.

This equation may now be integrated from 0 to R_o. Assuming that ρ, C_p, G, r and ΔH_r are not functions of R, this gives:

$$\rho\ C_p\ 2\pi\ \frac{\partial}{\partial t}(\int_0^{R_o} T\ R\ dR) = 2\pi\ k_{b,R}\int_0^{R_o}\frac{\partial}{\partial R}(R\ \frac{\partial T}{\partial R})\ dR + 2\pi\ k_{b,x}\ \frac{\partial^2}{\partial x^2}(\int_0^{R_o} T\ R\ dR)$$

$$- G\ \hat{c}\ 2\pi\ \frac{\partial}{\partial x}(\int_0^{R_o} T\ R\ dR) + ry(-\Delta H_r)2\pi(\int_0^{R_o} R\ dR)$$

Defining $T' = \frac{2}{R_o^2}\int_0^{R_o} T\ R\ dR$ and substituting gives

$$\rho\ C_p\ \pi\ R_o^2\ \frac{\partial T'}{\partial t} = 2\pi\ k_{b,R}\ \ R\ \frac{\partial T}{\partial R}\Big]_{R=R_o} + \pi\ R_o^2\ k_{b,x}\ \frac{\partial^2 T'}{\partial x^2}$$

$$- G\ \hat{c}\ \pi\ R_o^2\ \frac{\partial T'}{\partial x} + ry(-\Delta H_r)\ \pi\ R_o^2$$

The radial boundary conditions is:

$$k_{b,R}\ \frac{\partial T}{\partial R} = -h_R\ (T(R=R_o)-T_\infty)$$

Substituting this in the above equation gives:

$$\rho C_p \pi R_o^2 \frac{\partial T'}{\partial t} = -2\pi R_o h_R (T(R=R_o)-T_\infty) + \pi R_o^2 k_{b,x} \frac{\partial^2 T'}{\partial x^2}$$

$$- G \hat{c} \pi R_o^2 \frac{\partial T'}{\partial x} + r y(-\Delta H_r) \pi R_o^2$$

If the radial gradients are not too large, $T(R=R_o)$ will not be very different from T'. Assuming this to be the case the above equation may be written as:

$$\rho C_p \frac{\partial T'}{\partial t} = -2h_R/R_o (T'-T_\infty) + k_{b,x} \frac{\partial^2 T'}{\partial x^2} - G \hat{c} \frac{\partial T'}{\partial x} + r y(-\Delta H_r)$$

This equation is the same as equation 6.1.1 apart from the first term on the right hand side. This is the radial heat loss term.

Finally, the above equation is made dimensionless using the substitutions given in Section 6.1. The result is equation 6.1.5 i.e.

$$\frac{\partial \theta}{\partial \tau} = \frac{\partial^2 \theta}{\partial X^2} - a \frac{\partial \theta}{\partial X} + b y - C (\theta - 1) \qquad 6.1.5$$

where $C = 2 h_R L^2/(k_b R_o)$.

It should be noted that as R_o tends to infinity, C tends to zero.

APPENDIX 6 EXPLANATION FOR THE INSTABILITY OF THE RUNGE-KUTTA ALGORITHM

The equation is

$$0 = \frac{d^2\theta}{dX^2} - a\frac{d\theta}{dX} - b\,y \qquad \text{A6.1}$$

with boundary conditions:

at X=0 $\quad \frac{d\theta}{dX} = (Bi_0+a)(\theta-1)$

at X=1 $\quad \frac{d\theta}{dX} = -Bi_1(\theta-1)$

For the first step along the bed the coefficients of equation A6.1 may be assumed constant. In effect the Runge-Kutta algorithm is stepping along the solution of 6.2.1 but with boundary conditions both at X = 0 i.e.

$$\frac{d\theta}{dX} = (Bi_0+a)(\theta-1)$$

$$\theta(X=0) = \theta_0$$

The solution to A6.1 with these boundary conditions is:

$$\theta = \theta_0 + a(\exp(aX)-1)((Bi_0+a)(\theta_0-1)-b/a) + b\,X/a \qquad \text{A6.2}$$

It can be seen that the value of θ_0 is critical, since if

$(Bi_0+a)(\theta_0-1)-b/a > 0$ then the second term of equation A6.2 increases without bound. If on the other hand:

$(Bi_0+a)(\theta_0-1)-b/a < 0$

then the second term becomes very large negative.

The real problem is that the boundary condition at X = 1 is not included in the method of solution, and thus the method will always become unstable.

APPENDIX 7 SOLUTION OF EQUATION 6.2.1 WITH r CONSTANT

If r is assumed constant then equation 6.1.2 may be integrated

i.e. $$\frac{dy}{dx} = \frac{-r\ y}{G}$$

gives $$y = y_o \exp(-rx/G) = y_o \exp(\gamma_3 X) \qquad A7.1$$

Substituting this in equation 6.2.1 give:

$$0 = \frac{d^2\theta}{dX^2} - a\frac{d\theta}{dX} - b\ y_o \exp(\gamma_3 X) - C\ (\theta - 1) \qquad A7.2$$

The solution of this equation is

$$\theta(X) = 1 + C_1\exp(\gamma_1 X) + C_2\exp(\gamma_2 X) + C_3\exp(\gamma_3 X)$$

$$C_3 = -b/(\gamma_3^2 + a\gamma_3 - C)$$

$$\gamma_1 = (a - (a^2 + 4C))^{1/2})/2$$

$$\gamma_2 = (a + (a^2 + 4C))^{1/2})/2$$

C_1 and C_2 may be determined from the boundary conditions.

Equation 6.1.3 may be integrated to give

$$-\rho_\infty\ v^2/2 = -f\ G\ R\ T_\infty\ L/P(\int_o^1 \theta\ dX + \rho_\infty\ g\ L(\int_o^1 \theta^{-1}\ dX)) \qquad A7.3$$

or $$G = P\ \rho_\infty(v^2/2L + g\ L(1-\int_o^1 \theta^{-1}dX))/(f\ R\ T_\infty\ L\ \int_o^1 \theta dX) \qquad A7.4$$

APPENDIX 8 SOLUTION OF EQUATION 6.1.5 WITH r CONSTANT

The equation to be solved is:

$$\frac{\partial\theta}{\partial\tau} = \frac{\partial^2\theta}{\partial X^2} - a\frac{\partial\theta}{\partial X} + b\,y - C\,(\theta - 1) \qquad \text{A8.1}$$

with boundary conditions

at X=0 $\quad \frac{\partial\theta}{\partial X} = (Bi_0+a)(\theta-1)$

at X=1 $\quad \frac{\partial\theta}{\partial X} = -Bi_1(\theta-1)$

The initial condition is $\theta(X,0) = \theta_0(X)$

The first step in the solution is to write:

$$\theta(X,\tau) = u(X,\tau) + \phi(X) \qquad \text{A8.2}$$

Substituting equation A8.2 in equation A8.1 gives:

$$\frac{\partial u}{\partial\tau} = \frac{\partial^2 u}{\partial X^2} - a\frac{\partial u}{\partial X} - C\,u + \frac{d^2\phi}{dX^2} - a\frac{d\phi}{dX} + b\exp(\gamma_s X) - C(\phi-1) \qquad \text{A8.3}$$

This may be written as two equations:

$$\frac{\partial u}{\partial\tau} = \frac{\partial^2\theta}{\partial X^2} - a\frac{\partial u}{\partial X} - C\,u \qquad \text{A8.4}$$

and

$$0 = \frac{d^2\phi}{dX^2} - a\frac{d\phi}{dX} + b\exp(\gamma_s X) - C(\phi-1) \qquad \text{A8.5}$$

with boundary conditions:

at X=0 $\quad \frac{\partial u}{\partial X} = (Bi_0+a)\,u$ and $\frac{d\phi}{dX} = (Bi_0+a)(\phi-1)$

at X=1 $\quad \frac{\partial u}{\partial X} = -Bi_1\,u$ and $\frac{d\phi}{dX} = -Bi_1(\phi-1)$

and initial condition $u(X,0) = \theta_0(X) - \phi(X)$

Equation A8.5 with its associated boundary conditions is merely the steady-state temperature equation, whose solution has been dealt with in Appendix 7.

The problem has thus been reduced to solving equation A8.4 with its boundary and initial conditions.

Defining a new variable $v(X,\tau)$ as:

$$u(X,\tau) = v(X,\tau) \exp(-\tau(a^2/4-C) + aX/2)$$

and substituting in equation A8.4 gives the diffusion equation i.e

$$\frac{\partial v}{\partial \tau} = \frac{\partial^2 v}{\partial X^2} \qquad \text{A8.6}$$

The boundary conditions on v are:

At X=0 $\quad \frac{\partial v}{\partial \tau} = (Bi_0 + a/2)v$

At X=1 $\quad \frac{\partial v}{\partial \tau} = -(Bi_1 + a/2)v$

and initial condition:

$$v(X,0) = (\theta_0(X) - \phi(X)) \exp(-aX/2)$$

The solution to equation A8.6 may be found in Carslaw & Jaeger (1959), and is:

$$v(X,\tau) = \Sigma \left(Z_n(X) \exp(-\beta_n^2\tau) \int Z_n(X') g(X') dX'\right) \qquad \text{A8.7}$$

$$Z_n(X) = \frac{2(\beta_n^2+Bi_3^2)(\beta_n \cos(\beta_n X)+Bi_2 \sin(\beta_n X))}{((\beta_n^2+Bi_2^2)(\beta_n^2+Bi_3^2+Bi_3)+Bi_2(\beta_n^2+Bi_3^2))}$$

$$g(X) = (\theta_0(X) - \phi(X)) \exp(-aX/2)$$

$$Bi_2 = Bi_0 - a/2$$

$$Bi_3 = Bi_1 + a/2$$

and the β_n are the positive roots of

$$\tan(\beta) = \frac{\beta(Bi_3 + Bi_2)}{(Bi_2\, Bi_3 + \beta^2)}$$

APPENDIX 9 APPLICATION OF THE METHOD OF LINES TO THE SOLUTION OF EQUATION 6.1.5

Equation 6.4.1 is:

$$\frac{\partial\theta(X_i,\tau)}{\partial X} = \Sigma(a_{ij}\ \theta(X_j,\tau) \qquad i=1 \text{ to } N \qquad \text{A9.1}$$

where the X_i are the nodes of the Nth order shifted Legendre polynomial.

Similarly

$$\frac{\partial^2\theta(X_i,\tau)}{\partial X} = \Sigma(b_{ij}\ \theta(X_j,\tau) \qquad i=1 \text{ to } N \qquad \text{A9.2}$$

It may easily be shown that the matrix $\underline{A}$ of coefficients a_{ij} is related to the matrix $\underline{B}$ of coefficients b_{ij} by:

$$\underline{B} = \underline{A}^2$$

Using equations A9.1 and A9.2 equation 6.1.5 may be written as:

$$\frac{d\theta_i}{d\tau} = \Sigma((b_{ij}-a\ a_{ij})\theta_j)+by_i\exp\{-E/(RT_\infty\theta_i)\}-C(\theta_i-1) \qquad \text{A9.3}$$

where $\theta_i = \theta(X_i,\tau)$

$y_i = y(X_i)$

The bondary conditions are also discretized:

$$\Sigma\ a_{1j}\theta_j = (Bio + a)(\theta_1 - 1) \qquad \text{A9.4}$$

$$\Sigma\ a_{Nj}\theta_j = -Bi_1(\theta_N - 1) \qquad \text{A9.5}$$

It can be seen that the partial differential equation has been rteduced to N ordinary differentail equations. The procedure used to solve is to calculate all the derivatives $d\theta_i/d\tau$ for one time and then use a Runge-Kutta algorithm to calculate the value of θ_i at the next time. The boundary values are included explicitly by solving equations A9.4 and A9.5 for θ_1 and θ_N in [illegible] at each time step. In addition a

backward difference formula is used to calculate the oxygen profile at each time. If the effects of ageing are incuded it is neccessary to calculate the fractional conversion of the coal at each time and distance using equation 1.4.4.

APPENDIX 10 TABULATION OF RESULTS OF CHIMNEY EXPERIMENT

A10.1 Introduction

In this Appendix the measured data for the chimney experiment is presented in tabular form. In the printouts it will be noted that 10 channels were used to log data. Channel 1 is the thermocouple at the very bottom of the bed, while channel 9 is the thermocouple at the very top of the bed. Channel 10 is a thermocouple placed in the oven.

The printouts show the time at which the data was logged and the temperature in degrees centigrade (labelled as deg_C). It should be noted that in some instances the data logger was re-started, with a greater interval between scans.

A10.2 Cooling Run

This run was used to obtain the heat transfer coefficients necessary for the model. The bed was heated under nitrogen and then removed from the oven. The model parameters used to obtain figure 7.2 were:

Coal particle size range : -3.4 + 1.19 mm
Bed Length : 0.2 m
Bed Radius : 0.039 m
C : 23
Bi_o : 3.7
Bi_1 : 9.3
Bed voidage : 0.38
D_p : 2.5 mm

EXP 10--SCAN 01---24:01:08:58:03
"COOLING"

ch: 01	190.3	deg_C
ch: 02	194.1	deg_C
ch: 03	196.5	deg_C
ch: 04	198.3	deg_C
ch: 05	197.1	deg_C
ch: 06	192.8	deg_C
ch: 07	189.6	deg_C
ch: 08	185.3	deg_C
ch: 09	181.4	deg_C
ch: 10	55.2	deg_C

EXP 10--SCAN 02---24:01:09:17:1
"COOLING"

ch: 01	179.3	deg_C
ch: 02	189.0	deg_C
ch: 03	191.7	deg_C
ch: 04	194.2	deg_C
ch: 05	193.5	deg_C
ch: 06	188.9	deg_C
ch: 07	187.2	deg_C
ch: 08	179.0	deg_C
ch: 09	157.2	deg_C
ch: 10	32.6	deg_C

EXP 10--SCAN 03---24:01:09:28:
"COOLING"

ch: 01	155.1	deg_C
ch: 02	171.7	deg_C
ch: 03	178.0	deg_C
ch: 04	181.2	deg_C
ch: 05	181.1	deg_C
ch: 06	176.0	deg_C
ch: 07	174.7	deg_C
ch: 08	158.3	deg_C
ch: 09	129.4	deg_C
ch: 10	29.8	deg_C

EXP 10--SCAN 04---24:01:09:47:
"COOLING"

ch: 01	171.9	deg_C
ch: 02	150.2	deg_C
ch: 03	160.1	deg_C
ch: 04	165.5	deg_C
ch: 05	165.6	deg_C
ch: 06	160.4	deg_C
ch: 07	157.7	deg_C
ch: 08	136.6	deg_C
ch: 09	108.7	deg_C
ch: 10	25.5	deg_C

EXP 10--SCAN 05---24:01:09:58:02:
"COOLING"

ch: 01	112.7	deg_C
ch: 02	129.1	deg_C
ch: 03	141.2	deg_C
ch: 04	145.5	deg_C
ch: 05	150.1	deg_C
ch: 06	144.7	deg_C
ch: 07	140.2	deg_C
ch: 08	117.8	deg_C
ch: 09	92.9	deg_C
ch: 10	26.2	deg_C

EXP 10--SCAN ---24:01:10:38:20
"COOLING"

ch: 01	50.6	deg_C
ch: 02	57.3	deg_C
ch: 03	64.3	deg_C
ch: 04	72.8	deg_C
ch: 05	75.3	deg_C
ch: 06	71.0	deg_C
ch: 07	65.2	deg_C
ch: 08	54.0	deg_C
ch: 09	45.3	deg_C
ch: 10	22.8	deg_C

EXP 10--SCAN 03---24:01:10:58:20
"COOLING"

ch: 01	42.9	deg_C
ch: 02	47.6	deg_C
ch: 03	53.1	deg_C
ch: 04	59.9	deg_C
ch: 05	62.0	deg_C
ch: 06	59.6	deg_C
ch: 07	54.0	deg_C
ch: 08	45.6	deg_C
ch: 09	39.1	deg_C
ch: 10	22.1	deg_C

EXP 10--SCAN 07---24:01:11:28:20
"COOLING"

ch: 01	38.4	deg_C
ch: 02	41.0	deg_C
ch: 03	44.9	deg_C
ch: 04	50.1	deg_C
ch: 05	51.9	deg_C
ch: 06	49.2	deg_C
ch: 07	45.6	deg_C
ch: 08	39.4	deg_C
ch: 09	34.6	deg_C
ch: 10	22.4	deg_C

EXP 10--SCAN 04---24:01:13:08:20
"COOLING"

ch: 01	32.4	deg_C
ch: 02	26.0	deg_C
ch: 03	38.3	deg_C
ch: 04	42.6	deg_C
ch: 05	44.1	deg_C
ch: 06	42.2	deg_C
ch: 07	39.5	deg_C
ch: 08	34.9	deg_C
ch: 09	31.7	deg_C
ch: 10	21.9	deg_C

EXP 10--SCAN 08---24:01:15:08:20
"COOLING"

ch: 01	25.7	deg_C
ch: 02	26.4	deg_C
ch: 03	27.2	deg_C
ch: 04	28.3	deg_C
ch: 05	28.6	deg_C
ch: 06	28.1	deg_C
ch: 07	27.2	deg_C
ch: 08	25.9	deg_C
ch: 09	24.8	deg_C
ch: 10	22.3	deg_C

EXP 10--SCAN 05---24:01:13:38:20
"COOLING"

ch: 01	30.6	deg_C
ch: 02	32.4	deg_C
ch: 03	34.5	deg_C
ch: 04	37.4	deg_C
ch: 05	38.6	deg_C
ch: 06	37.9	deg_C
ch: 07	34.9	deg_C
ch: 08	31.5	deg_C
ch: 09	28.9	deg_C
ch: 10	22.3	deg_C

EXP 10--SCAN 09---24:01:15:38:20
"COOLING"

ch: 01	24.8	deg_C
ch: 02	25.3	deg_C
ch: 03	25.9	deg_C
ch: 04	26.6	deg_C
ch: 05	26.9	deg_C
ch: 06	26.5	deg_C
ch: 07	25.9	deg_C
ch: 08	24.9	deg_C
ch: 09	24.1	deg_C
ch: 10	22.2	deg_C

EXP 10--SCAN 06---24:01:14:08:20
"COOLING"

ch: 01	28.4	deg_C
ch: 02	29.8	deg_C
ch: 03	31.3	deg_C
ch: 04	33.4	deg_C
ch: 05	34.1	deg_C
ch: 06	33.1	deg_C
ch: 07	31.6	deg_C
ch: 08	29.1	deg_C
ch: 09	27.1	deg_C
ch: 10	21.9	deg_C

EXP 10--SCAN 10---24:01:16:08:20
"COOLING"

ch: 01	24.2	deg_C
ch: 02	24.5	deg_C
ch: 03	24.9	deg_C
ch: 04	25.5	deg_C
ch: 05	25.7	deg_C
ch: 06	25.3	deg_C
ch: 07	24.9	deg_C
ch: 08	24.2	deg_C
ch: 09	23.6	deg_C
ch: 10	21.9	deg_C

EXP 10--SCAN 07---24:01:14:38:20
"COOLING"

ch: 01	26.8	deg_C
ch: 02	27.8	deg_C
ch: 03	28.9	deg_C
ch: 04	30.4	deg_C
ch: 05	31.0	deg_C
ch: 06	30.2	deg_C
ch: 07	29.1	deg_C
ch: 08	27.2	deg_C
ch: 09	25.8	deg_C
ch: 10	22.0	deg_C

EXP 10--SCAN 11---24:01:16:38:20
"COOLING"

ch: 01	23.7	deg_C
ch: 02	24.0	deg_C
ch: 03	24.3	deg_C
ch: 04	24.6	deg_C
ch: 05	24.7	deg_C
ch: 06	24.5	deg_C
ch: 07	24.2	deg_C
ch: 08	23.6	deg_C
ch: 09	23.2	deg_C
ch: 10	21.9	deg_C

A10.3 Ageing Run 1

The results of this run were used to obtain the plot shown in figure 7.2. The experimental conditions and model parameters were:

Coal particle size range: -3.4 + 1.19 mm

C : 23

Bi_o : 3.7

Bi_1 : 9.3

Bed voidage: 0.38

K_o : 3.33 m/s

E/R : 7000 K

$D_e\rho_m$: 1.42×10^{-13}

D_p : 2.5 mm

O_2 flowrate: 1.14×10^{-4} kmol/m^2/s

Oven temperature : 135°C

EXP 10---------- 19:01:14:35:54

ch: 01	131.8	deg_C
ch: 02	130.8	deg_C
ch: 03	129.2	deg_C
ch: 04	126.9	deg_C
ch: 05	125.6	deg_C
ch: 06	125.6	deg_C
ch: 07	127.1	deg_C
ch: 08	128.9	deg_C
ch: 09	130.1	deg_C
ch: 10	129.5	deg_C

EXP 10--SCAN 01---19:01:14:43:05

ch: 01	132.0	deg_C
ch: 02	131.1	deg_C
ch: 03	129.5	deg_C
ch: 04	127.2	deg_C
ch: 05	126.0	deg_C
ch: 06	125.9	deg_C
ch: 07	127.4	deg_C
ch: 08	129.1	deg_C
ch: 09	130.2	deg_C
ch: 10	125.3	deg_C

EXP 10--SCAN 02---19:01:14:43:29

ch: 01	132.0	deg_C
ch: 02	131.1	deg_C
ch: 03	129.5	deg_C
ch: 04	127.3	deg_C
ch: 05	126.0	deg_C
ch: 06	125.9	deg_C
ch: 07	127.4	deg_C
ch: 08	129.1	deg_C
ch: 09	130.2	deg_C
ch: 10	127.2	deg_C

EXP 10--SCAN 03---19:01:15:43:05

ch: 01	139.1	deg_C
ch: 02	139.9	deg_C
ch: 03	138.4	deg_C
ch: 04	135.0	deg_C
ch: 05	132.5	deg_C
ch: 06	131.1	deg_C
ch: 07	131.7	deg_C
ch: 08	132.0	deg_C
ch: 09	132.0	deg_C
ch: 10	128.3	deg_C

EXP 10--SCAN 04---19:01:16:43:05

ch: 01	145.2	deg_C
ch: 02	147.9	deg_C
ch: 03	147.8	deg_C
ch: 04	144.1	deg_C
ch: 05	140.1	deg_C
ch: 06	137.1	deg_C
ch: 07	136.6	deg_C
ch: 08	135.3	deg_C
ch: 09	134.3	deg_C
ch: 10	128.2	deg_C

EXP 10--SCAN 05---19:01:17:43:05

ch: 01	147.7	deg_C
ch: 02	151.3	deg_C
ch: 03	152.3	deg_C
ch: 04	149.5	deg_C
ch: 05	145.1	deg_C
ch: 06	141.3	deg_C
ch: 07	140.0	deg_C
ch: 08	137.7	deg_C
ch: 09	136.0	deg_C
ch: 10	126.6	deg_C

EXP 10--SCAN 06---19:01:18:43:05

ch: 01	148.6	deg_C
ch: 02	152.5	deg_C
ch: 03	154.1	deg_C
ch: 04	152.3	deg_C
ch: 05	148.1	deg_C
ch: 06	143.9	deg_C
ch: 07	142.1	deg_C
ch: 08	139.1	deg_C
ch: 09	137.1	deg_C
ch: 10	127.4	deg_C

EXP 10--SCAN 07---19:01:19:43:05

ch: 01	148.8	deg_C
ch: 02	152.7	deg_C
ch: 03	154.8	deg_C
ch: 04	153.7	deg_C
ch: 05	149.8	deg_C
ch: 06	145.4	deg_C
ch: 07	143.3	deg_C
ch: 08	139.8	deg_C
ch: 09	137.6	deg_C
ch: 10	126.9	deg_C

EXP 10--SCAN 08---19:01:20:43:05

ch: 01	148.5	deg_C
ch: 02	152.5	deg_C
ch: 03	154.0	deg_C
ch: 04	154.3	deg_C
ch: 05	150.7	deg_C
ch: 06	146.3	deg_C
ch: 07	143.9	deg_C
ch: 08	140.2	deg_C
ch: 09	137.9	deg_C
ch: 10	126.2	deg_C

EXP 10--SCAN 09---19:01:21:43:05

ch: 01	148.3	deg_C
ch: 02	152.2	deg_C
ch: 03	154.4	deg_C
ch: 04	154.4	deg_C
ch: 05	151.1	deg_C
ch: 06	146.8	deg_C
ch: 07	144.2	deg_C
ch: 08	140.4	deg_C
ch: 09	138.0	deg_C
ch: 10	126.2	deg_C

EXP 10--SCAN 10---19:01:22:43:05

ch: 01	147.9	deg_C
ch: 02	151.7	deg_C
ch: 03	154.0	deg_C
ch: 04	154.3	deg_C
ch: 05	151.3	deg_C
ch: 06	147.0	deg_C
ch: 07	144.4	deg_C
ch: 08	140.5	deg_C
ch: 09	138.1	deg_C
ch: 10	127.0	deg_C

EXP 10--SCAN 11---19:01:23:43:05

ch: 01	147.5	deg_C
ch: 02	151.3	deg_C
ch: 03	153.6	deg_C
ch: 04	154.1	deg_C
ch: 05	151.3	deg_C
ch: 06	147.1	deg_C
ch: 07	144.5	deg_C
ch: 08	140.6	deg_C
ch: 09	138.2	deg_C
ch: 10	126.9	deg_C

EXP 10--SCAN 12---20:01:00:43:05

ch: 01	147.2	deg_C
ch: 02	150.8	deg_C
ch: 03	153.1	deg_C
ch: 04	153.7	deg_C
ch: 05	151.2	deg_C
ch: 06	147.2	deg_C
ch: 07	144.6	deg_C
ch: 08	140.6	deg_C
ch: 09	138.2	deg_C
ch: 10	127.8	deg_C

EXP 10--SCAN 13---20:01:01:43:05

ch: 01	146.8	deg_C
ch: 02	150.3	deg_C
ch: 03	152.6	deg_C
ch: 04	153.3	deg_C
ch: 05	151.0	deg_C
ch: 06	147.1	deg_C
ch: 07	144.6	deg_C
ch: 08	140.6	deg_C
ch: 09	138.1	deg_C
ch: 10	128.2	deg_C

EXP 10--SCAN 14---20:01:02:43:05

ch: 01	146.4	deg_C
ch: 02	149.9	deg_C
ch: 03	152.1	deg_C
ch: 04	152.9	deg_C
ch: 05	150.8	deg_C
ch: 06	147.0	deg_C
ch: 07	144.5	deg_C
ch: 08	140.5	deg_C
ch: 09	138.1	deg_C
ch: 10	129.0	deg_C

EXP 10--SCAN 15---20:01:03:43:05

ch: 01	146.1	deg_C
ch: 02	149.4	deg_C
ch: 03	151.6	deg_C
ch: 04	152.5	deg_C
ch: 05	150.6	deg_C
ch: 06	146.9	deg_C
ch: 07	144.4	deg_C
ch: 08	140.5	deg_C
ch: 09	138.1	deg_C
ch: 10	127.4	deg_C

EXP 10--SCAN 16---20:01:04:43:05

ch: 01	145.8	deg_C
ch: 02	149.0	deg_C
ch: 03	151.1	deg_C
ch: 04	152.2	deg_C
ch: 05	150.3	deg_C
ch: 06	146.8	deg_C
ch: 07	144.4	deg_C
ch: 08	140.4	deg_C
ch: 09	138.0	deg_C
ch: 10	125.4	deg_C

EXP 10--SCAN 17---20:01:05:43:05

ch: 01	145.5	deg_C
ch: 02	149.7	deg_C
ch: 03	150.8	deg_C
ch: 04	151.9	deg_C
ch: 05	150.1	deg_C
ch: 06	146.6	deg_C
ch: 07	144.3	deg_C
ch: 08	140.4	deg_C
ch: 09	138.0	deg_C
ch: 10	127.1	deg_C

EXP 10--SCAN 18---20:01:06:43:05

ch: 01	145.3	deg_C
ch: 02	148.4	deg_C
ch: 03	150.4	deg_C
ch: 04	151.5	deg_C
ch: 05	149.9	deg_C
ch: 06	146.5	deg_C
ch: 07	144.2	deg_C
ch: 08	140.3	deg_C
ch: 09	138.0	deg_C
ch: 10	125.9	deg_C

EXP 10--SCAN 19---20:01:07:43:05

ch: 01	145.1	deg_C
ch: 02	148.1	deg_C
ch: 03	150.1	deg_C
ch: 04	151.1	deg_C
ch: 05	149.7	deg_C
ch: 06	146.4	deg_C
ch: 07	144.2	deg_C
ch: 08	140.3	deg_C
ch: 09	137.9	deg_C
ch: 10	125.1	deg_C

A10.4 Ageing Run 2

The results of this run were used to obtain the plot shown in figure 7.3. The experimental conditions and model parameters used to obtain figure 7.3 were:

Coal particle size range : -3.4 + 1.19 mm
C : 23
Bi_0 : 3.7
Bi_1 : 9.3
Bed voidage: 0.38
K_o : 3.33 m/s
E/R : 7000 K
$D_e\rho_m$: 1.42×10^{-13}
D_p : 2.5 mm
O_2 flowrate: 1.14×10^{-4} kmol/m^2/s
Oven temperature : 88°C

ch: 01	83.7	deg_C
ch: 02	83.9	deg_C
ch: 03	83.2	deg_C
ch: 04	83.2	deg_C
ch: 05	82.5	deg_C
ch: 06	82.0	deg_C
ch: 07	82.0	deg_C
ch: 08	82.4	deg_C
ch: 09	82.3	deg_C
ch: 10	88.7	deg_C

EXP 10--SCAN 01---09:02:09:06 19

ch: 01	83.7	deg_C
ch: 02	83.9	deg_C
ch: 03	83.2	deg_C
ch: 04	83.2	deg_C
ch: 05	82.5	deg_C
ch: 06	82.0	deg_C
ch: 07	82.0	deg_C
ch: 08	82.4	deg_C
ch: 09	82.3	deg_C
ch: 10	90.2	deg_C

EXP 10--SCAN 02---09:02:08:21 19

ch: 01	86.7	deg_C
ch: 02	87.7	deg_C
ch: 03	86.9	deg_C
ch: 04	85.3	deg_C
ch: 05	85.9	deg_C
ch: 06	85.0	deg_C
ch: 07	84.3	deg_C
ch: 08	85.2	deg_C
ch: 09	84.5	deg_C
ch: 10	89.2	deg_C

EXP 10--SCAN 03---09:02:08:36 19

ch: 01	87.9	deg_C
ch: 02	89.9	deg_C
ch: 03	89.4	deg_C
ch: 04	89.3	deg_C
ch: 05	88.4	deg_C
ch: 06	87.2	deg_C
ch: 07	86.8	deg_C
ch: 08	87.1	deg_C
ch: 09	85.8	deg_C
ch: 10	89.1	deg_C

EXP 10--SCAN 04---09:02:09:51 19

ch: 01	88.7	deg_C
ch: 02	91.3	deg_C
ch: 03	91.2	deg_C
ch: 04	91.3	deg_C
ch: 05	90.3	deg_C
ch: 06	89.0	deg_C
ch: 07	88.4	deg_C
ch: 08	88.4	deg_C
ch: 09	86.8	deg_C
ch: 10	86.4	deg_C

EXP 10--SCAN 05---09:02:09:06 19

ch: 01	89.3	deg_C
ch: 02	92.3	deg_C
ch: 03	92.6	deg_C
ch: 04	93.0	deg_C
ch: 05	92.0	deg_C
ch: 06	90.5	deg_C
ch: 07	89.6	deg_C
ch: 08	89.5	deg_C
ch: 09	87.6	deg_C
ch: 10	87.9	deg_C

EXP 10--SCAN 06---09:02:09:21 19

ch: 01	89.7	deg_C
ch: 02	93.1	deg_C
ch: 03	93.7	deg_C
ch: 04	94.4	deg_C
ch: 05	93.5	deg_C
ch: 06	91.9	deg_C
ch: 07	90.7	deg_C
ch: 08	90.4	deg_C
ch: 09	88.2	deg_C
ch: 10	88.6	deg_C

EXP 10--SCAN 07---09:02:09:36 19

ch: 01	90.1	deg_C
ch: 02	93.6	deg_C
ch: 03	94.5	deg_C
ch: 04	96.6	deg_C
ch: 05	94.7	deg_C
ch: 06	93.0	deg_C
ch: 07	91.5	deg_C
ch: 08	90.2	deg_C
ch: 09	88.1	deg_C
ch: 10	89.2	deg_C

EXP 10--SCAN 09---09:02:09:51:19

ch: 01	90.4	deg_C
ch: 02	94.1	deg_C
ch: 03	95.2	deg_C
ch: 04	96.6	deg_C
ch: 05	95.0	deg_C
ch: 06	94.0	deg_C
ch: 07	92.3	deg_C
ch: 08	91.0	deg_C
ch: 09	89.3	deg_C
ch: 10	90.4	deg_C

EXP 10--SCAN 09---09:02:10:06:19

ch: 01	90.6	deg_C
ch: 02	94.4	deg_C
ch: 03	95.7	deg_C
ch: 04	97.4	deg_C
ch: 05	96.9	deg_C
ch: 06	94.9	deg_C
ch: 07	93.0	deg_C
ch: 08	92.4	deg_C
ch: 09	89.7	deg_C
ch: 10	90.0	deg_C

EXP 10--SCAN 10---09:02:10:21:19

ch: 01	90.7	deg_C
ch: 02	94.6	deg_C
ch: 03	96.1	deg_C
ch: 04	98.1	deg_C
ch: 05	97.7	deg_C
ch: 06	95.7	deg_C
ch: 07	93.6	deg_C
ch: 08	92.9	deg_C
ch: 09	90.1	deg_C
ch 10	88.8	deg_C

EXP 10--SCAN 11---09:02:10:36:19

ch: 01	90.9	deg_C
ch: 02	94.8	deg_C
ch: 03	96.4	deg_C
ch: 04	99.6	deg_C
ch: 05	98.4	deg_C
ch: 06	96.4	deg_C
ch: 07	94.1	deg_C
ch: 08	93.3	deg_C
ch: 09	90.3	deg_C
ch: 10	88.6	deg_C

EXP 10--SCAN 12---09:02:10:51:19

ch: 01	91.0	deg_C
ch: 02	94.9	deg_C
ch: 03	96.6	deg_C
ch: 04	99.0	deg_C
ch: 05	98.9	deg_C
ch: 06	96.9	deg_C
ch: 07	94.5	deg_C
ch: 08	93.6	deg_C
ch: 09	90.6	deg_C
ch: 10	89.4	deg_C

EXP 10--SCAN 13---09:02:11:06:19

ch: 01	91.0	deg_C
ch: 02	94.9	deg_C
ch: 03	96.8	deg_C
ch: 04	99.2	deg_C
ch: 05	99.3	deg_C
ch: 06	97.4	deg_C
ch: 07	94.8	deg_C
ch 08	93.9	deg_C

EXP 10--SCAN 14---09:02:11:21:19

ch: 01	91.0	deg_C
ch: 02	94.9	deg_C
ch: 03	96.8	deg_C
ch: 04	99.4	deg_C
ch: 05	99.5	deg_C
ch: 06	97.7	deg_C
ch: 07	95.1	deg_C
ch: 08	94.1	deg_C
ch: 09	90.9	deg_C
ch: 10	90.1	deg_C

EXP 10--SCAN 15---09:02:11:36:19

ch: 01	91.0	deg_C
ch: 02	94.9	deg_C
ch: 03	96.8	deg_C
ch: 04	99.5	deg_C
ch: 05	99.7	deg_C
ch: 06	97.9	deg_C
ch: 07	95.3	deg_C
ch: 08	94.3	deg_C
ch: 09	91.0	deg_C
ch 10	90.1	deg_C

EXP 10--SCAN 16---09:02:11:51:19

ch: 01	91.0	deg_C
ch: 02	94.8	deg_C
ch: 03	96.8	deg_C
ch: 04	99.5	deg_C
ch: 05	99.8	deg_C
ch: 06	98.0	deg_C
ch: 07	95.4	deg_C
ch: 08	94.2	deg_C
ch: 09	91.1	deg_C
ch 10	90.6	deg_C

EXP 10--SCAN 17---09:02:12:06:19

ch: 01	90.9	deg_C
ch: 02	94.7	deg_C
ch: 03	96.7	deg_C
ch: 04	99.4	deg_C
ch: 05	99.9	deg_C
ch: 06	98.1	deg_C
ch: 07	95.4	deg_C
ch 08	94.4	deg_C
ch: 09	91.1	deg_C
ch: 10	87.3	deg_C

EXP 10--SCAN 18---09:02:12:21:19

ch: 01	90.8	deg_C
ch: 02	94.6	deg_C
ch: 03	96.5	deg_C
ch: 04	99.3	deg_C
ch: 05	99.7	deg_C
ch: 06	98.1	deg_C
ch: 07	95.4	deg_C
ch: 08	94.4	deg_C
ch: 09	91.1	deg_C
ch: 10	89.0	deg_C

EXP 10--SCAN 19---09:02:12:36:19

ch: 01	90.8	deg_C
ch: 02	94.5	deg_C
ch: 03	96.4	deg_C
ch: 04	99.1	deg_C
ch: 05	99.5	deg_C
ch: 06	98.0	deg_C
ch: 07	95.3	deg_C
ch: 08	94.3	deg_C
ch: 09	91.0	deg_C
ch: 10	89.5	deg_C

EXP 10--SCAN 20---09:02:12:51:19

ch: 01	90.7	deg_C
ch: 02	94.3	deg_C
ch: 03	96.2	deg_C
ch: 04	98.9	deg_C
ch: 05	99.3	deg_C
ch: 06	97.8	deg_C
ch: 07	95.2	deg_C
ch: 08	94.2	deg_C
ch: 09	91.0	deg_C
ch: 10	90.6	deg_C

EXP 10--SCAN 21---09:02:13:06:19

ch: 01	90.6	deg_C
ch: 02	94.2	deg_C
ch: 03	96.0	deg_C
ch: 04	98.7	deg_C
ch: 05	99.1	deg_C
ch: 06	97.6	deg_C
ch: 07	95.0	deg_C
ch: 08	94.1	deg_C
ch: 09	90.9	deg_C
ch: 10	88.2	deg_C

EXP 10--SCAN 22---09:02:13:21:19

ch: 01	90.5	deg_C
ch: 02	94.0	deg_C
ch: 03	95.8	deg_C
ch: 04	98.4	deg_C
ch: 05	98.8	deg_C
ch: 06	97.4	deg_C
ch: 07	94.9	deg_C
ch: 08	93.9	deg_C
ch: 09	90.7	deg_C
ch: 10	87.4	deg_C

EXP 10--SCAN 23---09:02:13:36:19

ch: 01	90.4	deg_C
ch: 02	93.8	deg_C
ch: 03	95.5	deg_C
ch: 04	98.1	deg_C
ch: 05	98.5	deg_C
ch: 06	97.1	deg_C
ch: 07	94.6	deg_C
ch: 08	93.7	deg_C
ch: 09	90.6	deg_C
ch: 10	89.1	deg_C

EXP 10--SCAN 24---09:02:13:51:19

ch: 01	90.3	deg_C
ch: 02	93.6	deg_C
ch: 03	95.3	deg_C
ch: 04	97.8	deg_C
ch: 05	98.2	deg_C
ch: 06	96.9	deg_C
ch: 07	94.4	deg_C
ch: 08	93.5	deg_C
ch: 09	90.4	deg_C
ch: 10	89.8	deg_C

EXP 10--SCAN 01---09:02:14:07:24

ch: 01	90.2	deg_C
ch: 02	93.4	deg_C
ch: 03	95.0	deg_C
ch: 04	97.5	deg_C
ch: 05	98.0	deg_C
ch: 06	96.6	deg_C
ch: 07	94.1	deg_C
ch: 08	93.2	deg_C
ch: 09	90.2	deg_C
ch: 10	90.3	deg_C

EXP 10--SCAN 02---09:02:14:07:46

ch: 01	90.2	deg_C
ch: 02	93.4	deg_C
ch: 03	95.0	deg_C
ch: 04	97.5	deg_C
ch: 05	97.8	deg_C
ch: 06	96.5	deg_C
ch: 07	94.1	deg_C
ch: 08	93.2	deg_C
ch: 09	90.3	deg_C
ch: 10	88.5	deg_C

EXP 10--SCAN 03---09:02:15:07:24

ch: 01	89.7	deg_C
ch: 02	92.7	deg_C
ch: 03	94.0	deg_C
ch: 04	96.2	deg_C
ch: 05	96.5	deg_C
ch: 06	95.2	deg_C
ch: 07	93.1	deg_C
ch: 08	92.3	deg_C
ch: 09	89.6	deg_C
ch: 10	88.0	deg_C

EXP 10--SCAN 04---09:02:16:07:24

ch: 01	89.2	deg_C
ch: 02	92.0	deg_C
ch: 03	93.1	deg_C
ch: 04	95.0	deg_C
ch: 05	95.1	deg_C
ch: 06	93.9	deg_C
ch: 07	92.0	deg_C
ch: 08	91.4	deg_C
ch: 09	88.9	deg_C
ch: 10	87.7	deg_C

EXP 10--SCAN 05---09:02:17:07:24

ch: 01	88.8	deg_C
ch: 02	91.3	deg_C
ch: 03	92.2	deg_C
ch: 04	93.9	deg_C
ch: 05	93.9	deg_C
ch: 06	92.8	deg_C
ch: 07	91.1	deg_C
ch: 08	90.6	deg_C
ch: 09	88.4	deg_C
ch: 10	89.9	deg_C

EXP 10--SCAN 06---09:02:18:07:24

ch: 01	88.4	deg_C
ch: 02	90.9	deg_C
ch: 03	91.5	deg_C
ch: 04	93.0	deg_C
ch: 05	92.9	deg_C
ch: 06	91.9	deg_C
ch: 07	90.4	deg_C
ch: 08	90.0	deg_C
ch: 09	87.9	deg_C
ch: 10	90.4	deg_C

EXP 10--SCAN 07---09:02:19:07:24

ch: 01	88.1	deg_C
ch: 02	90.2	deg_C
ch: 03	90.9	deg_C
ch: 04	92.2	deg_C
ch: 05	92.1	deg_C
ch: 06	91.1	deg_C
ch: 07	89.8	deg_C
ch: 08	89.4	deg_C
ch: 09	87.5	deg_C
ch: 10	89.1	deg_C

EXP 10--SCAN 08---09:02:20:07:24

ch: 01	87.2	deg_C
ch: 02	89.9	deg_C
ch: 03	90.4	deg_C
ch: 04	91.5	deg_C
ch: 05	91.4	deg_C
ch: 06	90.5	deg_C
ch: 07	89.2	deg_C
ch: 08	88.9	deg_C
ch: 09	87.2	deg_C
ch: 10	87.5	deg_C

EXP 10--SCAN 09---09:02:21:07:24

ch: 01	87.6	deg_C
ch: 02	89.5	deg_C
ch: 03	89.9	deg_C
ch: 04	91.1	deg_C
ch: 05	89.9	deg_C
ch: 06	89.9	deg_C
ch: 07	88.8	deg_C
ch: 08	88.6	deg_C
ch: 09	85.9	deg_C
ch: 10	86.6	deg_C

EXP 10--SCAN 10---09:02:22:07:24

ch: 01	87.4	deg_C
ch: 02	89.2	deg_C
ch: 03	89.5	deg_C
ch: 04	90.6	deg_C
ch: 05	90.4	deg_C
ch: 06	89.5	deg_C
ch: 07	88.5	deg_C
ch: 08	88.3	deg_C
ch: 09	86.7	deg_C
ch: 10	90.0	deg_C

EXP 10--SCAN 11---09:02:27:07:24

ch: 01	87.2	deg_C
ch: 02	89.0	deg_C
ch: 03	89.2	deg_C
ch: 04	90.3	deg_C
ch: 05	90.0	deg_C
ch: 06	89.2	deg_C
ch: 07	88.2	deg_C
ch: 08	88.1	deg_C
ch: 09	86.5	deg_C
ch: 10	88.2	deg_C

EXP 10--SCAN 12---10:02:00:07:24

ch: 01	87.1	deg_C
ch: 02	88.8	deg_C
ch: 03	89.0	deg_C
ch: 04	90.0	deg_C
ch: 05	89.7	deg_C
ch: 06	88.9	deg_C
ch: 07	88.0	deg_C
ch: 08	87.9	deg_C
ch: 09	86.4	deg_C
ch: 10	88.9	deg_C

EXP 10--SCAN 13---10:02:01:07:24

ch: 01	87.0	deg_C
ch: 02	88.6	deg_C
ch: 03	88.9	deg_C
ch: 04	89.8	deg_C
ch: 05	89.5	deg_C
ch: 06	88.7	deg_C
ch: 07	87.9	deg_C
ch: 08	87.7	deg_C
ch: 09	86.3	deg_C
ch: 10	88.9	deg_C

EXP 10--SCAN 14---10:02:02:07:24

ch: 01	86.9	deg_C
ch: 02	88.4	deg_C
ch: 03	89.6	deg_C
ch: 04	89.5	deg_C
ch: 05	89.2	deg_C
ch: 06	88.5	deg_C
ch: 07	87.7	deg_C
ch: 08	87.6	deg_C
ch: 09	86.2	deg_C
ch: 10	90.5	deg_C

EXP 10--SCAN 15---10:02:03:07:24

ch: 01	86.8	deg_C
ch: 02	88.3	deg_C
ch: 03	89.5	deg_C
ch: 04	89.4	deg_C
ch: 05	89.1	deg_C
ch: 06	88.3	deg_C
ch: 07	87.5	deg_C
ch: 08	87.4	deg_C
ch: 09	86.1	deg_C
ch: 10	87.1	deg_C

EXP 10--SCAN 16---10:02:04:07:24

ch: 01	86.7	deg_C
ch: 02	88.2	deg_C
ch: 03	88.3	deg_C
ch: 04	89.2	deg_C
ch: 05	88.9	deg_C
ch: 06	88.1	deg_C
ch: 07	87.4	deg_C
ch: 08	87.3	deg_C
ch: 09	86.9	deg_C
ch: 10	89.7	deg_C

EXP 10--SCAN 17---10:02:05:07:24

ch: 01	86.6	deg_C
ch: 02	88.1	deg_C
ch: 03	88.2	deg_C
ch: 04	88.1	deg_C
ch: 05	88.0	deg_C
ch: 06	87.3	deg_C
ch: 07	87.2	deg_C
ch: 08	86.9	deg_C
ch: 09	86.4	deg_C
ch: 10		

EXP 10--SCAN 18---10:02:06:07:24

ch: 01	86.6	deg_C
ch: 02	88.0	deg_C
ch: 03	88.1	deg_C
ch: 04	89.0	deg_C
ch: 05	88.6	deg_C
ch: 06	87.9	deg_C
ch: 07	87.2	deg_C
ch: 08	87.2	deg_C
ch: 09	85.9	deg_C
ch: 10	88.3	deg_C

EXP 10--SCAN 19---10:02:07:07:24

ch: 01	86.5	deg_C
ch: 02	87.9	deg_C
ch: 03	89.0	deg_C
ch: 04	88.8	deg_C
ch: 05	88.5	deg_C
ch: 06	87.8	deg_C
ch: 07	87.1	deg_C
ch: 08	87.1	deg_C
ch: 09	85.8	deg_C
ch: 10	90.9	deg_C

EXP 10--SCAN 20---10:02:08:07:24

ch: 01	86.5	deg_C
ch: 02	87.9	deg_C
ch: 03	87.9	deg_C
ch: 04	88.7	deg_C
ch: 05	88.4	deg_C
ch: 06	87.7	deg_C
ch: 07	87.0	deg_C
ch: 08	87.0	deg_C
ch: 09	85.7	deg_C
ch: 10	88.7	deg_C

EXP 10--SCAN 21---10:02:09:07:24

ch: 01	86.4	deg_C
ch: 02	87.8	deg_C
ch: 03	87.9	deg_C
ch: 04	88.7	deg_C
ch: 05	88.3	deg_C
ch: 06	87.5	deg_C
ch: 07	87.0	deg_C
ch: 08	87.0	deg_C
ch: 09	85.7	deg_C
ch: 10	90.3	deg_C

EXP 10--SCAN 22---10:02:10:07:24

ch: 01	86.4	deg_C
ch: 02	87.8	deg_C
ch: 03	87.8	deg_C
ch: 04	88.6	deg_C
ch: 05	88.7	deg_C
ch: 06	87.5	deg_C
ch: 07	86.9	deg_C
ch: 08	86.9	deg_C
ch: 09	85.7	deg_C
ch: 10	87.7	deg_C

EXP 10--SCAN 23---10:02:11:07:24

ch: 01	86.4	deg_C
ch: 02	87.9	deg_C
ch: 03	87.9	deg_C
ch: 04	88.6	deg_C
ch: 05	88.7	deg_C
ch: 06	87.6	deg_C
ch: 07	86.9	deg_C
ch: 08	86.9	deg_C
ch: 09	85.7	deg_C
ch: 10	90.5	deg_C

EXP 10--SCAN 24---10:02:12:07:24

ch: 01	86.4	deg_C
ch: 02	87.8	deg_C
ch: 03	87.8	deg_C
ch: 04	88.6	deg_C
ch: 05	88.2	deg_C
ch: 06	87.6	deg_C
ch: 07	87.0	deg_C
ch: 08	87.0	deg_C
ch: 09	85.9	deg_C
ch: 10	87.6	deg_C

EXP 10--SCAN 25---10:02:13:07:24

ch: 01	86.5	deg_C
ch: 02	87.9	deg_C
ch: 03	87.8	deg_C
ch: 04	88.6	deg_C
ch: 05	88.2	deg_C
ch: 06	87.6	deg_C
ch: 07	86.9	deg_C
ch: 08	87.0	deg_C
ch: 09	85.8	deg_C
ch: 10	90.4	deg_C

A10.5 Ageing run 3

The results of this run have not been analyzed. The run conditions were as follows:

Coal particle size range	: - 3.4 + 1.19 mm
Oven temperature	: 180°C
Oxygen flowrate	: 1.42 x 10^{-5} kmol/m^2/s

EXP 10----------20:01 13:53:45

ch: 01	178.4	deg_C
ch: 02	178.2	deg_C
ch: 03	177.1	deg_C
ch: 04	175.5	deg_C
ch: 05	174.2	deg_C
ch: 06	173.5	deg_C
ch: 07	174.7	deg_C
ch: 08	175.2	deg_C
ch: 09	175.2	deg_C
ch: 10	174.8	deg_C

EXP 10--SCAN 01---20:01 13:55:24

ch: 01	178.5	deg_C
ch: 02	178.2	deg_C
ch: 03	177.2	deg_C
ch: 04	175.5	deg_C
ch: 05	174.3	deg_C
ch: 06	173.5	deg_C
ch: 07	174.8	deg_C
ch: 08	175.2	deg_C
ch: 09	175.2	deg_C
ch: 10	175.3	deg_C

EXP 10--SCAN 02---20:01 13:55:58

ch: 01	178.5	deg_C
ch: 02	178.2	deg_C
ch: 03	177.2	deg_C
ch: 04	175.5	deg_C
ch: 05	174.3	deg_C
ch: 06	173.5	deg_C
ch: 07	174.8	deg_C
ch: 08	175.2	deg_C
ch: 09	175.2	deg_C
ch: 10	174.6	deg_C

EXP 10--SCAN 03---20:01 14:10:34

ch: 01	179.3	deg_C
ch: 02	179.1	deg_C
ch: 03	178.0	deg_C
ch: 04	176.1	deg_C
ch: 05	174.9	deg_C
ch: 06	174.0	deg_C
ch: 07	175.3	deg_C
ch: 08	175.7	deg_C
ch: 09	175.4	deg_C
ch: 10	174.2	deg_C

EXP 10--SCAN 04---20:01 14:25:34

ch: 01	185.1	deg_C
ch: 02	185.6	deg_C
ch: 03	183.5	deg_C
ch: 04	179.8	deg_C
ch: 05	177.2	deg_C
ch: 06	175.6	deg_C
ch: 07	176.4	deg_C
ch: 08	176.4	deg_C
ch: 09	175.8	deg_C
ch: 10	174.5	deg_C

EXP 10--SCAN 05---20:01 14:40 34

ch: 01	190.9	deg_C
ch: 02	193.0	deg_C
ch: 03	190.4	deg_C
ch: 04	184.5	deg_C
ch: 05	180.3	deg_C
ch: 06	177.6	deg_C
ch: 07	178.0	deg_C
ch: 08	177.4	deg_C
ch: 09	176.4	deg_C
ch: 10	174.7	deg_C

EXP 10--SCAN 06---20:01 14 55 34

ch: 01	195.8	deg_C
ch: 02	198.4	deg_C
ch: 03	196.7	deg_C
ch: 04	188.8	deg_C
ch: 05	183.2	deg_C
ch: 06	179.6	deg_C
ch: 07	179.5	deg_C
ch: 08	178.4	deg_C
ch: 09	176.9	deg_C
ch: 10	173.1	deg_C

EXP 10--SCAN 07---20:01 15:10 34

ch: 01	199.6	deg_C
ch: 02	204.5	deg_C
ch: 03	202.0	deg_C
ch: 04	192.5	deg_C
ch: 05	185.6	deg_C
ch: 06	181.2	deg_C
ch: 07	180.7	deg_C
ch: 08	179.1	deg_C
ch: 09	177.4	deg_C
ch: 10	174.1	deg_C

EXP 10--SCAN 00---20:01:15:25:34

ch: 01	202.7	deg_C
ch: 02	208.7	deg_C
ch: 03	206.5	deg_C
ch: 04	195.6	deg_C
ch: 05	187.5	deg_C
ch: 06	182.6	deg_C
ch: 07	181.7	deg_C
ch: 08	179.7	deg_C
ch: 09	177.8	deg_C
ch: 10	173.8	deg_C

EXP 10--SCAN 09---20:01:15:40:3

ch: 01	205.2	deg_C
ch: 02	212.1	deg_C
ch: 03	210.1	deg_C
ch: 04	198.2	deg_C
ch: 05	189.1	deg_C
ch: 06	183.7	deg_C
ch: 07	182.5	deg_C
ch: 08	180.2	deg_C
ch: 09	178.2	deg_C
ch: 10	173.5	deg_C

EXP 10--SCAN 10---20:01:15:55:3

ch: 01	207.2	deg_C
ch: 02	214.7	deg_C
ch: 03	213.0	deg_C
ch: 04	200.4	deg_C
ch: 05	190.4	deg_C
ch: 06	184.5	deg_C
ch: 07	183.1	deg_C
ch: 08	180.6	deg_C
ch: 09	178.5	deg_C
ch: 10	172.9	deg_C

EXP 10--SCAN 01---20:01:16:10:0

ch: 01	208.7	deg_C
ch: 02	216.8	deg_C
ch: 03	215.4	deg_C
ch: 04	202.2	deg_C
ch: 05	191.4	deg_C
ch: 06	185.1	deg_C
ch: 07	183.5	deg_C
ch: 08	180.8	deg_C
ch: 09	178.6	deg_C
ch: 10	173.6	deg_C

EXP 10--SCAN 02---20:01:17:10:02

ch: 01	212.1	deg_C
ch: 02	221.5	deg_C
ch: 03	221.3	deg_C
ch: 04	207.2	deg_C
ch: 05	194.3	deg_C
ch: 06	186.5	deg_C
ch: 07	184.0	deg_C
ch: 08	180.9	deg_C
ch: 09	178.8	deg_C
ch: 10	173.9	deg_C

EXP 10--SCAN 03---20:01:18:10:02

ch: 01	212.9	deg_C
ch: 02	222.8	deg_C
ch: 03	223.6	deg_C
ch: 04	210.0	deg_C
ch: 05	196.0	deg_C
ch: 06	187.2	deg_C
ch: 07	184.0	deg_C
ch: 08	180.8	deg_C
ch: 09	178.7	deg_C
ch: 10	174.8	deg_C

EXP 10--SCAN 04---20:01:19:10:02

ch: 01	212.5	deg_C
ch: 02	222.6	deg_C
ch: 03	224.3	deg_C
ch: 04	211.7	deg_C
ch: 05	197.3	deg_C
ch: 06	187.8	deg_C
ch: 07	184.3	deg_C
ch: 08	180.8	deg_C
ch: 09	178.7	deg_C
ch: 10	175.2	deg_C

EXP 10--SCAN 05---20:01:20:10:02

ch: 01	211.7	deg_C
ch: 02	221.7	deg_C
ch: 03	224.2	deg_C
ch: 04	212.9	deg_C
ch: 05	198.4	deg_C
ch: 06	188.5	deg_C
ch: 07	184.6	deg_C
ch: 08	181.0	deg_C
ch: 09	178.8	deg_C
ch: 10	173.8	deg_C

EXP 10--SCAN 06---20:01:21:10:02

ch: 01	210.7	deg_C
ch: 02	220.6	deg_C
ch: 03	223.6	deg_C
ch: 04	213.5	deg_C
ch: 05	199.3	deg_C
ch: 06	189.2	deg_C
ch: 07	185.1	deg_C
ch: 08	181.2	deg_C
ch: 09	179.0	deg_C
ch: 10	173.4	deg_C

EXP 10--SCAN 07---20:01:22:10:02

ch: 01	209.7	deg_C
ch: 02	219.4	deg_C
ch: 03	222.9	deg_C
ch: 04	214.0	deg_C
ch: 05	200.3	deg_C
ch: 06	189.9	deg_C
ch: 07	185.6	deg_C
ch: 08	181.5	deg_C
ch: 09	179.2	deg_C
ch: 10	173.7	deg_C

EXP 10--SCAN 08---20:01:23:10:02

ch: 01	208.7	deg_C
ch: 02	218.2	deg_C
ch: 03	222.2	deg_C
ch: 04	214.4	deg_C
ch: 05	201.1	deg_C
ch: 06	190.6	deg_C
ch: 07	186.1	deg_C
ch: 08	181.8	deg_C
ch: 09	179.4	deg_C
ch: 10	175.6	deg_C

EXP 10--SCAN 09---21:01:00:10:02

ch: 01	207.9	deg_C
ch: 02	217.1	deg_C
ch: 03	221.3	deg_C
ch: 04	214.7	deg_C
ch: 05	201.9	deg_C
ch: 06	191.3	deg_C
ch: 07	186.6	deg_C
ch: 08	182.1	deg_C
ch: 09	179.6	deg_C
ch: 10	174.5	deg_C

EXP 10--SCAN 10---21:01:01:10:02

ch: 01	206.9	deg_C
ch: 02	216.9	deg_C
ch: 03	220.4	deg_C
ch: 04	214.8	deg_C
ch: 05	202.6	deg_C
ch: 06	191.9	deg_C
ch: 07	187.1	deg_C
ch: 08	182.4	deg_C
ch: 09	179.7	deg_C
ch: 10	174.8	deg_C

EXP 10--SCAN 11---21:01:02:10:02

ch: 01	206.1	deg_C
ch: 02	215.0	deg_C
ch: 03	219.6	deg_C
ch: 04	214.9	deg_C
ch: 05	203.2	deg_C
ch: 06	192.5	deg_C
ch: 07	187.5	deg_C
ch: 08	182.7	deg_C
ch: 09	179.9	deg_C
ch: 10	174.8	deg_C

EXP 10--SCAN 12---21:01:03:10:02

ch: 01	205.2	deg_C
ch: 02	214.0	deg_C
ch: 03	218.?	deg_C
ch: 04	214.8	deg_C
ch: 05	203.7	deg_C
ch: 06	193.1	deg_C
ch: 07	188.0	deg_C
ch: 08	182.9	deg_C
ch: 09	180.0	deg_C
ch: 10	174.2	deg_C

EXP 10--SCAN 13---21:01:04:10:02

ch: 01	204.4	deg_C
ch: 02	213.0	deg_C
ch: 03	217.8	deg_C
ch: 04	214.?	deg_C
ch: 05	204.2	deg_C
ch: 06	193.5	deg_C
ch: 07	188.4	deg_C
ch: 08	183.1	deg_C
ch: 09	180.1	deg_C
ch: 10	173.6	deg_C

EXP 10--SCAN 14---21:01:05:10:02

ch: 01	203.7	deg_C
ch: 02	212.1	deg_C
ch: 03	217.0	deg_C
ch: 04	214.5	deg_C
ch: 05	204.7	deg_C
ch: 06	194.2	deg_C
ch: 07	188.8	deg_C
ch: 08	183.4	deg_C
ch: 09	180.3	deg_C
ch: 10	174.7	deg_C

EXP 10--SCAN 15---21:01:06:10:02

ch: 01	203.1	deg_C
ch: 02	211.2	deg_C
ch: 03	216.1	deg_C
ch: 04	214.4	deg_C
ch: 05	205.1	deg_C
ch: 06	194.7	deg_C
ch: 07	189.3	deg_C
ch: 08	183.6	deg_C
ch: 09	180.5	deg_C
ch: 10	174.4	deg_C

EXP 10--SCAN 16---21:01:07:10:02

ch: 01	202.4	deg_C
ch: 02	210.4	deg_C
ch: 03	215.4	deg_C
ch: 04	214.1	deg_C
ch: 05	205.4	deg_C
ch: 06	195.2	deg_C
ch: 07	189.7	deg_C
ch: 08	183.9	deg_C
ch: 09	180.6	deg_C
ch: 10	174.4	deg_C

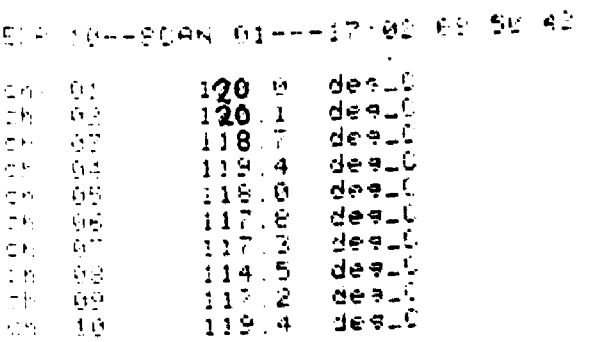
EXP 10--SCAN 17---21:01:08:10:02

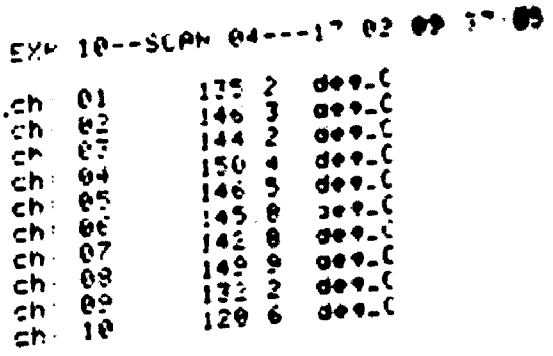
ch: 01	201.9	deg_C
ch: 02	209.7	deg_C
ch: 03	214.6	deg_C
ch: 04	213.9	deg_C
ch: 05	205.7	deg_C
ch: 06	195.6	deg_C
ch: 07	190.1	deg_C
ch: 08	184.1	deg_C
ch: 09	180.8	deg_C
ch: 10	175.2	deg_C

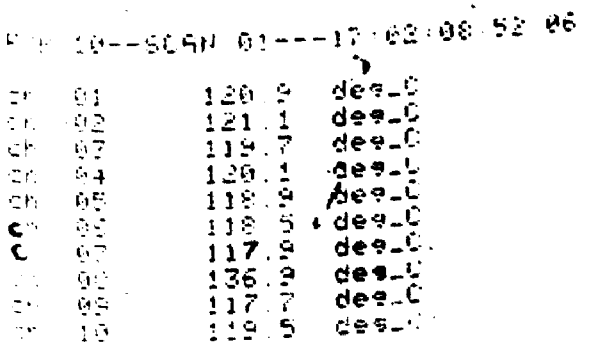
A10.6 Ignition run 1

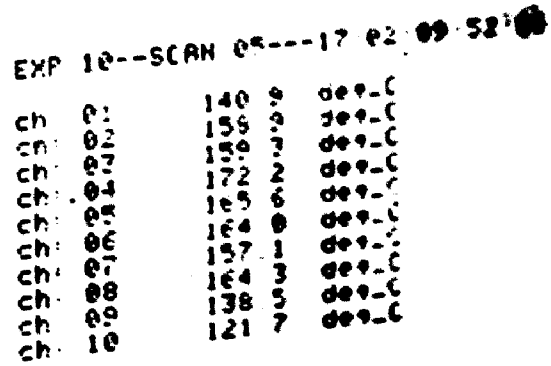
The results from this run were used in figure 7.4. The experimental conditions and model parameters used were as follows:

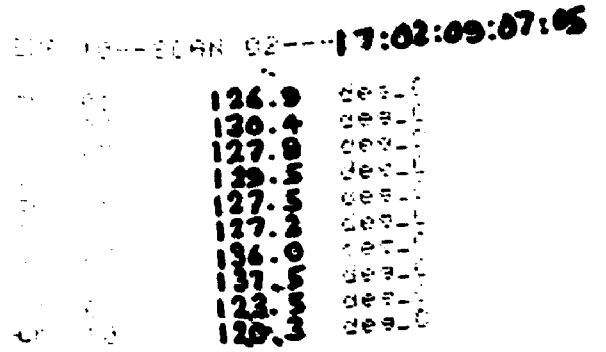
Coal particle size range	: -1.19 mm
Oven temperature	: 120 ^{o}C
Oxygen flowrate	: 4.33 x 10^{-5} kmol/m^2/s
C	: 23
Bi_o	: 3.7
Bi_1	: 9.3
Bed voidage	: 0.38
K_o	: 4.84 m/s
E/R	: 7000 K
$D_e \rho_m$	: 1.42 x 10^{-13}
D_p	: 0.5 mm

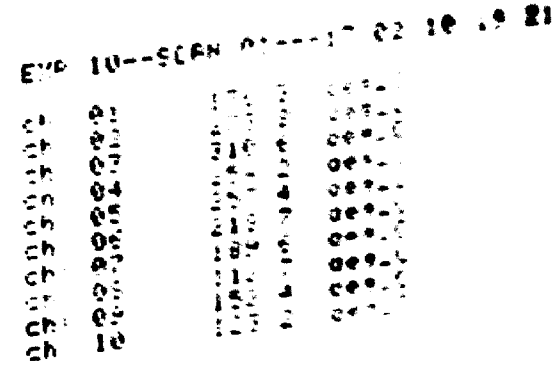

EXP 10--SCAN 01---17 02 09 52 42
CH 01 120.9 deg_C
CH 02 120.1 deg_C
CH 03 118.7 deg_C
CH 04 119.4 deg_C
CH 05 118.0 deg_C
CH 06 117.8 deg_C
CH 07 117.3 deg_C
CH 08 114.5 deg_C
CH 09 117.2 deg_C
CH 10 119.4 deg_C

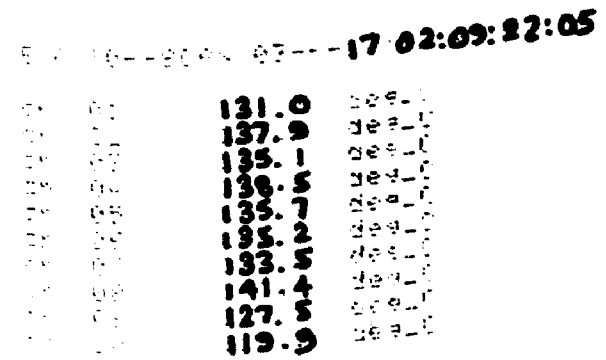

EXP 10--SCAN 04---17 02 09 1? 05
CH 01 175.2 deg_C
CH 02 146.3 deg_C
CH 03 144.2 deg_C
CH 04 150.4 deg_C
CH 05 146.5 deg_C
CH 06 145.8 deg_C
CH 07 142.8 deg_C
CH 08 140.9 deg_C
CH 09 132.2 deg_C
CH 10 120.6 deg_C

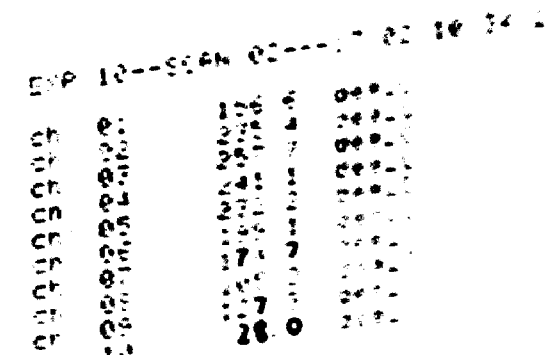

EXP 10--SCAN 01---17 02 09 52 06
CH 01 120.9 deg_C
CH 02 121.1 deg_C
CH 03 119.7 deg_C
CH 04 120.1 deg_C
CH 05 119.9 deg_C
CH 06 118.5 deg_C
CH 07 117.9 deg_C
CH 08 136.9 deg_C
CH 09 117.7 deg_C
CH 10 119.5 deg_C


EXP 10--SCAN 05---17 02 09 52 08
CH 01 140.9 deg_C
CH 02 155.9 deg_C
CH 03 159.7 deg_C
CH 04 172.2 deg_C
CH 05 165.6 deg_C
CH 06 164.0 deg_C
CH 07 157.1 deg_C
CH 08 164.3 deg_C
CH 09 138.5 deg_C
CH 10 121.7 deg_C


EXP 10--SCAN 02---17:02:09:07:05
126.9 deg_C
130.4 deg_C
127.8 deg_C
129.5 deg_C
127.5 deg_C
127.4 deg_C
136.0 deg_C
137.5 deg_C
122.3 deg_C
120.3 deg_C


EXP 10--SCAN 01---17 02 10 09 21


EXP 10--SCAN 07---17:02:09:22:05
131.0 deg_C
137.9 deg_C
135.1 deg_C
136.5 deg_C
135.7 deg_C
135.2 deg_C
133.5 deg_C
141.4 deg_C
127.5 deg_C
119.9 deg_C


EXP 10--SCAN 01---17 02 10 14 ??
26.0

A10.7 Ignition run 2

The results from this run were used in figure 7.4. The experimental conditions and model parameters used were as follows:

Coal particle size range	: -1.19 mm
Oven temeprature	: 100 ^{o}C
Oxygen flowrate	: 4.33 x 10^{-5} kmol/m^2/s
C	: 23
Bi_o	: 3.7
Bi_1	: 9.3
Bed voidage	: 0.38
k_o	: 4.9 m/s
E/R	: 7000 K
$D_e\rho_m$	: 1.42 x 10^{-13}
D_p	: 0.5 mm

25 02 10:15:50

ch:	01	deg_C
ch:	02	deg_C
ch:	03	deg_C
ch:	04	deg_C
ch:	05	deg_C
ch:	06	deg_C
ch:	07	deg_C
ch:	08	deg_C
ch:	09	deg_C
ch:	10	deg_C

EXP 05--SCAN 06---25 02 10 45 50

ch:	01	deg_C
ch:	02	deg_C
ch:	03	deg_C
ch:	04	deg_C
ch:	05	deg_C
ch:	06	deg_C
ch:	07	deg_C
ch:	08	deg_C
ch:	09	deg_C
ch:	10	

EXP 05--SCAN 07---25 02 11 15 50

ch:	01	deg_C
ch:	02	deg_C
ch:	03	deg_C
ch:	04	deg_C
ch:	05	deg_C
ch:	06	deg_C
ch:	07	deg_C
ch:	08	deg_C
ch:	09	deg_C
ch:	10	

EXP 05--SCAN 08---25 02 11 45 50

ch:	01	deg_C
ch:	02	deg_C
ch:	03	deg_C
ch:	04	deg_C
ch:	05	deg_C
ch:	06	deg_C
ch:	07	deg_C
ch:	08	deg_C
ch:	09	deg_C
ch:	10	

EXP 05--SCAN 09---25 02 12 15 50

ch:	01	deg_C
ch:	02	deg_C
ch:	03	deg_C
ch:	04	deg_C
ch:	05	deg_C
ch:	06	deg_C
ch:	07	deg_C
ch:	08	deg_C
ch:	09	deg_C
ch:	10	

APPENDIX 11 **MODEL PARAMETERS USED AS 'BASE CASE'**

The following model parameters have been used as the base-case:

k_o = 10 m/s

E_a/R = 7000 K

ϵ = .3

ΔH_r = 3 x 10^8 J/kmol

k_b = 0.2 W/m/K

$\hat{c}$ = 3 x 10^4 J/kmol/K

ρ_b = 900 kg/m^3

C_b = 1000 J/kg/K

P = 1.013 x 10^5 Pa

y_o = .21

L = 5 m

$h_1 = \sigma\,(T_\infty+T_o)(T_\infty^2+T_o^2)$

$h_2 = \sigma\,(T_\infty+T_e)(T_\infty^2+T_e^2)$

C = 0

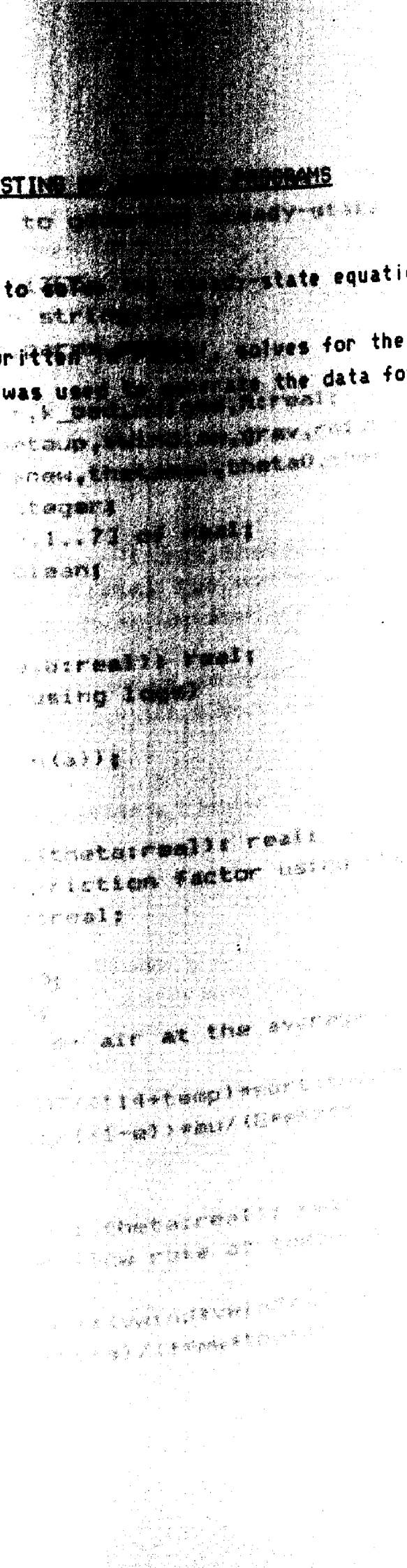
V = 0

APPENDIX 12 **LISTING**

A12.1 Program to

This program, written

solutions. It was used



```
program coal;
{Pascal program to generate steady-state stable solutions}

const pres = 1.013E5;
type string255 = string[255];
label startloop,parms,endp;
var
g,DelH,L,YO,Tinf,k_bed,msigma,R:real;
tad,thetalow,thetaup,vwind,mw,grav,roi,Eor,E,k0,S,dp,cp:real;
diff,theta,thetanew,thetamax,theta0,theta1,lhs,rhs:real;
imax,imin,i,j:integer;
tem:array[-1..10,1..7] of real;
ok,increased:boolean;
ch:char;

function power(a,b:real): real;
{calculates a^b using logs}
begin
  power:=exp(b*ln(a));
end;

function fricfac(theta:real): real;
{calculates the friction factor using the Ergun equation}
var mu,thet,temp:real;
begin
  temp:=theta*300;
  thet:=temp/273;
  {the viscosity of air at the average temperature}
  {Perry 3rd ed}
  mu:=1.709e-5*387/(114+temp)*sqrt(thet*thet*thet);
  FricFac:=180*sqr((1-e))*mu/(E*e*e*sqr(dp));
end;

function flowrate(f,theta:real): real;
{calculates molar flow rate at temperature theta}
begin
 flowrate:=sqr(roi)*(vwind*vwind/(2*1)+
 grav*(theta-1)/theta)/(f*mw*theta);
end;
```

```
procedure printparms;
{Prints the parameters with a heading}
var heading:string255;
begin
write('Heading for this run ? ');readln(heading);
writeln(lst,heading);
writeln(lst,'Voidage: ',e:4:1,' k0: ',k0:6:1,' E/R: ',eor*tinf:6:0);
writeln(lst,'Wind speed: ',vwind:4:1,' k_bed: ',k_bed*1000:4:1,
' Bed length: ',l:2:0);
writeln(lst);
end;

procedure calcall(var theta,thetabar,difference:real;flag:boolean);
{This routine calculates the difference between the LHS and}
{RHS of the equation at an average temperature theta}
label 330;
var expc,w,heat,deltheta0,deltheta1,Bi0,Bi1,f,p,
theta0n,theta1n,a2,a,c,a1,c2p,t,expma2,expa,c2a,c2,c1overam:real;
begin

  {Set up the parameters required}

  theta0:=theta;
  theta1:=theta;
  f:=fricfac(theta);
  p:=sqr(roi)*grav/(f*mw);
  w:=k0*6*(1-e)*l*f/(dp*grav*roi);
  heat:=msigma/(p*cp*mw);
  g:=flowrate(f,theta);
  a2:=w*theta*exp(-eor/theta)/(theta-1);
  a:=g*cp*l*mw/(k_bed);
  c:=delh*g*l/(tinf*k_bed);
  a1:=c*y0/(a2+a);
  if a2>80 then expma2:=0 else expma2:=exp(-a2);
  if abs(a)>80 then expa:=0 else expa:=exp(a);

  {Jump back here if the end temperatures don't converge}

330:  bi0:=msigma*((theta0)+1)*(sqr(theta0)+1)*l/k_bed;
  bi1:=msigma*((theta1)+1)*(sqr(theta1)+1)*l/k_bed;
```

```
c2a:=-a1*a2*exp                    (bi0+a)+a1*(1-expma2));
if a>80 then c2
c2:=c2a/(a*expa-                   +expa*bi1);
cloveram:=a1*a2/                   )*a1-c2+1;
if a>80 then c2p                   else c2p:=c2*expa;
theta0n:=clover
theta1n:=clover
t:=sqr(theta-1);
deltheta0:=abs(t
deltheta1:=abs(

{Check for conver                  temperatures}

if (1.e5/t*(sqr(                   sqr(deltheta1)))>1 then begin
  theta0:=(theta0n
  theta1:=(theta1n
  goto 330;
end;

{Calculate the LHS                 the energy balance}

lhs:=bi0*(theta0n-                 theta1n-1)/a+theta1n-1;
if a2>80 then rhs
rhs:=tad*(1-exp(-                  theta-1)*exp(-eor/theta)));

{Write answers on screen as a check for the operator}

writeln('Mean temperature guessed: ',theta*tinf:6:2);
thetabar:=cloveram*a2/a2*(expma2-1)+c2p/a-c2/a;
writeln('Mean temperature calculated ',thetabar*tinf:6:2);
difference:=lhs-rhs;
if ((a*a2/(a+a2))>80) then expc:=0 else expc:=exp(-a*a2/(a2+a));
thetamax:=cloveram*power((c*y0/a),(a/(a+a2)))*
          power((-c2p*(1+a/a2)),(a2/(a2+a)))*expc;
writeln('Flowrate ',g);
writeln('Inlet & outlet temps ',theta0n*tinf:6:2,' ',theta1n*tinf:6:

writeln('LHS ',lhs,' RHS  ',rhs);
writeln('Difference ',difference);
writeln('Maximum temperature  ',thetamax*tinf:6:2);
writeln;
end;
```

```
procedure PrintAnswers;
begin
  writeln(lst,'Mean temperature ',thetanew*tinf:6:2,
  '  Flowrate ',g);
  writeln(lst,'Inlet & outlet temps ',theta0*tinf:6:2,
  ' ',theta1*tinf:6:2);
  writeln(lst,'LHS ',lhs,' RHS ',rhs);
  writeln(lst,'Difference ',lhs-rhs);
  writeln(lst,'Maximum temperature ',thetamax*tinf:6:2);
  writeln(lst);
end;

{**** MAIN PROGRAM *****}
begin
  parms:
  {Parameters for the model}
  Tinf:=300;          {Ambient temperature}
  delh:=3.e5;         {Delta H reaction in kJ/kmol}
  mw:=30.;            {Molecular weight}
  l:=5;               {Bed length in metres}
  y0:=0.21;           {Mole fraction of oxygen in air}
  k_bed:=0.2e-3;      {Thermal conductivity in kW/m/K}
  Eor:=7000./tinf;    {Activation energy divided by (R T_ambient)}
  E:=0.3;             {Bed voidage}
  k0:=10.0;           {Surface rate constant in m/s}
  cp:=1.;             {Gas specific heat in kJ/kgK}
  roi:=1.2;           {density of ambient air in kg/m^3}
  {modified Stefan-Boltzmann constant}
  msigma:=5.67e-11*tinf*tinf*tinf;
  grav:=9.81;         {acceleration due to gravity}
  vwind:=0.1;         {wind velocity in m/s}
  R:=8.314e3;         {gas constant in kJ/kmol/K}
  gotoxy(1,1);
  writeLN('Do you want to print a heading ? ');read(kbd,ch);
  if upcase(ch)='Y'then printparms;      {Print the parameters}
  {Adiabatic dimensionless temperature rise}
  tad:=delh*y0/(cp*tinf*mw);
  write('Minimum loop counter ? ');readln(imin);
  write('Maximum loop counter ? ');readln(imax);
  if imin=imax then begin
     write('Particle size in mm ? ');readln(dp);
     dp:=dp/1000;
  end;

                                    answers are stored}
                                    i,j]:=0;
```

```
for j:=1 to 2 do begin

{if j=1 then calculations done on the upper branch
 if j=2 then calculations done on the lower branch}

theta:=3.0;if j=2 then theta:=1.01;  {initial guesses}
increased:=false;
for i:=imax downto imin do begin;
 if imin<>imax then begin
    dp:=i*2;
    if i=0 then dp:=0.4;
    if i=-1 then dp:=0.5;
    dp:=dp/1000;
 end;
 startloop:
 ClrScr;
 tem[i,4]:=dp;
 writeln('Particle size ',dp*1000:4:2);writeln;
 thetanew:=0;
 while (sqr(abs(theta-thetanew))>1.e-6) do begin
  calcall(theta,thetanew,diff,true);
  if (((thetanew*tin(j)>360) and (j=2)) then begin

  {The program was moving along the lower branch and then}
  {jumped onto the upper branch.}
  {Increase dp by 1mm and try again}

    if not(increased) then
    begin
      dp:=dp+1.e-3;
      increased:=true;
      theta:=1.05;          {initial guess}
      goto startloop;
    end else goto endp;   {if dp was already increased, exit}
  end;
  {Repeat calculation with new theta}
  theta:=0.4*thetanew+0.6*theta;
 end;
 tem[i,j]:=thetanew;
 tem[i,j+4]:=thetamax;
end;
end;
```

```
p:
teln(lst,'SUMMARY OF SOLUTIONS');
teln(lst);
teln(lst,'DP':5,'LOWER':9,'LOWER MAX':9,'UPPER':9,'UPPE
teln(lst);
 i:=imax downto imin do begin
riteln(lst,tem[i,4]*1000:5:1,tem[i,2]*tinf:9:2,tem[i,3]
ea[i,1]*tinf:9:2,tem[i,5]*tinf:9:2);
;
.
```

A12.2 Program to solve the unsteady-state equations for constant r

This program, written in BASIC, uses the analytical solution to solve for the time varying behaviour of the bed.

```
10    ! PROGRAM "                    YTIC SOLUTION
20    ! WITH A
30    OPTION BASE
40    DIM Beta(50)                   (50)
50    COM C(3),Dat                   (11),B(4),Phi(4)
60    PRINTER IS
70 Values:    ! THI                  all the constants and data used
80    MAT READ Cp                    ! N2
90    DATA 6.524,                    ! O2
100   DATA 6.148,
110   DATA 6.214,1                   ! CO2
120   DATA 4.18,                     ! C  NB:Cp=a + bT + c/T^2
130   ! THIS DATA I
140   MAT Cp=Cp*(4.                  J/kmol K
150   P=1.013E5 ! N/
160   ! Initial mole
170   C(1)=.79
180   C(2)=.21
190   C(3)=0
200   ! INITIAL
210    INPUT "Enter                  ,Te,Tavss
220   ! Convert                      atures
230   Ti=300                         nt temperature
240   T0=T0/Ti
250   Te=Te/Ti
260   Tavss=Tavss/
270   ! T0 is the
280   ! Tavss is
290   ! Te is the                    is the density of the ambient air in kg/m^3
300   CALL Density(Ti,               constant in J/kmol/K
310   R=8.314E3
320   E=.4                           particle size in mm
330   Dp=2                           !Surface per volume in m^-1
340   S=6000/Dp                      !Effective thermal conductivity in W/mK
350   Ke=.2                          !Path length in m
360   L=1                            !Modified Stefan-Boltzmann constant
370   Msig=5.67E-8                   !Density of bed in kg/m^3
380   Rho=900                        !Specific heat of bed in J/kg/K
390   Cps=1000                       !Viscosity in m^2/hr
400   ! Effective
410   Kappa=Ke*3600/(Rho*Cps)        !+.448*((.35/.25)^2-1)*500*Cps)
420   K0=0/3600                      !Pre-exponential factor in m/s
430   Eor=0                          !Activation energy/R in K
440   G=9.81                         !Acceleration due to gravity in m/s^2
450   Hc=.76                         !Heat transfer coefficient in W/m^2/K
460   Radius=.25                     !Radius of bed
470   C=0                            !Heat loss coefficient
480   Power=0                        !Power input to heater in W
490   Df=Power*L/(PI*Radius^2*Msig*Ti) !Dimensionless flux
```

```
500  ! Write data into array Dat for passing to subroutines
510  Dat(1)=Roi
520  Dat(2)=R
530  Dat(3)=E
540  Dat(4)=Dp
550  Dat(5)=S
560  Dat(6)=P
570  Dat(7)=Ke
580  Dat(8)=Msig
590  Dat(9)=K0
600  Dat(10)=Eor
610  Dat(11)=L
620  Dat(12)=G
630  Dat(13)=C
640  Dat(14)=Ti
650  Dat(15)=Df!
660  ! Input name of file into which values are written
670  INPUT "Name of data file",Name$
680  ! Print initial values and constants
690  PRINTER IS 7,1,WIDTH(80)
700  PRINT CHR$(27);"&dD";"METHOD OF SOLUTION:";CHR$(27);"&dE";" ANALYTIC SOLU
ON WITH RATE CONSTANT AT I ev"
710  PRINT LIN(2);"Rav set to a constant to check methods"
720  PRINT LIN(2);CHR$(27);"&dD";"BED CONSTANTS";CHR$(27);"&dE"
730  PRINT LIN(1);"Particle size=";Dp;"mm",,"Voidage=";E
740  PRINT LIN(1);"Bed radius=";Radius;"m",,"Bed length=";L;"m"
750  PRINT LIN(1);"Power input=";Power;"W",,"Loss coefficient=";C
760  PRINT USING "/4A,X,4D,X,A,29X,4A,X,D.DDDE,X,4A";"E/R=";Eor;"K",,"K0=";K0
0;"m/hr"
770  PRINT LIN(1);"Bed density=";Rho;"kg/m^3","Cp of bed=";Cps;"J/kg/K"
780  PRINT USING "/12A,X,D.DDDE,X,6A";"Diffusivity=";Kappa;"m^2/hr"
790  ! PRINT LIN(1);"Name of data file is ";Name$
800  ! PRINT PAGE
810  PRINTER IS 16
820  ! Calculate  predicted steady state profile
830  CALL Tsteady(Tavss,T0,Te,Tmax)
850  ! Tmax is used to give upper limit for "PLOT"
860  Tup=100*INT(Tmax*Ti/100+.5)
870  ! Write steady state profile into matrix T as first element
880  FOR I=1 TO 11
890     T(I,1)=Z(1)
900  NEXT I
910  ! Input Tin which is the initial bed temperature
920  INPUT "Initial temperature?",Tin
930  Tin=Tin/Ti
940  T0=Tin
950  Te=Tin
960   PRINTER IS 7,1,WIDTH(80)
970  PRINT CHR$(27);"&dD";"UNSTEADY STATE SOLUTION";CHR$(27);"&dE"   Initial tem
erature=";INT(Tin*Ti+.5);"K"
980  PRINTER IS 16
990  Ta=Tin          !For the first time slice
1010 ! Decide on time scaling
1020 Dtmax=Ti*ABS(Tavss-Tin)
1030 PRINT "The difference in average temperatures is ";Dtmax
1040 Reinput:  INPUT "Maximum temperature rise per time slice?",Delt
1050    Lastj=INT(Dtmax/Delt)+1  !Lastj is the number of curves
1060    PRINT "This gives ";Lastj;" curves (including steady state). Is this O K
?"
1070    A$=""
1080    INPUT A$
1090 IF A$="N" THEN Reinput !
```

```
1100 ! Initialize the array Beta to (N-1)*PI except for the first value
1110 Beta(1)=PI/2
1120 FOR N=2 TO 50
1130    Beta(N)=(N-1)*PI
1140 NEXT N
1150 Time=2              !First time at which calculation is done
1160 Lastj=50
1170 FOR J=2 TO Lastj    !Outer loop for time increments
1180    ! Put time into matrix
1190    Tim(J)=Time
1200    ! Calculate flowrate and reaction rate based on average temperature
1210    Tai=Ta*Ti
1220    CALL Darcy(Tai,Fr)
1230    CALL Cp(Tai,Cpav)
1240    CALL H_react(Tai,Delh)
1250    ! Calculate dimensionless flow number
1260    Dfn=L*Roi*G*P*Cpav/(Fr*R*Ti*Ke)
1270    A=Dfn*((Ta-1)/Ta/Ta)
1280    Gg=A*Ke/(Cpav*L)
1290    ! Calculate dimensionless reaction number
1300    Rav=K0*EXP(-Eor/Tai)*P*(1-E)*S/(R*Tai)
1310  ! Rav=5E-7
1320    B=Rav*Delh*L*L*C(2)/(Ke*Ti)
1330    M=Rav*L/Gg
1340    ! Calculate values for 'steady state' coefficients
1350    IF Df=0 THEN CALL Coe(A,B,C,R1,R2,M,T0,Te,C1,C2,C3,Bi0,Bi1,0)
1360    IF Df<>0 THEN CALL Coe2(A,B,C,R1,R2,M,T0,Te,C1,C2,C3,Bi0,Bi1,Df)
1370    Hi=Bi0+A/2
1380    H2=Bi1+A/2
1390    ! Calculte constants needed for unsteady state profile
1400    Kt=Kappa*Time
1410    Inter=EXP(-Kt*A*A/4-C*Kt)
1420    V=0
1430    FOR N=1 TO 20
1440            CALL Integral(Beta(N),N,H1,H2,A,B,C,R1,R2,M,C1,C2,C3,Tin,In(N))
1450            ! Calculate and print 'V' at 1 as a check for convergence
1460            Zn=Beta(N)*COS(Beta(N))+H1*SIN(Beta(N))
1470            V=V+In(N)*Zn*EXP(-Kt*Beta(N)^2)
1480            PRINT N,V
1490    NEXT N
1500    V1=V
1510     ! Calculate unsteady state profile
1520     FOR I=0 TO 9
1530        X=I/10
1540        V=0
1550        FOR N=1 TO 20
1560              Betax=Beta(N)*X
1570              Zn=Beta(N)*COS(Betax)+H1*SIN(Betax)
1580              V=V+In(N)*Zn*EXP(-Kt*Beta(N)^2)
1590        NEXT N
1600        CALL Temp(X,Tss,R1,R2,M,C1,C2,C3)!Tss is the steady state temperature
1610        Z(I+1)=Tss
1620        T(I+1,J)=Tss+V*Inter*EXP(A*X/2)
1630     NEXT I
1640     ! The value of 'V' at the exit is V1
1650     CALL Temp(1,Tss,R1,R2,M,C1,C2,C3)
1660     Z(11)=Tss
1670     T(11,J)=Tss+V1*Inter*EXP(A/2)
1680     T0=T(1,J)
1690     Te=T(11,J)!
```

```
1700     ! Print heading on printer
1710      PRINTER IS 7,1,WIDTH(80)
1720     PRINT LIN(2);CHR$(27);"&dD";"TIME=";Time;"hrs";CHR$(27);"&d@"
1730     ! Call subroutine to print 'constants'
1740     CALL Print(Ta*Ti,Rav,Delh,Cpav,Fr,Gg,Bi0,Bi1,A,B)
1750     ! Calculate average bed temperature & print profile
1760     PRINT LIN(1);"X (m)","TEMPERATURE (K)","   T ss(K)","    Y02"
1770     FOR I=1 TO 11
1780        Y(I)=T(I,J)
1790        Xx=I/10-.1
1800        PRINT Xx,Y(I)*Ti,Z(I)*Ti,.21*EXP(-M*Xx)
1810     NEXT I
1820     ! Throw a page if J is odd
1830     IF FRACT(J/2)<>0 THEN PRINT PAGE
1840     PRINTER IS 16
1850     CALL Simpson(Ta)
1860     ! Calculate time step using exponential scaling
1870    Del_time=LOG((Lastj+2-J)/(Lastj+1-J))/(Kappa*Beta(1)^2)
1880    Time=Time+PROUND(Del_time,0)
1900    PRINT "NEXT TIME IS";Time;"hrs","TAV=";Ta*Ti
1910 NEXT J
1920 STOP
1930 ! Write temperature profiles onto tape for plotting
1940 Record: Recl=INT((11+23*Lastj)/32)+1   !This number is the record length
1950 GOTO 2150
1960 CREATE Name$,Recl
1970 ASSIGN #1 TO Name$
1980 PRINT #1;Lastj+2
1990 ! Set upper and lower limits
2000 PRINT #1;2
2010 PRINT #1;0,Ti
2020 PRINT #1;1,Tup
2030 ! Put initial temperature on tape
2040     PRINT #1;2
2050     PRINT #1;0,Tin*Ti
2060     PRINT #1;1,Tin*Ti
2070 ! Put array T onto tape                !Lastj is the number of curves
2080 FOR J=1 TO Lastj                      !Number of points
2090     PRINT #1;11
2100     FOR I=1 TO 11                     !Point
2110        PRINT #1;I/10-.1,T(I,J)*Ti
2120     NEXT I
2130 NEXT J
2140 ASSIGN #1 TO *
2150 ! Put temperature vs. time plot on tape
2160 CREATE Name$&"T",Recl
2170 ASSIGN #2 TO Name$&"T"
2180 PRINT #2;12
2190 PRINT #2;2
2200 PRINT #2;0,300
2210 PRINT #2;Tim(Lastj),Tup
2220 FOR I=1 TO 11
2230 PRINT #2;Lastj
2240 PRINT #2;0,Tin*Ti
2250 FOR J=2 TO Lastj
2260 PRINT #2;Tim(J),T(I,J)*Ti
2270 NEXT J
2280 NEXT I
2290 ASSIGN #2 TO *
2300 STOP !
```

```
2310 Tsteady:  SUB Tsteady(Ta,T0,Te,Tmax)
2320 OPTION BASE 1
2330 ! This subroutine calculates the steady state temperature profile
2340 ! It is quite separate to the calculation of the unsteady state profiles
2350 COM C(3),Data(20),Cp(4,3),Y(11),T(11)
2360 ! Give variables in array 'Data' desriptive names
2370 Roi=Data(1)
2380 R=Data(2)
2390 E=Data(3)
2400 Dp=Data(4)
2410 S=Data(5)
2420 P=Data(6)
2430 Ke=Data(7)
2440 Msig=Data(8)
2450 K0=Data(9)
2460 Eor=Data(10)
2470 L=Data(11)
2480 G=Data(12)
2490 C=Data(13)
2500 Ti=Data(14)
2510 Df=Data(15)
2520 ! Make estimates of flowrate & reaction rate constant
2530 Tai=Ta*Ti
2540 Rav=K0*EXP(-Eor/Tai)*P*(1-E)*S/(R*Tai)
2550 Rav=1E-5
2560 CALL Darcy(Tai,Fr)
2570 Gg=P*Roi*G/(Fr*R*Tai)*(1-1/Ta)
2580 ! Outer loop which iterates for reaction rate constant
2590 Calc_rate: Tai=Ta*Ti
2600   CALL Darcy(Tai,Fr)
2610   CALL Cp(Tai,Cpav)
2620   CALL H_react(Tai,Delh)
2630   B=Rav*Delh*C(2)*L*L/(Ke*Ti)
2640   ! Inner loop to calculate flowrate
2650 Calc_flow:     A=Gg*Cpav*L/Ke
2660     M=Rav*L/Gg
2670     IF Df=0 THEN CALL Coe(A,B,C,R1,R2,M,T0,Te,C1,C2,C3,Bi0,Bi1,1)
2680     IF Df<>0 THEN CALL Coe2(A,B,C,R1,R2,M,T0,Te,C1,C2,C3,Bi0,Bi1,Df)
2690     PRINT "T0=";T0*Ti,"G=";Gg
2700     ! Calculate temperature at 11 points
2710     FOR I=0 TO 10
2720       X=I/10
2730       CALL Temp(X,T,R1,R2,M,C1,C2,C3)
2740       T(I+1)=T
2750       Y(I+1)=1/T
2760     NEXT I
2770     ! Calculate integral of T^-1 using Simpson's Rule
2780     CALL Simpson(Di1)
2790     ! Calculate integral of T analytically
2800     CALL Intt(It,R1,R2,M,C1,C2,C3,C)
2810     ! Calclulate new flowrate
2820     Gg1=P*G*Roi*(1-Di1)/(Fr*R*It*Ti)
2830     Dif=ABS(Gg1-Gg)
2840     Gg=.8*Gg1+.2*Gg
2850     ! Check for convergence of flowrate
2860     IF Dif>Gg/500 THEN GOTO Calc_flow
2870   ! Calculate new end temperature and rate expression
2880   Dif1=ABS(Te-T(11))
2890   Te=T(11)!
```

```
2900   GOTO 3000
2910   ! Evaluate exp(-E/(RT))/T numerically
2920    FOR I=1 TO 11
2930       Temp=T(I)*Ti
2940       Y(I)=EXP(-Eor/Temp)/Temp
2950    NEXT I
2960    CALL Simpson(Di2)
2970    Rav1=K0*P*Di2*S*(1-E)/R
2980    Dif=ABS(Rav-Rav1)
2990    Rav=.8*Rav1+.2*Rav
3000    Ta=It
3010    PRINT "T av=";Ta*Ti,,"RAV=";Rav
3020 ! Check for convergence
3030 IF (Dif)Rav/500) OR (Dif1).001) THEN GOTO Calc_rate
3040 ! The iteration is finished
3050 Tmax=T(1)
3060 ! Calculate maximum temperature if Flux=0
3070 IF Df=0 THEN CALL Tmax(Xmax,Tmax,R1,R2,M,C1,C2,C3)
3080 ! Print steady state profile & constants
3090  PRINTER IS 7,1,WIDTH(80)
3100 PRINT LIN(2);CHR$(27);"&dD";"STEADY STATE SOLUTION";CHR$(27);"&d@"
3110 CALL Print(Ta*Ti,Rav,Delh,Cpav,Fr,Gg,Bi0,Bi1,A,B)
3120 PRINT LIN(1);"X    ","TEMPERATURE (K)"
3130 FOR I=0 TO 10
3140 PRINT I/10,T(I+1)*Ti
3150 NEXT I
3160 PRINT LIN(1);"T max=";Tmax*Ti;"K @ X=";Xmax;
3170 ! Check on overall energy balance
3180 Hr=Bi0*(T0-1)+Bi1*(Te-1)+A*(Te-1)+C*(It-1)
3190 Hg=B/M*(1-EXP(-M))+Df
3200 PRINT LIN(1);"HR=";Hr,,"HG=";Hg
3210  PRINT PAGE
3220  PRINTER IS 16
3230 SUBEND !
```

```
3240 SUB Cp(T,Cpav)
3250 OPTION BASE 1
3260 COM C(3),Data(20),Cp0(4,3)
3270 DIM Cp(3)
3280 ! Cp's in J/kmol K FOR T IN K:
3290 MAT Cp=(0)
3300 FOR I=1 TO 3
3310 FOR J=1 TO 3
3320 Cp(I)=Cp(I)+Cp0(I,J)*T^(J-1)
3330 NEXT J
3340 NEXT I
3350 ! C(*) IS VECTOR OF MOL FRACTIONS, SO
3360 Cpav=DOT(C,Cp)
3370 SUBEND !


3380 SUB Density(T,P,Ro,Mass)
3390 OPTION BASE 1
3400 COM C(3)
3410 DIM Mwt(3)
3420 Mwt(1)=28   ! N2
3430 Mwt(2)=32   ! O2
3440 Mwt(3)=44   ! CO2
3450 ! C(*) IS VECTOR OF MOL FRACTIONS, SO FOR 1 MOL:
3460 Mass=DOT(C,Mwt)
3470 R=8.3E3    ! J/kmol K
3480 Vol=R*T/P
3490 Ro=Mass/Vol    ! kg/m3
3500 SUBEND !


3510 SUB Darcy(T,Darcy)
3520 OPTION BASE 1
3530 COM C(3),Data(20)
3540 E=Data(3)
3550 D=Data(4)
3560 S=Data(5)
3570 ! T = TEMP K
3580 ! D = PARTICLE DIAM m
3590 ! E = VOIDAGE
3600 ! S = PARTICLE AREA/VOLUME
3610 CALL Viscosity(T,Mu)
3620 K=5
3630 Darcy=K*(1-E)^2*Mu*S^2/E^3
3640 SUBEND !


3650 SUB Viscosity(T,Mu)
3660 ! VISCOSITY OF AIR
3670 ! PERRY THIRD ED P 370
3680 C=114
3690 Mu0=.01709                                    ! IN cp FOR T IN K
3700 Mu=Mu0*(273.1+C)/(T+C)*(T/273.1)^1.5
3710 Mu=Mu/1000    ! IN kg/m s
3720 SUBEND !
```

```
3730 SUB H_react(T,Delh)
3740 ! Subroutine to calculate Delta H reaction
3750 OPTION BASE 1
3760 COM X(3),Data(20),Cp(4,3)
3770 Delta_h_0=-9.4E7*4.18  !J/kmol !Enthalpy of formation of CO2
3780 Ho2=0
3790 Hco2=0
3800 T0=298
3810 I=2  !2 refers to CO2
3820 FOR J=1 TO 3     ! CP = CP(I,1)+CP(I,2)*T+CP(1,3)*T^2
3830 Ho2=Ho2+Cp(I,J)*(T^J-T0^J)/J
3840 NEXT J
3850 I=3 !3 refers to O2
3860 FOR J=1 TO 3     ! CP = CP(I,1)+CP(I,2)*T+CP(I,3)*T^2
3870 Hco2=Hco2+Cp(I,J)*(T^J-T0^J)/J
3880 NEXT J
3890 ! Enthalpy of Carbon with Cp=Cp(4,1)+Cp(4,2)*T+Cp(4,3)*T^-2
3900 Hc=Cp(4,1)*(T-T0)+Cp(4,2)/2*(T^2-T0^2)-Cp(4,3)*(1/T-1/T0)
3910 Delh=Ho2-Hco2+Hc-Delta_h_0
3920 ! This is actually -Delta H reaction
3930 SUBEND !


3940 Temp: SUB Temp(X,T,R1,R2,M,C1,C2,C3)
3950 ! Steady state temperature expression
3960 T=1+C1*EXP(R1*X)+C2*EXP(R2*X)+C3*EXP(-M*X)
3970 SUBEND !


3980 SUB Intt(It,R1,R2,M,C1,C2,C3,C)
3990 ! Calculates the integral of T
4000 It=1+C1+C2/R2*(EXP(R2)-1)-C3/M*(EXP(-M)-1)
4010 IF C<>0 THEN It=It-C1*(1-(EXP(R1)-1)/R1)
4020 SUBEND!


4030 Simp: SUB Simpson(Di)
4040    ! Simpson's Rule for 11 evenly spaced points on interval length 1
4050    OPTION BASE 1
4060    COM C(3),Dat(20),Cp(4,3),Y(11),T(11)
4070    LET Di=Y(1)+Y(11)
4080    FOR J=2 TO 10
4090       Di=Di+2*Y(J)
4100       IF J/2-INT(J/2)=0 THEN Di=Di+2*Y(J)
4110    NEXT J
4120    Di=Di/30
4130 SUBEND !
```

```
4140 In: SUB Integral(Beta,N,H1,H2,A,B,C,R1,R2,M,C1,C2,C3,Tin,In)
4150 ! Calculates the coefficient of the series
4160 OPTION BASE 1
4170 COM C(3),Dat(20),Cp(4,3),Y(11),Z(11),B(4),Phi(4)
4180 ! Calculate value of Beta  using succesive substitution
4190 ! Best estimate for Beta  is the one from the previous time slice
4200 Mult=H1*H2
4210 Add=H1+H2
4220 Pre=N*PI-PI/2
4230 Again: X1=Pre-ATN((Beta*Beta-Mult)/(Add*Beta))
4240    Dif=ABS(X1-Beta)
4250    Beta=X1
4260    ! Note strict convergence criterion for acceptable accuracy
4270 IF Dif)1E-8 THEN Again
4280 B(1)=-C1
4290 B(2)=-C2
4300 B(3)=-C3
4310 B(4)=Tin-1
4320 Phi(1)=R1-A/2
4330 Phi(2)=R2-A/2
4340 Phi(3)=-M-A/2
4350 Phi(4)=-A/2
4360 An=2*(Beta^2+H2^2)/((Beta^2+H1^2)*(Beta^2+H2^2+H2)+H1*(Beta^2+H2^2))
4370 In=0
4380 FOR I=1 TO 4
4390    Im=Beta*(EXP(Phi(I))*(Phi(I)*COS(Beta)+Beta*SIN(Beta))-Phi(I))
4400    Im=Im+H1*(EXP(Phi(I))*(Phi(I)*SIN(Beta)-Beta*COS(Beta))+Beta)
4410    Im=Im*B(I)/(Phi(I)^2+Beta^2)
4420    In=In+Im
4430 NEXT I
4440 In=In*An
4450 SUBEND !


4460 Coe: SUB Coe(A,B,C,R1,R2,M,T0,Te,C1,C2,C3,Bi0,Bi1,Flag)
4470 ! Calculates the coefficients in the steady state temperature equation
4480 OPTION BASE 1
4490 COM C(3),Data(20)
4500 Ke=Data(7)
4510 Msig=Data(8)
4520 Bi1=Msig*(Te*Te+1)*(Te+1)
4530 R1=(A-SQR(A*A+4*C))/2
4540 R2=(A+SQR(A*A+4*C))/2
4550 Again: Bi0=(T0+1)*(T0*T0+1)*Msig
4560    C3=-B/(M*M+A*M-C)
4570    C2=1/((R1+Bi1)*(A+Bi0-R2)*EXP(R1)+(R2+Bi1)*(R1-A-Bi0)*EXP(R2))
4580    C2=C2*C3*((M-Bi1)*(R1-A-Bi0)*EXP(-M)-(R1+Bi1)*(M+Bi0+A)*EXP(R1))
4590    C1=(C2*(A+Bi0-R2)+C3*(A+Bi0+M))/(R1-A-Bi0)
4600    CALL Temp(0,T,R1,R2,M,C1,C2,C3)
4610    Dif=ABS(T-T0)
4620    T0=T
4630    ! Check for convergence but  only iterate if doing 'proper'
4640    ! steady state calculation
4650 IF (Dif).001) AND (Flag=1) THEN Again
4660 SUBEND !
```

```
4670 Tmax: SUB Tmax(X,Tmax,R1,R2,M,C1,C2,C3)
4680 ! Subprogram to find maximum temperature and where it occurs
4690 ! Method used is Newton-Raphson
4700 X=.5
4710 Recalc: D2tdx2=C1*R1*R1*EXP(R1*X)+C2*R2*R2*EXP(R2*X)+C3*M*M*EXP(-M*X)
4720         Dtdx=C1*R1*EXP(R1*X)+C2*R2*EXP(R2*X)-C3*M*EXP(-M*X)
4730         X1=X-Dtdx/D2tdx2
4740         Dif=ABS(X1-X)
4750         X=X1
4760 IF Dif).01 THEN Recalc
4770 CALL Temp(X,Tmax,R1,R2,M,C1,C2,C3)
4780 SUBEND !


4790 Prnt: SUB Print(Ta,Rav,Delh,Cp,Fr,Gg,Bi0,Bi1,A,B)
4800 ! Subroutine to print 'constants'
4810 PRINT LIN(1);"T average=";PROUND(Ta,-2);"K",,"RAV=";Rav;"kmol/m^3/s"
4820 PRINT LIN(1);"DELTA H REACTION=";INT(Delh+.5);"J/kmol","CP=";INT(Cp+.5);"J/
kmol/K"
4830 PRINT LIN(1);"DARCY'S CONSTANT=";INT(Fr+.5);"kg/m^2/s"  !?
4840 PRINT LIN(1);"FLOWRATE=";Gg;"kmol/m^2/s"
4850 PRINT LIN(1);"BI0=";Bi0,"BIi=";Bi1
4860 PRINT LIN(1);"A=";A,,"B=";B
4870 SUBEND !


4880 Coe2: SUB Coe2(A,B,C,R1,R2,M,T0,Te,C1,C2,C3,Bi0,Bi1,Df)
4890 ! Calculates the coefficients in the steady state temperature equation
4900 ! for the case of heating on the bottom
4910 OPTION BASE 1
4920 COM C(3),Data(20)
4930 Ke=Data(7)
4940 Msig=Data(8)
4950 ! Bi0 is due to the glass wool insulation
4960 Bi0=120
4970 Bi1=Msig*(Te*Te+1)*(Te+1)
4980 R1=(A-SQR(A*A+4*C))/2
4990 R2=(A+SQR(A*A+4*C))/2
5000 C3=-B/(M*M+A*M-C)
5010 C2=C3*((M-Bi1)*(R1-A-Bi0)*EXP(-M)-(R1+Bi1)*(A+Bi0+M)*EXP(R1))+Df*(R1+Bi1)*E
XP(R1)
5020 C2=C2/((R1+Bi1)*(A+Bi0-R2)*EXP(R1)+(R2+Bi1)*(R1-A-Bi0)*EXP(R2))
5030 C1=(C2*(A+Bi0-R2)+C3*(A+Bi0+M)-Df)/(R1-A-Bi0)
5040 CALL Temp(0,T0,R1,R2,M,C1,C2,C3)
5050 SUBEND !
```

A12.3 Program to solve the equations numerically

This program, written in BASIC, uses the method of lines to solve the equations without the assumption of constant r.

```
10   ! PROGRAM "LIN" WHICH DOES CALCULATIONS AT THE ROOTS OF THE NITH
20   ! ORDER LEGENDRE POLYNOMIAL
30    OPTION BASE 1
40    DIM Th(15),Yo2(15),Z(15),Temp(15,25),Tim(25)
60    N1=15                          !Number of lines
70    REDIM Th(N1),Yo2(N1),Z(N1),Temp(N1,20),X(N1),Aw(N1,N1),A2w(N1,N1)
75    COM Cc(3),Dat(25),Cp(4,3),Aw(15,15),A2w(15,15),X(15),U(15),Ks(15),Rate(15)
80   ! Read the matrix of the nodes of the polynomial from tape
81    OFF ERROR
90    ASSIGN @F1 TO "X"&VAL$(N1)
100   ENTER @F1;X(*)
101   ASSIGN @F1 TO *
110  ! Read the matrix of coefficients from tape
120   ASSIGN @F1 TO "MAT"&VAL$(N1)
130   ENTER @F1;Aw(*)
131   ASSIGN @F1 TO *
140  ! Calculate the matrix AW*AW for 2nd derivatives
150   MAT A2w= Aw*Aw
160   Dif=X(N1)-X(1)          !Scaling factor since nodes are not at 0 and 1
170  ! Calculate the matrix Z which contains rescaled x values
180   FOR I=1 TO N1
190     Z(I)=(X(I)-X(1))/Dif
200   NEXT I
210 Values:  ! This section contains all the constants and data used
290   P=1.013E+5                      ! N/m2 = 1 ATM
300  ! Initial mole fractions
310   Cc(1)=.79                       !N2
320   Cc(2)=.21                       !O2
330   Cc(3)=0                         !CO2
340 Restart:PRINTER IS 1
350   MAT U= (0)
360   Ti=300                          !Ambient temperature
370   CALL Density(Ti,P,Roi,W)        !Roi is the density of the ambient air in kg/m^3
380   R=8.314E+3                      !Gas Constant in J/kmol/K
390   E=.3                            !Voidage
400   Dp=6                            !Particle size in mm
410   S=6000/Dp                       !Surface per volume in m^-1
420   Ke=.2                           !Effective thermal conductivity in W/mK
430   L=5                             !Bed length in m
440   Msig=5.67E-8*Ti^3*L/Ke          !Modified Stefan-Boltzmann constant
450   Rho=900                         !Density of bed in kg/m^3
460   Cps=1000                        !Specific heat of bed in J/kg/K
470   Kappa=Ke*3600/(Rho*Cps)         !Effective thermal diffusivity in m^2/hr
480   Drho=1.E+99                     !Constant for shrinking core (1E99 = no ageing)
490   K0=10                           !Pre-exponential factor in m/s
500   Eor=7000                        !Activation energy/R in K
510   Vwind=0                         !Wind velocity in m/s
520   G=9.81                          !Acceleration due to gravity in m/s^2
530   Radius=0                        !Radius of bed
540   C=0                             !Heat loss coefficient
550 Time:Delt=60                      !Size of time step in hours
560    Deltau=Delt*Kappa/L/L          !Dimensionless time step
```

```
561   Time0=0
570   Time=Time0                    !First time at which calculation is done
580   Lastj=50                      !Number of times calculation is performed
590   Skip=10                       !Not every point is stored and recorded
600   Lastr=Lastj/Skip              !Number of profiles to be recorded
610   REDIM Tim(Lastr+1)
611   REDIM Temp(N1,Lastr+1)
620 ! Write data into array Dat for passing to subroutines
630   Dat(1)=Roi
640   Dat(2)=R
650   Dat(3)=E
660   Dat(4)=Dp
670   Dat(5)=S
680   Dat(6)=P
690   Dat(7)=Ke
700   Dat(8)=Msig
710   Dat(9)=K0
720   Dat(10)=Eor
730   Dat(11)=L
740   Dat(12)=G
750   Dat(13)=C
760   Dat(14)=Ti
770   Dat(15)=Df
780   Dat(16)=N1
790   Dat(19)=Kappa
800   Dat(20)=Dif
810   Dat(21)=Vwind
820   Dat(25)=Drho
830 ! Input name of file into which values are written
840   INPUT "Name of data file",Name$
850 ! Print initial values and constants
860 Prntc:  PRINTER IS 9;WIDTH (2000)
870   PRINT RPT$("
                 ",2);N1;"TH ORDER LEGENDRE POLYNOMIAL-MARCHING BY RUNGE-KUTTA"
880   PRINT RPT$("
                 ",2);"BED CONSTANTS"
890   PRINT RPT$("
                 ",1);"Particle size=";Dp;"mm","Voidage=";E
900   PRINT RPT$("
                 ",1);"Bed length=";L;"m"
910   IF Drho()1.E+99 THEN PRINT USING "/16A,D.DDE";"Ageing factor=";Drho
920   PRINT USING "/,4A,X,4D,X,A,29X,3A,X,DDDD.DD,X,4A";"E/R=";Eor;"K","K0=";K0 "
930   PRINT RPT$("
                 ",1);"Bed density=";Rho;"kg/m^3","Cp of bed=";Cps;"J/kg/K"
940   PRINT USING "/,21A,D.DDDE,X,6A";"Thermal Diffusivity=";Kappa;"m^2/hr"
950 ! PRINT RPT$("
                 ",1);"Wind velocity=";Vwind;"m/s"
960   PRINT RPT$("
                 ",1);"Name of data file:";Name$
970   PRINT RPT$("
                 ",1);"Size of time step:";Delt;"hrs","Number of lines:";N1
971   PRINT RPT$("
                 ",1);"Number of time steps=";Lastj,"Every";Skip;"th recorded"
980   PRINT CHR$(12)
990   PRINTER IS 1
991   A$=""
992   Time0=0
1000  INPUT "DO YOU WANT TO INPUT A TEMPERATURE PROFILE?",A$
1010  IF A$()"Y" THEN GOTO 1100
1020  FOR I=1 TO N1
1030    PRINT "T(";I;") IN K?"
1040    INPUT Th(I)
```

```
1060  MAT Th= Th/(Ti)
1070  INPUT "TIME0 IN HOURS?",Time0
1071  Time=Time0
1080  CALL Tav(Th(*),Ta)
1090  GOTO 1150
1100 ! Input Tin which is the initial bed temperature
1110  INPUT "Initial temperature?",Tin
1120  Tin=Tin/Ti  !Made dimensionless
1130  Ta=Tin!For the first time slice the average temperature is the initial
1140  MAT Th= (Tin)!Th is the matrix that contains the dimensionless temperature
1150  MAT Yo2= (Cc(2))  !Yo2 is the matrix that contains the oxygen profile
1160 ! Store initial temperature profile
1170  FOR I=1 TO N1
1180    Temp(I,1)=Th(I)*Ti
1190  NEXT I
1200  Tim(1)=Time0        !First time
1210  Pflag=1             !Flag to control printing
1220  Nprint=0            !Counter to control output
1250 !
1260 Startloop:FOR J=1 TO Lastj    !Outer loop for time increments
1270    PRINTER IS 9;WIDTH (2000)
1280    ! Calculate flowrate based on average temperature
1290    Tai=Ta*Ti
1300    CALL Darcy(Tai,Fr)
1310    Gg=P*Roi/(Fr*R*Tai)*(G*(1-Ti/Tai)+Vwind^2/L/2)
1320    Dat(18)=Gg
1330    ! Call program to march forward
1340    ! March2 marches forward using forward differences
1350    ! March uses a 4th order Runge Kutta algorithm
1360    CALL March2(Th(*),Yo2(*),Deltau)
1370    ! Call subroutine to calculate O2 profile
1380    CALL Newo2(Yo2(*),Th(*))!
```

```
1381    IF (Th(1))1) AND (Th(N1))1) THEN GOTO 1390!CHECK TO SE IF UNSTABLE
1382    PRINTER IS 1
1383    BEEP
1385    PRINT "WARNING: TIME=";Time;"T0=";Th(1)*Ti;"TE=";Th(N1)*Ti
1386    Th(1)=1
1387    Th(N1)=1
1389    PRINTER IS 9;WIDTH (2000)
1390    IF J MOD Skip()0 THEN GOTO 1560
1400    FOR I=1 TO N1
1410      Temp(I,J/Skip+1)=Th(I)*Ti
1420    NEXT I
1430    IF Pflag=0 THEN GOTO 1560
1440    PRINT RPT$("
                   ",2);"TIME=";Time+Delt;"hrs"
1450    ! The Biot numbers are now in the matrix Dat
1460    Bi0=Dat(21)
1470    Bi1=Dat(22)
1480    ! Call subroutine to print 'constants'
1490    CALL Print(Ta*Ti,Fr,Gg,Bi0,Bi1)
1500    ! Calculate average bed temperature & print profile
1510    PRINT RPT$("
                   ",1);"  X","TEMPERATURE (K)","  Y02"
1520    FOR I=1 TO N1
1530      PRINT USING "Z.DDD,17X,DDDD.DDD,11X,.DDDD,4D,5X,4D";Z(1),Temp(I,J/Skip+
1540    NEXT I
1550    ! Calculate the average dimensionless temperature
1560    CALL Tav(Th(*),Ta)
1570    ! Rescale Ta
1580    Ta=Ta/Dif
1590    ! Throw a page if J is a multiple of 2
1600    IF (J/Skip MOD 3=0) AND (Pflag=1) THEN PRINT CHR$(12)
1610    IF Pflag=0 THEN PRINT USING "#,X,5A,DD.D,X,2A,DDD.DDD";"DAY=",Time/24,"!=
1620    Nprint=Nprint+1
1630    IF (Nprint MOD 4=0) AND (Pflag=0) THEN PRINT
1640 !  DISP J,Ta*Ti,Th(1)*Ti,Th(N1)*Ti
1641    IF Time<1800 THEN GOTO 1650
1642    Delt=5
1643    Deltau=Delt*Kappa/L/L
1650    Time=Time+Delt
1660    IF J MOD Skip=0 THEN Tim(J/Skip+1)=Time
1670 Endloop:NEXT J
1680 ! Print stored temperatures
1681  GOTO 1800
1690  PRINTER IS 9;WIDTH (2000)
1700  PRINT CHR$(12)
1710  FOR J=1 TO Lastr+1
1720    PRINT RPT$("
                   ",2);"TIME=";Tim(J);"days"
1730    PRINT RPT$("
                   ",1);"  X","TEMPERATURE (K)"
1740    FOR I=1 TO N1
1750      PRINT USING "Z.DDD,17X,DDDD.DDD,";Z(I),Temp(I,J)
1760    NEXT I
1770    IF J MOD 3=0 THEN PRINT CHR$(12)
1780  NEXT J
1790  PRINT CHR$(12)
1800  PRINTER IS 1
1810 Qrec:A$=""
1820  INPUT "DO YOU WANT TO RECORD RESULTS?",A$
1830  IF A$="Y" THEN CALL Record(Name$,Temp(*),Z(*),Tim(*),Lastr,N1)
1840  STOP!
1841  END
```

```
1850 Cp:SUB Cp(T,Cpav)
1860    OPTION BASE 1
1890    Cpav=28930
2000  SUBEND!
2010 Dens:SUB Density(T,P,Ro,Mass)
2020    OPTION BASE 1
2030    COM Cc(3),Dat(25),Cp(4,3),Aw(15,15),A2w(15,15),X(15),U(15),Ks(15),Rate(15
2040    DIM Mwt(3)
2050    Mwt(1)=28! N2
2060    Mwt(2)=32! O2
2070    Mwt(3)=44! CO2
2080 ! CC(*) IS VECTOR OF MOL FRACTIONS, SO FOR 1 MOL:
2090    Mass=DOT(Cc,Mwt)
2100    R=8.3E+3! J/kmol K
2110    Vol=R*T/P
2120    Ro=Mass/Vol! kg/m3
2130  SUBEND!


2140 Darcy:SUB Darcy(T,Darcy)
2150    OPTION BASE 1
2160    COM Cc(3),Data(25),Cp(4,3),Aw(15,15),A2w(15,15),X(15),U(15),Ks(15),Rate(
2170    E=Data(3)
2180    D=Data(4)
2190    S=Data(5)
2200 ! T = TEMP K
2210 ! D = PARTICLE DIAM m
2220 ! E = VOIDAGE
2230 ! S = PARTICLE AREA/VOLUME
2240    CALL Viscosity(T,Mu)
2250    K=5
2260    Darcy=K*(1-E)^2*Mu*S^2/E^3
2270  SUBEND!
2280 Visc:SUB Viscosity(T,Mu)
2290 ! VISCOSITY OF AIR
2300 ! PERRY THIRD ED P 370
2310    C=114
2320    Mu0=.01709
2330    Mu=Mu0*(273.1+C)/(T+C)*(T/273.1)^1.5 ! IN cp FOR T IN K
2340    Mu=Mu/1000! IN kg/m s
2350  SUBEND!
2360 Delh:SUB H_react(T,Delh)
2370 ! Subroutine to calculate Delta H reaction
2380    OPTION BASE 1
2400    Delh=3.E+8
2580  SUBEND!
2590 Prnt:SUB Print(Ta,Fr,Gg,Bi0,Bi1)
2600 ! Subroutine to print 'constants'
2610    PRINT RPT$("
                  ",1);"T average=";PROUND(Ta,-2);"K"
2620    PRINT "DARCY'S CONSTANT=";INT(Fr+.5);"kg/m^2/s" !?
2630    PRINT "FLOWRATE=";Gg;"kmol/m^2/s"
2640    PRINT "BI0=";Bi0,"BI1=";Bi1
2650  SUBEND!
```

```
2660 02:SUB Newo2(Y(*),Th(*))
2670 ! Calculates oxygen profile using backward differences
2680    OPTION BASE 1
2690    COM Cc(3),Data(25),Cp(4,3),Aw(15,15),A2w(15,15),X(15),U(15),Ks(15),Rat
2700    L=Data(11)
2710    Delx=Data(17)
2720    N1=Data(16)
2730    Dif=Data(20)
2740    G=Data(18)!Flowrate
2750    Ti=Data(14)
2760    Drho=Data(25)
2770    S=Data(5)
2780    E=Data(3)
2790    FOR I=1 TO N1
2800       T=Th(I)*Ti
2810       CALL React(T,Ratei,Ks(I),U(I))
2820       IF I=1 THEN 2850
2830       Delx=(X(I)-X(I-1))/Dif
2840       Y(I)=Y(I-1)/(1+Delx*Ratei*L/G)
2850       U(I)=U(I)+Ratei*Y(I)/(S*(1-E)*Drho)
2860    NEXT I
2870  SUBEND!
2880 Func:SUB Func(Dydt,Y(*),Ix,Yo2(*))
2890 ! Subroutine to calculate dY/dt
2900    OPTION BASE 1
2910    COM Cc(3),Data(25),Cp(4,3),Aw(15,15),A2w(15,15),X(15),U(15),Ks(15),Rat
2920    Ti=Data(14)
2930    L=Data(11)
2940    C=Data(13)
2950    Ke=Data(7)
2960    G=Data(18)
2970    N1=Data(16)
2980    Dif=Data(20)
2990    T=Y(Ix)*Ti
3000    CALL Cp(T,Cpav)
3010    CALL H_react(T,Delh)
3020    CALL React(T,Ratei,Ks(Ix),U(Ix))
3030    Rate(Ix)=Ratei
3040    A=G*Cpav*L/Ke
3050    B=Delh*Ratei*L*L*Yo2(Ix)/(Ti*Ke)
3060    CALL Deriv(Y(*),Ix,Dydx,D2ydx2)
3070    Dydt=Dif*Dif*D2ydx2-A*Dif*Dydx+B-C*(Y(Ix)-1)
3080  SUBEND!
3090 Deriv:SUB Deriv(Y(*),Ix,Dydx,D2ydx2)
3100 ! Derivatives of Y by calculation at the roots of the
3110 ! shifted Legendre polynomial of order N1
3120    OPTION BASE 1
3130    COM Cc(3),Data(25),Cp(4,3),Aw(15,15),A2w(15,15),X(15),U(15),Ks(15),Rate(1
3140    N1=Data(16)
3150    Dydx=0
3160    D2ydx2=0
3170    FOR J=1 TO N1
3180       Dydx=Dydx+Aw(Ix,J)*Y(J)
3190       D2ydx2=D2ydx2+A2w(Ix,J)*Y(J)
3200    NEXT J
3210  SUBEND!
```

```
3220 Bvals:SUB Bvals(Y(*))
3230 ! Subroutine to calculate the end temperatures
3240    OPTION BASE 1
3250    COM Cc(3),Data(25),Cp(4,3),Aw(15,15),A2w(15,15),X(15),U(15),K<(15),Rat<(
3260    Ke=Data(7)
3270    Msig=Data(8)
3280    L=Data(11)
3290    Ti=Data(14)
3300    Df=Data(15)
3310    N1=Data(16)
3320    Diff=Data(20)
3330    Gg=Data(18)
3340    T0=Y(1)
3350    Te=Y(N1)
3360 Again:CALL Cp(T0*Ti,Cpav)
3370    Af=Gg*Cpav*L/Ke
3380    Bi0=Msig*(T0+1)*(T0*T0+1)
3390    Bi1=Msig*(Te+1)*(Te*Te+1)
3400    S1=0
3410    S2=0
3420    FOR J=2 TO N1-1
3430      S1=S1+Aw(1,J)*Y(J)
3440      S2=S2+Aw(N1,J)*Y(J)
3450    NEXT J
3460    A1=(Bi0+Af)/Diff
3470    A2=Aw(N1,N1)+Bi1/Diff
3480    Numer=A1+Df/Diff+S1+Aw(1,N1)*(Bi1/Diff-S2)/A2
3490    Den=A1+Aw(1,N1)*Aw(N1,1)/A2-Aw(1,1)
3500    T01=Numer/Den
3501    IF T01<1 THEN T01=1
3510    Te1=(Bi1/Diff-S2-Aw(N1,1)*T01)/A2
3511    IF Te1<1 THEN Te1=1
3520    Dif1=ABS(T01-T0)
3530    Dif2=ABS(Te1-Te)
3540    T0=.5*(T01+T0)
3550    Te=.5*(Te1+Te)
3560 ! Check for convergence of the two end temperatures
3570    IF (Dif1>1.E-3) OR (Dif2>1.E-3) THEN Again
3580    Y(1)=T0
3590    Y(N1)=Te
3600 ! Write the Biot numbers into the matrix Data for passing back
3610    Data(21)=Bi0
3620    Data(22)=Bi1
3630  SUBEND!
```

```
3220 Bvals:SUB Bvals(Y(*))
3230 ! Subroutine to calculate the end temperatures
3240    OPTION BASE 1
3250    COM Cc(3),Data(25),Cp(4,3),Aw(15,15),A2w(15,15),X(15),U(15),K<(15),Rate((
3260    Ke=Data(7)
3270    Msig=Data(8)
3280    L=Data(11)
3290    Ti=Data(14)
3300    Df=Data(15)
3310    N1=Data(16)
3320    Diff=Data(20)
3330    Gg=Data(18)
3340    T0=Y(1)
3350    Te=Y(N1)
3360 Again:CALL Cp(T0*Ti,Cpav)
3370    Af=Gg*Cpav*L/Ke
3380    Bi0=Msig*(T0+1)*(T0*T0+1)
3390    Bi1=Msig*(Te+1)*(Te*Te+1)
3400    S1=0
3410    S2=0
3420    FOR J=2 TO N1-1
3430      S1=S1+Aw(1,J)*Y(J)
3440      S2=S2+Aw(N1,J)*Y(J)
3450    NEXT J
3460    A1=(Bi0+Af)/Diff
3470    A2=Aw(N1,N1)+Bi1/Diff
3480    Numer=A1+Df/Diff+S1+Aw(1,N1)*(Bi1/Diff-S2)/A2
3490    Den=A1+Aw(1,N1)*Aw(N1,1)/A2-Aw(1,1)
3500    T01=Numer/Den
3501    IF T01<1 THEN T01=1
3510    Te1=(Bi1/Diff-S2-Aw(N1,1)*T01)/A2
3511    IF Te1<1 THEN Te1=1
3520    Dif1=ABS(T01-T0)
3530    Dif2=ABS(Te1-Te)
3540    T0=.5*(T01+T0)
3550    Te=.5*(Te1+Te)
3560 ! Check for convergence of the two end temperatures
3570    IF (Dif1)1.E-3) OR (Dif2)1.E-3) THEN Again
3580    Y(1)=T0
3590    Y(N1)=Te
3600 ! Write the Biot numbers into the matrix Data for passing back
3610    Data(21)=Bi0
3620    Data(22)=Bi1
3630  SUBEND!
```

```
3640 March:SUB March(Y(*),Yo2(*),Deltau)
3650 ! Marching forward using 4th order Runge Kutta
3660    OPTION BASE 1
3670    COM Cc(3),Data(25),Cp(4,3),Aw(15,15),A2w(15,15),X(15),U(15),Ks(15),Rate
3680    DIM Z(15),Dy(15)
3690    N1=Data(16)
3700    REDIM Z(N1),Dy(N1)
3710    CALL Bvals(Y(*))
3720    FOR I=2 TO N1-1
3730      CALL Func(Dt,Y(*),I,Yo2(*))
3740      Yk=Deltau*Dt
3750      Dy(I)=Yk
3760      Z(I)=Y(I)+Yk/2
3770    NEXT I
3780    Z(1)=Y(1)
3790    Z(N1)=Y(N1)
3800    FOR I=2 TO N1-1
3810      CALL Func(Dt,Z(*),I,Yo2(*))
3820      Yk=Deltau*Dt
3830      Dy(I)=Dy(I)+2*Yk
3840      Z(I)=Y(I)+Yk/2
3850    NEXT I
3860    FOR I=2 TO N1-1
3870      CALL Func(Dt,Z(*),I,Yo2(*))
3880      Yk=Deltau*Dt
3890      Dy(I)=Dy(I)+2*Yk
3900      Z(I)=Y(I)+Yk
3910    NEXT I
3920    FOR I=2 TO N1-1
3930      CALL Func(Dt,Z(*),I,Yo2(*))
3940      Yk=Deltau*Dt
3950      Dy(I)=(Dy(I)+Yk)/6
3960      Y(I)=Y(I)+Dy(I)
3970    NEXT I
3980    Y(1)=Z(1)
3990    Y(N1)=Z(N1)
4000  SUBEND!
4010 React:SUB React(T,Rate,Ks,U)
4020    OPTION BASE 1
4030 ! Rate of oxidation for unity O2 mole fraction
4040    COM Cc(3),Data(25),Cp(4,3),Aw(15,15),A2w(15,15),X(15),Ui(15),Ksi(15),Rate
4050    R=Data(2)
4060    S=Data(5)
4070    P=Data(6)
4080    E=Data(3)
4090    K0=Data(9)
4100    Eor=Data(10)
4110    Ks=K0*EXP(-Eor/T)
4120    Rate=P*(1-E)*S/(R*T)/(1/Ks+U)
4130  SUBEND!
```

```
4140 March2:SUB March2(Y(*),Yo2(*),Deltau)
4150 ! Marching using forward differences
4160    OPTION BASE 1
4170    COM Cc(3),Data(25),Cp(4,3),Aw(15,15),A2w(15,15),X(15),Ui(15),Ks(15),Rat
4180    DIM Z(15)
4190    N1=Data(16)
4200    REDIM Z(N1)
4210    CALL Bvals(Y(*))
4220    Z(1)=Y(1)
4230    Z(N1)=Y(N1)
4240    FOR I=2 TO N1-1
4250      CALL Func(Dt,Y(*),I,Yo2(*))
4260      Z(I)=Y(I)+Dt*Deltau
4270    NEXT I
4280    MAT Y= Z
4290  SUBEND!
4300 Tav:SUB Tav(Y(*),Ta)
4310 ! Average temperature using trapezium rule
4320    OPTION BASE 1
4330    COM Cc(3),Data(25),Cp(4,3),Aw(15,15),A2w(15,15),X(15),U(15),Ks(15),Rate
4340    N=Data(16)
4350    Ta=0
4360    FOR I=1 TO N-1
4370      Ta=Ta+(Y(I)+Y(I+1))*(X(I+1)-X(I))/2
4380    NEXT I
4390  SUBEND!
4400 Record:SUB Record(N$,T(*),Z(*),Tim(*),Lj,N1)
4410 ! Subroutine to record profile on tape for plotting
4420    OPTION BASE 1
4430    GOTO 4480
4440    INPUT "T,X OR B?",A$
4450    INPUT "TMIN IN KELVIN?",Tmin
4460    INPUT "TMAX IN KELVIN?",Tmax
4470    IF A$="T" THEN GOTO Time
4480    A$="X"
4490    Tmin=300
4500    Tmax=320
4510    Nrec=INT((12+2*(1+N1)*(Lj+1))/32)+1!Number of records
4520    CREATE BDAT N$,Nrec
4530    ASSIGN @F1 TO N$
4540    OUTPUT @F1;INT(Lj+1)          !Number of curves
4580    FOR J=1 TO Lj+1       !Now the temperature profiles are stored
4590      OUTPUT @F1;INT(N1)
4600      FOR I=1 TO N1
4610        OUTPUT @F1;Z(I),T(I,J)
4620      NEXT I
4630    NEXT J
4640    ASSIGN @F1 TO *
4650    IF A$="X" THEN SUBEXIT
4660 !Time: CREATE N$&"T",Nrec
4670    ASSIGN @F2 TO N$&"T"
4680    OUTPUT @F2;N1+1
4690    OUTPUT @F2;2
4700    OUTPUT @F2;0,Tmin
4710    OUTPUT @F2;Tim(Lj+1),Tmax
4720    FOR I=1 TO N1
4730      OUTPUT @F2;Lj+1
4740      FOR J=1 TO Lj+1
4750        OUTPUT @F2;Tim(J),T(I,J)
4760      NEXT J
4770    NEXT I
4780    ASSIGN @F2 TO *
4790  SUBEND!
```

REFERENCES

ARGO, W.B., & Smith, J.M., Heat transfer in packed beds - Prediction of radial rates in gas-solid beds. Chem. Eng. Prog., 49, 443 (1953)

ASTM C177, ASTM Stand. (1963)

BADZIOCH, S., Gregory, D.R., & Field, M.A., Investigation of the thermal conductivity and thermal diffusivity of coal. Fuel, 43(4), 267 (1964)

BALAKOTAIAH, V., & Luss, D., Global Analysis of the Multiplicity Features of Multi-Reaction Lumped-Parameter Systems. Chem. Eng. Sci. 39(5), 865 (1984)

BELLMAN, R., Kashef, B.G., & Casti, J., Differential quadrature: A technique for the rapid solution of non-linear partial differential equatins. Journal of Computational Physics 10, 40 (1972)

BEJAN, A., Natural convection in an infinite porous medium with a concentrated heat source. J. Fluid Mech. 89(1) 97 (1978)

BEVERIDGE, G.S.G & Haughey, D.P., Axial Heat Transfer In Packed Beds. Stagnant Beds Between 20 And 750 °C.
Int. J. Mass Heat Transfer, 14, 1093 (1971)

BEVERIDGE, G.S.G & Haughey, D.P., Axial Heat Transfer In Packed Beds. Gas Flow Through Beds Between 20 and 650 °C.
Int. J. Mass Heat Transfer, 15, 953 (1972)

BHATTACHARRYA, K.K., Effect of humidity on oxidation of coal and its spontaneous heatng. J. Mines Metal Fuel, 18(1), 5 (1970)

BIRD, R.B., Stewart, W.E. & Lightfoot, E.N., Transport Phenomena, Wiley, New York (1960)

BOSWORTH, R.C.L., Heat Transfer Phenomena, Wiley, New York (1952)

BROOKS, K.S. & Woods, E.G.K., Thermal Conductivity of a Coal Bed Laboratory Report, Department of Chemical Engineering, University of the Witwatersrand (1980)

BS 874, British Standards Institution , London (1956)

CARSLAW, H.S., & Jager, J.C., Conduction of Heat in Solids. 3rd Ed., Clarendon Press, Oxford (1959)

CHEN, J.C. & Churchill, S.W., Radiant heat transfer in packed beds. AIChE J. 9, 35 (1963)

DEISSLER, R.G. & Eian, C.S., Investigation of effective thermal conductivities of powders. N.A.C.A., Washington, RME52C05 (1952)

ECKERT, E.R.G., & Drake, R.M., Analysis of Heat & Mass Transfer, Mcgraw-Hill, New York (1972)

EDWARDS, J.C., Mathematical modelling of spontaneous combustion of coal. Presented at the 112th Annual meeting of A.I.M>E., (1983)

GIJBELS M.R., & Bruining J., Spontaneous ignition time of underground coal - Estimation from oxidation rates determined in the laboratory. Erdoel und Kohle, 8, 376, (1982)

GUNEY, M. & Hodges, D.J., Adiabatic apparatus designed to study self-heating rates of coal. Chem & Industry, 42, 1429 (1968)

GUNEY, M., Oxidation and spontaneous heating of coal. J. of Pure And Applied Sciences, 5, 1, (1972)

GUNN, D.J. & Khalid, M., Thermal dispersion and wall heat transfer in packed beds. Chem. Eng. Sci., 30, 261 (1975)

KIBRIA, J., Effect of properties and enviromental variables on self heating tendencies of lignite. M.Sc. Thesis, University of North Dakota (1972)

KRAMERS, H. & Westerterp, K., Elements of Chemical Reactor Design & Operation, Academic Press, New York (1963)

KUNII, D. & Smith, J.M., Heat Transfer characteristics of porous rocks. AIChE J., 6(1), 71, (1960)

LAPWOOD, E.R., Convection of a fluid in a porous medium. Proc. Cam. Phil. Soc., 44, 508, (1948)

LEVENSPIEL, O., Chemical Reaction Engineering, Wiley, New York (1962)

LUSS, D., Sufficient Conditions for Uniqueness of the Steady State Solutions in Distributed Parameter Systems. Chem. Eng. Sci., 23, 1249, (1968)

LUSS, D. & Amundson, N.R., Uniqueness of the Steady State Solutions For Chemical Reaction Occcurring in a Catalyst Particle or in a Tubular Reactor with Axial Diffusion. Chem. Eng. Sci. 22, 253, (1967)

MURTAGH, B.A., The spontaneous heating of coal. M.Eng Thesis, Department of Chemical Engineering, University of Canterbury (1966)

NORDON, P., Model for the self-heating reaction of coal and char. Fuel, 58, 456 (1979)

NORDON, P., Young, B.C. & Bainbridge, N.W., The rate of oxidation of char and coal in relation to their tendency to self-heat. Fuel, 58, 443 (1979)

PERRY, R.H., & Chilton, C.H., editors of Chemical Engineer's Handbook, 5th edition, Mcgraw Hill, Tokyo (1973)

SCHMIDT, L.D., in Chemistry of Coal Utilization, Wiley, New York (1945)

SCHOTTE, W., Thermal conductivity of packed beds. AIChE J. 3, 373 (1960)

SONDREAL, E.A. & Ellman, R.C., Laboratory Determination of factors affecting storage of North Dakota Lignite. Bureau of Mines Report. R.I. 7887, (1974)

TYE, R.P., Thermal Conductivity, Academic Press, London (1969)

VAN DOORNUM, G.A.W., The spontaneous heating of coal. J. Inst Fuel, 27, 482 (1954)

VAN KREVELEN, D.W., Coal, 2nd Edit., Elsevier, Amsterdam, (1981)

WEBER, J.E, Convection in a porous medium with horizontal and vertical temperature gradients. Int. J. Heat Mass Transfer, 17(2), 241 (1974)

Yagi, S. & Kunii, D., Studies on effective thermal conductivities in packed beds AIChE J., 3, 373 (1957)

YOUNG, B.D., Two-dimensional conduction and convection in a porous medium: Application to spontaneous combustion of coal. M.Sc. Thesis, University of the Witwatersrand, Johannesburg, South Africa (1985)

YOUNG, M.L., Heat transfer in chromite ores. M.Sc. Thesis, University of the Witwatersrand, Johannesburg, South Africa (1975)

A SIMPLIFIED MODEL FOR SPONTANEOUS COMBUSTION IN COAL STOCKPILES

Kevin Seth Brooks

A thesis submitted to the Faculty of Engineering, University of the Witwatersrand, Johannesburg, in fulfilment of the requirements for the degree of Doctor of Philosophy.

July 1985

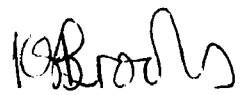
Johannesburg

NK 6717/1

DECLARATION

The work described in this thesis was carried out in the Department of Chemical Engineering of the University of the Witwatersrand, Johannesburg, and is the original and independent work of the author except where specifically acknowledged in the text.

No part of the thesis has previously been submitted for a degree in the University of the Witwatersrand, or is being submitted to any other University.



K S BROOKS

July 1985

ABSTRACT

Based on a study of the fundamental processes of heat,mass and momentum transfer, a one-dimensional model to predict the behaviour of coal dumps with respect to spontaneous combustion is presented.

Heat transfer within the dump is modelled using an effective thermal conductivity. This quantity has been measured for a typical coal sample using a guarded hot ring apparatus. Mass transfer is considered to occur by natural convection and wind pressure. Diffusion is shown to be unimportant except for very fine material.

A shrinking-core model for the low temperature oxidation of coal is proposed; the model explains the fact that the coal reactivity decreases with time. The effects of moisture on the coal reactivity are neglected due to lack of data.

Estimates of the parameters required for the model have been obtained experimentally. The equations are solved analytically in both the steady and unsteady-state under the assumption of unchanging rate constant. A numerical method has been used to solve the equations without this assumption.

It has been shown that coal dumps may be classified as either safe, unsafe or conditionally safe. Safe coal dumps are either oxygen limited or heat transfer limited. The former is the case for fine reactive coal; the high reactivity of the coal means that all the oxygen reacts close to the surface where the heat produced can easily be dissipated. The latter is the case for for coarse, unreactive material; although the oxygen is freely available throughout the dump, the reactivity per unit volume of the coal is sufficiently low such that heat produced can be dissipated without the temperature rising significantly.

It is shown that the important parameters in predicting the behaviour of a coal bed are the particle size distribution of the coal, the bed voidage and the reaction rate parameters. The effect on the temperature in a coal bed of changing each of parameter is presented graphically. The unsteady-state behaviour of the model shows that the time taken to reach a certain critical temperature may be the best way of arriving at a safe stockpiling time.

For my wife, Ilana:

A good typist and an even better cook

ACKNOWLEDGEMENTS

I should like to express my gratitude to my supervisor, Professor David Glasser, for his help, interest and encouragement during the course of this work.

As well as being a good friend, Mr (now Dr) Michael Itay performed the experimental work described in Chapter 2.

Mr L Schwartz and Mr A C Harris were of great assistance in the building of experimental apparatus.

The work described in this thesis was made possible by the financial assistance of the Iron and Steel Corporation of South Africa.

CONTENTS

	Page
DECLARATION	ii
ABSTRACT	iii
DEDICATION	iv
ACKNOWLEDGEMENTS	v
CONTENTS	vi
LIST OF FIGURES	x
LIST OF TABLES	xii
LIST OF SYMBOLS	xiii
1. AN OVERVIEW OF SPONTANEOUS COMBUSTION	1
1.1 Introduction	1
1.2 Previous Investigations into Spontaneous Combustion	3
1.3 Transport in a Coal Dump	6
1.4 The Chemical Reactivity of Coal	6
1.4.1 Reaction between Coal and Water	7
1.4.2 Low Temperature Oxidation of Coal	8
1.5 Heat Transfer within a Coal Dump	12
1.6 A Mathematical Model for Spontaneous Combustion	12
1.7 Experimental Investigation	13
1.8 Results and Conclusions	13
2. ANALYSIS OF SUGGESTED MECHANISMS FOR INGRESS OF REACTANTS	14
2.1 Introduction	14
2.2 Natural Convection and Wind Pressure	14
2.3 Analysis of Molecular Diffusion	18
2.4 Barometric Breathing	21
2.5 Thermal Breathing	22
2.6 Conclusions	23
3. THEORETICAL MODELS FOR HEAT TRANSFER IN PACKED BEDS	25
3.1 Introduction	25
3.2 Mechanisms of Energy Transfer in Packed Beds	25
3.3 Describing the Overall Energy Transfer in a Packed Bed	26

3.4 Models for Energy Transfer in which only conduction is considered 26

3.5 Models for Energy Transfer in which conduction and radiation are considered 31

3.5.1 Conditions under which radiation in a packed bed is likely to be significant 33

3.6 Theoretical Studies of Natural Convection 34

3.7 The Effect of flow on Energy Transfer in a Packed Bed 37

3.8 Conclusions 37

4. MEASUREMENT OF THE EFFECTIVE THERMAL CONDUCTIVITY OF A PACKED BED OF COAL 39

4.1 Introduction 39

4.2 Theory of the Measurement of Thermal Conductivity 39

4.3 Steady-state Methods for Measuring Thermal Conductivity 40

4.3.1 Measurements in the rectangular system 41

4.3.2 Measurements in the cylindrical system 43

4.3.3 Measurements in the spherical system 44

4.4 Unsteady-state or Dynamic Methods 44

4.5 Choice of Measurement Method for Packed Bed of Coal 45

4.6 Design and Construction of Guarded Hot Ring Apparatus 46

4.6.1 General Design Considerations 46

4.6.2 Heat Sinks 46

4.6.3 Heating Elements 48

4.6.4 Outer Containing Vessel 48

4.6.5 Water supply to heat sinks 50

4.6.6 Measurement Techniques 50

4.7 Experimental Procedure 51

4.8 Results and Discussion 52

5. MATHEMATICAL MODELLING OF A ONE-DIMENSIONAL ANALOGUE OF A COAL DUMP 54

5.1 Introduction 54

5.2 Literature survey of mathematical models 54

5.3 A One-dimensional Analogue of a Coal Dump 61

5.4 Model Equations 63

5.5 Discussion of the Model Equations 65

5.6 Boundary and Initial Conditions 66

6. SIMPLIFICATION OF THE MODEL EQUATIONS AND THEIR SOLUTION 67

6.1 Introduction 67
6.2 The Steady-State form of the Equations 69
6.3 The Solution of the Unsteady-State Equations with a constant rate 71
6.4 A Numerical Method for Solving the Unsteady-State Equations 72

7. EXPERIMENTAL INVESTIGATION OF THE BEHAVIOUR OF A ONE-DIMENSIONAL ANALOGUE OF A COAL DUMP 75

7.1 Introduction 75
7.2 Experimental 75
7.3 Results 78
7.4 Discussion 81

8. RESULTS OF SOLVING THE MODEL EQUATIONS 82

8.1 Introduction 82
8.2 Steady-State Solution for constant r 82
8.2.1 The Character of the Solutions 83
8.2.2 Effect of varying the voidage 90
8.2.3 Effect of varying the pre-exponential Factor 92
8.2.4 Effect of varying the activation energy 94
8.2.5 Effect of different assumptions about the reactive surface area of coal 94
8.2.6 The Meaning of Particle Size 95
8.2.7 Effect of wind on maximum Temperature 98
8.2.8 Effect of Thermal Conductivity on maximum Temperature 98
8.2.9 Effect of Changing the Bed Length 98
8.3 Unsteady-State solutions for r constant 101
8.3.1 Introduction 101
8.3.2 The Character of the Solutions 101
8.3.3 Discussion 107
8.4 Results of solving the equations numerically 107
8.4.1 Introduction 107
8.4.2 Comparison Between the Numerical Method and the Analytical Method 108
8.5 Conclusions 110

9. CONCLUSIONS 111

Appendix 1 Derivation of a rate equation for the low temperature oxidation of coal 116

Appendix 2 Tabulation of measured thermal conductivities 120

Appendix 3 Derivation of model equations 122

Appendix 4 The continuum and pseudo steady-state assumptions 130

Appendix 5 The inclusion of a radial heat loss term in equation 6.1.4 132

Appendix 6 Explanation for the Instability of the Runge-Kutta algorithm 135

Appendix 7 Solution of equation 6.2.2 with r constant 136

Appendix 8 Solution of equation 6.1.5 with r constant 137

Appendix 9 Application of the method of lines to the solution of equation 6.1.5 140

Appendix 10 Results of chimney experiment 142

Appendix 11 Model Parameters used as base case 165

Appendix 12 Listing of computer programs 166

REFERENCES 194

LIST OF FIGURES

Figure		Page
1.1	Temperature, Oxygen and Carbon Dioxide Versus Time	9
3.1	Geometrical Conduction Models (Beveridge & Haughey, 1971)	28
4.1	Guarded hot ring apparatus - Heat sink	47
4.2	Guarded hot ring apparatus - Assembled apparatus	49
5.1	Streamlines in a packed bed containing a line source	62
7.1	Chimney experiment - Apparatus	76
7.2	Chimney experiment - Fitting heat transfer coefficients	79
7.3	Chimney experiment - Fitting ageing run 1	79
7.4	Chimney experiment - Fitting ageing run 2	80
7.5	Chimney experiment - Fitting ignition runs	80
8.1	LHS and RHS of equation 8.2 as a function of θ	86
8.2	Locus of solutions to equation 8.2	86
8.3	Stable and unstable solutions for the base-case	91
8.4	Effect of varying voidage on the maximum temperature	91
8.5	Effect of varying the pre-exponential factor on the maximum temperature	93
8.6	Effect of varying the activation energy on the maximum temperature	93
8.7	Pre-exponential factor versus particle size for the two cases considered	96
8.8	Effect of different assumptions about surface area on the maximum temperature	96
8.9	Effect of wind on the maximum temperature	99
8.10	Effect of varying bed thermal conductivity on the maximum temperature	99
8.11	Effect of varying bed length on the maximum temperature	100
8.12	Temperature-time curves in the centre of a coal bed for different initial temperatures	102
8.13	Temperature profiles in a coal bed Particle size 10 mm - Analytical solution	102
8.14	Temperature-time behaviour at bed centre Particle size 6 mm - Analytical solution	106
8.15	Temperature profiles in a coal bed Particle size 10 mm - Numerical Method	106

Figure		Page
8.16	Temperature profiles with ignition Particle size 2 mm - 5 m/s wind - Numerical method	109
8.17	Cross plot of Figure 8.16 at bed centre	109
A1.1	Simplified coal particle geometry	116
A2.1	Measured thermal conductivities versus difference between guard and main heater temperatures	121
A3.1	Differential element of a coal bed	122
A5.1	Differential element in the form of a ring	132

LIST OF TABLES

Table		Page
2.1	Molar Flowrates for Various Particle Sizes	17
2.2	Comparison of Molecular Diffusion and Convection	21
5.1	Values of ΔT L Required for Ra = 4 π^2	59
5.2	Unknowns in the model equations	65
8.1	Particle Size Distribution for a typical sample	97
8.2	Model Parameters for Figure 8.12	101
8.3	The Quantity 'a' For Various Particle Sizes	105
A2.1	Measured Thermal Conductivities	120

LIST OF SYMBOLS

a: Dimensionless quantity in equation 6.1.4

a': Fitting constant in equation 5.2.1

a_{ij}: Weighting coefficients for first derivatives

A: Area

A': Fitting constant in equation 5.2.1

A^*: Arrhenius pre-exponential factor

$\underline{A}$: Matrix of coefficeints a_{ij}

A_o: Pre-exponential factor in equation 5.2.8

b: Dimensionless quantity in equation 6.1.4

b_{ij}: Weighting coefficients for second derivatives

B: Elovich constant

$\underline{B}$: Matrix of coefficients b_{ij}

Bi_o: Biot number at $X = 0$

Bi_1: Biot number at $X = 1$

Bi_2: $Bi_o + a/2$

Bi_3: $Bi_1 + a/2$

c: Heat loss coefficient

$\bar{c}$: Heat capacity per unit mass

$\bar{c}_s$: Heat capacity per unit mass of solid

$\bar{c}_w$: Heat capacity per unit mass of liquid water

$\bar{c}_j$: Heat capacity per unit mass of component j in the solid

$\bar{c}_b$: Heat capacity per unit mass of bed

$\hat{c}$: Molar heat capacity of the gas

$\hat{c}_i$: Molar heat capacity of component i in the gas

C_p: Specific heat capacity

C: Oxygen concentration

C_s: Oxygen concentration at reaction surface

C_1: Integration constant

C_2: Integration constant

C_3: Integration constant

D: Molecular diffusion coefficient

D_e: Effective diffusivity of oxycoal

D_p: Particle diameter

E: Activation energy

f: d'Arcy's law constant

f_j: Mass fraction of component j in the solid

g: Acceleration due to gravity

$g(X)$: Auxilary temperature function

G: Molar flowrate per unit area

h_o, h_1: Heat transfer coefficients

h_R: Heat transfer coefficient on radial surface

$\hat{H}$: molar enthalpy of gas

$\hat{H}_i$: molar enthalpy of component i in the gas

$\bar{H}$: Solid enthalpy per unit mass

$\bar{H}_j$: Enthalpy per unit mass of component j in solid

I_m: Main heater current

J_i: ith order Bessel function of the first kind

k: Thermal Conductivity

k_g: Gas thermal conductivity

k_s: Solid thermal conductivity

k_b: Bed thermal conductivity

$k_{b,x}$: Bed thermal conductivity in axial direction

$k_{b,R}$: Bed thermal conductivity in radial direction

k_o: Pre-exponential factor

k_r: $k_o \exp(-E/(RT))$

l: sample thickness

l_1, l_2: Distances between heater and sinks (equation 4.6.2)

L: Bed length or height

L_e: Effective particle length

m: Moles of oxygen per moles of nitrogen in the gas

m: Water flowrate

M: number of components in the solid phase

M_c: Mass of coal

M_w: Mass of absorbed water in the coal

M_p: Percent moisture in the coal

M_n: n th root of the equation $J_o(M_n)=0$

M': Dimensionless quantity defined by equation 5.2.3

n: Order of the Legendre polynomial P_n

N: Number of components in the gas phase

N': Dimensionless quantity defined by equation 5.2.4

p_j: Rate of Formation per unit bed volume of component j in the solid

P: Pressure

P_∞: ambient pressure

$\hat{P}$: $P - P_\infty$

$P_n(X)$: n th order Legendre polynomial

$P_n^*(X)$: n th order shifted Legendre polynomial

q: Amount of O_2 taken up per unit mass of coal

q_g: Flux in gas

q_s: Flux in solid

q': Source term in Diffusion Equation

Q': Rate of energy transfer by Conduction

Q_c: Rate of Convection from Solid to Gas

Q: Rate of energy input

Q_q: Rate of Energy absorption

Q_R: Radial Flux

Q_x: Axial Flux

r_i: Rate of formation per unit bed volume of i in the gas phase

r_o: Rate of oxidation at T_∞ for fresh coal

r: Rate of oxygen adsorption per unit bed volume for unity mole fraction oxygen

R: Gas constant

r: Radial co-ordinate (Chapter 4)

R: Spherical co-ordinate (Chapter 4)

R: Radial Distance (Appendix 5)

R_o: Bed Radius (Appendix 5)

S_t: Total reactive surface per particle volume

S: Total external surface per particle volume

S_m: External surface area per unit mass

S': Total surface area for reaction

t: Time

T: Temperature

T_∞: Ambient Temperature

T_g: Gas Temperature

T_s: Solid temperature

T': Temperature averaged radially

T_∞: Ambient Temperature

T_{av}: Average temperature = $L/\int_0^L T^{-1}dx$

$T_o(X)$: Initial temperature profile

U: Flow velocity

U_g: Gas internal energy

U_s: Solid internal energy

$\hat{U}$: Molar internal energy of the gas

$\bar{U}_s$: Internal energy of the solid per unit mass

$u(X,\tau)$: Auxilary temperature function (equation A8.2)

V: Wind velocity

v: Temperature above ambient

$v(X,\tau)$: Auxilary temperature function (equation 6.3.2)

V_b: Bed volume

V_p: Particle volume

V_m: Main heater voltage
x: Distance along bed
X: Dimensionless distance = x/L
y: Rectangular co-ordinate (Chapter 4)
y_i: Mole fraction of i in the gas phase
y_o: Mole fraction of oxygen at X=0
y: Mole fraction oxygen in the gas phase
z: Rectangular co-ordinate (Chapter 4)
z: Thickness of oxycoal layer
Z: Fractional conversion of coal
$Z_n(X)$: See equaiton 6.3.3

Greek Symbols

α: Fitting constant in equation 5.2.1
β: Roots of equation 6.3.4
γ_1,γ_2: $((a\pm(a^2+4C))^{1/2})/2$
γ_3: $-rL/G$
ΔH_w: Latent heat + heat of wetting
ΔH_r^i: Enthalpy of reaction
ΔH_r: Enthalpy of reaction for oxygen adsorption
ΔT: Temperature rise or temperature difference
ϵ: Voidage
η: Tortuosity factor
θ: Dimensionless temperature
$\theta_o(X)$: Initial dimensionless temperature profile
$\theta_{ss}(X)$: Steady-state dimensionless temperature profile
κ: Thermal diffusivity
μ: Gas viscosity
ν: D P/(R T)
ξ: $1/\tau'$
ρ: Density
ρ_s: Solid density
ρ_b: Bed density
ρ_g: Molar density of gas
ρ_∞: Density of gas at T_∞,P_∞
ρ_m: Molar density of oxycoal
σ: Stefan-Boltzmann constant
τ: Dimensionless time
τ_o: Period of oscillation
τ': Time constant for heat loss (Equation 5.2.5)
$\phi(X)$: Auxilary temperature function (equation A8.2)
ϕ_1,ϕ_2: Fitting constants in equation 8.1
τ_d: Time constant for equilibration of gas and solid

temperatures

τ_c: Time constant for conduction

τ_f: Time constant for flow

τ_p: Time constant for pressure change

1. AN OVERVIEW OF SPONTANEOUS COMBUSTION OF COAL

1.1 Introduction

The need to stockpile coal arises in many situations, most importantly in the following fields:

a) The generation of electricity

b) The coal mining industry

c) Coal transport

d) Steel making

It is well known that certain types of coal, when stockpiled, are liable to spontaneous combustion. Coal may undergo spontaneos combustion in many storage situations, among them:

a) In coal dumps

b) Underground

c) In the holds of ships

d) In storage silos or bunkers

The work described in this thesis concerns mainly spontaneous combustion as it relates to coal dumps. However, many of the conclusions reached are of significance, to a greater or lesser extent, in all of the storage situations mentioned above.

Spontaneous combustion of coal may lead to some or all of the following problems:

a) Loss of all or part of the coal dump. If the coal dump is a large one, as is the case at many mines and power stations, the economic effects of spontaneous combustion may well be disastrous.

b) Pollution. A burning coal dump presents a very real environmental problem, with noxious gases and particulate matter

being introduced into the atmosphere. This can present serious problems to communities in the vicinity of the burning dump.

c) Danger to human lives. Burning coal dumps can give rise to a dangerously high level of carbon monoxide, which may affect people working in the vicinity. Similarly, fires in ship's holds or underground can be extremely dangerous as well as costly.

Methods have been suggested, and are in use, for making coal dumps less liable to spontaneous combustion. These methods include compacting the dump, covering the dump with tar or sand, or spraying a cement-like substance on the surface of the dump. In addition much discussion has revolved around the monitoring of coal dumps, in order to obtain early warning of potential problems. Temperature monitoring by means of thermocouples, the taking of infra-red photographs and gas sampling have all been suggested and used as means of monitoring coal dumps.

One of the problems with the methods discussed above is that they tend to be costly, and the economic justification for their use is often not immediately obvious. The reason for this is that the knowledge that has been obtained in the field of spontaneous combustion is largely empirical, being based on experience gained by people working in the field. Although this knowledge is exteremely valuable, it is not always of great use when new stockpiling situations arise, or when a new mine is opened and the newly mined coal's liability to spontaneous combustion is an unknown quantity.

It seems clear that what is required is a sound scientific analysis of spontaneous combustion, on which decisions as to stockpiling practice can be based. The aim of this thesis is to provide this analysis, by analyzing the fundamental processes occuring in a coal dump, and synthesizing their effects in a mathematical model. The model can then be used as a basis on which predicitions about the behaviour of a certain coal in a certain stockpiling situation can be made. Hopefully this will lead to the construction of stockpiles in which the chances of spontaneous combustion occuring are minimized.

1.2 Previous Investigations into Spontaneous Combustion

A comprehensive reviews of spontaneous combustion of coal has been presented by Itay (1984). The aim of this section is to provide a critical review in which the important facts that have emerged are summarised. These facts will then be further discussed.

Many workers have concerned themselves with oxidation of coal (Van Krevelen,1981) and the literature on the subject has been reviewed by Guney (1968). The main conclusions reached are

a) The oxidation of coal appears to be a chemisorption reaction at temperatures under 70 ^{o}C; oxygen is taken up without water or carbon dioxide being formed.

b) The enthalpy of reaction is of the order of 300 kJ per mole of oxygen adsorbed (Edwards, 1983 and Sondreal & Ellman, 1974). This may be compared with an enthalpy of reaction of 390 kJ/mole for the reaction

$$C(graphite) + O_2(g) = CO_2(g).$$

c) The rate of oxidation decreases with time i.e. the coal ages.

d) The reaction rate appears to be of order ½ to 1 with respect to the oxygen concentration.

A series of investigators have reported different activation energies for the oxidation; these discrepancies appear to be due to the various ranges of temperature covered.

Van Krevelen (1981) believed that the primary reaction of chemisorption of oxygen has a relatively low activation energy of approximately 3 - 4 Kcal/mole.

Above a temperature of 70 ^{o}C decomposition of the adsorption complex may occur, with an activation energy of approximatley 6.5 Kcal/mole. However, chemisoption of oxygen occurs up to a temperature of 350 ^{o}C.

Many other investigators, notably Guney (1972) and Bhattacharyya

(1970) have investigated the effect ot moisture in the coal and reacting gas. The absorption of water is, not surprisingly, associated with a large enthalpy of reaction. In addition it appears that the absorbed moisture in the coal plays a part in the oxidation reaction, for dry coal oxidises at a far lower rate than moist coal. However, the effect of moisture on self heating of coal is still a subject of intense debate, mainly because different investigators have reported different results. This appears to be due to different apparatus and analysis methods being used, as well as different sample preparation techniques (e.g. vacuum drying, oil drying and air drying all at room temperature or elevated temperatures).

One important point has emerged from the studies performed by Murtagh (1966) who used a computer simulation technique. His main conclusion is that at low temperature moisture transfer is the dominant heat transfer mechanism in a dump, but that spontaneous ignition does not occur when only moisture is considered. His explanation for this is that at about 100 ^{o}C inherent moisture is driven from the coal, causing a cooling. Since there can be no further absorption of water, the maximum temperature that can occur is approximately 100 ^{o}C. It should be pointed out that should a coal dump reach a temperature of 100 ^{o}C, then it might be well on the way to combustion, since the rate of oxidation could be very high at this temperature.

It thus appears from the literature that moisture effects, especially the absorption of water by dry coal, can lead to an increase in the temperature of a coal dump to the point where the rate of oxidation becomes appreciable. In this situation the coal dump could be at risk.

This conclusion has a important consequence when one considers spontaneous combustion underground as opposed to spontaneous combustion above ground. In the underground situation the coal is likely to be dry, especially if it is newly mined. In addition the humidity of the air in the mine is high. Thus underground spontaneous combustion could be largely triggered by moisture absorption. However, when considering coal stockpiles, it should be remembered that these are normally laid down with water to facilitate compaction. In addition the coal that is stockpiled has generally come from a washing plant, and is thus wet. Thus the effect of moisture on a newly laid down coal dump is likely

(1970) have investigated the effect ot moisture in the coal and reacting gas. The absorption of water is, not surprisingly, associated with a large enthalpy of reaction. In addition it appears that the absorbed moisture in the coal plays a part in the oxidation reaction, for dry coal oxidises at a far lower rate than moist coal. However, the effect of moisture on self heating of coal is still a subject of intense debate, mainly because different investigators have reported different results. This appears to be due to different apparatus and analysis methods being used, as well as different sample preparation techniques (e.g. vacuum drying, oil drying and air drying all at room temperature or elevated temperatures).

One important point has emerged from the studies performed by Murtagh (1966) who used a computer simulation technique. His main conclusion is that at low temperature moisture transfer is the dominant heat transfer mechanism in a dump, but that spontaneous ignition does not occur when only moisture is considered. His explanation for this is that at about 100 ^{o}C inherent moisture is driven from the coal, causing a cooling. Since there can be no further absorption of water, the maximum temperature that can occur is approximately 100 ^{o}C. It should be pointed out that should a coal dump reach a temperature of 100 ^{o}C, then it might be well on the way to combustion, since the rate of oxidation could be very high at this temperature.

It thus appears from the literature that moisture effects, especially the absorption of water by dry coal, can lead to an increase in the temperature of a coal dump to the point where the rate of oxidation becomes appreciable. In this situation the coal dump could be at risk.

This conclusion has a important consequence when one considers spontaneous combustion underground as opposed to spontaneous combustion above ground. In the underground situation the coal is likely to be dry, especially if it is newly mined. In addition the humidity of the air in the mine is high. Thus underground spontaneous combustion could be largely triggered by moisture absorption. However, when considering coal stockpiles, it should be remembered that these are normally laid down with water to facilitate compaction. In addition the coal that is stockpiled has generally come from a washing plant, and is thus wet. Thus the effect of moisture on a newly laid down coal dump is likely

to be a beneficial one i.e. the evaporation of water will cause cooling. However, should there be very dry conditions causing drying out of the coal, followed by humid conditions, moisture absorption may well occur.

It is neccessary to look at the other factors involved in spontaneous combustion. These have been shown by many investigators (Sondreal & Ellman, 1974, Nordon, 1979) to be:

a) Transport into the dump and
b) Heat transfer within the dump.

As many investigators have pointed out, the importance of these two effects should not be underestimated. No matter how reactive a given coal is it will not undergo spontaneous combustion if

a) The reactants cannot get to it or
b) The heat generated by reaction can be readily transferred out of the dump.

Investigators have previously used mathematical models, based on energy balances for a reacting bed of coal, to try and predict the onset of spontaneous combustion. Notable among these investigators are Van Doornum (1954), Murtagh (1966), Sondreal & Ellman (1974) and Nordon (1979). The work of Murtagh (1966) has been discussed, and the work of the other three investigators will be further discussed in section 5.2. It is shown that the models used by these investigators suffer from the shortcoming that the effect of natural convection is ignored. The justification for ignoring this effect has been based on conclusions drawn by these researchers from the work of Lapwood (1948). The validity of these conclusions will be discussed in section 5.2.

Having reviewed the literature on the subject of spontaneous combustion of coal, it is felt that three main areas of importance in predicting the behaviour of a coal dump have been identified.

They are:

a) Mechanisms whereby reactants such as oxygen and water are transported into a dump.

b) The chemical reactions that occur betwen coal and these reactants, in particular the thermal effects of these reactions.

c) Heat transfer within the dump.

These three areas will now be discussed separately.

1.3 Transport in a Coal Dump

Five mechanisms whereby reactants may be transported into a coal dump have been identified. They are:

a) Natural convection caused by self heating of the dump.

b) Wind pressure on the inclined surfaces of the dump which causes flow.

c) Molecular diffusion caused by concentration gradients.

d) Barometric breathing caused by changes in barometric pressure.

e) Thermal breathing caused by the daily variation in temperature.

In order to decide which, if any, of these mechanisms is the most important source of reactants to a coal dump it was felt necessary to derive simple models to describe each mechanism. These models give an idea of the order of magnitude of each of the effects and lead to important conclusions regarding which mechanisms may be neglected and which may not. A full discussion of these models is given in Chapter 2.

1.4 The Chemical Reactivity of Coal

Spontaneous combustion of coal occurs due to reaction between atmospheric gases and coal. The gases that are of importance are water vapour and oxygen. A discussion of the reactivity of coal towards these reactants follows.

1.4.1 Reaction between Coal and Water

Much experimental effort has been devoted to the elucidation of the effect of moisture on spontaneous combustion of coal. Nordon, Young & Bainbridge (1979) have pointed out that the effect of moisture on the self heating of coal is two-fold. Firstly absorbed water exerts a catalytic effect on the oxidation rate, and secondly there is a transient effect which occurs as moisture is absorbed or desorbed. This partly explains why so many apparently contradictory results in connection with the effect of gas and coal moisture on self heating of coal have been obtained, since confusion arises due to the different ways in which the coal is dried, and the coal and atmospheric moisture contents are reported.

The catalytic effect of coal moisture content on the oxidation rate is well documented in the literature. Sondreal & Ellman (1974) report oxidation rates of lignite as being proportional to

$$1 + 0.674\ M_p - 0.01634\ M_p^2$$

where M_p is the moisture content expressed in percent. This expression implies that the rate of oxidation is a maximum when M_p is equal to twenty percent. This value is close to the equilibrium moisture content of coal.

The second effect mentioned is the transient absorption and desorption of moisture. The heat effect associated with the absorption of moisture is the latent heat of vaporization plus the heat of wetting. The former has a value of 500 cal/g at 25 °C and the latter has been reported by Sondreal & Ellman (1974) to be of the order of 24 cal/g. A simple energy balance may be written to calculate the temperature rise due to absorption of moisture by dry coal.

1.4.1

$$M_c\ \bar{c}_b\ \Delta T = M_w\ \Delta H_w$$

where M_c = mass of coal
$\bar{c}_b$ = specific heat capacity of coal
ΔT = temperature rise
M_w = mass of water absorbed
ΔH_w = latent heat + heat of wetting

Therefore $\Delta T = \frac{M_w \Delta H_w}{M_c \bar{c}_b}$ 1.4.2

Assume $M_w/M_c = 0,05$ i.e the coal absorbs five percent of its mass of moisture. The specific heat of a typical coal is 0,25 cal/g/K. By equation 1.4.2

$$\Delta T = \frac{0,05 \times 524}{0,25} = 104,8 \text{ K}$$

This is a substantial temperature rise, which will never be achieved in practise since as the coal absorbs moisture and the temperature increases the vapour pressure of the water above the coal increases and the reaction rapidly comes to equilibrium.

As has been pointed out by Kibria (1972) heating due to moisture absorption may bring coal to a temperature where oxidation occurs at a dangerous rate. This point is extremely important; water absorption may well be a starting mechanism whereby the tempe- rature inside a coal pile which is at risk starts rising leading to the onset of a large amount of oxidation and eventual com- bustion. The opposite is also true; if a coal dump is inherently safe no amount of water absorption will start it burning; com- bustion occurs due to oxidation, and not due to moisture effects.

1.4.2 Low Temperature Oxidation of Coal

The amount of literature on the chemical reactivity of coal, and in particular its low temperature oxidation, is vast. However, for the reason that every coal is likely to have a different reactivity, it was felt that a new study had to be undertaken. This work was performed by M. Itay, at the department of Chemical Engineering at the University of the Witwatersrand. A summary of the conclusions reached by Itay (1984) is presented in this section.

The experimental apparatus used to conduct these studies was a nearly adiabatic reaction vessel into which coal is packed and oxygen introduced. The temperature-time history of the reaction is recorded, and gas samples are taken periodically and analyzed for O_2, N_2, CO, CO_2, and H_2O. The measured temperature time

curve is used to back calculate the adiabatic temperature time curve, and this curve is used to obtain information on the rate of reaction and on the thermal effects associated with the reaction.

The data obtained thus far points very strongly to the conclusion that the chemical reactivity of the coal falls off with the degree of oxidation of the sample. This effect is well known and has been much reported in the literature (see for example Van Krevelen, 1981). However few plausible explanations for the effect have been given.

Another important conclusion is that the disappearance of oxygen is not neccessarily accompanied by the appearance of reaction products e.g. CO_2. It appears that at a low temperature coal adsorbs O_2 strongly and desorbs CO_2 at a far lower rate. This has also been noted in the literature, and the increase in density of reacting coal samples strongly supports this fact (Van Krevelen, 1981). In addition the desorption of the CO_2 appears to have a small enthalpy of reaction. This behaviour is shown graphically in Figure 1.1.

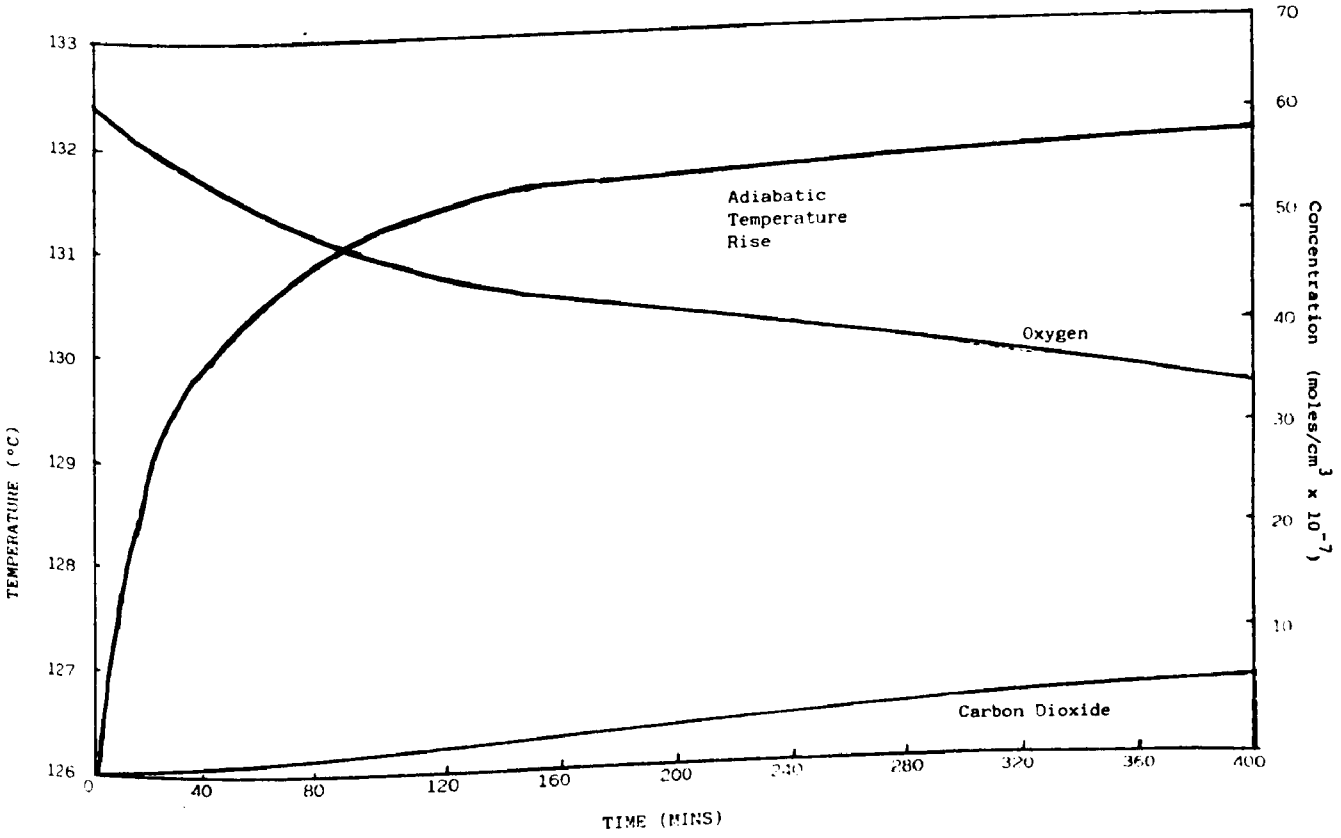


Figure 1.1 Temperature, Oxygen and Carbon Dioxide Versus Time

(After Itay, 1984)

In order to explain these effects a model for the reaction of coal with oxygen has been jointly derived by this researcher and Itay . The model is based on the hypothesis that coal absorbs oxygen to form a complex, which may be called oxycoal, without the formation of any gaseous products. The formation of an oxycoal layer on the surface of the coal has been demonstrated in the literature, and photographs showing this effect have been published by Van Krevelen (1981). As the oxycoal layer builds up the reaction rate slows down due to the fact that oxygen now has to diffuse through the oxycoal to react with the coal. This reaction model is an example of the so called shrinking core model, which is thoroughly discussed by Levenspiel (1962).

The derivation of the rate equation that follows from these assumptions is given in Appendix 1. The equations take the form:

Rate of adsorption of oxygen / unit volume of bed =

$$r = \frac{S_t\ (1-\epsilon)\ C}{1/k_r + Z/(S_t\ D_e)} \qquad 1.4.3$$

$$\frac{dZ}{dt} = \frac{S_t\ C}{\rho_m\ (1/k_r + Z/(S_t\ D_e))} \qquad 1.4.4$$

Where $S_t = \dfrac{\text{total surface area of particle}}{\text{volume of particle}}$

ϵ = bed voidage

C = O_2 concentration

k_r = surface rate constant

Z = fractional conversion of coal

D_e = effective diffusivity of oxycoal layer

ρ_m = molar density of coal

The temperature dependence of the reaction is given by the usual Arrhenius relationship i.e.

$$k_r = k_o \exp(-E/(R\,T)) \qquad 1.4.5$$

k_o = pre-exponential factor
E = activation energy
R = gas constant
T = temperature

In order to better understand the behaviour of this reaction model, the equations were solved under the assumptions of constant O_2 concentration and a constant value of k_r, the surface rate constant.

Under this assumption equation 1.4.4 gives

$$Z/(S_t\,D_e) = -1/k_r^2 + (1/k_r^2 + 2Ct/(\rho_m\,D_e))^{1/2} \qquad 1.4.6$$

Back substitution in equation 1.4.5 gives

$$r = S_t\,(1-\epsilon)\,C\,/(1/k_r^2 + 2Ct/(\rho_m\,D_e))^{1/2} \qquad 1.4.7$$

Two limiting cases were considered. In the early stages of reaction the oxycoal layer has not built up and the rate of the chemical reaction is limiting. In this case

$$1/k_r^2 \gg 2Ct/(\rho_m\,D_e)$$

$$\text{and } r = k_r S_t (1-\epsilon) C \qquad 1.4.8$$

i.e. in the early stages of reaction the rate is first order with respect to the O_2 concentration and is time independent.

However when more reaction has taken place it is reasonable to assume that the diffusion through the oxycoal layer is limiting. In this case

$$1/k_r^2 \ll 2Ct/(\rho_m\,D_e)$$

$$\text{and} \qquad r = ((\rho_m\,D_e\,C/(2t))^{1/2}\,S_t\,(1-\epsilon) \qquad 1.4.9$$

In the later stages of the reaction the rate is half order with respect to the O_2 concentration and exhibits a $1/t^{1/2}$ dependence on time.

This model therefore is in agreement with the observed behaviour of coal reactivity i.e. that the reactivity shows a definite falling off with time, which is in fact a falling off with degree of oxidation, and that the reaction order with respect to oxygen varies between one and a half . Fractional reaction orders have been reported by Sondreal & Ellman (1974).

It is therefore felt that a reaction model has been derived which is consistent with the available evidence. The problem that remains is to use the available experimental data to derive the model constants, in order that the model may be checked and used with confidence.

1.5 Heat Transfer within a coal dump

The safety or otherwise of a coal dump is likely to depend upon the balance between the rate of temperature rise due to reaction and the rate at which this energy is transferred away from the hot zone. It is known that coal is a fairly good insulator, but little data is available on the physical characteristics of heat transfer in coal beds. In addition these characteristics are likely to be dependent on both the voidage and particle size of the coal bed. For these reasons a literature survey was performed on the subject of heat transfer in packed beds; the results of this survey are presented in Chapter 3.

Following from this work, it was felt worth while to design and construct an apparatus to measure the so called effective thermal conductivity of a packed bed of coal. This aspect of the work is also discussed in Chapter 4 together with the results obtained.

1.6 A Mathematical Model For Spontaneous Combustion

In Chapter 5 a literature survey of existing mathematical models for spontaneous combustion of coal is presented. It is shown that all of these models suffer from one or more shortcomings. A set of equations, describing the behaviour of a so-called one-dimensional analogue of a coal dump is thus derived and discussed. In Chapter 6 certain simplifications to the model are discussed and justified. The methods used to solve this simplified set of equations are discussed.

1.7 Experimental Investigation

In Chapter 7 an experiment used to test the model as well as to obtain parameters for the model is discussed. The conclusion is reached that the model accurately describes the behaviour of a one-dimensional analogue of a coal dump.

1.8 Results and Conclusions

The large majority of Chapter 8 is devoted to a parameter study on the effect of on the model of changing certain parameters. The results obtained are discussed and the implications for the practising engineer pointed out. A simplified analysis is performed in order to deduce the temperature-time behaviour of the model, and the practical implications discussed. Shortcomings of the model are also discussed, together with suggestions for further research. Finally, in Chapter 9, the important conclusions reached in the thesis are summarised.

2. ANALYSIS OF SUGGESTED MECHANISMS FOR INGRESS OF REACTANTS

2.1 Introduction

The various mechanisms suggested for transport into a coal dump have been mentioned in section 1.2. They are repeated here for convenience.

a) Natural convection caused by self heating of the dump.

b) Flow caused by differential pressure between inclined and flat surfaces of the dump.

c) Molecular diffusion caused by concentration gradients.

d) Barometric breathing caused by changes in barometric pressure.

e) Thermal breathing caused by the daily variation in temperature.

In order to decide which of these mechanisms are important simple models were used to obtain order of magnitude estimates of their effect. It proves convenient to analyze mechanisms a) and b) together.

2.2 Natural Convection and Wind Pressure

In Chapter 5 a so-called one-dimensional model of the processes occuring in a coal dump is discussed. In Appendix 3 it is shown that the following momentum balance, for a vertically aligned bed open at both ends, may be written:

$$\frac{d\hat{P}}{dx} = -f\,U + \rho_\infty\, g\,(1 - T_\infty/T) \qquad 2.2.1$$

$\hat{P}$ = Pressure - ambient pressure
f = D'Arcy's law constant for the packed bed.
U = Superficial flow velocity
ρ_∞ = density of ambient air
g = acceleration due to gravity
T_∞ = ambient air temperature
T = bed temperature

Bird, Stuart & Lightfoot (1960) have discussed equations that attempt to correlate the factor f. One such equation is the Ergun equation which is

$$f = \frac{150\ (1-\epsilon)^2\ \mu\ S^2}{36\ \epsilon^3} + \frac{10.5\ (1-\epsilon)\ \rho\ U\ S}{\epsilon^3} \qquad 2.2.2$$

ϵ = bed voidage
μ = gas viscosity
ρ = gas density
$S = \frac{\text{total particle external surface area}}{\text{volume of particle}}$

It has been shown that for small flowrates the second term on the R.H.S. is negligible giving:

$$f = \frac{150\ (1-\epsilon)^2\ \mu\ S^2}{36\ \epsilon^3} \qquad 2.2.3$$

Note that no assumption need be made on the geometry of the particles or the bed packing. A mean particle diameter may be defined to be

$$D_p = 6/S \qquad 2.2.4$$

Under still air conditions the following boundary conditions are used for equation 2.2.1:

$$\hat{P}\ (x=0) = 0 \qquad 2.2.5$$

$$\hat{P}\ (x=L) = 0 \qquad 2.2.6$$

These boundary conditions merely reflect the fact that the ends of the bed are at atmospheric pressure.

In an attempt to compare the magnitude of natural convection induced flows with those of flows due to pressure differences, it is assumed that the stagnation pressure of a wind flow of velocity U may be use as an upper bound on the pressure difference that can arise between any two points on the surface of a coal dump. It is thus assumed that an estimate of the flows due to wind pressure may be obtained by assuming that the pressure at the bottom of the bed is increased by the stagnation pressure of the wind of velocity U.

Therefore

$$P(x=0) = P_\infty + \rho_\infty U^2/2 \qquad 2.2.7$$

and

$$\hat{P}(x=0) = \rho_\infty U^2/2 \qquad 2.2.8$$

Therefore the effect of wind is to change the boundary condition at $x = 0$ to

$$\hat{P} = \rho_\infty U^2/2 \qquad 2.2.9$$

Assuming U constant for small variations in temperature, equation 2.2.1 may be integrated to give:

$$\hat{P}(x=L)-\hat{P}(x=0) = -f\ U\ L + \rho_\infty\ g\ (L - \int_0^L (T_\infty/T\ dx)) \qquad 2.2.10$$

or

$$-\rho_\infty U^2/2 = -f\ U\ L + \rho_\infty\ g\ L\ (1 - (T_\infty/T_{aU})) \qquad 2.2.11$$

where

$$1/T_{aU} = 1/L \int_0^L T^{-1}\ dx \qquad 2.2.12$$

Therefore

$$U = \frac{\rho_\infty U^2}{2\ f\ L} + \frac{\rho_\infty g}{f}\ (1-T_\infty/T_{aU}) \qquad 2.2.13$$

or $$U = U(\text{Wind pressure}) + U(\text{Natural convection}) \quad 2.2.14$$

therefore

$$\frac{U(\text{Wind})}{U(\text{convection})} = \frac{v^2}{2\,L\,g\,(1-T_\infty/T_{av})} \quad 2.2.15$$

To illustrate the use of this equation, it will be used to calculate the wind velocity required to cause the same flow through a 10 m bed as a temperature rise of 20 ^{o}C.

i.e. $$1 = \frac{v^2}{2 \times 10 \times 9.8 \times (1-300/320)} \quad 2.2.16$$

or $$v = 3.5 \text{ m/s} = 12.6 \text{ km/hr}$$

This implies that for a windspeed of 12.6 km/hr natural convection will supply as much oxygen to the dump as will the differential wind pressure effect.

In order to compare these effects with the effects of molecular diffusion it is neccesary to calculate the molar flow rate per unit area for various average particle sizes. The relationships used are

$$G = \frac{P\,U}{R\,T} \quad 2.2.17$$

together with equations 2.2.2 and 2.2.15.

This calculation has been performed for L = 10 m, T_{av} = 320 K and ϵ = 0.3. The results are presented in Table 2.1.

TABLE 2.1 MOLAR FLOWRATES FOR VARIOUS PARTICLE SIZES

D_p (mm)	f (kg/m^2/s)	G (kmol/m^2/s)
1	5.6×10^{4}	5.1×10^{-7}
2	1.4×10^{4}	2.0×10^{-6}
5	2.2×10^{3}	1.3×10^{-4}

2.3 Analysis of Molecular Diffusion

In order to analyze the importance of diffusion as a mechanism for oxygen ingress a simplified analysis was performed. Considering diffusion as the only transport mechanism for oxygen into the dump the following energy and mass balances may be written:

Energy balance: $$K_b \frac{\partial^2 T}{\partial x^2} - r \Delta H = 0 \qquad 2.3.1$$

Mass balance: $$D\epsilon \frac{\partial^2 C}{\partial x^2} - r = 0 \qquad 2.3.2$$

The boundary conditions are:

$$\text{At } x=0 \quad T = T_\infty \quad C = C_\infty$$

$$\text{At } x=L \quad \frac{\partial T}{\partial x} = 0 \quad \frac{\partial C}{\partial x} = 0$$

These correspond to ambient conditions on the top surface of the dump, and a bottom surface that is perfectly insulating and impervious. These conditions will lead to a maximum temperature rise. Although this geometry is somewhat different to the geometry used in section 2.2, and thus the results obtained will not be directly comparable, it should be stressed that all that is required is an upper bound for comparison purposes; the geometry is unlikely to make a large difference on the bound.

Multiplying 2.3.2 by ΔH and subtracting the result from 2.3.1 gives:

$$K_b \frac{\partial^2 T}{\partial x^2} - D\epsilon\Delta H \frac{\partial^2 C}{\partial x^2} = 0 \qquad 2.3.3$$

or $$\frac{\partial^2}{\partial x^2}\left(T - \frac{D\epsilon\Delta H}{K_b} C\right) = 0 \qquad 2.3.4$$

This equation may be integrated to give:

$$T - \frac{D\epsilon\Delta H}{K_b} C = Ax + B \qquad 2.3.5$$

A and B may be determined from the boundary conditions as

follows:

At $x=0$ $T=T_\infty$ $C=C_\infty$

Therefore $$T_\infty - \frac{D\epsilon\Delta H}{k_b} C_\infty = B$$

and $$T - T_\infty - \frac{D\epsilon\Delta H}{k_b} (C - C_\infty) = Ax \qquad 2.3.6$$

Differentiating 2.3.5 wrt x gives:

$$\frac{\partial T}{\partial x} - \frac{D\epsilon\Delta H}{k_b} \frac{\partial C}{\partial x} = A \qquad 2.3.7$$

but at $x=L$ both derivatives in 2.3.7 are 0, therefore $A=0$.

Therefore $$T - T_\infty = \frac{D\epsilon\Delta H}{k_b} (C_\infty - C) \qquad 2.3.8$$

From 2.3.8 the maximum temperature rise with diffusion as the only transport mechanism may be calculated. This maximum temperature rise will occur at a point where $C=0$. Then:

$$T - T_\infty = \frac{D\epsilon\Delta H C_\infty}{k_b} \qquad 2.3.9$$

Typical values for the quantites in this equation are:

$$D = 2 \times 10^{-5} \text{ m}^2/\text{s}$$
$$\epsilon = 0.3$$
$$\Delta H = 3 \times 10^{8} \text{ J/kmol}$$
$$C_\infty = 8 \times 10^{-3} \text{ kmol/m}^3$$
$$k_b = 0.2 \text{ W/m/K}$$

Therefore

$$T - T_\infty = \frac{2\times10^{-5}\times0.3\times3\times10^{8}\times8\times10^{-3}}{0.2}$$

$$= 72 \text{ K}$$

This temperature rise, though appreciable, is not sufficient to explain the high temperatures observed in burning coal dumps. It is thus suggested that, in the same way that moisture absorption can act as a trigger for the oxidation reaction, diffusion can act as a trigger whereby the temperature in a coal dump starts rising, eventually giving rise to stable natural convection flows. These flows supply more oxygen to the dump than diffusion can, and eventually lead to spontaneous combustion.

Having concluded that diffusion can not explain spontaneous combustion, it is felt important to attempt to calculate the flowrates that diffusion causes. This facilitates the comparison of the magnitude of the flowrate caused by diffusion with the flowrates already calculated for wind and natural convection. To model molecular diffusion the coal is considered to adsorb oxygen, as discussed in section 1.3, and the isothermal steady state material balance for oxygen is

$$0 = \frac{D\ P}{R\ T}\frac{d^2y}{dx^2} - G\frac{dy}{dx} - r\ y \qquad 2.3.10$$

D = molecular diffusion coefficient
y = mole fraction oxygen
r = reaction rate per unit bed volume

The boundary conditions for equation 2.3.1 are:

$$y(x = 0) = .21 \qquad 2.3.11$$

and $$y(x \to \infty) = 0 \qquad 2.3.12$$

The solution is:

$$y = .21\ \exp((G - (G^2 + 4\ r\ \nu)^{1/2})\ x/\nu) \qquad 2.3.13$$

where $$\nu = D\ P/(R\ T)$$

The oxygen flux at x = 0 is

$$\frac{D\ P}{R\ T}\frac{dy}{dx} = .21\ ((G^2/4 + r\ \nu)^{1/2} - G/2) \qquad 2.3.14$$

Using the simplified equation

$$r = k_o\ S_t\ (1-\epsilon)\ \exp(-E/(R\ T))\ P/(R\ T) \qquad 2.3.15$$

with the values

k_o = 10 m/s
E/R = 7000 K
$S_t = 6/D_p$
ϵ = 0.3

$$D = 1.8 \times 10^{-8} \ m^2/s$$

and the data from Table 2.1 the entries in Table 2.2 have been calculated.

TABLE 2.2 COMPARISON OF MOLECULAR DIFFUSION AND CONVECTION

D_D (mm)	r (kmol/m^3/s)	Diffusional O_2 Flux (kmol/m^2/s)	Convective O_2 Flux (kmol/m^2/s)
1	1.2×10^{-7}	2.8×10^{-8}	1.0×10^{-7}
2	6.2×10^{-8}	4.4×10^{-9}	4.0×10^{-6}
5	2.5×10^{-8}	2.8×10^{-10}	2.6×10^{-5}

It can be seen from Table 2.2 that the effect of molecular diffusion is very much less pronounced for larger particles. For a particle size of 1 mm molecular diffusion supplies approximately 1/4 as much O_2 as a natural convection flow driven by a 20 ^oC temperature rise. In addition the molecular diffusion flux decreases with increasing particle size, while the convective flux increases. Although the analysis presented above may be criticized on the grounds that the transport equations have been decoupled, it can be seen that, except for the smallest particle sizes, the convective flux is orders of magnitude larger than the diffusional flux. This result justifies the use of the decoupled analysis to obtain order of magnitude estimates.

In the absence of wind or any temperature rise molecular diffusion may well be the only mechanism for O_2 transport into the dump. However it can be seen that as soon as there is any temperature rise in the dump natural convection will take over as the mechanism of O_2 transport.

2.4 Barometric Breathing

Barometric breathing occurs when the barometric pressure changes, causing a change in the volume of air that was in the dump. If the barometric pressure increases, this will cause a flow of air into the dump.

Consider a dump of 100 m x 50 m x 20 m high. Assume the barometric pressure increases from 620 mm Hg to 630 mm Hg in a time period of 24 hrs.

The air in the dump has a volume

$$100 \times 20 \times 50 \times 0.3 = 3 \times 10^4 \text{ m}^3$$

assuming $\epsilon = 0.3$.

This amount of air would shrink to a volume of

$3 \times 10^4 \times 620/630 \text{ m}^3 = 2.95 \times 10^4 \text{ m}^3$

and thus $4{,}76 \times 10^2 \text{ m}^3$ of air will flow in.

This flow will occur through the sides and the top of the dump i.e. a surface area of

$100 \times 50 + 2 \times 20 \times 50 + 2 \times 100 \times 20 = 11\,000 \text{ m}^2$

Thus the flowrate of air into the dump will be

$$\frac{4.76 \times 10^2}{11\,000 \times 24 \times 3600} = 5 \times 10^{-7} \text{ m/s}$$

This corresponds to a flux of 2×10^{-8} kmol/m^2/s which is an extremely small flux, and can safely be ignored.

Under certain weather conditions the barometric pressure may change far more rapidly than 10 mm Hg over a 24 hr period. This is the case for instance after a thunderstorm. These rapid changes may supply the dump with an appreciable amount of gas over a short period of time. The effect of this may well be to increase local temperatures in the dump and lead to the onset of natural convection flows. Thus rapid changes in barometric pressure may be a starting mechanism for the onset of spontaneous combustion in a dump that is in an unsafe condition.

2.5 Thermal Breathing

It has been hypothesized that the daily variation in temperature may lead to breathing of the dump i.e. hot air may leave the dump at night and be replaced by cold air thus supplying the dump with fresh reactants.

Measurements made at Grootegeluk coal mine indicate that surface temperature variations extend into the dump only a short distance; typically 325 mm.

A theoretical analysis of a problem of a semi-infinite solid with the surface temperature varying sinusoidally with time is discussed by Eckert & Drake (1972) who draw the conclusion that the oscillations are unimportant when

$$\frac{x}{2\,(\pi K \tau_o)^{1/2}} > 0.8 \qquad 2.5.1$$

Where K = thermal diffusivity of medium
τ_o = period of oscillation
x = distance into medium

For the case of daily fluctuations τ_o = 24 hrs. A typical value for the diffusivity of a coal bed is 8×10^{-4} m^2 / hr.

Therefore equation 2.5.1 gives

$$x > 2 \times 0.8 \times (\pi \times 8 \times 10^{-4} \times 24)^{1/2}$$

or $$x = 0.37 \text{ m}$$

This value agrees well with the measurements made on coal dumps discussed above.

It can be seen that thermal breathing will only supply reactants to the surface of the dump. Since any temperature rise near the surface of the dump is likely to be dissipated to the surface, it is unlikely that thermal breathing need be considered as an important reactant transport mechanism.

2.6 Conclusions

It may be concluded from the admittedly simplified analyses presented above that both wind pressure and natural convection must be considered as important mechanisms of O_2 transport into a coal dump. Molecular diffusion and barometric breathing may well be starting mechanisms, whereby the temperature begins rising in a coal dump. Natural convection soon becomes the dominant mech-

anism supplying O_2. This process may lead to eventual spontaneous combustion of a coal dump that is in an unsafe situation.

3. THEORETICAL MODELS FOR HEAT TRANSFER IN PACKED BEDS

3.1 Introduction

Thermal transfer of energy in packed beds is a field in which much work has been performed. The main reason for this is the importance of heat transfer in the design of packed bed catalytic chemical reactors. Other fields in which this knowledge is required include drying, nuclear reaction engineering and powder technology.

The literature survey that follows is very general, with no specific reference to coal beds. This is because the processes occuring in a packed bed of coal are no different to those occuring in packed beds of other materials.

3.2 Mechanisms of Energy Transfer in Packed Beds

In general energy transfer in a packed bed containing stagnant or moving fluid occurs by conduction, convection and radiation. The following potential mechanisms can be identified in the general case (Beveridge & Haughey, 1971).

Conductions Mechanisms

1. Conduction through the solid particles
2. Conduction across the gas in the voids
3. Conduction across the stagnant gas surrounding the points of contact between particles.
4. Conduction through the points of contact between particles

Radiation Mechanisms

5. Radiation between adjacent particle surfaces
6. Radiation between particle surfaces seen through more than one void space
7. Radiation absorption by the gas

Convection Mechanisms

8. Natural convection in the gas
9. Forced convection solid-gas transfer
10. Forced convection due to bulk flow, turbulent diffusion or mixing of the gas.

Of these mechanisms, mechanisms 1,2,4,5,6 and 7 are independent of fluid flow, while the other mechanisms depend to a greater or lesser extent on fluid flow, especially at low Reynolds numbers (Yagi & Kunii, 1957).

In general, thermal transfer of energy will take place by various combinations of series and parallel paths of these mechanisms.

3.3 Describing the overall energy transfer in a packed bed

The most common way of describing the overall transfer in a packed bed is by means of the so called effective thermal conductivity of the bed (Beveridge & Haughey, 1971). This quantity has also been called the thermal dispersion coefficient in the literature (Gunn & Khaled, 1975).

This formulation treats the system as homogeneous allowing the Fourier equation for the flux per unit area Q to be written

$$Q' = -k_b \frac{\partial T}{\partial X}$$

where $\partial T/\partial X$ is the temperature gradient in the required direction (axial or radial).

It can be seen from the discussion in 3.2 that k_b, the effective thermal conductivity, is in fact a function of many parameters including gas velocity, gas and solid temperatures, relative directions of gas and energy flow, fluid and solid properties as well as bed voidage and structural characteristics. It is the elucidation of this functional relationship that has been the goal of much of the work, both theoretical and experimental, that has been done in this field.

3.4 Models for energy transfer in which only conduction is considered

Many researchers have used as their starting point a model of a packed bed in which only conduction is considered. Models so derived should give good results provided the following conditions are met:

1. There is no gas flow
2. The particles are sufficiently small, and the temperature

sufficiently low, so that natural convection and radiation may be ignored.

Exactly what is meant by sufficiently small and sufficiently low will be discussed in greater detail later. Suffice it to say that if these conditions are met then the effective thermal conductivity, k_b, will be primarily a function of the thermal conductivities of the solid particle and stagnant gas. k_s and k_g respectively, and the structure of the bed.

Many models have been published to account for the four conduction mechanisms discussed in section 2, most of which describe the system in terms of its fluid and solid phase elements arranged in some regular array.

These models have been summarized by Beveridge & Haughey (1971), and their geometric significance is shown in figure 3.1

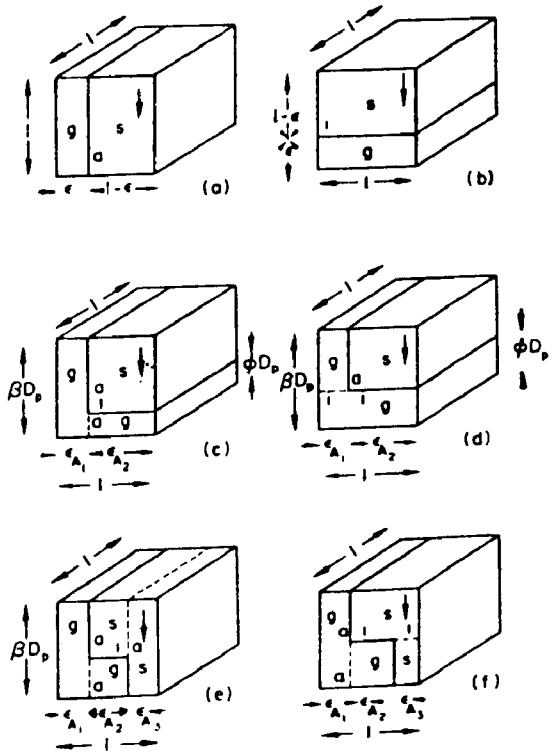


FIGURE 3.1 GEOMETRICAL CONDUCTION MODELS

a. adiabatic plane

i. isothermal plane

g. gas phase

s. solid phase

→ direction of energy transfer

(Beveridge & Haughey, 1971)

The simplest model is that represented by Fig 3.1a which postulates that conduction through the solid (mechanism 1) acts over a solid volume $1-\epsilon$, and the conduction across the gas in the voids and the stagnant gas round the points of contact (mechanisms 2 and 3) act over a gas volume ϵ. An arithmetic mean corresponding to a parallel arrangement of the two phases gives

$$\frac{k_b}{k_g} = \epsilon + (1 - \epsilon) \frac{k_s}{k_g} \qquad 3.4.1$$

The harmonic mean which corresponds to a series arrangement of the phases (Fig 3.1b) yields

$$\frac{k_b}{k_g} = \frac{k_s}{\epsilon\, k_s + (1 - \epsilon)\, k_g} \qquad 3.4.2$$

In attempting the formulation of more realistic models the concept of the unit cell is introduced, i.e. a representative element which is repeated throughout the packing. The basic geometric cell is that of Fig 3.1c with a cell of unit area perpendicular to the energy flow and height equal to the particle layer thickness $\beta' D_p$ where D_p = average diameter of particles.

Energy flow is one dimensional in parallel paths which are insulated from each other, and the distribution on the two phases is handled only by a two dimensional variation. This system then gives (see Fig 3.1c)

$$k_b = k_g\, \epsilon_{a1} + \frac{(1 - \epsilon_{a1})\, k_s}{\alpha' X + 1 - \alpha'} \qquad 3.4.3$$

where $\alpha' = \frac{\phi}{\beta'}$

and $\epsilon_{a1} = \frac{\epsilon - \alpha'}{1 - \alpha'}$

Modifications include that shown in Fig 3.1d which gives

$$k_b = \left[\alpha' k_g + \frac{1 - \alpha'}{k_g\, \epsilon_{a1} + k_s\, (1 - \epsilon_{a1})} \right]^{-1} \qquad 3.4.4$$

However, none of these models take into account the point to point

contact resistance (mechanism 4). One approach to this problem is that one used by Kunii & Smith (1960) who define a "heat" transfer coefficient h_p, accounting for an energy transfer contact resistance in parallel with the gas phase portion of the gas-solid series mechanism yielding:

$$\frac{k_b}{k_g} = \epsilon_{a1} + \frac{(1 - \epsilon_{a1})\, k_s/k_g}{(1 - \alpha) + \dfrac{\alpha\, k_s/k_g}{1 + \dfrac{h_p\, D_p}{k_g}}} \qquad 3.4.5$$

The quantity h_p has not been well correlated in the literature.

A more logical approach is the inclusion of the contact resistance in the idealized cell model as a solid energy flux path (represented by an area fraction ϵ_{a3}) arranged parallel to the gas path (Fig 3.1e) giving:

$$k_b = \epsilon_{a1}\, k_g + \frac{\epsilon_{a2}\, k_s}{\alpha' \dfrac{k_s}{k_g} + 1 - \alpha'} + \epsilon_{a3}\, k_s \qquad 3.4.6$$

A further extension to this approach is the one presented by Beveridge & Haughey (1971) in which the adiabatic boundary between the two parallel paths is replaced by an isothermal boundary (Fig 3.1f). This yields

$$\frac{k_b}{k_g} = \epsilon_{a1} + \left[\frac{1 - \alpha'}{\dfrac{k_s}{k_g}(1 - \epsilon_{a1})} + \frac{\alpha'}{\epsilon_{a2} + \epsilon_{a3}}\right]^{-1} \qquad 3.4.7$$

This approach has the advantage of allowing flux line bending in the solid phase.

It is shown by Beveridge & Haughey (1971) that k_b is a function of k_s/k_g, ϵ and ϵ_{a3} only. While k_s/k_g and ϵ are definable physical properties the parameter ϵ_{a3} must be determined experimentally for a given set of particles, since it will be affected by the particle loading and deformation as well as the surface

characteristics of the solid. It is also important to note that the effect of pressure on the thermal conductivity of the gas, k_g, must be properly taken into account.

3.5 Models for energy transfer in which conduction and radiation are considered.

Although radiant energy transfer will occur only through the voids of a packed bed of opaque solid pseudo-homogenous models have beem proposed which consider the solid and the gas as a single homogenous medium. The solution of the resultant integro-differential equations for conduction and radiation in absorbing and scattering models has been examined, most notably by Chan & Churchill (1963). They found that in an optically thick bed that the so called radiant conductivity $k_{b,r}$ could be written as

$$k_{b,r} = \frac{8 \sigma T^3}{a' + 2b'} \qquad 3.5.1$$

where σ = Stephan - Boltzmann constant
T = average bed temperature
a' = absorption cross section per unit volume of packing
b' = back scattering cross seciton per unit volume of packing

Note that the radiant conductivity is defined as the radiant energy flux density divided by the temperature gradient.

The radiant contribution has also been calculated by Bosworth (1952) from a random walk model giving

$$k_{b,r} = \frac{4 D_p T^3}{3}$$

The simplest radiation geometric model is that with two radiating plane surfaces at temperature T_1 and T_2, the radiant energy flux Q_r' being given by

$$Q'_r = \chi \sigma (T_1^4 - T_2^4) \qquad 3.5.3$$

where χ = view factor and emmisivity function

The elucidation of the function χ is difficult both theoretically and experimentally.

The energy flux Q'_r can be related to a radiation thermal conductivity $k_{b,r}$, and to a radiation coefficient $h_{b,r}$, by

$$Q'_r = -k_{b,r} \frac{\partial T}{\partial x} = h_{b,r} (T_1 - T_2) \qquad 3.5.4$$

When $T_1 - T_2$ is small compared to the absolute value of $T = T_1$ then:

$$\frac{k_{b,r}}{\beta D_p} = h_{b,r} = 4 \chi \sigma T^3 \qquad 3.5.5$$

The parameters in these models have a highly complex interaction with the structural and physical properties of the bed, and for this reason Beveridge & Haughey (1971) feel that there is little justification in representing the radiation mechanism other than by adding suitable terms to the simplest model such as the geometrical conduction models of Fig 1. Schotte (1960) used an analysis similar to that of Argo & Smith (1953) accounting for both the radiation between adjacent particle surfaces (mechanism 5) and the radiation between particle surfaces seen through more than one void space (mechanism 6) giving

$$Y_r = \epsilon X_{r,g} + \frac{1 - \epsilon}{\frac{k_g}{k_s} + \frac{1}{X_{r,s}}} \qquad 3.5.6$$

where $Y_r = \frac{k_{b,r}}{k_g}$

$$X_{r,g} = X_{r,s} = \frac{h_r D_p}{k_g} = \frac{4 D_p \chi \sigma T^3}{k_g} \qquad 3.5.7$$

The thermal conductivity of the bed is then given by

$$Y_t = Y_c + Y_r$$

In fact there is an interaction between the radiation and other energy transfer mechanisms and the contribution Yr cannot be added simply to the conduction terms. It is more satisfactory to utilize h_r within the conduction type model (Fig 3.1e). This was done by Yagi & Kunii (1957) who obtained

$$y_t = \epsilon_{a1}\,(1+ X_{r,g}) + \frac{\epsilon_{a2}}{\frac{\alpha'}{1 + \alpha' X_{r,s}} + \frac{1-\alpha'}{X}} + \epsilon_{a3} X \qquad 3.5.9$$

Normally no distinction is made between the Nusselt Numbers $X_{r,s}$ and $X_{r,g}$, although Yagi and Kunii (1957) used

$$X_{r,s} = \frac{4D_p}{k_g}\left[\frac{e}{2-\epsilon}\right] T^3 \qquad 3.5.10$$

$$X_{r,g} = \frac{4D_p}{k_g}\left[1 + \frac{\epsilon(1-e)}{2(1-\epsilon)e}\right]^{-1} \qquad 3.5.11$$

The model used by Beveridge and Haughey (1971) results in the expression

$$Y = \epsilon_{a1}(1+H_r) + \left[\frac{1-\alpha'}{X(1-\epsilon_{a1})} + \frac{\alpha'}{\epsilon_{a2}(1+H_r) + X\epsilon_{a3}}\right]^{-1}$$

$$H_r = \frac{\beta h_r D_p}{k_g} = \frac{4\beta D_p X \sigma T^3}{k_g} \qquad 3.5.12$$

Beveridge & Haughey (1971) treated X as an unknown function of temperature, and deduced the functional form experimentally.

3.5.1 Conditions under which radiation in a packed bed is likely to be significant

Young (1975) has performed calculations of the radiation contribution to the effective thermal conductivity of packed beds. The calculations were based on the radiation model of Schotte (1960) in conjunction with the correlation of Deissler and Eian (1952). The calculations show that radiation will become important for 1 mm particles about 400 °C and for 0,1 mm particles above 1500 °C. For

5 mm particles at an average bed temperature of 400 ^{o}C radiation will account for approximately 20 % of the total energy transfer.

3.6 A Theoretical Study of Natural Convection.

The first theoretical study of natural convection in packed beds is that of Lapwood (1948). This author formulated the equations describing natural convection in a porous medium with an imposed vertical temperature gradient as follows:

Equation of motion:

$$\rho \frac{D}{Dt}(U,V,W) = -\left[\frac{\partial}{\partial x},\frac{\partial}{\partial y},\frac{\partial}{\partial z}\right] P - \frac{\rho g}{K'}(U,V,W) - (0,0,\rho g) \qquad 3.6.1$$

Equation of continuity:

$$\frac{1}{\rho}\frac{D\rho}{Dt} = \frac{\partial U}{\partial x} + \frac{\partial V}{\partial y} + \frac{\partial W}{\partial z} \qquad 3.6.2$$

Conservation of energy:

$$\frac{DT}{Dt} = \kappa \nabla^2 T \qquad 3.6.3$$

Equation of state:

$$\rho = \rho_{\infty}[1 - \alpha(T-T_{\infty})] \qquad 3.6.4$$

(U,V,W) = the macroscopic velocity components of an element of fluid at (x,y,z)

P = pressure at (x,y,z).

T = temperature at (x,y,z)

ρ = gas density at (x,y,z)

g = acceleration due to gravity

κ = thermal diffusivity = $k_b/(\rho\, c_g)$

k_b = effective thermal conductivity of medium

c_g = specific heat capacity of gas

α = coefficient of thermal expansion of fluid

K' = coefficient of permeability of medium for fluid concerned
= Kg/ν

ρ_{∞} = density at ambient temperature

ν = kinematic viscosity of fluid

K = permeability of medium

Note that Darcy's law has been used in the equation of motion in place of the usual viscosity term.

In order to reduce these equations to a more manageable form Lapwood (1948) makes the following assumptions:

1) All velocities, and departures of temperature, density, and pressure from the equilibrium state, are small enough to neglect second order terms and to formulate a useful first order theory.

2) Variations of density can be neglected, except in so far as they modify the action of gravity (the Boussinesq assumption).

These assumptions mean that D/Dt can be replaced everywhere except in the energy equation to give

Equation of motion:

$$\rho \frac{\partial}{\partial t}(U,V,W) = -\left(\frac{\partial}{\partial x},\frac{\partial}{\partial y},\frac{\partial}{\partial z}\right) P - \frac{\rho g}{K'}(U,V,W) - (0,0,\rho g)$$

Equation of continuity:

$$\frac{\partial U}{\partial x} + \frac{\partial V}{\partial y} + \frac{\partial W}{\partial z} = 0$$

Conservation of energy:

$$\frac{DT}{Dt} = \kappa \nabla^2 T$$

Equation of state:

$$\rho = \rho_\infty [1 - \alpha(T-T_\infty)] = \rho_\infty \frac{T}{T_\infty} \quad \text{for an ideal gas}$$

Lapwood (1948) reworks this set of equations for small disturbances from equilibrium, and obtains the 4th order differential equation

$$\left(\frac{\partial}{\partial t} + \frac{Q}{K}\right)\left(\frac{\partial}{\partial t} - K'^2\right)\nabla^2\theta = g\frac{\Delta T}{L}\nabla^2\theta$$

where $\theta = T-T_0$, $T_0 = -\Delta T(z/L)$

The equation is solved for the following boundary conditions:

$$T, \quad \frac{\partial^2 T}{\partial z^2} = 0 \qquad \text{at } z=0 \text{ and } z=L$$

It is shown that the solution obtained leads to exponential decay for

$$Ra = \frac{\Delta T \ \rho_0 K \ L \ g}{\kappa \ \mu \ T_\infty} < 4\pi^2 \qquad 3.6.5$$

where Ra = Rayleigh Number

Lapwood (1948) thus states that $Ra = 4\pi^2$ is the criterion for convective flow; if Ra is less than this value the disturbance dies away, but if it reaches this value steady convection becomes possible.

These results also show that the temperature depth relationship is, except in the vicinity of the boundaries,

$$T = T_0 - \frac{\Delta T}{L} z + A \sin\left(\frac{\pi z}{L}\right) \sin(lx) \sin(my) \qquad 3.6.6$$

Where A,l,m are constants.

This equation shows that in the presence of convection the temperature is no longer a linear function of z.

3.7 The Effect of Flow on Energy Transfer in Packed Beds

When there is bulk flow of gas through a packed bed, the thermal transfer of energy becomes many times more complicated. It has been mentioned in section 2 that of the 10 proposed mechanisms of energy transfer, only 6 are completely independent of fluid flow. Briefly the mechanisms which are believed to be dependent on the fluid flow are:

1) Conduction across the stagnant gas surrounding the contact points. (This is likely to be a weak function of fluid flow).
2) Natural convection in the gas.
3) Forced convection in the gas.
4) Forced convection due to bulk flow, turbulent diffusion or mixing of the gas.

Mechanisms 3 and 4 are unlikely to be of importance for a coal bed, since forced convection is not being considered except for the case of wind. The flowrates through packed beds of coal are in any case very small. The flow velocity may be calculated from the entries in Table 2.1. For a particle size of 5 mm the velocity is of the order of 10 m/hr.

It may thus be concluded that the effects of flow on heat transfer in packed beds of coal is likely to be negligible.

3.8 Conclusions

A variety of theoretical models have been presented in this chapter. In order to apply the results of this literature survey to reacting coal beds, the following should be borm in mind:

a) The temperature range considered to be important is 100 ^{o}C and below. From practical experience as well as from considerations of the oxidation rate once a coal bed reaches 100 ^{o}C it is well on its way to combustion, and the model developed in this work no longer describes the situation accurately.

b) The flowrate through a bed of coal is sufficiently small (as shown above) that the effect of flow on the effective thermal conductivity is likely to be negligible.

The first point means that radiation can for all practical purposes be ignored as a significant mechanism for heat transfer in coal beds. The second point suggests that the effects of flow on the effective thermal conductivity can be ignored.

The conclusion is that only conduction type models need be considered for describing the effective thermal conductivity. Thus an equation like 3.4.5 could be rewritten

$$k_b = \epsilon k_g + (1-\epsilon)\ \eta k_s \qquad 3.8.1$$

where η = tortuosity factor

and η can be determined experimentally, with the expectation that η will not be a strong function of temperature.

Having reached this conclusion it was decided to measure k_b for a packed bed of coal. This is the subject of the next chapter.

4. MEASUREMENT OF THE EFFECTIVE THERMAL CONDUCTIVITY OF A PACKED BED OF COAL

4.1 Introduction

Very broadly speaking, methods for measuring thermal conductivities fall into one of two categories, i.e. steady-state or unsteady-state methods. The vast majority of unsteady-state methods do not measure the thermal conductivity directly, but instead measure the thermal diffusivity, κ, where:

$$\kappa = \frac{k}{\rho C_p} \qquad 4.1.1$$

k = thermal conductivity
ρ = density
C_p = specific heat capacity

One exception to this is the hot wire method which measures both the thermal conductivity and the thermal diffusivity. Steady state methods, on the other hand, measure the thermal conductivity directly.

4.2 Theory of the Measurement of Thermal Conductivity

Thermal conductivity is defined by Fourier's law:

$$Q' = -kA \frac{dT}{dx} \qquad 4.2.1$$

Q' is the rate of energy transfer by conduction

A is the area at right angles to the direction of transfer

$\frac{dT}{dx}$ is the temperature gradient in the direction of transfer

This equation may be combined with an energy balance for a solid or static fluid to give:

$$\rho C_p \frac{\partial T}{\partial t} = \frac{\partial}{\partial x}\left[k \frac{\partial T}{\partial x}\right] + \frac{\partial}{\partial y}\left[k \frac{\partial T}{\partial y}\right] + \frac{\partial}{\partial z}\left[k \frac{\partial T}{\partial z}\right] + q' \qquad 4.2.2$$

T is the temperature
q' is a source term, which may be due to chemical or nuclear reaction or the passage of a current.

In general in the measurment of thermal conductivities an attempt is made to ensure that only one dimensional conduction takes place. In this case equation 4.2.2 becomes:

$$\rho C_p \frac{\partial T}{\partial t} = k \frac{\partial^2 T}{\partial x^2} + q' \qquad 4.2.3$$

This equation may be written for cylindrical or spherical coordinate systems giving:

Cylindrical co-ordinates: $$\rho C_p \frac{\partial T}{\partial t} = \frac{k}{r} \frac{\partial}{\partial r}\left[r \frac{\partial T}{\partial r}\right] + q' \qquad 4.2.4$$

Spherical co-ordinates: $$\rho C_p \frac{\partial T}{\partial t} = \frac{k}{R^2} \frac{\partial}{\partial R}\left[R^2 \frac{\partial T}{\partial R}\right] + q' \qquad 4.2.5$$

4.3 Steady-State Methods for Measuring Thermal Conductivity

The second order differential equations 4.2.3 - 4.2.5 may be solved in the steady-state to give:

Rectangular co-ordinates: $$T = \frac{-q'x^2}{2k} + C_1 x + C_2 \qquad 4.3.1$$

Cylindrical co-ordinates: $$T = \frac{-q'r^2}{4k} + C_1 \ln(r) + C_2 \qquad 4.3.2$$

Spherical co-ordinates: $$T = \frac{-q'R^2}{6k} - \frac{C_1}{R} + C_2 \qquad 4.3.3$$

The constants of integration are found from known boundary conditions. In writing the above equations k has been assumed to be independent of temperature. In general in attempting to

measure thermal conductivity one would avoid introducing sources into the sample i.e. q′ would be zero in the above equations.

4.3.1 Measurements in the Rectangular System

The temperature-position equation in the rectangular system with q′=0 is:

$$T = C_1 x + C_2 \qquad 4.3.4$$

This equation implies a linear temperature profile.

In order to use equation 4.3.4 to measure thermal conductivity a heater is used to provide a known energy input Q. The boundary condition at x=0 is therefore:

$$Q = -kA \left.\frac{dT}{dx}\right]_{x=0} \qquad 4.3.5$$

The sample is cooled at the end. The boundary condition at x = L is therefore:

$$T = T_o \qquad 4.3.6$$

Solving for the integration constants C_1 and C_2:

$$C_1 = \frac{Q}{-kA} \qquad 4.3.7$$

$$C_2 = T_o + \frac{QL}{kA} \qquad 4.3.8$$

Therefore $$T = T_o + \frac{Q}{kA}(L - x) \qquad 4.3.9$$

Suppose that the measured temperature at x = 0 is T_1. Then:

$$T_1 = T_o + \frac{QL}{kA} \qquad 4.3.10$$

$$K = \frac{QL}{A(T_1 - T_0)} \qquad 4.3.11$$

This formula is the basis for measurements of the thermal conductivity of a material in rod or slab form. It requires measurement of five quantities i.e

The power input	Q
The sample length	L
The sample area	A
The temperature	T_0
The temperature	T_1

An improved version of the apparatus is one in which two identical samples, heated in the middle are used. The apparatus has the advantage that no energy loss can occur through the ends provided $T_0 = T_\infty$.

The equation used to calculate the thermal conductivity is now:

$$K = \frac{QL}{2A\ (T_1 - T_0)} \qquad 4.3.12$$

Despite the advantages of this apparatus energy loss may still occur along the sides. For this reason the so called guarded hot ring method has been developed. In this apparatus a circular electrical heating element is used and it is surrounded by a heating element in the form of a ring. During the experiment the power input to this guard ring is adjusted so that the temperature measured on the ring is the same as that measured on the main heater. This implies that any energy losses are supplied by the guard heater, and that all the energy supplied by the main heater passes through the sample.

The design of guarded hot plate apparatus has been the subject of much study, and is covered in ASTM C177 (1963) and BS 874 (1956). This method has been used by many investigators in the field of thermal conductivity of packed beds; notably Beveridge & Haughey (1971).

4.3.2 Measurements in the Cylindrical System.

In radial flow methods use is made of equation 4.3.2 with $q' = 0$:

$$T = C_1 \ln (r) + C_2 \qquad 4.3.13$$

With boundary conditions:

$$Q = -2\pi r_1 l \, k \left.\frac{dT}{dr}\right]_{r_1} \quad \text{at } r = r_1 \qquad 4.3.14$$

$$T = T_2 \quad \text{at } r = r_2 \qquad 4.3.15$$

Solving equation 4.3.14 for the constants and rewriting in terms of k gives:

$$k = \frac{Q}{2\pi l \, (T_1 - T_2)} \ln \left[\frac{r_1}{r_2}\right] \qquad 4.3.16$$

Two different experimental apparatus may be designed in order to make use of equation 4.3.16. In the first type of apparatus the specimen is placed between an outer shell which is kept at temperature T_2, and is heated centrally. In the second type of apparatus the sample is heated on the outside surface, and the energy is removed at the centre of the sample.

In order to ensure that energy transfer is occuring only in the radial direction it is neccesary either to use a large sample length to thickness ratio, or to make use of end guard heaters. If guard heaters are used a fairly complicated experimental apparatus is neccesary, involving movable thermocouples in order to measure axial temperature gradients. This aspect of the design of such equipment is covered by Tye (1969).

Examples of the use of such methods for measurements of thermal conductivity of packed beds are Yagi & Kunii (1957) who used a centrally heated specimen, and Young (1975) who used a centrally cooled specimen.

4.3.3 Measurements in the Spherical System

Equation 4.3.3 may be solved to give:

$$k = \frac{Q\ (1/r_1 - 1/r_2)}{4\pi(T_2 - T_1)} \qquad 4.3.17$$

The spherical system has the advantage that all the energy supplied by a central heater passes through the specimen. The disadvantages of the method include the difficulty of fabricating a uniform heater and specimen, and the fact that the thermo-couples used for temperature measurement cannot lie along isotherms.These disadvantages mean that the spherical system has not been used for the measurement of thermal conductivity of packed beds.

4.4 Unsteady-State or Dynamic Methods

In general dynamic methods involve the measurement of the thermal diffusivity. The experiment consists of measuring the temperature history of a heated sample of known geometry, and then using this data and the appropriate integrated form of equation 4.2.2 to solve for the thermal diffusivity.

These methods have the advantage that no measurement of power input need be made. The disadvantages include the fact that many temperature measurements must be made, and that solving for the diffusivity may require complex numerical techniques.

An example of the use of a dynamic method to measure the thermal conductivity of a coal bed is the investigation by Brooks & Woods (1980). These investigators used a cylindrical vessel of diameter 500 mm and height 1600 mm. The vessel was heated on the outside surface by steam and radial temperature profiles were measured as a function of time. These measurements were made every 15 minutes for periods of up to 8 hrs.

It can be shown that under the above experimental conditions equation 4.2.4 may be solved to give

$$\frac{T - T_s}{T_o - T_s} = 2 \sum_{n=1}^{\infty} \frac{\exp \frac{-M_n^2 K t}{R^2} \; J_o \frac{M_n r}{R}}{M_n \; J_1(M_n)} \qquad 4.4.1$$

where T = temperature at radial position r

T_s = surface temperature

T_o = initial bed temperature

R = radius of cylinder

r = radius measured from axis of cylinder

t = time

J_i = i th order Bessel function of the first kind

M_n = n th root of the equation $Jo(M_n) = 0$

A computer program was used to minimize the sum of squared errors between the measured and predicted temperatures by choice of K. It can be appreciated that this process is far more complicated than the direct application of an equation such as 4.3.12.

Although only one dynamic method has been discussed it should be appreciated that all such methods involve the same sort of experiment and analysis, and differ only in the sample geometry chosen. One of the problems with applying these methods to coal beds is the small value of K of such beds which leads to long experiments.

4.5 Choice of Measurement Method for a Packed Bed of Coal

From experience gained by Brooks & Woods (1980) in trying to measure this quantity by use of an unsteady-state method, it was felt that a steady-state method would be better. The reason for this is that it is far easier to analyze the effect of a temperature dependent thermal conductivity in the case of a simple equation such as 4.3.12, whereas this task may be extremely difficult in the case of an equation such as 4.4.1. Put another way, it was felt that a thermal conductivity calculated by equation 4.3.12 is far better defined than one calculated from equation 4.4.1.

Having decided on a steady-state method the choice had to be made between axial or radial energy transfer. Again experience gained

in a previous study led to the choice of axial energy transfer. The reason for this was that the previous study indicated that convection may be a significant mechanism of energy transfer. If this is the case the axial method would lead to the determination of the "correct" thermal conductivity i.e the one in which the energy transfer by conduction and convection are in the same direction (This of course assumes that the apparatus has the heater horizontal).

It was also felt that, by designing the equipment in such a way that the energy absorbed at the two sinks could be measured, the presence or absence of convection could be detected, and its effect measured. To do this would be much more difficult in a radial type of apparatus.

4.6 Design and Construction of Guarded Hot Ring Apparatus

4.6.1 General Design Considerations

Although standards exist for the design of guarded hot ring apparatus, it was felt in the present case that accuracy of measurement could be sacrificed for ease of experimental design and construction, and for versatility of the apparatus. It was felt that due to the inhomogeneous nature of coal and variations in packing geometry, accurate and repeatable values for the thermal conductivity would not in any case be achieved.

In order to make measurements on coal up to 20 mm in size it was decided to make the test section of the apparatus of diameter 200 mm and length 200 mm. These dimensions should be sufficient to make end and edge effects negligible. However it was noted that the recommended D/L ratio is three or more, and that using a smaller ratio would lead to a loss in accuracy (Tye ,1969).

4.6.2 Heat Sinks

As mentioned before the sinks are designed in such a way that the energy absorbed by the sinks can be measured. This is achieved by placing thermistors in the inlet and outlet streams from the sinks, in order to measure the temperature difference in the water flowing through the sinks. The rate of energy absorption

is calculated as

$$Q = m\ \bar{c}\ \Delta T_w \qquad 4.6.1$$

Q = rate of energy absorption
m = water flowrate
$\bar{c}$ = specific heat capacity of water
ΔT_w = temperature difference of water

The sinks are provided with spiral baffles in order to ensure good mixing of the cooling fluid, which was in all cases water. The sinks are surrounded by guard sinks in order to prevent radial energy losses.

A sketch of one heat sink is shown in Figure 4.1.

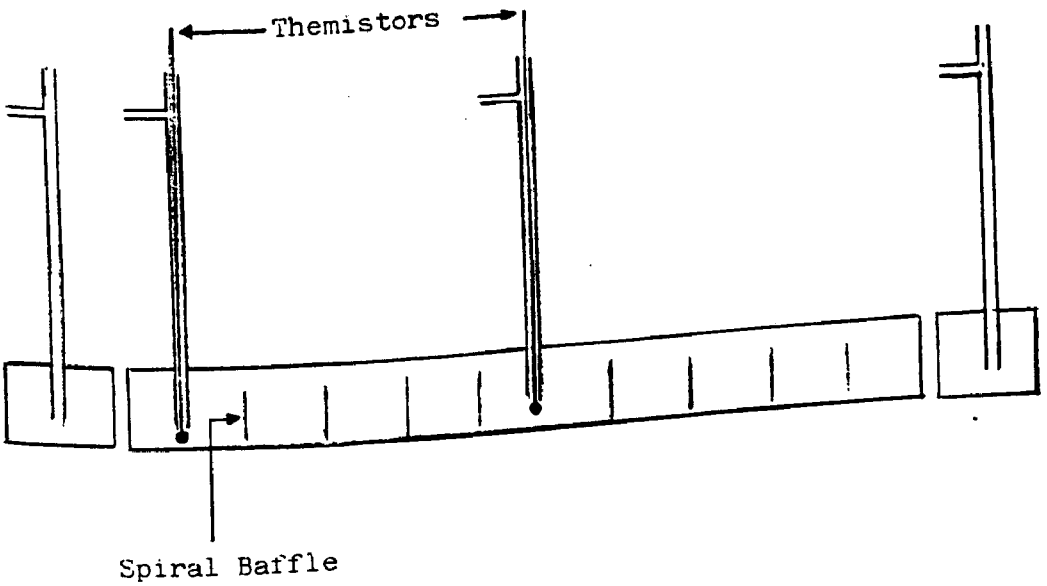


Figure 4.1 Guarded hot ring apparatus - Heat sink

4.6.3 Heating Elements

The heating elements were fabricated commercially, and consist of Nichrome wire ribbon wrapped around mica formers, which assembly is then sandwiched between more mica. The heaters are clad in light aluminium, and the whole assembly then sandwiched between 2 mm steel plates which are bolted together. The steel plates are used to prevent buckling.

The central heater has a diameter of 145 mm and the guard ring has an internal diameter of 150 mm and an external diameter of 200 mm. There is thus a 2.5 mm gap between the main and guard heaters.

4.6.4 Outer containing Vessel

The vessel has a diameter of 600 mm and a length of 600 mm. It is constructed from 6 mm mild steel. The ends of the vessel have 10 mm mild steel flanges in order to support the 10 mm MS end plates. The flanges are fitted with 5 mm rubber ring gaskets, and the endplates are held on with 18 bolts.

In order to facilitate electrical connections to the heaters as well as the placement of the thermocouples, six bushes have been placed on the midline of the apparatus. The bushes are shown in figure 4.2 and have proved satisfactory in sealing.

The end plates are provided with four similar bushes in order that the cooling sink pipes may pass through them. In addition the bottom end plate has an additional bush for connection of a vacuum pump or gas cylinder.

A sketch of the assembled apparatus is shown in Figure 4.2.

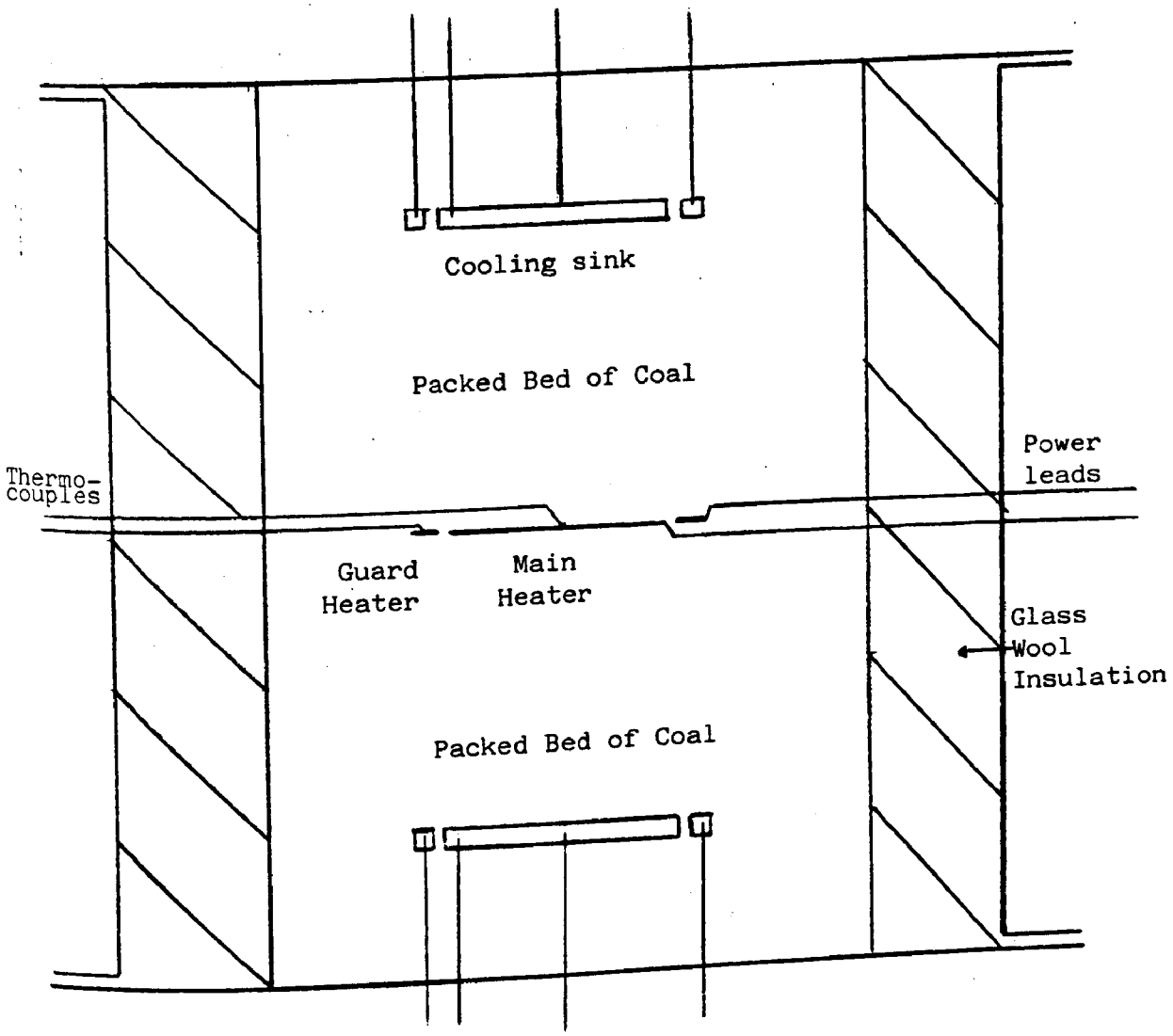


Figure 4.2 Guarded hot ring apparatus - Assembled apparatus

4.6.5 Water Supply to Heat Sinks

The apparatus is designed so that the temperature rise of the water flowing through the sinks is approximately 1 ^{o}C. A larger temperature rise is not used as this would upset the accuracy of the measurement of the temperature difference between the hot and cold faces. In order to measure this 1 ^{o}C temperature rise accurately it is neccessary to control the temperature of the water entering the sinks to at least 0.05 ^{o}C and preferably to 0.01 ^{o}C. To achieve this the following system is used:

Water flows from a constant head tank through a coil which is immersed in a constant termperature bath. The bath is controlled with a proportional controller. After leaving the bath the water flows through a jacketed copper pipe and hence to the heat sink. The jacketed pipe has water flowing in the jacket countercurrent to the flow to the sink. The water in the jacket is pumped from the constant temperature bath.

4.6.6 Measurement Techniques

The temperature of the main heater and guard heater are measured with chromel-alumel thermocouples. The cold junctions of the thermocouples are placed in glass tubes filled with glycerine, which are then placed in a "Thermos" flask filled with ice. The thermocouple voltage is measured using a Cambridge Slide Wire Potentiometer, i.e the voltage is measured at zero current.

The current supplied to the main heater is measured by a Fluke digital multimeter which is continuously in the circuit. This prevents the neccessity of correcting for the internal resistance of the meter. The voltage across the heaters is measured when required by another Fluke multimeter.

The resistances of the thermistors in the cooling sinks are measured in a Wheatstone bridge circuit, using a Kipp and Zonen recorder to measure the off balance voltage from the bridge.

The other values required to solve equation 4.3.12 for K are the heater area A and the length l. A is measured by measuring the diameter of the heater, and l is measured at the time of packing

the equipment with coal.

In fact the heater is not exactly betwen the two sinks, and thus l must be averaged. The correct average is

$$l = \frac{2\, l_1\, l_2}{l_1 + l_2} \qquad 4.6.2$$

where l_1, l_2 are the distances from the bottom and top sinks to the heater respectively.

4.7 Experimental Procedure

The experimental procedure is to switch on the main and guard heaters, setting the voltages so that there is no temperature difference between the guard and main heaters. The equipment takes approximately one week to reach steady-state, and each subsequent adjustment of the guard heater voltage requires further time for steady-state to be reached.

At the time of taking measurements the following are measured:

1) The voltage across the main heater and the guard heater.
2) The current through the main heater.
3) The thermocouple voltages on the main and guard heaters.
4) The resistance of the thermistors in the cooling sinks.

Once the thermocouple voltages and thermistor resistances have been converted to temperatures using calibration tables, the thermal conductivity is calculated from

$$k = \frac{V_m\, I_m\, l}{2\, A\, \Delta T} \qquad 4.6.3$$

V_m = main heater voltage
I_m = main heater current
ΔT = temperature difference between heater and sink

4.8 Results and Discussion

The results of the series of runs performed over the period March 1982 to August 1982 are tabulated in Appendix 2.

Although the resistances of the thermistors in the heat sinks were measured, it was not possible to calculate the energy absorbed at one heat sink. This was due to the fact that the thermistors are not identical i.e. they have slightly different resistances at the same temperature. An attempt was made to calibrate the thermistor pairs, but this was not succesful due to the fact that the calibration drifts with time. In addition problems were experienced with thermistors leaking and giving erratic readings. This facet of the experiment was consequently abandoned.

As can be seen from these results the thermal conductivity of the coal does not vary significantly in the temperature range considered. The mean value is 0.22 W/m/K.

It should be noted that for the largest tempeature difference used in the apparatus, the Rayleigh number as calculatedfrom equation 3.6.5 is 1.9. Therefore it may be safely assumed that only heat transfer by conduction was measured in this series of experiments, since this Rayleigh number is below the value required for the onset of natural convection.

The original intention of this experiment was to obtain experimental values for the so-called effective thermal conductivity of a coal bed, and deduce its functional relationship with particle size and voidage. However during the early stages of the mathematical modelling performed as part of this investigation, it was found that the thermal conductivity did not play as crucial a role in the equations as first believed. For this reason the experimental work was considered complete once a value of the thermal conductivity had been obtained for a typical sample of coal.

It is felt that a simple relationship for relating the thermal conductivity of the bed to that of the coal and the gas is all that is required. The relationship

$$k_b = \epsilon\, k_g + (1-\epsilon)\, \eta\, k_s \qquad 3.8.1$$

k_g = gas thermal conductivity
k_s = solid thermal conductivity
ϵ = voidage
η = tortuosity factor

which was presented and discussed in chapter 3 is probably satisfactory for a study of this type.

Using the values

k_g = 0.026 W/m/K (Perry & Chilton, 1973)
k_s = 0.28 W/m/K (Badzioch, Gregory & Field, 1964)
k_b = 0.22 W/m/K
ϵ = 0.38 (Appendix 2)

gives a value for η of 1.2.

5. MATHEMATICAL MODELLING OF A ONE-DIMENSIONAL ANALOGUE OF A COAL DUMP

5.1 Introduction

In any attempt to understand a natural phenomenon a model for the phenomenon is invaluable. In the case of a coal dump a mathematical model is required which has the ability to show the behaviour of a real coal dump, while still being simple enough to be solved. The full three dimensional equations for the transport processes occuring in a coal dump would be extremely complicated, and may indeed be impossible to solve without a tremendous amount of computation. A simpler model is required which may be solved without the excessive use of computation, but which nevertheless within its limits of applicability has the ability to predict whether a given coal dump may be considered to be safe or unsafe, and if unsafe what measures may be taken to render it safe. A model which is fundamentally based may be used to extrapolate measured data, which is not the case with models that are mainly empirical in nature. In addition the mathematical model points to the best experiments to measure the parameters required. It is believed that the mathematical model presented here has many of these desirable characteristics.

Mathematical models for coal dumps have been presented before, and in order to understand the reason for deriving a new one, a brief survey of these models and their shortcomings follows.

5.2 Literature survey of mathematical models for coal dumps

Much experimental effort has been devoted to measurement of physiochemical properties of coal over the last century. Less attention has been given to the development of a method to predict self heating.

An early model that attempts to predict safe conditions of storage of coal is that of Van Doornum (1954). The essential assumption of this model is that the coal may be considered to be a source of energy given by:

$$q' = A' \exp (a'v - \alpha t) \qquad 5.2.1$$

where q' = rate of generation
A' = fitting constant
a' = fitting constant
v = temperature above ambient
α = fitting constant
t = time

It should be noted that the form of equation 5.2.1 is in disagreement with the usual Arrhenius type temperature dependence of chemical reactions.

Van Doornum (1954) solves the conduction equation:

$$\rho_b \bar{c}_b \frac{\partial v}{\partial t} = \nabla^2(kv) + q' \qquad 5.2.2$$

where ρ_b = density of pile
$\bar{c}_b$ = specific heat capacity of coal
k = thermal conductivity
q' = source given by 5.2.1

for various geometries. From an analysis of the stability of the solutions the following is made that the safety or otherwise of a coal pile may be characterized by two dimensionless numbers M' and N' given by:

$$M' = \frac{A'a'}{\alpha \rho_b \bar{c}_b} \qquad 5.2.3$$

$$N' = \alpha \tau' \qquad 5.2.4$$

τ' = time constant for heat loss

τ' depends on the storage situation. For heat loss by conduction

$$\tau' = \frac{k \pi^2}{4 L^2 \rho_b \bar{c}_b} \qquad 5.2.5$$

L = height of pile

The criterion derived is as follows:

For $M' < 0.63$: a coal is unconditionally safe
$M' > 1.2$: the occurence of spontaneous combustion is very likely.

For the region $0.63 < M' < 1.2$ the situation, depending on the value of N', is normally manageable if care is taken.

This work has been adopted by the National Institute for Coal Research of South Africa as a test on the exportability of coal. The numbers M' and N' are found experimentally from a non-linear regression of the temperature-time curve at the centre of a 15 ton sample of coal which is aerated in a test bunker.

The chief disadvantage of this model is that no specific account is taken of the effect of oxygen depletion on the safety of a dump. In addition the constants in equation 5.2.1 have to be measured experimentally for every different coal; for instance, it is not possible to extrapolate measured data for one size grading of coal to a different size grading of the same coal.

Sondreal & Ellman (1974) performed exhaustive tests on North Dakota lignite, which data was used to perform computer simulations of spontaneous heating. The quantities measured by these investigators were the following:

a) The rate of oxidation of lignite, and the heat of reaction.
b) The specific heat of lignite.
c) The heat of wetting.
d) Airflow through a bed of compacted lignite.
e) The thermal conductivity of solid lignite.

In all case the quantities were measured at various moisture contents and bulk densities. The authors have used least squares techniques to fit the data to equations which are largely empirical in nature. These empirical equations have been used in computer simulations of spontaneous heating, using finite difference forms of the differential equation 5.2.2 together with a material balance equation for oxygen.

The authors present a large number of graphs showing the temperature rise in lignite under various assumptions. The cases

considered include the effects of prior oxidation, pressure gradients due to wind, porosity and moisutre content of the coal.

Although these investigators were most thorough in their approach, the chief disadvantage of this study is that it is highly specific to the particular lignite used. The authors state that the range of validity of their empirical correlations is limited to the range studied, and that extrapolations should only be made with caution. In addition Sondreal & Ellman (1974) take no account of airflow due to natural convection.

Nordon (1979) has presented a model for the self heating reactions of coal or char. The reactants considered are oxygen and water vapour, which are transported into the pile by molecular diffusion and forced convection due to differential wind pressure. A one-dimensional model is used in which the differential equations describing heat and mass transfer are:

$$(1-\epsilon)\,\rho_b\,\bar{c}_b\,\frac{\partial T}{\partial t} = \frac{(1-\epsilon)}{K}\,\frac{\partial^2 T}{\partial x^2} - \epsilon\,U\,\rho_g\,\hat{c}\,\frac{\partial T}{\partial x} - r\,\Delta H_r \qquad 5.2.6$$

where
K = thermal diffusivity
x = length along bed
U = flow velocity
ρ_g = density of gas
$\hat{c}$ = specific heat capacity of gas
r = reaction rate per volume of coal
ΔH_r = enthalpy of reaction

$$0 = \epsilon\,\frac{\partial m}{\partial t} + U\,\frac{\partial m}{\partial x} - D\,\frac{\partial^2 m}{\partial x^2} + \rho_g\,r \qquad 5.2.7$$

m = moles of oxygen per moles of nitrogen in gas
D = diffusion coefficient

These equations are solved using a finite difference method. No account is taken of natural convection flow. The reaction rate of the oxidation reaction is modelled using the so-called Elovich equation:

considered include the effects of prior oxidation, pressure gradients due to wind, porosity and moisutre content of the coal.

Although these investigators were most thorough in their approach, the chief disadvantage of this study is that it is highly specific to the particular lignite used. The authors state that the range of validity of their empirical correlations is limited to the range studied, and that extrapolations should only be made with caution. In addition Sondreal & Ellman (1974) take no account of airflow due to natural convection.

Nordon (1979) has presented a model for the self heating reactions of coal or char. The reactants considered are oxygen and water vapour, which are transported into the pile by molecular diffusion and forced convection due to differential wind pressure. A one-dimensional model is used in which the differential equations describing heat and mass transfer are:

$$(1-\epsilon)\,\rho_b\,\bar{c}_b\,\frac{\partial T}{\partial t} = \frac{(1-\epsilon)}{\kappa}\,\frac{\partial^2 T}{\partial x^2} - \epsilon\,U\,\rho_g\,\hat{c}\,\frac{\partial T}{\partial x} - r\,\Delta H_r \qquad 5.2.6$$

where
κ = thermal diffusivity
x = length along bed
U = flow velocity
ρ_g = density of gas
$\hat{c}$ = specific heat capacity of gas
r = reaction rate per volume of coal
ΔH_r = enthalpy of reaction

$$0 = \epsilon\,\frac{\partial m}{\partial t} + U\,\frac{\partial m}{\partial x} - D\,\frac{\partial^2 m}{\partial x^2} + \rho_g\,r \qquad 5.2.7$$

m = moles of oxygen per moles of nitrogen in gas
D = diffusion coefficient

These equations are solved using a finite difference method. No account is taken of natural convection flow. The reaction rate of the oxidation reaction is modelled using the so-called Elovich equation:

$$\frac{dq}{dt} = r_o A' \exp(-(E + Bq)/RT) \qquad 5.2.8$$

where q = amount of O_2 taken up per unit weight of char.
r_o = rate of oxidation at $T_\infty = 20^oC$ when q = 0.
A' = Arrhenius pre-exponential factor = $\exp(E/RT_\infty)$.
E = activation energy.
B = Elovich constant.

In the results by Nordon (1979) no account has been taken of the presence of moisture. As in the case of Sondreal & Ellman (1974) this author presents graphs showing the effect of various parameters on the temperature rise in char beds. The cases considered are:

a) Self heating for various bed lengths where diffusion is the only transport process.

b) Dependence of steady state temperature on critical bed size for various activation energies.

c) Self heating where diffusion and convection processes are present.

d) The moderating influence of Elovich kinetics.

The author concludes that there is a critical bed length above which spontaneous combustion will occur. He states that for bed lengths smaller that this critical value the steady state temperature rise is small and is limited by heat transfer. The high temperature steady state is caused by the reaction being limited by the rate of oxygen diffusion. With forced convection present this oxygen limitation may be removed; however when the forced convection becomes large loss of heat through flow will limit the reaction, leading to a low temperature steady state. Note however that the air flow required for this to occur is of the order of 10^{-4} m/s which is a fairly large flowrate for the fine (-3,35 mm) material considered in this study.

This study then is theoretically sound, and the author presents a

good discussion of the nature of self-heating. The main drawback of the model is the failure to take account of natural convection flows.

The omission by these researchers of natural convection deserves some explanation. It has been suggested by some researchers that the work of Lapwood (1948), as discussed in section 3.6, shows that natural convection is unimportant in coal dumps. The argument used is that Lapwood (1948) states that a Rayleigh number of $4\pi^2$ is a criterion for the onset of stable convection flows. This would seem to imply that the temperature rise required for natural convection flows to take place in a coal dump can be calculated using equation 3.6.5. The equation is

$$Ra = \frac{\Delta T \; \rho_g^2 \; L \; g \; c_g}{k_b \; f \; T_\infty}$$

where the identities $f = \mu/K$ and $\alpha = 1/T_\infty$ for an ideal gas have been used.

Setting the Rayleigh number equal to $4\pi^2$ in the above equation, the quantity $\Delta T \; L$ may be solved for. The results of doing this calculation are summarised in Table 5.1 below.

TABLE 5.1 VALUES OF $\Delta T \; L$ REQUIRED FOR $Ra = 4\pi^2$

D_p (mm)	f ($kg/m^3/s$)	$\Delta T \; L$ (K m)
1	5.6×10^4	9500
2	1.4×10^4	2375
5	2.2×10^3	380
20	1.4×10^2	24

These results have been taken by other researchers to indicate that for a 2 metre bed of 20 mm particles a 12 K temperature rise is necessary for the onset of natural convection flows, and that for 1 mm particles natural convection flows are very unlikely to occur.

There is however a fallacy in this argument. Lapwood investigated natural convection flows for the case of an imposed temperature gradient in the vertical direction, and with impermeable

horizontal faces. The problem is thus constrained to a one-dimensional temperature gradient. The boundary conditions that are implied are not appropriate for the case of a coal dump. A coal dump has no impermeable sides and has each of its surfaces at nearly ambient temperature, and experiences a three-dimensional temperature field.

Young (1985) has reworked this problem for the case of a coal bed open on the top surface, with impermeable sides and a two-dimensional temperature field. For this case it can be shown that the equation governing the stream function of the flow in the bed is:

$$\frac{\partial^2 \psi}{\partial X^2} + \frac{\partial^2 \psi}{\partial Y^2} = \frac{\partial \theta}{\partial X}$$

The right hand side of this equation represents the horizontal temperature gradient. If this quantity is 0 and the boundary conditions are such that ψ is zero everywhere, then this equation can be satisfied by the case of no flow. However, when the temperature gradient in the horizontal direction is non-zero, convection can be expected under all conditions.

Young (1985) has also shown experimentally that for his case as soon as there is any temperature rise in such a bed, natural convection will occur. There is thus no obvious critical Rayleigh number for this case.

Weber (1974) has studied theoretically a similar situation to Lapwood, but with a small horizontal temperature gradient. It appears from this work that there exists no critical Rayleigh number below which there is no flow, but rather that there is a critical Rayleigh number above which there is a fairly rapid increase in flow. The application of this work to coal beds is not completely obvious, because the infinite region considered requires infinite temperatures at the ends; hence only horizontal flows occcur at Rayleigh numbers below a certain critical value.

Bejan (1978) has studied convection in an infinite porous medium with a concentrated heat source; for this case there is no critical Rayleigh nmuber for the onset of convection. The steady-state flow pattern shows an upward flow that becomes very intense near the source. The upward flow extends throughout the medium, and as the Rayleigh number increases, the warmer region

moves upwards. It is felt that this case is likely to be more similar to the situation in a coal dump, than the situation modelled by Lapwood (1948) and Weber (1974).

In conclusion, having reviewed the available models for self-heating it is felt that a model similar to that used by Nordon (1979), but taking into account natural convection flows and neglecting diffusion, (as discussed in Chapter 2), should be developed in order to make predictions about the behaviour of stockpiled coal.

5.3 A one-dimensional analogue of a coal dump

In order to derive a mathematical model of a coal dump which will yield results fairly simply, certain simplifying assumptions have to be made. The main assumption in the model presented here is that the processes of heat, mass and momentum transfer occur in one direction only. Although this is known not to be true in a real coal dump, it does represent a limiting case which in many respects is the worst case. It can be seen that considering heat transfer in one direction only is likely to be the worst case, since the heat loss is limited to one direction only. Similarly considering flow in only one direction is the worst case, since reactant depletion is likely to be less in a one dimensional model than in one in which reactant flows from many directions.

In many important respects the one-dimensional model is accurate. A one-dimensional model is likely to be accurate for the case of coal stored in a silo, if proper allowance is made for radial heat losses that can occur. In the middle of a very large dump of coal heat transfer to the sides is unlikely to be significant because of the large distances involved; significant heat transfer will occur only to the surface of the dump. In addition should a "hot-spot" occur in a dump the flow due to natural convection will be in the same direction as the heat transfer. The existence of hot spots in coal dumps is well known; spontaneous combustion in its early stages is localized, as has been shown by infra-red photography. The reasons for the existence of hot-spots in coal dumps may include inhomogeneity of the bed in respect of degree of compaction, coal reactivity or moisture content. Experimental work by Young (1985), on natural convection in a porous bed containing a line source, shows

clearly that there is a region close to the source through which most of the flow passes. This is shown diagramatically in Figure 5.1, in which model streamlines are plotted for one half of a symmetrical bed, of infinite length in the Z direction, containing a line source located at X=0, Y=0.6. Note that the reason that no flow occurs through the side X=1 is that in solving the model equations Young assumed that this surface was impermeable. This assumption should not drastically effect the behaviour of the streamlines near the source. Although the situation modelled by Young (1985) is not identical to that in a coal bed, it is felt that the flow patterns near a hot-spot are unlikely to be very different to the flow patterns found near a line source.

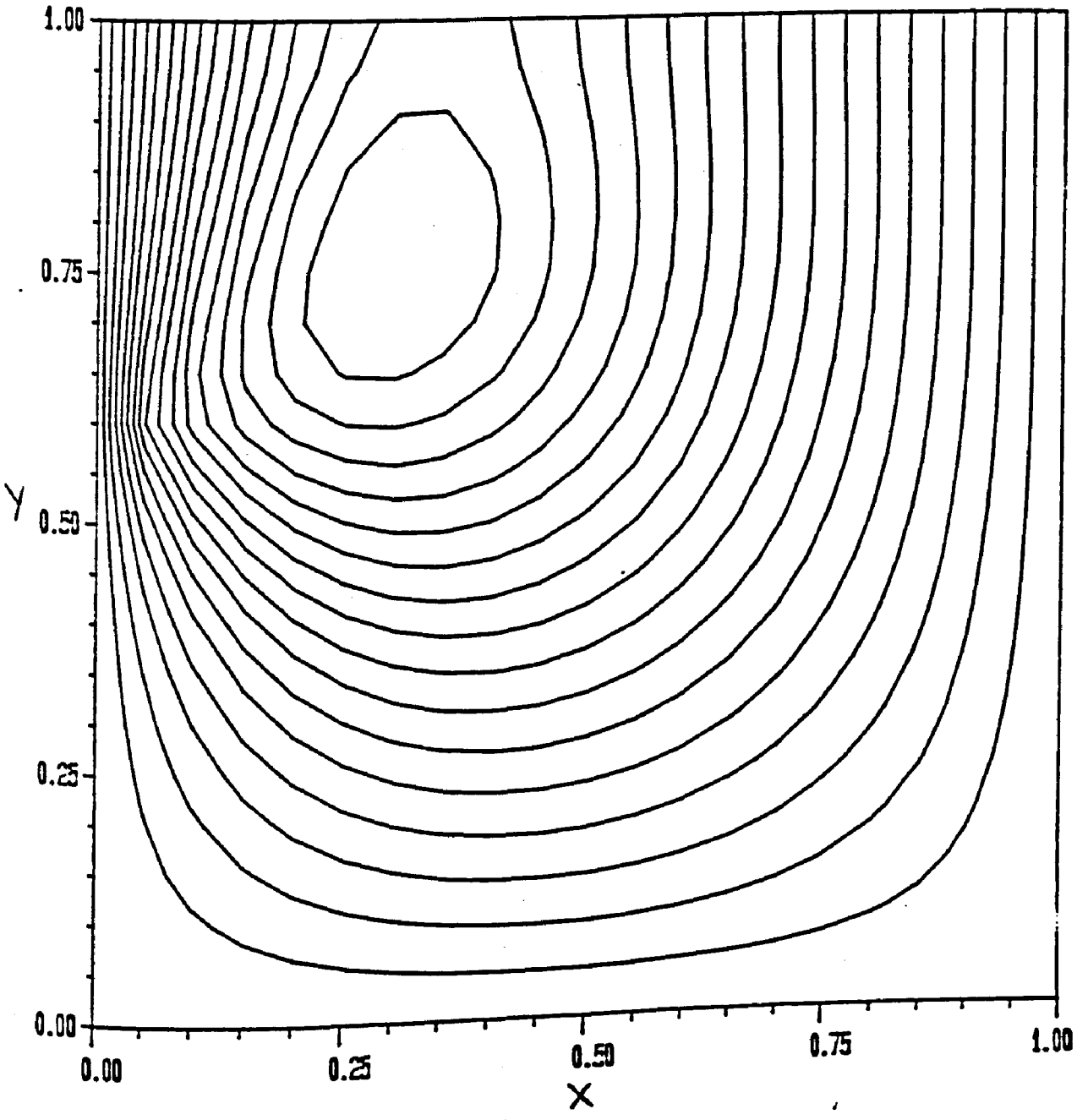


Figure 5.1 Streamlines in a Packed Bed Containing a Line Source (From Young, 1985)

Assuming that a hot spot arises in a coal dump for some reason, it can be reasoned that a chimney effect will take place. Air will flow up the chimney, and be replaced by air flowing in from the sides and top of the dump. If the behaviour of this chimney inside the coal dump can be modelled, then valuable insight into the nature of spontaneous combustion can be obtained. This is the physical basis for the model presented here.

To model the chimney inside the coal bed would be difficult. To make the model simpler the chimney is considered to be perfectly insulating radially. All the flow is considered to occur through the bottom of the bed, with no flow occurring through the sides. The bottom of the bed is considered to be open to atmosphere. These assumptions mean that the chimney can be modelled separately from the rest of the coal dump.

The disadvantages of this model are the following:

a) No simple relationship has been found relating the length of the chimney in the model to the size of the coal dump. Since the bed length is an important model parameter, this limits the applicability of the results obtained. This point will be further discussed in chapter 8.

b) It is assumed that the bottom of the chimney is open and thus loses heat to the atmosphere. In a real dump the bottom of the chimney loses heat to the surrounding coal. It is difficult to gauge how dissimilar these heat loss mechanisms are, and in what way this assumption will affect the results.

Despite these disadvantages the chimney or one-dimensional model may be considered to be a model that has a sound physical basis. The behaviour of the chimney should be similar to the behaviour of a coal dump in many important respects. The shortcomings of the the model are appreciated, but are not expected to invalidate the results obtained, provided these results are not taken to be directly applicable in a quantitative sense.

The great advantage of the model is that the equations derived may be solved fairly easily. A study of the parameters that are important in the prediction of spontaneous combustion may thus be performed without excessive computation.

The main assumptions in the mathematical model used in this study are therefore:

a) Flow and heat transfer occur in the same direction, and since the gas is assumed to flow in plug flow there are no radial gradients in the bed.

b) The reactions considered are

$$n\,C(s) + O_2(g) \rightarrow C_nO_2(s)$$
$$C_nO_2 \rightarrow CO_2 + (n-1)\,C(s)$$
$$\tfrac{1}{2}\,C_nO_2 \rightarrow CO(g) + (\tfrac{1}{2}n-1)\,C(s)$$
$$H_2O(g) \rightleftarrows H_2O(abs)$$

This reaction scheme is in agreement with the observed behaviour of the low temperature reactions of coal, as discussed in Chapter 1. C_nO_2 is oxycoal but note that no specific hypothesis about its structure needs to be made. The fourth reaction is water absorption, which has been reported to be of importance in spontaneous combustion of coal dumps, as has been discussed in chapter 2.

c) Flow is considered to be caused by natural convection and by differential pressure. Molecular diffusion is neglected as discussed in Chapter 2. Natural convection flows occur as soon as there is any temperature rise in the bed, since the bed is considered to be vertically aligned and open top and bottom.

Under these assumptions and some other minor assumptions which arise in the derivation of the equations a mathematical model has been derived. The full derivation is given in Appendix 3.

5.4 Model Equations

The model equations are:

5.4.1 Component mass balances (Gas phase)

$$G\frac{\partial y_i}{\partial x} + \frac{P\,\epsilon}{R\,T_g}\frac{\partial y_i}{\partial t} = r_i - y_i \sum r_j \qquad (i = 1 \text{ to } N)$$

G = molar flowrate per unit area

y_i = mole fraction of i in the gas phase

x = distance along bed

P = pressure

R = gas constant

ϵ = bed voidage

T_g = gas temperature

t = time

r_j = rate of formation of j in the gas phase per unit bed volume

N = number of components in gas phase

5.4.2 Overall gas mass balance

$$\frac{\partial G}{\partial x} + \frac{\epsilon}{R}\frac{\partial (P/T)}{\partial t} = \sum_{j=1}^{N} r_j$$

5.4.3 Component mass balances (Solid phase)

$$(1-\epsilon)\frac{\partial (\rho_s f_j)}{\partial t} = p_j \qquad (j = 1 \text{ to } M)$$

ρ_s = density of solid

f_j = mass fraction of j in the solid

p_j = rate of formation of j in the solid

M = number of components in solid phase

5.4.4 Overall solid mass balance

$$(1-\epsilon)\frac{\partial \rho_s}{\partial t} = \sum_{j=1}^{M} p_j$$

5.4.5 Gas phase energy balance

$$\frac{P\epsilon}{RT_g}\hat{c}\frac{\partial T_g}{\partial t} - \epsilon\frac{\partial P}{\partial t} = -G\hat{c}\frac{\partial T_g}{\partial x} + \epsilon K_g\frac{\partial^2 T_g}{\partial x^2} + Q_c$$

$\hat{c}$ = molar specific heat capacity of gas

K_g = thermal conductivity of gas

Q_c = rate of convection from solid to gas

5.4.6 Solid phase energy balance

$$(1-\epsilon)\,\rho_s\,\bar{c}_s\,\frac{\partial T_s}{\partial t} - (1-\epsilon)\,\frac{\partial P}{\partial t} = (1-\epsilon)\,\eta\,k_s\,\frac{\partial^2 T_s}{\partial x^2} - Q_c - \Sigma\,(r_i \Delta H_r^i)$$

T_s = solid temperature
η = tortuosity factor
k_s = thermal conductivity of solid
ΔH_r^i = enthalpy of reaction for formation of i

5.4.7 Momentum balance

$$\rho\,\frac{\partial U}{\partial t} = -f\,U + g\,\rho_\infty(1-T_\infty/T) - \frac{\partial(P-P_\infty)}{\partial x}$$

U = flow velocity
f = D'Arcy's law constant
ρ_∞ = density of ambient air
P_∞ = ambient air pressure

5.5 Discussion of the model equations

This is a set of M + N + 5 differential equations. The unknowns are tabulated in Table 5.2.

TABLE 5.2 UNKNOWNS IN THE MODEL EQUATIONS

UNKNOWN	DESCRIPTION	NUMBER
y_i	Gas mole fractions	N
G	Molar flowrate/area	1
f_i	Solid mass fractions	M
ρ_s	Solid density	1
T_g	Gas temperature	1
T_s	Solid temperature	1
P	Gas pressure	1

Although the equations have been derived for any number of gas and solid components, in the discussions that follow the gases considered are O_2, N_2, CO_2, CO and H_2O. The solid is considered to be composed of four fractions i.e. carbon, oxycoal, absorbed water and inert material.

5.6 Boundary and Initial Conditions

The following are the boundary conditions used: (x=0 refers to the bottom of the bed and x=L refers to the top).

$$y_i(0,t) = \text{Mole fraction of i in ambient air}$$

The pressure boundary conditions have been discussed in section 2.2 and are:

$$P(0,t) = P_\infty + \rho_\infty V^2/2$$

$$P(L,t) = P_\infty$$

$$V = \text{wind velocity}$$

For the gas phase energy balance

$$\epsilon k_g \frac{\partial T_g(0,t)}{\partial x} = G \hat{c} (T(0,t) - T_\infty)$$

$$\frac{\partial T_g(L,t)}{\partial x} = 0$$

The first boundary condition reflect the fact that the gas entering the bed is heated to the gas temperature. At the end of the bed it is assumed that there is no heat loss due to flow; the gas is assumed to leave the bed in plug-flow, implying that the temperature just outside the bed is equal to the temperature just inside the bed.

For the solid phase energy balance

$$(1-\epsilon) \eta k_s \frac{\partial T_s(0,t)}{\partial x} = h_1 (T_s(0,t) - T_\infty)$$

$$(1-\epsilon) \eta k_s \frac{\partial T_s(L,t)}{\partial x} = -h_2 (T_s(L,t) - T_\infty)$$

These are convective boundary conditions, but h_1 and h_2 may be interpreted as radiation heat transfer coefficients. Initial conditions for the equations involve assigning values to each of the variables at time zero for all x. In most cases ambient values would be used.

6. SIMPLIFICATON OF THE MODEL EQUATIONS AND THEIR SOLUTION

6.1 Introduction

Although a one-dimensional formulation has been used to simplify the equations and reduce their number, the equations remain complicated. In order to simplify them further to perform computation the following assumptions (which are discussed more fully in Appendix 4) were made:

a) The gas and solid temperatures are unlikely to be very different; therefore equations 5.4.5 and 5.4.6 may be combined to give one equation in temperature, ie a continuum assumption is made. The reason for deriving the gas and solid phase energy balances separately is that the boundary conditions for use in the continuum model are not clear; deriving the balances separately and then combining them allows the correct boundary conditions to be deduced mathematically.

b) Since the heat transfer is by far the slowest transfer process occuring in the bed, the other transfer processes may be considered to be at steady state i.e. a pseudo steady state formulation is used.

In order to simplify still further it is convenient to define a rate (ry) which is the rate at which oxygen disappears. Similarly an enthalpy of reaction ΔH_r is defined; this may be considered to be the enthalpy of reaction associated with the disappearance of oxygen. The reaction involving water is ignored for the following reasons:

a) It is likely to be only a starting mechanism whereby the temperature in a coal bed is raised to the point where natural convection flows and oxidation become the mechanisms whereby the dump combusts.

b) As yet no reliable data for this reaction is available, and it is in any case believed that the reaction is likely to be close to equilibrium in most cases.

It would appear from equation 5.4.2 that the change in flowrate due to reaction has to be considered. However, if air is the reactant then even if all the oxygen in the flow is removed the flowrate will only change by twenty percent. It is therefore

6. SIMPLIFICATON OF THE MODEL EQUATIONS AND THEIR SOLUTION

6.1 Introduction

Although a one-dimensional formulation has been used to simplify the equations and reduce their number, the equations remain complicated. In order to simplify them further to perform computation the following assumptions (which are discussed more fully in Appendix 4) were made:

a) The gas and solid temperatures are unlikely to be very different; therefore equations 5.4.5 and 5.4.6 may be combined to give one equation in temperature, ie a continuum assumption is made. The reason for deriving the gas and solid phase energy balances separately is that the boundary conditions for use in the continuum model are not clear; deriving the balances separately and then combining them allows the correct boundary conditions to be deduced mathematically.

b) Since the heat transfer is by far the slowest transfer process occuring in the bed, the other transfer processes may be considered to be at steady state i.e. a pseudo steady state formulation is used.

In order to simplify still further it is convenient to define a rate (ry) which is the rate at which oxygen disappears. Similarly an enthalpy of reaction ΔH_r is defined; this may be considered to be the enthalpy of reaction associated with the disappearance of oxygen. The reaction involving water is ignored for the following reasons:

a) It is likely to be only a starting mechanism whereby the temperature in a coal bed is raised to the point where natural convection flows and oxidation become the mechanisms whereby the dump combusts.

b) As yet no reliable data for this reaction is available, and it is in any case believed that the reaction is likely to be close to equilibrium in most cases.

It would appear from equation 5.4.2 that the change in flowrate due to reaction has to be considered. However, if air is the reactant then even if all the oxygen in the flow is removed the

6. SIMPLIFICATON OF THE MODEL EQUATIONS AND THEIR SOLUTION

6.1 Introduction

Although a one-dimensional formulation has been used to simplify the equations and reduce their number, the equations remain complicated. In order to simplify them further to perform computation the following assumptions (which are discussed more fully in Appendix 4) were made:

a) The gas and solid temperatures are unlikely to be very different; therefore equations 5.4.5 and 5.4.6 may be combined to give one equation in temperature, ie a continuum assumption is made. The reason for deriving the gas and solid phase energy balances separately is that the boundary conditions for use in the continuum model are not clear; deriving the balances separately and then combining them allows the correct boundary conditions to be deduced mathematically.

b) Since the heat transfer is by far the slowest transfer process occuring in the bed, the other transfer processes may be considered to be at steady state i.e. a pseudo steady state formulation is used.

In order to simplify still further it is convenient to define a rate (ry) which is the rate at which oxygen disappears. Similarly an enthalpy of reaction ΔH_r is defined; this may be considered to be the enthalpy of reaction associated with the disappearance of oxygen. The reaction involving water is ignored for the following reasons:

a) It is likely to be only a starting mechanism whereby the temperature in a coal bed is raised to the point where natural convection flows and oxidation become the mechanisms whereby the dump combusts.

b) As yet no reliable data for this reaction is available, and it is in any case believed that the reaction is likely to be close to equilibrium in most cases.

It would appear from equation 5.4.2 that the change in flowrate due to reaction has to be considered. However, if air is the reactant then even if all the oxygen in the flow is removed the flowrate will only change by twenty percent. It is therefore considered adequate to regard the flowrate as a constant to be considered adequate to regard the flowrate as a constant to be calculated from equation 5.4.7.

Under these assumptions the number of equations to be solved is reduced to three i.e. a temperature equation, an oxygen equation and a flowrate equation. These equations are given below.

Temperature: $$\rho C_b \frac{\partial T}{\partial t} = k_b \frac{\partial^2 T}{\partial x^2} - G \hat{c} \frac{\partial T}{\partial x} + r\, y\, \Delta H_r \qquad 6.1.1$$

ρ_b = density of bed
C_b = specific heat capacity of bed
k_b = thermal conductivity of bed
y = mole fraction oxygen
ΔH_r = enthalpy of reaction for oxygen disappearance

Oxygen: $$G \frac{dy}{dx} = -r\, y \qquad 6.1.2$$

Flowrate: $$\frac{d(P-P_\infty)}{dx} = -f\, G\, R\, T/P + g(\rho_\infty - \rho) \qquad 6.1.3$$

One possible functional form for the rate of reaction r has been discussed in Section 1.3, but should a superior rate expression for the oxidation be proposed it would be a simple matter to use this expression in the model.

The boundary conditions on the equations are:

$$k_b \frac{\partial T(0,t)}{\partial x} = (h_0 + G \hat{c})\,(T(0,t)-T_\infty)$$

$$k_b \frac{\partial T(L,t)}{\partial x} = -h_1\,(T(L,t)-T_\infty)$$

$y(x=0)$ = mole fraction of oxygen in air

$P(x=0) = P_\infty + \rho_\infty V^2/2$

$P(x=L) = P_\infty$

The initial condition for equation 6.1.1 is a given temperature profile e.g. $T(x,0) = T_0(x)$.

It is convenient in what follows to make equation 6.1.1 dimen-

sionless. To do this the following substitutions are made:

$$\theta = T/T_\infty$$
$$X = x/L$$
$$\tau = \kappa t/L^2$$
$$a = G\,\hat{c}\,L/k_b$$
$$b = L^2\,r\,(-\Delta H_r)/(T_\infty\,k_b)$$
$$\gamma_s = -r/G$$
$$Bi_0 = h_0\,L/k_b$$
$$Bi_1 = h_1\,L/k_b$$

Equation 6.1.1 becomes:

$$\frac{\partial\theta}{\partial\tau} = \frac{\partial^2\theta}{\partial X^2} - a\,\frac{\partial\theta}{\partial X} - b\,\gamma \qquad 6.1.4$$

with boundary conditions

at X=0 $$\frac{\partial\theta}{\partial X} = (Bi_0+a)(\theta-1)$$

at X=1 $$\frac{\partial\theta}{\partial X} = -Bi_1(\theta-1)$$

The initial condition is $\theta(X,0) = \theta_0(X)$

This equation may be improved by including a heat loss term. This heat loss term takes into account radial heat losses that are not taken into account in the original model. The term, as is shown in Appendix 5, may be written as $C(\theta - 1)$. In a sense C is a free parameter. It does however have real meaning in simulating a coal dump as will be seen in Chapter 7. Equation 6.1.4 becomes:

$$\frac{\partial\theta}{\partial\tau} = \frac{\partial^2\theta}{\partial X^2} - a\,\frac{\partial\theta}{\partial X} - b\,\gamma - C\,(\theta - 1) \qquad 6.1.5$$

with boundary and initial conditions as above.

6.2 The Steady-State form of the Equations

It may be argued that the set of equations does not have a steady-state solution since the reaction rate r is a function of the amount of oxidation and therefore of time. If the reaction rate is constantly falling off with time, i.e. the coal is

ageing, then there is no steady state. However it is convenient to study the behaviour of the equations in the limit of steady state, and for this purpose the ageing of the coal is ignored, and the so-called reaction rate of fresh coal is used. This is in a sense the worst case since the fresh coal has the highest reaction rate.

The temperature equation then becomes

$$0 = \frac{d^2\theta}{dX^2} - a\frac{d\theta}{dX} - b\,y - C\,(\theta - 1) \qquad 6.2.1$$

First attempts to solve equation 6.2.1 with equation 6.1.2 and 6.1.3 involved the use of a Runge - Kutta algorithm. The method used was a shooting one i.e. a temperature at X = 0 and flowrate were guessed, and the equations integrated forward to try and meet the boundary conditions at X = 1. This method met with no success at all, since the calculated temperature was very sensitive to the assumed value of the inlet temperature. Changing the value of this temperature led either to the temperature increasing without bound or becoming negative. An explanation for this behaviour is given in Appendix 6.

An alternative method of solving equation 6.2.1 involves making the assumption that the reaction rate r may be considered constant throughout the bed. This is a very large assumption since the form of r involves an exponential of the temperature, and thus r cannot in fact be constant unless the bed temperature is constant. However over a fairly small range of temperature the assumption of an average rate in the bed is acceptable, even though the answers it gives will not be quite correct. A further justification for making this assumption is that an analytic form for the temperature profile in the coal bed may be obtained, and thus the characteristics of the solution may be quickly investigated.

The details of the solution are given in Appendix 7, and the temperature equation has the form:

$$\theta_{ss}(X) = 1 + C_1\exp(\gamma_1 X) + C_2\exp(\gamma_2 X) + C_3\exp(\gamma_3 X) \qquad 6.2.2$$

The coefficients γ_1, γ_2, C_1, C_2, and C_3 are given functions of the known parameters.

The solution of the equation set is in fact iterative, since some average temperature is assumed and the flowrate and average reaction rate calculated. This in turn leads to a new temperature profile, flowrate, and average reaction rate and so on till the process converges. The computer code to perform this calculation is given in Appendix 12.

The character of the solutions so obtained and their significance is discussed in Chapter 8.

6.3 The Solution of the Unsteady-State Equations with a Constant Rate

The unsteady state behaviour of the equation set is of great practical importance. If a coal dump is going to be reclaimed in a relatively short time, then its long time or steady-state behaviour is of little importance in predicting the safety or otherwise of the dump. In addition it is only possible to decide whether a given dump will achieve a safe or unsafe steady-state by considering the behaviour of the temperature with time.

As a continuation of the work in which the equation set is solved using a constant rate, a solution was sought for the unsteady state behaviour under the same assumption.

The equation to be solved is equation 6.1.5 and the details of the solution are given in Appendix 8. The solution is:

$$\theta(X,\tau) = \theta_{ss}(X) + v(X,\tau)\exp(-\tau(a^2/4-C) + aX/2) \qquad 6.3.1$$

where $$v(X,\tau) = \Sigma \{Z_n(X)\exp(-\beta_n^2\tau)\ Z_n(X')\ g(X')\ dX'\} \qquad 6.3.2$$

$$Z_n(X) = \frac{2(\beta_n^2+Bi_3^2)(\beta_n\cos(\beta_n X)+Bi_2\sin(\beta_n X))}{((\beta_n^2+Bi_2^2)(\beta_n^2+Bi_3^2+Bi_3)+Bi_2(\beta_n^2+Bi_3^2))}$$

$$g(X) = (\theta_o(X) - \phi_{ss}(X))\exp(-aX/2) \qquad 6.3.3$$

$$Bi_2 = Bi_0 + a/2$$

$$Bi_3 = Bi_1 + a/2$$

and the β_n are the positive roots of

$$\tan(\beta) = \frac{\beta(Bi_3 + Bi_2)}{(Bi_2\, Bi_3 + \beta^2)} \qquad 6.3.4$$

Obtaining the final solution (equation 6.3.1) at a given X and τ is a stepwise process, since starting with the initial condition $\theta_0(X)$ the coefficients a, b, and γ_3 are calculated. A time step is then taken and the temperature profile calculated. This in turn gives new values of a, b, and γ_3 and the process continued.

The solution has been programmed in BASIC on a HP 9835 computer, and the code is given in Appendix 12. In practice it has been found that only twenty terms of the series need be taken. Nevertheless obtaining the solution is a fairly lengthy process, since for each time step $Z_n(X)$ and the integral in equation 6.3.2 must be calculated for a number of X values.

The character of the solutions obtained by this method is discussed in Chapter 8.

6.4 A Numerical Method for Solving the Unsteady State Equations

A numerical method for solving the equation set has the following advantages:

a) The variation of the reaction rate with temperature and amount of oxidation of coal can be taken into account.

b) The model can be used to fit data obtained from experiments such as the one described in Chapter 7. This data can then be used to make predictions about the behaviour of a given coal in a given stockpiling situation.

The disadvantage of a numerical method is that no general observations can be made about the form of the solution, as is possible with an analytic solution. Also the amount of computation may become prohibitive.

The method chosen for solving the equations in this case is one first presented by Bellman, Kashef & Casti (1972), which has been

termed the method of lines. The technique involves the use of a Legendre polynomial to fit the temperature profile at any given time t. This has the effect of reducing the partial differential equation to a set of ordinary differential equations, which may then be solved by one of many available methods e.g. Runge-Kutta or Adams-Moulton.

The advantage of this method over the more normally used finite difference approach is that the finite difference methods require calcualtion at a large number of points in order to obtain accurate results at the points of interest. Consequently both the computing time and storage required are large. In contrast, the approach of doing the calculation at the nodes of the shifted Legendre polynomial offers a moderately accurate solution at a few points, and the solution may be calculated rapidly.

The essence of the method rests in writing

$$\frac{\partial\theta(X_j,\tau)}{\partial X} = \Sigma(a_{ij}\ \theta(X_j,\tau)) \qquad \text{for } i=1 \text{ to } n \qquad 6.4.1$$

The X_j are chosen to be the nodes of the shifted Legendre polynomial

$$P_n^*(X) = P_n(1-2X) \qquad 6.4.2$$

and the matrix a_{ij} of weighting factors may be calculated once and for all.

The details of the application of the technique to the particular set of equations under consideration are given in Appendix 9. In many respects the solution procedure is similar to that discussd in Section 6.3, since the coefficients a, b, and γ_3 are recalculated at each time step.

This solution method has also been programmed in BASIC on an HP 9816 computer, and the code is given in Appendix 12. The choice of the length of the time step chosen is critical to the stability of the method, but apart from this the method is very effective. Calculational time is in fact shorter than that required to obtain the solution 6.3.1 and it has been found that using a ninth order Legendre Polynomial is entirely adequate.

Further discussion of the method and the results obtained is given in Chapter 8.

7. EXPERIMENTAL INVESTIGATION OF THE BEHAVIOUR OF A ONE DIMENSIONAL ANALOGUE OF A COAL DUMP

7.1 Introduction

In order to attempt to validate the equations derived in the previous sections, as well as to obtain data to use in a parameter study, it was decided to build a coal chimney. The apparatus used and results obtained are discussed in this chapter.

7.2 Experimental

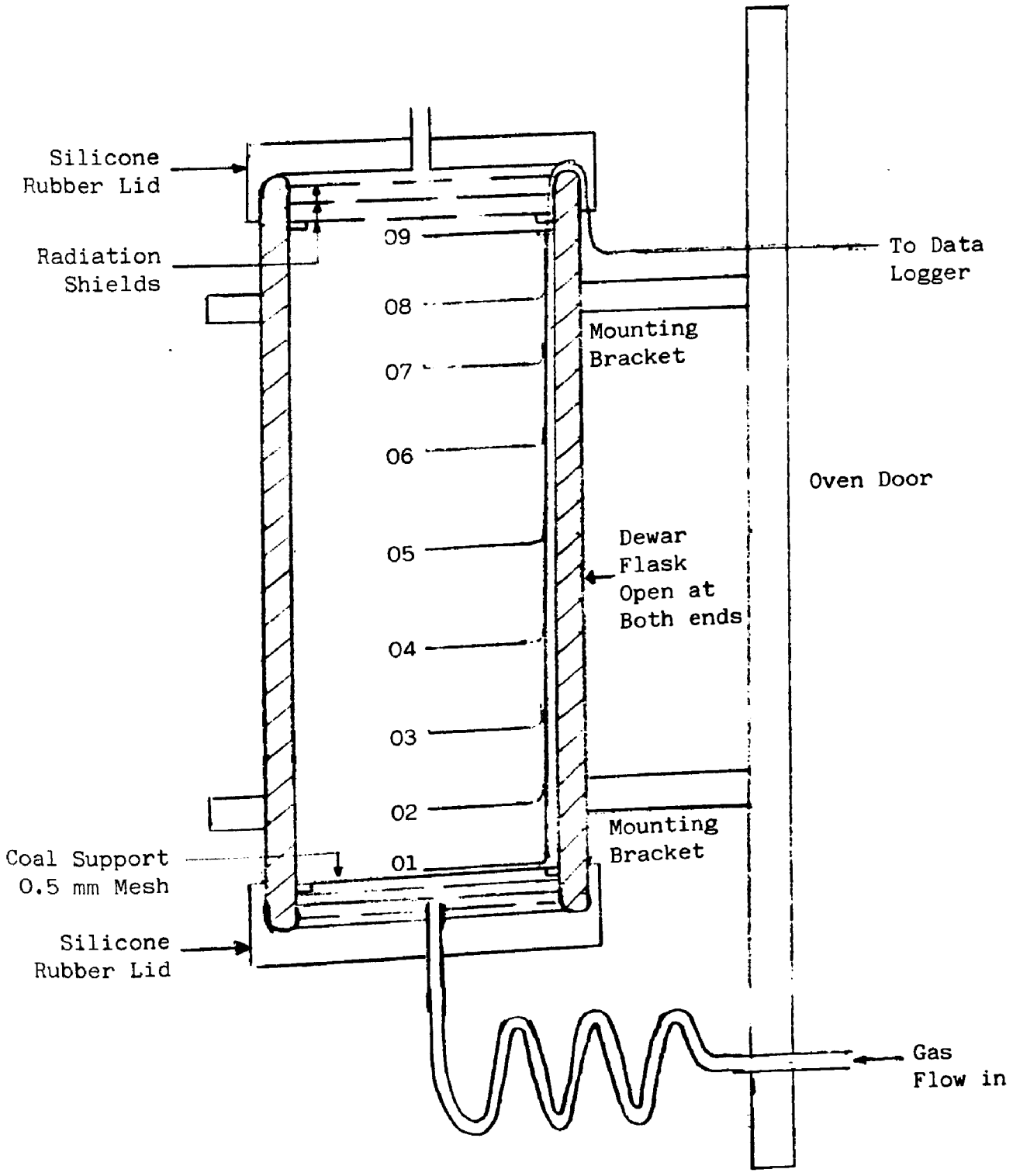
A skethch of the apparatus used is shown in figure 7.1. The coal chimney is constructed from an open ended Dewar Flask of 78 mm internal diameter and 240 mm height. Dimples of glass 20 mm from the bottom of the apparatus provide support for a piece of thin mesh, which in turn supports the coal. The chimney is provided with removable silicone rubber lids above and below. Both lids have 6 mm copper tubing moulded in, to provide for flow of gas in and out.

To minimize heat losses radiation shields manufactured from aluminium foil covered balsa wood discs are used. 10 mm Holes are punched in these discs in such a way that if three discs are assembled 5 mm apart, no direct rays of radiation can escape.

Thermocouples are manufactured by sparking together 20 SWG fabric coverd copper and constantan. The thermocouples are tested at 0°C and at the boiling point of water.

At the time of packing the bed with coal, the thermocouples are placed with their exposed ends on the centre line of the apparatus. Nine thermocouples are placed in the apparatus at positions corresponding to the nodes of the ninth order Legendre polynomial used in the solution method discussed in section 6.4.

In order to record the temperature-time behaviour of the chimney, these nine thermocouples, together with a tenth thermocouple placed in the oven containing the apparatus, are connected to a HP 3054 Data Aquisition Unit controlled by an HP 85 computer. A program



01 - 09: Copper Constantan Theromcouples

Figure 7.1 Chimney Experiment - Apparatus

supplied by Hewlett Packard is used to record the temperatures at a suitable time interval, as well as to print the temperatures and record them on tape. The program converts thermocouple voltages to temperatures using a fourth order polynomial; a silicon device built in to the data logger provides the cold junction reference temperature.

The apparatus is contained within a thermostatically controlled oven. Considerable care is taken to ensure that the temperature variations within the oven are small. The temperature in the oven is continually recorded using an eleventh thermocouple and a recorder. The temperature control of the oven is better than one degree centigrade.

The bed is supplied with gas (either nitrogen and oxygen) from cylinders. A series of valves are used to drop the pressure from the cylinder to the inlet of the bed, and to provide control over the flowrate of gas into the bed. This flowrate is measured usng a Tri Flat Variable Area Floe Meter. The manufacturer's curves are used to convert a reading on the meter to a volumetric flowrate. The barometric pressure is recorded in order that the volumetric flowrate can be converted to a molar flowrate. In order to ensure that the gas entering the bed is at oven temperature, a coil of length 0.5 m of 6 mm copper pipe is provided within the oven. enables the temperature time and temperature distance profiles to be automatically logged at any suitable time interval.

Experimental procedure consists of setting the oven temperature to the desired level, and placing the apparatus in the oven with a flow of nitrogen through the bed. Temperatures are recorded until they are considered to be steady. The flow is then switched to oxygen, and the temperature-time data recorded. For each run fresh coal that has been stored under water is used, in order to minimize the amount of prior oxidation of the coal. The coal is allowed to dry in a thin layer overnight at ambient temperature.

The experimental data obtained is tabulated in Appendix 10.

7.3 Experimental Results

The accuracy of results obtained from this experiment is limited by the accuracy to which the heat transfer characteristics of the apparatus are known. In order to calculate the numbers Bi_o, Bi_1, and C required for the model the bed was heated under nitrogen and then removed from the oven while continuing the nitrogen flow. The temperature time curve was then recorded, and a trial and error method used to calculate the values of the coefficients which best fit the data. The results of this fitting procedure are shown in Figure 7.2.

It can be seen that the experimental data is fitted very well at the centre of the bed but rather poorly at the ends of the bed. This indicates that the heat transfer mechanism at the ends of the bed is not well modelled by a heat transfer coefficient. However it was felt that if the rest of the fitting was done with temperature time curves at the centre of the bed the results would at least yield suitable values to use in a parameter study.

Two different sorts of behaviour have been observed during the experiments in which oxygen is flowed through a preheated coal bed. The different sorts of behaviour depend on the particle size of the coal used and the oven temperature.

The first type of behaviour which is observed is a fairly gentle rise of the temperature in the bed, with some maximum temperature being reached, after which the temperature begins to fall off again. This behaviour can only occur if the reactivity of the coal is falling off with time; this implies that the coal is ageing. This behaviour, observed for the larger particle sizes at oven temperatures of approximately 90 ^{o}C, has been used to calculate the various constants in the shrinking core model discussed in Section 1.3; these fits are shown in Figures 7.3 and 7.4.

The second type of behaviour observed is a fairly rapid temperature increase in the coal bed with the rate of temperature rise increasing with time. This behaviour may be considered to be combustion. When this occurs the coal bed has to be cooled down by taking the apparatus out of the oven and restoring the

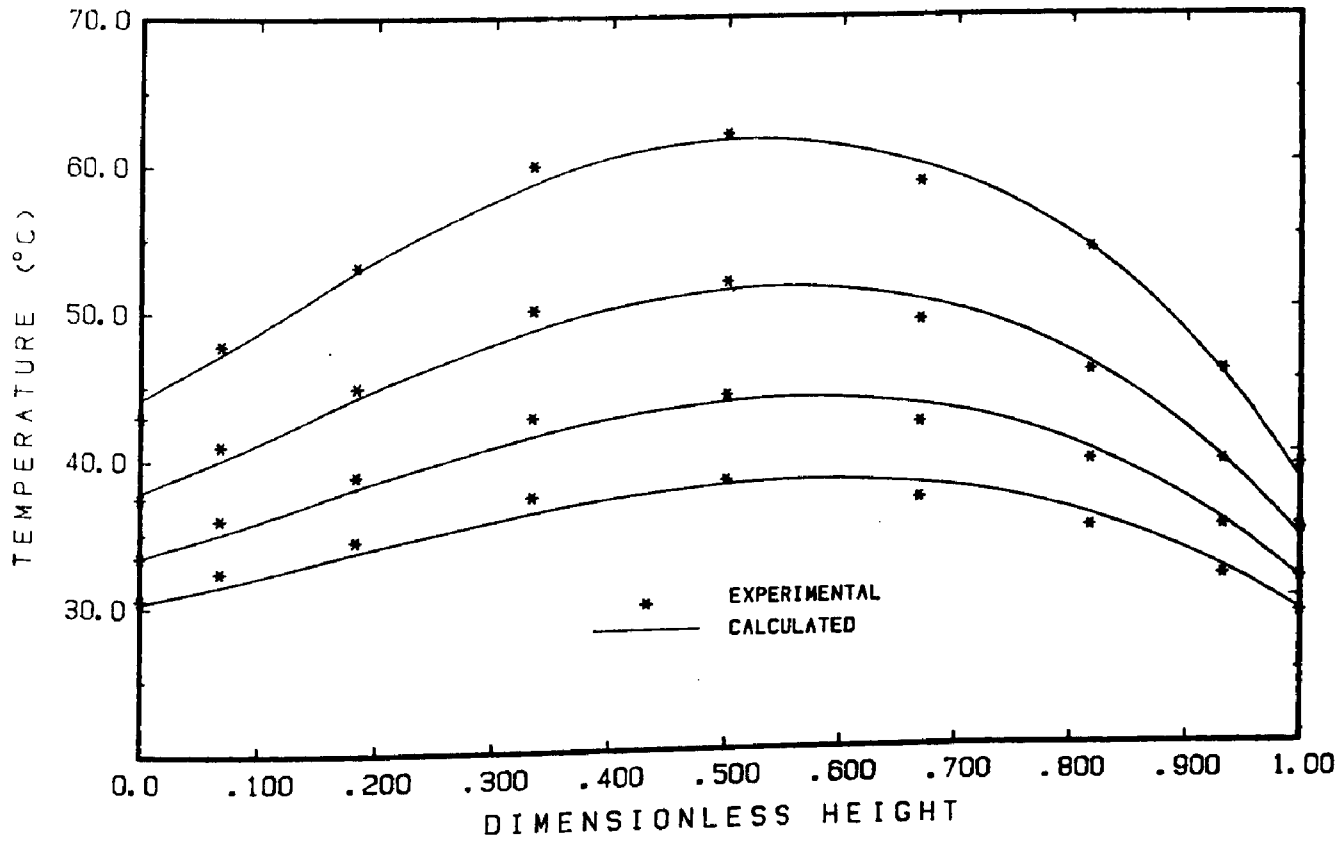


Figure 7.2 Chimney experiment - Fitting heat transfer coefficients

Profiles plotted every 30 minutes

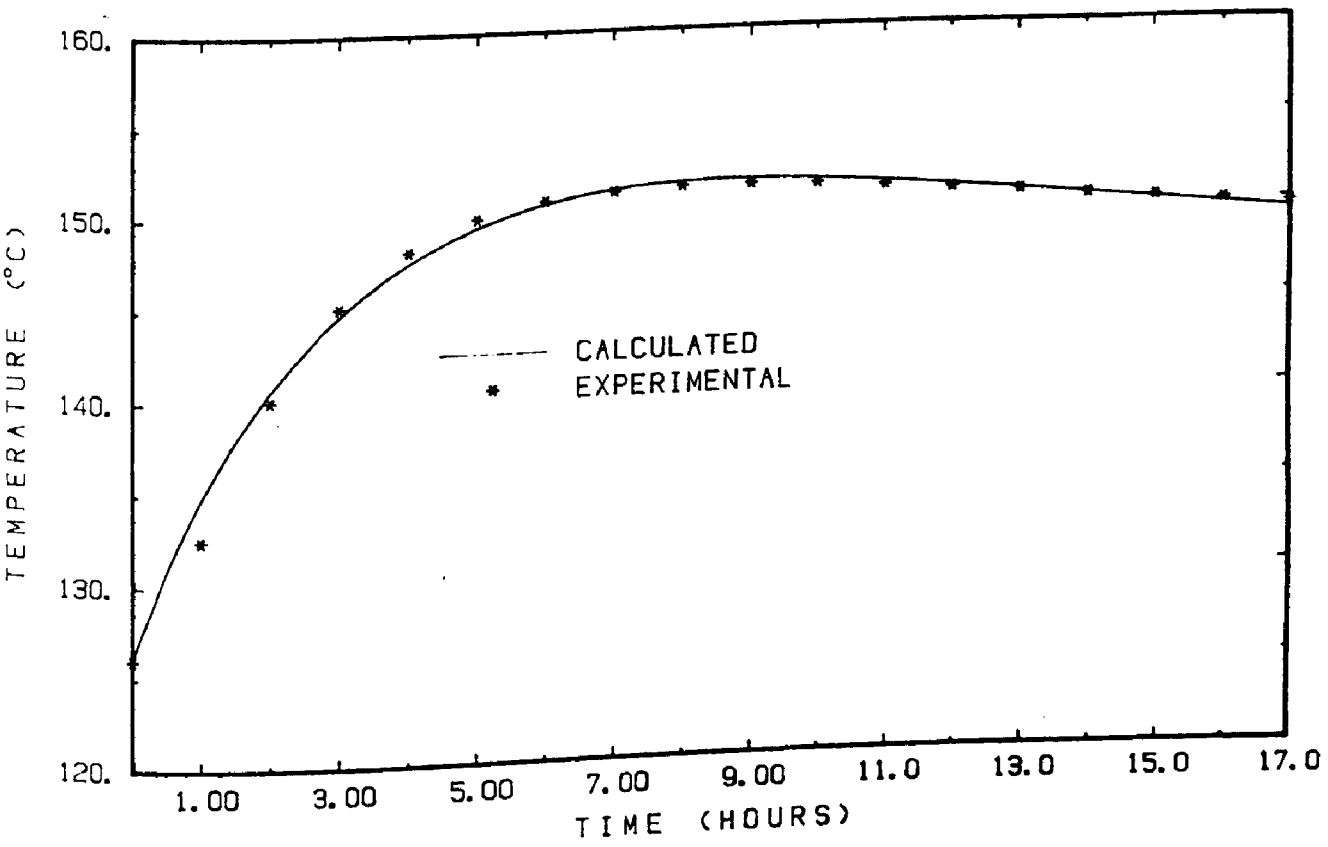


Figure 7.3 Chimney experiment - Fitting ageing run 1

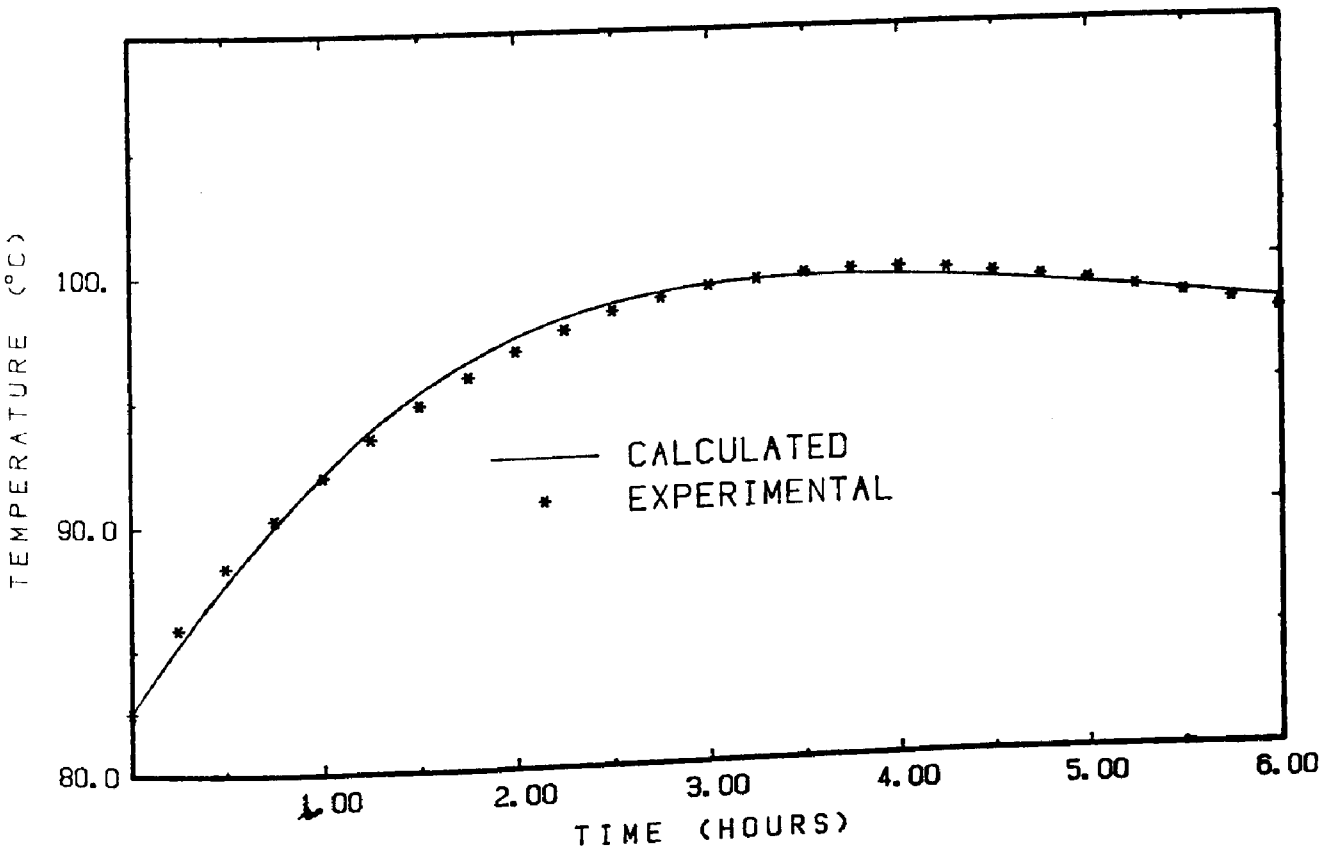


Figure 7.4 Chimney experiment - Fitting ageing run 2

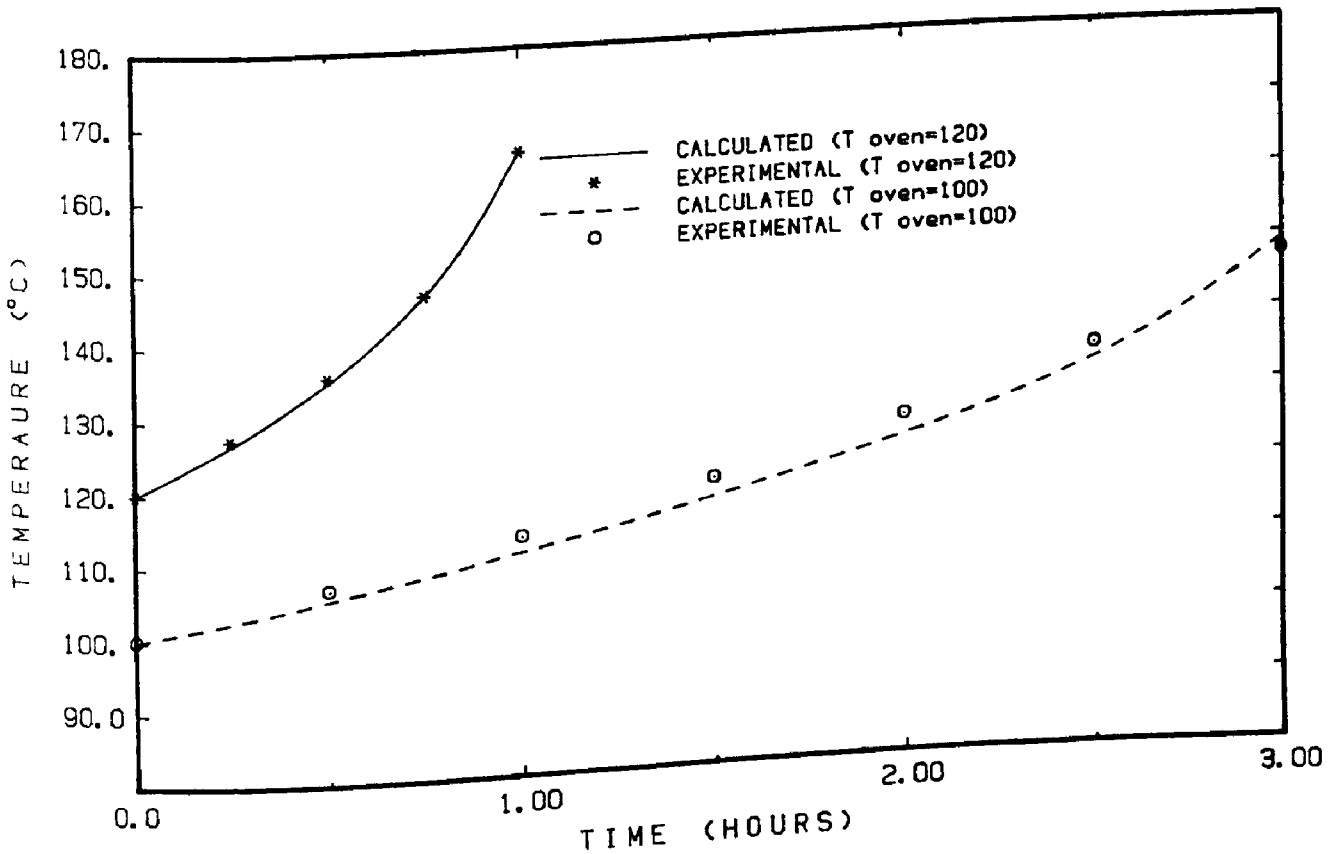


Figure 7.5 Chimney experiment - Fitting ignition runs

nitrogen flow.

These ignition runs yield very valuable information since it proves simpler to deduce the kinetic data from these runs then from the runs in which there is a gentle temperature rise. The reasons for this are that the temperature rises are much larger, meaning that ageing is a smaller effect. An example of the fitting of this data is shown in Figure 7.5 where two different experimental runs are fitted with the same data. The fit is fair but tends to be poorer as the temperature increases more rapidly. The reason for this is that at these higher temperature some of the model assumptions breakdown.

The values of the parameters used to obtain the fits shown in figures 7.2 to 7.5 are tabulated in Appendix 10. It must be stressed that these parameters, in particular the reaction rate values, are likely to be very different for different coals.

7.4 Discussion

The experiment used to derive the results in this section is not a good experiment from the point of view of analyzing the results to obtain the parameters required. This is partly because many of the parameters required in the model need to be estimated, and there may be a high cross correlation between the estimated parameters, and those found by curve fitting. However it is felt that the parameters calculated are accurate enough to give starting values for the parameter analysis discussed in the next chapter.

The analysis of the experiment may be improved in many respects e.g. by the use of a minimization routine to calculate the parameters. This was not felt neccessary in the present study.

8. RESULTS OF SOLVING THE MODEL EQUATIONS

8.1 Introduction

In this chapter the results of solving the model equations are presented. The three cases considered are:

a) Solving the steady-state equations with constant r.
b) Solving the unsteady-state equations with constant r.
c) Solving the equations with no assumptions, using a numerical method.

8.2 Steady-State Solution for constant r

Since an analytic solution exists for the temperature profile in this case, it has been used to perform a parameter study of the effect that changing the model parameters has on the calculated temperature profiles. In order to perform this parameter study a base set of parameter values had to be chosen, and certain assumptions made. The values of the parameters for this base case are given in Appendix 11. The assumptions made were the following:

a) The coal may be characterized by a single particle diameter, D_p, where

$$D_p = 6/S$$

S = external surface area per particle volume

b) The surface area for reaction, S_t, is set equal to the external surface area, S. However, the effect of changing this assumption has been investigated.

c) The wind velocity is set to zero, as is the heat loss coefficient, C.

d) Radiation heat transfer coefficients are used for h_1 and h_2; these could easily be replaced by natural convection heat transfer coefficients, if these were found to be more appropriate.

8.2.1 The Character of the Solutions

In order to investigate the character of the solutions, the following analysis was used:

Equaton 6.1.5 with C set equal to zero (i.e. no radial heat loss) is :

$$\frac{\partial\theta}{\partial\tau} = \frac{\partial^2\theta}{\partial X^2} - a\frac{\partial\theta}{\partial X} - by$$

Integrating from X = 0 to X = 1 gives

$$\int_0^1 \frac{\partial\theta}{\partial\tau}\,dX = \int_0^1 \frac{\partial^2\theta}{\partial X^2}\,dX - \int_0^1 a\frac{\partial\theta}{\partial X} - \int_0^1 by\,dX \qquad 8.1$$

Now, as shown in Appendix 4, $y = y_o \exp(\gamma_3 X)$. In addition a and b are not functions of X since they are calculated at an average temperature.

Thus equation 8.1 becomes

$$\frac{\partial\bar{\theta}}{\partial\tau} = \frac{\partial\theta}{\partial X}\Big]_1 - \frac{\partial\theta}{\partial X}\Big]_0 - a\,[\theta_1 - \theta_0] - \frac{by_o}{\gamma_3}[\exp(\gamma_3) - 1]$$

$$\frac{\partial\bar{\theta}}{\partial\tau} = -Bi_1(\theta_1 - 1) - (Bi_o + a)(\theta_0 - 1) - \frac{by_o}{\gamma_3}[\exp(\gamma_3) - 1]$$

$$\frac{1}{a}\frac{\partial\bar{\theta}}{\partial\tau} = -\frac{Bi_1}{a}(\theta_1 - 1) - \left(\frac{Bi_o}{a} + 1\right)(\theta_0 - 1) + \frac{by_o}{a\gamma_3}[1-\exp(\gamma_3)]$$

This equation may be written as

$$\frac{1}{a}\frac{\partial\bar{\theta}}{\partial\tau} = RHS - LHS \qquad 8.2$$

where

$$LHS = \frac{Bi_1}{a}(\theta_1 - 1) + \left(\frac{Bi_o}{a} + 1\right)(\theta_0 - 1)$$

$$RHS = \frac{by_o}{a\gamma_3}[1-\exp(\gamma_3)]$$

Equation 8.2 is the overall energy balance for the bed.

The quantity $by_o/(a\gamma_3)$ may be evaluated by substituting for a,b and γ_3 to give $(-\Delta H_r y_0) / (\hat{c}T_\infty)$. This quantity is the dimensionless adiabatic temperature rise i.e. the temperature rise that would occur if there was total conversion and no heat loss.

The steady-state solutions to equation 8.2 may be found by plotting LHS and RHS against θ , and observing where the two curves cross, since where the two curves cross

$$\frac{\partial\theta}{\partial\tau} = 0$$

The advantage of this procedure over solving the equation directly is that both stable and unstable steady-state solutions may be easily found.

A problem that occurs in using equation 8.2 is that , in the absence of wind, $T = T_\infty$ is always a solution of the equation. This is not a realistic solution, and arises from the assumpton in the model that natural convection is the only flow mechanism. In reality some diffusion will occur, and in this case this solution will vanish. In order to avoid numerical difficulties that arise, and also to make the solutions more realistic, in what follows it is assumed that the flowrate G may be written as

$$G = G_0 + G_{convection} \qquad 8.3$$

where G_0 is small but non-zero.

In the programs used to generate the figures in this section G_0 is assumed to caused by a 0.1 m/s wind. Equation 2.2.13 can be used to show that for a 5m long bed, this wind velocity causes the same flow as a temperature rise of 10^{-4} K, which is of course entirely negligible.

Several general points may be deduced from the definitions of RHS and LHS. In particular it is instructive to take limits of both the RHS and LHS as θ tends to 1 and to infinity.

When θ tends to 1, r tends to a finite quantity and G tends

to G_o by equation 8.3. (When $\theta = 1$ $G_{convection} = 0$). However since G_o can be chosen arbitrarily small the quantity exp(-rL/G) tends to 0. No other quantities in equation 8.2 are functions of θ , therefore

$$\lim_{\theta \to 0} (RHS) = - \frac{\Delta H_r y_o}{\hat{c}\, T_\infty}$$

For the values tabulated in Appendix 11 this quantity, which is the dimensionless adiabatic temperature rise, evaluates to 7.

When θ tends to 1 the LHS tends to zero by equation 8.2 , since both θ_o and θ_1 and tend to 1 as θ tends to 1.

When θ tends to infinity, the RHS tends to 0. This may be seen by considering the behaviour of rL/G for this case.

When θ tends to inifinity the LHS is not bounded, since both θ_o and θ_1 tend to infinity.

This suggests that the behaviour of the graph of RHS and LHS versus θ is as sketched in Figure 8.1.

From figure 8.1 it is clear that there must be an odd number of solutions to equation 8.2, and that the curves intersect at least once.

A further analysis of equation 8.2 leads to the ability to predict whether a cetain solution is an unstable or stable solution. Referring to equation 8.2 it may be seen that if LHS < RHS then $\partial\theta/\partial\tau > 0$ i.e. the bed tempeature is increasing. Referring to figure 8.1, and in particular to point B, it can be seen that at a temperature just above the temperature at which LHS and RHS intesect RHS is greater then LHS i.e. the derivative is positive. This implies that should the bed be at point B and the temperature rise, it will carry on rising since the derivative remains positive. Only at point C when this derivative is again 0 will the temperature stop rising. This implies that point B represents an unstable steady-state. A similar analysis can be performed to show that points A and C are stable steady-states.

The general conclusion from this analysis is:

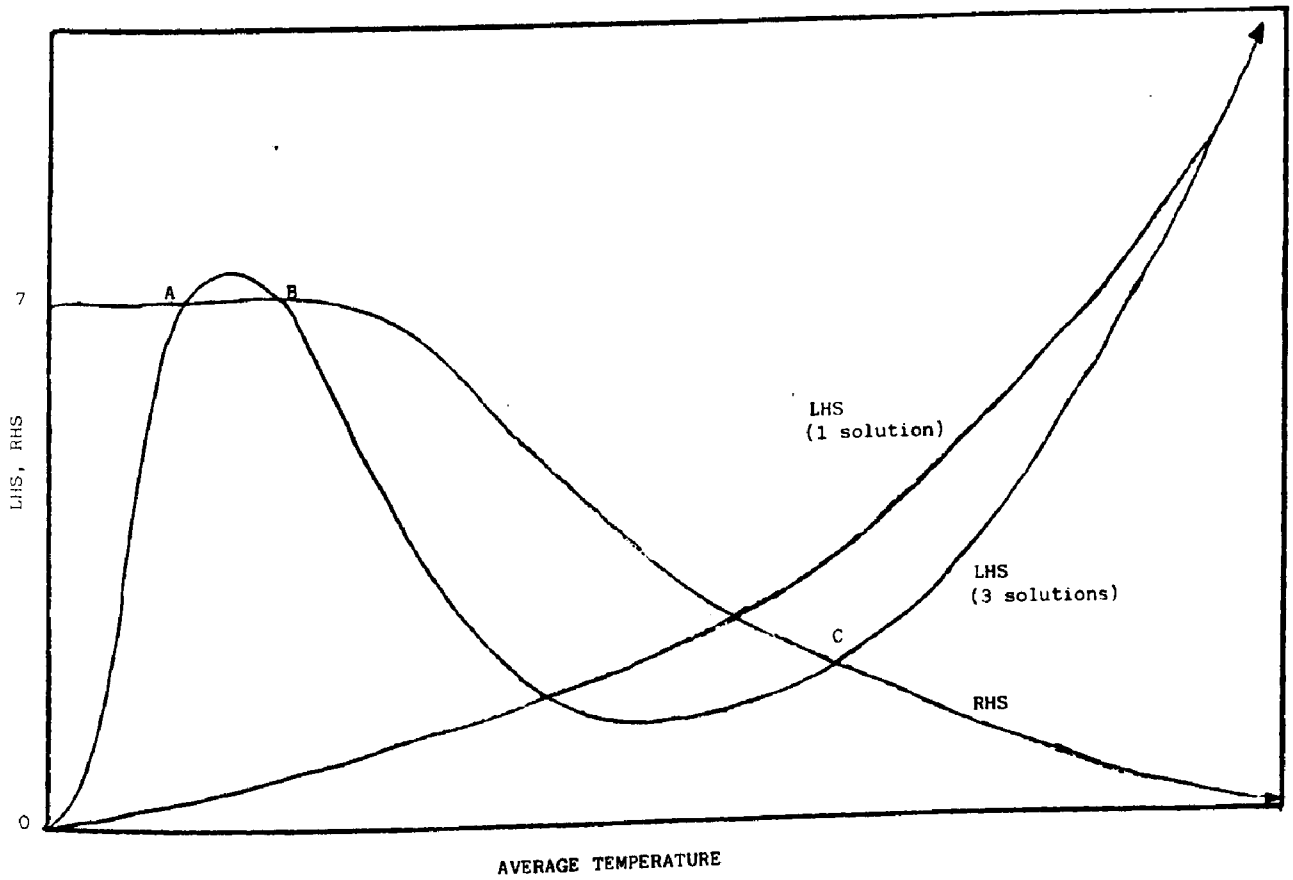


Figure 8.1 LHS and RHS of equation 8.2 as a function of θ

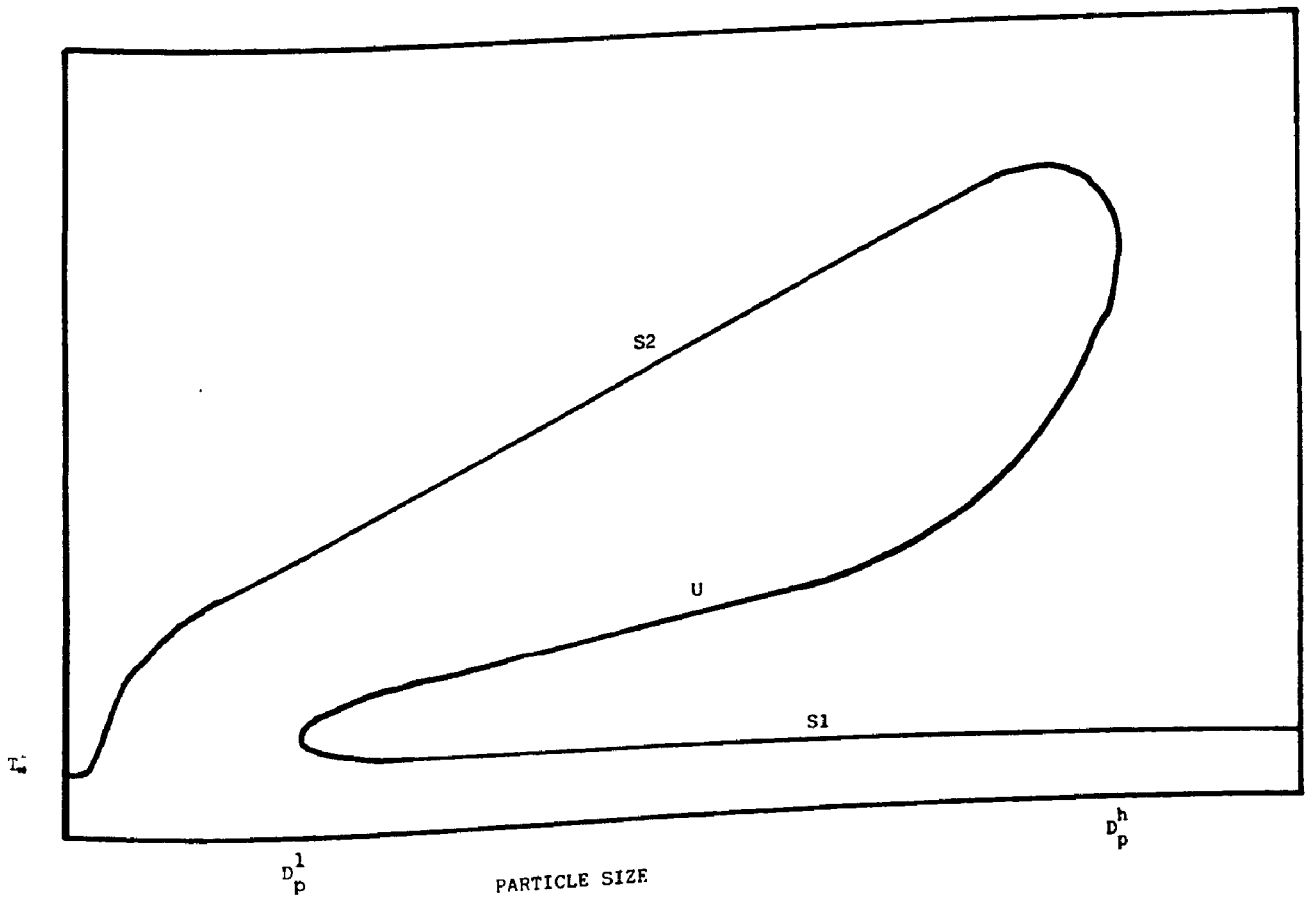


Figure 8.2 Locus of solutions to equation 8.2

For a stable solution at crossing θ_c the following condition must be true:

$$\left.\frac{d\ RHS}{d\bar{\theta}}\right]_{\theta_c} < \left.\frac{d\ LHS}{d\bar{\theta}}\right]_{\theta_c}$$

and conversely for an unstable solution:

Referring to figure 8.1 it is clear that the solutions A and C are stable solutions, while B is an unstable solution. In general the first and last solutions must be stable, and in between the solutions occur as unstable-stable-unstable etc. If there is only one solution it is stable.

This discussion serves to relate the behaviour of coal beds, as deduced in this study, to the behaviour of autothermal chemical reactors, and is extremaly valuable in understanding the nature of the solutions. A further discussion of the behaviour of autothermal reactors is given by Kramers & Westerterp (1963). In the beds investigated in this study, only beds with 1 or 3 solutions have been found. This does not mean that it is not possible that a certain coal bed may have more solutions; indeed this may be possible depending on the parameters in the model.

The procedure of plotting LHS and RHS versus θ has been performed for the base case, for different particle sizes. The graphs obtained are summarized in figure 8.2, in which is sketched the locus of solutions to equation 8.2, with particle size along the x-axis and average temperature on the y-axis.

The following conclusions may be drawn from figure 8.2:

a) Below a certain particle size, which may be called D_p^l, there exists only only 1 solution to equation 8.2.

b) Above D_p^l, but below a certain particle size D_p^h, there exist 3 solutions to equation 8.2.

c) Above D_p^h there exists only one solution to the equation.

Referring to figure 8.2 it can be seen that two different types of stable solution exist, labelled S1 and S2 respectively. The branch labelled S1 is characterized by a temperature rise of less than 30 ^{o}C. This implies that the assumption of a constant rate is a good one in this region. This solution is associated with little use up of oxygen. Beds in this region may be considered to be heat-transfer limited, i.e. they do not experience a large temperature rise because the heat transfer is high enough to remove most of the sensible heat of reaction. This solution ceases to exist below D_p^l since the heat transfer is no longer high enough to remove the sensible heat.

The branch labelled S2 is characterized by total consumption of oxygen. It should be noted that the values of the temperature on this branch are likely to be quite wrong, since the assumption of a constant rate used to calculate these values is a poor one. This is not of great practical importance since these beds may be considered to be burning, and the temperature at which the burning occurs is not of great importance. What is of importance is that for small temperature rises, ie safe beds, the model is accurate, and it is safe beds that are of interest. This high temperature solution ceases to exist above D_p^h since the surface area available for reaction becomes too small to support combustion. It should be pointed out that the values of D_p^h obtained in this study are in the region of 100 mm, which is above the particle size at which coal is normally stockpiled. A further point to note is that the details of the kinetics on branch S2 are also not of great importance. The reason for this is that when there is total consumption of oxygen the energy balance no longer contains any kinetic parameters ie the RHS of the energy balances reduces to the dimensionless adiabatic temperature rise.

Of great practical importance is the behaviour of branch S2 for small particle sizes. Below a certain particle size, which for the base-case parameters is of the order of 1 mm, the average temperature rise falls to less than 70 ^{o}C. Practical experience has shown that these beds, although experiencing a substantial temperature rise, are safe. In many practical cases, the effective particle size of a sample of coal will be below this value, and the bed will be safe. The meaning of particle size, as used in this study, is further discussed in section 8.2.6.,

It should be pointed out that neglecting molecular diffusion as a transport mechanism for oxygen is not a good assumption for particles in the sub 1mm range. Thus the temperatures the model predicts for these particle sizes in likely to be in error. However as has been shown in Chapter 2, the maximum temperature rise due to diffusion is of the order of 70 K. This temperature rise will not occur in practice due to the fact that that heat losses will occur. It is important to realise that even if there is a 70 K rise, the natural convection flows will be extremely small for these fine particles, implying that the beds will remain safe.

It can be seen from figure 8.2 that between D_p^1 and some small particle size the only solution to equation 8.2 is one in which the average temperature in the bed is dangerously high. Thus the model agrees with the often noted fact that certain coals cannot be safely stockpiled, and will, given enough time, spontaneously combust.

Also of practical importance is the branch labelled u in Figure 8.2. This is the locus of the unstable solutions, and serves to separate the stable solutions. The implication of this curve is that should a bed reach an average temperature above the average temperature given by the curve u, then the bed will combust. On the other hand, should the average temperature stay below u, then the temperature of the bed cannot reach the value given by the branch S2.

The possibility of multiple steady-states occurring in fixed bed chemical reactors has been noted in the literature. Luss (1968) and Luss & Amundson (1967) have used bifurcation theory to derive sufficient conditions for the existence of a unique steady-state in a fixed bed chemical reactor. This knowledge would be very valuable in the present study. The problem solved by Luss (1968) is similar, but not identical, to the problem studied in the present work. Unfortunately, the results obtained are not directly applicable to the model presented here, due to the differing mechanisms for reactant transport. This factor makes the application of the method presented by Luss (1968) to the present problem somewhat less than straightforward.

It would indeed be very useful to predict parameter values for which there are a given number of solutions to equation 8.2.

Balakotaiah & Luss (1984) have presented methods for determining the regions of parameters for which a given number of steady-state solutions exist in reacting systems. This work hhas been applied to the problem of predicting multiple steady-states in continuous stirred tank chemical reactors. In these cases the systems are described by algebraic rather than differential equations. The extension of the methods presented by Balakotaiah & Luss (1984) to differential equations is in principle simple; in practice the mathematics soon become intractable.

For the purposes of this study a less mathematically involved, albeit simple minded, approach has been used to determine how many steady-states exist for a given set of parameter values. The approach taken is to calculate the low temperature solution for particle size 20 mm. The particle size is then reduced by 1 mm and the calculation repeated. Eventually no low temperature solution to the equation can be found; thus the particle size at which the low temperature solution ceases to exist is found to an accuracy of 1 mm. The high temperature solution to the equation is then calculated. Although it is known that the model is poor for high temperatures, it is nevertheless important to calculate along this branch since, for sufficiently small particle sizes, the calculated temperatures are below 340 K. These beds may be considered to be safe. It should be noted that if a calculational scheme had been adopted whereby only the number of solutions to equation 8.2 was calculated, then these safe oxygen limited dumps would not have been identified.

The computational effort in performing the calculation described above is minor, even for a large range of parameter values. A computer program to perform the calculation is listed in Appendix 12. In figure 8.3 the results of calculating the locus of solutions to equation 8.2 for the parameter values given in Appendix 11, is presented. The results have been calculated in steps of 1 mm up to particle size 20 mm. Figure 8.3 is the base case, and is used in what follows as a means of comparing the effects of changing the parameters in the model.

The results presented in this section are critical to understanding the behaviour of coal dumps, and will therefore now be summarised:

a) Coal dumps may be classified as either safe, unsafe or con-

ditionally safe.

b) Dumps that are safe are composed of either fine reactive material in which case they are oxygen limited, or coarse unreactive material, in which case they are heat transfer limited.

c) Dumps which are conditionally safe may burn if the temperature of the dump rises above a certain critical temperature. If the temperature of the dump stays below this critical value, the dump remains safe.

d) There are cases in which the dump will, given enough time, undergo spontaneous combustion.

In this study particle size has been chosen as the independent variable for the purposes of presenting in a graphical form the results of solving the model equations. The reason for this is that by varying the particle size, the behaviour of different coal dumps may be observed. However, the other physical parameters of the bed are of extreme importance. For this reason the effect of changing one parameter in the model at a time was investigated. The results are presented graphically in figures 8.3 - 8.11 , and discussed in depth below.

It will be noted that the different branches on the curves are labelled 'small temperature rise' and 'combustion'. It may seem contradictory that for fine material the temperatures on the combustion curve are relatively low. However, combustion may be regarded as a situation in which the large majority of available oxygen is reacting, and in this sense the label combustion is accurate for these curves.

In the discussions below 340 K is used as a dividing value between safe and unsafe coal beds. This value must not be taken too literally, since it has been arbitarily chosen. Its use merley proves convenient in comparing the results obtained for different parameter values.

8.2.2 Effect of varying the voidage

Voidage is a parameter which may be varied in practice by means of compaction. The effect of this is shown in Figure 8.4, from which the following conclusions may be drawn:

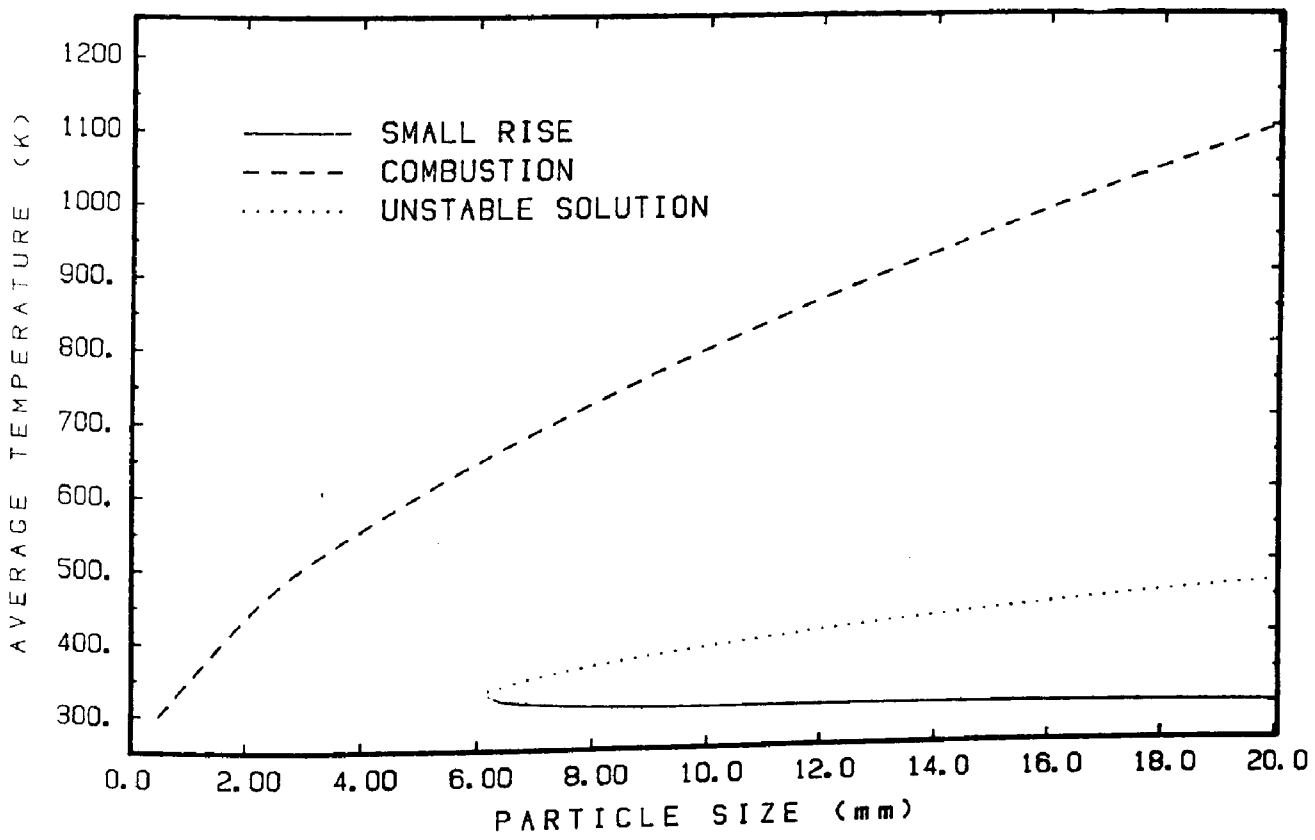


Figure 8.3 Stable and unstable solutions for the base-case

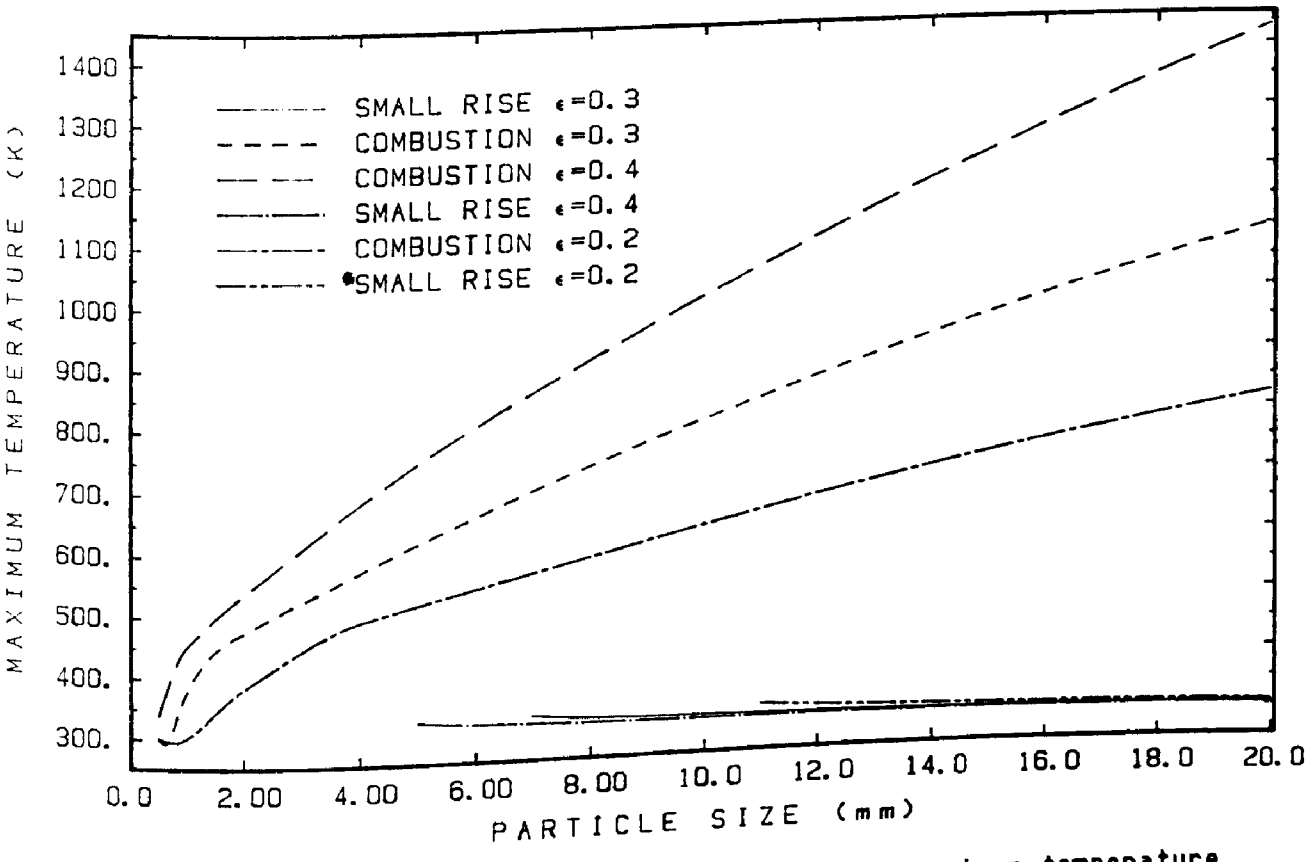


Figure 8.4 Effect of varying voidage on the maximum temperature

a) For fine material, compacting the bed will help make it safer. This can be seen from the fact that the combustion or oxygen limited curve is lower in temperature for lower voidages. Put another way, a fine coal may be safely stockpiled uncompacted, whereas a slightly coarser coal may have to be compacted when stockpiled in order for it to be safe. Using the rough criterion of 340 K then for this particular case material of voidage 0.2 is safe up to particle size 1.8 mm, while for voidage 0.3 the material is safe only up to particle size 0.8 mm.

b) Compacting coarse material may be detrimental. This is shown by the fact that the small temperature rise solution ceases to exist at $D_p = 11$ for $\epsilon = 0.2$, $D_p = 8$ for $\epsilon = 0.3$ and at $D_p = 5$ for $\epsilon = 0.4$.

The last conclusion may seen odd, and deserves some explanation. By compacting the bed the surface area per unit volume of the bed is increased. This in turn has two effects:

a) The resistance to flow is greater and
b) The mass of reactive material per unit bed volume is greater.

For the heat-transfer limited beds, i.e. the ones that experience a small temperature rise, the second result of more reactive material per bed volume more than outweighs the first of reducing oxygen ingress, since the bed was not in any case oxygen limited. (In fact, the reduction in flow also causes a rise in temperature since the heat loss due to flow is decreased). However for the case of oxygen limited beds compaction makes them safer by increasing the rate at which oxygen is scavenged from the air by reaction, as well as increasing the resistance to flow and therefore reducing the flowrate.

8.2.3 Effect of varying the pre-exponential factor

The purpose of varying the pre-exponential factor K_o is to try and simulate the fact that different coals will have different reactivities. Figure 8.5 indicates very clearly that for heat transfer limited beds, the larger K_o, the less safe the bed is. However, the opposite is true for oxygen limited beds. This surprising result can be understood in terms of the fact that

a) For fine material, compacting the bed will help make it safer. This can be seen from the fact that the combustion or oxygen limited curve is lower in temperature for lower voidages. Put another way, a fine coal may be safely stockpiled uncompacted, whereas a slightly coarser coal may have to be compacted when stockpiled in order for it to be safe. Using the rough criterion of 340 K then for this particular case material of voidage 0.2 is safe up to particle size 1.8 mm, while for voidage 0.3 the material is safe only up to particle size 0.8 mm.

b) Compacting coarse material may be detrimental. This is shown by the fact that the small temperature rise solution ceases to exist at $D_p = 11$ for $\epsilon = 0.2$, $D_p = 8$ for $\epsilon = 0.3$ and at $D_p = 5$ for $\epsilon = 0.4$.

The last conclusion may seen odd, and deserves some explanation. By compacting the bed the surface area per unit volume of the bed is increased. This in turn has two effects:

a) The resistance to flow is greater and
b) The mass of reactive material per unit bed volume is greater.

For the heat-transfer limited beds, i.e. the ones that experience a small temperature rise, the second result of more reactive material per bed volume more than outweighs the first of reducing oxygen ingress, since the bed was not in any case oxygen limited. (In fact, the reduction in flow also causes a rise in temperature since the heat loss due to flow is decreased). However for the case of oxygen limited beds compaction makes them safer by increasing the rate at which oxygen is scavenged from the air by reaction, as well as increasing the resistance to flow and therefore reducing the flowrate.

8.2.3 Effect of varying the pre-exponential factor

The purpose of varying the pre-exponential factor k_o is to try and simulate the fact that different coals will have different reactivities. Figure 8.5 indicates very clearly that for heat transfer limited beds, the larger k_o, the less safe the bed is. However, the opposite is true for oxygen limited beds. This surprising result can be understood in terms of the fact that

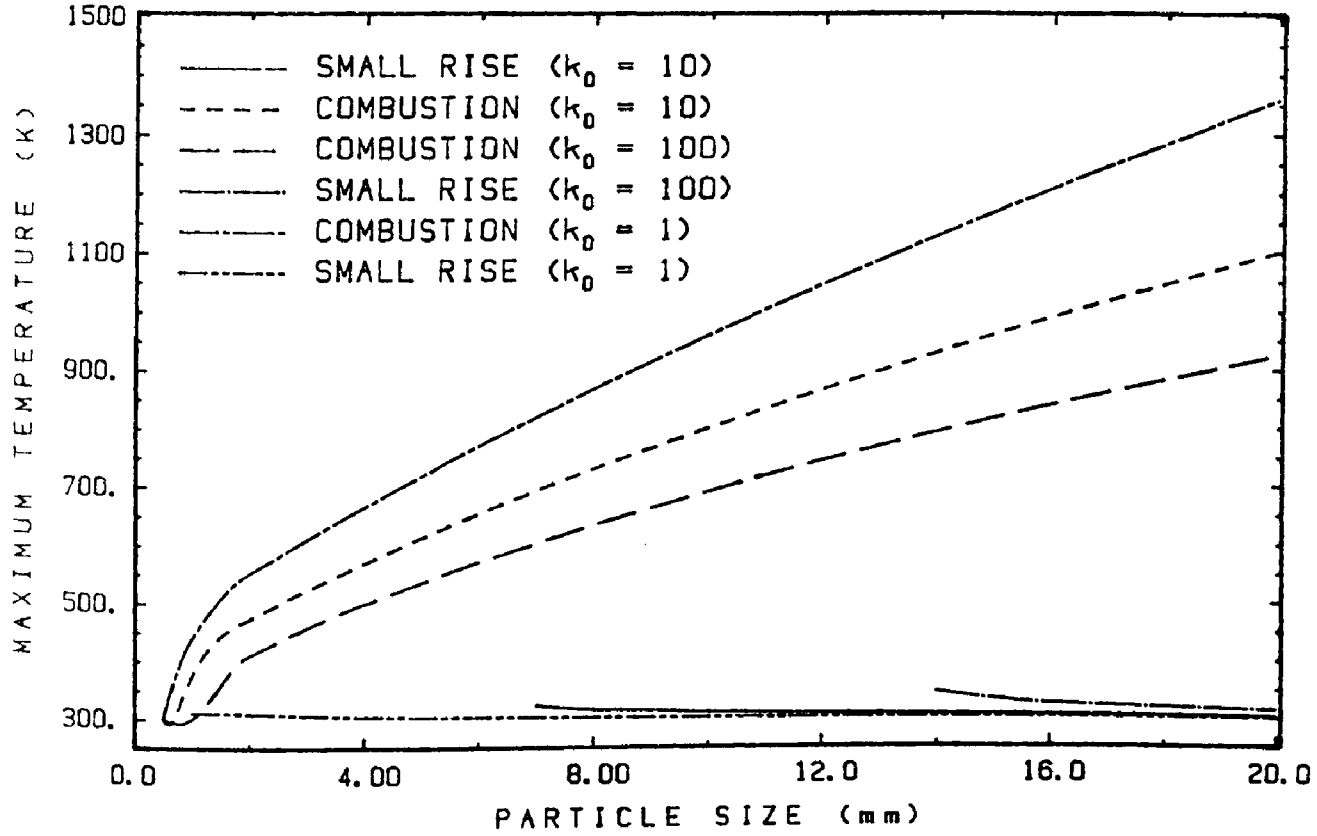


Figure 8.5 Effect of varying the pre-exponential factor on the maximum temperature

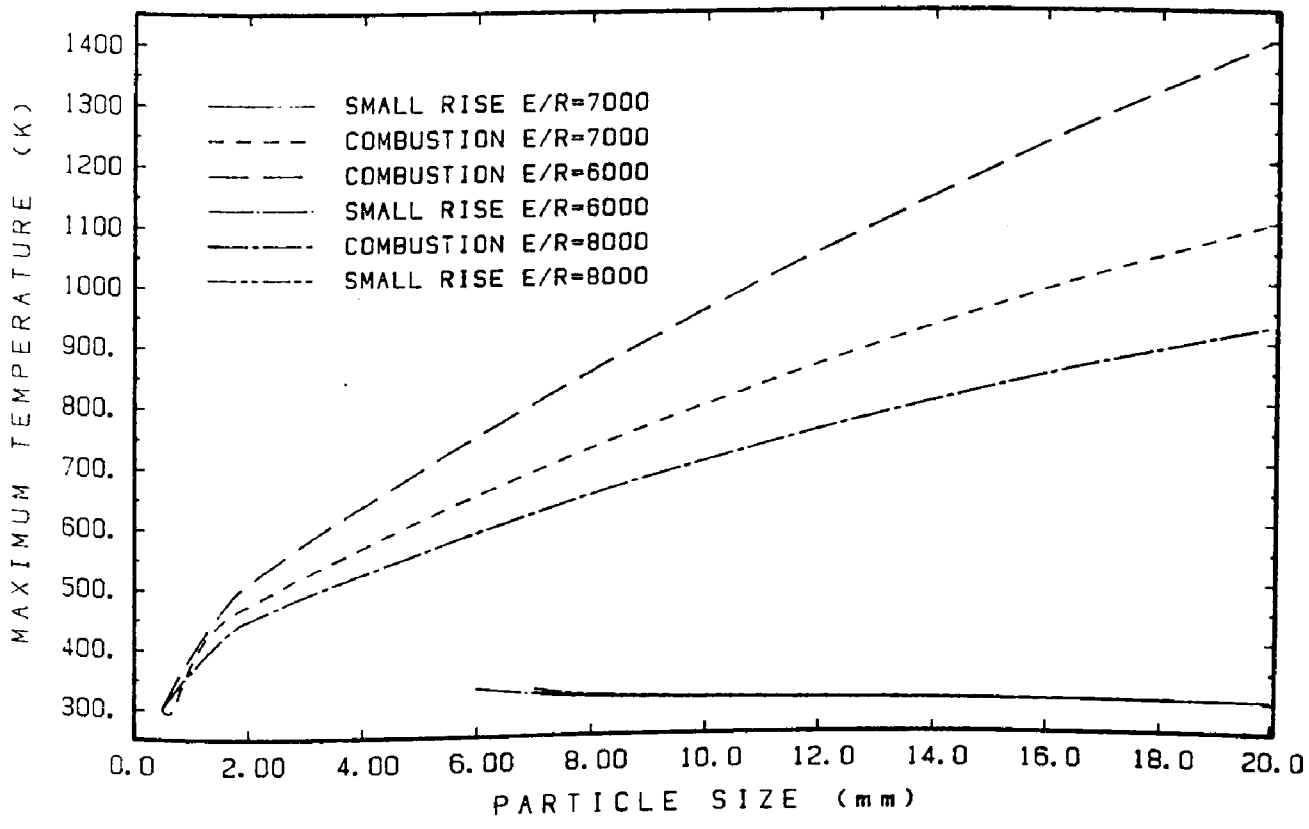


Figure 8.6 Effect of varying the activation energy on the maximum temperature

the oxygen depletion is less when k_o is lower, implying that the oxygen in the bed can penetrate further, leading to a larger temperature rise. When k_o is very large, all the oxygen is consumed close to the surface, where the sensible heat of reaction is easily conducted away.

Using the criterion of 340 K then for k_o = 1 m/s beds are safe below approximately 0.5 mm particle size, whhile for k_o = 100 m/s beds are safe below 1.5 mm particle size. This shows that for these small particle sizes, the more reactive the coal, the safer it is to stockpile.

Also of interest in Figure 8.5 is the fact that that for k_o=1 there is only a small range of particle sizes for which the bed is unsafe. This is a logical conclusion since it is to be expected that very unreactive material will not combust spontaneously.

Figure 8.5 indicates very clearly that k_o is a critical model parameter, and as such needs to be accurately measured.

8.2.4 Effect of varying the activation energy

To study the effect of changing the activation energy, it is necessary at the same time to vary k_o, so that the reactivity is the same at some base temperature. In this case a base temperature of 300 K was chosen. Figure 8.6 thus shows the behaviour of three different coals with the same room temperature reactivity but different activation energies. It can be seen from Figure 8.5 that there is little effect on both the curves. This then indicates that the activation energy is not a critical parameter for coals which have the same room temperature reactivity. However, two coals which have both different activation energies and different room temperature reactivities will have different liabilities toward self heating. The activation energy must thus be measured, and used in conjuction with k_o as a measure of the reactivity of the coal.

8.2.5 Effect of different assumptions about the reactive surface area of coal

The relationship between the particle size of coal and its reactive surface area has been discussed by Sondreal & Ellman (1974). They state that low-temperature oxidation rates have reported to

the oxygen depletion is less when k_o is lower, implying that the oxygen in the bed can penetrate further, leading to a larger temperature rise. When k_o is very large, all the oxygen is consumed close to the surface, where the sensible heat of reaction is easily conducted away.

Using the criterion of 340 K then for k_o = 1 m/s beds are safe below approximately 0.5 mm particle size, whhile for k_o = 100 m/s beds are safe below 1.5 mm particle size. This shows that for these small particle sizes, the more reactive the coal, the safer it is to stockpile.

Also of interest in Figure 8.5 is the fact that that for k_o=1 there is only a small range of particle sizes for which the bed is unsafe. This is a logical conclusion since it is to be expected that very unreactive material will not combust spontaneously.

Figure 8.5 indicates very clearly that k_o is a critical model parameter, and as such needs to be accurately measured.

8.2.4 Effect of varying the activation energy

To study the effect of changing the activation energy, it is necessary at the same time to vary k_o, so that the reactivity is the same at some base temperature. In this case a base temperature of 300 K was chosen. Figure 8.6 thus shows the behaviour of three different coals with the same room temperature reactivity but different activation energies. It can be seen from Figure 8.5 that there is little effect on both the curves. This then indicates that the activation energy is not a critical parameter for coals which have the same room temperature reactivity. However, two coals which have both different activation energies and different room temperature reactivities will have different liabilities toward self heating. The activation energy must thus be measured, and used in conjuction with k_o as a measure of the reactivity of the coal.

8.2.5 Effect of different assumptions about the reactive surface area of coal

The relationship between the particle size of coal and its reactive surface area has been discussed by Sondreal & Ellman (1974). They state that low-temperature oxidation rates have reported to

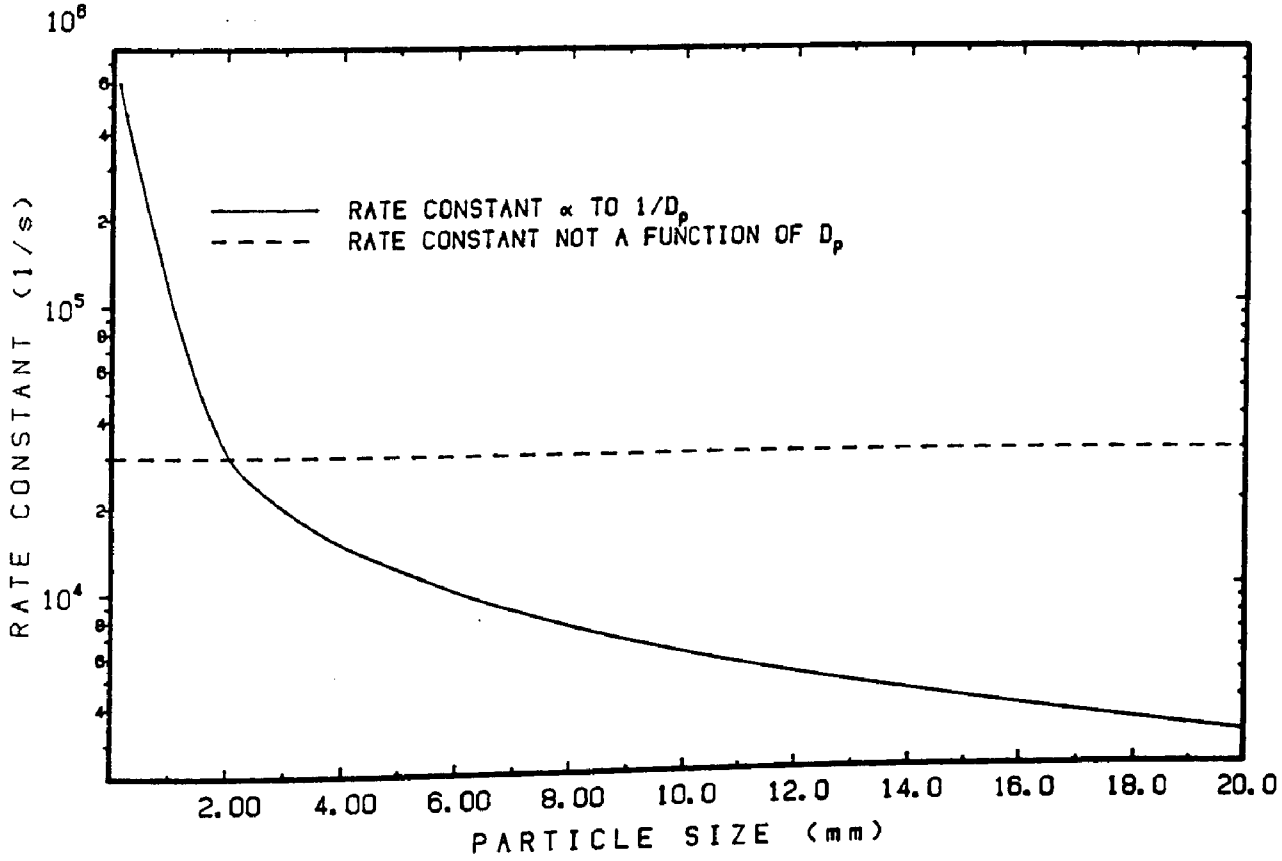


Figure 8.7 Pre-exponential factor versus particle size for the two cases considerd

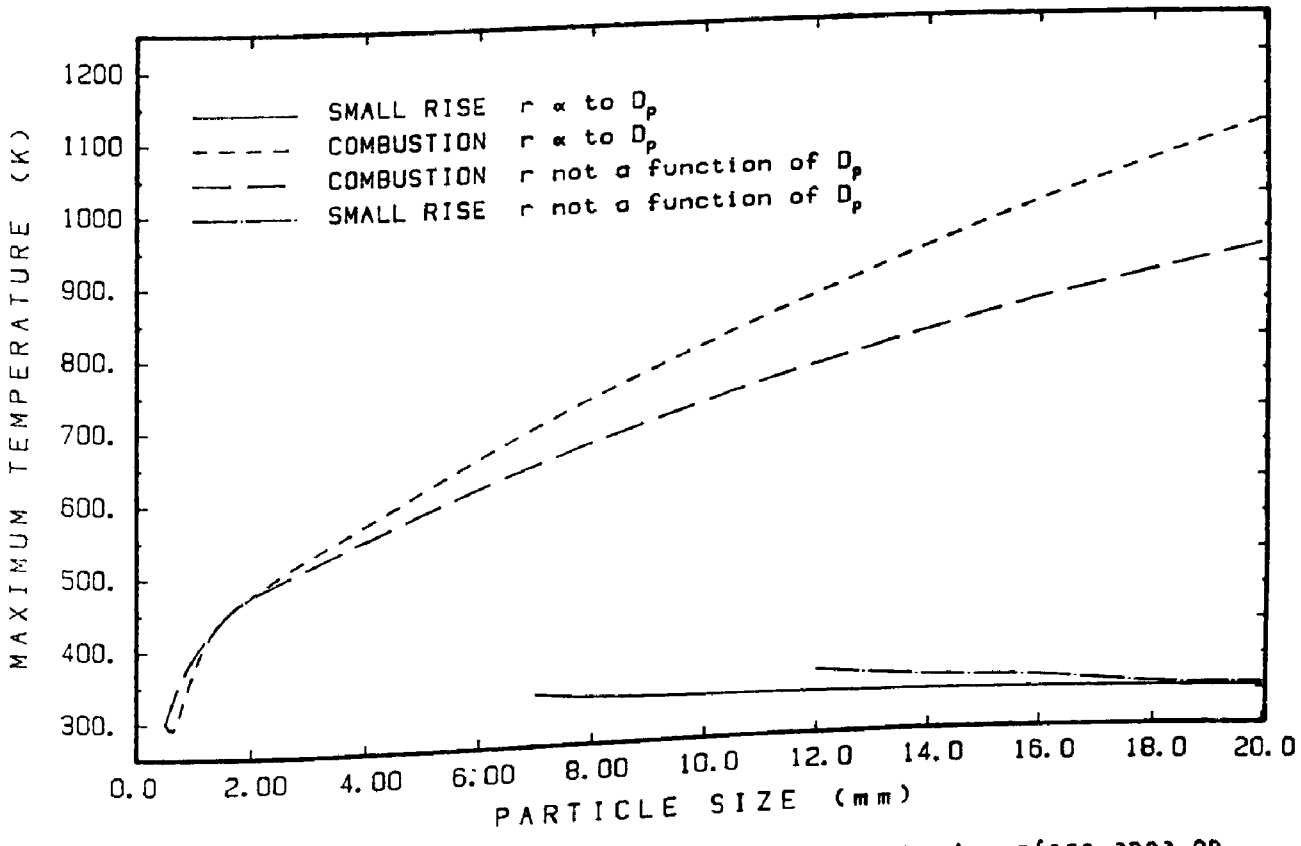


Figure 8.8 Effect of different assumptions about surface area on the maximum temperature

8.2.6 The Meaning of Particle Size

It should be noted that the particle size as used in the graphs presented in this section is defined by:

$$D_p = 6/S_t \qquad 8.5$$

and that this is of great importance when calculating the particle size of a coal sample with a particle size distribution. The correct particle size to use is the one defined by

$$S_t = 6 \sum_{i=1}^{N} \frac{m_i}{D_{p_i}} \qquad 8.6$$

together with equation 8.5

where D_{p_i} = average particle size of class i

m_i = mass fraction of coal in class i

N = number of classes

$$D_p = \sum_{i=1}^{N} D_{p_i} m_i \qquad 8.7$$

is not the correct average for this case.

Should a full particle size distribution be available, the summation in the above equations may be replaced by integrals.

To demonstrate the importance of the above discussion consider a coal with the size distribution given in Table 8.1.

TABLE 8.1 PARTICLE SIZE DISTRIBUTION FOR A TYPICAL SAMPLE

PARTICLE SIZE IN mm		MASS %
	+6.68	26,9
-6.68	+4.70	12.3
-4.70	+2.36	20.2
-2.36	+1.20	12.9
-1.20	+0.59	10.1
-0.59	+0.10	15.7
-.10		1.9

Calculating Dp by equation 8.7 gives a value of 4.5 mm while using equations 8.5 and 8.6 gives 0.9 mm. It can be seen that even a relatively small amount of fine material has the effect of drastically changing the effective particle size of the coal. This is of great importance when considering the liability towards spontaneous combustion of so-called segregated coal

8.2.7 Effect of Wind on Maximum Temperature

The effect of wind on the maximum temperature in the coal bed is shown in Figure 8.9. It appears from this figure that the presence or absence of wind has little effect on the calculated temperatures. However the curve plotted in Figure 8.9 assumes the wind blows constantly until steady-state is reached. This is highly unlikely to occur in practice. The more likely case is a wind which blows for a while, and then dies away. This is obviously on unsteady-state phenomenon, and as such will be discussed in section 8.3.

8.2.8 Effect of Thermal Conductivity on Maximum Temperature

Although the effective thermal conductivity of a packed bed of coal has been measured, it was felt worthwhile to investigate the effect of changing this parameter. It can be seen from Figure 8.10 that both halving and doubling this parameter have little effect on the calculated curves. It thus appears satisfactory to use the measured value of the effective thermal conductivity in all calculations.

8.2.9 Effect of Changing the Bed Length

The bed length is the most difficult model parameter to relate to a real coal dump. It is incorrect to assume that this bed length bears a fixed relationship to the physical size of a coal dump, e.g. its height or width. The bed length in the one-dimensional model in fact corresponds to the path length for flow in the real situation. This path length in general will not be known, although the physical size of the dump sets an upper bound on this quantity.

For the purposes of this study three bed lengths were chosen, in order to see the effect of changing this quantity. From Figure 8.11 it can be seen that the effect of bed length is very pro-

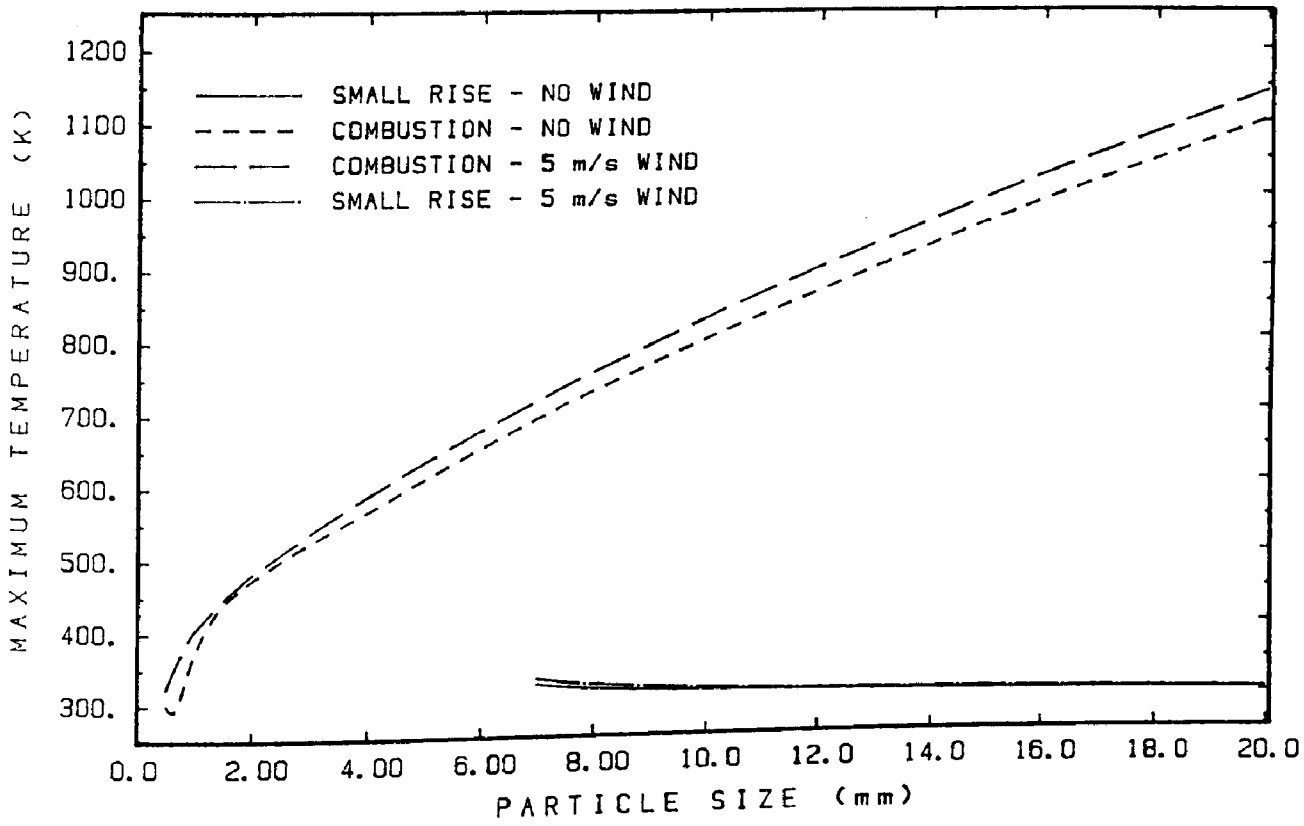


Figure 8.9 Effect of wind on the maximum temperature

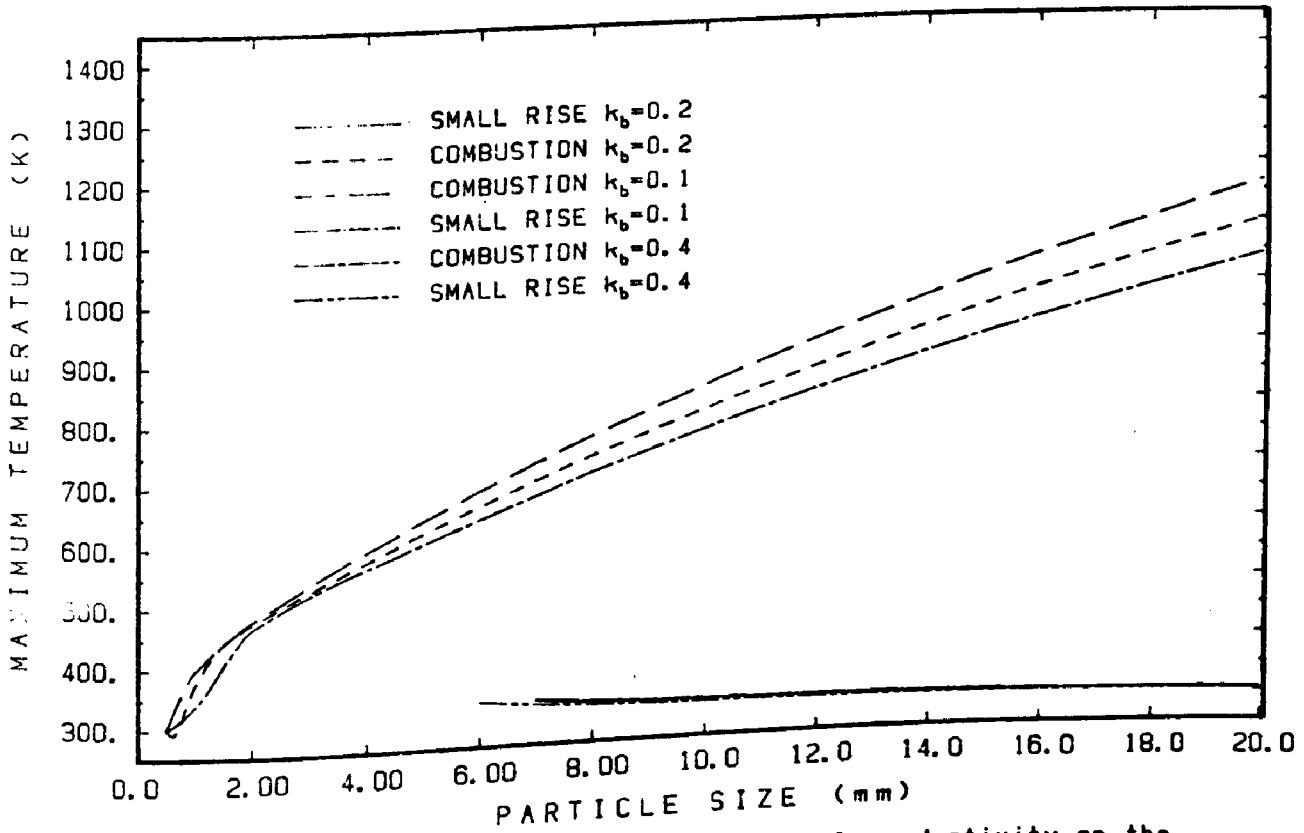


Figure 8.10 Effect of varying bed thermal conductivity on the maximum temperature

nounced on the low temperature solution curves. For the oxygen limited beds, there is little difference between the curves for bed length 5 and 10 m. The curve for bed length 1 m has a somewhat different shape, and for particle sizes less than 1 mm the temperature rise is negligible. In addition the range of particle sizes for which the bed can be considered to be unsafe is between approximately 1.5 and 2 mm.

The fact that the curves for 5 m and 10 m are so similar can be explained as follows: For an oxygen limited bed the oxygen in the flow is used up very close to the inlet to the bed. From that point in the bed where there is to all intents and purposes no oxygen, no more reaction can occur. The temperature profile in the rest of the bed is thus governed by conduction, especially for the beds of finer particles for which the flowrates are low. This implies that making the bed longer will have little effect on the maximum temperature in the bed, since all the temperature rise occurs very close to the inlet.

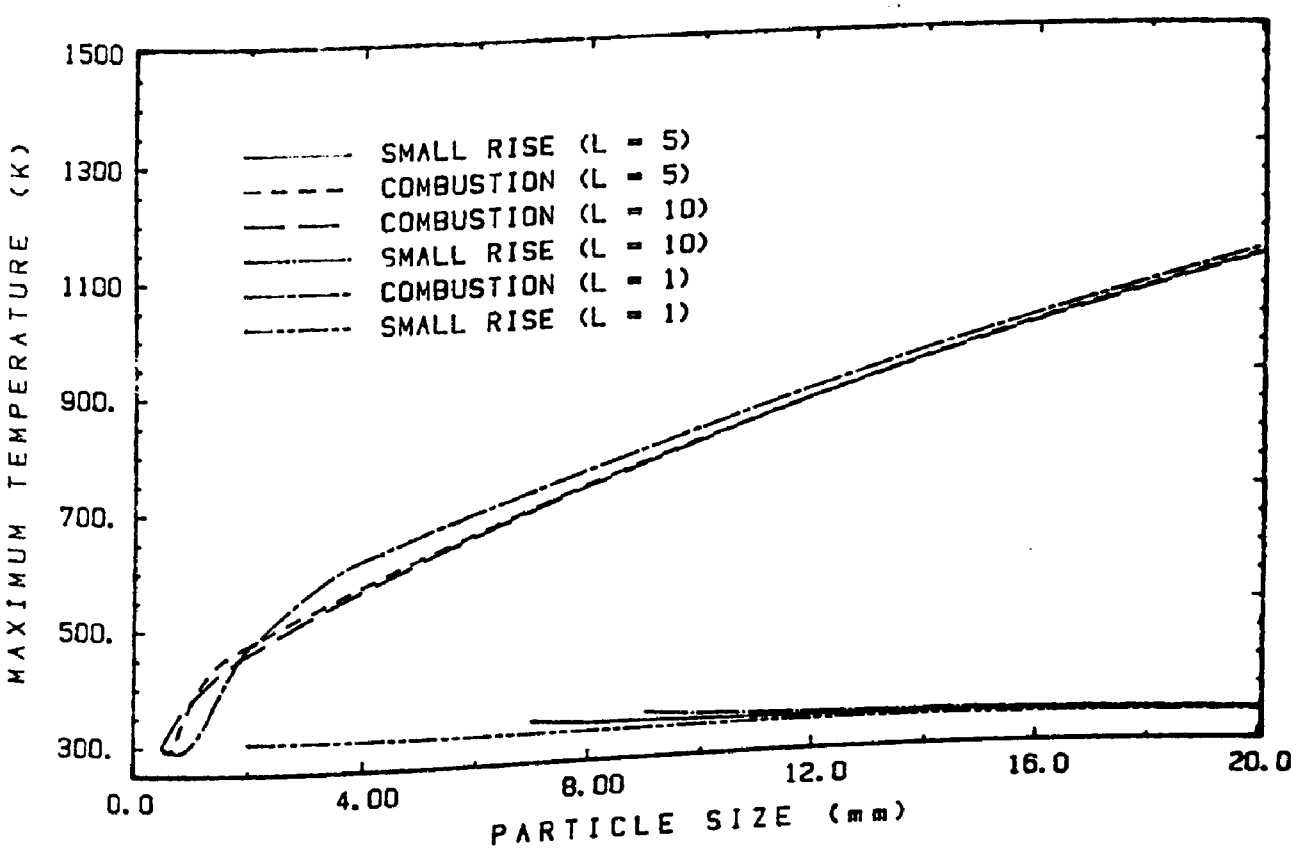


Figure 8.11 Effect of varying bed length on the maximum temperature

8.3 Unsteady-State Solutions for r constant

8.3.1 Introduction

The unsteady-state solution for r constant has been discussed in section 6.3. The resulting solution has been programmed in BASIC on an HP 9835 computer, and a lsiting of the program is given in Appendix 12.

It has been found that obtaining the solution to the analytical equation is in fact slower than obtaining the solution using the numerical method discussed in section 6.4. The aim of what follows is thus to point out the pertinent facts that emerge from solving the equation, without presenting an extensive array of graphs.

8.3.2 The Character of the Solutions

It is already known from calculations in the previous section what the steady-state temperature profiles for a given bed will look like. The advantage of the unsteady-state method thus lies in the fact that should the bed be conditionally safe, the unsteady-state solution will be able to predict from the initial condition what the final steady-state will be.

The temperature time curves in the centre of a coal bed using three different initial conditions are plotted in figure 8.12. The initial condition used is the somewhat artificial one of a coal bed with an initial uniform temperature.

The model parameters used to obtain the curves shown in Figure 8.12 are given in Table 8.2.

TABLE 8.2 MODEL PARAMETERS FOR FIGURE 8.12

Particle Size	5 mm
Voidage	0.4
Bed Length	1 m
K_o	0.7 m/hr
E/R	2889 K

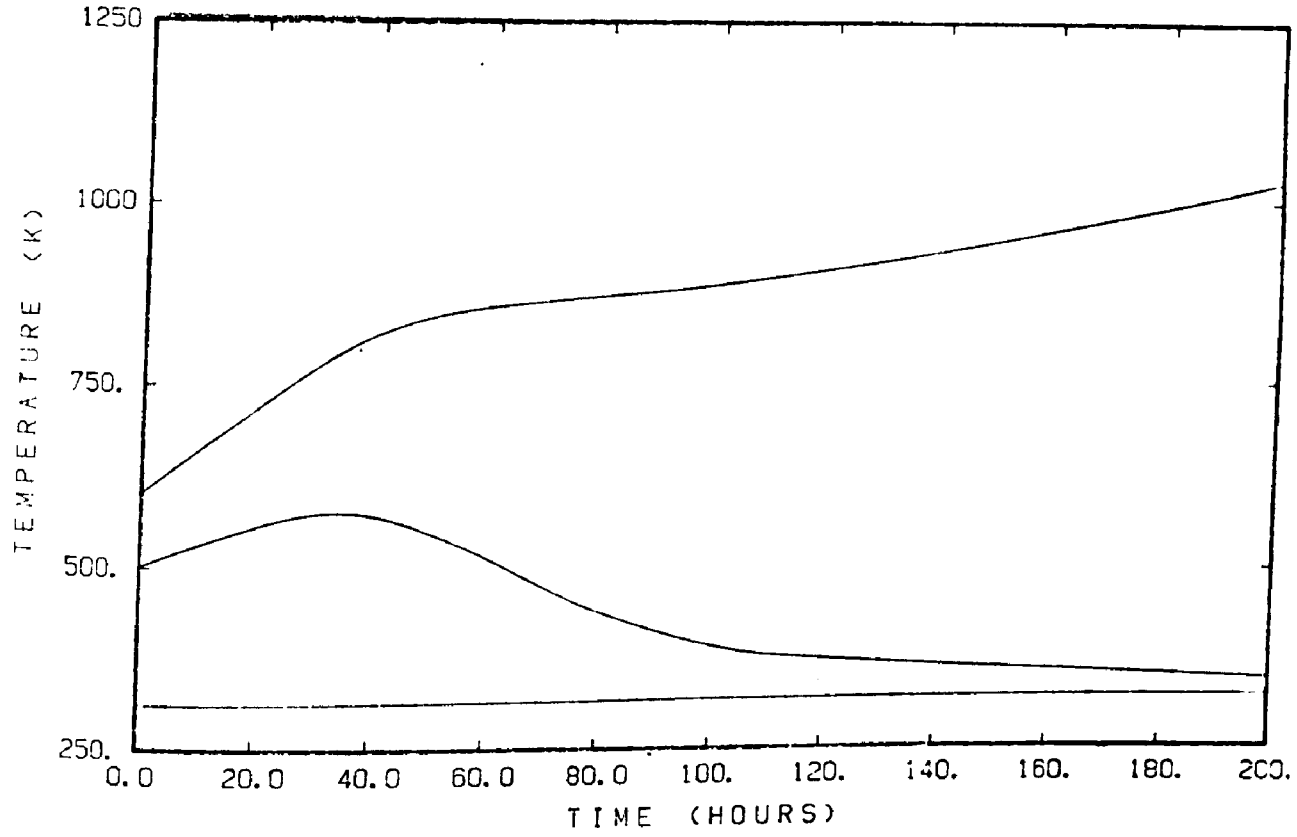


Figure 8.12 Temperature-time curves in the centre of a coal bed for different initial temperatures

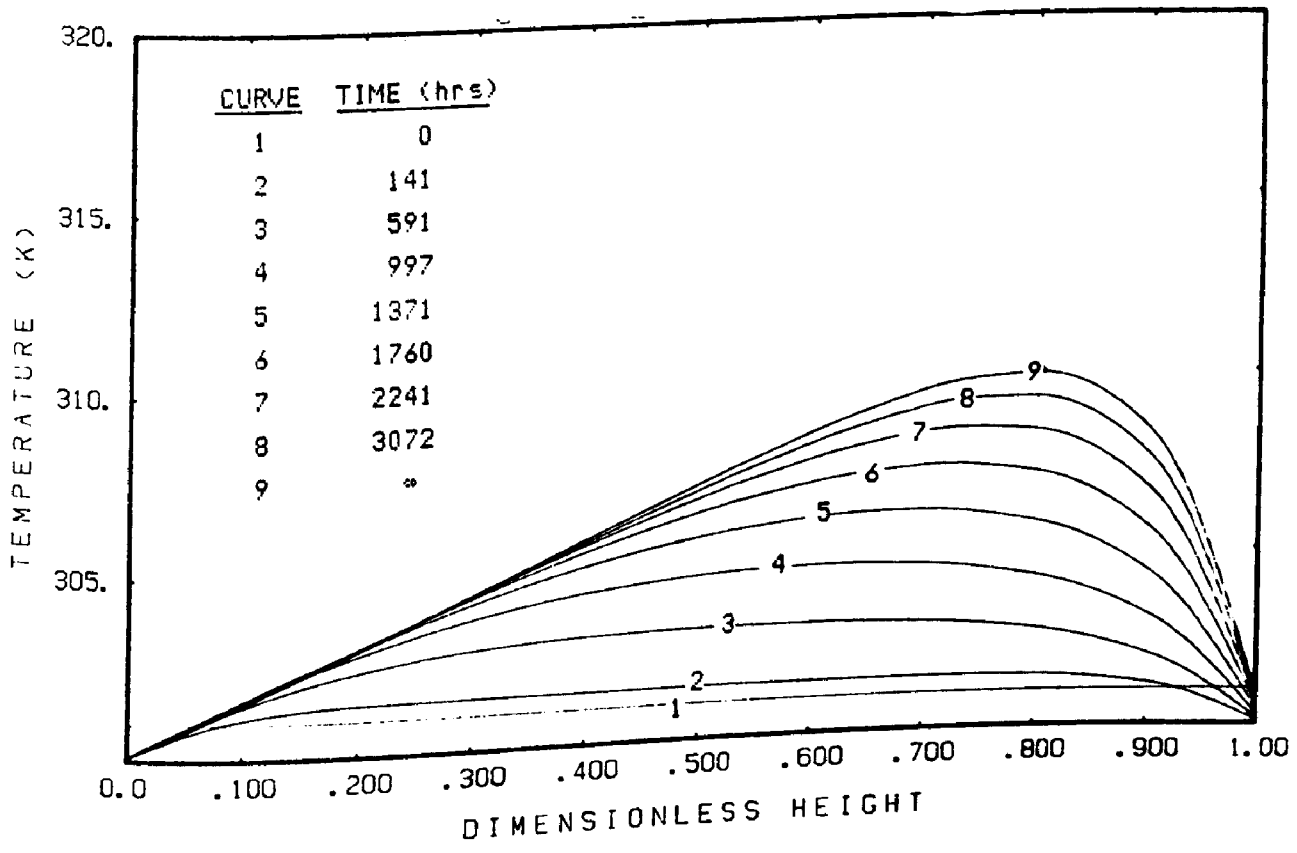


Figure [illegible] Temperature profiles in a coal bed

It can be observed from figure 8.12 that starting with an initial temperature of 301 K the temperature in the bed gradually rises to eventually reach a stable low temperature steady-state. Starting with a bed temperature of 500 K the temperature initially increases but then decreases to eventually again reach the low temperature stable steady-state. However starting at 600 K the temperature increases monotonically, leading to combustion. Thus for this particular bed the critical temperature appears to be between 500 & 600 K. This temperature would in fact correspond to the unstable solution temperature discussed in section 8.2.

Temperature profiles for a coal bed with parameters as given in Appendix 11, for a particle size of 10 mm and length of 5 m are shown in figure 8.13. Referring to figure 8.3 it can be seen that such a bed has a stable steady-state at a maximum temperature of 310 K. In figure 8.13 it can be observed that starting with a temperature of 301 K the bed gradually heats up to its final steady-state temperature. Although in theory the bed reaches steady-state after only an infinite time, it can be seen that after 3568 hrs or nearly 150 days, the bed is to all intents and purposes at steady-state.

It is tempting to try and define a time constant for a coal bed, in order that predictions may be made on safe stockpiling times. In order to do this one would hypothesize that the temperature in a coal bed could be described by an equation of the form

$$\frac{\theta(X,\tau) - \theta_{ss}(X)}{\theta(X,0) - \theta_{ss}(X)} = \exp(-\frac{\tau}{\tau_c}) = \exp(-\frac{t}{t_c}) \qquad 8.3.1$$

where τ_c is a dimensionless time constant, and t_c is a time constant.

In fact using equation 6.3.2, and assuming that only the first term in the series $V(X,\tau)$ need be considered it can be shown that

$$\tau_c = (\beta_1^2 + a^2/4)^{-1} \qquad 8.3.2$$

It is thus immediately obvious that τ_c is not constant, but in fact a function of time, since the quantity, a, which is proportional to the flowrate, is a function of time.

For cases when $\beta_1^2 \gg a^2/4$, the use of a time constant is justified. It can be shown that $\beta_1 \approx \pi$, therefore $a/2 \ll \pi$ is the criterion for using a time constant.

Converting τ_c to time units using the relationship

$$\tau_c = \frac{\kappa t_c}{L^2} \qquad 8.3.3$$

In the case when $a/2 \ll \pi$

$$\tau_c = \frac{1}{\beta_1^2} = \frac{1}{\pi^2}$$

$$t_c = \frac{L^2}{\pi^2 \kappa} \qquad 8.3.4$$

The time constant in this case is governed by the thermal diffusivity of the bed, which implies that the heat transfer in the bed is mainly by conduction.

Then

$$t_c = \frac{L^2}{\pi^2 \times 8 \times 10^{-4}} = 126L^2 \text{ hrs} \approx 5L^2 \text{ days}$$

This implies that for cases where the heat transfer in the bed is governed by conduction, the bed will be 37 % away from its steady-state temperature after $5L^2$ days and 14 % after $10L^2$ days.

A similar calculation for the case $a/2 \gg \pi$ is not justifiable, since a is a function of time. However, using the definition of of the quantity a

$$a = \frac{\hat{G}cL}{k_b}$$

and using the simplified formula for the flowrate G

$$G = \frac{q}{fM_w}\left[\frac{\theta-1}{\bar{\theta}^2}\right]$$

Is is possible to calculate the quantity a, and compare it to 2π to deduce whether the dominant transfer mechanism is conduction or flow.

Using values from Table 2.1 and Appendix 11, and assuming an average dimensionless temperature of 1,1 ie an average temperature of 330 K the values in Table 8.3 have been calculated

TABLE 8.3 THE QUANTITY 'a' FOR VARIOUS PARTICLE SIZES

Particle Size (mm)	a
1	0.1L
2	0.4L
5	2.5L
20	40L

It thus appears that for a 5 m bed of 5 mm particles at an average temperature of 330 K that flow is a more important heat transfer mechanism than conduction. For finer particles in shorter beds conduction will dominate, and then equation 8.3.1 together with 8.3.4 may be used to calculate the time varying behaviour of the coal bed.

Plotted in figure 8.14 is the temperature-time behaviour at the centre of a bed composed of 6 mm particle and 5 m in length. All the other model parameters are base case values. Referring to Figure 8.3 it can be seen that for this coal bed there is no low temperature solution. This conclusion is confirmed by the unsteady-state calculation.

It can be seen that the temperature rise in the centre of this bed is gradual with a value of 0.24 K/day until approximately 80 days. At this time the temperature increases dramatically

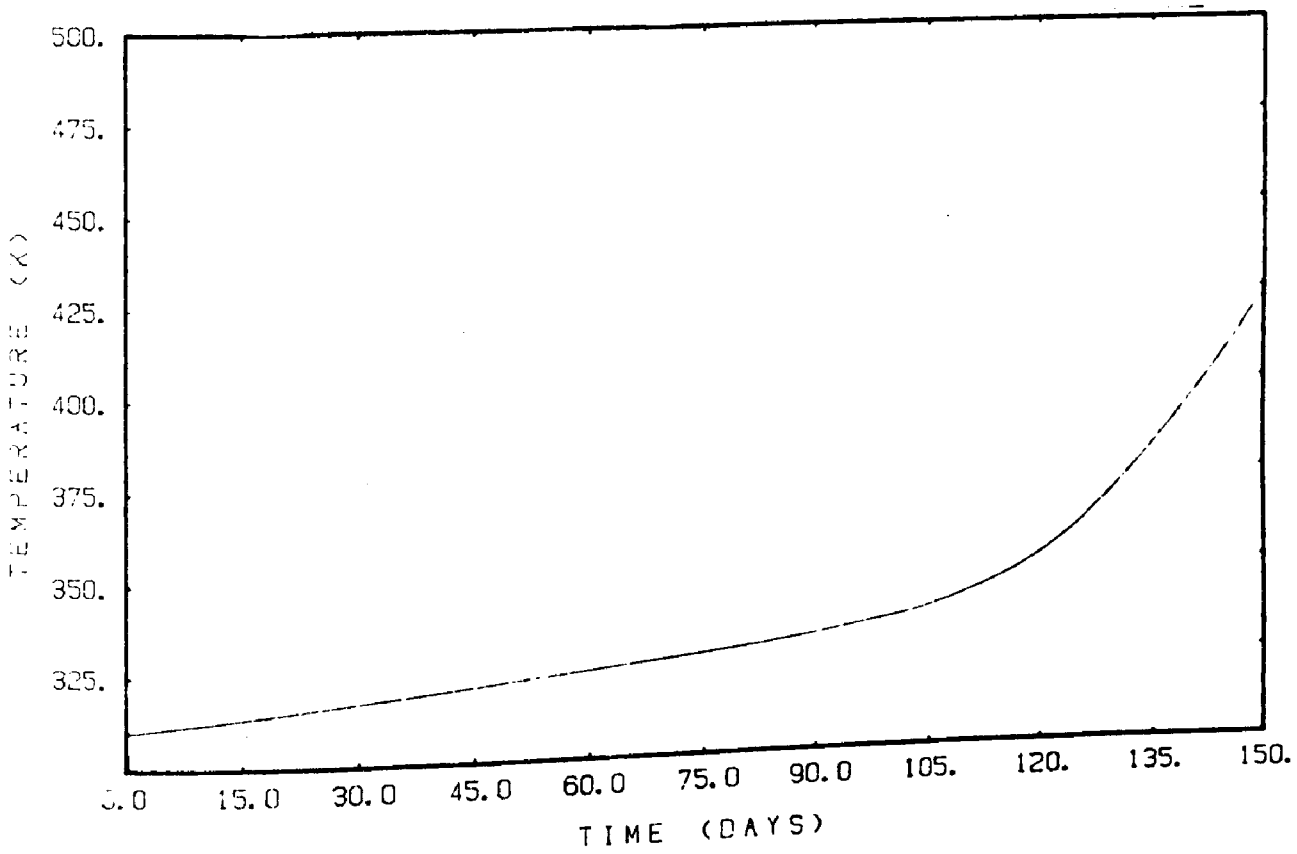


Figure 8.14 Temperature-time behaviour at bed centre
Particle size 6 mm - Analytical solution

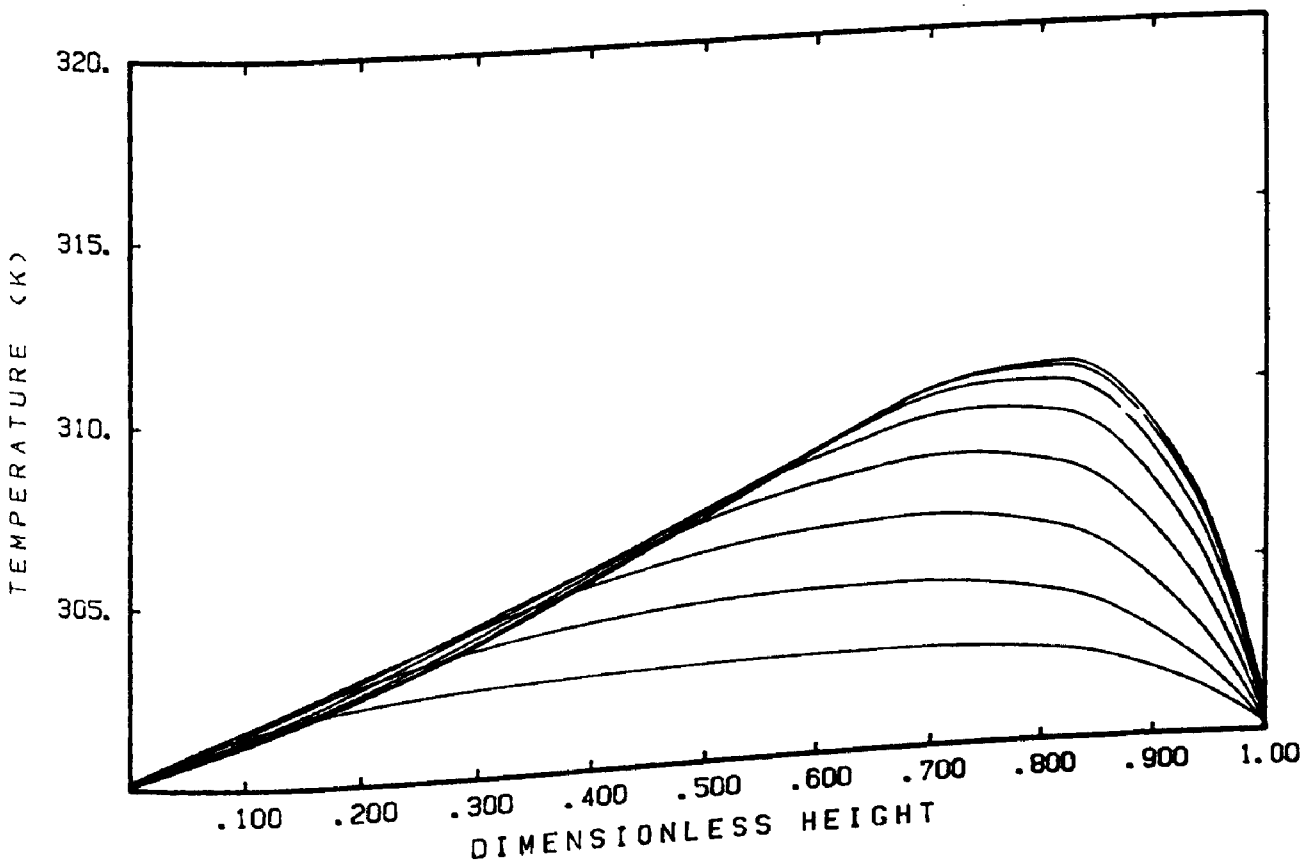


Figure 8.15 Temperature profiles in a coal bed
size 10 mm - Numerical Method

leading to eventual combustion. From this plot 60 ^{o}C appears to be a critical temperature. It is interesting to note that from Table 8.3, at 57 ^{o}C flow is already dominating conduction as the significant heat transfer mechanism, since the value of the quantity 'a' is 3.6L or 18 which is significantly greater than 2π.

8.3.3 Discussion

The results presented in this section confirm the validity of the plots presented in section 8.2. The following are the important conclusions from the section.

a) Depending on the initial condition, a coal bed may either attain a low or high temperature steady state.

b) For coal beds in which conduction is the dominating heat transfer mechanism, a simple formula may be used to calculate the temperature of a coal bed as a function of time.

c) A method has been presented whereby it may be calculated whether conduction or flow is the dominant heat transfer mechanism in a coal bed. In general conduction will only be dominant for short coal beds of fine particles, in which the temperature rise remains small.

d) Results have been presented showing the temperature time behaviour of a coal bed on its way to spontaneous combustion. The bed is characterized by a gradual temperature rise until 60 ^{o}C at which point the temperature rise becomes more dramatic. It has been pointed out that at 60 ^{o}C flow is the dominant heat transfer mechanism in the bed.

8.4 Results of Solving the Equations Numerically

8.4.1 Introduction

As has been discussed, the numerical method for solving the equations involves no assumptions about the reaction rate being constant, and allows for the effect of prior oxidation on the reaction rate. The solutions can be found quickly, even using a fairly unsophisticated microcomputer, and if programmed on a more powerful mainframe computer, the computer time involved would be small.

8.4.2 Comparison Beteewn the Numerical Method and the Analytical Method

The results presented in Figures 8.13 were recalculated using the numerical method. In figure 8.15 the results for the case D_p = 10 mm are presented. It can be seen that for this low temperature case the results obtained are very similar. This is to be expected since the temperature variation in the bed is only of the order of 10 K, and therefore the assumption of a constant rate constant is fairly good.

In figure 8.16 temperature profiles through a reacting bed of coal of size 2 mm with a wind velocity of 5 m/s. A glance at Figure 8.9 will show that for this range of the parameters the bed is unsafe, with a final predicted maximum temperature of 450 K. In fact, as can be seem from figure 8.16 the maximum temperature reached is approximately 1100 K, indicating that the assumption of constant rate constant used to generate the curves in Figure 8.9 is a poor one for this case.

A point of interest in Figure 8.16 is the way in which ignition appears to occur. Between day 40 and day 45 a hump appears in the temperature profile, subsequently the maximim temperature in the bed moves toward the entrance of the bed. This effect is due to the fact that as the temperature increases so does the rate of reaction, leading to the oxygen being depleted near the entrance of the bed. The curves between day 55 and day 80 show some evidence that the numerical method does not cope very well with the ingition, which is in fact a shock phemomenon. In particular the curve for day 55, which exhibits two maxima is unrealistic, Nevertheless the temperature profile after 80 days appears to be in agreement with what one would expect, except for a slightly concave shape.

In Figure 8.17 is shown a cross plot of the results in Figure 8.16 at the bed centre. This curve shows a dramatic increase in temperature between 40 and 45 days of 130 K. The critical temperature from this plot appears to be in the region of 75 ^{o}C.

This bed appears to "take-off" after 40 days whereas the results shown in Figure 8.14 appears to become dangerous after 80 days. The difference between these two cases is the particle sizes of the coal and the fact that that for the results shown in Figure

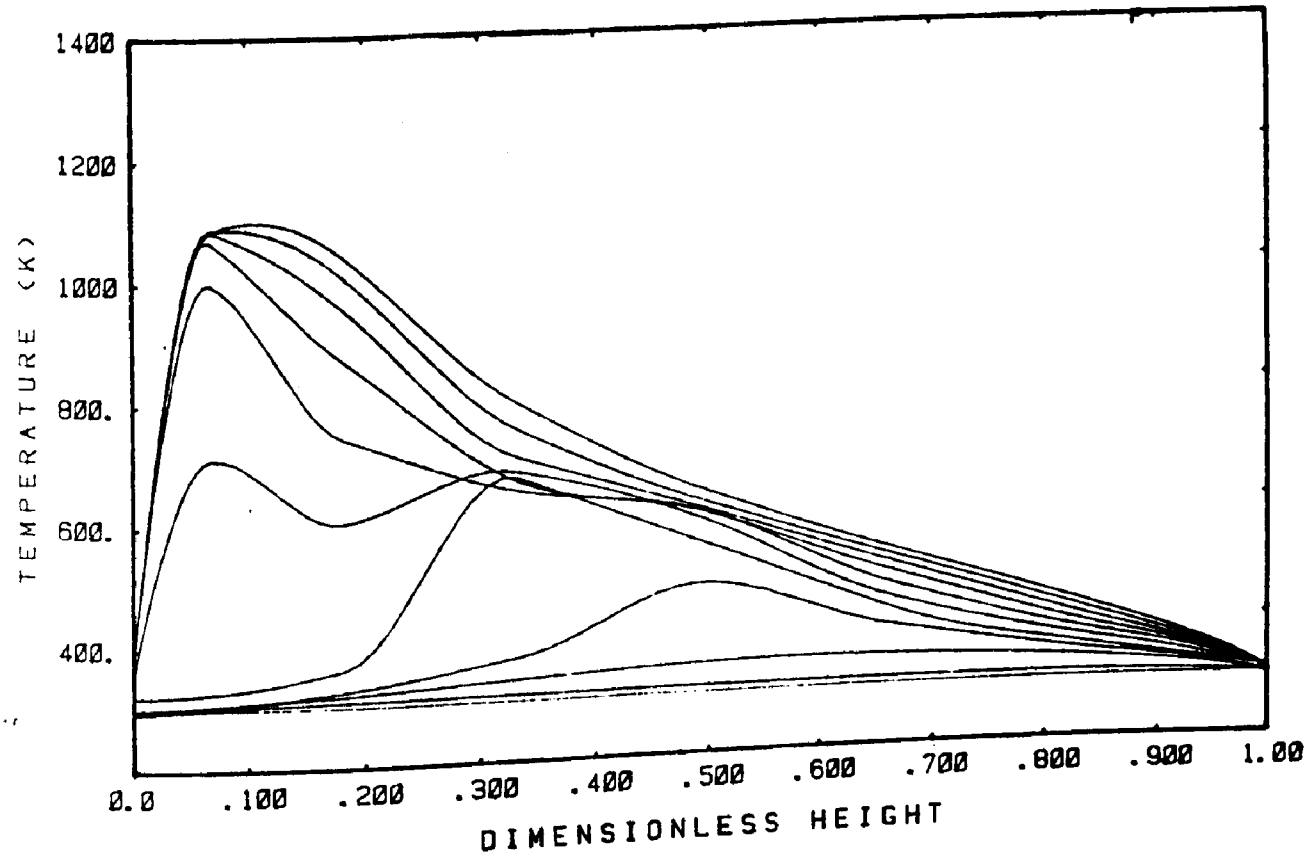
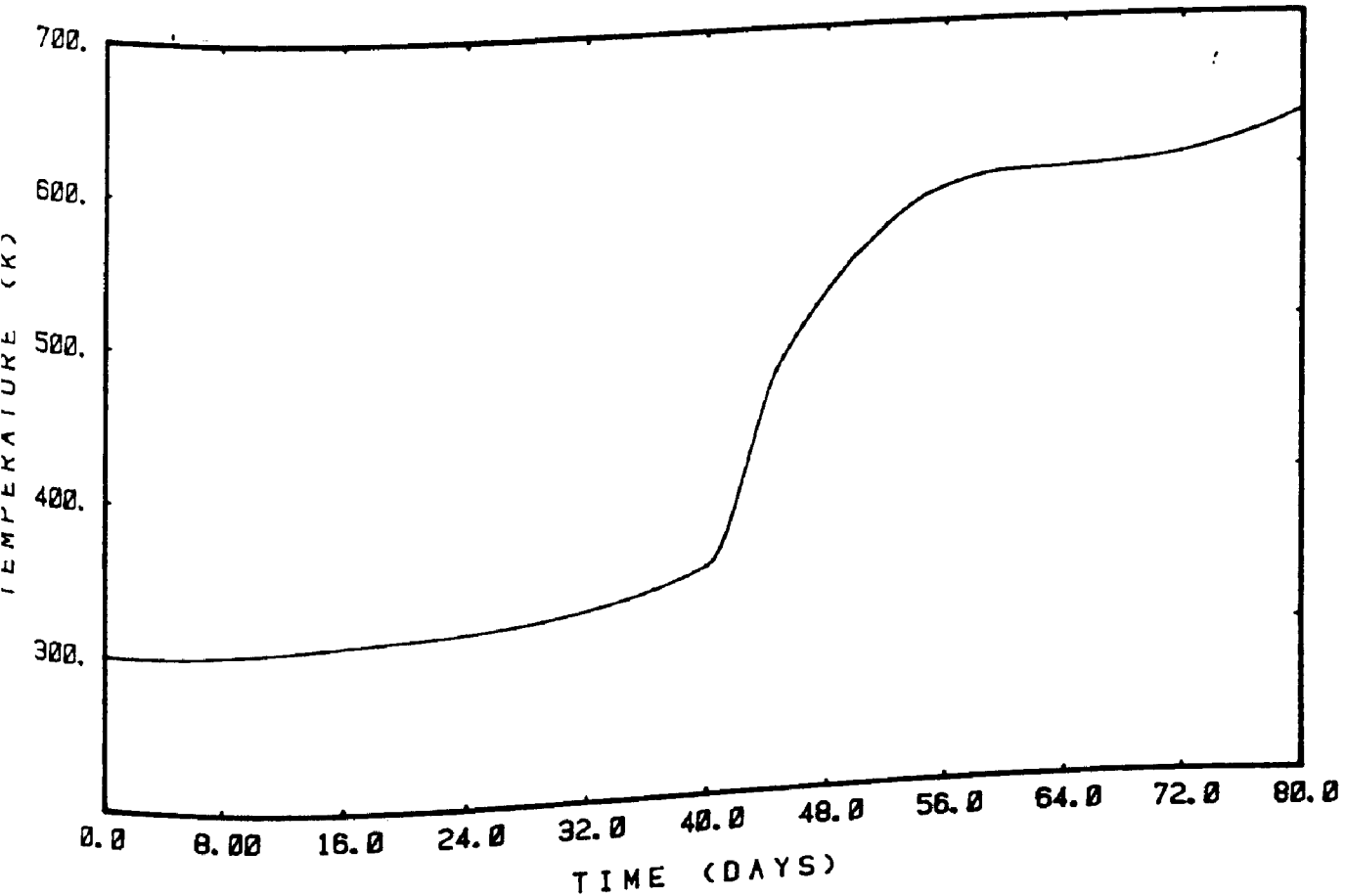


Figure 8.16 Temperature profiles with ignition
Particle size 2 mm - 5 m/s wind - Numerical method
First three curves 20 days apart
Subsequent curves 5 days apart



8.16 a 5 m/s wind has been assumed to blow constantly. It would be expected that the finer, more reactive coal would combust in a shorter time provided is is supplied with enough oxygen, as is the case here with the wind blowing.

8.6 Conclusions

The results presented in this chapter represent the results of solving the model equations for various values of the model parameters. It is felt that the parameters used are realistic, and therefore that the results obtained can be regarded as at the worst semi-quantitative.

The results of solving the equations for both the steady and unsteady-states have been presented. The results are consistent with practical experience. It has been shown that the assumption of a constant rate constant is a good one for beds in which the temperature remains less than approximately 350 K. The results of solving the unsteady-state equations numerically show that the model can predict the onset of spontaneous combustion, although numerical difficulties occur when the temperature gradients become large.

9. CONCLUSIONS

The important physical processes occuring in coal dumps have been identified and modelled. They are:

a. The ingress of reactants into the dump

b. The reaction between these reactants and coal

c. Heat transfer in the coal dump

It has been shown that natural convection and wind pressure are the most imprtant mechanisms whereby reactants are transported into a coal dump, with molecular diffusion only being of importance for fine material.

A shrinking-core model for the oxidation of coal at low temperatures has been proposed. This model explains the well known but little understood fact that the reactivity of the coal falls off with time.

It has been shown that heat transfer in a coal dump may be modelled using an effective thermal conductivity; the effective thermal conductivity of a typical coal bed has been measured.

All these effects have been incorporated into a one-dimensional model, with the aim of studying their combined effect on spontaneous combustion of coal. The model has been shown to have the correct characteristics in the prediction of the onset of spontaneous combustion. The model equations exhibit multiple solutions for certain values of the model parameters; it is concluded that stockpiles may be classified as safe, unsafe or conditionally safe.

Safe coal dumps have been shown to be either oxygen limited or heat transfer limited. In both cases the dump is safe because the sensible heat of reaction can be dissipated at temperatures near ambient. For oxygen limited beds the high reactivity of the coal toward oxygen causes oxygen to be consumed and thus the sensible heat to be produced close to the surface of the dump, where it is easily dissipated. For heat transfer limited beds, oxygen is readily available throughout the bed, but the reactivi-

ty per unit bed volume of the coal is sufficiently low that the sensible heat of reaction may be dissipated even from deep within the dump at near ambient temperatures.

The important parameters that must be known in order to make qualitative predictions about the safety of coal dumps have been shown to be:

a. The particle size distribution of the coal.

b. The voidage of the bed.

c. The pre-exponential factor and activation energy for the oxidation of the coal.

The model presented here may be used to qualitatively determine the effect of changing certain parameters which are under the control of the persons responsible for coal plant operation and particular dumping practise. In particular the effects of particle size distribution and compaction have been clearly pointed out. Compaction makes oxygen limited dumps safer, but appears to be ineffective in improving the safety of heat transfer limited dumps.

The efect of particle size distribution on the safety of dumps may be summarized as follows:

If the dump is oxygen limited adding fines may help make the dump safer, both by reducing the voidage and increasing the rate of oxygen depletion. If the dump is heat transfer limited then removing fine material may help make it safer.

An important practical implication of this work is that there is a dump size for an oxygen limited coal dump, above which the dump is effectively no more liable to spontaneous combustion. For very reactive coals this is a comforting result, since it implies that very reactive coals may be safely stockpiled on very large dumps, with obvious economic advantages. Caution must be exercised to ensure that the dump is oxygen limited, and that the oxygen levels below a certain depth remain negligible. At this stage the quantification of what this depth is, is not possible, but it appears from practical experience that 2 metres is a sensible upper limit on the depth at which the percentage oxygen in a safe

coal dump should be negligible.

Safe stockpiling times are not available from the model, and there is reason to believe that the concept of a safe stockpiling time can be misleading. It has been shown, both in practise and from the model, that a slow rise in temperature may suddenly become a rapid rise in temperature. The critical temperature appears to be in the region of 60 to 100 ^{o}C. The time taken to reach this critical temperature might be a better way of arriving at a safe stockpiling time.

The concepts presented in this thesis may also help to answer questions about stockpiling practise. In particular the following points are of practical importance:

Segregated coal dumps i.e. dumps in which particle size segregation occurs due to stacking methods employed, are potentially dangerous. It can clearly be seen from the results presented in this thesis that such dumps are dangerous because air can penetrate the dump through the coarse material, and react deep in the dump with finer material, that is inherently more reactive, thus leading to a temperature rise deep within the dump where the energy cannot easily be dissipated.

Covering dumps of coal has been suggested as a means of preventing spontaneous combustion. Broadly speaking a dump may be covered with either an inert or reactive material. An inert covering may be permeable or impermeable. In the case of an inert permeable covering such as sand, the fact that there is a balance between oxygen ingress and heat loss must always be borne in mind. Enough sand must be put down to substantially reduce the amount of oxygen ingress, recognising that the dump is being insulated at the same time. If an attempt is made to cover the dump with an impermeable layer of a material such as tar, it must be recognized that cracks in the covering may lead to large localized flows of oxygen into the dump, possibly giving rise to a hot spot.

Schmidt (1945) states that covering a coal dump with a layer of very fine coal and then with a layer of coarser coal provides an efficient coating. The coarse coal is packed on top of the fine coal to prevent wind and water erosion. In the light of the results presented in this chapter, this is an eminently

reasonable suggestion provided all the oxygen can be removed close to the surface.

In the case of dumps that are safe due to the fact that they are oxygen limited, the danger exists that with time the outer layer of coal will become unreactive due to the ageing effect, and that oxygen will penetrate deeper into the dump where any reaction that occurs may lead to a dangerous temperature rise. One of the practical conclusions that arises out of this analysis is that analysing for oxygen at various depths in a coal dump is an excellent way of monitoring the dump. It has been found in practise that in oxygen limited type of dump, the gas in the dump will contain virtually no oxygen at a depth of 2m. It has therefore been suggested that should appreciable oxygen be found at this depth an attempt be made to recompact the dump. Should this fail to rectify the situation the next logical step is the laying down of fresh coal on the dump. This would have the effect of limiting the amount of oxygen that is able to penetrate to appreciable depths. In the light of the model presented here, these suggestions seem sensible as well as practical.

A limitation of the model presented here is the inability at this stage to easily translate the size of a coal dump to the parameter of bed length used in the model. It can be demonstrated that there is a worst depth associated with natural convection, and a worst path length associated with wind driven flows. However at this stage it has not been possible to calculate these distances. A full three- dimensional analysis of the situation could give an idea of the magnitude of these distances; these could then be used in the simpler one-dimensional model for predictive purposes.

The omission of moisture effects in the model is simply rectified as has been demonstrated by Murtagh (1966). It must be borne in mind that in addition to the heat transfer mechanism of condensation and vaporization, moisture appears to exert a catalytic effect on the oxidation reaction. Schmidt (1945) discusses moisture effects in some detail; the ommision of these effects in the model presented here is mainly due to lack of data. There is thus scope for further work in determining the effects of both atmospheric and coal moisture content on the rate of oxidation.

One of the main areas of uncertainty in the field of spontaneous combustion of coal is the functional relationship between rates of oxidation and coal particle size. Much conflicting data has been published in ths regard (Schmidt, 1945, Sondreal & Ellman, 1974). It is felt that there is much need for further study in this regard.

APPENDIX 1 DERIVATION OF A RATE EQUATION FOR THE LOW TEMPERATURE OXIDATION OF COAL

The reaction mechanism considered here is one of diffusion of O_2 through an inert layer of oxycoal followed by reaction between the O_2 and the coal. No reaction products are formed and reaction at the reaction zone is considered to first order with respect to the O_2 concentration

In order to account for the fact that coal has both internal and external surface, the simplification is made that this surface area S′ may be considered to behave as if it was all external i.e. pore diffusion is neglected. This is a good assumption provided the particle size is not too large, as has been mentioned by Gijbels & Bruining (1982).

The coal particle is thus considered to have the geometry shown in Figure A1.1.

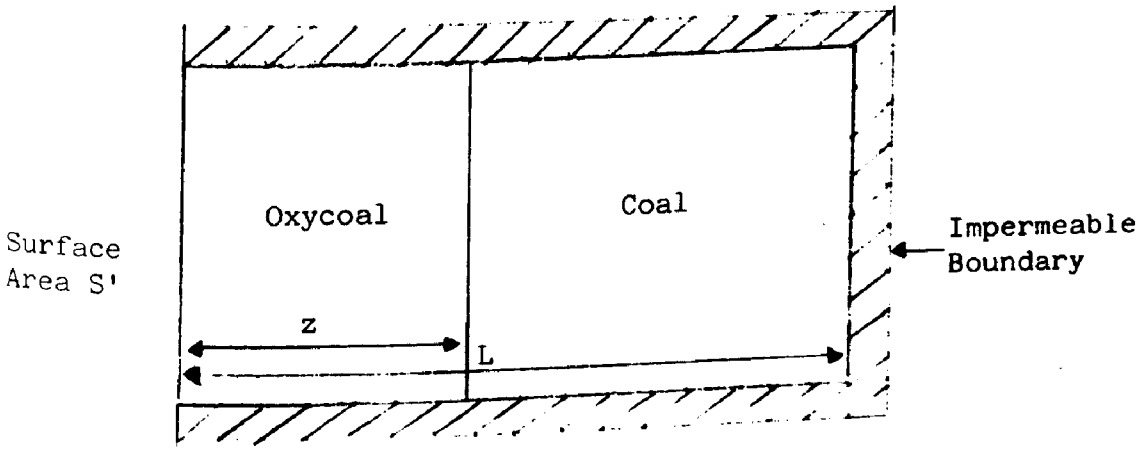


Figure A1.1 Simplified coal particle geometry

A particle length L is defined such that

$$S'L = V_p \qquad \text{A1.1}$$

where V_p = particle volume

At a time when the oxycoal layer has a thickness x the following equations may be written:

$$\text{Rate of diffuson of } O_2 \text{ through oxycoal} = S'D_e\,(C-C_s)/x \qquad \text{A1.2}$$

Rate of reaction of O_2 at reaction front = $S' k_s C_s$ A1.3

where D_e = effective diffusivity of oxycoal layer
C = free stream oxygen concentration
C_s = oxygen concentration at reaction boundary
k_r = surface rate constant

Under the pseudo steady state assumption that there is no accumulation of O_2 in the oxycoal these two rates must be equal i.e.

$$D_e (C - C_s)/x = k_r C_s \qquad \text{A1.4}$$

and solving for C_s gives

$$C_s = \frac{C}{1 + k_r x/D_e} \qquad \text{A1.5}$$

Back substitution in equation A1.2 gives

Rate of adsorption of O_2 by one particle $= \dfrac{S' k_r c}{1 + k_r x/D_e}$ A1.6

Now in a time Δt let the reaction front move a distance Δx.

Volume of coal reacted $= S' \Delta x$ A1.7

Moles of coal reacted $= \rho_m S' \Delta x$ A1.8

where ρ_m = molar density of reactive unit.

However the moles of coal reacted must equal the rate of adsorption times the time interval i.e.

$$\rho_m S' \Delta x = \frac{k_r C S' \Delta t}{1 + k_r x/D_e} \qquad \text{A1.9}$$

letting Δt, Δx tend to zero gives

$$\rho_m \frac{dx}{dt} = \frac{k_r C}{1 + k_r x/D_e} \qquad \text{A1.10}$$

In order to write the equations in terms of fractional

conversion of the coal, rather than the thickness of the oxycoal layer, it is noted that the volume of reacted material is S′x and the total volume is S′L.

Therefore the fractional conversion X is $S'x/(S'L) = x/L$

However L as defined by equation A1.1 is equal to V_p/S'.

Therefore $L = V_p/S' = 1/S_t$ A1.11

where S_t is now the total particle surface area per unit volume of particle.

Therefore, fractional conversion $X = xS_t$ A1.12

and substituting in equation A1.10 gives

Rate of adsorption of O_2 by one particle $= \dfrac{S_t\ V_p\ k_r\ C}{1 + k_r\ X/(S_t\ D_e)}$ A1.13

$$\rho_m\ S'\ \frac{dX}{dt} = \frac{k_r\ C\ S_t}{1 + k_r\ X/(S_t\ D_e)} \qquad \text{A1.14}$$

The rate that is required is however the rate per unit bed volume.

Rate / unit bed volume = Rate per particle x $\dfrac{\text{no of particles}}{\text{unit bed volume}}$

A volume V of the bed contains a volume $V(1-\epsilon)$ of coal where ϵ is the bed voidage.

The number of particles in the volume is therefore

$$V(1 - \epsilon)/V_p$$

and the number of particles per unit volume is

$$(1 - \epsilon)/V_p$$

Therefore the rate per unit bed volume is

$$r = \frac{S_t\, k_r\, C\, (1-\epsilon)}{1 + k_r\, X/(S_t\, D_e)} \qquad \text{A1.15}$$

APPENDIX 2 TABULATION OF MEASURED THERMAL CONDUCTIVITIES

A2.1 Details of Coal Used

Particle size range: -6.32 + 3.4 mm

Mass of coal: 67 Kg

Density of coal (measured): 1.36 g/cm^3

Volume of apparatus: .08 m^3

Voidage of bed: 0.38

A2.2 Measured Values

The values measured during 1982 are given in Table A2.1.

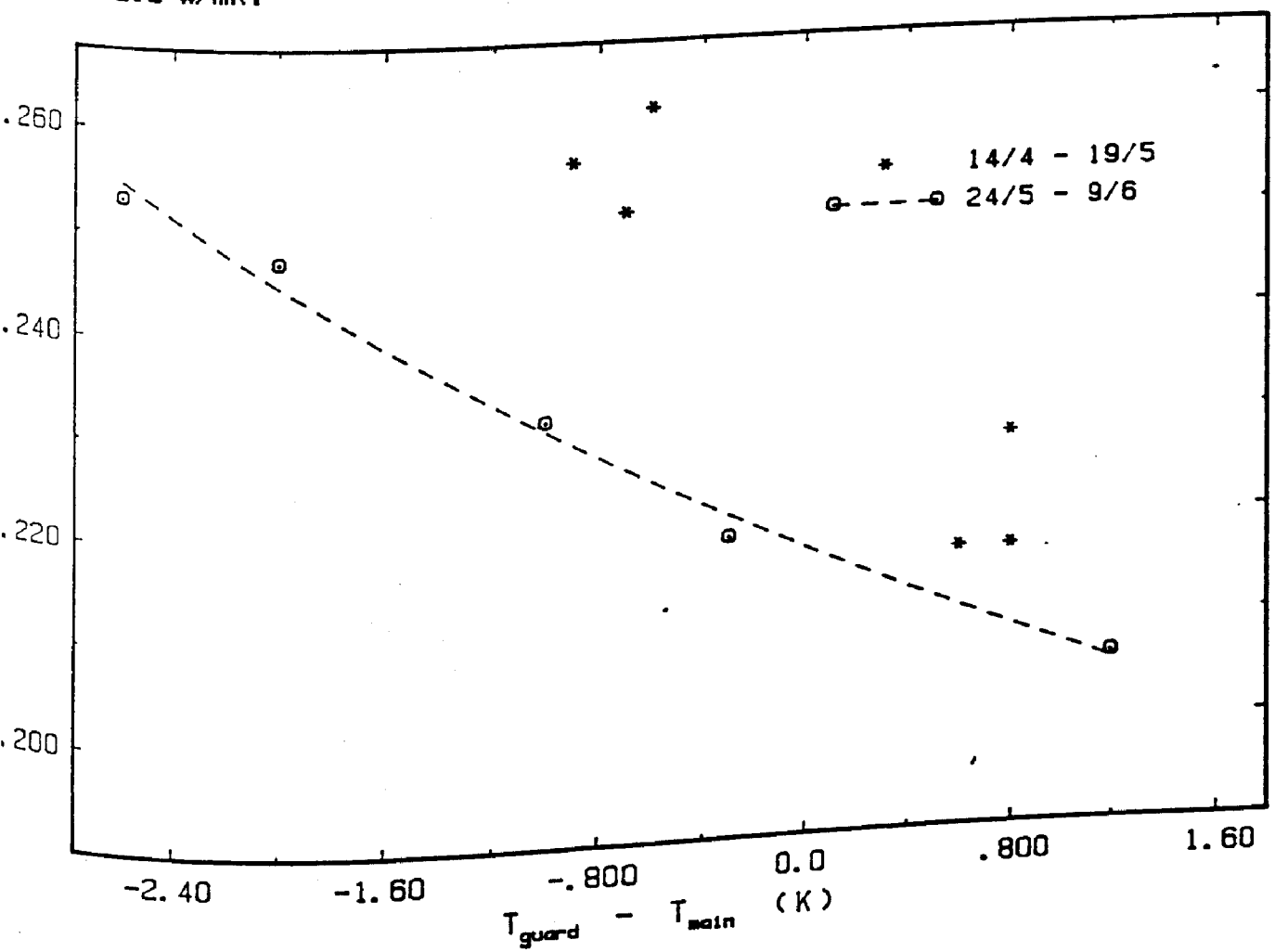
TABLE A2.1 MEASURED THERMAL CONDUCTIVITIES

DATE	MAIN TEMP(^{o}C)	GUARD TEMP(^{o}C)	MAIN VOLTAGE(V)	MAIN CURRENT(mA)	WATER TEMP(^{o}C)	k_b(W/mK)
14/4	67.8	68.6	11.66	139.8	23.0	0.217
16/4	68.7	69.5	11.66	139.8	24.0	0.228
6/5	57.8	58.4	11.64	139.5	24.0	0.286
10/5	62.2	61.6	11.64	139.7	25.0	0.261
18/5	60.2	59.5	11.69	140.2	22.0	0.251
19/5	60.0	59.1	11.69	140.2	22.5	0.256
24/5	98.2	95.6	16.46	196.7	23.0	0.253
27/5	99.7	97.7	16.45	196.7	23.0	0.247
28/5	104.9	103.9	16.46	196.6	23.0	0.231
4/6	109.2	108.9	16.45	196.4	23.0	0.219
9/6	114.8	116.0	16.45	196.5	23.0	0.206
25/6	86.8	88.6	13.94	166.6	23.0	0.213
23/7	91.3	91.1	14.00	167.2	23.0	0.201

The thermal conductivities measured between 14/4 and 9/6 are graphed against the temperature difference between the main and guard heaters on Figure A2.1. The reason for this choice

of plot is that in theory the guarded hot ring apparatus should be operated with the guard ring and main heater temperatures equal. Since this is impossible to achieve in practice, and since the calculated thermal conductivity is sensitive to differences between the main and guard heater temperatures, some form of interpolation must be used in calculating the thermal conductivty for the case of equal guard and main heater temperatures.

In figure A2.1 the data is plotted for the two different power inputs used. As can be seen, the data for the period 14/4 to 19/5, at the lower power input, shows considerable scatter. This could be due to a number of factors including failure to allow the apparatus to come to steady-state, as well as the variations in the cooling water temperature which are evident from Table A2.1. Due to the scatter in the data no attempt has been made to interpolate to $T_{guard} = T_{main}$. The data for the period 24/5 - 9/6 shows far more consistency. A quadratic least squares curve fits this data well, as can be seen from the graph. The interpolated value for $T_{guard} = T_{main}$ is 0.216 W/mK. The value obtained by linear interpolation between the values measured on 25/6 and 23/7 (which are not shown on the graph) is 0.202 W/mK.



APPENDIX 3 DERIVATION OF MODEL EQUATIONS

A3.1 Mass Balances

A3.1.1 Gas Phase Mass Balances

Consider the element of a bed of coal shown in Figure A3.1. The element has cross sectional area A and height Δx. The volume of gas in the element is $A \Delta x \epsilon$. The molar flowrate per unit area of the gas through the voids is G .

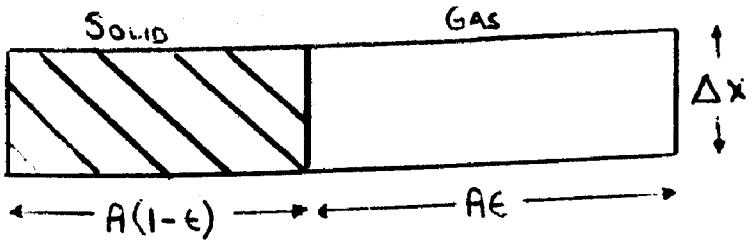


Figure A3.1 Differential element of a coal bed

The mass balance for component i in the gas phase is:

$$(\text{Moles of i in gas})\big|_{t+\Delta t} - (\text{Moles of i in gas})\big|_{t}$$

$$= (\text{Moles in})\big|_{x} - (\text{Moles in})\big|_{x+\Delta x} + \text{Moles produced in time } \Delta t$$

or

$$\left(\frac{P \epsilon}{R T_g} A \Delta x \, y_i\right)\Big|_{t+\Delta t} - \left(\frac{P \epsilon}{R T_g} A \Delta x \, y_i\right)\Big|_{t}$$

$$= (A G y_i \Delta t)\big|_{x} - (A G y_i \Delta t)\big|_{x+\Delta x} + r_i A \Delta x \Delta t$$

where
- G = molar flowrate per unit area
- y_i = mole fraction of i in the gas phase
- x = distance along bed
- P = pressure
- R = gas constant
- ϵ = bed voidage
- T_g = gas temperature
- t = time
- r_i = rate of formation of i per unit bed volume

Dividing by A Δx Δt and letting Δx and Δt tend to zero gives:

$$\frac{\partial}{\partial t}\left(\frac{P \epsilon}{R T_g} y_i\right) + \frac{\partial}{\partial x}(G y_i) = r_i \qquad \text{A3.1.1}$$

Equation A3.1.1 may be summed over all i to give:

$$\frac{\partial G}{\partial x} + \frac{\epsilon}{R} \frac{\partial}{\partial t} \frac{P}{T_g} = \sum_{i=1}^{N} r_i \qquad \text{A3.1.2}$$

where N = number of components in gas phase

Substitution of equation A3.1.1 in A3.1.2 gives:

$$G \frac{\partial y_i}{\partial x} + \frac{P \epsilon}{R T_g} \frac{\partial y_i}{\partial t} = r_i - y_i \sum_{j=1}^{N} r_j \qquad (i = 1 \text{ to } N) \qquad \text{A3.1.3}$$

A3.2 Solid Phase Mass Balances

Let the mass fraction of component j in the solid phase be f_j, and the rate of formation of j per bed volume be p_j.

The mass balance for the solid phase is:

Increase of mass of j in time Δt
= rate of formation of j x bed volume x Δt

or: $(A \Delta x \rho (1-\epsilon) f_j)_{t+\Delta t} - (A \Delta x \rho (1-\epsilon) f_j)_t = p_j \Delta t A \Delta x$

Dividing by A Δx Δt and letting Δt tend to zero gives:

$$(1-\epsilon) \frac{\partial (\rho f_j)}{\partial t} = p_j \qquad (j = 1 \text{ to } M) \qquad \text{A3.1.4}$$

ρ = density of solid
f_j = mass fraction of j in the solid
p_j = rate of formation of j in the solid
M = number of components in solid phase

where it has been assumed that the voidage of the bed does not change with time.

Summing over all j gives:

$$(1-\epsilon)\frac{\partial \rho}{\partial t} = \sum_{j=1}^{M} p_j \qquad \text{A3.1.5}$$

A3.2 Energy Balances

The general energy balance used in this section is:

Rate of change of internal energy of the volume =

Internal energy in - Internal energy out +

energy transferred thermally + energy transferred mechanically

In the derivations that follow changes in kinetic and potential energy have been neglected.

A3.2.1 Gas Phase Energy Balance

Application of the above formula to the gas in the volume shown in Figure A3.1 gives:

$\frac{\partial U_g}{\partial t}$ Rate of change of internal energy

$= (A\ \epsilon\ q_g)_{/x} - (A\ \epsilon\ q_g)_{/x+\Delta x}$ conduction/radiation

$+ (A\ G\ \hat{H})_{/x} - (A\ G\ \hat{H})_{/x+\Delta x}$ flow

$+ A\ \Delta x \sum_{i=1}^{N} r_i\ \hat{H}_i$ Reaction

$+ Q_c\ A\ \Delta x$ Convection from solid to gas

where U_g = Internal energy of gas in volume

q_g = flux due to conduction and radiation in gas

$\hat{H}$ = molar enthalpy of flowing gas

$\hat{H}_i$ = molar enthalpy of gas leaving or entering by reaction

Q_c = rate of convection from gas to solid

It should be noted that the flow and reaction terms involve enthalpies and not internal energies. This is because the process is to all intents and purposes constant pressure and reversible, and therefore the mechanical work term may be combined with the flow and reaction terms which then may be written as enthalpies.

Now:

$$U_g = A\,\Delta x\,\epsilon\,\rho_g\,\hat{U} = A\,\Delta x\,\epsilon\,P\,\hat{U}/(R\,T_g)$$

where the ideal gas law

$$\rho_g = P/(R\,T_g)$$

has been used.

Substituting this in the above energy balance, dividing by $A\,\Delta x$ and letting Δx tend to zero gives:

$$\epsilon\,\frac{\partial}{\partial t}\,\frac{P\,\hat{U}}{R\,T_g} = -\,\epsilon\,\frac{\partial q_g}{\partial x} - \frac{\partial}{\partial x}\,(G\,\hat{H}) + \sum_{i=1}^{N} r_i\,\hat{H}_i + Q_c \qquad \text{A3.2.1}$$

But

$$\hat{U} = \hat{H} - R\,T_g$$

since the ideal gas assumption has been made. Substituting this in Equation A3.2.1 gives:

$$\epsilon\,\frac{\partial}{\partial t}\,\frac{P\,\hat{H}}{R\,T_g} - \epsilon\,\frac{\partial P}{\partial x} = -\,\epsilon\,\frac{\partial q_g}{\partial x} - \frac{\partial}{\partial x}\,(G\,\hat{H}) + \sum_{i=1}^{N} r_i\,\hat{H}_i + Q_c \qquad \text{A3.2.2}$$

For an ideal gas

$$\hat{H} = \sum_{i=1}^{N} y_i\,\hat{H}_i$$

and

$$d\hat{H} = \sum_{i=1}^{N} (y_i\,d\hat{H}_i + \hat{H}_i\,dy_i)$$

Therefore

$$\epsilon \frac{\partial}{\partial t}\frac{P\hat{H}}{R T_g} + \frac{\partial}{\partial x}(G\hat{H}) = \frac{\epsilon P}{R T_g}\frac{\partial \hat{H}}{\partial t} + G\frac{\partial \hat{H}}{\partial x} + \epsilon \hat{H}\frac{\partial}{\partial t}\frac{P}{R T_g} + \hat{H}\frac{\partial G}{\partial x}$$

$$= \frac{P\epsilon}{R T_g}\sum_{i=1}^{N}\left(y_i\frac{\partial \hat{H}_i}{\partial t} + \hat{H}_i\frac{\partial y_i}{\partial t}\right) + G\sum_{i=1}^{N}\left(y_i\frac{\partial \hat{H}_i}{\partial x} + \hat{H}_i\frac{\partial y_i}{\partial x}\right) + \hat{H}\left(\epsilon\frac{\partial}{\partial t}\frac{P}{R T_g} + \frac{\partial G}{\partial x}\right)$$

Combining terms and using the gas phase mass balance (equation A3.1.3) the right hand side of the above equation may be written as

$$\sum_{i=1}^{N}\left(\hat{H}_i\left(r_i - y_i\sum_{j=1}^{N} r_j\right)\right) + \frac{P\epsilon}{R T_g}\sum_{i=1}^{N}\left(y_i\frac{\partial \hat{H}_i}{\partial T}\frac{\partial T}{\partial t}\right)$$

$$+ G\sum_{i=1}^{N}\left(y_i\frac{\partial \hat{H}_i}{\partial T}\frac{\partial T}{\partial t}\right) + \hat{H}\sum_{i=1}^{N} r_i$$

For an ideal gas $\frac{\partial \hat{H}_i}{\partial T} = \hat{c}_i$ by definition

and $$\sum_{i=1}^{N} y_i\,\hat{c}_i = \hat{c}$$

Substituting in the above expression gives:

$$RHS = \sum_{j=1}^{N}\hat{H}_i\,r_i + \frac{P\epsilon}{RT_g}\hat{c}\frac{\partial T_g}{\partial t} + G\,\hat{c}\frac{\partial T_g}{\partial x}$$

Finally, back substitution in A3.2.2 gives the gas phase energy balance:

$$\frac{P\epsilon}{RT_g}\hat{c}\frac{\partial T_g}{\partial t} - \epsilon\frac{\partial P}{\partial t} = -G\,\hat{c}\frac{\partial T_g}{\partial x} + \epsilon k_g\frac{\partial^2 T_g}{\partial x^2} + Q_c$$

where use has been made of Fourier's law in writing

$$\frac{\partial q_g}{\partial x} = -k_g\frac{\partial^2 T_g}{\partial x^2}$$

A3.2.2 Solid Phase Energy Balance

The approach taken is to write an energy balance for the whole system, and then to subtract the gas phase energy balance to leave the solid phase energy balance.

Thus, using equation A3.2.1

$$(U_s + U_g)/_{t+\Delta t} - (U_s + U_g)/_t$$

$$= [A\epsilon q^g_{cr}/_x - A\epsilon q^g_{cr}/_{x+\Delta x}]\Delta t \qquad \text{(Conduction and radiation in gas)}$$

$$+ [A(1-\epsilon)q^s_c/_x - A(1-\epsilon)q^s_c/_{x+\Delta x}]\Delta t \qquad \text{(Conduction in solid)}$$

$$+ [A\hat{G}\hat{H}/_x - A\hat{G}\hat{H}/_{x+\Delta x}]\Delta t \qquad \text{(Bulk Flow)} \quad \text{A3.2.6}$$

Note that there are no reaction or convection terms since these terms are associated with transport between the phases.

Subtracting the appropriate gas-phase energy balance leaves:

$$U_s/_{t+\Delta t} - U_s/_t$$

$$= [A(1-\epsilon)q^s_c/_x - A(1-\epsilon)q^s_c/_{x+\Delta x}]\Delta t$$

$$- Q_c A\Delta x\Delta t \qquad \text{A3.2.7}$$

Now $U_s = \rho A\Delta x(1-\epsilon)\bar{U}_s$ since $A\Delta x(1-\epsilon)$ is the volume of the solid phase and $\bar{U}_s$ is the specific mass internal energy of the solid.

Substituting this in equation A3.2.7, dividing by $A\Delta x\Delta t$ and letting Δx and Δt tend to zero gives:

$$\frac{\partial}{\partial t}(\rho\bar{U}_s) = -(1-\epsilon)\frac{\partial q^s_c}{\partial x} - Q_c \qquad \text{A3.2.8}$$

Now

$$\bar{U}_s = \bar{H}_s - \frac{P}{\rho} \qquad \text{A3.2.9}$$

Therefore

$$\frac{\partial}{\partial t}(\rho\bar{U_s}) = \frac{\partial}{\partial t}(\rho\bar{H_s}) - \frac{\partial P}{\partial t} \qquad \text{A3.2.10}$$

$$= \bar{H}_s\frac{\partial\rho}{\partial t} + \rho\frac{\partial\bar{H}}{\partial t}s - \frac{\partial P}{\partial t} \qquad \text{A3.2.11}$$

Assuming $\bar{H}_s$ may be written as the sum of pure component enthalpies ie:

$$\bar{H}_s = \sum_{j=1}^{N} f_j\bar{H}_j \qquad \text{A3.2.12}$$

Therefore

$$\frac{\partial\bar{H}}{\partial t}s = \sum_{j=1}^{N}\frac{\partial}{\partial t}(f_j\bar{H}_j) = \sum_{j=1}^{N}(\bar{H}_j\frac{\partial f}{\partial t}j + f_j\frac{\partial\bar{H}}{\partial t}j) \qquad \text{A3.2.13}$$

Now, using equation A3.2.13 and the solid phase mass balance A3.1.5 it may be shown that:

$$(1-\epsilon)\frac{\partial}{\partial t}(\rho\bar{H}_s) = \sum_{j=1}^{N}\bar{H}_j\rho_j + (1-\epsilon)\rho\sum_{j=1}^{N}f_j\frac{\partial\bar{H}}{\partial t}j \qquad \text{A3.2.14}$$

Now

$$\frac{\partial\bar{H}}{\partial t}j = \left(\frac{\partial\bar{H}}{\partial T}j\right)_p\frac{\partial T}{\partial t}s + \left(\frac{\partial\bar{H}}{\partial P}j\right)_{T_s}\frac{\partial P}{\partial t} \qquad \text{A3.2.15}$$

$$= \bar{c}_j\frac{\partial T}{\partial t}s + \left(\frac{\partial H}{\partial P}j\right)_{T_s}\frac{\partial P}{\partial t} \qquad \text{A3.2.16}$$

Therefore

$$\sum_{j=1}^{N}f_j\frac{\partial\bar{H}}{\partial t}j = \sum_{j=1}^{N}\left(f_j\bar{c}_j\frac{\partial T}{\partial t}s + f_j\left(\frac{\partial\bar{H}}{\partial t}j\right)_{T_s}\frac{\partial P}{\partial t}\right) \qquad \text{A3.2.17}$$

$$= \bar{c}_s\frac{\partial T}{\partial t}s + \frac{\partial P}{\partial t}\sum_{j=1}^{N}f_j\left(\frac{\partial\bar{H}}{\partial P}j\right)_{T_s} \qquad \text{A3.2.18}$$

At this point the assumption is made that the solid enthalpy is not a function of pressure. Thus the last term of equation

A3.2.18 can be dropped. Substitution of the above results in equation A3.2.18 yields:

$$(1-\epsilon)\rho_s \bar{c}_s \frac{\partial T_s}{\partial t} - (1-\epsilon)\frac{\partial P}{\partial t} = (1-\epsilon)\frac{\partial q^s_c}{\partial x} - Q_c - \sum_{j=1}^{N} p_j H_j$$

Finally, use is made of Fourier's Law in writing

$$\frac{\partial q^s_c}{\partial x} = \eta k_s \frac{\partial^2 T_s}{\partial x^2}$$

where η is a tortuosity factor allowing for the fact that the conduction in the solid does not occur in a straight line.

A3.3 Momentum Balance

The equation of motion for the one-dimensional flow of a Newtonian fluid is given by Bird, Stewart & Lightfoot (1960) to be:

$$\rho \frac{\partial U}{\partial t} = -\rho U \frac{\partial U}{\partial x} + \mu \frac{\partial^2 U}{\partial x^2} - \rho g - \frac{\partial P}{\partial x} \qquad \text{A3.3.1}$$

Bird et al (1960) state that for flow through packed beds the steady-state equation of motion may be simplified to:

$$0 = -fU - \rho g - \frac{\partial P}{\partial x} \qquad \text{A3.3.2}$$

This implies that the unsteady-state equation of motion in the case of a packed bed is:

$$\rho \frac{\partial U}{\partial t} = -fU - \rho g - \frac{\partial P}{\partial x} \qquad \text{A3.3.3}$$

The equation of motion for the air far from the bed is:

$$0 = -\rho_\infty g - \frac{\partial P_\infty}{\partial x} \qquad \text{A3.3.4}$$

Subtracting A3.3.4 from A3.3.3 gives:

$$\rho \frac{\partial U}{\partial t} = -fU + g(\rho_\infty - \rho) - \frac{\partial}{\partial x}(P - P_\infty) \qquad \text{A3.3.5}$$

If the gas is assumed to behave ideally, and its molecular weight is constant then

$$\frac{\rho}{\rho_\infty} = \frac{T_\infty}{T}$$

Substituting this in equation A3.3.5 gives, for the steady-state:

$$\frac{\partial}{\partial x}(P-P_\infty) = -fU + g\,\rho_\infty\left(1 - \frac{T}{T_\infty}\right) \qquad 2.2.1$$

APPENDIX 4 THE CONTINUUM AND PSEUDO STEADY-STATE ASSUMPTIONS

The continuum assumption for a packed bed may be made when the solid and gas temperatures are not very different. In this case equations 5.4.5 and 5.6.4 may be added to give equation 6.1.1.

Edwards (1983) has discussed the conditions under which the particle and gas temperatures tend to equilibrate, and has shown that this will occur within a time τ_d given by:

$$\tau_d = \frac{\rho_s \, C_s \, D_p^2}{4 \, k_s} \qquad \text{A4.1}$$

This author's calculations indicate that the particle surface and air temperatures are nearly in equlibrium. This can be understood if τ_d is evaluated for the following values:

$$\rho_s = 1200 \text{ kg/m}^3$$
$$C_s = 1000 \text{ J/kg/K}$$
$$k_s = 0.4 \text{ W/m/K}$$

Then $\tau_d = 750 \times 10^3 \, D_p^2$

For $D_p = 1$ mm $\qquad \tau_d = 750 \times 10^{-3}$ s

For $D_p = 20$ mm $\qquad \tau_d = 300$ s

Both of these times are small in comparison to the residence time of the gas in the bed, and therefore thermal equilibrium between gas and solid should be reached.

The pseudo-steady state assumption may be made when the time constant for one process is very much larger than the time constant for the other process. In the case of a coal bed the time constant for conduction is given by

$$\tau_c = \frac{4L^2 \, \rho_b \, C_b}{\pi^2 \, k_b} = \frac{4 \, L^2}{\pi^2 \, \kappa}$$

Using a typical value for κ of 8×10^{-4} m^2/hr gives

$$\tau_c = \frac{4 \, L^2}{\pi^2 \, 8 \times 10^{-4}} = 500 \, L^2 \text{ hours}$$

The time constant for gas flow and gas composition is the residence time of the gas i.e.

$$\tau_f = \frac{L}{U} = \frac{P\,L}{G\,R\,T}$$

Using values from Table 2.1 for D_p = 5 mm gives

$$\tau_f = \frac{8.3 \times 10^3 \times 320 \times 1.3 \times 10^{-4}\,L}{1 \times 10^5} = 0.08\,L \text{ hours}$$

The time constant associated with the momentum balance is

$$\tau_p = \frac{\rho_g L}{f} = \frac{1.173\,L}{2.2 \times 10^3} = 5.3 \times 10^{-4}\,L \text{ seconds}$$

It can be seen that the time constants for gas flow and composition and for pressure changes are very much smaller than that for conduction. Furthermore the time constant for conduction depends on L^2 while the other time constants depend on L. For these reasons the pseudo-steady state assumption on the gas mass balances and the momentum balance is a good one.

APPENDIX 5 THE INCLUSION OF A RADIAL HEAT LOSS TERM IN EQUATION 6.1.4

In order to include radial heat losses in equation 6.1.4, an alternative derivation of the temperature equation is used.

Consider an element in the form of a ring, as shown in Figure A5.1:

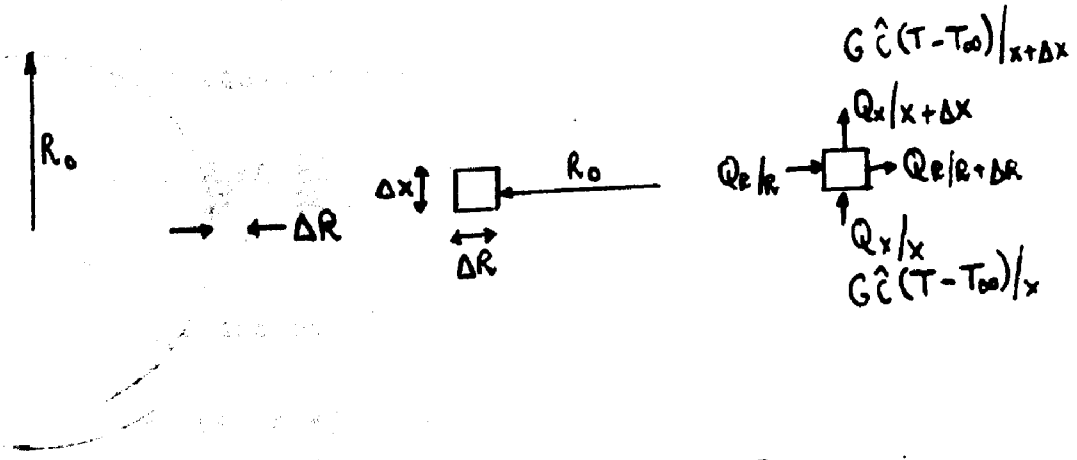


FIGURE A5.1 ELEMENT IN THE FORM OF A RING

The following energy balance may be written:

Rate of accumulation of energy in the volume =

Rate of energy transfer into volume +

Rate of generation in volume -

Rate of energy transfer out of volume

or

$$\rho C_p \frac{\partial}{\partial t}(T\ 2\pi R\ \Delta R\ \Delta x)$$

$$= (Q_R\ 2\pi R\ \Delta x)|_R + (Q_x\ 2\pi R\ \Delta R)|_x + G\hat{c}\ 2\pi R\ \Delta R\ (T-T_\infty)|_x$$

$$+ r_x(-\Delta H_r)\ 2\pi R\ \Delta R\ \Delta x$$

$$- (Q_R\ 2\pi R\ \Delta x)|_{R+\Delta R} - (Q_x\ 2\pi R\ \Delta R)|_{x+\Delta x} - G\hat{c}\ 2\pi R\ \Delta R\ (T-T_\infty)|_{x+\Delta x}$$

Dividing by $\Delta R\ \Delta x$ and letting them tend to zero gives:

$$\rho\ C_p\ 2\pi R\ \frac{\partial T}{\partial t} = -\frac{\partial}{\partial R}(Q_R\ 2\pi R) - \frac{\partial}{\partial x}(Q_x\ 2\pi R) - G\ \hat{c}\ 2\pi R\ \frac{\partial T}{\partial x} + ry(-\Delta H_r)2\pi R$$

Using Fourier's law $\quad Q_R = -k_{b,R}\ \frac{\partial T}{\partial R}$

and $\quad Q_x = -k_{b,x}\ \frac{\partial T}{\partial x}$

Substituting in above equation gives:

$$\rho\ C_p\ 2\pi R\ \frac{\partial T}{\partial t} = 2\pi\ k_{b,R}\ \frac{\partial}{\partial R}(R\ \frac{\partial T}{\partial R}) + 2\pi R\ k_{b,x}\ \frac{\partial^2 T}{\partial^2 x} - G\ \hat{c}\ 2\pi R\ \frac{\partial T}{\partial x} + ry(-\Delta H_r)2\pi R$$

assuming $k_{b,R}$ and $k_{b,x}$ are not functions of R and x respectively.

This equation may now be integrated from 0 to R_o. Assuming that ρ, C_p, G, r and ΔH_r are not functions of R, this gives:

$$\rho\ C_p\ 2\pi\ \frac{\partial}{\partial t}(\int_0^{R_o} T\ R\ dR) = 2\pi\ k_{b,R}\int_0^{R_o}\frac{\partial}{\partial R}(R\ \frac{\partial T}{\partial R})\ dR + 2\pi\ k_{b,x}\ \frac{\partial^2}{\partial x^2}(\int_0^{R_o} T\ R\ dR)$$

$$- G\ \hat{c}\ 2\pi\ \frac{\partial}{\partial x}(\int_0^{R_o} T\ R\ dR) + ry(-\Delta H_r)2\pi(\int_0^{R_o} R\ dR)$$

Defining $T' = \frac{2}{R_o^2}\int_0^{R_o} T\ R\ dR$ and substituting gives

$$\rho\ C_p\ \pi\ R_o^2\ \frac{\partial T'}{\partial t} = 2\pi\ k_{b,R}\ \ R\ \frac{\partial T}{\partial R}\Big]_{R=R_o} + \pi\ R_o^2\ k_{b,x}\ \frac{\partial^2 T'}{\partial x^2}$$

$$- G\ \hat{c}\ \pi\ R_o^2\ \frac{\partial T'}{\partial x} + ry(-\Delta H_r)\ \pi\ R_o^2$$

The radial boundary conditions is:

$$k_{b,R}\ \frac{\partial T}{\partial R} = -h_R\ (T(R=R_o)-T_\infty)$$

Substituting this in the above equation gives:

$$\rho C_p \pi R_o^2 \frac{\partial T'}{\partial t} = -2\pi R_o h_R (T(R=R_o)-T_\infty) + \pi R_o^2 k_{b,x} \frac{\partial^2 T'}{\partial x^2}$$

$$- G \hat{c} \pi R_o^2 \frac{\partial T'}{\partial x} + r y(-\Delta H_r) \pi R_o^2$$

If the radial gradients are not too large, $T(R=R_o)$ will not be very different from T'. Assuming this to be the case the above equation may be written as:

$$\rho C_p \frac{\partial T'}{\partial t} = -2h_R/R_o (T'-T_\infty) + k_{b,x} \frac{\partial^2 T'}{\partial x^2} - G \hat{c} \frac{\partial T'}{\partial x} + r y(-\Delta H_r)$$

This equation is the same as equation 6.1.1 apart from the first term on the right hand side. This is the radial heat loss term.

Finally, the above equation is made dimensionless using the substitutions given in Section 6.1. The result is equation 6.1.5 i.e.

$$\frac{\partial \theta}{\partial \tau} = \frac{\partial^2 \theta}{\partial X^2} - a \frac{\partial \theta}{\partial X} + b y - C (\theta - 1) \qquad 6.1.5$$

where $C = 2 h_R L^2/(k_b R_o)$.

It should be noted that as R_o tends to infinity, C tends to zero.

APPENDIX 6 EXPLANATION FOR THE INSTABILITY OF THE RUNGE-KUTTA ALGORITHM

The equation is

$$0 = \frac{d^2\theta}{dX^2} - a\frac{d\theta}{dX} - b\,y \qquad \text{A6.1}$$

with boundary conditions:

at X=0 $\quad \frac{d\theta}{dX} = (Bi_0+a)(\theta-1)$

at X=1 $\quad \frac{d\theta}{dX} = -Bi_1(\theta-1)$

For the first step along the bed the coefficients of equation A6.1 may be assumed constant. In effect the Runge-Kutta algorithm is stepping along the solution of 6.2.1 but with boundary conditions both at X = 0 i.e.

$$\frac{d\theta}{dX} = (Bi_0+a)(\theta-1)$$

$$\theta(X=0) = \theta_0$$

The solution to A6.1 with these boundary conditions is:

$$\theta = \theta_0 + a(\exp(aX)-1)((Bi_0+a)(\theta_0-1)-b/a) + b\,X/a \qquad \text{A6.2}$$

It can be seen that the value of θ_0 is critical, since if

$(Bi_0+a)(\theta_0-1)-b/a > 0$ then the second term of equation A6.2 increases without bound. If on the other hand:

$(Bi_0+a)(\theta_0-1)-b/a < 0$

then the second term becomes very large negative.

The real problem is that the boundary condition at X = 1 is not included in the method of solution, and thus the method will always become unstable.

APPENDIX 7 SOLUTION OF EQUATION 6.2.1 WITH r CONSTANT

If r is assumed constant then equation 6.1.2 may be integrated

i.e. $$\frac{dy}{dx} = \frac{-r\ y}{G}$$

gives $$y = y_o \exp(-rx/G) = y_o \exp(\gamma_3 X) \qquad A7.1$$

Substituting this in equation 6.2.1 give:

$$0 = \frac{d^2\theta}{dX^2} - a\frac{d\theta}{dX} - b\ y_o \exp(\gamma_3 X) - C\ (\theta - 1) \qquad A7.2$$

The solution of this equation is

$$\theta(X) = 1 + C_1\exp(\gamma_1 X) + C_2\exp(\gamma_2 X) + C_3\exp(\gamma_3 X)$$

$$C_3 = -b/(\gamma_3^2 + a\gamma_3 - C)$$

$$\gamma_1 = (a - (a^2 + 4C))^{1/2})/2$$

$$\gamma_2 = (a + (a^2 + 4C))^{1/2})/2$$

C_1 and C_2 may be determined from the boundary conditions.

Equation 6.1.3 may be integrated to give

$$-\rho_\infty\ v^2/2 = -f\ G\ R\ T_\infty\ L/P(\int_o^1 \theta\ dX + \rho_\infty\ g\ L(\int_o^1 \theta^{-1}\ dX)) \qquad A7.3$$

or $$G = P\ \rho_\infty(v^2/2L + g\ L(1-\int_o^1 \theta^{-1}dX))/(f\ R\ T_\infty\ L\ \int_o^1 \theta dX) \qquad A7.4$$

APPENDIX 8 SOLUTION OF EQUATION 6.1.5 WITH r CONSTANT

The equation to be solved is:

$$\frac{\partial\theta}{\partial\tau} = \frac{\partial^2\theta}{\partial X^2} - a\frac{\partial\theta}{\partial X} + b\,y - C\,(\theta - 1) \qquad \text{A8.1}$$

with boundary conditions

at X=0 $\quad \frac{\partial\theta}{\partial X} = (Bi_0+a)(\theta-1)$

at X=1 $\quad \frac{\partial\theta}{\partial X} = -Bi_1(\theta-1)$

The initial condition is $\theta(X,0) = \theta_0(X)$

The first step in the solution is to write:

$$\theta(X,\tau) = u(X,\tau) + \phi(X) \qquad \text{A8.2}$$

Substituting equation A8.2 in equation A8.1 gives:

$$\frac{\partial u}{\partial\tau} = \frac{\partial^2 u}{\partial X^2} - a\frac{\partial u}{\partial X} - C\,u + \frac{d^2\phi}{dX^2} - a\frac{d\phi}{dX} + b\exp(\gamma_s X) - C(\phi-1) \qquad \text{A8.3}$$

This may be written as two equations:

$$\frac{\partial u}{\partial\tau} = \frac{\partial^2\theta}{\partial X^2} - a\frac{\partial u}{\partial X} - C\,u \qquad \text{A8.4}$$

and

$$0 = \frac{d^2\phi}{dX^2} - a\frac{d\phi}{dX} + b\exp(\gamma_s X) - C(\phi-1) \qquad \text{A8.5}$$

with boundary conditions:

at X=0 $\quad \frac{\partial u}{\partial X} = (Bi_0+a)\,u$ and $\frac{d\phi}{dX} = (Bi_0+a)(\phi-1)$

at X=1 $\quad \frac{\partial u}{\partial X} = -Bi_1\,u$ and $\frac{d\phi}{dX} = -Bi_1(\phi-1)$

and initial condition $u(X,0) = \theta_0(X) - \phi(X)$

Equation A8.5 with its associated boundary conditions is merely the steady-state temperature equation, whose solution has been dealt with in Appendix 7.

The problem has thus been reduced to solving equation A8.4 with its boundary and initial conditions.

Defining a new variable $v(X,\tau)$ as:

$$u(X,\tau) = v(X,\tau) \exp(-\tau(a^2/4-C) + aX/2)$$

and substituting in equation A8.4 gives the diffusion equation i.e

$$\frac{\partial v}{\partial \tau} = \frac{\partial^2 v}{\partial X^2} \qquad \text{A8.6}$$

The boundary conditions on v are:

At X=0 $\quad \frac{\partial v}{\partial \tau} = (Bi_0 + a/2)v$

At X=1 $\quad \frac{\partial v}{\partial \tau} = -(Bi_1 + a/2)v$

and initial condition:

$$v(X,0) = (\theta_0(X) - \phi(X)) \exp(-aX/2)$$

The solution to equation A8.6 may be found in Carslaw & Jaeger (1959), and is:

$$v(X,\tau) = \Sigma \left(Z_n(X) \exp(-\beta_n^2\tau) \int Z_n(X') g(X') dX'\right) \qquad \text{A8.7}$$

$$Z_n(X) = \frac{2(\beta_n^2+Bi_3^2)(\beta_n \cos(\beta_n X)+Bi_2 \sin(\beta_n X))}{((\beta_n^2+Bi_2^2)(\beta_n^2+Bi_3^2+Bi_3)+Bi_2(\beta_n^2+Bi_3^2))}$$

$$g(X) = (\theta_0(X) - \phi(X)) \exp(-aX/2)$$

$$Bi_2 = Bi_0 - a/2$$

$$Bi_3 = Bi_1 + a/2$$

and the β_n are the positive roots of

$$\tan(\beta) = \frac{\beta(Bi_3 + Bi_2)}{(Bi_2\, Bi_3 + \beta^2)}$$

APPENDIX 9 APPLICATION OF THE METHOD OF LINES TO THE SOLUTION OF EQUATION 6.1.5

Equation 6.4.1 is:

$$\frac{\partial\theta(X_i,\tau)}{\partial X} = \Sigma(a_{ij}\ \theta(X_j,\tau) \qquad i=1 \text{ to } N \qquad \text{A9.1}$$

where the X_i are the nodes of the Nth order shifted Legendre polynomial.

Similarly

$$\frac{\partial^2\theta(X_i,\tau)}{\partial X} = \Sigma(b_{ij}\ \theta(X_j,\tau) \qquad i=1 \text{ to } N \qquad \text{A9.2}$$

It may easily be shown that the matrix $\underline{A}$ of coefficients a_{ij} is related to the matrix $\underline{B}$ of coefficients b_{ij} by:

$$\underline{B} = \underline{A}^2$$

Using equations A9.1 and A9.2 equation 6.1.5 may be written as:

$$\frac{d\theta_i}{d\tau} = \Sigma((b_{ij}-a\ a_{ij})\theta_j)+by_i\exp\{-E/(RT_\infty\theta_i)\}-C(\theta_i-1) \qquad \text{A9.3}$$

where $\theta_i = \theta(X_i,\tau)$

$y_i = y(X_i)$

The bondary conditions are also discretized:

$$\Sigma\ a_{1j}\theta_j = (Bio + a)(\theta_1 - 1) \qquad \text{A9.4}$$

$$\Sigma\ a_{Nj}\theta_j = -Bi_1(\theta_N - 1) \qquad \text{A9.5}$$

It can be seen that the partial differential equation has been rteduced to N ordinary differentail equations. The procedure used to solve is to calculate all the derivatives $d\theta_i/d\tau$ for one time and then use a Runge-Kutta algorithm to calculate the value of θ_i at the next time. The boundary values are included explicitly by solving equations A9.4 and A9.5 for θ_1 and θ_N in [illegible] at each time step. In addition a

backward difference formula is used to calculate the oxygen profile at each time. If the effects of ageing are incuded it is neccessary to calculate the fractional conversion of the coal at each time and distance using equation 1.4.4.

APPENDIX 10 TABULATION OF RESULTS OF CHIMNEY EXPERIMENT

A10.1 Introduction

In this Appendix the measured data for the chimney experiment is presented in tabular form. In the printouts it will be noted that 10 channels were used to log data. Channel 1 is the thermocouple at the very bottom of the bed, while channel 9 is the thermocouple at the very top of the bed. Channel 10 is a thermocouple placed in the oven.

The printouts show the time at which the data was logged and the temperature in degrees centigrade (labelled as deg_C). It should be noted that in some instances the data logger was re-started, with a greater interval between scans.

A10.2 Cooling Run

This run was used to obtain the heat transfer coefficients necessary for the model. The bed was heated under nitrogen and then removed from the oven. The model parameters used to obtain figure 7.2 were:

Coal particle size range : -3.4 + 1.19 mm
Bed Length : 0.2 m
Bed Radius : 0.039 m
C : 23
Bi_o : 3.7
Bi_1 : 9.3
Bed voidage : 0.38
D_p : 2.5 mm

EXP 10--SCAN 01---24:01:08:58:03
"COOLING"

ch: 01	190.3	deg_C
ch: 02	194.1	deg_C
ch: 03	196.5	deg_C
ch: 04	198.3	deg_C
ch: 05	197.1	deg_C
ch: 06	192.8	deg_C
ch: 07	189.6	deg_C
ch: 08	185.3	deg_C
ch: 09	181.4	deg_C
ch: 10	55.2	deg_C

EXP 10--SCAN 02---24:01:09:17:1
"COOLING"

ch: 01	179.3	deg_C
ch: 02	189.0	deg_C
ch: 03	191.7	deg_C
ch: 04	194.2	deg_C
ch: 05	193.5	deg_C
ch: 06	188.9	deg_C
ch: 07	187.2	deg_C
ch: 08	179.0	deg_C
ch: 09	157.2	deg_C
ch: 10	32.6	deg_C

EXP 10--SCAN 03---24:01:09:28:
"COOLING"

ch: 01	155.1	deg_C
ch: 02	171.7	deg_C
ch: 03	178.0	deg_C
ch: 04	181.2	deg_C
ch: 05	181.1	deg_C
ch: 06	176.0	deg_C
ch: 07	174.7	deg_C
ch: 08	158.3	deg_C
ch: 09	129.4	deg_C
ch: 10	29.8	deg_C

EXP 10--SCAN 04---24:01:09:47:
"COOLING"

ch: 01	171.9	deg_C
ch: 02	150.2	deg_C
ch: 03	160.1	deg_C
ch: 04	165.5	deg_C
ch: 05	165.6	deg_C
ch: 06	160.4	deg_C
ch: 07	157.7	deg_C
ch: 08	136.6	deg_C
ch: 09	108.7	deg_C
ch: 10	25.5	deg_C

EXP 10--SCAN 05---24:01:09:58:02:
"COOLING"

ch: 01	112.7	deg_C
ch: 02	129.1	deg_C
ch: 03	141.2	deg_C
ch: 04	145.5	deg_C
ch: 05	150.1	deg_C
ch: 06	144.7	deg_C
ch: 07	140.2	deg_C
ch: 08	117.8	deg_C
ch: 09	92.9	deg_C
ch: 10	26.2	deg_C

EXP 10--SCAN ---24:01:10:38:20
"COOLING"

ch: 01	50.6	deg_C
ch: 02	57.3	deg_C
ch: 03	64.3	deg_C
ch: 04	72.8	deg_C
ch: 05	75.3	deg_C
ch: 06	71.0	deg_C
ch: 07	65.2	deg_C
ch: 08	54.0	deg_C
ch: 09	45.3	deg_C
ch: 10	22.8	deg_C

EXP 10--SCAN 03---24:01:10:58:20
"COOLING"

ch: 01	42.9	deg_C
ch: 02	47.6	deg_C
ch: 03	53.1	deg_C
ch: 04	59.9	deg_C
ch: 05	62.0	deg_C
ch: 06	59.6	deg_C
ch: 07	54.0	deg_C
ch: 08	45.6	deg_C
ch: 09	39.1	deg_C
ch: 10	22.1	deg_C

EXP 10--SCAN 07---24:01:11:28:20
"COOLING"

ch: 01	38.4	deg_C
ch: 02	41.0	deg_C
ch: 03	44.9	deg_C
ch: 04	50.1	deg_C
ch: 05	51.9	deg_C
ch: 06	49.2	deg_C
ch: 07	45.6	deg_C
ch: 08	39.4	deg_C
ch: 09	34.6	deg_C
ch: 10	22.4	deg_C

EXP 10--SCAN 04---24:01:13:08:20
"COOLING"

ch: 01	32.4	deg_C
ch: 02	26.0	deg_C
ch: 03	38.3	deg_C
ch: 04	42.6	deg_C
ch: 05	44.1	deg_C
ch: 06	42.2	deg_C
ch: 07	39.5	deg_C
ch: 08	34.9	deg_C
ch: 09	31.7	deg_C
ch: 10	21.9	deg_C

EXP 10--SCAN 08---24:01:15:08:20
"COOLING"

ch: 01	25.7	deg_C
ch: 02	26.4	deg_C
ch: 03	27.2	deg_C
ch: 04	28.3	deg_C
ch: 05	28.6	deg_C
ch: 06	28.1	deg_C
ch: 07	27.2	deg_C
ch: 08	25.9	deg_C
ch: 09	24.8	deg_C
ch: 10	22.3	deg_C

EXP 10--SCAN 05---24:01:13:38:20
"COOLING"

ch: 01	30.6	deg_C
ch: 02	32.4	deg_C
ch: 03	34.5	deg_C
ch: 04	37.4	deg_C
ch: 05	38.6	deg_C
ch: 06	37.9	deg_C
ch: 07	34.9	deg_C
ch: 08	31.5	deg_C
ch: 09	28.9	deg_C
ch: 10	22.3	deg_C

EXP 10--SCAN 09---24:01:15:38:20
"COOLING"

ch: 01	24.8	deg_C
ch: 02	25.3	deg_C
ch: 03	25.9	deg_C
ch: 04	26.6	deg_C
ch: 05	26.9	deg_C
ch: 06	26.5	deg_C
ch: 07	25.9	deg_C
ch: 08	24.9	deg_C
ch: 09	24.1	deg_C
ch: 10	22.2	deg_C

EXP 10--SCAN 06---24:01:14:08:20
"COOLING"

ch: 01	28.4	deg_C
ch: 02	29.8	deg_C
ch: 03	31.3	deg_C
ch: 04	33.4	deg_C
ch: 05	34.1	deg_C
ch: 06	33.1	deg_C
ch: 07	31.6	deg_C
ch: 08	29.1	deg_C
ch: 09	27.1	deg_C
ch: 10	21.9	deg_C

EXP 10--SCAN 10---24:01:16:08:20
"COOLING"

ch: 01	24.2	deg_C
ch: 02	24.5	deg_C
ch: 03	24.9	deg_C
ch: 04	25.5	deg_C
ch: 05	25.7	deg_C
ch: 06	25.3	deg_C
ch: 07	24.9	deg_C
ch: 08	24.2	deg_C
ch: 09	23.6	deg_C
ch: 10	21.9	deg_C

EXP 10--SCAN 07---24:01:14:38:20
"COOLING"

ch: 01	26.8	deg_C
ch: 02	27.8	deg_C
ch: 03	28.9	deg_C
ch: 04	30.4	deg_C
ch: 05	31.0	deg_C
ch: 06	30.2	deg_C
ch: 07	29.1	deg_C
ch: 08	27.2	deg_C
ch: 09	25.8	deg_C
ch: 10	22.0	deg_C

EXP 10--SCAN 11---24:01:16:38:20
"COOLING"

ch: 01	23.7	deg_C
ch: 02	24.0	deg_C
ch: 03	24.3	deg_C
ch: 04	24.6	deg_C
ch: 05	24.7	deg_C
ch: 06	24.5	deg_C
ch: 07	24.2	deg_C
ch: 08	23.6	deg_C
ch: 09	23.2	deg_C
ch: 10	21.9	deg_C

A10.3 Ageing Run 1

The results of this run were used to obtain the plot shown in figure 7.2. The experimental conditions and model parameters were:

Coal particle size range: -3.4 + 1.19 mm

C : 23

Bi_o : 3.7

Bi_1 : 9.3

Bed voidage: 0.38

K_o : 3.33 m/s

E/R : 7000 K

$D_e\rho_m$: 1.42×10^{-13}

D_p : 2.5 mm

O_2 flowrate: 1.14×10^{-4} kmol/m^2/s

Oven temperature : 135°C

EXP 10---------- 19:01:14:35:54

ch: 01	131.8	deg_C
ch: 02	130.8	deg_C
ch: 03	129.2	deg_C
ch: 04	126.9	deg_C
ch: 05	125.6	deg_C
ch: 06	125.6	deg_C
ch: 07	127.1	deg_C
ch: 08	128.9	deg_C
ch: 09	130.1	deg_C
ch: 10	129.5	deg_C

EXP 10--SCAN 01---19:01:14:43:05

ch: 01	132.0	deg_C
ch: 02	131.1	deg_C
ch: 03	129.5	deg_C
ch: 04	127.2	deg_C
ch: 05	126.0	deg_C
ch: 06	125.9	deg_C
ch: 07	127.4	deg_C
ch: 08	129.1	deg_C
ch: 09	130.2	deg_C
ch: 10	125.3	deg_C

EXP 10--SCAN 02---19:01:14:43:29

ch: 01	132.0	deg_C
ch: 02	131.1	deg_C
ch: 03	129.5	deg_C
ch: 04	127.3	deg_C
ch: 05	126.0	deg_C
ch: 06	125.9	deg_C
ch: 07	127.4	deg_C
ch: 08	129.1	deg_C
ch: 09	130.2	deg_C
ch: 10	127.2	deg_C

EXP 10--SCAN 03---19:01:15:43:05

ch: 01	139.1	deg_C
ch: 02	139.9	deg_C
ch: 03	138.4	deg_C
ch: 04	135.0	deg_C
ch: 05	132.5	deg_C
ch: 06	131.1	deg_C
ch: 07	131.7	deg_C
ch: 08	132.0	deg_C
ch: 09	132.0	deg_C
ch: 10	128.3	deg_C

EXP 10--SCAN 04---19:01:16:43:05

ch: 01	145.2	deg_C
ch: 02	147.9	deg_C
ch: 03	147.8	deg_C
ch: 04	144.1	deg_C
ch: 05	140.1	deg_C
ch: 06	137.1	deg_C
ch: 07	136.6	deg_C
ch: 08	135.3	deg_C
ch: 09	134.3	deg_C
ch: 10	128.2	deg_C

EXP 10--SCAN 05---19:01:17:43:05

ch: 01	147.7	deg_C
ch: 02	151.3	deg_C
ch: 03	152.3	deg_C
ch: 04	149.5	deg_C
ch: 05	145.1	deg_C
ch: 06	141.3	deg_C
ch: 07	140.0	deg_C
ch: 08	137.7	deg_C
ch: 09	136.0	deg_C
ch: 10	126.6	deg_C

EXP 10--SCAN 06---19:01:18:43:05

ch: 01	148.6	deg_C
ch: 02	152.5	deg_C
ch: 03	154.1	deg_C
ch: 04	152.3	deg_C
ch: 05	148.1	deg_C
ch: 06	143.9	deg_C
ch: 07	142.1	deg_C
ch: 08	139.1	deg_C
ch: 09	137.1	deg_C
ch: 10	127.4	deg_C

EXP 10--SCAN 07---19:01:19:43:05

ch: 01	148.8	deg_C
ch: 02	152.7	deg_C
ch: 03	154.8	deg_C
ch: 04	153.7	deg_C
ch: 05	149.8	deg_C
ch: 06	145.4	deg_C
ch: 07	143.3	deg_C
ch: 08	139.8	deg_C
ch: 09	137.6	deg_C
ch: 10	126.9	deg_C

EXP 10--SCAN 08---19:01:20:43:05

ch: 01	148.5	deg_C
ch: 02	152.5	deg_C
ch: 03	154.0	deg_C
ch: 04	154.3	deg_C
ch: 05	150.7	deg_C
ch: 06	146.3	deg_C
ch: 07	143.9	deg_C
ch: 08	140.2	deg_C
ch: 09	137.9	deg_C
ch: 10	126.2	deg_C

EXP 10--SCAN 09---19:01:21:43:05

ch: 01	148.3	deg_C
ch: 02	152.2	deg_C
ch: 03	154.4	deg_C
ch: 04	154.4	deg_C
ch: 05	151.1	deg_C
ch: 06	146.8	deg_C
ch: 07	144.2	deg_C
ch: 08	140.4	deg_C
ch: 09	138.0	deg_C
ch: 10	126.2	deg_C

EXP 10--SCAN 10---19:01:22:43:05

ch: 01	147.9	deg_C
ch: 02	151.7	deg_C
ch: 03	154.0	deg_C
ch: 04	154.3	deg_C
ch: 05	151.3	deg_C
ch: 06	147.0	deg_C
ch: 07	144.4	deg_C
ch: 08	140.5	deg_C
ch: 09	138.1	deg_C
ch: 10	127.0	deg_C

EXP 10--SCAN 11---19:01:23:43:05

ch: 01	147.5	deg_C
ch: 02	151.3	deg_C
ch: 03	153.6	deg_C
ch: 04	154.1	deg_C
ch: 05	151.3	deg_C
ch: 06	147.1	deg_C
ch: 07	144.5	deg_C
ch: 08	140.6	deg_C
ch: 09	138.2	deg_C
ch: 10	126.9	deg_C

EXP 10--SCAN 12---20:01:00:43:05

ch: 01	147.2	deg_C
ch: 02	150.8	deg_C
ch: 03	153.1	deg_C
ch: 04	153.7	deg_C
ch: 05	151.2	deg_C
ch: 06	147.2	deg_C
ch: 07	144.6	deg_C
ch: 08	140.6	deg_C
ch: 09	138.2	deg_C
ch: 10	127.8	deg_C

EXP 10--SCAN 13---20:01:01:43:05

ch: 01	146.8	deg_C
ch: 02	150.3	deg_C
ch: 03	152.6	deg_C
ch: 04	153.3	deg_C
ch: 05	151.0	deg_C
ch: 06	147.1	deg_C
ch: 07	144.6	deg_C
ch: 08	140.6	deg_C
ch: 09	138.1	deg_C
ch: 10	128.2	deg_C

EXP 10--SCAN 14---20:01:02:43:05

ch: 01	146.4	deg_C
ch: 02	149.9	deg_C
ch: 03	152.1	deg_C
ch: 04	152.9	deg_C
ch: 05	150.8	deg_C
ch: 06	147.0	deg_C
ch: 07	144.5	deg_C
ch: 08	140.5	deg_C
ch: 09	138.1	deg_C
ch: 10	129.0	deg_C

EXP 10--SCAN 15---20:01:03:43:05

ch: 01	146.1	deg_C
ch: 02	149.4	deg_C
ch: 03	151.6	deg_C
ch: 04	152.5	deg_C
ch: 05	150.6	deg_C
ch: 06	146.9	deg_C
ch: 07	144.4	deg_C
ch: 08	140.5	deg_C
ch: 09	138.1	deg_C
ch: 10	127.4	deg_C

EXP 10--SCAN 16---20:01:04:43:05

ch: 01	145.8	deg_C
ch: 02	149.0	deg_C
ch: 03	151.1	deg_C
ch: 04	152.2	deg_C
ch: 05	150.3	deg_C
ch: 06	146.8	deg_C
ch: 07	144.4	deg_C
ch: 08	140.4	deg_C
ch: 09	138.0	deg_C
ch: 10	125.4	deg_C

EXP 10--SCAN 17---20:01:05:43:05

ch: 01	145.5	deg_C
ch: 02	149.7	deg_C
ch: 03	150.8	deg_C
ch: 04	151.9	deg_C
ch: 05	150.1	deg_C
ch: 06	146.6	deg_C
ch: 07	144.3	deg_C
ch: 08	140.4	deg_C
ch: 09	138.0	deg_C
ch: 10	127.1	deg_C

EXP 10--SCAN 18---20:01:06:43:05

ch: 01	145.3	deg_C
ch: 02	148.4	deg_C
ch: 03	150.4	deg_C
ch: 04	151.5	deg_C
ch: 05	149.9	deg_C
ch: 06	146.5	deg_C
ch: 07	144.2	deg_C
ch: 08	140.3	deg_C
ch: 09	138.0	deg_C
ch: 10	125.9	deg_C

EXP 10--SCAN 19---20:01:07:43:05

ch: 01	145.1	deg_C
ch: 02	148.1	deg_C
ch: 03	150.1	deg_C
ch: 04	151.1	deg_C
ch: 05	149.7	deg_C
ch: 06	146.4	deg_C
ch: 07	144.2	deg_C
ch: 08	140.3	deg_C
ch: 09	137.9	deg_C
ch: 10	125.1	deg_C

A10.4 Ageing Run 2

The results of this run were used to obtain the plot shown in figure 7.3. The experimental conditions and model parameters used to obtain figure 7.3 were:

Coal particle size range : -3.4 + 1.19 mm
C : 23
Bi_0 : 3.7
Bi_1 : 9.3
Bed voidage: 0.38
K_o : 3.33 m/s
E/R : 7000 K
$D_e\rho_m$: 1.42×10^{-13}
D_p : 2.5 mm
O_2 flowrate: 1.14×10^{-4} kmol/m^2/s
Oven temperature : 88°C

ch: 01	83.7	deg_C
ch: 02	83.9	deg_C
ch: 03	83.2	deg_C
ch: 04	83.2	deg_C
ch: 05	82.5	deg_C
ch: 06	82.0	deg_C
ch: 07	82.0	deg_C
ch: 08	82.4	deg_C
ch: 09	82.3	deg_C
ch: 10	88.7	deg_C

EXP 10--SCAN 01---09:02:09:06 19

ch: 01	83.7	deg_C
ch: 02	83.9	deg_C
ch: 03	83.2	deg_C
ch: 04	83.2	deg_C
ch: 05	82.5	deg_C
ch: 06	82.0	deg_C
ch: 07	82.0	deg_C
ch: 08	82.4	deg_C
ch: 09	82.3	deg_C
ch: 10	90.2	deg_C

EXP 10--SCAN 02---09:02:08:21 19

ch: 01	86.7	deg_C
ch: 02	87.7	deg_C
ch: 03	86.9	deg_C
ch: 04	85.3	deg_C
ch: 05	85.9	deg_C
ch: 06	85.0	deg_C
ch: 07	84.3	deg_C
ch: 08	85.2	deg_C
ch: 09	84.5	deg_C
ch: 10	89.2	deg_C

EXP 10--SCAN 03---09:02:08:36 19

ch: 01	87.9	deg_C
ch: 02	89.9	deg_C
ch: 03	89.4	deg_C
ch: 04	89.3	deg_C
ch: 05	88.4	deg_C
ch: 06	87.2	deg_C
ch: 07	86.8	deg_C
ch: 08	87.1	deg_C
ch: 09	85.8	deg_C
ch: 10	89.1	deg_C

EXP 10--SCAN 04---09:02:09:51 19

ch: 01	88.7	deg_C
ch: 02	91.3	deg_C
ch: 03	91.2	deg_C
ch: 04	91.3	deg_C
ch: 05	90.3	deg_C
ch: 06	89.0	deg_C
ch: 07	88.4	deg_C
ch: 08	88.4	deg_C
ch: 09	86.8	deg_C
ch: 10	86.4	deg_C

EXP 10--SCAN 05---09:02:09:06 19

ch: 01	89.3	deg_C
ch: 02	92.3	deg_C
ch: 03	92.6	deg_C
ch: 04	93.0	deg_C
ch: 05	92.0	deg_C
ch: 06	90.5	deg_C
ch: 07	89.6	deg_C
ch: 08	89.5	deg_C
ch: 09	87.6	deg_C
ch: 10	87.9	deg_C

EXP 10--SCAN 06---09:02:09:21 19

ch: 01	89.7	deg_C
ch: 02	93.1	deg_C
ch: 03	93.7	deg_C
ch: 04	94.4	deg_C
ch: 05	93.5	deg_C
ch: 06	91.9	deg_C
ch: 07	90.7	deg_C
ch: 08	90.4	deg_C
ch: 09	88.2	deg_C
ch: 10	88.6	deg_C

EXP 10--SCAN 07---09:02:09:36 19

ch: 01	90.1	deg_C
ch: 02	93.6	deg_C
ch: 03	94.5	deg_C
ch: 04	96.6	deg_C
ch: 05	94.7	deg_C
ch: 06	93.0	deg_C
ch: 07	91.5	deg_C
ch: 08	90.2	deg_C
ch: 09	88.1	deg_C
ch: 10	89.2	deg_C

EXP 10--SCAN 09---09:02:09:51:19

ch: 01	90.4	deg_C
ch: 02	94.1	deg_C
ch: 03	95.2	deg_C
ch: 04	96.6	deg_C
ch: 05	95.0	deg_C
ch: 06	94.0	deg_C
ch: 07	92.3	deg_C
ch: 08	91.0	deg_C
ch: 09	89.3	deg_C
ch: 10	90.4	deg_C

EXP 10--SCAN 09---09:02:10:06:19

ch: 01	90.6	deg_C
ch: 02	94.4	deg_C
ch: 03	95.7	deg_C
ch: 04	97.4	deg_C
ch: 05	96.9	deg_C
ch: 06	94.9	deg_C
ch: 07	93.0	deg_C
ch: 08	92.4	deg_C
ch: 09	89.7	deg_C
ch: 10	90.0	deg_C

EXP 10--SCAN 10---09:02:10:21:19

ch: 01	90.7	deg_C
ch: 02	94.6	deg_C
ch: 03	96.1	deg_C
ch: 04	98.1	deg_C
ch: 05	97.7	deg_C
ch: 06	95.7	deg_C
ch: 07	93.6	deg_C
ch: 08	92.9	deg_C
ch: 09	90.1	deg_C
ch 10	88.8	deg_C

EXP 10--SCAN 11---09:02:10:36:19

ch: 01	90.9	deg_C
ch: 02	94.8	deg_C
ch: 03	96.4	deg_C
ch: 04	99.6	deg_C
ch: 05	98.4	deg_C
ch: 06	96.4	deg_C
ch: 07	94.1	deg_C
ch: 08	93.3	deg_C
ch: 09	90.3	deg_C
ch: 10	88.6	deg_C

EXP 10--SCAN 12---09:02:10:51:19

ch: 01	91.0	deg_C
ch: 02	94.9	deg_C
ch: 03	96.6	deg_C
ch: 04	99.0	deg_C
ch: 05	98.9	deg_C
ch: 06	96.9	deg_C
ch: 07	94.5	deg_C
ch: 08	93.6	deg_C
ch: 09	90.6	deg_C
ch: 10	89.4	deg_C

EXP 10--SCAN 13---09:02:11:06:19

ch: 01	91.0	deg_C
ch: 02	94.9	deg_C
ch: 03	96.8	deg_C
ch: 04	99.2	deg_C
ch: 05	99.3	deg_C
ch: 06	97.4	deg_C
ch: 07	94.8	deg_C
ch 08	93.9	deg_C

EXP 10--SCAN 14---09:02:11:21:19

ch: 01	91.0	deg_C
ch: 02	94.9	deg_C
ch: 03	96.8	deg_C
ch: 04	99.4	deg_C
ch: 05	99.5	deg_C
ch: 06	97.7	deg_C
ch: 07	95.1	deg_C
ch: 08	94.1	deg_C
ch: 09	90.9	deg_C
ch: 10	90.1	deg_C

EXP 10--SCAN 15---09:02:11:36:19

ch: 01	91.0	deg_C
ch: 02	94.9	deg_C
ch: 03	96.8	deg_C
ch: 04	99.5	deg_C
ch: 05	99.7	deg_C
ch: 06	97.9	deg_C
ch: 07	95.3	deg_C
ch: 08	94.3	deg_C
ch: 09	91.0	deg_C
ch 10	90.1	deg_C

EXP 10--SCAN 16---09:02:11:51:19

ch: 01	91.0	deg_C
ch: 02	94.8	deg_C
ch: 03	96.8	deg_C
ch: 04	99.5	deg_C
ch: 05	99.8	deg_C
ch: 06	98.0	deg_C
ch: 07	95.4	deg_C
ch: 08	94.2	deg_C
ch: 09	91.1	deg_C
ch 10	90.6	deg_C

EXP 10--SCAN 17---09:02:12:06:19

ch: 01	90.9	deg_C
ch: 02	94.7	deg_C
ch: 03	96.7	deg_C
ch: 04	99.4	deg_C
ch: 05	99.9	deg_C
ch: 06	98.1	deg_C
ch: 07	95.4	deg_C
ch 08	94.4	deg_C
ch: 09	91.1	deg_C
ch: 10	87.3	deg_C

EXP 10--SCAN 18---09:02:12:21:19

ch: 01	90.8	deg_C
ch: 02	94.6	deg_C
ch: 03	96.5	deg_C
ch: 04	99.3	deg_C
ch: 05	99.7	deg_C
ch: 06	98.1	deg_C
ch: 07	95.4	deg_C
ch: 08	94.4	deg_C
ch: 09	91.1	deg_C
ch: 10	89.0	deg_C

EXP 10--SCAN 19---09:02:12:36:19

ch: 01	90.8	deg_C
ch: 02	94.5	deg_C
ch: 03	96.4	deg_C
ch: 04	99.1	deg_C
ch: 05	99.5	deg_C
ch: 06	98.0	deg_C
ch: 07	95.3	deg_C
ch: 08	94.3	deg_C
ch: 09	91.0	deg_C
ch: 10	89.5	deg_C

EXP 10--SCAN 20---09:02:12:51:19

ch: 01	90.7	deg_C
ch: 02	94.3	deg_C
ch: 03	96.2	deg_C
ch: 04	98.9	deg_C
ch: 05	99.3	deg_C
ch: 06	97.8	deg_C
ch: 07	95.2	deg_C
ch: 08	94.2	deg_C
ch: 09	91.0	deg_C
ch: 10	90.6	deg_C

EXP 10--SCAN 21---09:02:13:06:19

ch: 01	90.6	deg_C
ch: 02	94.2	deg_C
ch: 03	96.0	deg_C
ch: 04	98.7	deg_C
ch: 05	99.1	deg_C
ch: 06	97.6	deg_C
ch: 07	95.0	deg_C
ch: 08	94.1	deg_C
ch: 09	90.9	deg_C
ch: 10	88.2	deg_C

EXP 10--SCAN 22---09:02:13:21:19

ch: 01	90.5	deg_C
ch: 02	94.0	deg_C
ch: 03	95.8	deg_C
ch: 04	98.4	deg_C
ch: 05	98.8	deg_C
ch: 06	97.4	deg_C
ch: 07	94.9	deg_C
ch: 08	93.9	deg_C
ch: 09	90.7	deg_C
ch: 10	87.4	deg_C

EXP 10--SCAN 23---09:02:13:36:19

ch: 01	90.4	deg_C
ch: 02	93.8	deg_C
ch: 03	95.5	deg_C
ch: 04	98.1	deg_C
ch: 05	98.5	deg_C
ch: 06	97.1	deg_C
ch: 07	94.6	deg_C
ch: 08	93.7	deg_C
ch: 09	90.6	deg_C
ch: 10	89.1	deg_C

EXP 10--SCAN 24---09:02:13:51:19

ch: 01	90.3	deg_C
ch: 02	93.6	deg_C
ch: 03	95.3	deg_C
ch: 04	97.8	deg_C
ch: 05	98.2	deg_C
ch: 06	96.9	deg_C
ch: 07	94.4	deg_C
ch: 08	93.5	deg_C
ch: 09	90.4	deg_C
ch: 10	89.8	deg_C

EXP 10--SCAN 01---09:02:14:07:24

ch: 01	90.2	deg_C
ch: 02	93.4	deg_C
ch: 03	95.0	deg_C
ch: 04	97.5	deg_C
ch: 05	98.0	deg_C
ch: 06	96.6	deg_C
ch: 07	94.1	deg_C
ch: 08	93.2	deg_C
ch: 09	90.2	deg_C
ch: 10	90.3	deg_C

EXP 10--SCAN 02---09:02:14:07:46

ch: 01	90.2	deg_C
ch: 02	93.4	deg_C
ch: 03	95.0	deg_C
ch: 04	97.5	deg_C
ch: 05	97.8	deg_C
ch: 06	96.5	deg_C
ch: 07	94.1	deg_C
ch: 08	93.2	deg_C
ch: 09	90.3	deg_C
ch: 10	88.5	deg_C

EXP 10--SCAN 03---09:02:15:07:24

ch: 01	89.7	deg_C
ch: 02	92.7	deg_C
ch: 03	94.0	deg_C
ch: 04	96.2	deg_C
ch: 05	96.5	deg_C
ch: 06	95.2	deg_C
ch: 07	93.1	deg_C
ch: 08	92.3	deg_C
ch: 09	89.6	deg_C
ch: 10	88.0	deg_C

EXP 10--SCAN 04---09:02:16:07:24

ch: 01	89.2	deg_C
ch: 02	92.0	deg_C
ch: 03	93.1	deg_C
ch: 04	95.0	deg_C
ch: 05	95.1	deg_C
ch: 06	93.9	deg_C
ch: 07	92.0	deg_C
ch: 08	91.4	deg_C
ch: 09	88.9	deg_C
ch: 10	87.7	deg_C

EXP 10--SCAN 05---09:02:17:07:24

ch: 01	88.8	deg_C
ch: 02	91.3	deg_C
ch: 03	92.2	deg_C
ch: 04	93.9	deg_C
ch: 05	93.9	deg_C
ch: 06	92.8	deg_C
ch: 07	91.1	deg_C
ch: 08	90.6	deg_C
ch: 09	88.4	deg_C
ch: 10	89.9	deg_C

EXP 10--SCAN 06---09:02:18:07:24

ch: 01	88.4	deg_C
ch: 02	90.9	deg_C
ch: 03	91.5	deg_C
ch: 04	93.0	deg_C
ch: 05	92.9	deg_C
ch: 06	91.9	deg_C
ch: 07	90.4	deg_C
ch: 08	90.0	deg_C
ch: 09	87.9	deg_C
ch: 10	90.4	deg_C

EXP 10--SCAN 07---09:02:19:07:24

ch: 01	88.1	deg_C
ch: 02	90.2	deg_C
ch: 03	90.9	deg_C
ch: 04	92.2	deg_C
ch: 05	92.1	deg_C
ch: 06	91.1	deg_C
ch: 07	89.8	deg_C
ch: 08	89.4	deg_C
ch: 09	87.5	deg_C
ch: 10	89.1	deg_C

EXP 10--SCAN 08---09:02:20:07:24

ch: 01	87.2	deg_C
ch: 02	89.9	deg_C
ch: 03	90.4	deg_C
ch: 04	91.5	deg_C
ch: 05	91.4	deg_C
ch: 06	90.5	deg_C
ch: 07	89.2	deg_C
ch: 08	88.9	deg_C
ch: 09	87.2	deg_C
ch: 10	87.5	deg_C

EXP 10--SCAN 09---09:02:21:07:24

ch: 01	87.6	deg_C
ch: 02	89.5	deg_C
ch: 03	89.9	deg_C
ch: 04	91.1	deg_C
ch: 05	89.9	deg_C
ch: 06	89.9	deg_C
ch: 07	88.8	deg_C
ch: 08	88.6	deg_C
ch: 09	85.9	deg_C
ch: 10	86.6	deg_C

EXP 10--SCAN 10---09:02:22:07:24

ch: 01	87.4	deg_C
ch: 02	89.2	deg_C
ch: 03	89.5	deg_C
ch: 04	90.6	deg_C
ch: 05	90.4	deg_C
ch: 06	89.5	deg_C
ch: 07	88.5	deg_C
ch: 08	88.3	deg_C
ch: 09	86.7	deg_C
ch: 10	90.0	deg_C

EXP 10--SCAN 11---09:02:27:07:24

ch: 01	87.2	deg_C
ch: 02	89.0	deg_C
ch: 03	89.2	deg_C
ch: 04	90.3	deg_C
ch: 05	90.0	deg_C
ch: 06	89.2	deg_C
ch: 07	88.2	deg_C
ch: 08	88.1	deg_C
ch: 09	86.5	deg_C
ch: 10	88.2	deg_C

EXP 10--SCAN 12---10:02:00:07:24

ch: 01	87.1	deg_C
ch: 02	88.8	deg_C
ch: 03	89.0	deg_C
ch: 04	90.0	deg_C
ch: 05	89.7	deg_C
ch: 06	88.9	deg_C
ch: 07	88.0	deg_C
ch: 08	87.9	deg_C
ch: 09	86.4	deg_C
ch: 10	88.9	deg_C

EXP 10--SCAN 13---10:02:01:07:24

ch: 01	87.0	deg_C
ch: 02	88.6	deg_C
ch: 03	88.9	deg_C
ch: 04	89.8	deg_C
ch: 05	89.5	deg_C
ch: 06	88.7	deg_C
ch: 07	87.9	deg_C
ch: 08	87.7	deg_C
ch: 09	86.3	deg_C
ch: 10	88.9	deg_C

EXP 10--SCAN 14---10:02:02:07:24

ch: 01	86.9	deg_C
ch: 02	88.4	deg_C
ch: 03	89.6	deg_C
ch: 04	89.5	deg_C
ch: 05	89.2	deg_C
ch: 06	88.5	deg_C
ch: 07	87.7	deg_C
ch: 08	87.6	deg_C
ch: 09	86.2	deg_C
ch: 10	90.5	deg_C

EXP 10--SCAN 15---10:02:03:07:24

ch: 01	86.8	deg_C
ch: 02	88.3	deg_C
ch: 03	89.5	deg_C
ch: 04	89.4	deg_C
ch: 05	89.1	deg_C
ch: 06	88.3	deg_C
ch: 07	87.5	deg_C
ch: 08	87.4	deg_C
ch: 09	86.1	deg_C
ch: 10	87.1	deg_C

EXP 10--SCAN 16---10:02:04:07:24

ch: 01	86.7	deg_C
ch: 02	88.2	deg_C
ch: 03	88.3	deg_C
ch: 04	89.2	deg_C
ch: 05	88.9	deg_C
ch: 06	88.1	deg_C
ch: 07	87.4	deg_C
ch: 08	87.3	deg_C
ch: 09	86.9	deg_C
ch: 10	89.7	deg_C

EXP 10--SCAN 17---10:02:05:07:24

ch: 01	86.6	deg_C
ch: 02	88.1	deg_C
ch: 03	88.2	deg_C
ch: 04	88.1	deg_C
ch: 05	88.0	deg_C
ch: 06	87.3	deg_C
ch: 07	87.2	deg_C
ch: 08	86.9	deg_C
ch: 09	86.4	deg_C
ch: 10		

EXP 10--SCAN 18---10:02:06:07:24

ch: 01	86.6	deg_C
ch: 02	88.0	deg_C
ch: 03	88.1	deg_C
ch: 04	89.0	deg_C
ch: 05	88.6	deg_C
ch: 06	87.9	deg_C
ch: 07	87.2	deg_C
ch: 08	87.2	deg_C
ch: 09	85.9	deg_C
ch: 10	88.3	deg_C

EXP 10--SCAN 19---10:02:07:07:24

ch: 01	86.5	deg_C
ch: 02	87.9	deg_C
ch: 03	89.0	deg_C
ch: 04	88.8	deg_C
ch: 05	88.5	deg_C
ch: 06	87.8	deg_C
ch: 07	87.1	deg_C
ch: 08	87.1	deg_C
ch: 09	85.8	deg_C
ch: 10	90.9	deg_C

EXP 10--SCAN 20---10:02:08:07:24

ch: 01	86.5	deg_C
ch: 02	87.9	deg_C
ch: 03	87.9	deg_C
ch: 04	88.7	deg_C
ch: 05	88.4	deg_C
ch: 06	87.7	deg_C
ch: 07	87.0	deg_C
ch: 08	87.0	deg_C
ch: 09	85.7	deg_C
ch: 10	88.7	deg_C

EXP 10--SCAN 21---10:02:09:07:24

ch: 01	86.4	deg_C
ch: 02	87.8	deg_C
ch: 03	87.9	deg_C
ch: 04	88.7	deg_C
ch: 05	88.3	deg_C
ch: 06	87.5	deg_C
ch: 07	87.0	deg_C
ch: 08	87.0	deg_C
ch: 09	85.7	deg_C
ch: 10	90.3	deg_C

EXP 10--SCAN 22---10:02:10:07:24

ch: 01	86.4	deg_C
ch: 02	87.8	deg_C
ch: 03	87.8	deg_C
ch: 04	88.6	deg_C
ch: 05	88.7	deg_C
ch: 06	87.5	deg_C
ch: 07	86.9	deg_C
ch: 08	86.9	deg_C
ch: 09	85.7	deg_C
ch: 10	87.7	deg_C

EXP 10--SCAN 23---10:02:11:07:24

ch: 01	86.4	deg_C
ch: 02	87.9	deg_C
ch: 03	87.9	deg_C
ch: 04	88.6	deg_C
ch: 05	88.7	deg_C
ch: 06	87.6	deg_C
ch: 07	86.9	deg_C
ch: 08	86.9	deg_C
ch: 09	85.7	deg_C
ch: 10	90.5	deg_C

EXP 10--SCAN 24---10:02:12:07:24

ch: 01	86.4	deg_C
ch: 02	87.8	deg_C
ch: 03	87.8	deg_C
ch: 04	88.6	deg_C
ch: 05	88.2	deg_C
ch: 06	87.6	deg_C
ch: 07	87.0	deg_C
ch: 08	87.0	deg_C
ch: 09	85.9	deg_C
ch: 10	87.6	deg_C

EXP 10--SCAN 25---10:02:13:07:24

ch: 01	86.5	deg_C
ch: 02	87.9	deg_C
ch: 03	87.8	deg_C
ch: 04	88.6	deg_C
ch: 05	88.2	deg_C
ch: 06	87.6	deg_C
ch: 07	86.9	deg_C
ch: 08	87.0	deg_C
ch: 09	85.8	deg_C
ch: 10	90.4	deg_C

A10.5 Ageing run 3

The results of this run have not been analyzed. The run conditions were as follows:

Coal particle size range	: - 3.4 + 1.19 mm
Oven temperature	: 180°C
Oxygen flowrate	: 1.42 x 10^{-5} kmol/m^2/s

EXP 10----------20:01 13:53:45

ch: 01	178.4	deg_C
ch: 02	178.2	deg_C
ch: 03	177.1	deg_C
ch: 04	175.5	deg_C
ch: 05	174.2	deg_C
ch: 06	173.5	deg_C
ch: 07	174.7	deg_C
ch: 08	175.2	deg_C
ch: 09	175.2	deg_C
ch: 10	174.8	deg_C

EXP 10--SCAN 01---20:01 13:55:24

ch: 01	178.5	deg_C
ch: 02	178.2	deg_C
ch: 03	177.2	deg_C
ch: 04	175.5	deg_C
ch: 05	174.3	deg_C
ch: 06	173.5	deg_C
ch: 07	174.8	deg_C
ch: 08	175.2	deg_C
ch: 09	175.2	deg_C
ch: 10	175.3	deg_C

EXP 10--SCAN 02---20:01 13:55:58

ch: 01	178.5	deg_C
ch: 02	178.2	deg_C
ch: 03	177.2	deg_C
ch: 04	175.5	deg_C
ch: 05	174.3	deg_C
ch: 06	173.5	deg_C
ch: 07	174.8	deg_C
ch: 08	175.2	deg_C
ch: 09	175.2	deg_C
ch: 10	174.6	deg_C

EXP 10--SCAN 03---20:01 14:10:34

ch: 01	179.3	deg_C
ch: 02	179.1	deg_C
ch: 03	178.0	deg_C
ch: 04	176.1	deg_C
ch: 05	174.9	deg_C
ch: 06	174.0	deg_C
ch: 07	175.3	deg_C
ch: 08	175.7	deg_C
ch: 09	175.4	deg_C
ch: 10	174.2	deg_C

EXP 10--SCAN 04---20:01 14:25:34

ch: 01	185.1	deg_C
ch: 02	185.6	deg_C
ch: 03	183.5	deg_C
ch: 04	179.8	deg_C
ch: 05	177.2	deg_C
ch: 06	175.6	deg_C
ch: 07	176.4	deg_C
ch: 08	176.4	deg_C
ch: 09	175.8	deg_C
ch: 10	174.5	deg_C

EXP 10--SCAN 05---20:01 14:40 34

ch: 01	190.9	deg_C
ch: 02	193.0	deg_C
ch: 03	190.4	deg_C
ch: 04	184.5	deg_C
ch: 05	180.3	deg_C
ch: 06	177.6	deg_C
ch: 07	178.0	deg_C
ch: 08	177.4	deg_C
ch: 09	176.4	deg_C
ch: 10	174.7	deg_C

EXP 10--SCAN 06---20:01 14 55 34

ch: 01	195.8	deg_C
ch: 02	198.4	deg_C
ch: 03	196.7	deg_C
ch: 04	188.8	deg_C
ch: 05	183.2	deg_C
ch: 06	179.6	deg_C
ch: 07	179.5	deg_C
ch: 08	178.4	deg_C
ch: 09	176.9	deg_C
ch: 10	173.1	deg_C

EXP 10--SCAN 07---20:01 15:10 34

ch: 01	199.6	deg_C
ch: 02	204.5	deg_C
ch: 03	202.0	deg_C
ch: 04	192.5	deg_C
ch: 05	185.6	deg_C
ch: 06	181.2	deg_C
ch: 07	180.7	deg_C
ch: 08	179.1	deg_C
ch: 09	177.4	deg_C
ch: 10	174.1	deg_C

EXP 10--SCAN 00---20:01:15:25:34

ch: 01	202.7	deg_C
ch: 02	208.7	deg_C
ch: 03	206.5	deg_C
ch: 04	195.6	deg_C
ch: 05	187.5	deg_C
ch: 06	182.6	deg_C
ch: 07	181.7	deg_C
ch: 08	179.7	deg_C
ch: 09	177.8	deg_C
ch: 10	173.8	deg_C

EXP 10--SCAN 09---20:01:15:40:3

ch: 01	205.2	deg_C
ch: 02	212.1	deg_C
ch: 03	210.1	deg_C
ch: 04	198.2	deg_C
ch: 05	189.1	deg_C
ch: 06	183.7	deg_C
ch: 07	182.5	deg_C
ch: 08	180.2	deg_C
ch: 09	178.2	deg_C
ch: 10	173.5	deg_C

EXP 10--SCAN 10---20:01:15:55:3

ch: 01	207.2	deg_C
ch: 02	214.7	deg_C
ch: 03	213.0	deg_C
ch: 04	200.4	deg_C
ch: 05	190.4	deg_C
ch: 06	184.5	deg_C
ch: 07	183.1	deg_C
ch: 08	180.6	deg_C
ch: 09	178.5	deg_C
ch: 10	172.9	deg_C

EXP 10--SCAN 01---20:01:16:10:0

ch: 01	208.7	deg_C
ch: 02	216.8	deg_C
ch: 03	215.4	deg_C
ch: 04	202.2	deg_C
ch: 05	191.4	deg_C
ch: 06	185.1	deg_C
ch: 07	183.5	deg_C
ch: 08	180.8	deg_C
ch: 09	178.6	deg_C
ch: 10	173.6	deg_C

EXP 10--SCAN 02---20:01:17:10:02

ch: 01	212.1	deg_C
ch: 02	221.5	deg_C
ch: 03	221.3	deg_C
ch: 04	207.2	deg_C
ch: 05	194.3	deg_C
ch: 06	186.5	deg_C
ch: 07	184.0	deg_C
ch: 08	180.9	deg_C
ch: 09	178.8	deg_C
ch: 10	173.9	deg_C

EXP 10--SCAN 03---20:01:18:10:02

ch: 01	212.9	deg_C
ch: 02	222.8	deg_C
ch: 03	223.6	deg_C
ch: 04	210.0	deg_C
ch: 05	196.0	deg_C
ch: 06	187.2	deg_C
ch: 07	184.0	deg_C
ch: 08	180.8	deg_C
ch: 09	178.7	deg_C
ch: 10	174.8	deg_C

EXP 10--SCAN 04---20:01:19:10:02

ch: 01	212.5	deg_C
ch: 02	222.6	deg_C
ch: 03	224.3	deg_C
ch: 04	211.7	deg_C
ch: 05	197.3	deg_C
ch: 06	187.8	deg_C
ch: 07	184.3	deg_C
ch: 08	180.8	deg_C
ch: 09	178.7	deg_C
ch: 10	175.2	deg_C

EXP 10--SCAN 05---20:01:20:10:02

ch: 01	211.7	deg_C
ch: 02	221.7	deg_C
ch: 03	224.2	deg_C
ch: 04	212.9	deg_C
ch: 05	198.4	deg_C
ch: 06	188.5	deg_C
ch: 07	184.6	deg_C
ch: 08	181.0	deg_C
ch: 09	178.8	deg_C
ch: 10	173.8	deg_C

EXP 10--SCAN 06---20:01:21:10:02

ch: 01	210.7	deg_C
ch: 02	220.6	deg_C
ch: 03	223.6	deg_C
ch: 04	213.5	deg_C
ch: 05	199.3	deg_C
ch: 06	189.2	deg_C
ch: 07	185.1	deg_C
ch: 08	181.2	deg_C
ch: 09	179.0	deg_C
ch: 10	173.4	deg_C

EXP 10--SCAN 07---20:01:22:10:02

ch: 01	209.7	deg_C
ch: 02	219.4	deg_C
ch: 03	222.9	deg_C
ch: 04	214.0	deg_C
ch: 05	200.3	deg_C
ch: 06	189.9	deg_C
ch: 07	185.6	deg_C
ch: 08	181.5	deg_C
ch: 09	179.2	deg_C
ch: 10	173.7	deg_C

EXP 10--SCAN 08---20:01:23:10:02

ch: 01	208.7	deg_C
ch: 02	218.2	deg_C
ch: 03	222.2	deg_C
ch: 04	214.4	deg_C
ch: 05	201.1	deg_C
ch: 06	190.6	deg_C
ch: 07	186.1	deg_C
ch: 08	181.8	deg_C
ch: 09	179.4	deg_C
ch: 10	175.6	deg_C

EXP 10--SCAN 09---21:01:00:10:02

ch: 01	207.9	deg_C
ch: 02	217.1	deg_C
ch: 03	221.3	deg_C
ch: 04	214.7	deg_C
ch: 05	201.9	deg_C
ch: 06	191.3	deg_C
ch: 07	186.6	deg_C
ch: 08	182.1	deg_C
ch: 09	179.6	deg_C
ch: 10	174.5	deg_C

EXP 10--SCAN 10---21:01:01:10:02

ch: 01	206.9	deg_C
ch: 02	216.9	deg_C
ch: 03	220.4	deg_C
ch: 04	214.8	deg_C
ch: 05	202.6	deg_C
ch: 06	191.9	deg_C
ch: 07	187.1	deg_C
ch: 08	182.4	deg_C
ch: 09	179.7	deg_C
ch: 10	174.8	deg_C

EXP 10--SCAN 11---21:01:02:10:02

ch: 01	206.1	deg_C
ch: 02	215.0	deg_C
ch: 03	219.6	deg_C
ch: 04	214.9	deg_C
ch: 05	203.2	deg_C
ch: 06	192.5	deg_C
ch: 07	187.5	deg_C
ch: 08	182.7	deg_C
ch: 09	179.9	deg_C
ch: 10	174.8	deg_C

EXP 10--SCAN 12---21:01:03:10:02

ch: 01	205.2	deg_C
ch: 02	214.0	deg_C
ch: 03	218.?	deg_C
ch: 04	214.8	deg_C
ch: 05	203.7	deg_C
ch: 06	193.1	deg_C
ch: 07	188.0	deg_C
ch: 08	182.9	deg_C
ch: 09	180.0	deg_C
ch: 10	174.2	deg_C

EXP 10--SCAN 13---21:01:04:10:02

ch: 01	204.4	deg_C
ch: 02	213.0	deg_C
ch: 03	217.8	deg_C
ch: 04	214.?	deg_C
ch: 05	204.2	deg_C
ch: 06	193.5	deg_C
ch: 07	188.4	deg_C
ch: 08	183.1	deg_C
ch: 09	180.1	deg_C
ch: 10	173.6	deg_C

EXP 10--SCAN 14---21:01:05:10:02

ch: 01	203.7	deg_C
ch: 02	212.1	deg_C
ch: 03	217.0	deg_C
ch: 04	214.5	deg_C
ch: 05	204.7	deg_C
ch: 06	194.2	deg_C
ch: 07	188.8	deg_C
ch: 08	183.4	deg_C
ch: 09	180.3	deg_C
ch: 10	174.7	deg_C

EXP 10--SCAN 15---21:01:06:10:02

ch: 01	203.1	deg_C
ch: 02	211.2	deg_C
ch: 03	216.1	deg_C
ch: 04	214.4	deg_C
ch: 05	205.1	deg_C
ch: 06	194.7	deg_C
ch: 07	189.3	deg_C
ch: 08	183.6	deg_C
ch: 09	180.5	deg_C
ch: 10	174.4	deg_C

EXP 10--SCAN 16---21:01:07:10:02

ch: 01	202.4	deg_C
ch: 02	210.4	deg_C
ch: 03	215.4	deg_C
ch: 04	214.1	deg_C
ch: 05	205.4	deg_C
ch: 06	195.2	deg_C
ch: 07	189.7	deg_C
ch: 08	183.9	deg_C
ch: 09	180.6	deg_C
ch: 10	174.4	deg_C

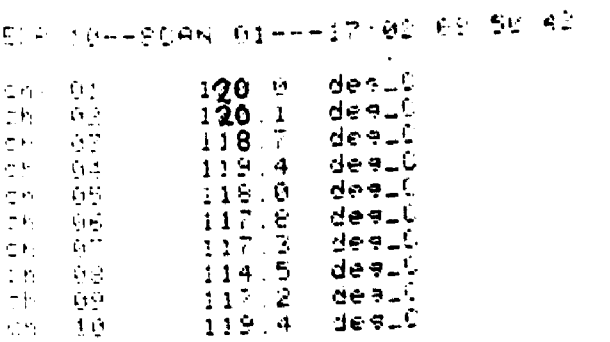
EXP 10--SCAN 17---21:01:08:10:02

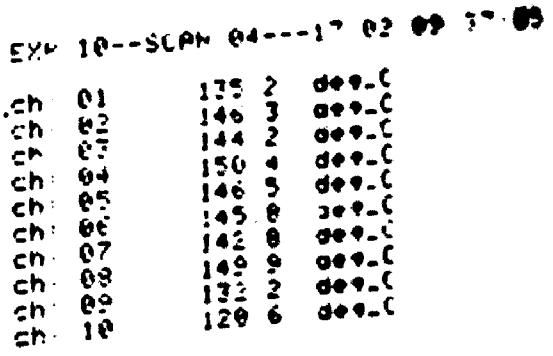
ch: 01	201.9	deg_C
ch: 02	209.7	deg_C
ch: 03	214.6	deg_C
ch: 04	213.9	deg_C
ch: 05	205.7	deg_C
ch: 06	195.6	deg_C
ch: 07	190.1	deg_C
ch: 08	184.1	deg_C
ch: 09	180.8	deg_C
ch: 10	175.2	deg_C

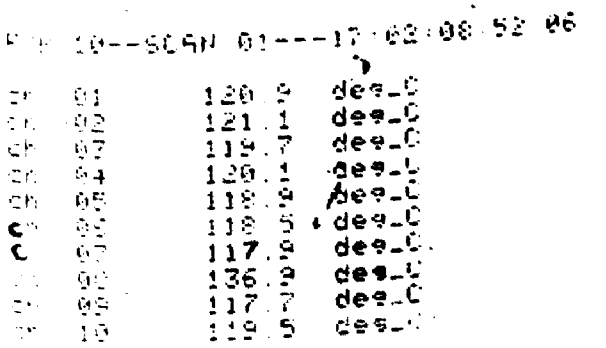
A10.6 Ignition run 1

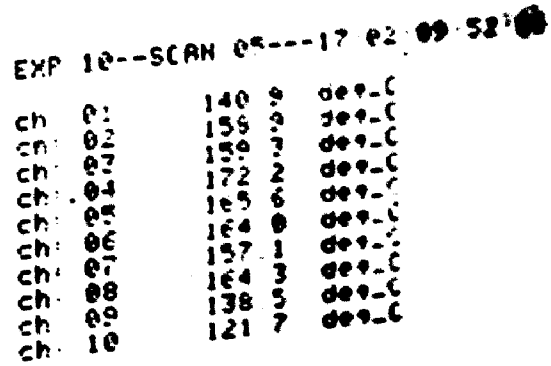
The results from this run were used in figure 7.4. The experimental conditions and model parameters used were as follows:

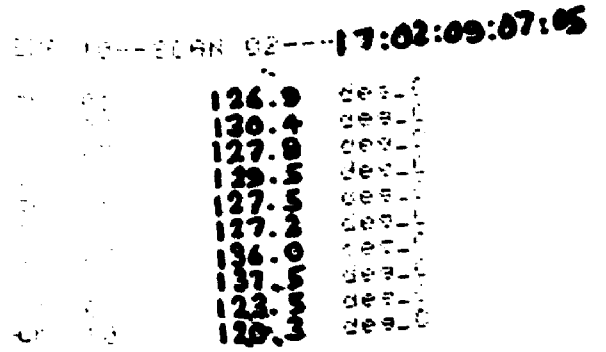
Coal particle size range	: -1.19 mm
Oven temperature	: 120 ^{o}C
Oxygen flowrate	: 4.33 x 10^{-5} kmol/m^2/s
C	: 23
Bi_o	: 3.7
Bi_1	: 9.3
Bed voidage	: 0.38
K_o	: 4.84 m/s
E/R	: 7000 K
$D_e \rho_m$	: 1.42 x 10^{-13}
D_p	: 0.5 mm

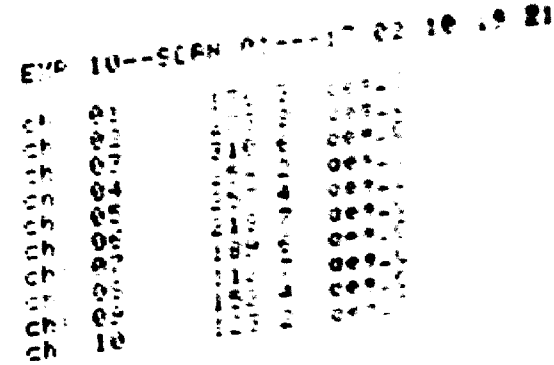

EXP 10--SCAN 01---17 02 09 52 42
CH 01 120.9 deg_C
CH 02 120.1 deg_C
CH 03 118.7 deg_C
CH 04 119.4 deg_C
CH 05 118.0 deg_C
CH 06 117.8 deg_C
CH 07 117.3 deg_C
CH 08 114.5 deg_C
CH 09 117.2 deg_C
CH 10 119.4 deg_C

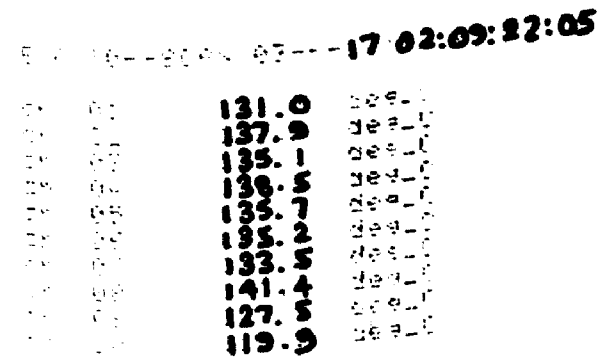

EXP 10--SCAN 04---17 02 09 1? 05
CH 01 175.2 deg_C
CH 02 146.3 deg_C
CH 03 144.2 deg_C
CH 04 150.4 deg_C
CH 05 146.5 deg_C
CH 06 145.8 deg_C
CH 07 142.8 deg_C
CH 08 140.9 deg_C
CH 09 132.2 deg_C
CH 10 120.6 deg_C

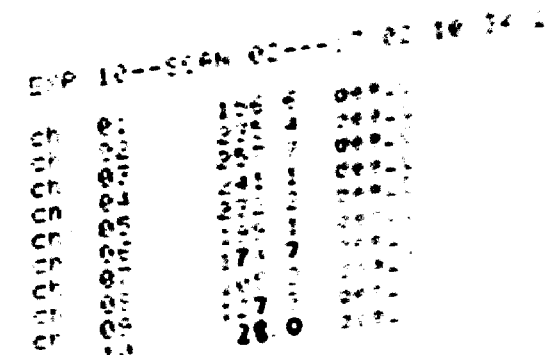

EXP 10--SCAN 01---17 02 09 52 06
CH 01 120.9 deg_C
CH 02 121.1 deg_C
CH 03 119.7 deg_C
CH 04 120.1 deg_C
CH 05 119.9 deg_C
CH 06 118.5 deg_C
CH 07 117.9 deg_C
CH 08 136.9 deg_C
CH 09 117.7 deg_C
CH 10 119.5 deg_C


EXP 10--SCAN 05---17 02 09 52 08
CH 01 140.9 deg_C
CH 02 155.9 deg_C
CH 03 159.7 deg_C
CH 04 172.2 deg_C
CH 05 165.6 deg_C
CH 06 164.0 deg_C
CH 07 157.1 deg_C
CH 08 164.3 deg_C
CH 09 138.5 deg_C
CH 10 121.7 deg_C


EXP 10--SCAN 02---17:02:09:07:05
126.9 deg_C
130.4 deg_C
127.8 deg_C
129.5 deg_C
127.5 deg_C
127.4 deg_C
136.0 deg_C
137.5 deg_C
122.3 deg_C
120.3 deg_C


EXP 10--SCAN 01---17 02 10 09 21


EXP 10--SCAN 07---17:02:09:22:05
131.0 deg_C
137.9 deg_C
135.1 deg_C
136.5 deg_C
135.7 deg_C
135.2 deg_C
133.5 deg_C
141.4 deg_C
127.5 deg_C
119.9 deg_C


EXP 10--SCAN 01---17 02 10 14 ??
26.0

A10.7 Ignition run 2

The results from this run were used in figure 7.4. The experimental conditions and model parameters used were as follows:

Coal particle size range	: -1.19 mm
Oven temeprature	: 100 ^{o}C
Oxygen flowrate	: 4.33 x 10^{-5} kmol/m^2/s
C	: 23
Bi_o	: 3.7
Bi_1	: 9.3
Bed voidage	: 0.38
k_o	: 4.9 m/s
E/R	: 7000 K
$D_e\rho_m$	: 1.42 x 10^{-13}
D_p	: 0.5 mm

25 02 10:15:50

ch:	01	deg_C
ch:	02	deg_C
ch:	03	deg_C
ch:	04	deg_C
ch:	05	deg_C
ch:	06	deg_C
ch:	07	deg_C
ch:	08	deg_C
ch:	09	deg_C
ch:	10	deg_C

EXP 05--SCAN 06---25 02 10 45 50

ch:	01	deg_C
ch:	02	deg_C
ch:	03	deg_C
ch:	04	deg_C
ch:	05	deg_C
ch:	06	deg_C
ch:	07	deg_C
ch:	08	deg_C
ch:	09	deg_C
ch:	10	

EXP 05--SCAN 07---25 02 11 15 50

ch:	01	deg_C
ch:	02	deg_C
ch:	03	deg_C
ch:	04	deg_C
ch:	05	deg_C
ch:	06	deg_C
ch:	07	deg_C
ch:	08	deg_C
ch:	09	deg_C
ch:	10	

EXP 05--SCAN 08---25 02 11 45 50

ch:	01	deg_C
ch:	02	deg_C
ch:	03	deg_C
ch:	04	deg_C
ch:	05	deg_C
ch:	06	deg_C
ch:	07	deg_C
ch:	08	deg_C
ch:	09	deg_C
ch:	10	

EXP 05--SCAN 09---25 02 12 15 50

ch:	01	deg_C
ch:	02	deg_C
ch:	03	deg_C
ch:	04	deg_C
ch:	05	deg_C
ch:	06	deg_C
ch:	07	deg_C
ch:	08	deg_C
ch:	09	deg_C
ch:	10	

APPENDIX 11 **MODEL PARAMETERS USED AS 'BASE CASE'**

The following model parameters have been used as the base-case:

k_o = 10 m/s

E_a/R = 7000 K

ϵ = .3

ΔH_r = 3 x 10^8 J/kmol

k_b = 0.2 W/m/K

$\hat{c}$ = 3 x 10^4 J/kmol/K

ρ_b = 900 kg/m^3

C_b = 1000 J/kg/K

P = 1.013 x 10^5 Pa

y_o = .21

L = 5 m

$h_1 = \sigma\,(T_\infty+T_o)(T_\infty^2+T_o^2)$

$h_2 = \sigma\,(T_\infty+T_e)(T_\infty^2+T_e^2)$

C = 0

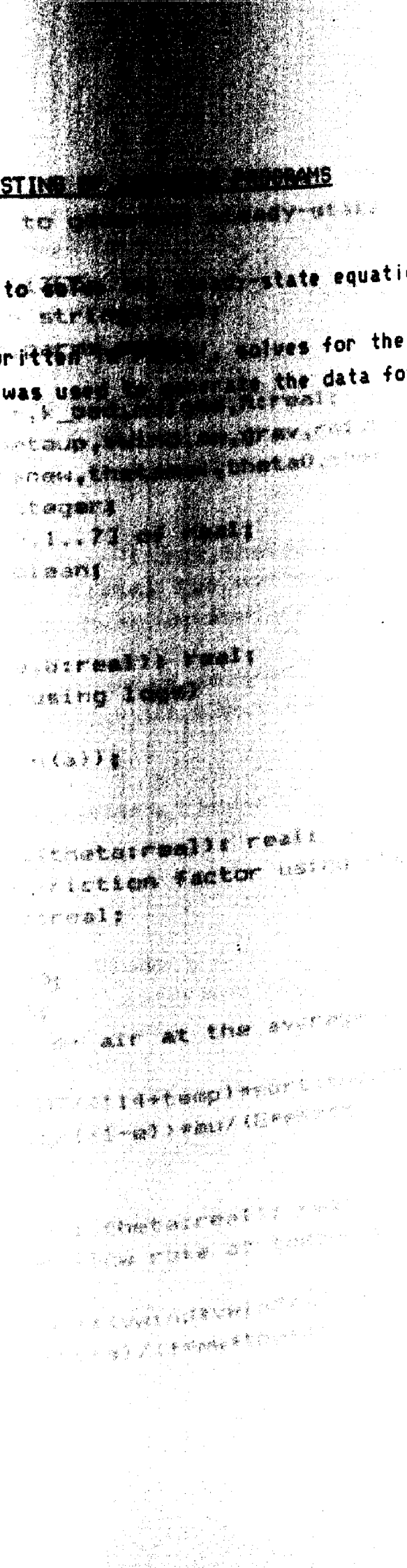
V = 0

APPENDIX 12 **LISTING**

A12.1 Program to

This program, written

solutions. It was used



```
program coal;
{Pascal program to generate steady-state stable solutions}

const pres = 1.013E5;
type string255 = string[255];
label startloop,parms,endp;
var
g,DelH,L,YO,Tinf,k_bed,msigma,R:real;
tad,thetalow,thetaup,vwind,mw,grav,roi,Eor,E,k0,S,dp,cp:real;
diff,theta,thetanew,thetamax,theta0,theta1,lhs,rhs:real;
imax,imin,i,j:integer;
tem:array[-1..10,1..7] of real;
ok,increased:boolean;
ch:char;

function power(a,b:real): real;
{calculates a^b using logs}
begin
  power:=exp(b*ln(a));
end;

function fricfac(theta:real): real;
{calculates the friction factor using the Ergun equation}
var mu,thet,temp:real;
begin
  temp:=theta*300;
  thet:=temp/273;
  {the viscosity of air at the average temperature}
  {Perry 3rd ed}
  mu:=1.709e-5*387/(114+temp)*sqrt(thet*thet*thet);
  FricFac:=180*sqr((1-e))*mu/(E*e*e*sqr(dp));
end;

function flowrate(f,theta:real): real;
{calculates molar flow rate at temperature theta}
begin
 flowrate:=sqr(roi)*(vwind*vwind/(2*1)+
 grav*(theta-1)/theta)/(f*mw*theta);
end;
```

```
procedure printparms;
{Prints the parameters with a heading}
var heading:string255;
begin
write('Heading for this run ? ');readln(heading);
writeln(lst,heading);
writeln(lst,'Voidage: ',e:4:1,' k0: ',k0:6:1,' E/R: ',eor*tinf:6:0);
writeln(lst,'Wind speed: ',vwind:4:1,' k_bed: ',k_bed*1000:4:1,
' Bed length: ',l:2:0);
writeln(lst);
end;

procedure calcall(var theta,thetabar,difference:real;flag:boolean);
{This routine calculates the difference between the LHS and}
{RHS of the equation at an average temperature theta}
label 330;
var expc,w,heat,deltheta0,deltheta1,Bi0,Bi1,f,p,
theta0n,theta1n,a2,a,c,a1,c2p,t,expma2,expa,c2a,c2,c1overam:real;
begin

  {Set up the parameters required}

  theta0:=theta;
  theta1:=theta;
  f:=fricfac(theta);
  p:=sqr(roi)*grav/(f*mw);
  w:=k0*6*(1-e)*l*f/(dp*grav*roi);
  heat:=msigma/(p*cp*mw);
  g:=flowrate(f,theta);
  a2:=w*theta*exp(-eor/theta)/(theta-1);
  a:=g*cp*l*mw/(k_bed);
  c:=delh*g*l/(tinf*k_bed);
  a1:=c*y0/(a2+a);
  if a2>80 then expma2:=0 else expma2:=exp(-a2);
  if abs(a)>80 then expa:=0 else expa:=exp(a);

  {Jump back here if the end temperatures don't converge}

330:  bi0:=msigma*((theta0)+1)*(sqr(theta0)+1)*l/k_bed;
  bi1:=msigma*((theta1)+1)*(sqr(theta1)+1)*l/k_bed;
```

```
c2a:=-a1*a2*exp                    (bi0+a)+a1*(1-expma2));
if a>80 then c2
c2:=c2a/(a*expa-                   +expa*bi1);
cloveram:=a1*a2/                   )*a1-c2+1;
if a>80 then c2p                   else c2p:=c2*expa;
theta0n:=clover
theta1n:=clover
t:=sqr(theta-1);
deltheta0:=abs(t
deltheta1:=abs(

{Check for conver                  temperatures}

if (1.e5/t*(sqr(                   sqr(deltheta1)))>1 then begin
  theta0:=(theta0n
  theta1:=(theta1n
  goto 330;
end;

{Calculate the LHS                 the energy balance}

lhs:=bi0*(theta0n-                 theta1n-1)/a+theta1n-1;
if a2>80 then rhs
rhs:=tad*(1-exp(-                  theta-1)*exp(-eor/theta)));

{Write answers on screen as a check for the operator}

writeln('Mean temperature guessed: ',theta*tinf:6:2);
thetabar:=cloveram*a2/a2*(expma2-1)+c2p/a-c2/a;
writeln('Mean temperature calculated ',thetabar*tinf:6:2);
difference:=lhs-rhs;
if ((a*a2/(a+a2))>80) then expc:=0 else expc:=exp(-a*a2/(a2+a));
thetamax:=cloveram*power((c*y0/a),(a/(a+a2)))*
          power((-c2p*(1+a/a2)),(a2/(a2+a)))*expc;
writeln('Flowrate ',g);
writeln('Inlet & outlet temps ',theta0n*tinf:6:2,' ',theta1n*tinf:6:

writeln('LHS ',lhs,' RHS  ',rhs);
writeln('Difference ',difference);
writeln('Maximum temperature  ',thetamax*tinf:6:2);
writeln;
end;
```

```
procedure PrintAnswers;
begin
  writeln(lst,'Mean temperature ',thetanew*tinf:6:2,
  '  Flowrate ',g);
  writeln(lst,'Inlet & outlet temps ',theta0*tinf:6:2,
  ' ',theta1*tinf:6:2);
  writeln(lst,'LHS ',lhs,' RHS ',rhs);
  writeln(lst,'Difference ',lhs-rhs);
  writeln(lst,'Maximum temperature ',thetamax*tinf:6:2);
  writeln(lst);
end;

{**** MAIN PROGRAM *****}
begin
  parms:
  {Parameters for the model}
  Tinf:=300;          {Ambient temperature}
  delh:=3.e5;         {Delta H reaction in kJ/kmol}
  mw:=30.;            {Molecular weight}
  l:=5;               {Bed length in metres}
  y0:=0.21;           {Mole fraction of oxygen in air}
  k_bed:=0.2e-3;      {Thermal conductivity in kW/m/K}
  Eor:=7000./tinf;    {Activation energy divided by (R T_ambient)}
  E:=0.3;             {Bed voidage}
  k0:=10.0;           {Surface rate constant in m/s}
  cp:=1.;             {Gas specific heat in kJ/kgK}
  roi:=1.2;           {density of ambient air in kg/m^3}
  {modified Stefan-Boltzmann constant}
  msigma:=5.67e-11*tinf*tinf*tinf;
  grav:=9.81;         {acceleration due to gravity}
  vwind:=0.1;         {wind velocity in m/s}
  R:=8.314e3;         {gas constant in kJ/kmol/K}
  gotoxy(1,1);
  writeLN('Do you want to print a heading ? ');read(kbd,ch);
  if upcase(ch)='Y'then printparms;      {Print the parameters}
  {Adiabatic dimensionless temperature rise}
  tad:=delh*y0/(cp*tinf*mw);
  write('Minimum loop counter ? ');readln(imin);
  write('Maximum loop counter ? ');readln(imax);
  if imin=imax then begin
     write('Particle size in mm ? ');readln(dp);
     dp:=dp/1000;
  end;

                                    answers are stored}
                                    i,j]:=0;
```

```
for j:=1 to 2 do begin

{if j=1 then calculations done on the upper branch
 if j=2 then calculations done on the lower branch}

theta:=3.0;if j=2 then theta:=1.01;  {initial guesses}
increased:=false;
for i:=imax downto imin do begin;
 if imin<>imax then begin
    dp:=i*2;
    if i=0 then dp:=0.4;
    if i=-1 then dp:=0.5;
    dp:=dp/1000;
 end;
 startloop:
 ClrScr;
 tem[i,4]:=dp;
 writeln('Particle size ',dp*1000:4:2);writeln;
 thetanew:=0;
 while (sqr(abs(theta-thetanew))>1.e-6) do begin
  calcall(theta,thetanew,diff,true);
  if (((thetanew*tin(j)>360) and (j=2)) then begin

  {The program was moving along the lower branch and then}
  {jumped onto the upper branch.}
  {Increase dp by 1mm and try again}

    if not(increased) then
    begin
      dp:=dp+1.e-3;
      increased:=true;
      theta:=1.05;          {initial guess}
      goto startloop;
    end else goto endp;   {if dp was already increased, exit}
  end;
  {Repeat calculation with new theta}
  theta:=0.4*thetanew+0.6*theta;
 end;
 tem[i,j]:=thetanew;
 tem[i,j+4]:=thetamax;
end;
end;
```

```
p:
teln(lst,'SUMMARY OF SOLUTIONS');
teln(lst);
teln(lst,'DP':5,'LOWER':9,'LOWER MAX':9,'UPPER':9,'UPPE
teln(lst);
 i:=imax downto imin do begin
riteln(lst,tem[i,4]*1000:5:1,tem[i,2]*tinf:9:2,tem[i,3]
ea[i,1]*tinf:9:2,tem[i,5]*tinf:9:2);
;
.
```

A12.2 Program to solve the unsteady-state equations for constant r

This program, written in BASIC, uses the analytical solution to solve for the time varying behaviour of the bed.

```
10    ! PROGRAM "                    YTIC SOLUTION
20    ! WITH A
30    OPTION BASE
40    DIM Beta(50)                   (50)
50    COM C(3),Dat                   (11),B(4),Phi(4)
60    PRINTER IS
70 Values:    ! THI                  all the constants and data used
80    MAT READ Cp                    ! N2
90    DATA 6.524,                    ! O2
100   DATA 6.148,
110   DATA 6.214,1                   ! CO2
120   DATA 4.18,                     ! C  NB:Cp=a + bT + c/T^2
130   ! THIS DATA I
140   MAT Cp=Cp*(4.                  J/kmol K
150   P=1.013E5 ! N/
160   ! Initial mole
170   C(1)=.79
180   C(2)=.21
190   C(3)=0
200   ! INITIAL
210    INPUT "Enter                  ,Te,Tavss
220   ! Convert                      atures
230   Ti=300                         nt temperature
240   T0=T0/Ti
250   Te=Te/Ti
260   Tavss=Tavss/
270   ! T0 is the
280   ! Tavss is
290   ! Te is the                    is the density of the ambient air in kg/m^3
300   CALL Density(Ti,               constant in J/kmol/K
310   R=8.314E3
320   E=.4                           particle size in mm
330   Dp=2                           !Surface per volume in m^-1
340   S=6000/Dp                      !Effective thermal conductivity in W/mK
350   Ke=.2                          !Path length in m
360   L=1                            !Modified Stefan-Boltzmann constant
370   Msig=5.67E-8                   !Density of bed in kg/m^3
380   Rho=900                        !Specific heat of bed in J/kg/K
390   Cps=1000                       !Viscosity in m^2/hr
400   ! Effective
410   Kappa=Ke*3600/(Rho*Cps)        !+.448*((.35/.25)^2-1)*500*Cps)
420   K0=0/3600                      !Pre-exponential factor in m/s
430   Eor=0                          !Activation energy/R in K
440   G=9.81                         !Acceleration due to gravity in m/s^2
450   Hc=.76                         !Heat transfer coefficient in W/m^2/K
460   Radius=.25                     !Radius of bed
470   C=0                            !Heat loss coefficient
480   Power=0                        !Power input to heater in W
490   Df=Power*L/(PI*Radius^2*Msig*Ti) !Dimensionless flux
```

```
500  ! Write data into array Dat for passing to subroutines
510  Dat(1)=Roi
520  Dat(2)=R
530  Dat(3)=E
540  Dat(4)=Dp
550  Dat(5)=S
560  Dat(6)=P
570  Dat(7)=Ke
580  Dat(8)=Msig
590  Dat(9)=K0
600  Dat(10)=Eor
610  Dat(11)=L
620  Dat(12)=G
630  Dat(13)=C
640  Dat(14)=Ti
650  Dat(15)=Df!
660  ! Input name of file into which values are written
670  INPUT "Name of data file",Name$
680  ! Print initial values and constants
690  PRINTER IS 7,1,WIDTH(80)
700  PRINT CHR$(27);"&dD";"METHOD OF SOLUTION:";CHR$(27);"&dE";" ANALYTIC SOLU
ON WITH RATE CONSTANT AT I ev"
710  PRINT LIN(2);"Rav set to a constant to check methods"
720  PRINT LIN(2);CHR$(27);"&dD";"BED CONSTANTS";CHR$(27);"&dE"
730  PRINT LIN(1);"Particle size=";Dp;"mm",,"Voidage=";E
740  PRINT LIN(1);"Bed radius=";Radius;"m",,"Bed length=";L;"m"
750  PRINT LIN(1);"Power input=";Power;"W",,"Loss coefficient=";C
760  PRINT USING "/4A,X,4D,X,A,29X,4A,X,D.DDDE,X,4A";"E/R=";Eor;"K",,"K0=";K0
0;"m/hr"
770  PRINT LIN(1);"Bed density=";Rho;"kg/m^3","Cp of bed=";Cps;"J/kg/K"
780  PRINT USING "/12A,X,D.DDDE,X,6A";"Diffusivity=";Kappa;"m^2/hr"
790  ! PRINT LIN(1);"Name of data file is ";Name$
800  ! PRINT PAGE
810  PRINTER IS 16
820  ! Calculate  predicted steady state profile
830  CALL Tsteady(Tavss,T0,Te,Tmax)
850  ! Tmax is used to give upper limit for "PLOT"
860  Tup=100*INT(Tmax*Ti/100+.5)
870  ! Write steady state profile into matrix T as first element
880  FOR I=1 TO 11
890     T(I,1)=Z(1)
900  NEXT I
910  ! Input Tin which is the initial bed temperature
920  INPUT "Initial temperature?",Tin
930  Tin=Tin/Ti
940  T0=Tin
950  Te=Tin
960   PRINTER IS 7,1,WIDTH(80)
970  PRINT CHR$(27);"&dD";"UNSTEADY STATE SOLUTION";CHR$(27);"&dE"   Initial tem
erature=";INT(Tin*Ti+.5);"K"
980  PRINTER IS 16
990  Ta=Tin          !For the first time slice
1010 ! Decide on time scaling
1020 Dtmax=Ti*ABS(Tavss-Tin)
1030 PRINT "The difference in average temperatures is ";Dtmax
1040 Reinput:  INPUT "Maximum temperature rise per time slice?",Delt
1050    Lastj=INT(Dtmax/Delt)+1  !Lastj is the number of curves
1060    PRINT "This gives ";Lastj;" curves (including steady state). Is this O K
?"
1070    A$=""
1080    INPUT A$
1090 IF A$="N" THEN Reinput !
```

```
1100 ! Initialize the array Beta to (N-1)*PI except for the first value
1110 Beta(1)=PI/2
1120 FOR N=2 TO 50
1130    Beta(N)=(N-1)*PI
1140 NEXT N
1150 Time=2              !First time at which calculation is done
1160 Lastj=50
1170 FOR J=2 TO Lastj    !Outer loop for time increments
1180    ! Put time into matrix
1190    Tim(J)=Time
1200    ! Calculate flowrate and reaction rate based on average temperature
1210    Tai=Ta*Ti
1220    CALL Darcy(Tai,Fr)
1230    CALL Cp(Tai,Cpav)
1240    CALL H_react(Tai,Delh)
1250    ! Calculate dimensionless flow number
1260    Dfn=L*Roi*G*P*Cpav/(Fr*R*Ti*Ke)
1270    A=Dfn*((Ta-1)/Ta/Ta)
1280    Gg=A*Ke/(Cpav*L)
1290    ! Calculate dimensionless reaction number
1300    Rav=K0*EXP(-Eor/Tai)*P*(1-E)*S/(R*Tai)
1310  ! Rav=5E-7
1320    B=Rav*Delh*L*L*C(2)/(Ke*Ti)
1330    M=Rav*L/Gg
1340    ! Calculate values for 'steady state' coefficients
1350    IF Df=0 THEN CALL Coe(A,B,C,R1,R2,M,T0,Te,C1,C2,C3,Bi0,Bi1,0)
1360    IF Df<>0 THEN CALL Coe2(A,B,C,R1,R2,M,T0,Te,C1,C2,C3,Bi0,Bi1,Df)
1370    Hi=Bi0+A/2
1380    H2=Bi1+A/2
1390    ! Calculte constants needed for unsteady state profile
1400    Kt=Kappa*Time
1410    Inter=EXP(-Kt*A*A/4-C*Kt)
1420    V=0
1430    FOR N=1 TO 20
1440            CALL Integral(Beta(N),N,H1,H2,A,B,C,R1,R2,M,C1,C2,C3,Tin,In(N))
1450            ! Calculate and print 'V' at 1 as a check for convergence
1460            Zn=Beta(N)*COS(Beta(N))+H1*SIN(Beta(N))
1470            V=V+In(N)*Zn*EXP(-Kt*Beta(N)^2)
1480            PRINT N,V
1490    NEXT N
1500    V1=V
1510    ! Calculate unsteady state profile
1520    FOR I=0 TO 9
1530       X=I/10
1540       V=0
1550       FOR N=1 TO 20
1560             Betax=Beta(N)*X
1570             Zn=Beta(N)*COS(Betax)+H1*SIN(Betax)
1580             V=V+In(N)*Zn*EXP(-Kt*Beta(N)^2)
1590       NEXT N
1600       CALL Temp(X,Tss,R1,R2,M,C1,C2,C3)!Tss is the steady state temperature
1610       Z(I+1)=Tss
1620       T(I+1,J)=Tss+V*Inter*EXP(A*X/2)
1630    NEXT I
1640    ! The value of 'V' at the exit is V1
1650    CALL Temp(1,Tss,R1,R2,M,C1,C2,C3)
1660    Z(11)=Tss
1670    T(11,J)=Tss+V1*Inter*EXP(A/2)
1680    T0=T(1,J)
1690    Te=T(11,J)!
```

```
1700     ! Print heading on printer
1710      PRINTER IS 7,1,WIDTH(80)
1720     PRINT LIN(2);CHR$(27);"&dD";"TIME=";Time;"hrs";CHR$(27);"&d@"
1730     ! Call subroutine to print 'constants'
1740     CALL Print(Ta*Ti,Rav,Delh,Cpav,Fr,Gg,Bi0,Bi1,A,B)
1750     ! Calculate average bed temperature & print profile
1760     PRINT LIN(1);"X (m)","TEMPERATURE (K)","   T ss(K)","    Y02"
1770     FOR I=1 TO 11
1780        Y(I)=T(I,J)
1790        Xx=I/10-.1
1800        PRINT Xx,Y(I)*Ti,Z(I)*Ti,.21*EXP(-M*Xx)
1810     NEXT I
1820     ! Throw a page if J is odd
1830     IF FRACT(J/2)<>0 THEN PRINT PAGE
1840     PRINTER IS 16
1850     CALL Simpson(Ta)
1860     ! Calculate time step using exponential scaling
1870    Del_time=LOG((Lastj+2-J)/(Lastj+1-J))/(Kappa*Beta(1)^2)
1880    Time=Time+PROUND(Del_time,0)
1900    PRINT "NEXT TIME IS";Time;"hrs","TAV=";Ta*Ti
1910 NEXT J
1920 STOP
1930 ! Write temperature profiles onto tape for plotting
1940 Record: Recl=INT((11+23*Lastj)/32)+1   !This number is the record length
1950 GOTO 2150
1960 CREATE Name$,Recl
1970 ASSIGN #1 TO Name$
1980 PRINT #1;Lastj+2
1990 ! Set upper and lower limits
2000 PRINT #1;2
2010 PRINT #1;0,Ti
2020 PRINT #1;1,Tup
2030 ! Put initial temperature on tape
2040     PRINT #1;2
2050     PRINT #1;0,Tin*Ti
2060     PRINT #1;1,Tin*Ti
2070 ! Put array T onto tape                !Lastj is the number of curves
2080 FOR J=1 TO Lastj                      !Number of points
2090     PRINT #1;11
2100     FOR I=1 TO 11                     !Point
2110        PRINT #1;I/10-.1,T(I,J)*Ti
2120     NEXT I
2130 NEXT J
2140 ASSIGN #1 TO *
2150 ! Put temperature vs. time plot on tape
2160 CREATE Name$&"T",Recl
2170 ASSIGN #2 TO Name$&"T"
2180 PRINT #2;12
2190 PRINT #2;2
2200 PRINT #2;0,300
2210 PRINT #2;Tim(Lastj),Tup
2220 FOR I=1 TO 11
2230 PRINT #2;Lastj
2240 PRINT #2;0,Tin*Ti
2250 FOR J=2 TO Lastj
2260 PRINT #2;Tim(J),T(I,J)*Ti
2270 NEXT J
2280 NEXT I
2290 ASSIGN #2 TO *
2300 STOP !
```

```
2310 Tsteady:  SUB Tsteady(Ta,T0,Te,Tmax)
2320 OPTION BASE 1
2330 ! This subroutine calculates the steady state temperature profile
2340 ! It is quite separate to the calculation of the unsteady state profiles
2350 COM C(3),Data(20),Cp(4,3),Y(11),T(11)
2360 ! Give variables in array 'Data' desriptive names
2370 Roi=Data(1)
2380 R=Data(2)
2390 E=Data(3)
2400 Dp=Data(4)
2410 S=Data(5)
2420 P=Data(6)
2430 Ke=Data(7)
2440 Msig=Data(8)
2450 K0=Data(9)
2460 Eor=Data(10)
2470 L=Data(11)
2480 G=Data(12)
2490 C=Data(13)
2500 Ti=Data(14)
2510 Df=Data(15)
2520 ! Make estimates of flowrate & reaction rate constant
2530 Tai=Ta*Ti
2540 Rav=K0*EXP(-Eor/Tai)*P*(1-E)*S/(R*Tai)
2550 Rav=1E-5
2560 CALL Darcy(Tai,Fr)
2570 Gg=P*Roi*G/(Fr*R*Tai)*(1-1/Ta)
2580 ! Outer loop which iterates for reaction rate constant
2590 Calc_rate: Tai=Ta*Ti
2600   CALL Darcy(Tai,Fr)
2610   CALL Cp(Tai,Cpav)
2620   CALL H_react(Tai,Delh)
2630   B=Rav*Delh*C(2)*L*L/(Ke*Ti)
2640   ! Inner loop to calculate flowrate
2650 Calc_flow:     A=Gg*Cpav*L/Ke
2660     M=Rav*L/Gg
2670     IF Df=0 THEN CALL Coe(A,B,C,R1,R2,M,T0,Te,C1,C2,C3,Bi0,Bi1,1)
2680     IF Df<>0 THEN CALL Coe2(A,B,C,R1,R2,M,T0,Te,C1,C2,C3,Bi0,Bi1,Df)
2690     PRINT "T0=";T0*Ti,"G=";Gg
2700     ! Calculate temperature at 11 points
2710     FOR I=0 TO 10
2720       X=I/10
2730       CALL Temp(X,T,R1,R2,M,C1,C2,C3)
2740       T(I+1)=T
2750       Y(I+1)=1/T
2760     NEXT I
2770     ! Calculate integral of T^-1 using Simpson's Rule
2780     CALL Simpson(Di1)
2790     ! Calculate integral of T analytically
2800     CALL Intt(It,R1,R2,M,C1,C2,C3,C)
2810     ! Calclulate new flowrate
2820     Gg1=P*G*Roi*(1-Di1)/(Fr*R*It*Ti)
2830     Dif=ABS(Gg1-Gg)
2840     Gg=.8*Gg1+.2*Gg
2850     ! Check for convergence of flowrate
2860     IF Dif>Gg/500 THEN GOTO Calc_flow
2870   ! Calculate new end temperature and rate expression
2880   Dif1=ABS(Te-T(11))
2890   Te=T(11)!
```

```
2900   GOTO 3000
2910   ! Evaluate exp(-E/(RT))/T numerically
2920    FOR I=1 TO 11
2930       Temp=T(I)*Ti
2940       Y(I)=EXP(-Eor/Temp)/Temp
2950    NEXT I
2960    CALL Simpson(Di2)
2970    Rav1=K0*P*Di2*S*(1-E)/R
2980    Dif=ABS(Rav-Rav1)
2990    Rav=.8*Rav1+.2*Rav
3000    Ta=It
3010    PRINT "T av=";Ta*Ti,,"RAV=";Rav
3020 ! Check for convergence
3030 IF (Dif)Rav/500) OR (Dif1).001) THEN GOTO Calc_rate
3040 ! The iteration is finished
3050 Tmax=T(1)
3060 ! Calculate maximum temperature if Flux=0
3070 IF Df=0 THEN CALL Tmax(Xmax,Tmax,R1,R2,M,C1,C2,C3)
3080 ! Print steady state profile & constants
3090  PRINTER IS 7,1,WIDTH(80)
3100 PRINT LIN(2);CHR$(27);"&dD";"STEADY STATE SOLUTION";CHR$(27);"&d@"
3110 CALL Print(Ta*Ti,Rav,Delh,Cpav,Fr,Gg,Bi0,Bi1,A,B)
3120 PRINT LIN(1);"X    ","TEMPERATURE (K)"
3130 FOR I=0 TO 10
3140 PRINT I/10,T(I+1)*Ti
3150 NEXT I
3160 PRINT LIN(1);"T max=";Tmax*Ti;"K @ X=";Xmax;
3170 ! Check on overall energy balance
3180 Hr=Bi0*(T0-1)+Bi1*(Te-1)+A*(Te-1)+C*(It-1)
3190 Hg=B/M*(1-EXP(-M))+Df
3200 PRINT LIN(1);"HR=";Hr,,"HG=";Hg
3210  PRINT PAGE
3220  PRINTER IS 16
3230 SUBEND !
```

```
3240 SUB Cp(T,Cpav)
3250 OPTION BASE 1
3260 COM C(3),Data(20),Cp0(4,3)
3270 DIM Cp(3)
3280 ! Cp's in J/kmol K FOR T IN K:
3290 MAT Cp=(0)
3300 FOR I=1 TO 3
3310 FOR J=1 TO 3
3320 Cp(I)=Cp(I)+Cp0(I,J)*T^(J-1)
3330 NEXT J
3340 NEXT I
3350 ! C(*) IS VECTOR OF MOL FRACTIONS, SO
3360 Cpav=DOT(C,Cp)
3370 SUBEND !


3380 SUB Density(T,P,Ro,Mass)
3390 OPTION BASE 1
3400 COM C(3)
3410 DIM Mwt(3)
3420 Mwt(1)=28   ! N2
3430 Mwt(2)=32   ! O2
3440 Mwt(3)=44   ! CO2
3450 ! C(*) IS VECTOR OF MOL FRACTIONS, SO FOR 1 MOL:
3460 Mass=DOT(C,Mwt)
3470 R=8.3E3    ! J/kmol K
3480 Vol=R*T/P
3490 Ro=Mass/Vol    ! kg/m3
3500 SUBEND !


3510 SUB Darcy(T,Darcy)
3520 OPTION BASE 1
3530 COM C(3),Data(20)
3540 E=Data(3)
3550 D=Data(4)
3560 S=Data(5)
3570 ! T = TEMP K
3580 ! D = PARTICLE DIAM m
3590 ! E = VOIDAGE
3600 ! S = PARTICLE AREA/VOLUME
3610 CALL Viscosity(T,Mu)
3620 K=5
3630 Darcy=K*(1-E)^2*Mu*S^2/E^3
3640 SUBEND !


3650 SUB Viscosity(T,Mu)
3660 ! VISCOSITY OF AIR
3670 ! PERRY THIRD ED P 370
3680 C=114
3690 Mu0=.01709                                    ! IN cp FOR T IN K
3700 Mu=Mu0*(273.1+C)/(T+C)*(T/273.1)^1.5
3710 Mu=Mu/1000    ! IN kg/m s
3720 SUBEND !
```

```
3730 SUB H_react(T,Delh)
3740 ! Subroutine to calculate Delta H reaction
3750 OPTION BASE 1
3760 COM X(3),Data(20),Cp(4,3)
3770 Delta_h_0=-9.4E7*4.18  !J/kmol !Enthalpy of formation of CO2
3780 Ho2=0
3790 Hco2=0
3800 T0=298
3810 I=2  !2 refers to CO2
3820 FOR J=1 TO 3     ! CP = CP(I,1)+CP(I,2)*T+CP(1,3)*T^2
3830 Ho2=Ho2+Cp(I,J)*(T^J-T0^J)/J
3840 NEXT J
3850 I=3 !3 refers to O2
3860 FOR J=1 TO 3     ! CP = CP(I,1)+CP(I,2)*T+CP(I,3)*T^2
3870 Hco2=Hco2+Cp(I,J)*(T^J-T0^J)/J
3880 NEXT J
3890 ! Enthalpy of Carbon with Cp=Cp(4,1)+Cp(4,2)*T+Cp(4,3)*T^-2
3900 Hc=Cp(4,1)*(T-T0)+Cp(4,2)/2*(T^2-T0^2)-Cp(4,3)*(1/T-1/T0)
3910 Delh=Ho2-Hco2+Hc-Delta_h_0
3920 ! This is actually -Delta H reaction
3930 SUBEND !


3940 Temp: SUB Temp(X,T,R1,R2,M,C1,C2,C3)
3950 ! Steady state temperature expression
3960 T=1+C1*EXP(R1*X)+C2*EXP(R2*X)+C3*EXP(-M*X)
3970 SUBEND !


3980 SUB Intt(It,R1,R2,M,C1,C2,C3,C)
3990 ! Calculates the integral of T
4000 It=1+C1+C2/R2*(EXP(R2)-1)-C3/M*(EXP(-M)-1)
4010 IF C<>0 THEN It=It-C1*(1-(EXP(R1)-1)/R1)
4020 SUBEND!


4030 Simp: SUB Simpson(Di)
4040    ! Simpson's Rule for 11 evenly spaced points on interval length 1
4050    OPTION BASE 1
4060    COM C(3),Dat(20),Cp(4,3),Y(11),T(11)
4070    LET Di=Y(1)+Y(11)
4080    FOR J=2 TO 10
4090       Di=Di+2*Y(J)
4100       IF J/2-INT(J/2)=0 THEN Di=Di+2*Y(J)
4110    NEXT J
4120    Di=Di/30
4130 SUBEND !
```

```
4140 In: SUB Integral(Beta,N,H1,H2,A,B,C,R1,R2,M,C1,C2,C3,Tin,In)
4150 ! Calculates the coefficient of the series
4160 OPTION BASE 1
4170 COM C(3),Dat(20),Cp(4,3),Y(11),Z(11),B(4),Phi(4)
4180 ! Calculate value of Beta  using succesive substitution
4190 ! Best estimate for Beta  is the one from the previous time slice
4200 Mult=H1*H2
4210 Add=H1+H2
4220 Pre=N*PI-PI/2
4230 Again: X1=Pre-ATN((Beta*Beta-Mult)/(Add*Beta))
4240    Dif=ABS(X1-Beta)
4250    Beta=X1
4260    ! Note strict convergence criterion for acceptable accuracy
4270 IF Dif)1E-8 THEN Again
4280 B(1)=-C1
4290 B(2)=-C2
4300 B(3)=-C3
4310 B(4)=Tin-1
4320 Phi(1)=R1-A/2
4330 Phi(2)=R2-A/2
4340 Phi(3)=-M-A/2
4350 Phi(4)=-A/2
4360 An=2*(Beta^2+H2^2)/((Beta^2+H1^2)*(Beta^2+H2^2+H2)+H1*(Beta^2+H2^2))
4370 In=0
4380 FOR I=1 TO 4
4390    Im=Beta*(EXP(Phi(I))*(Phi(I)*COS(Beta)+Beta*SIN(Beta))-Phi(I))
4400    Im=Im+H1*(EXP(Phi(I))*(Phi(I)*SIN(Beta)-Beta*COS(Beta))+Beta)
4410    Im=Im*B(I)/(Phi(I)^2+Beta^2)
4420    In=In+Im
4430 NEXT I
4440 In=In*An
4450 SUBEND !


4460 Coe: SUB Coe(A,B,C,R1,R2,M,T0,Te,C1,C2,C3,Bi0,Bi1,Flag)
4470 ! Calculates the coefficients in the steady state temperature equation
4480 OPTION BASE 1
4490 COM C(3),Data(20)
4500 Ke=Data(7)
4510 Msig=Data(8)
4520 Bi1=Msig*(Te*Te+1)*(Te+1)
4530 R1=(A-SQR(A*A+4*C))/2
4540 R2=(A+SQR(A*A+4*C))/2
4550 Again: Bi0=(T0+1)*(T0*T0+1)*Msig
4560    C3=-B/(M*M+A*M-C)
4570    C2=1/((R1+Bi1)*(A+Bi0-R2)*EXP(R1)+(R2+Bi1)*(R1-A-Bi0)*EXP(R2))
4580    C2=C2*C3*((M-Bi1)*(R1-A-Bi0)*EXP(-M)-(R1+Bi1)*(M+Bi0+A)*EXP(R1))
4590    C1=(C2*(A+Bi0-R2)+C3*(A+Bi0+M))/(R1-A-Bi0)
4600    CALL Temp(0,T,R1,R2,M,C1,C2,C3)
4610    Dif=ABS(T-T0)
4620    T0=T
4630    ! Check for convergence but  only iterate if doing 'proper'
4640    ! steady state calculation
4650 IF (Dif).001) AND (Flag=1) THEN Again
4660 SUBEND !
```

```
4670 Tmax: SUB Tmax(X,Tmax,R1,R2,M,C1,C2,C3)
4680 ! Subprogram to find maximum temperature and where it occurs
4690 ! Method used is Newton-Raphson
4700 X=.5
4710 Recalc: D2tdx2=C1*R1*R1*EXP(R1*X)+C2*R2*R2*EXP(R2*X)+C3*M*M*EXP(-M*X)
4720         Dtdx=C1*R1*EXP(R1*X)+C2*R2*EXP(R2*X)-C3*M*EXP(-M*X)
4730         X1=X-Dtdx/D2tdx2
4740         Dif=ABS(X1-X)
4750         X=X1
4760 IF Dif).01 THEN Recalc
4770 CALL Temp(X,Tmax,R1,R2,M,C1,C2,C3)
4780 SUBEND !


4790 Prnt: SUB Print(Ta,Rav,Delh,Cp,Fr,Gg,Bi0,Bi1,A,B)
4800 ! Subroutine to print 'constants'
4810 PRINT LIN(1);"T average=";PROUND(Ta,-2);"K",,"RAV=";Rav;"kmol/m^3/s"
4820 PRINT LIN(1);"DELTA H REACTION=";INT(Delh+.5);"J/kmol","CP=";INT(Cp+.5);"J/
kmol/K"
4830 PRINT LIN(1);"DARCY'S CONSTANT=";INT(Fr+.5);"kg/m^2/s"  !?
4840 PRINT LIN(1);"FLOWRATE=";Gg;"kmol/m^2/s"
4850 PRINT LIN(1);"BI0=";Bi0,"BIi=";Bi1
4860 PRINT LIN(1);"A=";A,,"B=";B
4870 SUBEND !


4880 Coe2: SUB Coe2(A,B,C,R1,R2,M,T0,Te,C1,C2,C3,Bi0,Bi1,Df)
4890 ! Calculates the coefficients in the steady state temperature equation
4900 ! for the case of heating on the bottom
4910 OPTION BASE 1
4920 COM C(3),Data(20)
4930 Ke=Data(7)
4940 Msig=Data(8)
4950 ! Bi0 is due to the glass wool insulation
4960 Bi0=120
4970 Bi1=Msig*(Te*Te+1)*(Te+1)
4980 R1=(A-SQR(A*A+4*C))/2
4990 R2=(A+SQR(A*A+4*C))/2
5000 C3=-B/(M*M+A*M-C)
5010 C2=C3*((M-Bi1)*(R1-A-Bi0)*EXP(-M)-(R1+Bi1)*(A+Bi0+M)*EXP(R1))+Df*(R1+Bi1)*E
XP(R1)
5020 C2=C2/((R1+Bi1)*(A+Bi0-R2)*EXP(R1)+(R2+Bi1)*(R1-A-Bi0)*EXP(R2))
5030 C1=(C2*(A+Bi0-R2)+C3*(A+Bi0+M)-Df)/(R1-A-Bi0)
5040 CALL Temp(0,T0,R1,R2,M,C1,C2,C3)
5050 SUBEND !
```

A12.3 Program to solve the equations numerically

This program, written in BASIC, uses the method of lines to solve the equations without the assumption of constant r.

```
10   ! PROGRAM "LIN" WHICH DOES CALCULATIONS AT THE ROOTS OF THE NITH
20   ! ORDER LEGENDRE POLYNOMIAL
30    OPTION BASE 1
40    DIM Th(15),Yo2(15),Z(15),Temp(15,25),Tim(25)
60    N1=15                          !Number of lines
70    REDIM Th(N1),Yo2(N1),Z(N1),Temp(N1,20),X(N1),Aw(N1,N1),A2w(N1,N1)
75    COM Cc(3),Dat(25),Cp(4,3),Aw(15,15),A2w(15,15),X(15),U(15),Ks(15),Rate(15)
80   ! Read the matrix of the nodes of the polynomial from tape
81    OFF ERROR
90    ASSIGN @F1 TO "X"&VAL$(N1)
100   ENTER @F1;X(*)
101   ASSIGN @F1 TO *
110  ! Read the matrix of coefficients from tape
120   ASSIGN @F1 TO "MAT"&VAL$(N1)
130   ENTER @F1;Aw(*)
131   ASSIGN @F1 TO *
140  ! Calculate the matrix AW*AW for 2nd derivatives
150   MAT A2w= Aw*Aw
160   Dif=X(N1)-X(1)          !Scaling factor since nodes are not at 0 and 1
170  ! Calculate the matrix Z which contains rescaled x values
180   FOR I=1 TO N1
190     Z(I)=(X(I)-X(1))/Dif
200   NEXT I
210 Values:  ! This section contains all the constants and data used
290   P=1.013E+5                      ! N/m2 = 1 ATM
300  ! Initial mole fractions
310   Cc(1)=.79                       !N2
320   Cc(2)=.21                       !O2
330   Cc(3)=0                         !CO2
340 Restart:PRINTER IS 1
350   MAT U= (0)
360   Ti=300                          !Ambient temperature
370   CALL Density(Ti,P,Roi,W)        !Roi is the density of the ambient air in kg/m^3
380   R=8.314E+3                      !Gas Constant in J/kmol/K
390   E=.3                            !Voidage
400   Dp=6                            !Particle size in mm
410   S=6000/Dp                       !Surface per volume in m^-1
420   Ke=.2                           !Effective thermal conductivity in W/mK
430   L=5                             !Bed length in m
440   Msig=5.67E-8*Ti^3*L/Ke          !Modified Stefan-Boltzmann constant
450   Rho=900                         !Density of bed in kg/m^3
460   Cps=1000                        !Specific heat of bed in J/kg/K
470   Kappa=Ke*3600/(Rho*Cps)         !Effective thermal diffusivity in m^2/hr
480   Drho=1.E+99                     !Constant for shrinking core (1E99 = no ageing)
490   K0=10                           !Pre-exponential factor in m/s
500   Eor=7000                        !Activation energy/R in K
510   Vwind=0                         !Wind velocity in m/s
520   G=9.81                          !Acceleration due to gravity in m/s^2
530   Radius=0                        !Radius of bed
540   C=0                             !Heat loss coefficient
550 Time:Delt=60                      !Size of time step in hours
560    Deltau=Delt*Kappa/L/L          !Dimensionless time step
```

```
561   Time0=0
570   Time=Time0                    !First time at which calculation is done
580   Lastj=50                      !Number of times calculation is performed
590   Skip=10                       !Not every point is stored and recorded
600   Lastr=Lastj/Skip              !Number of profiles to be recorded
610   REDIM Tim(Lastr+1)
611   REDIM Temp(N1,Lastr+1)
620 ! Write data into array Dat for passing to subroutines
630   Dat(1)=Roi
640   Dat(2)=R
650   Dat(3)=E
660   Dat(4)=Dp
670   Dat(5)=S
680   Dat(6)=P
690   Dat(7)=Ke
700   Dat(8)=Msig
710   Dat(9)=K0
720   Dat(10)=Eor
730   Dat(11)=L
740   Dat(12)=G
750   Dat(13)=C
760   Dat(14)=Ti
770   Dat(15)=Df
780   Dat(16)=N1
790   Dat(19)=Kappa
800   Dat(20)=Dif
810   Dat(21)=Vwind
820   Dat(25)=Drho
830 ! Input name of file into which values are written
840   INPUT "Name of data file",Name$
850 ! Print initial values and constants
860 Prntc:  PRINTER IS 9;WIDTH (2000)
870   PRINT RPT$("
                 ",2);N1;"TH ORDER LEGENDRE POLYNOMIAL-MARCHING BY RUNGE-KUTTA"
880   PRINT RPT$("
                 ",2);"BED CONSTANTS"
890   PRINT RPT$("
                 ",1);"Particle size=";Dp;"mm","Voidage=";E
900   PRINT RPT$("
                 ",1);"Bed length=";L;"m"
910   IF Drho()1.E+99 THEN PRINT USING "/16A,D.DDE";"Ageing factor=";Drho
920   PRINT USING "/,4A,X,4D,X,A,29X,3A,X,DDDD.DD,X,4A";"E/R=";Eor;"K","K0=";K0 "
930   PRINT RPT$("
                 ",1);"Bed density=";Rho;"kg/m^3","Cp of bed=";Cps;"J/kg/K"
940   PRINT USING "/,21A,D.DDDE,X,6A";"Thermal Diffusivity=";Kappa;"m^2/hr"
950 ! PRINT RPT$("
                 ",1);"Wind velocity=";Vwind;"m/s"
960   PRINT RPT$("
                 ",1);"Name of data file:";Name$
970   PRINT RPT$("
                 ",1);"Size of time step:";Delt;"hrs","Number of lines:";N1
971   PRINT RPT$("
                 ",1);"Number of time steps=";Lastj,"Every";Skip;"th recorded"
980   PRINT CHR$(12)
990   PRINTER IS 1
991   A$=""
992   Time0=0
1000  INPUT "DO YOU WANT TO INPUT A TEMPERATURE PROFILE?",A$
1010  IF A$()"Y" THEN GOTO 1100
1020  FOR I=1 TO N1
1030    PRINT "T(";I;") IN K?"
1040    INPUT Th(I)
```

```
1060  MAT Th= Th/(Ti)
1070  INPUT "TIME0 IN HOURS?",Time0
1071  Time=Time0
1080  CALL Tav(Th(*),Ta)
1090  GOTO 1150
1100 ! Input Tin which is the initial bed temperature
1110  INPUT "Initial temperature?",Tin
1120  Tin=Tin/Ti  !Made dimensionless
1130  Ta=Tin!For the first time slice the average temperature is the initial
1140  MAT Th= (Tin)!Th is the matrix that contains the dimensionless temperature
1150  MAT Yo2= (Cc(2))  !Yo2 is the matrix that contains the oxygen profile
1160 ! Store initial temperature profile
1170  FOR I=1 TO N1
1180    Temp(I,1)=Th(I)*Ti
1190  NEXT I
1200  Tim(1)=Time0        !First time
1210  Pflag=1             !Flag to control printing
1220  Nprint=0            !Counter to control output
1250 !
1260 Startloop:FOR J=1 TO Lastj    !Outer loop for time increments
1270    PRINTER IS 9;WIDTH (2000)
1280    ! Calculate flowrate based on average temperature
1290    Tai=Ta*Ti
1300    CALL Darcy(Tai,Fr)
1310    Gg=P*Roi/(Fr*R*Tai)*(G*(1-Ti/Tai)+Vwind^2/L/2)
1320    Dat(18)=Gg
1330    ! Call program to march forward
1340    ! March2 marches forward using forward differences
1350    ! March uses a 4th order Runge Kutta algorithm
1360    CALL March2(Th(*),Yo2(*),Deltau)
1370    ! Call subroutine to calculate O2 profile
1380    CALL Newo2(Yo2(*),Th(*))!
```

```
1381    IF (Th(1))1) AND (Th(N1))1) THEN GOTO 1390!CHECK TO SE IF UNSTABLE
1382    PRINTER IS 1
1383    BEEP
1385    PRINT "WARNING: TIME=";Time;"T0=";Th(1)*Ti;"TE=";Th(N1)*Ti
1386    Th(1)=1
1387    Th(N1)=1
1389    PRINTER IS 9;WIDTH (2000)
1390    IF J MOD Skip()0 THEN GOTO 1560
1400    FOR I=1 TO N1
1410      Temp(I,J/Skip+1)=Th(I)*Ti
1420    NEXT I
1430    IF Pflag=0 THEN GOTO 1560
1440    PRINT RPT$("
                   ",2);"TIME=";Time+Delt;"hrs"
1450    ! The Biot numbers are now in the matrix Dat
1460    Bi0=Dat(21)
1470    Bi1=Dat(22)
1480    ! Call subroutine to print 'constants'
1490    CALL Print(Ta*Ti,Fr,Gg,Bi0,Bi1)
1500    ! Calculate average bed temperature & print profile
1510    PRINT RPT$("
                   ",1);"  X","TEMPERATURE (K)","  Y02"
1520    FOR I=1 TO N1
1530      PRINT USING "Z.DDD,17X,DDDD.DDD,11X,.DDDD,4D,5X,4D";Z(1),Temp(I,J/Skip+
1540    NEXT I
1550    ! Calculate the average dimensionless temperature
1560    CALL Tav(Th(*),Ta)
1570    ! Rescale Ta
1580    Ta=Ta/Dif
1590    ! Throw a page if J is a multiple of 2
1600    IF (J/Skip MOD 3=0) AND (Pflag=1) THEN PRINT CHR$(12)
1610    IF Pflag=0 THEN PRINT USING "#,X,5A,DD.D,X,2A,DDD.DDD";"DAY=",Time/24,"!=
1620    Nprint=Nprint+1
1630    IF (Nprint MOD 4=0) AND (Pflag=0) THEN PRINT
1640 !  DISP J,Ta*Ti,Th(1)*Ti,Th(N1)*Ti
1641    IF Time<1800 THEN GOTO 1650
1642    Delt=5
1643    Deltau=Delt*Kappa/L/L
1650    Time=Time+Delt
1660    IF J MOD Skip=0 THEN Tim(J/Skip+1)=Time
1670 Endloop:NEXT J
1680 ! Print stored temperatures
1681  GOTO 1800
1690  PRINTER IS 9;WIDTH (2000)
1700  PRINT CHR$(12)
1710  FOR J=1 TO Lastr+1
1720    PRINT RPT$("
                   ",2);"TIME=";Tim(J);"days"
1730    PRINT RPT$("
                   ",1);"  X","TEMPERATURE (K)"
1740    FOR I=1 TO N1
1750      PRINT USING "Z.DDD,17X,DDDD.DDD,";Z(I),Temp(I,J)
1760    NEXT I
1770    IF J MOD 3=0 THEN PRINT CHR$(12)
1780  NEXT J
1790  PRINT CHR$(12)
1800  PRINTER IS 1
1810 Qrec:A$=""
1820  INPUT "DO YOU WANT TO RECORD RESULTS?",A$
1830  IF A$="Y" THEN CALL Record(Name$,Temp(*),Z(*),Tim(*),Lastr,N1)
1840  STOP!
1841  END
```

```
1850 Cp:SUB Cp(T,Cpav)
1860    OPTION BASE 1
1890    Cpav=28930
2000  SUBEND!
2010 Dens:SUB Density(T,P,Ro,Mass)
2020    OPTION BASE 1
2030    COM Cc(3),Dat(25),Cp(4,3),Aw(15,15),A2w(15,15),X(15),U(15),Ks(15),Rate(15
2040    DIM Mwt(3)
2050    Mwt(1)=28! N2
2060    Mwt(2)=32! O2
2070    Mwt(3)=44! CO2
2080 ! CC(*) IS VECTOR OF MOL FRACTIONS, SO FOR 1 MOL:
2090    Mass=DOT(Cc,Mwt)
2100    R=8.3E+3! J/kmol K
2110    Vol=R*T/P
2120    Ro=Mass/Vol! kg/m3
2130  SUBEND!


2140 Darcy:SUB Darcy(T,Darcy)
2150    OPTION BASE 1
2160    COM Cc(3),Data(25),Cp(4,3),Aw(15,15),A2w(15,15),X(15),U(15),Ks(15),Rate(
2170    E=Data(3)
2180    D=Data(4)
2190    S=Data(5)
2200 ! T = TEMP K
2210 ! D = PARTICLE DIAM m
2220 ! E = VOIDAGE
2230 ! S = PARTICLE AREA/VOLUME
2240    CALL Viscosity(T,Mu)
2250    K=5
2260    Darcy=K*(1-E)^2*Mu*S^2/E^3
2270  SUBEND!
2280 Visc:SUB Viscosity(T,Mu)
2290 ! VISCOSITY OF AIR
2300 ! PERRY THIRD ED P 370
2310    C=114
2320    Mu0=.01709
2330    Mu=Mu0*(273.1+C)/(T+C)*(T/273.1)^1.5 ! IN cp FOR T IN K
2340    Mu=Mu/1000! IN kg/m s
2350  SUBEND!
2360 Delh:SUB H_react(T,Delh)
2370 ! Subroutine to calculate Delta H reaction
2380    OPTION BASE 1
2400    Delh=3.E+8
2580  SUBEND!
2590 Prnt:SUB Print(Ta,Fr,Gg,Bi0,Bi1)
2600 ! Subroutine to print 'constants'
2610    PRINT RPT$("
                  ",1);"T average=";PROUND(Ta,-2);"K"
2620    PRINT "DARCY'S CONSTANT=";INT(Fr+.5);"kg/m^2/s" !?
2630    PRINT "FLOWRATE=";Gg;"kmol/m^2/s"
2640    PRINT "BI0=";Bi0,"BI1=";Bi1
2650  SUBEND!
```

```
2660 02:SUB Newo2(Y(*),Th(*))
2670 ! Calculates oxygen profile using backward differences
2680    OPTION BASE 1
2690    COM Cc(3),Data(25),Cp(4,3),Aw(15,15),A2w(15,15),X(15),U(15),Ks(15),Rat
2700    L=Data(11)
2710    Delx=Data(17)
2720    N1=Data(16)
2730    Dif=Data(20)
2740    G=Data(18)!Flowrate
2750    Ti=Data(14)
2760    Drho=Data(25)
2770    S=Data(5)
2780    E=Data(3)
2790    FOR I=1 TO N1
2800       T=Th(I)*Ti
2810       CALL React(T,Ratei,Ks(I),U(I))
2820       IF I=1 THEN 2850
2830       Delx=(X(I)-X(I-1))/Dif
2840       Y(I)=Y(I-1)/(1+Delx*Ratei*L/G)
2850       U(I)=U(I)+Ratei*Y(I)/(S*(1-E)*Drho)
2860    NEXT I
2870  SUBEND!
2880 Func:SUB Func(Dydt,Y(*),Ix,Yo2(*))
2890 ! Subroutine to calculate dY/dt
2900    OPTION BASE 1
2910    COM Cc(3),Data(25),Cp(4,3),Aw(15,15),A2w(15,15),X(15),U(15),Ks(15),Rat
2920    Ti=Data(14)
2930    L=Data(11)
2940    C=Data(13)
2950    Ke=Data(7)
2960    G=Data(18)
2970    N1=Data(16)
2980    Dif=Data(20)
2990    T=Y(Ix)*Ti
3000    CALL Cp(T,Cpav)
3010    CALL H_react(T,Delh)
3020    CALL React(T,Ratei,Ks(Ix),U(Ix))
3030    Rate(Ix)=Ratei
3040    A=G*Cpav*L/Ke
3050    B=Delh*Ratei*L*L*Yo2(Ix)/(Ti*Ke)
3060    CALL Deriv(Y(*),Ix,Dydx,D2ydx2)
3070    Dydt=Dif*Dif*D2ydx2-A*Dif*Dydx+B-C*(Y(Ix)-1)
3080  SUBEND!
3090 Deriv:SUB Deriv(Y(*),Ix,Dydx,D2ydx2)
3100 ! Derivatives of Y by calculation at the roots of the
3110 ! shifted Legendre polynomial of order N1
3120    OPTION BASE 1
3130    COM Cc(3),Data(25),Cp(4,3),Aw(15,15),A2w(15,15),X(15),U(15),Ks(15),Rate(1
3140    N1=Data(16)
3150    Dydx=0
3160    D2ydx2=0
3170    FOR J=1 TO N1
3180       Dydx=Dydx+Aw(Ix,J)*Y(J)
3190       D2ydx2=D2ydx2+A2w(Ix,J)*Y(J)
3200    NEXT J
3210  SUBEND!
```

```
3220 Bvals:SUB Bvals(Y(*))
3230 ! Subroutine to calculate the end temperatures
3240    OPTION BASE 1
3250    COM Cc(3),Data(25),Cp(4,3),Aw(15,15),A2w(15,15),X(15),U(15),K<(15),Rat<(
3260    Ke=Data(7)
3270    Msig=Data(8)
3280    L=Data(11)
3290    Ti=Data(14)
3300    Df=Data(15)
3310    N1=Data(16)
3320    Diff=Data(20)
3330    Gg=Data(18)
3340    T0=Y(1)
3350    Te=Y(N1)
3360 Again:CALL Cp(T0*Ti,Cpav)
3370    Af=Gg*Cpav*L/Ke
3380    Bi0=Msig*(T0+1)*(T0*T0+1)
3390    Bi1=Msig*(Te+1)*(Te*Te+1)
3400    S1=0
3410    S2=0
3420    FOR J=2 TO N1-1
3430      S1=S1+Aw(1,J)*Y(J)
3440      S2=S2+Aw(N1,J)*Y(J)
3450    NEXT J
3460    A1=(Bi0+Af)/Diff
3470    A2=Aw(N1,N1)+Bi1/Diff
3480    Numer=A1+Df/Diff+S1+Aw(1,N1)*(Bi1/Diff-S2)/A2
3490    Den=A1+Aw(1,N1)*Aw(N1,1)/A2-Aw(1,1)
3500    T01=Numer/Den
3501    IF T01<1 THEN T01=1
3510    Te1=(Bi1/Diff-S2-Aw(N1,1)*T01)/A2
3511    IF Te1<1 THEN Te1=1
3520    Dif1=ABS(T01-T0)
3530    Dif2=ABS(Te1-Te)
3540    T0=.5*(T01+T0)
3550    Te=.5*(Te1+Te)
3560 ! Check for convergence of the two end temperatures
3570    IF (Dif1>1.E-3) OR (Dif2>1.E-3) THEN Again
3580    Y(1)=T0
3590    Y(N1)=Te
3600 ! Write the Biot numbers into the matrix Data for passing back
3610    Data(21)=Bi0
3620    Data(22)=Bi1
3630  SUBEND!
```

```
3220 Bvals:SUB Bvals(Y(*))
3230 ! Subroutine to calculate the end temperatures
3240    OPTION BASE 1
3250    COM Cc(3),Data(25),Cp(4,3),Aw(15,15),A2w(15,15),X(15),U(15),K<(15),Rate((
3260    Ke=Data(7)
3270    Msig=Data(8)
3280    L=Data(11)
3290    Ti=Data(14)
3300    Df=Data(15)
3310    N1=Data(16)
3320    Diff=Data(20)
3330    Gg=Data(18)
3340    T0=Y(1)
3350    Te=Y(N1)
3360 Again:CALL Cp(T0*Ti,Cpav)
3370    Af=Gg*Cpav*L/Ke
3380    Bi0=Msig*(T0+1)*(T0*T0+1)
3390    Bi1=Msig*(Te+1)*(Te*Te+1)
3400    S1=0
3410    S2=0
3420    FOR J=2 TO N1-1
3430      S1=S1+Aw(1,J)*Y(J)
3440      S2=S2+Aw(N1,J)*Y(J)
3450    NEXT J
3460    A1=(Bi0+Af)/Diff
3470    A2=Aw(N1,N1)+Bi1/Diff
3480    Numer=A1+Df/Diff+S1+Aw(1,N1)*(Bi1/Diff-S2)/A2
3490    Den=A1+Aw(1,N1)*Aw(N1,1)/A2-Aw(1,1)
3500    T01=Numer/Den
3501    IF T01<1 THEN T01=1
3510    Te1=(Bi1/Diff-S2-Aw(N1,1)*T01)/A2
3511    IF Te1<1 THEN Te1=1
3520    Dif1=ABS(T01-T0)
3530    Dif2=ABS(Te1-Te)
3540    T0=.5*(T01+T0)
3550    Te=.5*(Te1+Te)
3560 ! Check for convergence of the two end temperatures
3570    IF (Dif1)1.E-3) OR (Dif2)1.E-3) THEN Again
3580    Y(1)=T0
3590    Y(N1)=Te
3600 ! Write the Biot numbers into the matrix Data for passing back
3610    Data(21)=Bi0
3620    Data(22)=Bi1
3630  SUBEND!
```

```
3640 March:SUB March(Y(*),Yo2(*),Deltau)
3650 ! Marching forward using 4th order Runge Kutta
3660    OPTION BASE 1
3670    COM Cc(3),Data(25),Cp(4,3),Aw(15,15),A2w(15,15),X(15),U(15),Ks(15),Rate
3680    DIM Z(15),Dy(15)
3690    N1=Data(16)
3700    REDIM Z(N1),Dy(N1)
3710    CALL Bvals(Y(*))
3720    FOR I=2 TO N1-1
3730      CALL Func(Dt,Y(*),I,Yo2(*))
3740      Yk=Deltau*Dt
3750      Dy(I)=Yk
3760      Z(I)=Y(I)+Yk/2
3770    NEXT I
3780    Z(1)=Y(1)
3790    Z(N1)=Y(N1)
3800    FOR I=2 TO N1-1
3810      CALL Func(Dt,Z(*),I,Yo2(*))
3820      Yk=Deltau*Dt
3830      Dy(I)=Dy(I)+2*Yk
3840      Z(I)=Y(I)+Yk/2
3850    NEXT I
3860    FOR I=2 TO N1-1
3870      CALL Func(Dt,Z(*),I,Yo2(*))
3880      Yk=Deltau*Dt
3890      Dy(I)=Dy(I)+2*Yk
3900      Z(I)=Y(I)+Yk
3910    NEXT I
3920    FOR I=2 TO N1-1
3930      CALL Func(Dt,Z(*),I,Yo2(*))
3940      Yk=Deltau*Dt
3950      Dy(I)=(Dy(I)+Yk)/6
3960      Y(I)=Y(I)+Dy(I)
3970    NEXT I
3980    Y(1)=Z(1)
3990    Y(N1)=Z(N1)
4000  SUBEND!
4010 React:SUB React(T,Rate,Ks,U)
4020    OPTION BASE 1
4030 ! Rate of oxidation for unity O2 mole fraction
4040    COM Cc(3),Data(25),Cp(4,3),Aw(15,15),A2w(15,15),X(15),Ui(15),Ksi(15),Rate
4050    R=Data(2)
4060    S=Data(5)
4070    P=Data(6)
4080    E=Data(3)
4090    K0=Data(9)
4100    Eor=Data(10)
4110    Ks=K0*EXP(-Eor/T)
4120    Rate=P*(1-E)*S/(R*T)/(1/Ks+U)
4130  SUBEND!
```

```
4140 March2:SUB March2(Y(*),Yo2(*),Deltau)
4150 ! Marching using forward differences
4160    OPTION BASE 1
4170    COM Cc(3),Data(25),Cp(4,3),Aw(15,15),A2w(15,15),X(15),Ui(15),Ks(15),Rat
4180    DIM Z(15)
4190    N1=Data(16)
4200    REDIM Z(N1)
4210    CALL Bvals(Y(*))
4220    Z(1)=Y(1)
4230    Z(N1)=Y(N1)
4240    FOR I=2 TO N1-1
4250      CALL Func(Dt,Y(*),I,Yo2(*))
4260      Z(I)=Y(I)+Dt*Deltau
4270    NEXT I
4280    MAT Y= Z
4290  SUBEND!
4300 Tav:SUB Tav(Y(*),Ta)
4310 ! Average temperature using trapezium rule
4320    OPTION BASE 1
4330    COM Cc(3),Data(25),Cp(4,3),Aw(15,15),A2w(15,15),X(15),U(15),Ks(15),Rate
4340    N=Data(16)
4350    Ta=0
4360    FOR I=1 TO N-1
4370      Ta=Ta+(Y(I)+Y(I+1))*(X(I+1)-X(I))/2
4380    NEXT I
4390  SUBEND!
4400 Record:SUB Record(N$,T(*),Z(*),Tim(*),Lj,N1)
4410 ! Subroutine to record profile on tape for plotting
4420    OPTION BASE 1
4430    GOTO 4480
4440    INPUT "T,X OR B?",A$
4450    INPUT "TMIN IN KELVIN?",Tmin
4460    INPUT "TMAX IN KELVIN?",Tmax
4470    IF A$="T" THEN GOTO Time
4480    A$="X"
4490    Tmin=300
4500    Tmax=320
4510    Nrec=INT((12+2*(1+N1)*(Lj+1))/32)+1!Number of records
4520    CREATE BDAT N$,Nrec
4530    ASSIGN @F1 TO N$
4540    OUTPUT @F1;INT(Lj+1)          !Number of curves
4580    FOR J=1 TO Lj+1       !Now the temperature profiles are stored
4590      OUTPUT @F1;INT(N1)
4600      FOR I=1 TO N1
4610        OUTPUT @F1;Z(I),T(I,J)
4620      NEXT I
4630    NEXT J
4640    ASSIGN @F1 TO *
4650    IF A$="X" THEN SUBEXIT
4660 !Time: CREATE N$&"T",Nrec
4670    ASSIGN @F2 TO N$&"T"
4680    OUTPUT @F2;N1+1
4690    OUTPUT @F2;2
4700    OUTPUT @F2;0,Tmin
4710    OUTPUT @F2;Tim(Lj+1),Tmax
4720    FOR I=1 TO N1
4730      OUTPUT @F2;Lj+1
4740      FOR J=1 TO Lj+1
4750        OUTPUT @F2;Tim(J),T(I,J)
4760      NEXT J
4770    NEXT I
4780    ASSIGN @F2 TO *
4790  SUBEND!
```

REFERENCES

ARGO, W.B., & Smith, J.M., Heat transfer in packed beds - Prediction of radial rates in gas-solid beds. Chem. Eng. Prog., 49, 443 (1953)

ASTM C177, ASTM Stand. (1963)

BADZIOCH, S., Gregory, D.R., & Field, M.A., Investigation of the thermal conductivity and thermal diffusivity of coal. Fuel, 43(4), 267 (1964)

BALAKOTAIAH, V., & Luss, D., Global Analysis of the Multiplicity Features of Multi-Reaction Lumped-Parameter Systems. Chem. Eng. Sci. 39(5), 865 (1984)

BELLMAN, R., Kashef, B.G., & Casti, J., Differential quadrature: A technique for the rapid solution of non-linear partial differential equatins. Journal of Computational Physics 10, 40 (1972)

BEJAN, A., Natural convection in an infinite porous medium with a concentrated heat source. J. Fluid Mech. 89(1) 97 (1978)

BEVERIDGE, G.S.G & Haughey, D.P., Axial Heat Transfer In Packed Beds. Stagnant Beds Between 20 And 750 °C.
Int. J. Mass Heat Transfer, 14, 1093 (1971)

BEVERIDGE, G.S.G & Haughey, D.P., Axial Heat Transfer In Packed Beds. Gas Flow Through Beds Between 20 and 650 °C.
Int. J. Mass Heat Transfer, 15, 953 (1972)

BHATTACHARRYA, K.K., Effect of humidity on oxidation of coal and its spontaneous heatng. J. Mines Metal Fuel, 18(1), 5 (1970)

BIRD, R.B., Stewart, W.E. & Lightfoot, E.N., Transport Phenomena, Wiley, New York (1960)

BOSWORTH, R.C.L., Heat Transfer Phenomena, Wiley, New York (1952)

BROOKS, K.S. & Woods, E.G.K., Thermal Conductivity of a Coal Bed Laboratory Report, Department of Chemical Engineering, University of the Witwatersrand (1980)

BS 874, British Standards Institution , London (1956)

CARSLAW, H.S., & Jager, J.C., Conduction of Heat in Solids. 3rd Ed., Clarendon Press, Oxford (1959)

CHEN, J.C. & Churchill, S.W., Radiant heat transfer in packed beds. AIChE J. 9, 35 (1963)

DEISSLER, R.G. & Eian, C.S., Investigation of effective thermal conductivities of powders. N.A.C.A., Washington, RME52C05 (1952)

ECKERT, E.R.G., & Drake, R.M., Analysis of Heat & Mass Transfer, Mcgraw-Hill, New York (1972)

EDWARDS, J.C., Mathematical modelling of spontaneous combustion of coal. Presented at the 112th Annual meeting of A.I.M>E., (1983)

GIJBELS M.R., & Bruining J., Spontaneous ignition time of underground coal - Estimation from oxidation rates determined in the laboratory. Erdoel und Kohle, 8, 376, (1982)

GUNEY, M. & Hodges, D.J., Adiabatic apparatus designed to study self-heating rates of coal. Chem & Industry, 42, 1429 (1968)

GUNEY, M., Oxidation and spontaneous heating of coal. J. of Pure And Applied Sciences, 5, 1, (1972)

GUNN, D.J. & Khalid, M., Thermal dispersion and wall heat transfer in packed beds. Chem. Eng. Sci., 30, 261 (1975)

KIBRIA, J., Effect of properties and enviromental variables on self heating tendencies of lignite. M.Sc. Thesis, University of North Dakota (1972)

KRAMERS, H. & Westerterp, K., Elements of Chemical Reactor Design & Operation, Academic Press, New York (1963)

KUNII, D. & Smith, J.M., Heat Transfer characteristics of porous rocks. AIChE J., 6(1), 71, (1960)

LAPWOOD, E.R., Convection of a fluid in a porous medium. Proc. Cam. Phil. Soc., 44, 508, (1948)

LEVENSPIEL, O., Chemical Reaction Engineering, Wiley, New York (1962)

LUSS, D., Sufficient Conditions for Uniqueness of the Steady State Solutions in Distributed Parameter Systems. Chem. Eng. Sci., 23, 1249, (1968)

LUSS, D. & Amundson, N.R., Uniqueness of the Steady State Solutions For Chemical Reaction Occcurring in a Catalyst Particle or in a Tubular Reactor with Axial Diffusion. Chem. Eng. Sci. 22, 253, (1967)

MURTAGH, B.A., The spontaneous heating of coal. M.Eng Thesis, Department of Chemical Engineering, University of Canterbury (1966)

NORDON, P., Model for the self-heating reaction of coal and char. Fuel, 58, 456 (1979)

NORDON, P., Young, B.C. & Bainbridge, N.W., The rate of oxidation of char and coal in relation to their tendency to self-heat. Fuel, 58, 443 (1979)

PERRY, R.H., & Chilton, C.H., editors of Chemical Engineer's Handbook, 5th edition, Mcgraw Hill, Tokyo (1973)

SCHMIDT, L.D., in Chemistry of Coal Utilization, Wiley, New York (1945)

SCHOTTE, W., Thermal conductivity of packed beds. AIChE J. 3, 373 (1960)

SONDREAL, E.A. & Ellman, R.C., Laboratory Determination of factors affecting storage of North Dakota Lignite. Bureau of Mines Report. R.I. 7887, (1974)

TYE, R.P., Thermal Conductivity, Academic Press, London (1969)

VAN DOORNUM, G.A.W., The spontaneous heating of coal. J. Inst Fuel, 27, 482 (1954)

VAN KREVELEN, D.W., Coal, 2nd Edit., Elsevier, Amsterdam, (1981)

WEBER, J.E, Convection in a porous medium with horizontal and vertical temperature gradients. Int. J. Heat Mass Transfer, 17(2), 241 (1974)

Yagi, S. & Kunii, D., Studies on effective thermal conductivities in packed beds AIChE J., 3, 373 (1957)

YOUNG, B.D., Two-dimensional conduction and convection in a porous medium: Application to spontaneous combustion of coal. M.Sc. Thesis, University of the Witwatersrand, Johannesburg, South Africa (1985)

YOUNG, M.L., Heat transfer in chromite ores. M.Sc. Thesis, University of the Witwatersrand, Johannesburg, South Africa (1975)

A SIMPLIFIED MODEL FOR SPONTANEOUS COMBUSTION IN COAL STOCKPILES

Kevin Seth Brooks

A thesis submitted to the Faculty of Engineering, University of the Witwatersrand, Johannesburg, in fulfilment of the requirements for the degree of Doctor of Philosophy.

July 1985

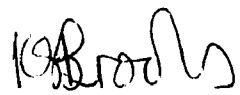
Johannesburg

NK 6717/1

DECLARATION

The work described in this thesis was carried out in the Department of Chemical Engineering of the University of the Witwatersrand, Johannesburg, and is the original and independent work of the author except where specifically acknowledged in the text.

No part of the thesis has previously been submitted for a degree in the University of the Witwatersrand, or is being submitted to any other University.



K S BROOKS

July 1985

ABSTRACT

Based on a study of the fundamental processes of heat,mass and momentum transfer, a one-dimensional model to predict the behaviour of coal dumps with respect to spontaneous combustion is presented.

Heat transfer within the dump is modelled using an effective thermal conductivity. This quantity has been measured for a typical coal sample using a guarded hot ring apparatus. Mass transfer is considered to occur by natural convection and wind pressure. Diffusion is shown to be unimportant except for very fine material.

A shrinking-core model for the low temperature oxidation of coal is proposed; the model explains the fact that the coal reactivity decreases with time. The effects of moisture on the coal reactivity are neglected due to lack of data.

Estimates of the parameters required for the model have been obtained experimentally. The equations are solved analytically in both the steady and unsteady-state under the assumption of unchanging rate constant. A numerical method has been used to solve the equations without this assumption.

It has been shown that coal dumps may be classified as either safe, unsafe or conditionally safe. Safe coal dumps are either oxygen limited or heat transfer limited. The former is the case for fine reactive coal; the high reactivity of the coal means that all the oxygen reacts close to the surface where the heat produced can easily be dissipated. The latter is the case for for coarse, unreactive material; although the oxygen is freely available throughout the dump, the reactivity per unit volume of the coal is sufficiently low such that heat produced can be dissipated without the temperature rising significantly.

It is shown that the important parameters in predicting the behaviour of a coal bed are the particle size distribution of the coal, the bed voidage and the reaction rate parameters. The effect on the temperature in a coal bed of changing each of parameter is presented graphically. The unsteady-state behaviour of the model shows that the time taken to reach a certain critical temperature may be the best way of arriving at a safe stockpiling time.

For my wife, Ilana:

A good typist and an even better cook

ACKNOWLEDGEMENTS

I should like to express my gratitude to my supervisor, Professor David Glasser, for his help, interest and encouragement during the course of this work.

As well as being a good friend, Mr (now Dr) Michael Itay performed the experimental work described in Chapter 2.

Mr L Schwartz and Mr A C Harris were of great assistance in the building of experimental apparatus.

The work described in this thesis was made possible by the financial assistance of the Iron and Steel Corporation of South Africa.

CONTENTS

	Page
DECLARATION	ii
ABSTRACT	iii
DEDICATION	iv
ACKNOWLEDGEMENTS	v
CONTENTS	vi
LIST OF FIGURES	x
LIST OF TABLES	xii
LIST OF SYMBOLS	xiii
1. AN OVERVIEW OF SPONTANEOUS COMBUSTION	1
1.1 Introduction	1
1.2 Previous Investigations into Spontaneous Combustion	3
1.3 Transport in a Coal Dump	6
1.4 The Chemical Reactivity of Coal	6
1.4.1 Reaction between Coal and Water	7
1.4.2 Low Temperature Oxidation of Coal	8
1.5 Heat Transfer within a Coal Dump	12
1.6 A Mathematical Model for Spontaneous Combustion	12
1.7 Experimental Investigation	13
1.8 Results and Conclusions	13
2. ANALYSIS OF SUGGESTED MECHANISMS FOR INGRESS OF REACTANTS	14
2.1 Introduction	14
2.2 Natural Convection and Wind Pressure	14
2.3 Analysis of Molecular Diffusion	18
2.4 Barometric Breathing	21
2.5 Thermal Breathing	22
2.6 Conclusions	23
3. THEORETICAL MODELS FOR HEAT TRANSFER IN PACKED BEDS	25
3.1 Introduction	25
3.2 Mechanisms of Energy Transfer in Packed Beds	25
3.3 Describing the Overall Energy Transfer in a Packed Bed	26

3.4 Models for Energy Transfer in which only conduction is considered 26

3.5 Models for Energy Transfer in which conduction and radiation are considered 31

3.5.1 Conditions under which radiation in a packed bed is likely to be significant 33

3.6 Theoretical Studies of Natural Convection 34

3.7 The Effect of flow on Energy Transfer in a Packed Bed 37

3.8 Conclusions 37

4. MEASUREMENT OF THE EFFECTIVE THERMAL CONDUCTIVITY OF A PACKED BED OF COAL 39

4.1 Introduction 39

4.2 Theory of the Measurement of Thermal Conductivity 39

4.3 Steady-state Methods for Measuring Thermal Conductivity 40

4.3.1 Measurements in the rectangular system 41

4.3.2 Measurements in the cylindrical system 43

4.3.3 Measurements in the spherical system 44

4.4 Unsteady-state or Dynamic Methods 44

4.5 Choice of Measurement Method for Packed Bed of Coal 45

4.6 Design and Construction of Guarded Hot Ring Apparatus 46

4.6.1 General Design Considerations 46

4.6.2 Heat Sinks 46

4.6.3 Heating Elements 48

4.6.4 Outer Containing Vessel 48

4.6.5 Water supply to heat sinks 50

4.6.6 Measurement Techniques 50

4.7 Experimental Procedure 51

4.8 Results and Discussion 52

5. MATHEMATICAL MODELLING OF A ONE-DIMENSIONAL ANALOGUE OF A COAL DUMP 54

5.1 Introduction 54

5.2 Literature survey of mathematical models 54

5.3 A One-dimensional Analogue of a Coal Dump 61

5.4 Model Equations 63

5.5 Discussion of the Model Equations 65

5.6 Boundary and Initial Conditions 66

6. SIMPLIFICATION OF THE MODEL EQUATIONS AND THEIR SOLUTION 67

6.1 Introduction 67
6.2 The Steady-State form of the Equations 69
6.3 The Solution of the Unsteady-State Equations with a constant rate 71
6.4 A Numerical Method for Solving the Unsteady-State Equations 72

7. EXPERIMENTAL INVESTIGATION OF THE BEHAVIOUR OF A ONE-DIMENSIONAL ANALOGUE OF A COAL DUMP 75

7.1 Introduction 75
7.2 Experimental 75
7.3 Results 78
7.4 Discussion 81

8. RESULTS OF SOLVING THE MODEL EQUATIONS 82

8.1 Introduction 82
8.2 Steady-State Solution for constant r 82
8.2.1 The Character of the Solutions 83
8.2.2 Effect of varying the voidage 90
8.2.3 Effect of varying the pre-exponential Factor 92
8.2.4 Effect of varying the activation energy 94
8.2.5 Effect of different assumptions about the reactive surface area of coal 94
8.2.6 The Meaning of Particle Size 95
8.2.7 Effect of wind on maximum Temperature 98
8.2.8 Effect of Thermal Conductivity on maximum Temperature 98
8.2.9 Effect of Changing the Bed Length 98
8.3 Unsteady-State solutions for r constant 101
8.3.1 Introduction 101
8.3.2 The Character of the Solutions 101
8.3.3 Discussion 107
8.4 Results of solving the equations numerically 107
8.4.1 Introduction 107
8.4.2 Comparison Between the Numerical Method and the Analytical Method 108
8.5 Conclusions 110

9. CONCLUSIONS 111

Appendix 1 Derivation of a rate equation for the low temperature oxidation of coal 116

Appendix 2 Tabulation of measured thermal conductivities 120

Appendix 3 Derivation of model equations 122

Appendix 4 The continuum and pseudo steady-state assumptions 130

Appendix 5 The inclusion of a radial heat loss term in equation 6.1.4 132

Appendix 6 Explanation for the Instability of the Runge-Kutta algorithm 135

Appendix 7 Solution of equation 6.2.2 with r constant 136

Appendix 8 Solution of equation 6.1.5 with r constant 137

Appendix 9 Application of the method of lines to the solution of equation 6.1.5 140

Appendix 10 Results of chimney experiment 142

Appendix 11 Model Parameters used as base case 165

Appendix 12 Listing of computer programs 166

REFERENCES 194

LIST OF FIGURES

Figure		Page
1.1	Temperature, Oxygen and Carbon Dioxide Versus Time	9
3.1	Geometrical Conduction Models (Beveridge & Haughey, 1971)	28
4.1	Guarded hot ring apparatus - Heat sink	47
4.2	Guarded hot ring apparatus - Assembled apparatus	49
5.1	Streamlines in a packed bed containing a line source	62
7.1	Chimney experiment - Apparatus	76
7.2	Chimney experiment - Fitting heat transfer coefficients	79
7.3	Chimney experiment - Fitting ageing run 1	79
7.4	Chimney experiment - Fitting ageing run 2	80
7.5	Chimney experiment - Fitting ignition runs	80
8.1	LHS and RHS of equation 8.2 as a function of θ	86
8.2	Locus of solutions to equation 8.2	86
8.3	Stable and unstable solutions for the base-case	91
8.4	Effect of varying voidage on the maximum temperature	91
8.5	Effect of varying the pre-exponential factor on the maximum temperature	93
8.6	Effect of varying the activation energy on the maximum temperature	93
8.7	Pre-exponential factor versus particle size for the two cases considered	96
8.8	Effect of different assumptions about surface area on the maximum temperature	96
8.9	Effect of wind on the maximum temperature	99
8.10	Effect of varying bed thermal conductivity on the maximum temperature	99
8.11	Effect of varying bed length on the maximum temperature	100
8.12	Temperature-time curves in the centre of a coal bed for different initial temperatures	102
8.13	Temperature profiles in a coal bed Particle size 10 mm - Analytical solution	102
8.14	Temperature-time behaviour at bed centre Particle size 6 mm - Analytical solution	106
8.15	Temperature profiles in a coal bed Particle size 10 mm - Numerical Method	106

Figure		Page
8.16	Temperature profiles with ignition Particle size 2 mm - 5 m/s wind - Numerical method	109
8.17	Cross plot of Figure 8.16 at bed centre	109
A1.1	Simplified coal particle geometry	116
A2.1	Measured thermal conductivities versus difference between guard and main heater temperatures	121
A3.1	Differential element of a coal bed	122
A5.1	Differential element in the form of a ring	132

LIST OF TABLES

Table		Page
2.1	Molar Flowrates for Various Particle Sizes	17
2.2	Comparison of Molecular Diffusion and Convection	21
5.1	Values of ΔT L Required for Ra = 4 π^2	59
5.2	Unknowns in the model equations	65
8.1	Particle Size Distribution for a typical sample	97
8.2	Model Parameters for Figure 8.12	101
8.3	The Quantity 'a' For Various Particle Sizes	105
A2.1	Measured Thermal Conductivities	120

LIST OF SYMBOLS

a: Dimensionless quantity in equation 6.1.4

a': Fitting constant in equation 5.2.1

a_{ij}: Weighting coefficients for first derivatives

A: Area

A': Fitting constant in equation 5.2.1

A^*: Arrhenius pre-exponential factor

$\underline{A}$: Matrix of coefficeints a_{ij}

A_o: Pre-exponential factor in equation 5.2.8

b: Dimensionless quantity in equation 6.1.4

b_{ij}: Weighting coefficients for second derivatives

B: Elovich constant

$\underline{B}$: Matrix of coefficients b_{ij}

Bi_o: Biot number at $X = 0$

Bi_1: Biot number at $X = 1$

Bi_2: $Bi_o + a/2$

Bi_3: $Bi_1 + a/2$

c: Heat loss coefficient

$\bar{c}$: Heat capacity per unit mass

$\bar{c}_s$: Heat capacity per unit mass of solid

$\bar{c}_w$: Heat capacity per unit mass of liquid water

$\bar{c}_j$: Heat capacity per unit mass of component j in the solid

$\bar{c}_b$: Heat capacity per unit mass of bed

$\hat{c}$: Molar heat capacity of the gas

$\hat{c}_i$: Molar heat capacity of component i in the gas

C_p: Specific heat capacity

C: Oxygen concentration

C_s: Oxygen concentration at reaction surface

C_1: Integration constant

C_2: Integration constant

C_3: Integration constant

D: Molecular diffusion coefficient

D_e: Effective diffusivity of oxycoal

D_p: Particle diameter

E: Activation energy

f: d'Arcy's law constant

f_j: Mass fraction of component j in the solid

g: Acceleration due to gravity

$g(X)$: Auxilary temperature function

G: Molar flowrate per unit area

h_o, h_1: Heat transfer coefficients

h_R: Heat transfer coefficient on radial surface

$\hat{H}$: molar enthalpy of gas

$\hat{H}_i$: molar enthalpy of component i in the gas

$\bar{H}$: Solid enthalpy per unit mass

$\bar{H}_j$: Enthalpy per unit mass of component j in solid

I_m: Main heater current

J_i: ith order Bessel function of the first kind

k: Thermal Conductivity

k_g: Gas thermal conductivity

k_s: Solid thermal conductivity

k_b: Bed thermal conductivity

$k_{b,x}$: Bed thermal conductivity in axial direction

$k_{b,R}$: Bed thermal conductivity in radial direction

k_o: Pre-exponential factor

k_r: $k_o \exp(-E/(RT))$

l: sample thickness

l_1, l_2: Distances between heater and sinks (equation 4.6.2)

L: Bed length or height

L_e: Effective particle length

m: Moles of oxygen per moles of nitrogen in the gas

m: Water flowrate

M: number of components in the solid phase

M_c: Mass of coal

M_w: Mass of absorbed water in the coal

M_p: Percent moisture in the coal

M_n: n th root of the equation $J_o(M_n)=0$

M': Dimensionless quantity defined by equation 5.2.3

n: Order of the Legendre polynomial P_n

N: Number of components in the gas phase

N': Dimensionless quantity defined by equation 5.2.4

p_j: Rate of Formation per unit bed volume of component j in the solid

P: Pressure

P_∞: ambient pressure

$\hat{P}$: $P - P_\infty$

$P_n(X)$: n th order Legendre polynomial

$P_n^*(X)$: n th order shifted Legendre polynomial

q: Amount of O_2 taken up per unit mass of coal

q_g: Flux in gas

q_s: Flux in solid

q': Source term in Diffusion Equation

Q': Rate of energy transfer by Conduction

Q_c: Rate of Convection from Solid to Gas

Q: Rate of energy input

Q_q: Rate of Energy absorption

Q_R: Radial Flux

Q_x: Axial Flux

r_i: Rate of formation per unit bed volume of i in the gas phase

r_o: Rate of oxidation at T_∞ for fresh coal

r: Rate of oxygen adsorption per unit bed volume for unity mole fraction oxygen

R: Gas constant

r: Radial co-ordinate (Chapter 4)

R: Spherical co-ordinate (Chapter 4)

R: Radial Distance (Appendix 5)

R_o: Bed Radius (Appendix 5)

S_t: Total reactive surface per particle volume

S: Total external surface per particle volume

S_m: External surface area per unit mass

S': Total surface area for reaction

t: Time

T: Temperature

T_∞: Ambient Temperature

T_g: Gas Temperature

T_s: Solid temperature

T': Temperature averaged radially

T_∞: Ambient Temperature

T_{av}: Average temperature = $L/\int_0^L T^{-1}dx$

$T_o(X)$: Initial temperature profile

U: Flow velocity

U_g: Gas internal energy

U_s: Solid internal energy

$\hat{U}$: Molar internal energy of the gas

$\bar{U}_s$: Internal energy of the solid per unit mass

$u(X,\tau)$: Auxilary temperature function (equation A8.2)

V: Wind velocity

v: Temperature above ambient

$v(X,\tau)$: Auxilary temperature function (equation 6.3.2)

V_b: Bed volume

V_p: Particle volume

V_m: Main heater voltage
x: Distance along bed
X: Dimensionless distance = x/L
y: Rectangular co-ordinate (Chapter 4)
y_i: Mole fraction of i in the gas phase
y_o: Mole fraction of oxygen at X=0
y: Mole fraction oxygen in the gas phase
z: Rectangular co-ordinate (Chapter 4)
z: Thickness of oxycoal layer
Z: Fractional conversion of coal
$Z_n(X)$: See equaiton 6.3.3

Greek Symbols

α: Fitting constant in equation 5.2.1
β: Roots of equation 6.3.4
γ_1,γ_2: $((a\pm(a^2+4C))^{1/2})/2$
γ_3: $-rL/G$
ΔH_w: Latent heat + heat of wetting
ΔH_r^i: Enthalpy of reaction
ΔH_r: Enthalpy of reaction for oxygen adsorption
ΔT: Temperature rise or temperature difference
ϵ: Voidage
η: Tortuosity factor
θ: Dimensionless temperature
$\theta_o(X)$: Initial dimensionless temperature profile
$\theta_{ss}(X)$: Steady-state dimensionless temperature profile
κ: Thermal diffusivity
μ: Gas viscosity
ν: D P/(R T)
ξ: $1/\tau'$
ρ: Density
ρ_s: Solid density
ρ_b: Bed density
ρ_g: Molar density of gas
ρ_∞: Density of gas at T_∞,P_∞
ρ_m: Molar density of oxycoal
σ: Stefan-Boltzmann constant
τ: Dimensionless time
τ_o: Period of oscillation
τ': Time constant for heat loss (Equation 5.2.5)
$\phi(X)$: Auxilary temperature function (equation A8.2)
ϕ_1,ϕ_2: Fitting constants in equation 8.1
τ_d: Time constant for equilibration of gas and solid

temperatures

τ_c: Time constant for conduction

τ_f: Time constant for flow

τ_p: Time constant for pressure change

1. AN OVERVIEW OF SPONTANEOUS COMBUSTION OF COAL

1.1 Introduction

The need to stockpile coal arises in many situations, most importantly in the following fields:

a) The generation of electricity

b) The coal mining industry

c) Coal transport

d) Steel making

It is well known that certain types of coal, when stockpiled, are liable to spontaneous combustion. Coal may undergo spontaneos combustion in many storage situations, among them:

a) In coal dumps

b) Underground

c) In the holds of ships

d) In storage silos or bunkers

The work described in this thesis concerns mainly spontaneous combustion as it relates to coal dumps. However, many of the conclusions reached are of significance, to a greater or lesser extent, in all of the storage situations mentioned above.

Spontaneous combustion of coal may lead to some or all of the following problems:

a) Loss of all or part of the coal dump. If the coal dump is a large one, as is the case at many mines and power stations, the economic effects of spontaneous combustion may well be disastrous.

b) Pollution. A burning coal dump presents a very real environmental problem, with noxious gases and particulate matter

being introduced into the atmosphere. This can present serious problems to communities in the vicinity of the burning dump.

c) Danger to human lives. Burning coal dumps can give rise to a dangerously high level of carbon monoxide, which may affect people working in the vicinity. Similarly, fires in ship's holds or underground can be extremely dangerous as well as costly.

Methods have been suggested, and are in use, for making coal dumps less liable to spontaneous combustion. These methods include compacting the dump, covering the dump with tar or sand, or spraying a cement-like substance on the surface of the dump. In addition much discussion has revolved around the monitoring of coal dumps, in order to obtain early warning of potential problems. Temperature monitoring by means of thermocouples, the taking of infra-red photographs and gas sampling have all been suggested and used as means of monitoring coal dumps.

One of the problems with the methods discussed above is that they tend to be costly, and the economic justification for their use is often not immediately obvious. The reason for this is that the knowledge that has been obtained in the field of spontaneous combustion is largely empirical, being based on experience gained by people working in the field. Although this knowledge is exteremely valuable, it is not always of great use when new stockpiling situations arise, or when a new mine is opened and the newly mined coal's liability to spontaneous combustion is an unknown quantity.

It seems clear that what is required is a sound scientific analysis of spontaneous combustion, on which decisions as to stockpiling practice can be based. The aim of this thesis is to provide this analysis, by analyzing the fundamental processes occuring in a coal dump, and synthesizing their effects in a mathematical model. The model can then be used as a basis on which predicitions about the behaviour of a certain coal in a certain stockpiling situation can be made. Hopefully this will lead to the construction of stockpiles in which the chances of spontaneous combustion occuring are minimized.

1.2 Previous Investigations into Spontaneous Combustion

A comprehensive reviews of spontaneous combustion of coal has been presented by Itay (1984). The aim of this section is to provide a critical review in which the important facts that have emerged are summarised. These facts will then be further discussed.

Many workers have concerned themselves with oxidation of coal (Van Krevelen,1981) and the literature on the subject has been reviewed by Guney (1968). The main conclusions reached are

a) The oxidation of coal appears to be a chemisorption reaction at temperatures under 70 ^{o}C; oxygen is taken up without water or carbon dioxide being formed.

b) The enthalpy of reaction is of the order of 300 kJ per mole of oxygen adsorbed (Edwards, 1983 and Sondreal & Ellman, 1974). This may be compared with an enthalpy of reaction of 390 kJ/mole for the reaction

$$C(graphite) + O_2(g) = CO_2(g).$$

c) The rate of oxidation decreases with time i.e. the coal ages.

d) The reaction rate appears to be of order ½ to 1 with respect to the oxygen concentration.

A series of investigators have reported different activation energies for the oxidation; these discrepancies appear to be due to the various ranges of temperature covered.

Van Krevelen (1981) believed that the primary reaction of chemisorption of oxygen has a relatively low activation energy of approximately 3 - 4 Kcal/mole.

Above a temperature of 70 ^{o}C decomposition of the adsorption complex may occur, with an activation energy of approximatley 6.5 Kcal/mole. However, chemisoption of oxygen occurs up to a temperature of 350 ^{o}C.

Many other investigators, notably Guney (1972) and Bhattacharyya

(1970) have investigated the effect ot moisture in the coal and reacting gas. The absorption of water is, not surprisingly, associated with a large enthalpy of reaction. In addition it appears that the absorbed moisture in the coal plays a part in the oxidation reaction, for dry coal oxidises at a far lower rate than moist coal. However, the effect of moisture on self heating of coal is still a subject of intense debate, mainly because different investigators have reported different results. This appears to be due to different apparatus and analysis methods being used, as well as different sample preparation techniques (e.g. vacuum drying, oil drying and air drying all at room temperature or elevated temperatures).

One important point has emerged from the studies performed by Murtagh (1966) who used a computer simulation technique. His main conclusion is that at low temperature moisture transfer is the dominant heat transfer mechanism in a dump, but that spontaneous ignition does not occur when only moisture is considered. His explanation for this is that at about 100 ^{o}C inherent moisture is driven from the coal, causing a cooling. Since there can be no further absorption of water, the maximum temperature that can occur is approximately 100 ^{o}C. It should be pointed out that should a coal dump reach a temperature of 100 ^{o}C, then it might be well on the way to combustion, since the rate of oxidation could be very high at this temperature.

It thus appears from the literature that moisture effects, especially the absorption of water by dry coal, can lead to an increase in the temperature of a coal dump to the point where the rate of oxidation becomes appreciable. In this situation the coal dump could be at risk.

This conclusion has a important consequence when one considers spontaneous combustion underground as opposed to spontaneous combustion above ground. In the underground situation the coal is likely to be dry, especially if it is newly mined. In addition the humidity of the air in the mine is high. Thus underground spontaneous combustion could be largely triggered by moisture absorption. However, when considering coal stockpiles, it should be remembered that these are normally laid down with water to facilitate compaction. In addition the coal that is stockpiled has generally come from a washing plant, and is thus wet. Thus the effect of moisture on a newly laid down coal dump is likely

(1970) have investigated the effect ot moisture in the coal and reacting gas. The absorption of water is, not surprisingly, associated with a large enthalpy of reaction. In addition it appears that the absorbed moisture in the coal plays a part in the oxidation reaction, for dry coal oxidises at a far lower rate than moist coal. However, the effect of moisture on self heating of coal is still a subject of intense debate, mainly because different investigators have reported different results. This appears to be due to different apparatus and analysis methods being used, as well as different sample preparation techniques (e.g. vacuum drying, oil drying and air drying all at room temperature or elevated temperatures).

One important point has emerged from the studies performed by Murtagh (1966) who used a computer simulation technique. His main conclusion is that at low temperature moisture transfer is the dominant heat transfer mechanism in a dump, but that spontaneous ignition does not occur when only moisture is considered. His explanation for this is that at about 100 ^{o}C inherent moisture is driven from the coal, causing a cooling. Since there can be no further absorption of water, the maximum temperature that can occur is approximately 100 ^{o}C. It should be pointed out that should a coal dump reach a temperature of 100 ^{o}C, then it might be well on the way to combustion, since the rate of oxidation could be very high at this temperature.

It thus appears from the literature that moisture effects, especially the absorption of water by dry coal, can lead to an increase in the temperature of a coal dump to the point where the rate of oxidation becomes appreciable. In this situation the coal dump could be at risk.

This conclusion has a important consequence when one considers spontaneous combustion underground as opposed to spontaneous combustion above ground. In the underground situation the coal is likely to be dry, especially if it is newly mined. In addition the humidity of the air in the mine is high. Thus underground spontaneous combustion could be largely triggered by moisture absorption. However, when considering coal stockpiles, it should be remembered that these are normally laid down with water to facilitate compaction. In addition the coal that is stockpiled has generally come from a washing plant, and is thus wet. Thus the effect of moisture on a newly laid down coal dump is likely

to be a beneficial one i.e. the evaporation of water will cause cooling. However, should there be very dry conditions causing drying out of the coal, followed by humid conditions, moisture absorption may well occur.

It is neccessary to look at the other factors involved in spontaneous combustion. These have been shown by many investigators (Sondreal & Ellman, 1974, Nordon, 1979) to be:

a) Transport into the dump and
b) Heat transfer within the dump.

As many investigators have pointed out, the importance of these two effects should not be underestimated. No matter how reactive a given coal is it will not undergo spontaneous combustion if

a) The reactants cannot get to it or
b) The heat generated by reaction can be readily transferred out of the dump.

Investigators have previously used mathematical models, based on energy balances for a reacting bed of coal, to try and predict the onset of spontaneous combustion. Notable among these investigators are Van Doornum (1954), Murtagh (1966), Sondreal & Ellman (1974) and Nordon (1979). The work of Murtagh (1966) has been discussed, and the work of the other three investigators will be further discussed in section 5.2. It is shown that the models used by these investigators suffer from the shortcoming that the effect of natural convection is ignored. The justification for ignoring this effect has been based on conclusions drawn by these researchers from the work of Lapwood (1948). The validity of these conclusions will be discussed in section 5.2.

Having reviewed the literature on the subject of spontaneous combustion of coal, it is felt that three main areas of importance in predicting the behaviour of a coal dump have been identified.

They are:

a) Mechanisms whereby reactants such as oxygen and water are transported into a dump.

b) The chemical reactions that occur betwen coal and these reactants, in particular the thermal effects of these reactions.

c) Heat transfer within the dump.

These three areas will now be discussed separately.

1.3 Transport in a Coal Dump

Five mechanisms whereby reactants may be transported into a coal dump have been identified. They are:

a) Natural convection caused by self heating of the dump.

b) Wind pressure on the inclined surfaces of the dump which causes flow.

c) Molecular diffusion caused by concentration gradients.

d) Barometric breathing caused by changes in barometric pressure.

e) Thermal breathing caused by the daily variation in temperature.

In order to decide which, if any, of these mechanisms is the most important source of reactants to a coal dump it was felt necessary to derive simple models to describe each mechanism. These models give an idea of the order of magnitude of each of the effects and lead to important conclusions regarding which mechanisms may be neglected and which may not. A full discussion of these models is given in Chapter 2.

1.4 The Chemical Reactivity of Coal

Spontaneous combustion of coal occurs due to reaction between atmospheric gases and coal. The gases that are of importance are water vapour and oxygen. A discussion of the reactivity of coal towards these reactants follows.

1.4.1 Reaction between Coal and Water

Much experimental effort has been devoted to the elucidation of the effect of moisture on spontaneous combustion of coal. Nordon, Young & Bainbridge (1979) have pointed out that the effect of moisture on the self heating of coal is two-fold. Firstly absorbed water exerts a catalytic effect on the oxidation rate, and secondly there is a transient effect which occurs as moisture is absorbed or desorbed. This partly explains why so many apparently contradictory results in connection with the effect of gas and coal moisture on self heating of coal have been obtained, since confusion arises due to the different ways in which the coal is dried, and the coal and atmospheric moisture contents are reported.

The catalytic effect of coal moisture content on the oxidation rate is well documented in the literature. Sondreal & Ellman (1974) report oxidation rates of lignite as being proportional to

$$1 + 0.674\ M_p - 0.01634\ M_p^2$$

where M_p is the moisture content expressed in percent. This expression implies that the rate of oxidation is a maximum when M_p is equal to twenty percent. This value is close to the equilibrium moisture content of coal.

The second effect mentioned is the transient absorption and desorption of moisture. The heat effect associated with the absorption of moisture is the latent heat of vaporization plus the heat of wetting. The former has a value of 500 cal/g at 25 °C and the latter has been reported by Sondreal & Ellman (1974) to be of the order of 24 cal/g. A simple energy balance may be written to calculate the temperature rise due to absorption of moisture by dry coal.

1.4.1

$$M_c\ \bar{c}_b\ \Delta T = M_w\ \Delta H_w$$

where M_c = mass of coal
$\bar{c}_b$ = specific heat capacity of coal
ΔT = temperature rise
M_w = mass of water absorbed
ΔH_w = latent heat + heat of wetting

Therefore $\Delta T = \frac{M_w \Delta H_w}{M_c \bar{c}_b}$ 1.4.2

Assume $M_w/M_c = 0,05$ i.e the coal absorbs five percent of its mass of moisture. The specific heat of a typical coal is 0,25 cal/g/K. By equation 1.4.2

$$\Delta T = \frac{0,05 \times 524}{0,25} = 104,8 \text{ K}$$

This is a substantial temperature rise, which will never be achieved in practise since as the coal absorbs moisture and the temperature increases the vapour pressure of the water above the coal increases and the reaction rapidly comes to equilibrium.

As has been pointed out by Kibria (1972) heating due to moisture absorption may bring coal to a temperature where oxidation occurs at a dangerous rate. This point is extremely important; water absorption may well be a starting mechanism whereby the tempe- rature inside a coal pile which is at risk starts rising leading to the onset of a large amount of oxidation and eventual com- bustion. The opposite is also true; if a coal dump is inherently safe no amount of water absorption will start it burning; com- bustion occurs due to oxidation, and not due to moisture effects.

1.4.2 Low Temperature Oxidation of Coal

The amount of literature on the chemical reactivity of coal, and in particular its low temperature oxidation, is vast. However, for the reason that every coal is likely to have a different reactivity, it was felt that a new study had to be undertaken. This work was performed by M. Itay, at the department of Chemical Engineering at the University of the Witwatersrand. A summary of the conclusions reached by Itay (1984) is presented in this section.

The experimental apparatus used to conduct these studies was a nearly adiabatic reaction vessel into which coal is packed and oxygen introduced. The temperature-time history of the reaction is recorded, and gas samples are taken periodically and analyzed for O_2, N_2, CO, CO_2, and H_2O. The measured temperature time

curve is used to back calculate the adiabatic temperature time curve, and this curve is used to obtain information on the rate of reaction and on the thermal effects associated with the reaction.

The data obtained thus far points very strongly to the conclusion that the chemical reactivity of the coal falls off with the degree of oxidation of the sample. This effect is well known and has been much reported in the literature (see for example Van Krevelen, 1981). However few plausible explanations for the effect have been given.

Another important conclusion is that the disappearance of oxygen is not neccessarily accompanied by the appearance of reaction products e.g. CO_2. It appears that at a low temperature coal adsorbs O_2 strongly and desorbs CO_2 at a far lower rate. This has also been noted in the literature, and the increase in density of reacting coal samples strongly supports this fact (Van Krevelen, 1981). In addition the desorption of the CO_2 appears to have a small enthalpy of reaction. This behaviour is shown graphically in Figure 1.1.

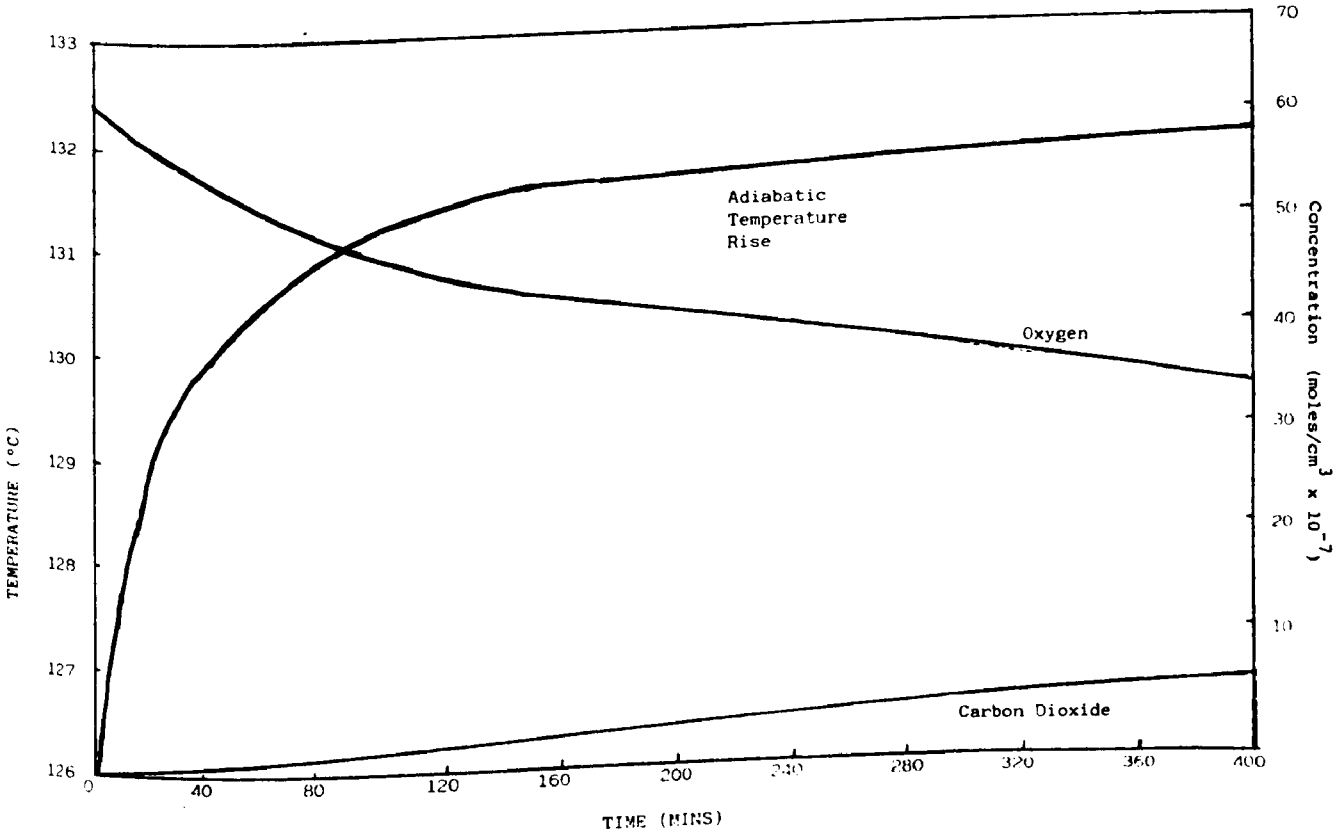


Figure 1.1 Temperature, Oxygen and Carbon Dioxide Versus Time

(After Itay, 1984)

In order to explain these effects a model for the reaction of coal with oxygen has been jointly derived by this researcher and Itay . The model is based on the hypothesis that coal absorbs oxygen to form a complex, which may be called oxycoal, without the formation of any gaseous products. The formation of an oxycoal layer on the surface of the coal has been demonstrated in the literature, and photographs showing this effect have been published by Van Krevelen (1981). As the oxycoal layer builds up the reaction rate slows down due to the fact that oxygen now has to diffuse through the oxycoal to react with the coal. This reaction model is an example of the so called shrinking core model, which is thoroughly discussed by Levenspiel (1962).

The derivation of the rate equation that follows from these assumptions is given in Appendix 1. The equations take the form:

Rate of adsorption of oxygen / unit volume of bed =

$$r = \frac{S_t\ (1-\epsilon)\ C}{1/k_r + Z/(S_t\ D_e)} \qquad 1.4.3$$

$$\frac{dZ}{dt} = \frac{S_t\ C}{\rho_m\ (1/k_r + Z/(S_t\ D_e))} \qquad 1.4.4$$

Where $S_t = \dfrac{\text{total surface area of particle}}{\text{volume of particle}}$

ϵ = bed voidage

C = O_2 concentration

k_r = surface rate constant

Z = fractional conversion of coal

D_e = effective diffusivity of oxycoal layer

ρ_m = molar density of coal

The temperature dependence of the reaction is given by the usual Arrhenius relationship i.e.

$$k_r = k_o \exp(-E/(R\,T)) \qquad 1.4.5$$

k_o = pre-exponential factor
E = activation energy
R = gas constant
T = temperature

In order to better understand the behaviour of this reaction model, the equations were solved under the assumptions of constant O_2 concentration and a constant value of k_r, the surface rate constant.

Under this assumption equation 1.4.4 gives

$$Z/(S_t\,D_e) = -1/k_r^2 + (1/k_r^2 + 2Ct/(\rho_m\,D_e))^{1/2} \qquad 1.4.6$$

Back substitution in equation 1.4.5 gives

$$r = S_t\,(1-\epsilon)\,C\,/(1/k_r^2 + 2Ct/(\rho_m\,D_e))^{1/2} \qquad 1.4.7$$

Two limiting cases were considered. In the early stages of reaction the oxycoal layer has not built up and the rate of the chemical reaction is limiting. In this case

$$1/k_r^2 \gg 2Ct/(\rho_m\,D_e)$$

$$\text{and } r = k_r S_t (1-\epsilon) C \qquad 1.4.8$$

i.e. in the early stages of reaction the rate is first order with respect to the O_2 concentration and is time independent.

However when more reaction has taken place it is reasonable to assume that the diffusion through the oxycoal layer is limiting. In this case

$$1/k_r^2 \ll 2Ct/(\rho_m\,D_e)$$

$$\text{and} \qquad r = ((\rho_m\,D_e\,C/(2t))^{1/2}\,S_t\,(1-\epsilon) \qquad 1.4.9$$

In the later stages of the reaction the rate is half order with respect to the O_2 concentration and exhibits a $1/t^{1/2}$ dependence on time.

This model therefore is in agreement with the observed behaviour of coal reactivity i.e. that the reactivity shows a definite falling off with time, which is in fact a falling off with degree of oxidation, and that the reaction order with respect to oxygen varies between one and a half . Fractional reaction orders have been reported by Sondreal & Ellman (1974).

It is therefore felt that a reaction model has been derived which is consistent with the available evidence. The problem that remains is to use the available experimental data to derive the model constants, in order that the model may be checked and used with confidence.

1.5 Heat Transfer within a coal dump

The safety or otherwise of a coal dump is likely to depend upon the balance between the rate of temperature rise due to reaction and the rate at which this energy is transferred away from the hot zone. It is known that coal is a fairly good insulator, but little data is available on the physical characteristics of heat transfer in coal beds. In addition these characteristics are likely to be dependent on both the voidage and particle size of the coal bed. For these reasons a literature survey was performed on the subject of heat transfer in packed beds; the results of this survey are presented in Chapter 3.

Following from this work, it was felt worth while to design and construct an apparatus to measure the so called effective thermal conductivity of a packed bed of coal. This aspect of the work is also discussed in Chapter 4 together with the results obtained.

1.6 A Mathematical Model For Spontaneous Combustion

In Chapter 5 a literature survey of existing mathematical models for spontaneous combustion of coal is presented. It is shown that all of these models suffer from one or more shortcomings. A set of equations, describing the behaviour of a so-called one-dimensional analogue of a coal dump is thus derived and discussed. In Chapter 6 certain simplifications to the model are discussed and justified. The methods used to solve this simplified set of equations are discussed.

1.7 Experimental Investigation

In Chapter 7 an experiment used to test the model as well as to obtain parameters for the model is discussed. The conclusion is reached that the model accurately describes the behaviour of a one-dimensional analogue of a coal dump.

1.8 Results and Conclusions

The large majority of Chapter 8 is devoted to a parameter study on the effect of on the model of changing certain parameters. The results obtained are discussed and the implications for the practising engineer pointed out. A simplified analysis is performed in order to deduce the temperature-time behaviour of the model, and the practical implications discussed. Shortcomings of the model are also discussed, together with suggestions for further research. Finally, in Chapter 9, the important conclusions reached in the thesis are summarised.

2. ANALYSIS OF SUGGESTED MECHANISMS FOR INGRESS OF REACTANTS

2.1 Introduction

The various mechanisms suggested for transport into a coal dump have been mentioned in section 1.2. They are repeated here for convenience.

a) Natural convection caused by self heating of the dump.

b) Flow caused by differential pressure between inclined and flat surfaces of the dump.

c) Molecular diffusion caused by concentration gradients.

d) Barometric breathing caused by changes in barometric pressure.

e) Thermal breathing caused by the daily variation in temperature.

In order to decide which of these mechanisms are important simple models were used to obtain order of magnitude estimates of their effect. It proves convenient to analyze mechanisms a) and b) together.

2.2 Natural Convection and Wind Pressure

In Chapter 5 a so-called one-dimensional model of the processes occuring in a coal dump is discussed. In Appendix 3 it is shown that the following momentum balance, for a vertically aligned bed open at both ends, may be written:

$$\frac{d\hat{P}}{dx} = -f\,U + \rho_\infty\, g\,(1 - T_\infty/T) \qquad 2.2.1$$

$\hat{P}$ = Pressure - ambient pressure
f = D'Arcy's law constant for the packed bed.
U = Superficial flow velocity
ρ_∞ = density of ambient air
g = acceleration due to gravity
T_∞ = ambient air temperature
T = bed temperature

Bird, Stuart & Lightfoot (1960) have discussed equations that attempt to correlate the factor f. One such equation is the Ergun equation which is

$$f = \frac{150\ (1-\epsilon)^2\ \mu\ S^2}{36\ \epsilon^3} + \frac{10.5\ (1-\epsilon)\ \rho\ U\ S}{\epsilon^3} \qquad 2.2.2$$

ϵ = bed voidage
μ = gas viscosity
ρ = gas density
$S = \frac{\text{total particle external surface area}}{\text{volume of particle}}$

It has been shown that for small flowrates the second term on the R.H.S. is negligible giving:

$$f = \frac{150\ (1-\epsilon)^2\ \mu\ S^2}{36\ \epsilon^3} \qquad 2.2.3$$

Note that no assumption need be made on the geometry of the particles or the bed packing. A mean particle diameter may be defined to be

$$D_p = 6/S \qquad 2.2.4$$

Under still air conditions the following boundary conditions are used for equation 2.2.1:

$$\hat{P}\ (x=0) = 0 \qquad 2.2.5$$

$$\hat{P}\ (x=L) = 0 \qquad 2.2.6$$

These boundary conditions merely reflect the fact that the ends of the bed are at atmospheric pressure.

In an attempt to compare the magnitude of natural convection induced flows with those of flows due to pressure differences, it is assumed that the stagnation pressure of a wind flow of velocity U may be use as an upper bound on the pressure difference that can arise between any two points on the surface of a coal dump. It is thus assumed that an estimate of the flows due to wind pressure may be obtained by assuming that the pressure at the bottom of the bed is increased by the stagnation pressure of the wind of velocity U.

Therefore

$$P(x=0) = P_\infty + \rho_\infty U^2/2 \qquad 2.2.7$$

and

$$\hat{P}(x=0) = \rho_\infty U^2/2 \qquad 2.2.8$$

Therefore the effect of wind is to change the boundary condition at $x = 0$ to

$$\hat{P} = \rho_\infty U^2/2 \qquad 2.2.9$$

Assuming U constant for small variations in temperature, equation 2.2.1 may be integrated to give:

$$\hat{P}(x=L)-\hat{P}(x=0) = -f\ U\ L + \rho_\infty\ g\ (L - \int_0^L (T_\infty/T\ dx)) \qquad 2.2.10$$

or

$$-\rho_\infty U^2/2 = -f\ U\ L + \rho_\infty\ g\ L\ (1 - (T_\infty/T_{aU})) \qquad 2.2.11$$

where

$$1/T_{aU} = 1/L \int_0^L T^{-1}\ dx \qquad 2.2.12$$

Therefore

$$U = \frac{\rho_\infty U^2}{2\ f\ L} + \frac{\rho_\infty g}{f}\ (1-T_\infty/T_{aU}) \qquad 2.2.13$$

or $$U = U(\text{Wind pressure}) + U(\text{Natural convection}) \quad 2.2.14$$

therefore

$$\frac{U(\text{Wind})}{U(\text{convection})} = \frac{v^2}{2\,L\,g\,(1-T_\infty/T_{av})} \quad 2.2.15$$

To illustrate the use of this equation, it will be used to calculate the wind velocity required to cause the same flow through a 10 m bed as a temperature rise of 20 ^{o}C.

i.e. $$1 = \frac{v^2}{2 \times 10 \times 9.8 \times (1-300/320)} \quad 2.2.16$$

or $$v = 3.5 \text{ m/s} = 12.6 \text{ km/hr}$$

This implies that for a windspeed of 12.6 km/hr natural convection will supply as much oxygen to the dump as will the differential wind pressure effect.

In order to compare these effects with the effects of molecular diffusion it is neccesary to calculate the molar flow rate per unit area for various average particle sizes. The relationships used are

$$G = \frac{P\,U}{R\,T} \quad 2.2.17$$

together with equations 2.2.2 and 2.2.15.

This calculation has been performed for L = 10 m, T_{av} = 320 K and ϵ = 0.3. The results are presented in Table 2.1.

TABLE 2.1 MOLAR FLOWRATES FOR VARIOUS PARTICLE SIZES

D_p (mm)	f (kg/m^2/s)	G (kmol/m^2/s)
1	5.6×10^{4}	5.1×10^{-7}
2	1.4×10^{4}	2.0×10^{-6}
5	2.2×10^{3}	1.3×10^{-4}

2.3 Analysis of Molecular Diffusion

In order to analyze the importance of diffusion as a mechanism for oxygen ingress a simplified analysis was performed. Considering diffusion as the only transport mechanism for oxygen into the dump the following energy and mass balances may be written:

Energy balance: $$K_b \frac{\partial^2 T}{\partial x^2} - r \Delta H = 0 \qquad 2.3.1$$

Mass balance: $$D\epsilon \frac{\partial^2 C}{\partial x^2} - r = 0 \qquad 2.3.2$$

The boundary conditions are:

$$\text{At } x=0 \quad T = T_\infty \quad C = C_\infty$$

$$\text{At } x=L \quad \frac{\partial T}{\partial x} = 0 \quad \frac{\partial C}{\partial x} = 0$$

These correspond to ambient conditions on the top surface of the dump, and a bottom surface that is perfectly insulating and impervious. These conditions will lead to a maximum temperature rise. Although this geometry is somewhat different to the geometry used in section 2.2, and thus the results obtained will not be directly comparable, it should be stressed that all that is required is an upper bound for comparison purposes; the geometry is unlikely to make a large difference on the bound.

Multiplying 2.3.2 by ΔH and subtracting the result from 2.3.1 gives:

$$K_b \frac{\partial^2 T}{\partial x^2} - D\epsilon\Delta H \frac{\partial^2 C}{\partial x^2} = 0 \qquad 2.3.3$$

or $$\frac{\partial^2}{\partial x^2}\left(T - \frac{D\epsilon\Delta H}{K_b} C\right) = 0 \qquad 2.3.4$$

This equation may be integrated to give:

$$T - \frac{D\epsilon\Delta H}{K_b} C = Ax + B \qquad 2.3.5$$

A and B may be determined from the boundary conditions as

follows:

At $x=0$ $T=T_\infty$ $C=C_\infty$

Therefore $$T_\infty - \frac{D\epsilon\Delta H}{k_b} C_\infty = B$$

and $$T - T_\infty - \frac{D\epsilon\Delta H}{k_b} (C - C_\infty) = Ax \qquad 2.3.6$$

Differentiating 2.3.5 wrt x gives:

$$\frac{\partial T}{\partial x} - \frac{D\epsilon\Delta H}{k_b} \frac{\partial C}{\partial x} = A \qquad 2.3.7$$

but at $x=L$ both derivatives in 2.3.7 are 0, therefore $A=0$.

Therefore $$T - T_\infty = \frac{D\epsilon\Delta H}{k_b} (C_\infty - C) \qquad 2.3.8$$

From 2.3.8 the maximum temperature rise with diffusion as the only transport mechanism may be calculated. This maximum temperature rise will occur at a point where $C=0$. Then:

$$T - T_\infty = \frac{D\epsilon\Delta H C_\infty}{k_b} \qquad 2.3.9$$

Typical values for the quantites in this equation are:

$$D = 2 \times 10^{-5} \text{ m}^2/\text{s}$$
$$\epsilon = 0.3$$
$$\Delta H = 3 \times 10^{8} \text{ J/kmol}$$
$$C_\infty = 8 \times 10^{-3} \text{ kmol/m}^3$$
$$k_b = 0.2 \text{ W/m/K}$$

Therefore

$$T - T_\infty = \frac{2\times10^{-5}\times0.3\times3\times10^{8}\times8\times10^{-3}}{0.2}$$

$$= 72 \text{ K}$$

This temperature rise, though appreciable, is not sufficient to explain the high temperatures observed in burning coal dumps. It is thus suggested that, in the same way that moisture absorption can act as a trigger for the oxidation reaction, diffusion can act as a trigger whereby the temperature in a coal dump starts rising, eventually giving rise to stable natural convection flows. These flows supply more oxygen to the dump than diffusion can, and eventually lead to spontaneous combustion.

Having concluded that diffusion can not explain spontaneous combustion, it is felt important to attempt to calculate the flowrates that diffusion causes. This facilitates the comparison of the magnitude of the flowrate caused by diffusion with the flowrates already calculated for wind and natural convection. To model molecular diffusion the coal is considered to adsorb oxygen, as discussed in section 1.3, and the isothermal steady state material balance for oxygen is

$$0 = \frac{D\ P}{R\ T}\frac{d^2y}{dx^2} - G\frac{dy}{dx} - r\ y \qquad 2.3.10$$

D = molecular diffusion coefficient
y = mole fraction oxygen
r = reaction rate per unit bed volume

The boundary conditions for equation 2.3.1 are:

$$y(x = 0) = .21 \qquad 2.3.11$$

and $$y(x \to \infty) = 0 \qquad 2.3.12$$

The solution is:

$$y = .21\ \exp((G - (G^2 + 4\ r\ \nu)^{1/2})\ x/\nu) \qquad 2.3.13$$

where $$\nu = D\ P/(R\ T)$$

The oxygen flux at x = 0 is

$$\frac{D\ P}{R\ T}\frac{dy}{dx} = .21\ ((G^2/4 + r\ \nu)^{1/2} - G/2) \qquad 2.3.14$$

Using the simplified equation

$$r = k_o\ S_t\ (1-\epsilon)\ \exp(-E/(R\ T))\ P/(R\ T) \qquad 2.3.15$$

with the values

k_o = 10 m/s
E/R = 7000 K
$S_t = 6/D_p$
ϵ = 0.3

$$D = 1.8 \times 10^{-8} \ m^2/s$$

and the data from Table 2.1 the entries in Table 2.2 have been calculated.

TABLE 2.2 COMPARISON OF MOLECULAR DIFFUSION AND CONVECTION

D_D (mm)	r (kmol/m^3/s)	Diffusional O_2 Flux (kmol/m^2/s)	Convective O_2 Flux (kmol/m^2/s)
1	1.2×10^{-7}	2.8×10^{-8}	1.0×10^{-7}
2	6.2×10^{-8}	4.4×10^{-9}	4.0×10^{-6}
5	2.5×10^{-8}	2.8×10^{-10}	2.6×10^{-5}

It can be seen from Table 2.2 that the effect of molecular diffusion is very much less pronounced for larger particles. For a particle size of 1 mm molecular diffusion supplies approximately 1/4 as much O_2 as a natural convection flow driven by a 20 ^oC temperature rise. In addition the molecular diffusion flux decreases with increasing particle size, while the convective flux increases. Although the analysis presented above may be criticized on the grounds that the transport equations have been decoupled, it can be seen that, except for the smallest particle sizes, the convective flux is orders of magnitude larger than the diffusional flux. This result justifies the use of the decoupled analysis to obtain order of magnitude estimates.

In the absence of wind or any temperature rise molecular diffusion may well be the only mechanism for O_2 transport into the dump. However it can be seen that as soon as there is any temperature rise in the dump natural convection will take over as the mechanism of O_2 transport.

2.4 Barometric Breathing

Barometric breathing occurs when the barometric pressure changes, causing a change in the volume of air that was in the dump. If the barometric pressure increases, this will cause a flow of air into the dump.

Consider a dump of 100 m x 50 m x 20 m high. Assume the barometric pressure increases from 620 mm Hg to 630 mm Hg in a time period of 24 hrs.

The air in the dump has a volume

$$100 \times 20 \times 50 \times 0.3 = 3 \times 10^4 \text{ m}^3$$

assuming $\epsilon = 0.3$.

This amount of air would shrink to a volume of

$3 \times 10^4 \times 620/630 \text{ m}^3 = 2.95 \times 10^4 \text{ m}^3$

and thus $4{,}76 \times 10^2 \text{ m}^3$ of air will flow in.

This flow will occur through the sides and the top of the dump i.e. a surface area of

$100 \times 50 + 2 \times 20 \times 50 + 2 \times 100 \times 20 = 11\,000 \text{ m}^2$

Thus the flowrate of air into the dump will be

$$\frac{4.76 \times 10^2}{11\,000 \times 24 \times 3600} = 5 \times 10^{-7} \text{ m/s}$$

This corresponds to a flux of 2×10^{-8} kmol/m^2/s which is an extremely small flux, and can safely be ignored.

Under certain weather conditions the barometric pressure may change far more rapidly than 10 mm Hg over a 24 hr period. This is the case for instance after a thunderstorm. These rapid changes may supply the dump with an appreciable amount of gas over a short period of time. The effect of this may well be to increase local temperatures in the dump and lead to the onset of natural convection flows. Thus rapid changes in barometric pressure may be a starting mechanism for the onset of spontaneous combustion in a dump that is in an unsafe condition.

2.5 Thermal Breathing

It has been hypothesized that the daily variation in temperature may lead to breathing of the dump i.e. hot air may leave the dump at night and be replaced by cold air thus supplying the dump with fresh reactants.

Measurements made at Grootegeluk coal mine indicate that surface temperature variations extend into the dump only a short distance; typically 325 mm.

A theoretical analysis of a problem of a semi-infinite solid with the surface temperature varying sinusoidally with time is discussed by Eckert & Drake (1972) who draw the conclusion that the oscillations are unimportant when

$$\frac{x}{2\,(\pi K \tau_o)^{1/2}} > 0.8 \qquad 2.5.1$$

Where K = thermal diffusivity of medium
τ_o = period of oscillation
x = distance into medium

For the case of daily fluctuations τ_o = 24 hrs. A typical value for the diffusivity of a coal bed is 8×10^{-4} m^2 / hr.

Therefore equation 2.5.1 gives

$$x > 2 \times 0.8 \times (\pi \times 8 \times 10^{-4} \times 24)^{1/2}$$

or $$x = 0.37 \text{ m}$$

This value agrees well with the measurements made on coal dumps discussed above.

It can be seen that thermal breathing will only supply reactants to the surface of the dump. Since any temperature rise near the surface of the dump is likely to be dissipated to the surface, it is unlikely that thermal breathing need be considered as an important reactant transport mechanism.

2.6 Conclusions

It may be concluded from the admittedly simplified analyses presented above that both wind pressure and natural convection must be considered as important mechanisms of O_2 transport into a coal dump. Molecular diffusion and barometric breathing may well be starting mechanisms, whereby the temperature begins rising in a coal dump. Natural convection soon becomes the dominant mech-

anism supplying O_2. This process may lead to eventual spontaneous combustion of a coal dump that is in an unsafe situation.

3. THEORETICAL MODELS FOR HEAT TRANSFER IN PACKED BEDS

3.1 Introduction

Thermal transfer of energy in packed beds is a field in which much work has been performed. The main reason for this is the importance of heat transfer in the design of packed bed catalytic chemical reactors. Other fields in which this knowledge is required include drying, nuclear reaction engineering and powder technology.

The literature survey that follows is very general, with no specific reference to coal beds. This is because the processes occuring in a packed bed of coal are no different to those occuring in packed beds of other materials.

3.2 Mechanisms of Energy Transfer in Packed Beds

In general energy transfer in a packed bed containing stagnant or moving fluid occurs by conduction, convection and radiation. The following potential mechanisms can be identified in the general case (Beveridge & Haughey, 1971).

Conductions Mechanisms

1. Conduction through the solid particles
2. Conduction across the gas in the voids
3. Conduction across the stagnant gas surrounding the points of contact between particles.
4. Conduction through the points of contact between particles

Radiation Mechanisms

5. Radiation between adjacent particle surfaces
6. Radiation between particle surfaces seen through more than one void space
7. Radiation absorption by the gas

Convection Mechanisms

8. Natural convection in the gas
9. Forced convection solid-gas transfer
10. Forced convection due to bulk flow, turbulent diffusion or mixing of the gas.

Of these mechanisms, mechanisms 1,2,4,5,6 and 7 are independent of fluid flow, while the other mechanisms depend to a greater or lesser extent on fluid flow, especially at low Reynolds numbers (Yagi & Kunii, 1957).

In general, thermal transfer of energy will take place by various combinations of series and parallel paths of these mechanisms.

3.3 Describing the overall energy transfer in a packed bed

The most common way of describing the overall transfer in a packed bed is by means of the so called effective thermal conductivity of the bed (Beveridge & Haughey, 1971). This quantity has also been called the thermal dispersion coefficient in the literature (Gunn & Khaled, 1975).

This formulation treats the system as homogeneous allowing the Fourier equation for the flux per unit area Q to be written

$$Q' = -k_b \frac{\partial T}{\partial X}$$

where $\partial T/\partial X$ is the temperature gradient in the required direction (axial or radial).

It can be seen from the discussion in 3.2 that k_b, the effective thermal conductivity, is in fact a function of many parameters including gas velocity, gas and solid temperatures, relative directions of gas and energy flow, fluid and solid properties as well as bed voidage and structural characteristics. It is the elucidation of this functional relationship that has been the goal of much of the work, both theoretical and experimental, that has been done in this field.

3.4 Models for energy transfer in which only conduction is considered

Many researchers have used as their starting point a model of a packed bed in which only conduction is considered. Models so derived should give good results provided the following conditions are met:

1. There is no gas flow
2. The particles are sufficiently small, and the temperature

sufficiently low, so that natural convection and radiation may be ignored.

Exactly what is meant by sufficiently small and sufficiently low will be discussed in greater detail later. Suffice it to say that if these conditions are met then the effective thermal conductivity, k_b, will be primarily a function of the thermal conductivities of the solid particle and stagnant gas. k_s and k_g respectively, and the structure of the bed.

Many models have been published to account for the four conduction mechanisms discussed in section 2, most of which describe the system in terms of its fluid and solid phase elements arranged in some regular array.

These models have been summarized by Beveridge & Haughey (1971), and their geometric significance is shown in figure 3.1

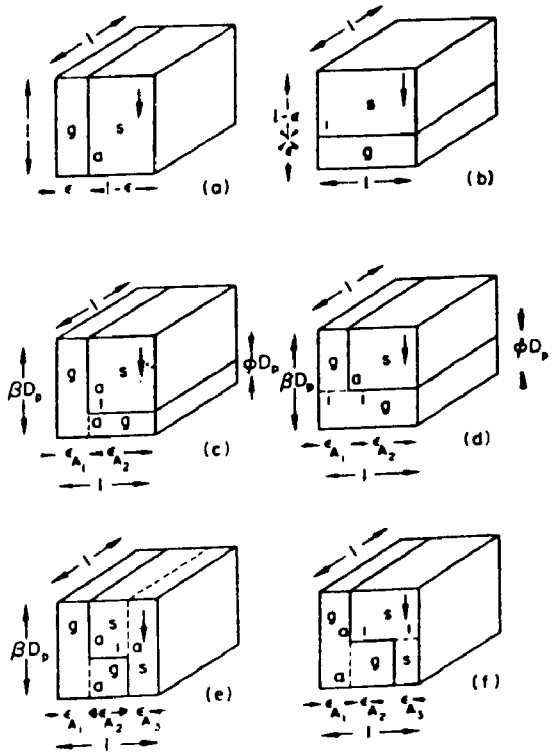


FIGURE 3.1 GEOMETRICAL CONDUCTION MODELS

a. adiabatic plane

i. isothermal plane

g. gas phase

s. solid phase

→ direction of energy transfer

(Beveridge & Haughey, 1971)

The simplest model is that represented by Fig 3.1a which postulates that conduction through the solid (mechanism 1) acts over a solid volume $1-\epsilon$, and the conduction across the gas in the voids and the stagnant gas round the points of contact (mechanisms 2 and 3) act over a gas volume ϵ. An arithmetic mean corresponding to a parallel arrangement of the two phases gives

$$\frac{k_b}{k_g} = \epsilon + (1 - \epsilon) \frac{k_s}{k_g} \qquad 3.4.1$$

The harmonic mean which corresponds to a series arrangement of the phases (Fig 3.1b) yields

$$\frac{k_b}{k_g} = \frac{k_s}{\epsilon\, k_s + (1 - \epsilon)\, k_g} \qquad 3.4.2$$

In attempting the formulation of more realistic models the concept of the unit cell is introduced, i.e. a representative element which is repeated throughout the packing. The basic geometric cell is that of Fig 3.1c with a cell of unit area perpendicular to the energy flow and height equal to the particle layer thickness $\beta' D_p$ where D_p = average diameter of particles.

Energy flow is one dimensional in parallel paths which are insulated from each other, and the distribution on the two phases is handled only by a two dimensional variation. This system then gives (see Fig 3.1c)

$$k_b = k_g\, \epsilon_{a1} + \frac{(1 - \epsilon_{a1})\, k_s}{\alpha' X + 1 - \alpha'} \qquad 3.4.3$$

where $\alpha' = \frac{\phi}{\beta'}$

and $\epsilon_{a1} = \frac{\epsilon - \alpha'}{1 - \alpha'}$

Modifications include that shown in Fig 3.1d which gives

$$k_b = \left[\alpha' k_g + \frac{1 - \alpha'}{k_g\, \epsilon_{a1} + k_s\, (1 - \epsilon_{a1})} \right]^{-1} \qquad 3.4.4$$

However, none of these models take into account the point to point

contact resistance (mechanism 4). One approach to this problem is that one used by Kunii & Smith (1960) who define a "heat" transfer coefficient h_p, accounting for an energy transfer contact resistance in parallel with the gas phase portion of the gas-solid series mechanism yielding:

$$\frac{k_b}{k_g} = \epsilon_{a1} + \frac{(1 - \epsilon_{a1})\, k_s/k_g}{(1 - \alpha) + \dfrac{\alpha\, k_s/k_g}{1 + \dfrac{h_p\, D_p}{k_g}}} \qquad 3.4.5$$

The quantity h_p has not been well correlated in the literature.

A more logical approach is the inclusion of the contact resistance in the idealized cell model as a solid energy flux path (represented by an area fraction ϵ_{a3}) arranged parallel to the gas path (Fig 3.1e) giving:

$$k_b = \epsilon_{a1}\, k_g + \frac{\epsilon_{a2}\, k_s}{\alpha' \dfrac{k_s}{k_g} + 1 - \alpha'} + \epsilon_{a3}\, k_s \qquad 3.4.6$$

A further extension to this approach is the one presented by Beveridge & Haughey (1971) in which the adiabatic boundary between the two parallel paths is replaced by an isothermal boundary (Fig 3.1f). This yields

$$\frac{k_b}{k_g} = \epsilon_{a1} + \left[\frac{1 - \alpha'}{\dfrac{k_s}{k_g}(1 - \epsilon_{a1})} + \frac{\alpha'}{\epsilon_{a2} + \epsilon_{a3}}\right]^{-1} \qquad 3.4.7$$

This approach has the advantage of allowing flux line bending in the solid phase.

It is shown by Beveridge & Haughey (1971) that k_b is a function of k_s/k_g, ϵ and ϵ_{a3} only. While k_s/k_g and ϵ are definable physical properties the parameter ϵ_{a3} must be determined experimentally for a given set of particles, since it will be affected by the particle loading and deformation as well as the surface

characteristics of the solid. It is also important to note that the effect of pressure on the thermal conductivity of the gas, k_g, must be properly taken into account.

3.5 Models for energy transfer in which conduction and radiation are considered.

Although radiant energy transfer will occur only through the voids of a packed bed of opaque solid pseudo-homogenous models have beem proposed which consider the solid and the gas as a single homogenous medium. The solution of the resultant integro-differential equations for conduction and radiation in absorbing and scattering models has been examined, most notably by Chan & Churchill (1963). They found that in an optically thick bed that the so called radiant conductivity $k_{b,r}$ could be written as

$$k_{b,r} = \frac{8 \sigma T^3}{a' + 2b'} \qquad 3.5.1$$

where σ = Stephan - Boltzmann constant
T = average bed temperature
a' = absorption cross section per unit volume of packing
b' = back scattering cross seciton per unit volume of packing

Note that the radiant conductivity is defined as the radiant energy flux density divided by the temperature gradient.

The radiant contribution has also been calculated by Bosworth (1952) from a random walk model giving

$$k_{b,r} = \frac{4 D_p T^3}{3}$$

The simplest radiation geometric model is that with two radiating plane surfaces at temperature T_1 and T_2, the radiant energy flux Q_r' being given by

$$Q'_r = \chi \sigma (T_1^4 - T_2^4) \qquad 3.5.3$$

where χ = view factor and emmisivity function

The elucidation of the function χ is difficult both theoretically and experimentally.

The energy flux Q'_r can be related to a radiation thermal conductivity $k_{b,r}$, and to a radiation coefficient $h_{b,r}$, by

$$Q'_r = -k_{b,r} \frac{\partial T}{\partial x} = h_{b,r} (T_1 - T_2) \qquad 3.5.4$$

When $T_1 - T_2$ is small compared to the absolute value of $T = T_1$ then:

$$\frac{k_{b,r}}{\beta D_p} = h_{b,r} = 4 \chi \sigma T^3 \qquad 3.5.5$$

The parameters in these models have a highly complex interaction with the structural and physical properties of the bed, and for this reason Beveridge & Haughey (1971) feel that there is little justification in representing the radiation mechanism other than by adding suitable terms to the simplest model such as the geometrical conduction models of Fig 1. Schotte (1960) used an analysis similar to that of Argo & Smith (1953) accounting for both the radiation between adjacent particle surfaces (mechanism 5) and the radiation between particle surfaces seen through more than one void space (mechanism 6) giving

$$Y_r = \epsilon X_{r,g} + \frac{1 - \epsilon}{\frac{k_g}{k_s} + \frac{1}{X_{r,s}}} \qquad 3.5.6$$

where $Y_r = \frac{k_{b,r}}{k_g}$

$$X_{r,g} = X_{r,s} = \frac{h_r D_p}{k_g} = \frac{4 D_p \chi \sigma T^3}{k_g} \qquad 3.5.7$$

The thermal conductivity of the bed is then given by

$$Y_t = Y_c + Y_r$$

In fact there is an interaction between the radiation and other energy transfer mechanisms and the contribution Yr cannot be added simply to the conduction terms. It is more satisfactory to utilize h_r within the conduction type model (Fig 3.1e). This was done by Yagi & Kunii (1957) who obtained

$$y_t = \epsilon_{a1}\,(1+ X_{r,g}) + \frac{\epsilon_{a2}}{\frac{\alpha'}{1 + \alpha' X_{r,s}} + \frac{1-\alpha'}{X}} + \epsilon_{a3} X \qquad 3.5.9$$

Normally no distinction is made between the Nusselt Numbers $X_{r,s}$ and $X_{r,g}$, although Yagi and Kunii (1957) used

$$X_{r,s} = \frac{4D_p}{k_g}\left[\frac{e}{2-\epsilon}\right] T^3 \qquad 3.5.10$$

$$X_{r,g} = \frac{4D_p}{k_g}\left[1 + \frac{\epsilon(1-e)}{2(1-\epsilon)e}\right]^{-1} \qquad 3.5.11$$

The model used by Beveridge and Haughey (1971) results in the expression

$$Y = \epsilon_{a1}(1+H_r) + \left[\frac{1-\alpha'}{X(1-\epsilon_{a1})} + \frac{\alpha'}{\epsilon_{a2}(1+H_r) + X\epsilon_{a3}}\right]^{-1}$$

$$H_r = \frac{\beta h_r D_p}{k_g} = \frac{4\beta D_p X \sigma T^3}{k_g} \qquad 3.5.12$$

Beveridge & Haughey (1971) treated X as an unknown function of temperature, and deduced the functional form experimentally.

3.5.1 Conditions under which radiation in a packed bed is likely to be significant

Young (1975) has performed calculations of the radiation contribution to the effective thermal conductivity of packed beds. The calculations were based on the radiation model of Schotte (1960) in conjunction with the correlation of Deissler and Eian (1952). The calculations show that radiation will become important for 1 mm particles about 400 °C and for 0,1 mm particles above 1500 °C. For

5 mm particles at an average bed temperature of 400 ^{o}C radiation will account for approximately 20 % of the total energy transfer.

3.6 A Theoretical Study of Natural Convection.

The first theoretical study of natural convection in packed beds is that of Lapwood (1948). This author formulated the equations describing natural convection in a porous medium with an imposed vertical temperature gradient as follows:

Equation of motion:

$$\rho \frac{D}{Dt}(U,V,W) = -\left[\frac{\partial}{\partial x},\frac{\partial}{\partial y},\frac{\partial}{\partial z}\right] P - \frac{\rho g}{K'}(U,V,W) - (0,0,\rho g) \qquad 3.6.1$$

Equation of continuity:

$$\frac{1}{\rho}\frac{D\rho}{Dt} = \frac{\partial U}{\partial x} + \frac{\partial V}{\partial y} + \frac{\partial W}{\partial z} \qquad 3.6.2$$

Conservation of energy:

$$\frac{DT}{Dt} = \kappa \nabla^2 T \qquad 3.6.3$$

Equation of state:

$$\rho = \rho_{\infty}[1 - \alpha(T-T_{\infty})] \qquad 3.6.4$$

(U,V,W) = the macroscopic velocity components of an element of fluid at (x,y,z)

P = pressure at (x,y,z).

T = temperature at (x,y,z)

ρ = gas density at (x,y,z)

g = acceleration due to gravity

κ = thermal diffusivity = $k_b/(\rho\, c_g)$

k_b = effective thermal conductivity of medium

c_g = specific heat capacity of gas

α = coefficient of thermal expansion of fluid

K' = coefficient of permeability of medium for fluid concerned
= Kg/ν

ρ_{∞} = density at ambient temperature

ν = kinematic viscosity of fluid

K = permeability of medium

Note that Darcy's law has been used in the equation of motion in place of the usual viscosity term.

In order to reduce these equations to a more manageable form Lapwood (1948) makes the following assumptions:

1) All velocities, and departures of temperature, density, and pressure from the equilibrium state, are small enough to neglect second order terms and to formulate a useful first order theory.

2) Variations of density can be neglected, except in so far as they modify the action of gravity (the Boussinesq assumption).

These assumptions mean that D/Dt can be replaced everywhere except in the energy equation to give

Equation of motion:

$$\rho \frac{\partial}{\partial t}(U,V,W) = -\left(\frac{\partial}{\partial x},\frac{\partial}{\partial y},\frac{\partial}{\partial z}\right) P - \frac{\rho g}{K'}(U,V,W) - (0,0,\rho g)$$

Equation of continuity:

$$\frac{\partial U}{\partial x} + \frac{\partial V}{\partial y} + \frac{\partial W}{\partial z} = 0$$

Conservation of energy:

$$\frac{DT}{Dt} = \kappa \nabla^2 T$$

Equation of state:

$$\rho = \rho_\infty [1 - \alpha(T-T_\infty)] = \rho_\infty \frac{T}{T_\infty} \quad \text{for an ideal gas}$$

Lapwood (1948) reworks this set of equations for small disturbances from equilibrium, and obtains the 4th order differential equation

$$\left(\frac{\partial}{\partial t} + \frac{Q}{K}\right)\left(\frac{\partial}{\partial t} - K'^2\right)\nabla^2\theta = g\frac{\Delta T}{L}\nabla^2\theta$$

where $\theta = T-T_0$, $T_0 = -\Delta T(z/L)$

The equation is solved for the following boundary conditions:

$$T, \quad \frac{\partial^2 T}{\partial z^2} = 0 \qquad \text{at } z=0 \text{ and } z=L$$

It is shown that the solution obtained leads to exponential decay for

$$Ra = \frac{\Delta T \ \rho_0 K \ L \ g}{\kappa \ \mu \ T_\infty} < 4\pi^2 \qquad 3.6.5$$

where Ra = Rayleigh Number

Lapwood (1948) thus states that $Ra = 4\pi^2$ is the criterion for convective flow; if Ra is less than this value the disturbance dies away, but if it reaches this value steady convection becomes possible.

These results also show that the temperature depth relationship is, except in the vicinity of the boundaries,

$$T = T_0 - \frac{\Delta T}{L} z + A \sin\left(\frac{\pi z}{L}\right) \sin(lx) \sin(my) \qquad 3.6.6$$

Where A,l,m are constants.

This equation shows that in the presence of convection the temperature is no longer a linear function of z.

3.7 The Effect of Flow on Energy Transfer in Packed Beds

When there is bulk flow of gas through a packed bed, the thermal transfer of energy becomes many times more complicated. It has been mentioned in section 2 that of the 10 proposed mechanisms of energy transfer, only 6 are completely independent of fluid flow. Briefly the mechanisms which are believed to be dependent on the fluid flow are:

1) Conduction across the stagnant gas surrounding the contact points. (This is likely to be a weak function of fluid flow).
2) Natural convection in the gas.
3) Forced convection in the gas.
4) Forced convection due to bulk flow, turbulent diffusion or mixing of the gas.

Mechanisms 3 and 4 are unlikely to be of importance for a coal bed, since forced convection is not being considered except for the case of wind. The flowrates through packed beds of coal are in any case very small. The flow velocity may be calculated from the entries in Table 2.1. For a particle size of 5 mm the velocity is of the order of 10 m/hr.

It may thus be concluded that the effects of flow on heat transfer in packed beds of coal is likely to be negligible.

3.8 Conclusions

A variety of theoretical models have been presented in this chapter. In order to apply the results of this literature survey to reacting coal beds, the following should be borm in mind:

a) The temperature range considered to be important is 100 ^{o}C and below. From practical experience as well as from considerations of the oxidation rate once a coal bed reaches 100 ^{o}C it is well on its way to combustion, and the model developed in this work no longer describes the situation accurately.

b) The flowrate through a bed of coal is sufficiently small (as shown above) that the effect of flow on the effective thermal conductivity is likely to be negligible.

The first point means that radiation can for all practical purposes be ignored as a significant mechanism for heat transfer in coal beds. The second point suggests that the effects of flow on the effective thermal conductivity can be ignored.

The conclusion is that only conduction type models need be considered for describing the effective thermal conductivity. Thus an equation like 3.4.5 could be rewritten

$$k_b = \epsilon k_g + (1-\epsilon)\ \eta k_s \qquad 3.8.1$$

where η = tortuosity factor

and η can be determined experimentally, with the expectation that η will not be a strong function of temperature.

Having reached this conclusion it was decided to measure k_b for a packed bed of coal. This is the subject of the next chapter.

4. MEASUREMENT OF THE EFFECTIVE THERMAL CONDUCTIVITY OF A PACKED BED OF COAL

4.1 Introduction

Very broadly speaking, methods for measuring thermal conductivities fall into one of two categories, i.e. steady-state or unsteady-state methods. The vast majority of unsteady-state methods do not measure the thermal conductivity directly, but instead measure the thermal diffusivity, κ, where:

$$\kappa = \frac{k}{\rho C_p} \qquad 4.1.1$$

k = thermal conductivity
ρ = density
C_p = specific heat capacity

One exception to this is the hot wire method which measures both the thermal conductivity and the thermal diffusivity. Steady state methods, on the other hand, measure the thermal conductivity directly.

4.2 Theory of the Measurement of Thermal Conductivity

Thermal conductivity is defined by Fourier's law:

$$Q' = -kA \frac{dT}{dx} \qquad 4.2.1$$

Q' is the rate of energy transfer by conduction

A is the area at right angles to the direction of transfer

$\frac{dT}{dx}$ is the temperature gradient in the direction of transfer

This equation may be combined with an energy balance for a solid or static fluid to give:

$$\rho C_p \frac{\partial T}{\partial t} = \frac{\partial}{\partial x}\left[k \frac{\partial T}{\partial x}\right] + \frac{\partial}{\partial y}\left[k \frac{\partial T}{\partial y}\right] + \frac{\partial}{\partial z}\left[k \frac{\partial T}{\partial z}\right] + q' \qquad 4.2.2$$

T is the temperature
q' is a source term, which may be due to chemical or nuclear reaction or the passage of a current.

In general in the measurment of thermal conductivities an attempt is made to ensure that only one dimensional conduction takes place. In this case equation 4.2.2 becomes:

$$\rho C_p \frac{\partial T}{\partial t} = k \frac{\partial^2 T}{\partial x^2} + q' \qquad 4.2.3$$

This equation may be written for cylindrical or spherical coordinate systems giving:

Cylindrical co-ordinates: $$\rho C_p \frac{\partial T}{\partial t} = \frac{k}{r} \frac{\partial}{\partial r}\left[r \frac{\partial T}{\partial r}\right] + q' \qquad 4.2.4$$

Spherical co-ordinates: $$\rho C_p \frac{\partial T}{\partial t} = \frac{k}{R^2} \frac{\partial}{\partial R}\left[R^2 \frac{\partial T}{\partial R}\right] + q' \qquad 4.2.5$$

4.3 Steady-State Methods for Measuring Thermal Conductivity

The second order differential equations 4.2.3 - 4.2.5 may be solved in the steady-state to give:

Rectangular co-ordinates: $$T = \frac{-q'x^2}{2k} + C_1 x + C_2 \qquad 4.3.1$$

Cylindrical co-ordinates: $$T = \frac{-q'r^2}{4k} + C_1 \ln(r) + C_2 \qquad 4.3.2$$

Spherical co-ordinates: $$T = \frac{-q'R^2}{6k} - \frac{C_1}{R} + C_2 \qquad 4.3.3$$

The constants of integration are found from known boundary conditions. In writing the above equations k has been assumed to be independent of temperature. In general in attempting to

measure thermal conductivity one would avoid introducing sources into the sample i.e. q′ would be zero in the above equations.

4.3.1 Measurements in the Rectangular System

The temperature-position equation in the rectangular system with q′=0 is:

$$T = C_1 x + C_2 \qquad 4.3.4$$

This equation implies a linear temperature profile.

In order to use equation 4.3.4 to measure thermal conductivity a heater is used to provide a known energy input Q. The boundary condition at x=0 is therefore:

$$Q = -kA \left.\frac{dT}{dx}\right]_{x=0} \qquad 4.3.5$$

The sample is cooled at the end. The boundary condition at x = L is therefore:

$$T = T_o \qquad 4.3.6$$

Solving for the integration constants C_1 and C_2:

$$C_1 = \frac{Q}{-kA} \qquad 4.3.7$$

$$C_2 = T_o + \frac{QL}{kA} \qquad 4.3.8$$

Therefore $$T = T_o + \frac{Q}{kA}(L - x) \qquad 4.3.9$$

Suppose that the measured temperature at x = 0 is T_1. Then:

$$T_1 = T_o + \frac{QL}{kA} \qquad 4.3.10$$

$$K = \frac{QL}{A(T_1 - T_0)} \qquad 4.3.11$$

This formula is the basis for measurements of the thermal conductivity of a material in rod or slab form. It requires measurement of five quantities i.e

The power input	Q
The sample length	L
The sample area	A
The temperature	T_0
The temperature	T_1

An improved version of the apparatus is one in which two identical samples, heated in the middle are used. The apparatus has the advantage that no energy loss can occur through the ends provided $T_0 = T_\infty$.

The equation used to calculate the thermal conductivity is now:

$$K = \frac{QL}{2A\ (T_1 - T_0)} \qquad 4.3.12$$

Despite the advantages of this apparatus energy loss may still occur along the sides. For this reason the so called guarded hot ring method has been developed. In this apparatus a circular electrical heating element is used and it is surrounded by a heating element in the form of a ring. During the experiment the power input to this guard ring is adjusted so that the temperature measured on the ring is the same as that measured on the main heater. This implies that any energy losses are supplied by the guard heater, and that all the energy supplied by the main heater passes through the sample.

The design of guarded hot plate apparatus has been the subject of much study, and is covered in ASTM C177 (1963) and BS 874 (1956). This method has been used by many investigators in the field of thermal conductivity of packed beds; notably Beveridge & Haughey (1971).

4.3.2 Measurements in the Cylindrical System.

In radial flow methods use is made of equation 4.3.2 with $q' = 0$:

$$T = C_1 \ln (r) + C_2 \qquad 4.3.13$$

With boundary conditions:

$$Q = -2\pi r_1 l \, k \left.\frac{dT}{dr}\right]_{r_1} \quad \text{at } r = r_1 \qquad 4.3.14$$

$$T = T_2 \quad \text{at } r = r_2 \qquad 4.3.15$$

Solving equation 4.3.14 for the constants and rewriting in terms of k gives:

$$k = \frac{Q}{2\pi l \, (T_1 - T_2)} \ln \left[\frac{r_1}{r_2}\right] \qquad 4.3.16$$

Two different experimental apparatus may be designed in order to make use of equation 4.3.16. In the first type of apparatus the specimen is placed between an outer shell which is kept at temperature T_2, and is heated centrally. In the second type of apparatus the sample is heated on the outside surface, and the energy is removed at the centre of the sample.

In order to ensure that energy transfer is occuring only in the radial direction it is neccesary either to use a large sample length to thickness ratio, or to make use of end guard heaters. If guard heaters are used a fairly complicated experimental apparatus is neccesary, involving movable thermocouples in order to measure axial temperature gradients. This aspect of the design of such equipment is covered by Tye (1969).

Examples of the use of such methods for measurements of thermal conductivity of packed beds are Yagi & Kunii (1957) who used a centrally heated specimen, and Young (1975) who used a centrally cooled specimen.

4.3.3 Measurements in the Spherical System

Equation 4.3.3 may be solved to give:

$$k = \frac{Q\ (1/r_1 - 1/r_2)}{4\pi(T_2 - T_1)} \qquad 4.3.17$$

The spherical system has the advantage that all the energy supplied by a central heater passes through the specimen. The disadvantages of the method include the difficulty of fabricating a uniform heater and specimen, and the fact that the thermo-couples used for temperature measurement cannot lie along isotherms.These disadvantages mean that the spherical system has not been used for the measurement of thermal conductivity of packed beds.

4.4 Unsteady-State or Dynamic Methods

In general dynamic methods involve the measurement of the thermal diffusivity. The experiment consists of measuring the temperature history of a heated sample of known geometry, and then using this data and the appropriate integrated form of equation 4.2.2 to solve for the thermal diffusivity.

These methods have the advantage that no measurement of power input need be made. The disadvantages include the fact that many temperature measurements must be made, and that solving for the diffusivity may require complex numerical techniques.

An example of the use of a dynamic method to measure the thermal conductivity of a coal bed is the investigation by Brooks & Woods (1980). These investigators used a cylindrical vessel of diameter 500 mm and height 1600 mm. The vessel was heated on the outside surface by steam and radial temperature profiles were measured as a function of time. These measurements were made every 15 minutes for periods of up to 8 hrs.

It can be shown that under the above experimental conditions equation 4.2.4 may be solved to give

$$\frac{T - T_s}{T_o - T_s} = 2 \sum_{n=1}^{\infty} \frac{\exp \frac{-M_n^2 K t}{R^2} \; J_o \frac{M_n r}{R}}{M_n \; J_1(M_n)} \qquad 4.4.1$$

where T = temperature at radial position r

T_s = surface temperature

T_o = initial bed temperature

R = radius of cylinder

r = radius measured from axis of cylinder

t = time

J_i = i th order Bessel function of the first kind

M_n = n th root of the equation $Jo(M_n) = 0$

A computer program was used to minimize the sum of squared errors between the measured and predicted temperatures by choice of K. It can be appreciated that this process is far more complicated than the direct application of an equation such as 4.3.12.

Although only one dynamic method has been discussed it should be appreciated that all such methods involve the same sort of experiment and analysis, and differ only in the sample geometry chosen. One of the problems with applying these methods to coal beds is the small value of K of such beds which leads to long experiments.

4.5 Choice of Measurement Method for a Packed Bed of Coal

From experience gained by Brooks & Woods (1980) in trying to measure this quantity by use of an unsteady-state method, it was felt that a steady-state method would be better. The reason for this is that it is far easier to analyze the effect of a temperature dependent thermal conductivity in the case of a simple equation such as 4.3.12, whereas this task may be extremely difficult in the case of an equation such as 4.4.1. Put another way, it was felt that a thermal conductivity calculated by equation 4.3.12 is far better defined than one calculated from equation 4.4.1.

Having decided on a steady-state method the choice had to be made between axial or radial energy transfer. Again experience gained

in a previous study led to the choice of axial energy transfer. The reason for this was that the previous study indicated that convection may be a significant mechanism of energy transfer. If this is the case the axial method would lead to the determination of the "correct" thermal conductivity i.e the one in which the energy transfer by conduction and convection are in the same direction (This of course assumes that the apparatus has the heater horizontal).

It was also felt that, by designing the equipment in such a way that the energy absorbed at the two sinks could be measured, the presence or absence of convection could be detected, and its effect measured. To do this would be much more difficult in a radial type of apparatus.

4.6 Design and Construction of Guarded Hot Ring Apparatus

4.6.1 General Design Considerations

Although standards exist for the design of guarded hot ring apparatus, it was felt in the present case that accuracy of measurement could be sacrificed for ease of experimental design and construction, and for versatility of the apparatus. It was felt that due to the inhomogeneous nature of coal and variations in packing geometry, accurate and repeatable values for the thermal conductivity would not in any case be achieved.

In order to make measurements on coal up to 20 mm in size it was decided to make the test section of the apparatus of diameter 200 mm and length 200 mm. These dimensions should be sufficient to make end and edge effects negligible. However it was noted that the recommended D/L ratio is three or more, and that using a smaller ratio would lead to a loss in accuracy (Tye ,1969).

4.6.2 Heat Sinks

As mentioned before the sinks are designed in such a way that the energy absorbed by the sinks can be measured. This is achieved by placing thermistors in the inlet and outlet streams from the sinks, in order to measure the temperature difference in the water flowing through the sinks. The rate of energy absorption

is calculated as

$$Q = m\ \bar{c}\ \Delta T_w \qquad 4.6.1$$

Q = rate of energy absorption
m = water flowrate
$\bar{c}$ = specific heat capacity of water
ΔT_w = temperature difference of water

The sinks are provided with spiral baffles in order to ensure good mixing of the cooling fluid, which was in all cases water. The sinks are surrounded by guard sinks in order to prevent radial energy losses.

A sketch of one heat sink is shown in Figure 4.1.

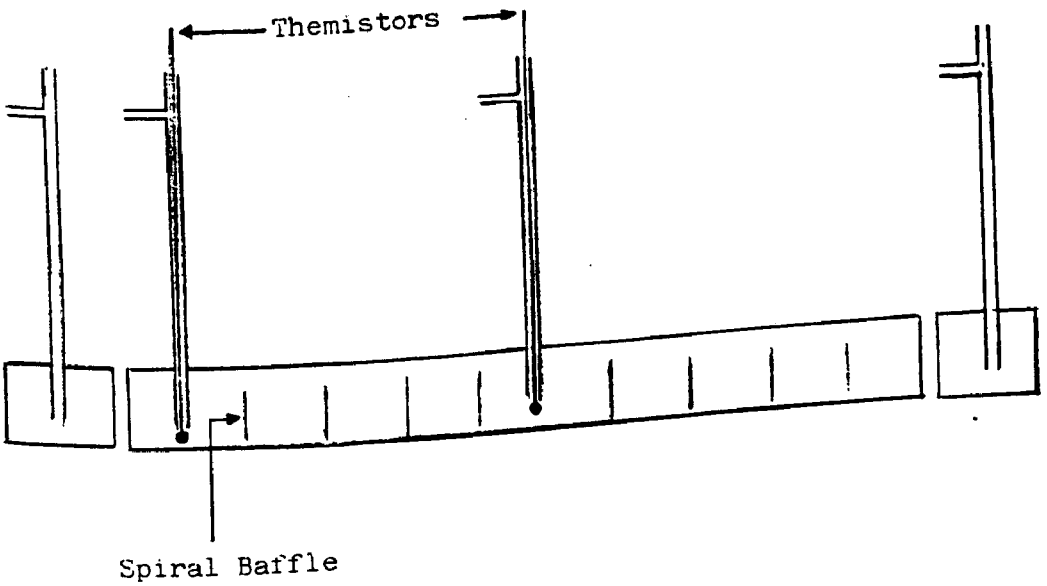


Figure 4.1 Guarded hot ring apparatus - Heat sink

4.6.3 Heating Elements

The heating elements were fabricated commercially, and consist of Nichrome wire ribbon wrapped around mica formers, which assembly is then sandwiched between more mica. The heaters are clad in light aluminium, and the whole assembly then sandwiched between 2 mm steel plates which are bolted together. The steel plates are used to prevent buckling.

The central heater has a diameter of 145 mm and the guard ring has an internal diameter of 150 mm and an external diameter of 200 mm. There is thus a 2.5 mm gap between the main and guard heaters.

4.6.4 Outer containing Vessel

The vessel has a diameter of 600 mm and a length of 600 mm. It is constructed from 6 mm mild steel. The ends of the vessel have 10 mm mild steel flanges in order to support the 10 mm MS end plates. The flanges are fitted with 5 mm rubber ring gaskets, and the endplates are held on with 18 bolts.

In order to facilitate electrical connections to the heaters as well as the placement of the thermocouples, six bushes have been placed on the midline of the apparatus. The bushes are shown in figure 4.2 and have proved satisfactory in sealing.

The end plates are provided with four similar bushes in order that the cooling sink pipes may pass through them. In addition the bottom end plate has an additional bush for connection of a vacuum pump or gas cylinder.

A sketch of the assembled apparatus is shown in Figure 4.2.

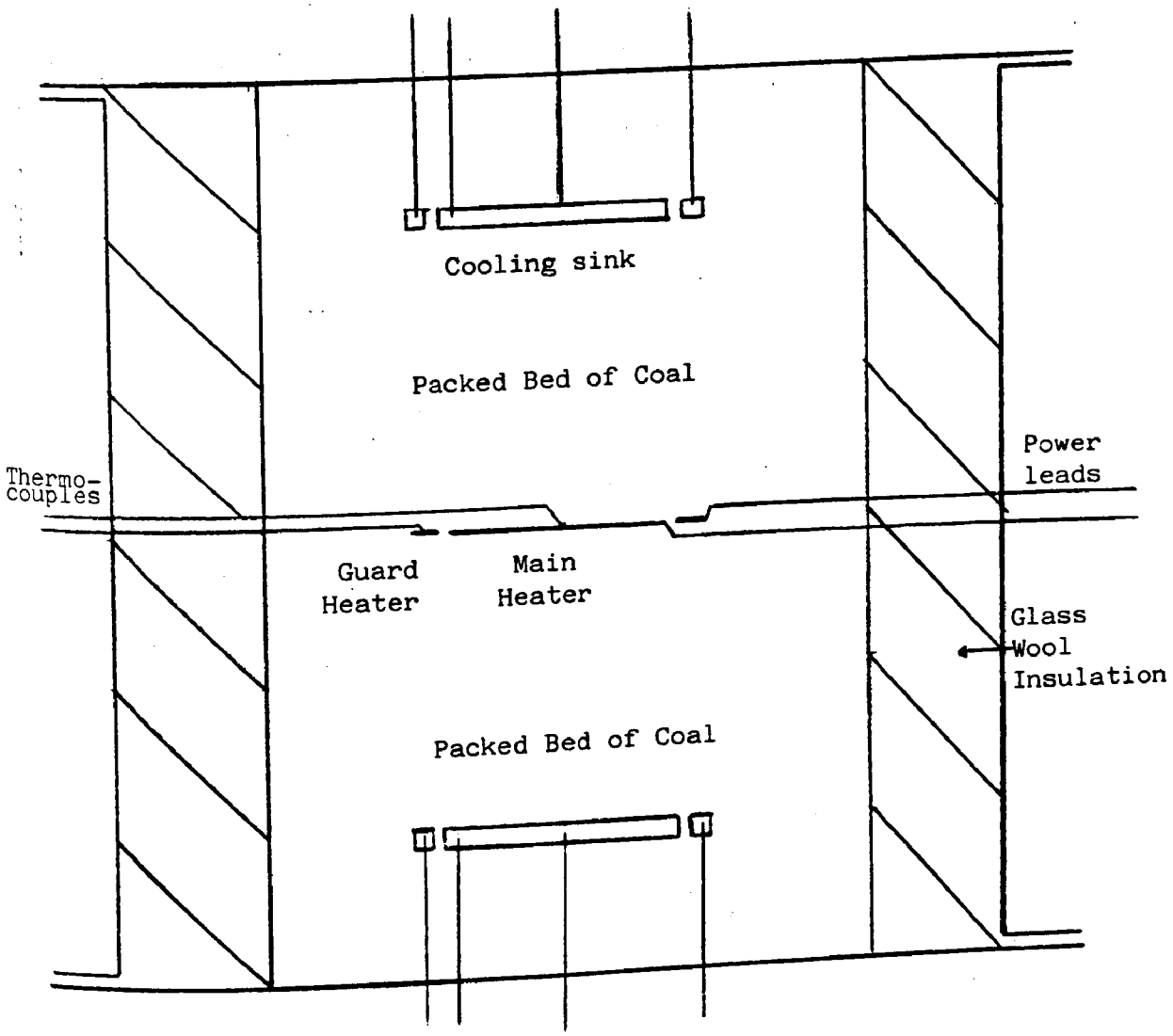


Figure 4.2 Guarded hot ring apparatus - Assembled apparatus

4.6.5 Water Supply to Heat Sinks

The apparatus is designed so that the temperature rise of the water flowing through the sinks is approximately 1 ^{o}C. A larger temperature rise is not used as this would upset the accuracy of the measurement of the temperature difference between the hot and cold faces. In order to measure this 1 ^{o}C temperature rise accurately it is neccessary to control the temperature of the water entering the sinks to at least 0.05 ^{o}C and preferably to 0.01 ^{o}C. To achieve this the following system is used:

Water flows from a constant head tank through a coil which is immersed in a constant termperature bath. The bath is controlled with a proportional controller. After leaving the bath the water flows through a jacketed copper pipe and hence to the heat sink. The jacketed pipe has water flowing in the jacket countercurrent to the flow to the sink. The water in the jacket is pumped from the constant temperature bath.

4.6.6 Measurement Techniques

The temperature of the main heater and guard heater are measured with chromel-alumel thermocouples. The cold junctions of the thermocouples are placed in glass tubes filled with glycerine, which are then placed in a "Thermos" flask filled with ice. The thermocouple voltage is measured using a Cambridge Slide Wire Potentiometer, i.e the voltage is measured at zero current.

The current supplied to the main heater is measured by a Fluke digital multimeter which is continuously in the circuit. This prevents the neccessity of correcting for the internal resistance of the meter. The voltage across the heaters is measured when required by another Fluke multimeter.

The resistances of the thermistors in the cooling sinks are measured in a Wheatstone bridge circuit, using a Kipp and Zonen recorder to measure the off balance voltage from the bridge.

The other values required to solve equation 4.3.12 for K are the heater area A and the length l. A is measured by measuring the diameter of the heater, and l is measured at the time of packing

the equipment with coal.

In fact the heater is not exactly betwen the two sinks, and thus l must be averaged. The correct average is

$$l = \frac{2\, l_1\, l_2}{l_1 + l_2} \qquad 4.6.2$$

where l_1, l_2 are the distances from the bottom and top sinks to the heater respectively.

4.7 Experimental Procedure

The experimental procedure is to switch on the main and guard heaters, setting the voltages so that there is no temperature difference between the guard and main heaters. The equipment takes approximately one week to reach steady-state, and each subsequent adjustment of the guard heater voltage requires further time for steady-state to be reached.

At the time of taking measurements the following are measured:

1) The voltage across the main heater and the guard heater.
2) The current through the main heater.
3) The thermocouple voltages on the main and guard heaters.
4) The resistance of the thermistors in the cooling sinks.

Once the thermocouple voltages and thermistor resistances have been converted to temperatures using calibration tables, the thermal conductivity is calculated from

$$k = \frac{V_m\, I_m\, l}{2\, A\, \Delta T} \qquad 4.6.3$$

V_m = main heater voltage
I_m = main heater current
ΔT = temperature difference between heater and sink

4.8 Results and Discussion

The results of the series of runs performed over the period March 1982 to August 1982 are tabulated in Appendix 2.

Although the resistances of the thermistors in the heat sinks were measured, it was not possible to calculate the energy absorbed at one heat sink. This was due to the fact that the thermistors are not identical i.e. they have slightly different resistances at the same temperature. An attempt was made to calibrate the thermistor pairs, but this was not succesful due to the fact that the calibration drifts with time. In addition problems were experienced with thermistors leaking and giving erratic readings. This facet of the experiment was consequently abandoned.

As can be seen from these results the thermal conductivity of the coal does not vary significantly in the temperature range considered. The mean value is 0.22 W/m/K.

It should be noted that for the largest tempeature difference used in the apparatus, the Rayleigh number as calculatedfrom equation 3.6.5 is 1.9. Therefore it may be safely assumed that only heat transfer by conduction was measured in this series of experiments, since this Rayleigh number is below the value required for the onset of natural convection.

The original intention of this experiment was to obtain experimental values for the so-called effective thermal conductivity of a coal bed, and deduce its functional relationship with particle size and voidage. However during the early stages of the mathematical modelling performed as part of this investigation, it was found that the thermal conductivity did not play as crucial a role in the equations as first believed. For this reason the experimental work was considered complete once a value of the thermal conductivity had been obtained for a typical sample of coal.

It is felt that a simple relationship for relating the thermal conductivity of the bed to that of the coal and the gas is all that is required. The relationship

$$k_b = \epsilon\, k_g + (1-\epsilon)\, \eta\, k_s \qquad 3.8.1$$

k_g = gas thermal conductivity
k_s = solid thermal conductivity
ϵ = voidage
η = tortuosity factor

which was presented and discussed in chapter 3 is probably satisfactory for a study of this type.

Using the values

k_g = 0.026 W/m/K (Perry & Chilton, 1973)
k_s = 0.28 W/m/K (Badzioch, Gregory & Field, 1964)
k_b = 0.22 W/m/K
ϵ = 0.38 (Appendix 2)

gives a value for η of 1.2.

5. MATHEMATICAL MODELLING OF A ONE-DIMENSIONAL ANALOGUE OF A COAL DUMP

5.1 Introduction

In any attempt to understand a natural phenomenon a model for the phenomenon is invaluable. In the case of a coal dump a mathematical model is required which has the ability to show the behaviour of a real coal dump, while still being simple enough to be solved. The full three dimensional equations for the transport processes occuring in a coal dump would be extremely complicated, and may indeed be impossible to solve without a tremendous amount of computation. A simpler model is required which may be solved without the excessive use of computation, but which nevertheless within its limits of applicability has the ability to predict whether a given coal dump may be considered to be safe or unsafe, and if unsafe what measures may be taken to render it safe. A model which is fundamentally based may be used to extrapolate measured data, which is not the case with models that are mainly empirical in nature. In addition the mathematical model points to the best experiments to measure the parameters required. It is believed that the mathematical model presented here has many of these desirable characteristics.

Mathematical models for coal dumps have been presented before, and in order to understand the reason for deriving a new one, a brief survey of these models and their shortcomings follows.

5.2 Literature survey of mathematical models for coal dumps

Much experimental effort has been devoted to measurement of physiochemical properties of coal over the last century. Less attention has been given to the development of a method to predict self heating.

An early model that attempts to predict safe conditions of storage of coal is that of Van Doornum (1954). The essential assumption of this model is that the coal may be considered to be a source of energy given by:

$$q' = A' \exp (a'v - \alpha t) \qquad 5.2.1$$

where q' = rate of generation
A' = fitting constant
a' = fitting constant
v = temperature above ambient
α = fitting constant
t = time

It should be noted that the form of equation 5.2.1 is in disagreement with the usual Arrhenius type temperature dependence of chemical reactions.

Van Doornum (1954) solves the conduction equation:

$$\rho_b \bar{c}_b \frac{\partial v}{\partial t} = \nabla^2(kv) + q' \qquad 5.2.2$$

where ρ_b = density of pile
$\bar{c}_b$ = specific heat capacity of coal
k = thermal conductivity
q' = source given by 5.2.1

for various geometries. From an analysis of the stability of the solutions the following is made that the safety or otherwise of a coal pile may be characterized by two dimensionless numbers M' and N' given by:

$$M' = \frac{A'a'}{\alpha \rho_b \bar{c}_b} \qquad 5.2.3$$

$$N' = \alpha \tau' \qquad 5.2.4$$

τ' = time constant for heat loss

τ' depends on the storage situation. For heat loss by conduction

$$\tau' = \frac{k \pi^2}{4 L^2 \rho_b \bar{c}_b} \qquad 5.2.5$$

L = height of pile

The criterion derived is as follows:

For $M' < 0.63$: a coal is unconditionally safe
$M' > 1.2$: the occurence of spontaneous combustion is very likely.

For the region $0.63 < M' < 1.2$ the situation, depending on the value of N', is normally manageable if care is taken.

This work has been adopted by the National Institute for Coal Research of South Africa as a test on the exportability of coal. The numbers M' and N' are found experimentally from a non-linear regression of the temperature-time curve at the centre of a 15 ton sample of coal which is aerated in a test bunker.

The chief disadvantage of this model is that no specific account is taken of the effect of oxygen depletion on the safety of a dump. In addition the constants in equation 5.2.1 have to be measured experimentally for every different coal; for instance, it is not possible to extrapolate measured data for one size grading of coal to a different size grading of the same coal.

Sondreal & Ellman (1974) performed exhaustive tests on North Dakota lignite, which data was used to perform computer simulations of spontaneous heating. The quantities measured by these investigators were the following:

a) The rate of oxidation of lignite, and the heat of reaction.
b) The specific heat of lignite.
c) The heat of wetting.
d) Airflow through a bed of compacted lignite.
e) The thermal conductivity of solid lignite.

In all case the quantities were measured at various moisture contents and bulk densities. The authors have used least squares techniques to fit the data to equations which are largely empirical in nature. These empirical equations have been used in computer simulations of spontaneous heating, using finite difference forms of the differential equation 5.2.2 together with a material balance equation for oxygen.

The authors present a large number of graphs showing the temperature rise in lignite under various assumptions. The cases

considered include the effects of prior oxidation, pressure gradients due to wind, porosity and moisutre content of the coal.

Although these investigators were most thorough in their approach, the chief disadvantage of this study is that it is highly specific to the particular lignite used. The authors state that the range of validity of their empirical correlations is limited to the range studied, and that extrapolations should only be made with caution. In addition Sondreal & Ellman (1974) take no account of airflow due to natural convection.

Nordon (1979) has presented a model for the self heating reactions of coal or char. The reactants considered are oxygen and water vapour, which are transported into the pile by molecular diffusion and forced convection due to differential wind pressure. A one-dimensional model is used in which the differential equations describing heat and mass transfer are:

$$(1-\epsilon)\,\rho_b\,\bar{c}_b\,\frac{\partial T}{\partial t} = \frac{(1-\epsilon)}{K}\,\frac{\partial^2 T}{\partial x^2} - \epsilon\,U\,\rho_g\,\hat{c}\,\frac{\partial T}{\partial x} - r\,\Delta H_r \qquad 5.2.6$$

where
K = thermal diffusivity
x = length along bed
U = flow velocity
ρ_g = density of gas
$\hat{c}$ = specific heat capacity of gas
r = reaction rate per volume of coal
ΔH_r = enthalpy of reaction

$$0 = \epsilon\,\frac{\partial m}{\partial t} + U\,\frac{\partial m}{\partial x} - D\,\frac{\partial^2 m}{\partial x^2} + \rho_g\,r \qquad 5.2.7$$

m = moles of oxygen per moles of nitrogen in gas
D = diffusion coefficient

These equations are solved using a finite difference method. No account is taken of natural convection flow. The reaction rate of the oxidation reaction is modelled using the so-called Elovich equation:

considered include the effects of prior oxidation, pressure gradients due to wind, porosity and moisutre content of the coal.

Although these investigators were most thorough in their approach, the chief disadvantage of this study is that it is highly specific to the particular lignite used. The authors state that the range of validity of their empirical correlations is limited to the range studied, and that extrapolations should only be made with caution. In addition Sondreal & Ellman (1974) take no account of airflow due to natural convection.

Nordon (1979) has presented a model for the self heating reactions of coal or char. The reactants considered are oxygen and water vapour, which are transported into the pile by molecular diffusion and forced convection due to differential wind pressure. A one-dimensional model is used in which the differential equations describing heat and mass transfer are:

$$(1-\epsilon)\,\rho_b\,\bar{c}_b\,\frac{\partial T}{\partial t} = \frac{(1-\epsilon)}{\kappa}\,\frac{\partial^2 T}{\partial x^2} - \epsilon\,U\,\rho_g\,\hat{c}\,\frac{\partial T}{\partial x} - r\,\Delta H_r \qquad 5.2.6$$

where
κ = thermal diffusivity
x = length along bed
U = flow velocity
ρ_g = density of gas
$\hat{c}$ = specific heat capacity of gas
r = reaction rate per volume of coal
ΔH_r = enthalpy of reaction

$$0 = \epsilon\,\frac{\partial m}{\partial t} + U\,\frac{\partial m}{\partial x} - D\,\frac{\partial^2 m}{\partial x^2} + \rho_g\,r \qquad 5.2.7$$

m = moles of oxygen per moles of nitrogen in gas
D = diffusion coefficient

These equations are solved using a finite difference method. No account is taken of natural convection flow. The reaction rate of the oxidation reaction is modelled using the so-called Elovich equation:

$$\frac{dq}{dt} = r_o A' \exp(-(E + Bq)/RT) \qquad 5.2.8$$

where q = amount of O_2 taken up per unit weight of char.
r_o = rate of oxidation at $T_\infty = 20^oC$ when q = 0.
A' = Arrhenius pre-exponential factor = $\exp(E/RT_\infty)$.
E = activation energy.
B = Elovich constant.

In the results by Nordon (1979) no account has been taken of the presence of moisture. As in the case of Sondreal & Ellman (1974) this author presents graphs showing the effect of various parameters on the temperature rise in char beds. The cases considered are:

a) Self heating for various bed lengths where diffusion is the only transport process.

b) Dependence of steady state temperature on critical bed size for various activation energies.

c) Self heating where diffusion and convection processes are present.

d) The moderating influence of Elovich kinetics.

The author concludes that there is a critical bed length above which spontaneous combustion will occur. He states that for bed lengths smaller that this critical value the steady state temperature rise is small and is limited by heat transfer. The high temperature steady state is caused by the reaction being limited by the rate of oxygen diffusion. With forced convection present this oxygen limitation may be removed; however when the forced convection becomes large loss of heat through flow will limit the reaction, leading to a low temperature steady state. Note however that the air flow required for this to occur is of the order of 10^{-4} m/s which is a fairly large flowrate for the fine (-3,35 mm) material considered in this study.

This study then is theoretically sound, and the author presents a

good discussion of the nature of self-heating. The main drawback of the model is the failure to take account of natural convection flows.

The omission by these researchers of natural convection deserves some explanation. It has been suggested by some researchers that the work of Lapwood (1948), as discussed in section 3.6, shows that natural convection is unimportant in coal dumps. The argument used is that Lapwood (1948) states that a Rayleigh number of $4\pi^2$ is a criterion for the onset of stable convection flows. This would seem to imply that the temperature rise required for natural convection flows to take place in a coal dump can be calculated using equation 3.6.5. The equation is

$$Ra = \frac{\Delta T \; \rho_g^2 \; L \; g \; c_g}{k_b \; f \; T_\infty}$$

where the identities $f = \mu/K$ and $\alpha = 1/T_\infty$ for an ideal gas have been used.

Setting the Rayleigh number equal to $4\pi^2$ in the above equation, the quantity $\Delta T \; L$ may be solved for. The results of doing this calculation are summarised in Table 5.1 below.

TABLE 5.1 VALUES OF $\Delta T \; L$ REQUIRED FOR $Ra = 4\pi^2$

D_p (mm)	f ($kg/m^3/s$)	$\Delta T \; L$ (K m)
1	5.6×10^4	9500
2	1.4×10^4	2375
5	2.2×10^3	380
20	1.4×10^2	24

These results have been taken by other researchers to indicate that for a 2 metre bed of 20 mm particles a 12 K temperature rise is necessary for the onset of natural convection flows, and that for 1 mm particles natural convection flows are very unlikely to occur.

There is however a fallacy in this argument. Lapwood investigated natural convection flows for the case of an imposed temperature gradient in the vertical direction, and with impermeable

horizontal faces. The problem is thus constrained to a one-dimensional temperature gradient. The boundary conditions that are implied are not appropriate for the case of a coal dump. A coal dump has no impermeable sides and has each of its surfaces at nearly ambient temperature, and experiences a three-dimensional temperature field.

Young (1985) has reworked this problem for the case of a coal bed open on the top surface, with impermeable sides and a two-dimensional temperature field. For this case it can be shown that the equation governing the stream function of the flow in the bed is:

$$\frac{\partial^2 \psi}{\partial X^2} + \frac{\partial^2 \psi}{\partial Y^2} = \frac{\partial \theta}{\partial X}$$

The right hand side of this equation represents the horizontal temperature gradient. If this quantity is 0 and the boundary conditions are such that ψ is zero everywhere, then this equation can be satisfied by the case of no flow. However, when the temperature gradient in the horizontal direction is non-zero, convection can be expected under all conditions.

Young (1985) has also shown experimentally that for his case as soon as there is any temperature rise in such a bed, natural convection will occur. There is thus no obvious critical Rayleigh number for this case.

Weber (1974) has studied theoretically a similar situation to Lapwood, but with a small horizontal temperature gradient. It appears from this work that there exists no critical Rayleigh number below which there is no flow, but rather that there is a critical Rayleigh number above which there is a fairly rapid increase in flow. The application of this work to coal beds is not completely obvious, because the infinite region considered requires infinite temperatures at the ends; hence only horizontal flows occcur at Rayleigh numbers below a certain critical value.

Bejan (1978) has studied convection in an infinite porous medium with a concentrated heat source; for this case there is no critical Rayleigh nmuber for the onset of convection. The steady-state flow pattern shows an upward flow that becomes very intense near the source. The upward flow extends throughout the medium, and as the Rayleigh number increases, the warmer region

moves upwards. It is felt that this case is likely to be more similar to the situation in a coal dump, than the situation modelled by Lapwood (1948) and Weber (1974).

In conclusion, having reviewed the available models for self-heating it is felt that a model similar to that used by Nordon (1979), but taking into account natural convection flows and neglecting diffusion, (as discussed in Chapter 2), should be developed in order to make predictions about the behaviour of stockpiled coal.

5.3 A one-dimensional analogue of a coal dump

In order to derive a mathematical model of a coal dump which will yield results fairly simply, certain simplifying assumptions have to be made. The main assumption in the model presented here is that the processes of heat, mass and momentum transfer occur in one direction only. Although this is known not to be true in a real coal dump, it does represent a limiting case which in many respects is the worst case. It can be seen that considering heat transfer in one direction only is likely to be the worst case, since the heat loss is limited to one direction only. Similarly considering flow in only one direction is the worst case, since reactant depletion is likely to be less in a one dimensional model than in one in which reactant flows from many directions.

In many important respects the one-dimensional model is accurate. A one-dimensional model is likely to be accurate for the case of coal stored in a silo, if proper allowance is made for radial heat losses that can occur. In the middle of a very large dump of coal heat transfer to the sides is unlikely to be significant because of the large distances involved; significant heat transfer will occur only to the surface of the dump. In addition should a "hot-spot" occur in a dump the flow due to natural convection will be in the same direction as the heat transfer. The existence of hot spots in coal dumps is well known; spontaneous combustion in its early stages is localized, as has been shown by infra-red photography. The reasons for the existence of hot-spots in coal dumps may include inhomogeneity of the bed in respect of degree of compaction, coal reactivity or moisture content. Experimental work by Young (1985), on natural convection in a porous bed containing a line source, shows

clearly that there is a region close to the source through which most of the flow passes. This is shown diagramatically in Figure 5.1, in which model streamlines are plotted for one half of a symmetrical bed, of infinite length in the Z direction, containing a line source located at X=0, Y=0.6. Note that the reason that no flow occurs through the side X=1 is that in solving the model equations Young assumed that this surface was impermeable. This assumption should not drastically effect the behaviour of the streamlines near the source. Although the situation modelled by Young (1985) is not identical to that in a coal bed, it is felt that the flow patterns near a hot-spot are unlikely to be very different to the flow patterns found near a line source.

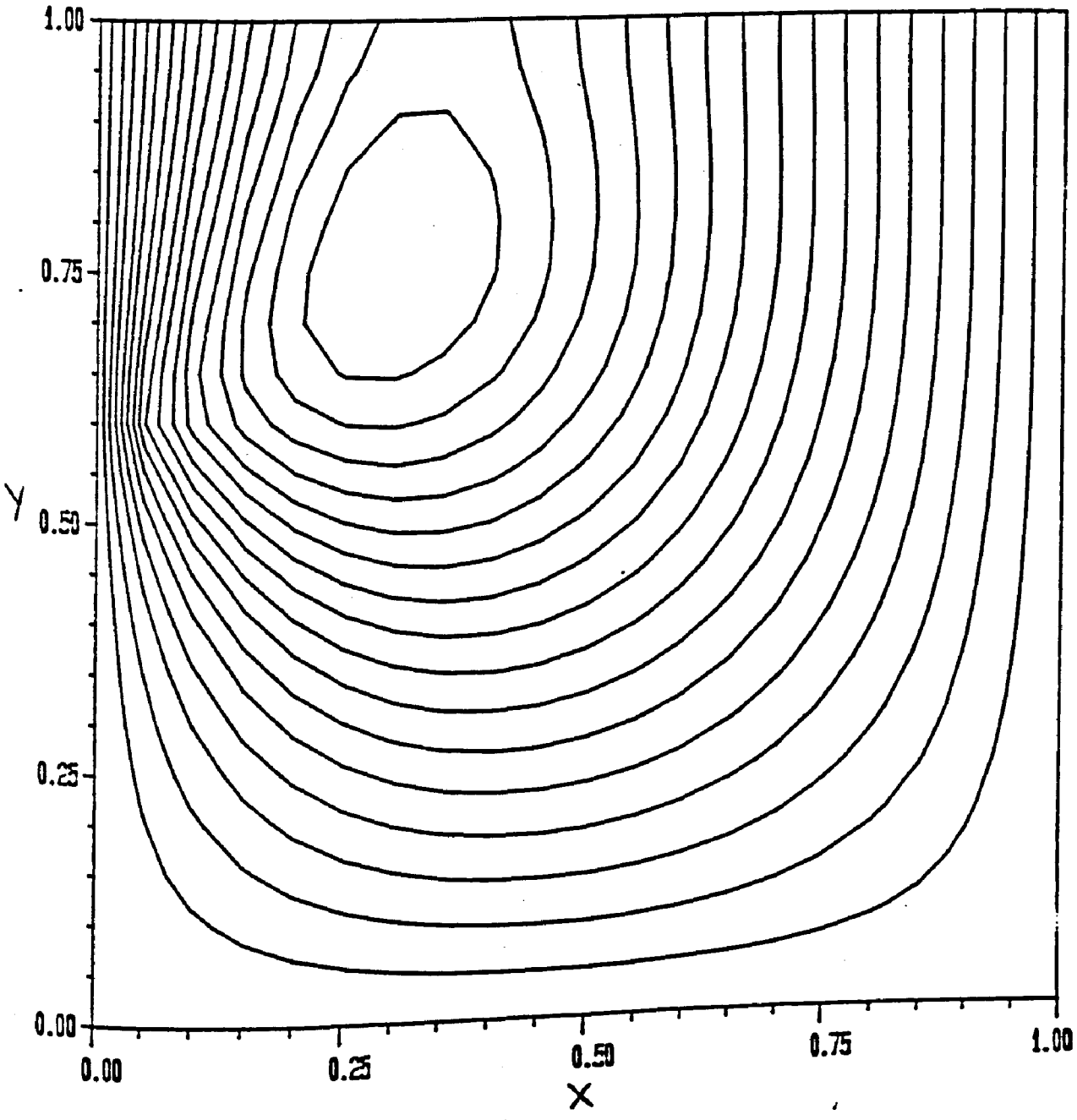


Figure 5.1 Streamlines in a Packed Bed Containing a Line Source (From Young, 1985)

Assuming that a hot spot arises in a coal dump for some reason, it can be reasoned that a chimney effect will take place. Air will flow up the chimney, and be replaced by air flowing in from the sides and top of the dump. If the behaviour of this chimney inside the coal dump can be modelled, then valuable insight into the nature of spontaneous combustion can be obtained. This is the physical basis for the model presented here.

To model the chimney inside the coal bed would be difficult. To make the model simpler the chimney is considered to be perfectly insulating radially. All the flow is considered to occur through the bottom of the bed, with no flow occurring through the sides. The bottom of the bed is considered to be open to atmosphere. These assumptions mean that the chimney can be modelled separately from the rest of the coal dump.

The disadvantages of this model are the following:

a) No simple relationship has been found relating the length of the chimney in the model to the size of the coal dump. Since the bed length is an important model parameter, this limits the applicability of the results obtained. This point will be further discussed in chapter 8.

b) It is assumed that the bottom of the chimney is open and thus loses heat to the atmosphere. In a real dump the bottom of the chimney loses heat to the surrounding coal. It is difficult to gauge how dissimilar these heat loss mechanisms are, and in what way this assumption will affect the results.

Despite these disadvantages the chimney or one-dimensional model may be considered to be a model that has a sound physical basis. The behaviour of the chimney should be similar to the behaviour of a coal dump in many important respects. The shortcomings of the the model are appreciated, but are not expected to invalidate the results obtained, provided these results are not taken to be directly applicable in a quantitative sense.

The great advantage of the model is that the equations derived may be solved fairly easily. A study of the parameters that are important in the prediction of spontaneous combustion may thus be performed without excessive computation.

The main assumptions in the mathematical model used in this study are therefore:

a) Flow and heat transfer occur in the same direction, and since the gas is assumed to flow in plug flow there are no radial gradients in the bed.

b) The reactions considered are

$$n\,C(s) + O_2(g) \rightarrow C_nO_2(s)$$
$$C_nO_2 \rightarrow CO_2 + (n-1)\,C(s)$$
$$\tfrac{1}{2}\,C_nO_2 \rightarrow CO(g) + (\tfrac{1}{2}n-1)\,C(s)$$
$$H_2O(g) \rightleftarrows H_2O(abs)$$

This reaction scheme is in agreement with the observed behaviour of the low temperature reactions of coal, as discussed in Chapter 1. C_nO_2 is oxycoal but note that no specific hypothesis about its structure needs to be made. The fourth reaction is water absorption, which has been reported to be of importance in spontaneous combustion of coal dumps, as has been discussed in chapter 2.

c) Flow is considered to be caused by natural convection and by differential pressure. Molecular diffusion is neglected as discussed in Chapter 2. Natural convection flows occur as soon as there is any temperature rise in the bed, since the bed is considered to be vertically aligned and open top and bottom.

Under these assumptions and some other minor assumptions which arise in the derivation of the equations a mathematical model has been derived. The full derivation is given in Appendix 3.

5.4 Model Equations

The model equations are:

5.4.1 Component mass balances (Gas phase)

$$G\frac{\partial y_i}{\partial x} + \frac{P\,\epsilon}{R\,T_g}\frac{\partial y_i}{\partial t} = r_i - y_i \sum r_j \qquad (i = 1 \text{ to } N)$$

G = molar flowrate per unit area

y_i = mole fraction of i in the gas phase

x = distance along bed

P = pressure

R = gas constant

ϵ = bed voidage

T_g = gas temperature

t = time

r_j = rate of formation of j in the gas phase per unit bed volume

N = number of components in gas phase

5.4.2 Overall gas mass balance

$$\frac{\partial G}{\partial x} + \frac{\epsilon}{R}\frac{\partial (P/T)}{\partial t} = \sum_{j=1}^{N} r_j$$

5.4.3 Component mass balances (Solid phase)

$$(1-\epsilon)\frac{\partial (\rho_s f_j)}{\partial t} = p_j \qquad (j = 1 \text{ to } M)$$

ρ_s = density of solid

f_j = mass fraction of j in the solid

p_j = rate of formation of j in the solid

M = number of components in solid phase

5.4.4 Overall solid mass balance

$$(1-\epsilon)\frac{\partial \rho_s}{\partial t} = \sum_{j=1}^{M} p_j$$

5.4.5 Gas phase energy balance

$$\frac{P\epsilon}{RT_g}\hat{c}\frac{\partial T_g}{\partial t} - \epsilon\frac{\partial P}{\partial t} = -G\hat{c}\frac{\partial T_g}{\partial x} + \epsilon K_g\frac{\partial^2 T_g}{\partial x^2} + Q_c$$

$\hat{c}$ = molar specific heat capacity of gas

K_g = thermal conductivity of gas

Q_c = rate of convection from solid to gas

5.4.6 Solid phase energy balance

$$(1-\epsilon)\,\rho_s\,\bar{c}_s\,\frac{\partial T_s}{\partial t} - (1-\epsilon)\,\frac{\partial P}{\partial t} = (1-\epsilon)\,\eta\,k_s\,\frac{\partial^2 T_s}{\partial x^2} - Q_c - \Sigma\,(r_i \Delta H_r^i)$$

T_s = solid temperature
η = tortuosity factor
k_s = thermal conductivity of solid
ΔH_r^i = enthalpy of reaction for formation of i

5.4.7 Momentum balance

$$\rho\,\frac{\partial U}{\partial t} = -f\,U + g\,\rho_\infty(1-T_\infty/T) - \frac{\partial(P-P_\infty)}{\partial x}$$

U = flow velocity
f = D'Arcy's law constant
ρ_∞ = density of ambient air
P_∞ = ambient air pressure

5.5 Discussion of the model equations

This is a set of M + N + 5 differential equations. The unknowns are tabulated in Table 5.2.

TABLE 5.2 UNKNOWNS IN THE MODEL EQUATIONS

UNKNOWN	DESCRIPTION	NUMBER
y_i	Gas mole fractions	N
G	Molar flowrate/area	1
f_i	Solid mass fractions	M
ρ_s	Solid density	1
T_g	Gas temperature	1
T_s	Solid temperature	1
P	Gas pressure	1

Although the equations have been derived for any number of gas and solid components, in the discussions that follow the gases considered are O_2, N_2, CO_2, CO and H_2O. The solid is considered to be composed of four fractions i.e. carbon, oxycoal, absorbed water and inert material.

5.6 Boundary and Initial Conditions

The following are the boundary conditions used: (x=0 refers to the bottom of the bed and x=L refers to the top).

$$y_i(0,t) = \text{Mole fraction of i in ambient air}$$

The pressure boundary conditions have been discussed in section 2.2 and are:

$$P(0,t) = P_\infty + \rho_\infty V^2/2$$

$$P(L,t) = P_\infty$$

$$V = \text{wind velocity}$$

For the gas phase energy balance

$$\epsilon k_g \frac{\partial T_g(0,t)}{\partial x} = G \hat{c} (T(0,t) - T_\infty)$$

$$\frac{\partial T_g(L,t)}{\partial x} = 0$$

The first boundary condition reflect the fact that the gas entering the bed is heated to the gas temperature. At the end of the bed it is assumed that there is no heat loss due to flow; the gas is assumed to leave the bed in plug-flow, implying that the temperature just outside the bed is equal to the temperature just inside the bed.

For the solid phase energy balance

$$(1-\epsilon) \eta k_s \frac{\partial T_s(0,t)}{\partial x} = h_1 (T_s(0,t) - T_\infty)$$

$$(1-\epsilon) \eta k_s \frac{\partial T_s(L,t)}{\partial x} = -h_2 (T_s(L,t) - T_\infty)$$

These are convective boundary conditions, but h_1 and h_2 may be interpreted as radiation heat transfer coefficients. Initial conditions for the equations involve assigning values to each of the variables at time zero for all x. In most cases ambient values would be used.

6. SIMPLIFICATON OF THE MODEL EQUATIONS AND THEIR SOLUTION

6.1 Introduction

Although a one-dimensional formulation has been used to simplify the equations and reduce their number, the equations remain complicated. In order to simplify them further to perform computation the following assumptions (which are discussed more fully in Appendix 4) were made:

a) The gas and solid temperatures are unlikely to be very different; therefore equations 5.4.5 and 5.4.6 may be combined to give one equation in temperature, ie a continuum assumption is made. The reason for deriving the gas and solid phase energy balances separately is that the boundary conditions for use in the continuum model are not clear; deriving the balances separately and then combining them allows the correct boundary conditions to be deduced mathematically.

b) Since the heat transfer is by far the slowest transfer process occuring in the bed, the other transfer processes may be considered to be at steady state i.e. a pseudo steady state formulation is used.

In order to simplify still further it is convenient to define a rate (ry) which is the rate at which oxygen disappears. Similarly an enthalpy of reaction ΔH_r is defined; this may be considered to be the enthalpy of reaction associated with the disappearance of oxygen. The reaction involving water is ignored for the following reasons:

a) It is likely to be only a starting mechanism whereby the temperature in a coal bed is raised to the point where natural convection flows and oxidation become the mechanisms whereby the dump combusts.

b) As yet no reliable data for this reaction is available, and it is in any case believed that the reaction is likely to be close to equilibrium in most cases.

It would appear from equation 5.4.2 that the change in flowrate due to reaction has to be considered. However, if air is the reactant then even if all the oxygen in the flow is removed the flowrate will only change by twenty percent. It is therefore

6. SIMPLIFICATON OF THE MODEL EQUATIONS AND THEIR SOLUTION

6.1 Introduction

Although a one-dimensional formulation has been used to simplify the equations and reduce their number, the equations remain complicated. In order to simplify them further to perform computation the following assumptions (which are discussed more fully in Appendix 4) were made:

a) The gas and solid temperatures are unlikely to be very different; therefore equations 5.4.5 and 5.4.6 may be combined to give one equation in temperature, ie a continuum assumption is made. The reason for deriving the gas and solid phase energy balances separately is that the boundary conditions for use in the continuum model are not clear; deriving the balances separately and then combining them allows the correct boundary conditions to be deduced mathematically.

b) Since the heat transfer is by far the slowest transfer process occuring in the bed, the other transfer processes may be considered to be at steady state i.e. a pseudo steady state formulation is used.

In order to simplify still further it is convenient to define a rate (ry) which is the rate at which oxygen disappears. Similarly an enthalpy of reaction ΔH_r is defined; this may be considered to be the enthalpy of reaction associated with the disappearance of oxygen. The reaction involving water is ignored for the following reasons:

a) It is likely to be only a starting mechanism whereby the temperature in a coal bed is raised to the point where natural convection flows and oxidation become the mechanisms whereby the dump combusts.

b) As yet no reliable data for this reaction is available, and it is in any case believed that the reaction is likely to be close to equilibrium in most cases.

It would appear from equation 5.4.2 that the change in flowrate due to reaction has to be considered. However, if air is the reactant then even if all the oxygen in the flow is removed the

6. SIMPLIFICATON OF THE MODEL EQUATIONS AND THEIR SOLUTION

6.1 Introduction

Although a one-dimensional formulation has been used to simplify the equations and reduce their number, the equations remain complicated. In order to simplify them further to perform computation the following assumptions (which are discussed more fully in Appendix 4) were made:

a) The gas and solid temperatures are unlikely to be very different; therefore equations 5.4.5 and 5.4.6 may be combined to give one equation in temperature, ie a continuum assumption is made. The reason for deriving the gas and solid phase energy balances separately is that the boundary conditions for use in the continuum model are not clear; deriving the balances separately and then combining them allows the correct boundary conditions to be deduced mathematically.

b) Since the heat transfer is by far the slowest transfer process occuring in the bed, the other transfer processes may be considered to be at steady state i.e. a pseudo steady state formulation is used.

In order to simplify still further it is convenient to define a rate (ry) which is the rate at which oxygen disappears. Similarly an enthalpy of reaction ΔH_r is defined; this may be considered to be the enthalpy of reaction associated with the disappearance of oxygen. The reaction involving water is ignored for the following reasons:

a) It is likely to be only a starting mechanism whereby the temperature in a coal bed is raised to the point where natural convection flows and oxidation become the mechanisms whereby the dump combusts.

b) As yet no reliable data for this reaction is available, and it is in any case believed that the reaction is likely to be close to equilibrium in most cases.

It would appear from equation 5.4.2 that the change in flowrate due to reaction has to be considered. However, if air is the reactant then even if all the oxygen in the flow is removed the flowrate will only change by twenty percent. It is therefore considered adequate to regard the flowrate as a constant to be considered adequate to regard the flowrate as a constant to be calculated from equation 5.4.7.

Under these assumptions the number of equations to be solved is reduced to three i.e. a temperature equation, an oxygen equation and a flowrate equation. These equations are given below.

Temperature: $$\rho C_b \frac{\partial T}{\partial t} = k_b \frac{\partial^2 T}{\partial x^2} - G \hat{c} \frac{\partial T}{\partial x} + r\, y\, \Delta H_r \qquad 6.1.1$$

ρ_b = density of bed
C_b = specific heat capacity of bed
k_b = thermal conductivity of bed
y = mole fraction oxygen
ΔH_r = enthalpy of reaction for oxygen disappearance

Oxygen: $$G \frac{dy}{dx} = -r\, y \qquad 6.1.2$$

Flowrate: $$\frac{d(P-P_\infty)}{dx} = -f\, G\, R\, T/P + g(\rho_\infty - \rho) \qquad 6.1.3$$

One possible functional form for the rate of reaction r has been discussed in Section 1.3, but should a superior rate expression for the oxidation be proposed it would be a simple matter to use this expression in the model.

The boundary conditions on the equations are:

$$k_b \frac{\partial T(0,t)}{\partial x} = (h_0 + G \hat{c})\,(T(0,t)-T_\infty)$$

$$k_b \frac{\partial T(L,t)}{\partial x} = -h_1\,(T(L,t)-T_\infty)$$

$y(x=0)$ = mole fraction of oxygen in air

$P(x=0) = P_\infty + \rho_\infty V^2/2$

$P(x=L) = P_\infty$

The initial condition for equation 6.1.1 is a given temperature profile e.g. $T(x,0) = T_0(x)$.

It is convenient in what follows to make equation 6.1.1 dimen-

sionless. To do this the following substitutions are made:

$$\theta = T/T_\infty$$
$$X = x/L$$
$$\tau = \kappa t/L^2$$
$$a = G\,\hat{c}\,L/k_b$$
$$b = L^2\,r\,(-\Delta H_r)/(T_\infty\,k_b)$$
$$\gamma_s = -r/G$$
$$Bi_0 = h_0\,L/k_b$$
$$Bi_1 = h_1\,L/k_b$$

Equation 6.1.1 becomes:

$$\frac{\partial\theta}{\partial\tau} = \frac{\partial^2\theta}{\partial X^2} - a\,\frac{\partial\theta}{\partial X} - b\,\gamma \qquad 6.1.4$$

with boundary conditions

at X=0 $$\frac{\partial\theta}{\partial X} = (Bi_0+a)(\theta-1)$$

at X=1 $$\frac{\partial\theta}{\partial X} = -Bi_1(\theta-1)$$

The initial condition is $\theta(X,0) = \theta_0(X)$

This equation may be improved by including a heat loss term. This heat loss term takes into account radial heat losses that are not taken into account in the original model. The term, as is shown in Appendix 5, may be written as $C(\theta - 1)$. In a sense C is a free parameter. It does however have real meaning in simulating a coal dump as will be seen in Chapter 7. Equation 6.1.4 becomes:

$$\frac{\partial\theta}{\partial\tau} = \frac{\partial^2\theta}{\partial X^2} - a\,\frac{\partial\theta}{\partial X} - b\,\gamma - C\,(\theta - 1) \qquad 6.1.5$$

with boundary and initial conditions as above.

6.2 The Steady-State form of the Equations

It may be argued that the set of equations does not have a steady-state solution since the reaction rate r is a function of the amount of oxidation and therefore of time. If the reaction rate is constantly falling off with time, i.e. the coal is

ageing, then there is no steady state. However it is convenient to study the behaviour of the equations in the limit of steady state, and for this purpose the ageing of the coal is ignored, and the so-called reaction rate of fresh coal is used. This is in a sense the worst case since the fresh coal has the highest reaction rate.

The temperature equation then becomes

$$0 = \frac{d^2\theta}{dX^2} - a\frac{d\theta}{dX} - b\,y - C\,(\theta - 1) \qquad 6.2.1$$

First attempts to solve equation 6.2.1 with equation 6.1.2 and 6.1.3 involved the use of a Runge - Kutta algorithm. The method used was a shooting one i.e. a temperature at X = 0 and flowrate were guessed, and the equations integrated forward to try and meet the boundary conditions at X = 1. This method met with no success at all, since the calculated temperature was very sensitive to the assumed value of the inlet temperature. Changing the value of this temperature led either to the temperature increasing without bound or becoming negative. An explanation for this behaviour is given in Appendix 6.

An alternative method of solving equation 6.2.1 involves making the assumption that the reaction rate r may be considered constant throughout the bed. This is a very large assumption since the form of r involves an exponential of the temperature, and thus r cannot in fact be constant unless the bed temperature is constant. However over a fairly small range of temperature the assumption of an average rate in the bed is acceptable, even though the answers it gives will not be quite correct. A further justification for making this assumption is that an analytic form for the temperature profile in the coal bed may be obtained, and thus the characteristics of the solution may be quickly investigated.

The details of the solution are given in Appendix 7, and the temperature equation has the form:

$$\theta_{ss}(X) = 1 + C_1\exp(\gamma_1 X) + C_2\exp(\gamma_2 X) + C_3\exp(\gamma_3 X) \qquad 6.2.2$$

The coefficients γ_1, γ_2, C_1, C_2, and C_3 are given functions of the known parameters.

The solution of the equation set is in fact iterative, since some average temperature is assumed and the flowrate and average reaction rate calculated. This in turn leads to a new temperature profile, flowrate, and average reaction rate and so on till the process converges. The computer code to perform this calculation is given in Appendix 12.

The character of the solutions so obtained and their significance is discussed in Chapter 8.

6.3 The Solution of the Unsteady-State Equations with a Constant Rate

The unsteady state behaviour of the equation set is of great practical importance. If a coal dump is going to be reclaimed in a relatively short time, then its long time or steady-state behaviour is of little importance in predicting the safety or otherwise of the dump. In addition it is only possible to decide whether a given dump will achieve a safe or unsafe steady-state by considering the behaviour of the temperature with time.

As a continuation of the work in which the equation set is solved using a constant rate, a solution was sought for the unsteady state behaviour under the same assumption.

The equation to be solved is equation 6.1.5 and the details of the solution are given in Appendix 8. The solution is:

$$\theta(X,\tau) = \theta_{ss}(X) + v(X,\tau)\exp(-\tau(a^2/4-C) + aX/2) \qquad 6.3.1$$

where $$v(X,\tau) = \Sigma \{Z_n(X)\exp(-\beta_n^2\tau)\ Z_n(X')\ g(X')\ dX'\} \qquad 6.3.2$$

$$Z_n(X) = \frac{2(\beta_n^2+Bi_3^2)(\beta_n\cos(\beta_n X)+Bi_2\sin(\beta_n X))}{((\beta_n^2+Bi_2^2)(\beta_n^2+Bi_3^2+Bi_3)+Bi_2(\beta_n^2+Bi_3^2))}$$

$$g(X) = (\theta_o(X) - \phi_{ss}(X))\exp(-aX/2) \qquad 6.3.3$$

$$Bi_2 = Bi_0 + a/2$$

$$Bi_3 = Bi_1 + a/2$$

and the β_n are the positive roots of

$$\tan(\beta) = \frac{\beta(Bi_3 + Bi_2)}{(Bi_2\, Bi_3 + \beta^2)} \qquad 6.3.4$$

Obtaining the final solution (equation 6.3.1) at a given X and τ is a stepwise process, since starting with the initial condition $\theta_0(X)$ the coefficients a, b, and γ_3 are calculated. A time step is then taken and the temperature profile calculated. This in turn gives new values of a, b, and γ_3 and the process continued.

The solution has been programmed in BASIC on a HP 9835 computer, and the code is given in Appendix 12. In practice it has been found that only twenty terms of the series need be taken. Nevertheless obtaining the solution is a fairly lengthy process, since for each time step $Z_n(X)$ and the integral in equation 6.3.2 must be calculated for a number of X values.

The character of the solutions obtained by this method is discussed in Chapter 8.

6.4 A Numerical Method for Solving the Unsteady State Equations

A numerical method for solving the equation set has the following advantages:

a) The variation of the reaction rate with temperature and amount of oxidation of coal can be taken into account.

b) The model can be used to fit data obtained from experiments such as the one described in Chapter 7. This data can then be used to make predictions about the behaviour of a given coal in a given stockpiling situation.

The disadvantage of a numerical method is that no general observations can be made about the form of the solution, as is possible with an analytic solution. Also the amount of computation may become prohibitive.

The method chosen for solving the equations in this case is one first presented by Bellman, Kashef & Casti (1972), which has been

termed the method of lines. The technique involves the use of a Legendre polynomial to fit the temperature profile at any given time t. This has the effect of reducing the partial differential equation to a set of ordinary differential equations, which may then be solved by one of many available methods e.g. Runge-Kutta or Adams-Moulton.

The advantage of this method over the more normally used finite difference approach is that the finite difference methods require calcualtion at a large number of points in order to obtain accurate results at the points of interest. Consequently both the computing time and storage required are large. In contrast, the approach of doing the calculation at the nodes of the shifted Legendre polynomial offers a moderately accurate solution at a few points, and the solution may be calculated rapidly.

The essence of the method rests in writing

$$\frac{\partial\theta(X_j,\tau)}{\partial X} = \Sigma(a_{ij}\ \theta(X_j,\tau)) \qquad \text{for } i=1 \text{ to } n \qquad 6.4.1$$

The X_j are chosen to be the nodes of the shifted Legendre polynomial

$$P_n^*(X) = P_n(1-2X) \qquad 6.4.2$$

and the matrix a_{ij} of weighting factors may be calculated once and for all.

The details of the application of the technique to the particular set of equations under consideration are given in Appendix 9. In many respects the solution procedure is similar to that discussd in Section 6.3, since the coefficients a, b, and γ_3 are recalculated at each time step.

This solution method has also been programmed in BASIC on an HP 9816 computer, and the code is given in Appendix 12. The choice of the length of the time step chosen is critical to the stability of the method, but apart from this the method is very effective. Calculational time is in fact shorter than that required to obtain the solution 6.3.1 and it has been found that using a ninth order Legendre Polynomial is entirely adequate.

Further discussion of the method and the results obtained is given in Chapter 8.

7. EXPERIMENTAL INVESTIGATION OF THE BEHAVIOUR OF A ONE DIMENSIONAL ANALOGUE OF A COAL DUMP

7.1 Introduction

In order to attempt to validate the equations derived in the previous sections, as well as to obtain data to use in a parameter study, it was decided to build a coal chimney. The apparatus used and results obtained are discussed in this chapter.

7.2 Experimental

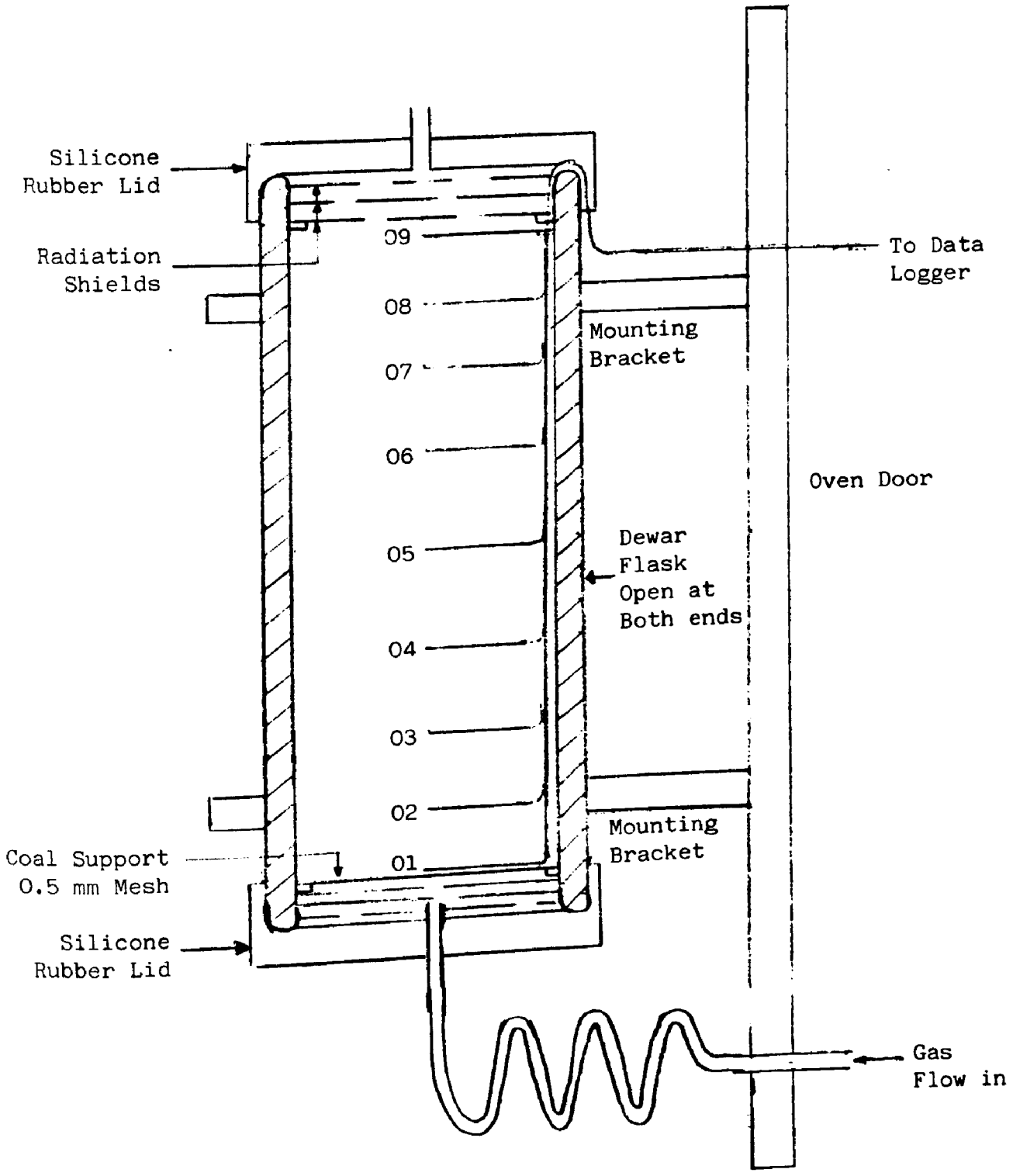
A skethch of the apparatus used is shown in figure 7.1. The coal chimney is constructed from an open ended Dewar Flask of 78 mm internal diameter and 240 mm height. Dimples of glass 20 mm from the bottom of the apparatus provide support for a piece of thin mesh, which in turn supports the coal. The chimney is provided with removable silicone rubber lids above and below. Both lids have 6 mm copper tubing moulded in, to provide for flow of gas in and out.

To minimize heat losses radiation shields manufactured from aluminium foil covered balsa wood discs are used. 10 mm Holes are punched in these discs in such a way that if three discs are assembled 5 mm apart, no direct rays of radiation can escape.

Thermocouples are manufactured by sparking together 20 SWG fabric coverd copper and constantan. The thermocouples are tested at 0°C and at the boiling point of water.

At the time of packing the bed with coal, the thermocouples are placed with their exposed ends on the centre line of the apparatus. Nine thermocouples are placed in the apparatus at positions corresponding to the nodes of the ninth order Legendre polynomial used in the solution method discussed in section 6.4.

In order to record the temperature-time behaviour of the chimney, these nine thermocouples, together with a tenth thermocouple placed in the oven containing the apparatus, are connected to a HP 3054 Data Aquisition Unit controlled by an HP 85 computer. A program



01 - 09: Copper Constantan Theromcouples

Figure 7.1 Chimney Experiment - Apparatus

supplied by Hewlett Packard is used to record the temperatures at a suitable time interval, as well as to print the temperatures and record them on tape. The program converts thermocouple voltages to temperatures using a fourth order polynomial; a silicon device built in to the data logger provides the cold junction reference temperature.

The apparatus is contained within a thermostatically controlled oven. Considerable care is taken to ensure that the temperature variations within the oven are small. The temperature in the oven is continually recorded using an eleventh thermocouple and a recorder. The temperature control of the oven is better than one degree centigrade.

The bed is supplied with gas (either nitrogen and oxygen) from cylinders. A series of valves are used to drop the pressure from the cylinder to the inlet of the bed, and to provide control over the flowrate of gas into the bed. This flowrate is measured usng a Tri Flat Variable Area Floe Meter. The manufacturer's curves are used to convert a reading on the meter to a volumetric flowrate. The barometric pressure is recorded in order that the volumetric flowrate can be converted to a molar flowrate. In order to ensure that the gas entering the bed is at oven temperature, a coil of length 0.5 m of 6 mm copper pipe is provided within the oven. enables the temperature time and temperature distance profiles to be automatically logged at any suitable time interval.

Experimental procedure consists of setting the oven temperature to the desired level, and placing the apparatus in the oven with a flow of nitrogen through the bed. Temperatures are recorded until they are considered to be steady. The flow is then switched to oxygen, and the temperature-time data recorded. For each run fresh coal that has been stored under water is used, in order to minimize the amount of prior oxidation of the coal. The coal is allowed to dry in a thin layer overnight at ambient temperature.

The experimental data obtained is tabulated in Appendix 10.

7.3 Experimental Results

The accuracy of results obtained from this experiment is limited by the accuracy to which the heat transfer characteristics of the apparatus are known. In order to calculate the numbers Bi_o, Bi_1, and C required for the model the bed was heated under nitrogen and then removed from the oven while continuing the nitrogen flow. The temperature time curve was then recorded, and a trial and error method used to calculate the values of the coefficients which best fit the data. The results of this fitting procedure are shown in Figure 7.2.

It can be seen that the experimental data is fitted very well at the centre of the bed but rather poorly at the ends of the bed. This indicates that the heat transfer mechanism at the ends of the bed is not well modelled by a heat transfer coefficient. However it was felt that if the rest of the fitting was done with temperature time curves at the centre of the bed the results would at least yield suitable values to use in a parameter study.

Two different sorts of behaviour have been observed during the experiments in which oxygen is flowed through a preheated coal bed. The different sorts of behaviour depend on the particle size of the coal used and the oven temperature.

The first type of behaviour which is observed is a fairly gentle rise of the temperature in the bed, with some maximum temperature being reached, after which the temperature begins to fall off again. This behaviour can only occur if the reactivity of the coal is falling off with time; this implies that the coal is ageing. This behaviour, observed for the larger particle sizes at oven temperatures of approximately 90 ^{o}C, has been used to calculate the various constants in the shrinking core model discussed in Section 1.3; these fits are shown in Figures 7.3 and 7.4.

The second type of behaviour observed is a fairly rapid temperature increase in the coal bed with the rate of temperature rise increasing with time. This behaviour may be considered to be combustion. When this occurs the coal bed has to be cooled down by taking the apparatus out of the oven and restoring the

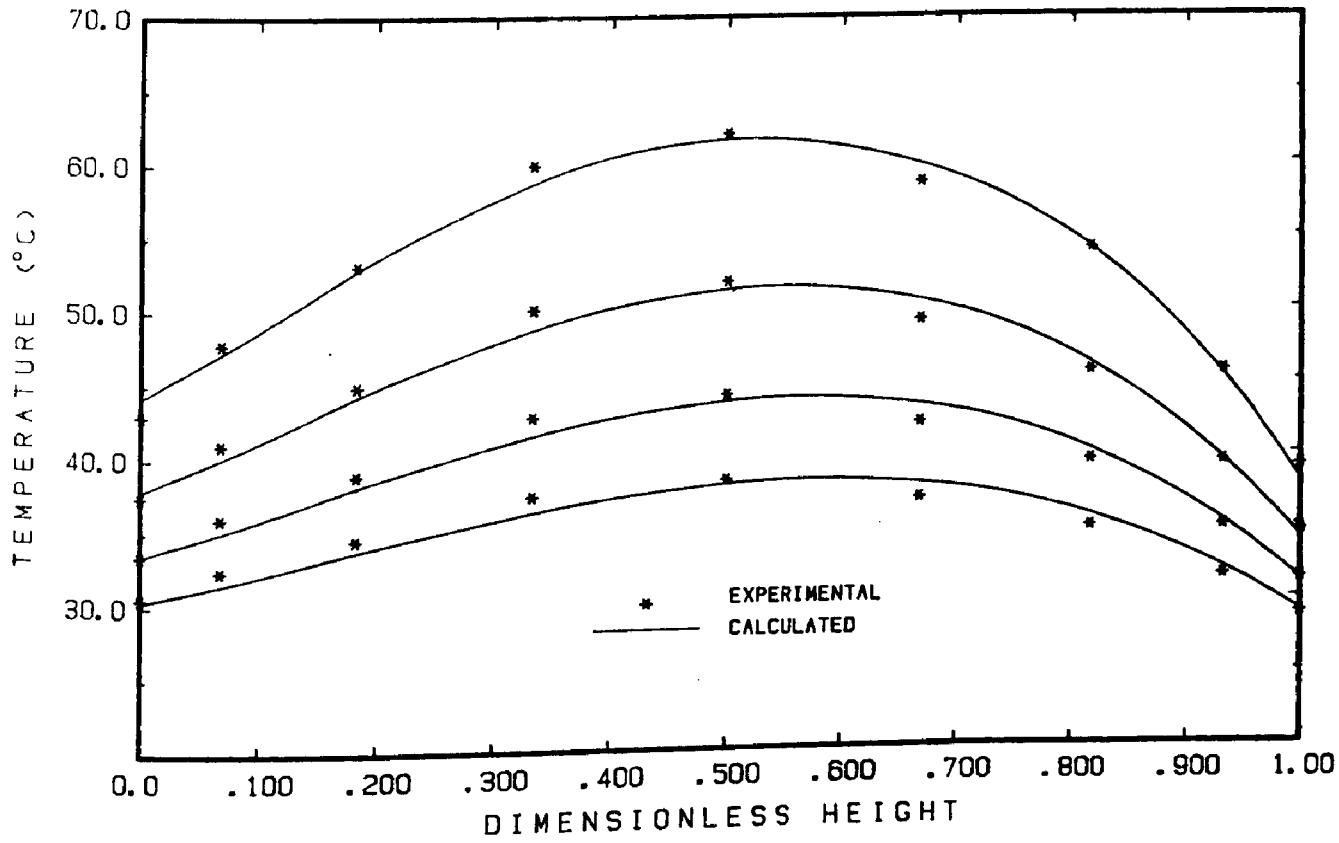


Figure 7.2 Chimney experiment - Fitting heat transfer coefficients

Profiles plotted every 30 minutes

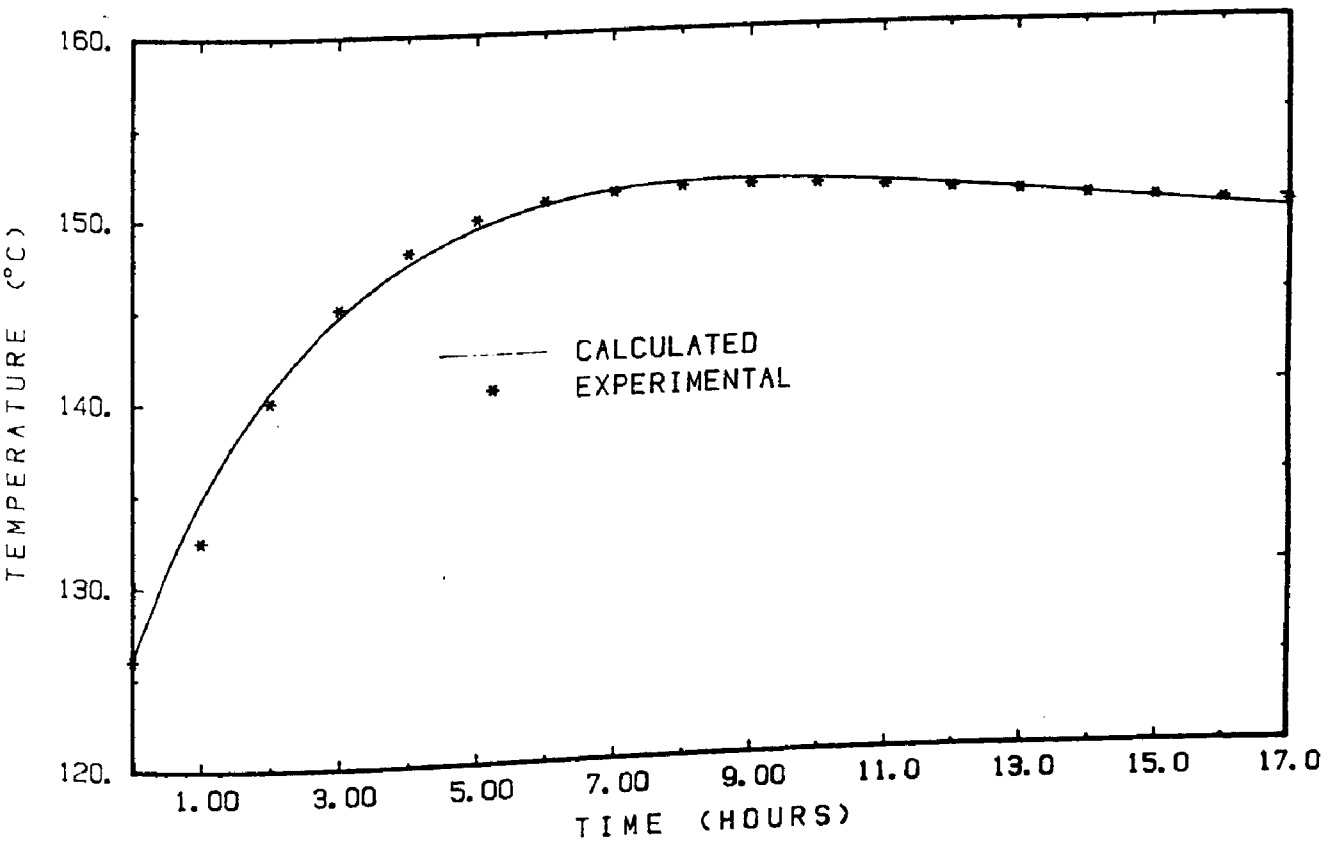


Figure 7.3 Chimney experiment - Fitting ageing run 1

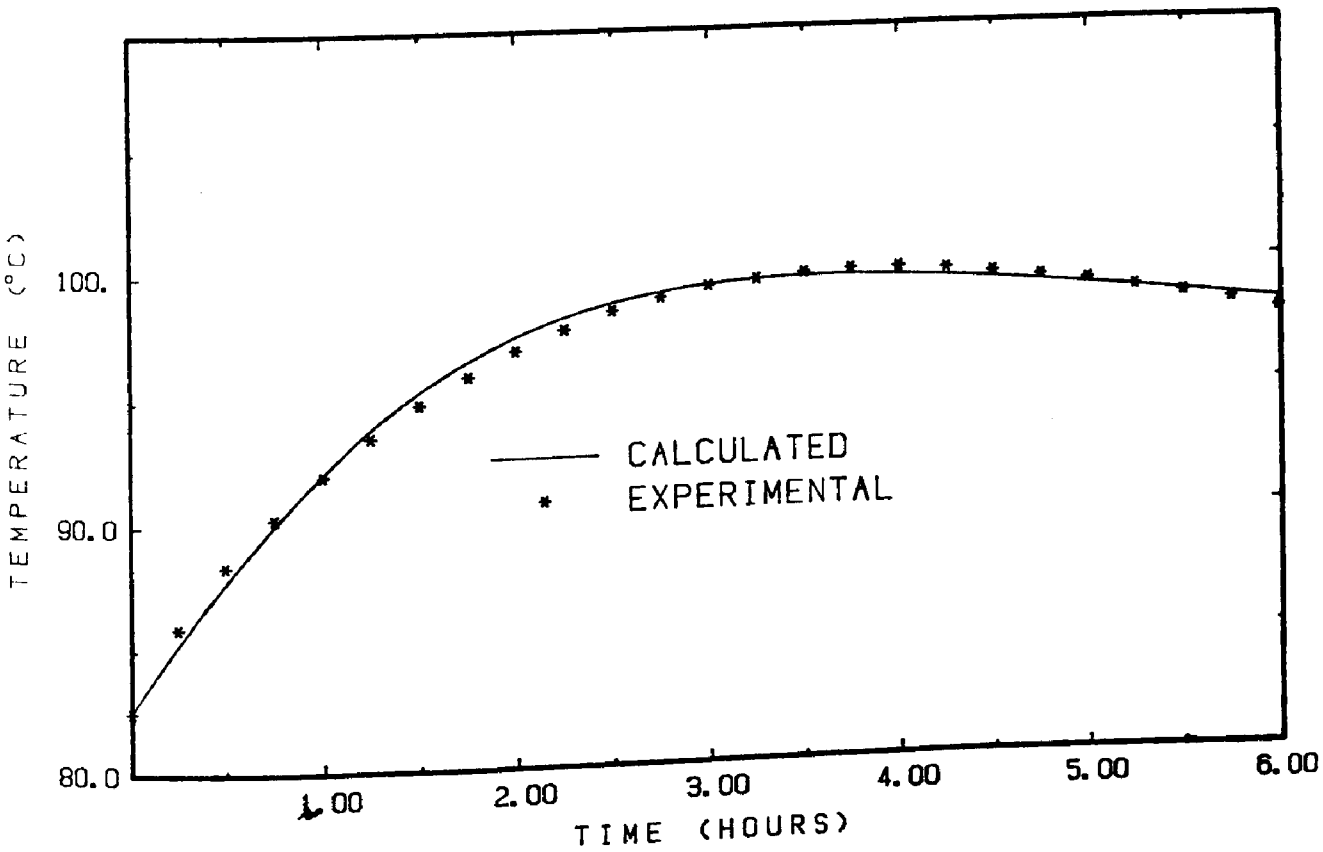


Figure 7.4 Chimney experiment - Fitting ageing run 2

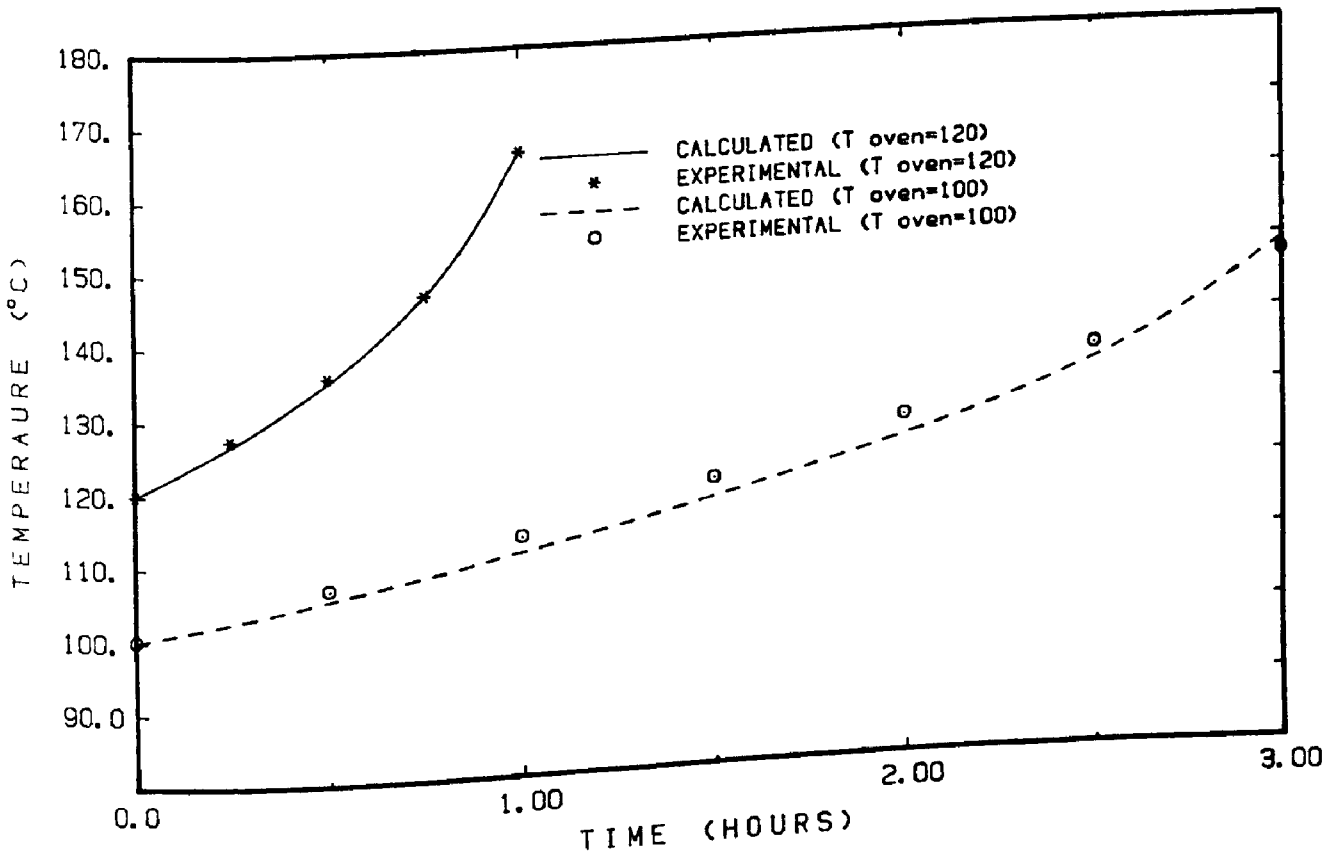


Figure 7.5 Chimney experiment - Fitting ignition runs

nitrogen flow.

These ignition runs yield very valuable information since it proves simpler to deduce the kinetic data from these runs then from the runs in which there is a gentle temperature rise. The reasons for this are that the temperature rises are much larger, meaning that ageing is a smaller effect. An example of the fitting of this data is shown in Figure 7.5 where two different experimental runs are fitted with the same data. The fit is fair but tends to be poorer as the temperature increases more rapidly. The reason for this is that at these higher temperature some of the model assumptions breakdown.

The values of the parameters used to obtain the fits shown in figures 7.2 to 7.5 are tabulated in Appendix 10. It must be stressed that these parameters, in particular the reaction rate values, are likely to be very different for different coals.

7.4 Discussion

The experiment used to derive the results in this section is not a good experiment from the point of view of analyzing the results to obtain the parameters required. This is partly because many of the parameters required in the model need to be estimated, and there may be a high cross correlation between the estimated parameters, and those found by curve fitting. However it is felt that the parameters calculated are accurate enough to give starting values for the parameter analysis discussed in the next chapter.

The analysis of the experiment may be improved in many respects e.g. by the use of a minimization routine to calculate the parameters. This was not felt neccessary in the present study.

8. RESULTS OF SOLVING THE MODEL EQUATIONS

8.1 Introduction

In this chapter the results of solving the model equations are presented. The three cases considered are:

a) Solving the steady-state equations with constant r.
b) Solving the unsteady-state equations with constant r.
c) Solving the equations with no assumptions, using a numerical method.

8.2 Steady-State Solution for constant r

Since an analytic solution exists for the temperature profile in this case, it has been used to perform a parameter study of the effect that changing the model parameters has on the calculated temperature profiles. In order to perform this parameter study a base set of parameter values had to be chosen, and certain assumptions made. The values of the parameters for this base case are given in Appendix 11. The assumptions made were the following:

a) The coal may be characterized by a single particle diameter, D_p, where

$$D_p = 6/S$$

S = external surface area per particle volume

b) The surface area for reaction, S_t, is set equal to the external surface area, S. However, the effect of changing this assumption has been investigated.

c) The wind velocity is set to zero, as is the heat loss coefficient, C.

d) Radiation heat transfer coefficients are used for h_1 and h_2; these could easily be replaced by natural convection heat transfer coefficients, if these were found to be more appropriate.

8.2.1 The Character of the Solutions

In order to investigate the character of the solutions, the following analysis was used:

Equaton 6.1.5 with C set equal to zero (i.e. no radial heat loss) is :

$$\frac{\partial\theta}{\partial\tau} = \frac{\partial^2\theta}{\partial X^2} - a\frac{\partial\theta}{\partial X} - by$$

Integrating from X = 0 to X = 1 gives

$$\int_0^1 \frac{\partial\theta}{\partial\tau}\,dX = \int_0^1 \frac{\partial^2\theta}{\partial X^2}\,dX - \int_0^1 a\frac{\partial\theta}{\partial X} - \int_0^1 by\,dX \qquad 8.1$$

Now, as shown in Appendix 4, $y = y_o \exp(\gamma_3 X)$. In addition a and b are not functions of X since they are calculated at an average temperature.

Thus equation 8.1 becomes

$$\frac{\partial\bar{\theta}}{\partial\tau} = \frac{\partial\theta}{\partial X}\Big]_1 - \frac{\partial\theta}{\partial X}\Big]_0 - a\,[\theta_1 - \theta_0] - \frac{by_o}{\gamma_3}[\exp(\gamma_3) - 1]$$

$$\frac{\partial\bar{\theta}}{\partial\tau} = -Bi_1(\theta_1 - 1) - (Bi_o + a)(\theta_0 - 1) - \frac{by_o}{\gamma_3}[\exp(\gamma_3) - 1]$$

$$\frac{1}{a}\frac{\partial\bar{\theta}}{\partial\tau} = -\frac{Bi_1}{a}(\theta_1 - 1) - \left(\frac{Bi_o}{a} + 1\right)(\theta_0 - 1) + \frac{by_o}{a\gamma_3}[1-\exp(\gamma_3)]$$

This equation may be written as

$$\frac{1}{a}\frac{\partial\bar{\theta}}{\partial\tau} = RHS - LHS \qquad 8.2$$

where

$$LHS = \frac{Bi_1}{a}(\theta_1 - 1) + \left(\frac{Bi_o}{a} + 1\right)(\theta_0 - 1)$$

$$RHS = \frac{by_o}{a\gamma_3}[1-\exp(\gamma_3)]$$

Equation 8.2 is the overall energy balance for the bed.

The quantity $by_o/(a\gamma_3)$ may be evaluated by substituting for a,b and γ_3 to give $(-\Delta H_r y_0) / (\hat{c}T_\infty)$. This quantity is the dimensionless adiabatic temperature rise i.e. the temperature rise that would occur if there was total conversion and no heat loss.

The steady-state solutions to equation 8.2 may be found by plotting LHS and RHS against θ , and observing where the two curves cross, since where the two curves cross

$$\frac{\partial\theta}{\partial\tau} = 0$$

The advantage of this procedure over solving the equation directly is that both stable and unstable steady-state solutions may be easily found.

A problem that occurs in using equation 8.2 is that , in the absence of wind, $T = T_\infty$ is always a solution of the equation. This is not a realistic solution, and arises from the assumpton in the model that natural convection is the only flow mechanism. In reality some diffusion will occur, and in this case this solution will vanish. In order to avoid numerical difficulties that arise, and also to make the solutions more realistic, in what follows it is assumed that the flowrate G may be written as

$$G = G_0 + G_{convection} \qquad 8.3$$

where G_0 is small but non-zero.

In the programs used to generate the figures in this section G_0 is assumed to caused by a 0.1 m/s wind. Equation 2.2.13 can be used to show that for a 5m long bed, this wind velocity causes the same flow as a temperature rise of 10^{-4} K, which is of course entirely negligible.

Several general points may be deduced from the definitions of RHS and LHS. In particular it is instructive to take limits of both the RHS and LHS as θ tends to 1 and to infinity.

When θ tends to 1, r tends to a finite quantity and G tends

to G_o by equation 8.3. (When $\theta = 1$ $G_{convection} = 0$). However since G_o can be chosen arbitrarily small the quantity exp(-rL/G) tends to 0. No other quantities in equation 8.2 are functions of θ , therefore

$$\lim_{\theta \to 0} (RHS) = - \frac{\Delta H_r y_o}{\hat{c}\, T_\infty}$$

For the values tabulated in Appendix 11 this quantity, which is the dimensionless adiabatic temperature rise, evaluates to 7.

When θ tends to 1 the LHS tends to zero by equation 8.2 , since both θ_o and θ_1 and tend to 1 as θ tends to 1.

When θ tends to infinity, the RHS tends to 0. This may be seen by considering the behaviour of rL/G for this case.

When θ tends to inifinity the LHS is not bounded, since both θ_o and θ_1 tend to infinity.

This suggests that the behaviour of the graph of RHS and LHS versus θ is as sketched in Figure 8.1.

From figure 8.1 it is clear that there must be an odd number of solutions to equation 8.2, and that the curves intersect at least once.

A further analysis of equation 8.2 leads to the ability to predict whether a cetain solution is an unstable or stable solution. Referring to equation 8.2 it may be seen that if LHS < RHS then $\partial\theta/\partial\tau > 0$ i.e. the bed tempeature is increasing. Referring to figure 8.1, and in particular to point B, it can be seen that at a temperature just above the temperature at which LHS and RHS intesect RHS is greater then LHS i.e. the derivative is positive. This implies that should the bed be at point B and the temperature rise, it will carry on rising since the derivative remains positive. Only at point C when this derivative is again 0 will the temperature stop rising. This implies that point B represents an unstable steady-state. A similar analysis can be performed to show that points A and C are stable steady-states.

The general conclusion from this analysis is:

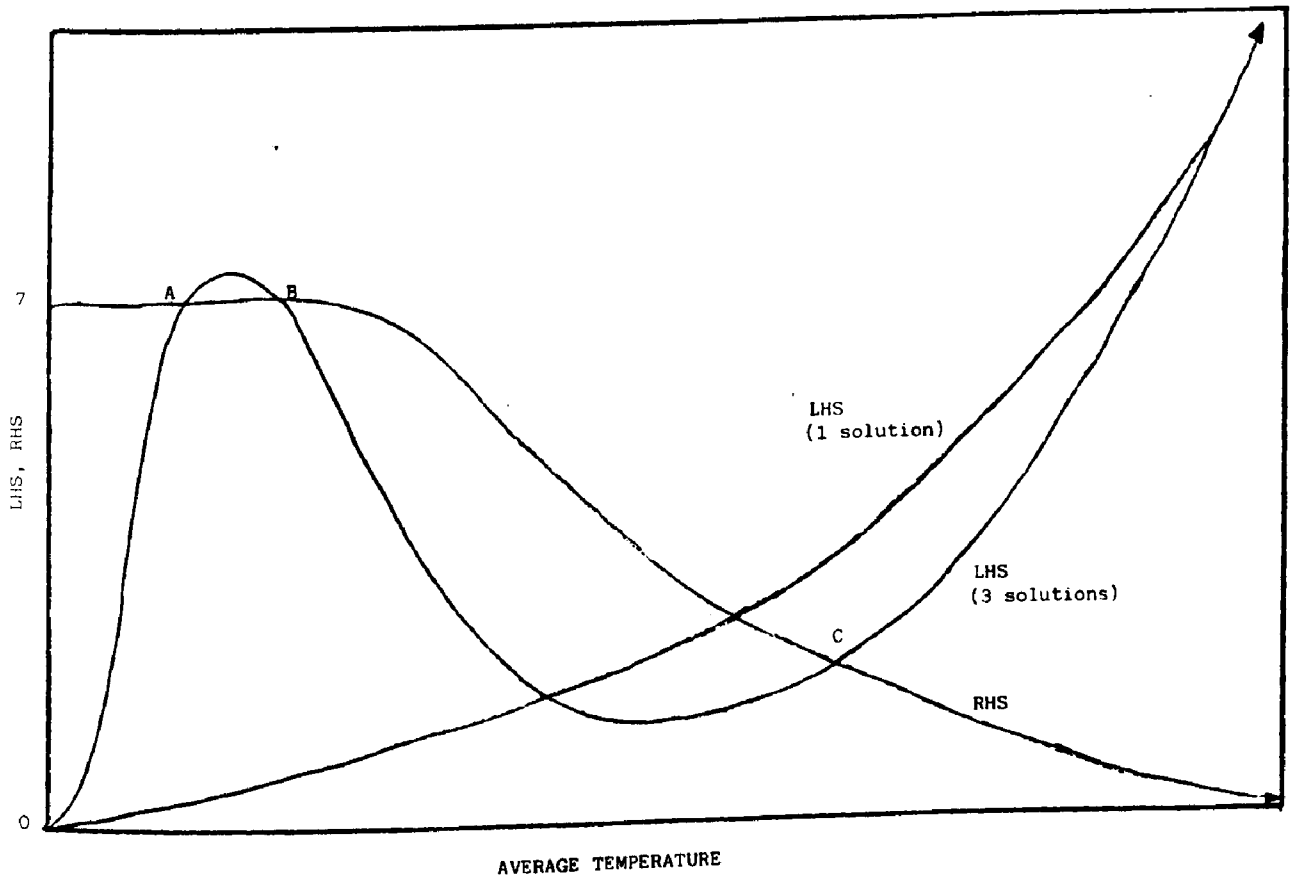


Figure 8.1 LHS and RHS of equation 8.2 as a function of θ

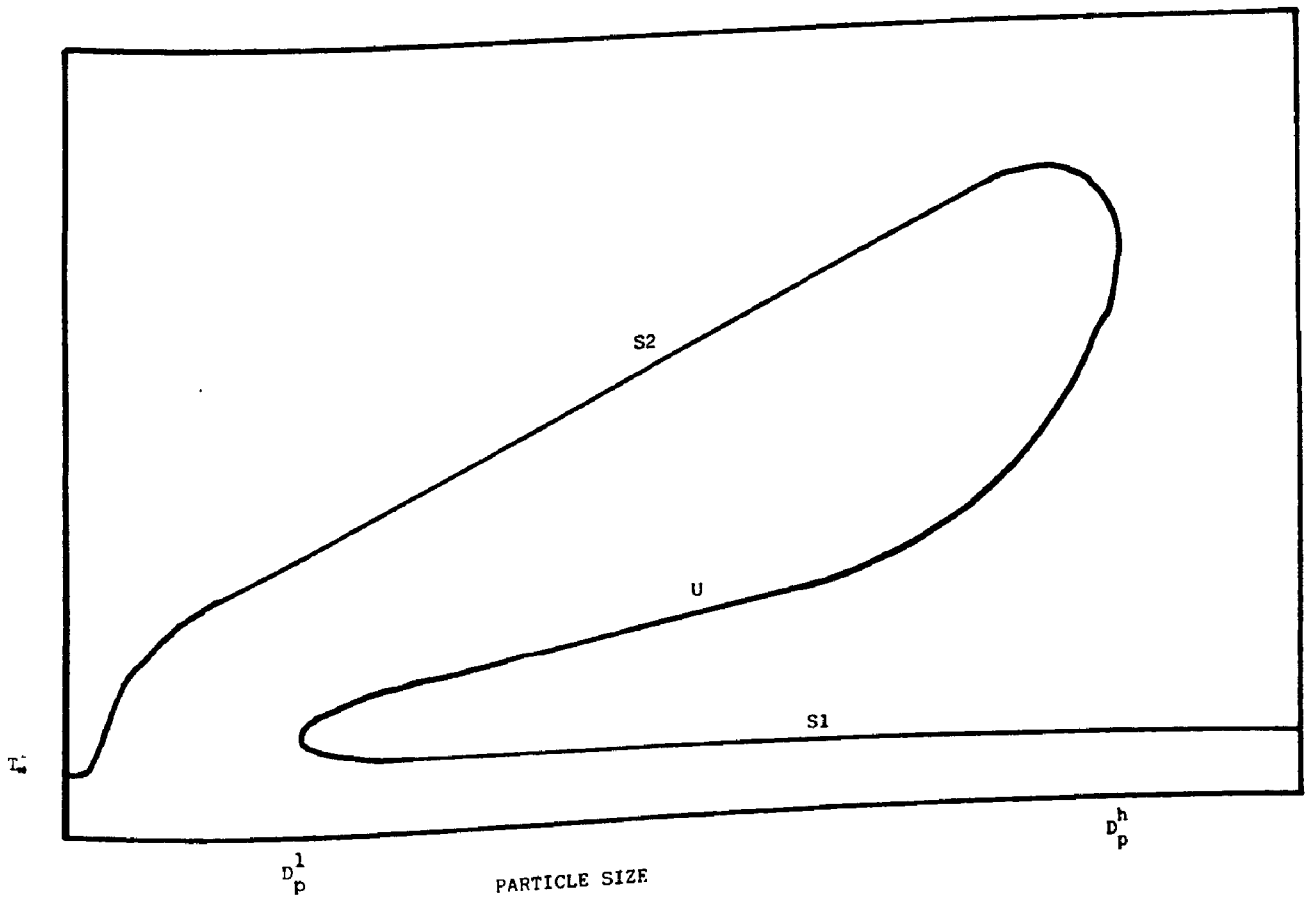


Figure 8.2 Locus of solutions to equation 8.2

For a stable solution at crossing θ_c the following condition must be true:

$$\left.\frac{d\ RHS}{d\bar{\theta}}\right]_{\theta_c} < \left.\frac{d\ LHS}{d\bar{\theta}}\right]_{\theta_c}$$

and conversely for an unstable solution:

Referring to figure 8.1 it is clear that the solutions A and C are stable solutions, while B is an unstable solution. In general the first and last solutions must be stable, and in between the solutions occur as unstable-stable-unstable etc. If there is only one solution it is stable.

This discussion serves to relate the behaviour of coal beds, as deduced in this study, to the behaviour of autothermal chemical reactors, and is extremaly valuable in understanding the nature of the solutions. A further discussion of the behaviour of autothermal reactors is given by Kramers & Westerterp (1963). In the beds investigated in this study, only beds with 1 or 3 solutions have been found. This does not mean that it is not possible that a certain coal bed may have more solutions; indeed this may be possible depending on the parameters in the model.

The procedure of plotting LHS and RHS versus θ has been performed for the base case, for different particle sizes. The graphs obtained are summarized in figure 8.2, in which is sketched the locus of solutions to equation 8.2, with particle size along the x-axis and average temperature on the y-axis.

The following conclusions may be drawn from figure 8.2:

a) Below a certain particle size, which may be called D_p^l, there exists only only 1 solution to equation 8.2.

b) Above D_p^l, but below a certain particle size D_p^h, there exist 3 solutions to equation 8.2.

c) Above D_p^h there exists only one solution to the equation.

Referring to figure 8.2 it can be seen that two different types of stable solution exist, labelled S1 and S2 respectively. The branch labelled S1 is characterized by a temperature rise of less than 30 ^{o}C. This implies that the assumption of a constant rate is a good one in this region. This solution is associated with little use up of oxygen. Beds in this region may be considered to be heat-transfer limited, i.e. they do not experience a large temperature rise because the heat transfer is high enough to remove most of the sensible heat of reaction. This solution ceases to exist below D_p^l since the heat transfer is no longer high enough to remove the sensible heat.

The branch labelled S2 is characterized by total consumption of oxygen. It should be noted that the values of the temperature on this branch are likely to be quite wrong, since the assumption of a constant rate used to calculate these values is a poor one. This is not of great practical importance since these beds may be considered to be burning, and the temperature at which the burning occurs is not of great importance. What is of importance is that for small temperature rises, ie safe beds, the model is accurate, and it is safe beds that are of interest. This high temperature solution ceases to exist above D_p^h since the surface area available for reaction becomes too small to support combustion. It should be pointed out that the values of D_p^h obtained in this study are in the region of 100 mm, which is above the particle size at which coal is normally stockpiled. A further point to note is that the details of the kinetics on branch S2 are also not of great importance. The reason for this is that when there is total consumption of oxygen the energy balance no longer contains any kinetic parameters ie the RHS of the energy balances reduces to the dimensionless adiabatic temperature rise.

Of great practical importance is the behaviour of branch S2 for small particle sizes. Below a certain particle size, which for the base-case parameters is of the order of 1 mm, the average temperature rise falls to less than 70 ^{o}C. Practical experience has shown that these beds, although experiencing a substantial temperature rise, are safe. In many practical cases, the effective particle size of a sample of coal will be below this value, and the bed will be safe. The meaning of particle size, as used in this study, is further discussed in section 8.2.6.,

It should be pointed out that neglecting molecular diffusion as a transport mechanism for oxygen is not a good assumption for particles in the sub 1mm range. Thus the temperatures the model predicts for these particle sizes in likely to be in error. However as has been shown in Chapter 2, the maximum temperature rise due to diffusion is of the order of 70 K. This temperature rise will not occur in practice due to the fact that that heat losses will occur. It is important to realise that even if there is a 70 K rise, the natural convection flows will be extremely small for these fine particles, implying that the beds will remain safe.

It can be seen from figure 8.2 that between D_p^1 and some small particle size the only solution to equation 8.2 is one in which the average temperature in the bed is dangerously high. Thus the model agrees with the often noted fact that certain coals cannot be safely stockpiled, and will, given enough time, spontaneously combust.

Also of practical importance is the branch labelled u in Figure 8.2. This is the locus of the unstable solutions, and serves to separate the stable solutions. The implication of this curve is that should a bed reach an average temperature above the average temperature given by the curve u, then the bed will combust. On the other hand, should the average temperature stay below u, then the temperature of the bed cannot reach the value given by the branch S2.

The possibility of multiple steady-states occurring in fixed bed chemical reactors has been noted in the literature. Luss (1968) and Luss & Amundson (1967) have used bifurcation theory to derive sufficient conditions for the existence of a unique steady-state in a fixed bed chemical reactor. This knowledge would be very valuable in the present study. The problem solved by Luss (1968) is similar, but not identical, to the problem studied in the present work. Unfortunately, the results obtained are not directly applicable to the model presented here, due to the differing mechanisms for reactant transport. This factor makes the application of the method presented by Luss (1968) to the present problem somewhat less than straightforward.

It would indeed be very useful to predict parameter values for which there are a given number of solutions to equation 8.2.

Balakotaiah & Luss (1984) have presented methods for determining the regions of parameters for which a given number of steady-state solutions exist in reacting systems. This work hhas been applied to the problem of predicting multiple steady-states in continuous stirred tank chemical reactors. In these cases the systems are described by algebraic rather than differential equations. The extension of the methods presented by Balakotaiah & Luss (1984) to differential equations is in principle simple; in practice the mathematics soon become intractable.

For the purposes of this study a less mathematically involved, albeit simple minded, approach has been used to determine how many steady-states exist for a given set of parameter values. The approach taken is to calculate the low temperature solution for particle size 20 mm. The particle size is then reduced by 1 mm and the calculation repeated. Eventually no low temperature solution to the equation can be found; thus the particle size at which the low temperature solution ceases to exist is found to an accuracy of 1 mm. The high temperature solution to the equation is then calculated. Although it is known that the model is poor for high temperatures, it is nevertheless important to calculate along this branch since, for sufficiently small particle sizes, the calculated temperatures are below 340 K. These beds may be considered to be safe. It should be noted that if a calculational scheme had been adopted whereby only the number of solutions to equation 8.2 was calculated, then these safe oxygen limited dumps would not have been identified.

The computational effort in performing the calculation described above is minor, even for a large range of parameter values. A computer program to perform the calculation is listed in Appendix 12. In figure 8.3 the results of calculating the locus of solutions to equation 8.2 for the parameter values given in Appendix 11, is presented. The results have been calculated in steps of 1 mm up to particle size 20 mm. Figure 8.3 is the base case, and is used in what follows as a means of comparing the effects of changing the parameters in the model.

The results presented in this section are critical to understanding the behaviour of coal dumps, and will therefore now be summarised:

a) Coal dumps may be classified as either safe, unsafe or con-

ditionally safe.

b) Dumps that are safe are composed of either fine reactive material in which case they are oxygen limited, or coarse unreactive material, in which case they are heat transfer limited.

c) Dumps which are conditionally safe may burn if the temperature of the dump rises above a certain critical temperature. If the temperature of the dump stays below this critical value, the dump remains safe.

d) There are cases in which the dump will, given enough time, undergo spontaneous combustion.

In this study particle size has been chosen as the independent variable for the purposes of presenting in a graphical form the results of solving the model equations. The reason for this is that by varying the particle size, the behaviour of different coal dumps may be observed. However, the other physical parameters of the bed are of extreme importance. For this reason the effect of changing one parameter in the model at a time was investigated. The results are presented graphically in figures 8.3 - 8.11 , and discussed in depth below.

It will be noted that the different branches on the curves are labelled 'small temperature rise' and 'combustion'. It may seem contradictory that for fine material the temperatures on the combustion curve are relatively low. However, combustion may be regarded as a situation in which the large majority of available oxygen is reacting, and in this sense the label combustion is accurate for these curves.

In the discussions below 340 K is used as a dividing value between safe and unsafe coal beds. This value must not be taken too literally, since it has been arbitarily chosen. Its use merley proves convenient in comparing the results obtained for different parameter values.

8.2.2 Effect of varying the voidage

Voidage is a parameter which may be varied in practice by means of compaction. The effect of this is shown in Figure 8.4, from which the following conclusions may be drawn:

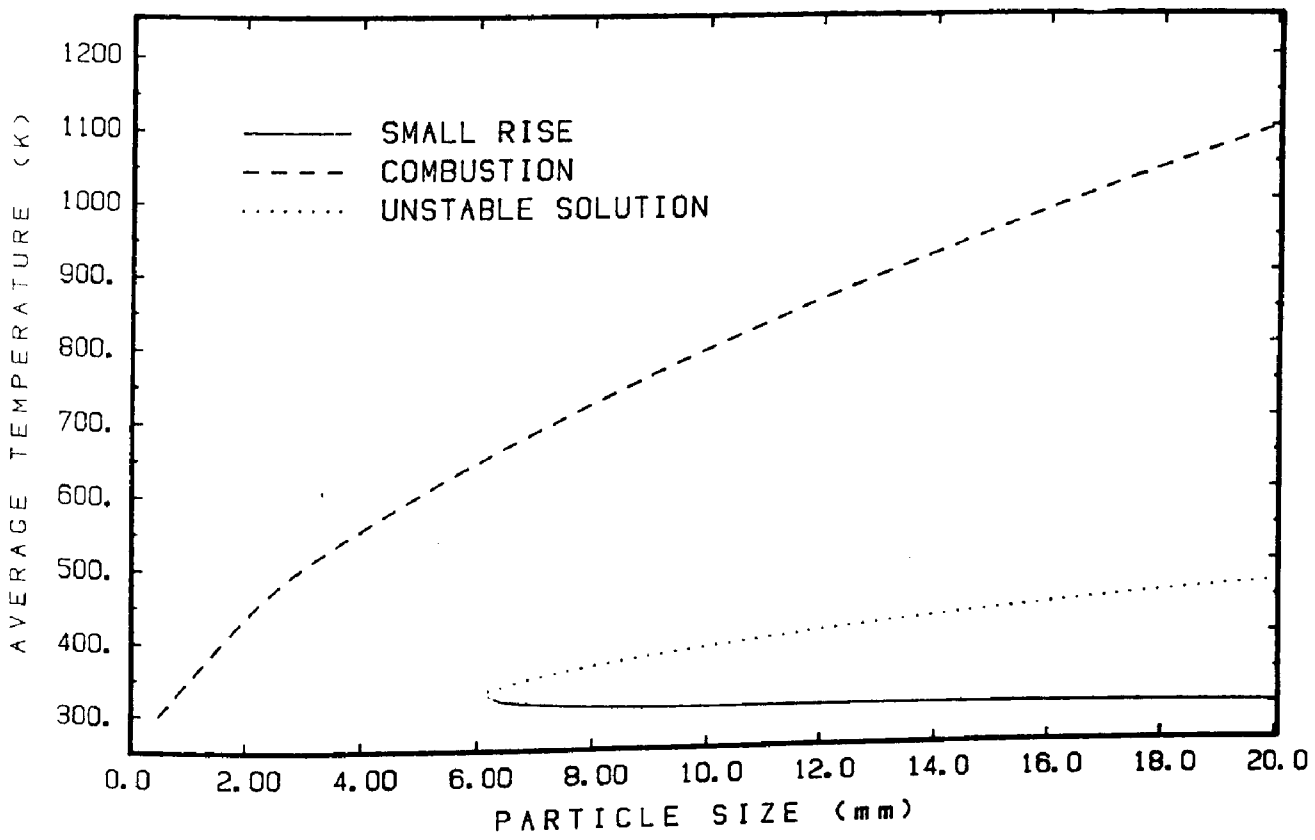


Figure 8.3 Stable and unstable solutions for the base-case

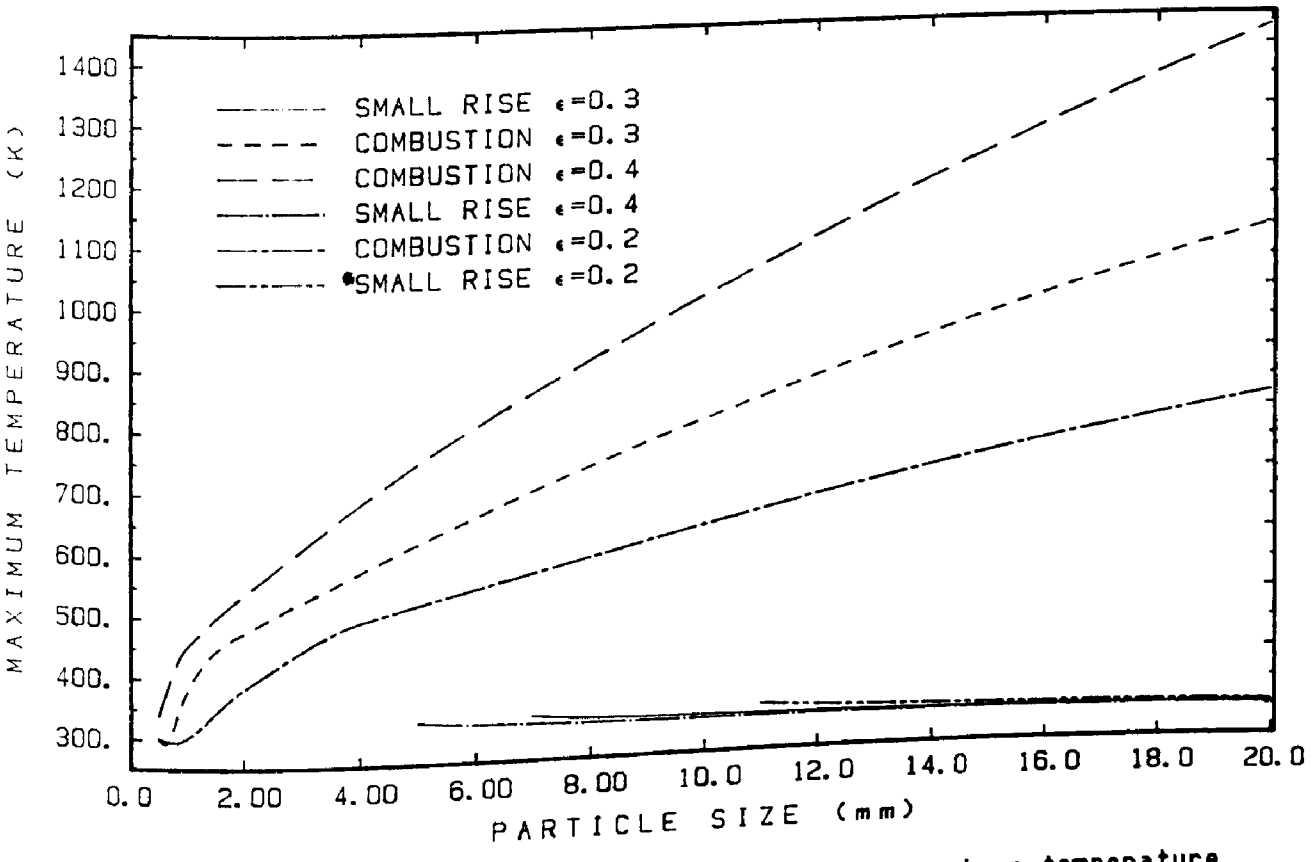


Figure 8.4 Effect of varying voidage on the maximum temperature

a) For fine material, compacting the bed will help make it safer. This can be seen from the fact that the combustion or oxygen limited curve is lower in temperature for lower voidages. Put another way, a fine coal may be safely stockpiled uncompacted, whereas a slightly coarser coal may have to be compacted when stockpiled in order for it to be safe. Using the rough criterion of 340 K then for this particular case material of voidage 0.2 is safe up to particle size 1.8 mm, while for voidage 0.3 the material is safe only up to particle size 0.8 mm.

b) Compacting coarse material may be detrimental. This is shown by the fact that the small temperature rise solution ceases to exist at $D_p = 11$ for $\epsilon = 0.2$, $D_p = 8$ for $\epsilon = 0.3$ and at $D_p = 5$ for $\epsilon = 0.4$.

The last conclusion may seen odd, and deserves some explanation. By compacting the bed the surface area per unit volume of the bed is increased. This in turn has two effects:

a) The resistance to flow is greater and
b) The mass of reactive material per unit bed volume is greater.

For the heat-transfer limited beds, i.e. the ones that experience a small temperature rise, the second result of more reactive material per bed volume more than outweighs the first of reducing oxygen ingress, since the bed was not in any case oxygen limited. (In fact, the reduction in flow also causes a rise in temperature since the heat loss due to flow is decreased). However for the case of oxygen limited beds compaction makes them safer by increasing the rate at which oxygen is scavenged from the air by reaction, as well as increasing the resistance to flow and therefore reducing the flowrate.

8.2.3 Effect of varying the pre-exponential factor

The purpose of varying the pre-exponential factor K_o is to try and simulate the fact that different coals will have different reactivities. Figure 8.5 indicates very clearly that for heat transfer limited beds, the larger K_o, the less safe the bed is. However, the opposite is true for oxygen limited beds. This surprising result can be understood in terms of the fact that

a) For fine material, compacting the bed will help make it safer. This can be seen from the fact that the combustion or oxygen limited curve is lower in temperature for lower voidages. Put another way, a fine coal may be safely stockpiled uncompacted, whereas a slightly coarser coal may have to be compacted when stockpiled in order for it to be safe. Using the rough criterion of 340 K then for this particular case material of voidage 0.2 is safe up to particle size 1.8 mm, while for voidage 0.3 the material is safe only up to particle size 0.8 mm.

b) Compacting coarse material may be detrimental. This is shown by the fact that the small temperature rise solution ceases to exist at $D_p = 11$ for $\epsilon = 0.2$, $D_p = 8$ for $\epsilon = 0.3$ and at $D_p = 5$ for $\epsilon = 0.4$.

The last conclusion may seen odd, and deserves some explanation. By compacting the bed the surface area per unit volume of the bed is increased. This in turn has two effects:

a) The resistance to flow is greater and
b) The mass of reactive material per unit bed volume is greater.

For the heat-transfer limited beds, i.e. the ones that experience a small temperature rise, the second result of more reactive material per bed volume more than outweighs the first of reducing oxygen ingress, since the bed was not in any case oxygen limited. (In fact, the reduction in flow also causes a rise in temperature since the heat loss due to flow is decreased). However for the case of oxygen limited beds compaction makes them safer by increasing the rate at which oxygen is scavenged from the air by reaction, as well as increasing the resistance to flow and therefore reducing the flowrate.

8.2.3 Effect of varying the pre-exponential factor

The purpose of varying the pre-exponential factor k_o is to try and simulate the fact that different coals will have different reactivities. Figure 8.5 indicates very clearly that for heat transfer limited beds, the larger k_o, the less safe the bed is. However, the opposite is true for oxygen limited beds. This surprising result can be understood in terms of the fact that

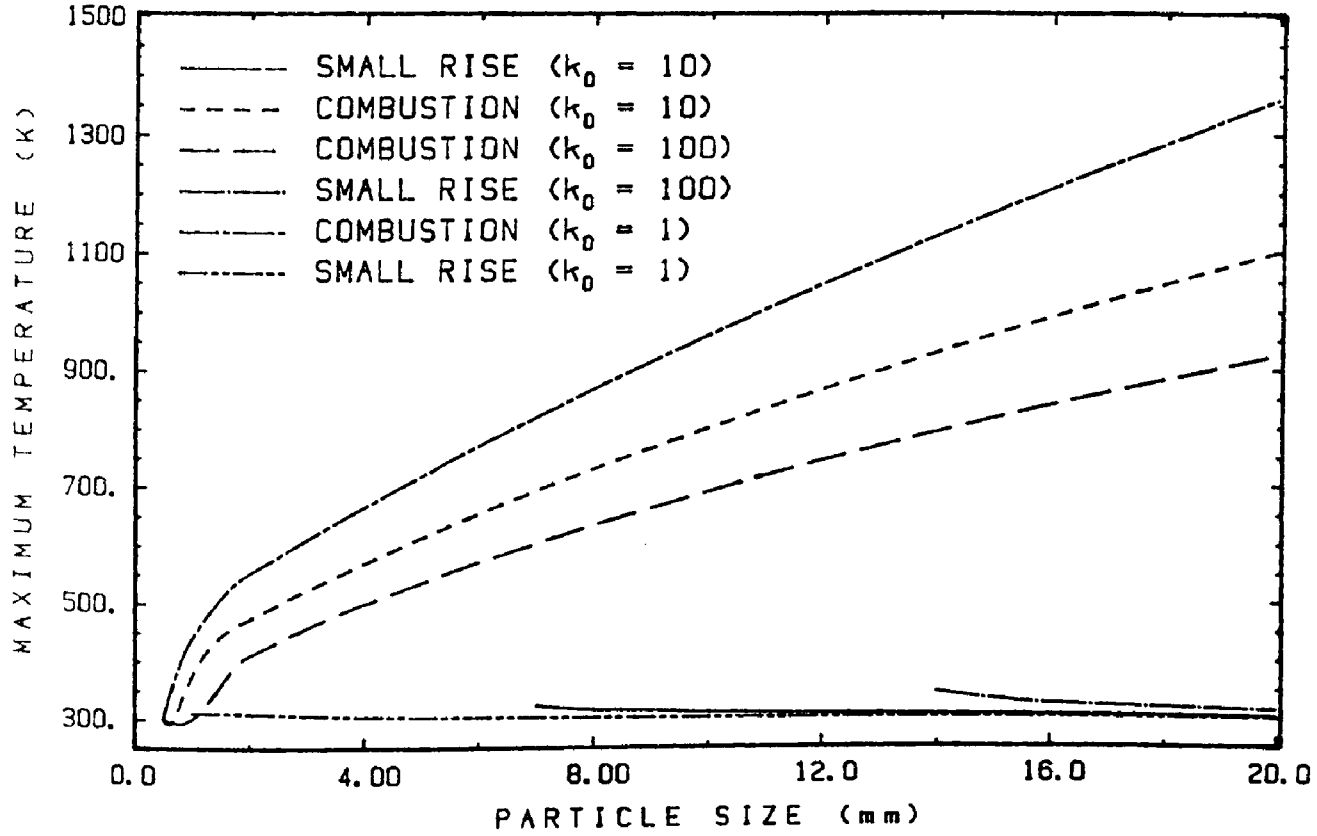


Figure 8.5 Effect of varying the pre-exponential factor on the maximum temperature

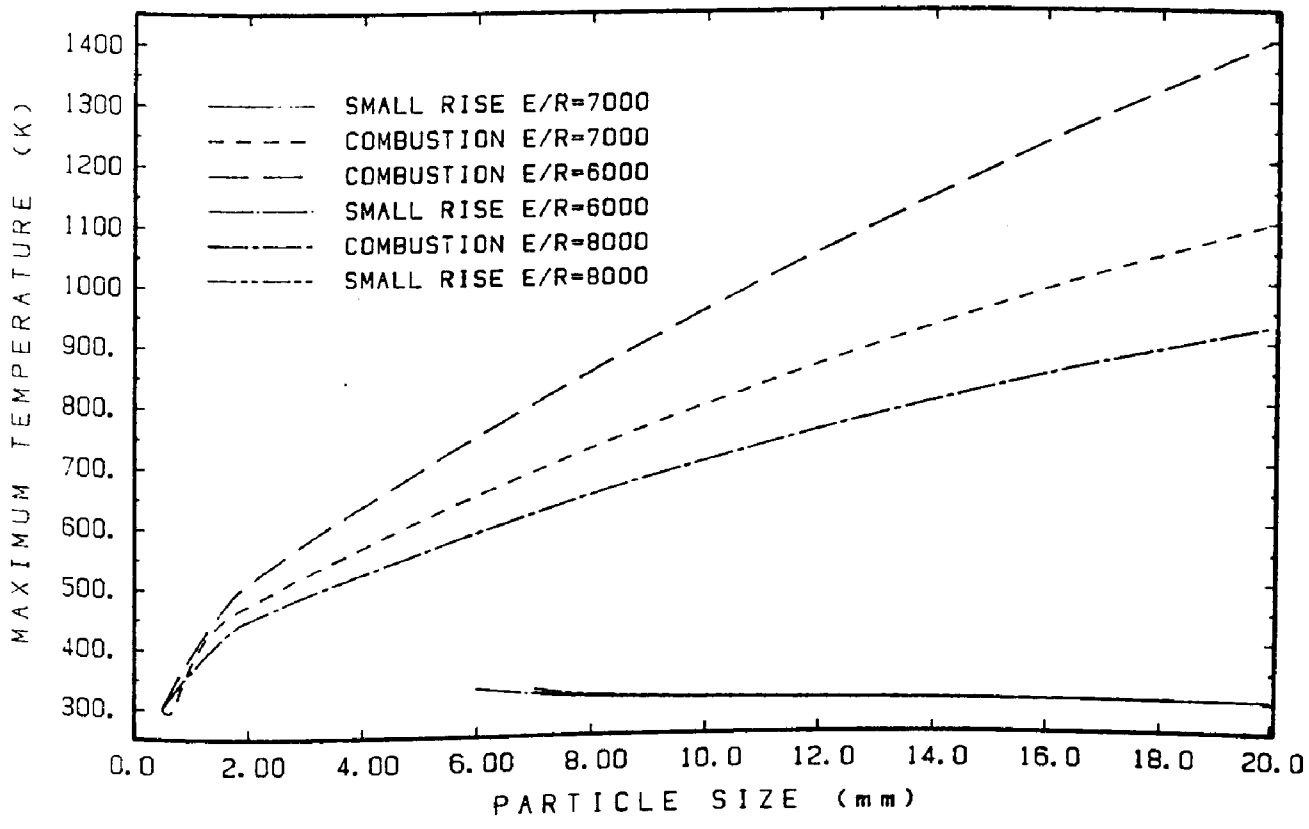


Figure 8.6 Effect of varying the activation energy on the maximum temperature

the oxygen depletion is less when k_o is lower, implying that the oxygen in the bed can penetrate further, leading to a larger temperature rise. When k_o is very large, all the oxygen is consumed close to the surface, where the sensible heat of reaction is easily conducted away.

Using the criterion of 340 K then for k_o = 1 m/s beds are safe below approximately 0.5 mm particle size, whhile for k_o = 100 m/s beds are safe below 1.5 mm particle size. This shows that for these small particle sizes, the more reactive the coal, the safer it is to stockpile.

Also of interest in Figure 8.5 is the fact that that for k_o=1 there is only a small range of particle sizes for which the bed is unsafe. This is a logical conclusion since it is to be expected that very unreactive material will not combust spontaneously.

Figure 8.5 indicates very clearly that k_o is a critical model parameter, and as such needs to be accurately measured.

8.2.4 Effect of varying the activation energy

To study the effect of changing the activation energy, it is necessary at the same time to vary k_o, so that the reactivity is the same at some base temperature. In this case a base temperature of 300 K was chosen. Figure 8.6 thus shows the behaviour of three different coals with the same room temperature reactivity but different activation energies. It can be seen from Figure 8.5 that there is little effect on both the curves. This then indicates that the activation energy is not a critical parameter for coals which have the same room temperature reactivity. However, two coals which have both different activation energies and different room temperature reactivities will have different liabilities toward self heating. The activation energy must thus be measured, and used in conjuction with k_o as a measure of the reactivity of the coal.

8.2.5 Effect of different assumptions about the reactive surface area of coal

The relationship between the particle size of coal and its reactive surface area has been discussed by Sondreal & Ellman (1974). They state that low-temperature oxidation rates have reported to

the oxygen depletion is less when k_o is lower, implying that the oxygen in the bed can penetrate further, leading to a larger temperature rise. When k_o is very large, all the oxygen is consumed close to the surface, where the sensible heat of reaction is easily conducted away.

Using the criterion of 340 K then for k_o = 1 m/s beds are safe below approximately 0.5 mm particle size, whhile for k_o = 100 m/s beds are safe below 1.5 mm particle size. This shows that for these small particle sizes, the more reactive the coal, the safer it is to stockpile.

Also of interest in Figure 8.5 is the fact that that for k_o=1 there is only a small range of particle sizes for which the bed is unsafe. This is a logical conclusion since it is to be expected that very unreactive material will not combust spontaneously.

Figure 8.5 indicates very clearly that k_o is a critical model parameter, and as such needs to be accurately measured.

8.2.4 Effect of varying the activation energy

To study the effect of changing the activation energy, it is necessary at the same time to vary k_o, so that the reactivity is the same at some base temperature. In this case a base temperature of 300 K was chosen. Figure 8.6 thus shows the behaviour of three different coals with the same room temperature reactivity but different activation energies. It can be seen from Figure 8.5 that there is little effect on both the curves. This then indicates that the activation energy is not a critical parameter for coals which have the same room temperature reactivity. However, two coals which have both different activation energies and different room temperature reactivities will have different liabilities toward self heating. The activation energy must thus be measured, and used in conjuction with k_o as a measure of the reactivity of the coal.

8.2.5 Effect of different assumptions about the reactive surface area of coal

The relationship between the particle size of coal and its reactive surface area has been discussed by Sondreal & Ellman (1974). They state that low-temperature oxidation rates have reported to

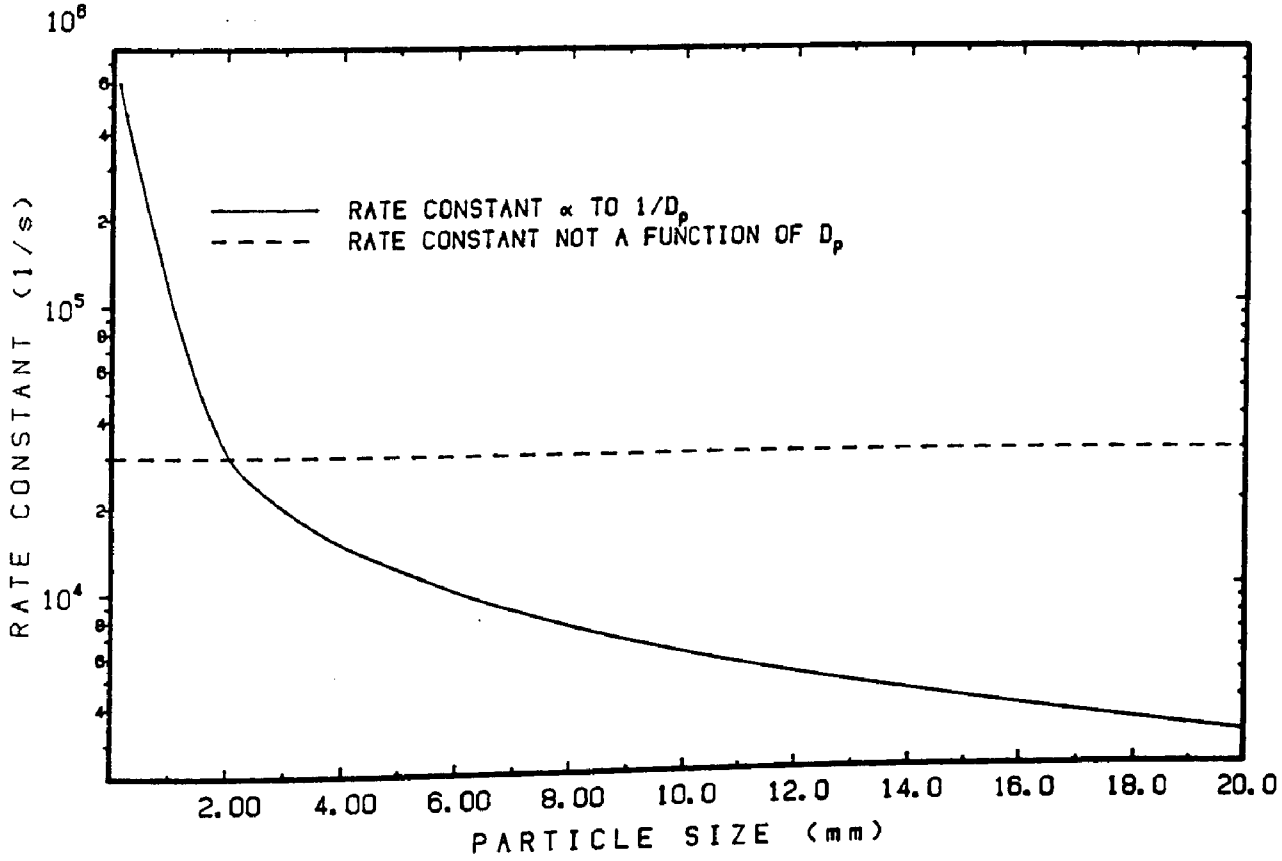


Figure 8.7 Pre-exponential factor versus particle size for the two cases considerd

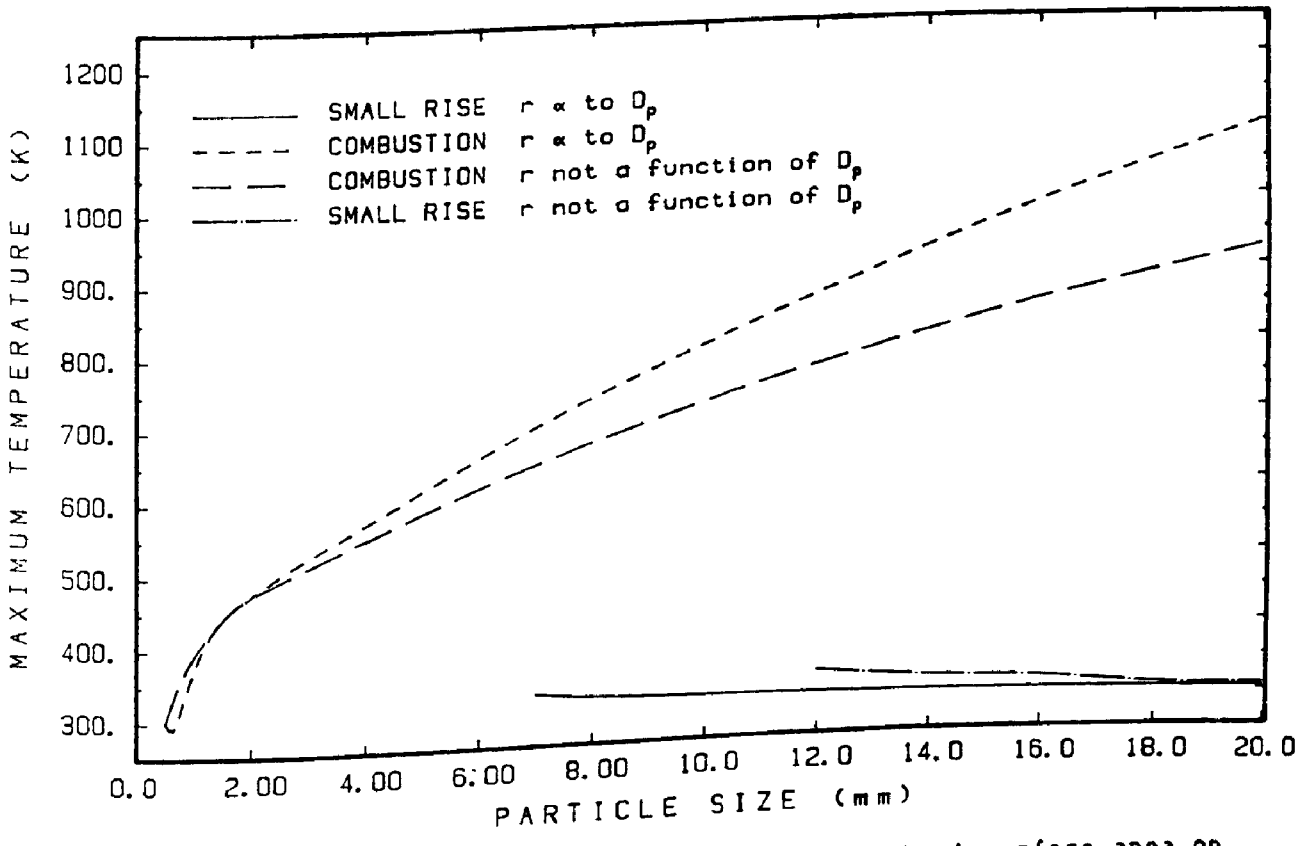


Figure 8.8 Effect of different assumptions about surface area on the maximum temperature

8.2.6 The Meaning of Particle Size

It should be noted that the particle size as used in the graphs presented in this section is defined by:

$$D_p = 6/S_t \qquad 8.5$$

and that this is of great importance when calculating the particle size of a coal sample with a particle size distribution. The correct particle size to use is the one defined by

$$S_t = 6 \sum_{i=1}^{N} \frac{m_i}{D_{p_i}} \qquad 8.6$$

together with equation 8.5

where D_{p_i} = average particle size of class i

m_i = mass fraction of coal in class i

N = number of classes

$$D_p = \sum_{i=1}^{N} D_{p_i} m_i \qquad 8.7$$

is not the correct average for this case.

Should a full particle size distribution be available, the summation in the above equations may be replaced by integrals.

To demonstrate the importance of the above discussion consider a coal with the size distribution given in Table 8.1.

TABLE 8.1 PARTICLE SIZE DISTRIBUTION FOR A TYPICAL SAMPLE

PARTICLE SIZE IN mm		MASS %
	+6.68	26,9
-6.68	+4.70	12.3
-4.70	+2.36	20.2
-2.36	+1.20	12.9
-1.20	+0.59	10.1
-0.59	+0.10	15.7
-.10		1.9

Calculating Dp by equation 8.7 gives a value of 4.5 mm while using equations 8.5 and 8.6 gives 0.9 mm. It can be seen that even a relatively small amount of fine material has the effect of drastically changing the effective particle size of the coal. This is of great importance when considering the liability towards spontaneous combustion of so-called segregated coal

8.2.7 Effect of Wind on Maximum Temperature

The effect of wind on the maximum temperature in the coal bed is shown in Figure 8.9. It appears from this figure that the presence or absence of wind has little effect on the calculated temperatures. However the curve plotted in Figure 8.9 assumes the wind blows constantly until steady-state is reached. This is highly unlikely to occur in practice. The more likely case is a wind which blows for a while, and then dies away. This is obviously on unsteady-state phenomenon, and as such will be discussed in section 8.3.

8.2.8 Effect of Thermal Conductivity on Maximum Temperature

Although the effective thermal conductivity of a packed bed of coal has been measured, it was felt worthwhile to investigate the effect of changing this parameter. It can be seen from Figure 8.10 that both halving and doubling this parameter have little effect on the calculated curves. It thus appears satisfactory to use the measured value of the effective thermal conductivity in all calculations.

8.2.9 Effect of Changing the Bed Length

The bed length is the most difficult model parameter to relate to a real coal dump. It is incorrect to assume that this bed length bears a fixed relationship to the physical size of a coal dump, e.g. its height or width. The bed length in the one-dimensional model in fact corresponds to the path length for flow in the real situation. This path length in general will not be known, although the physical size of the dump sets an upper bound on this quantity.

For the purposes of this study three bed lengths were chosen, in order to see the effect of changing this quantity. From Figure 8.11 it can be seen that the effect of bed length is very pro-

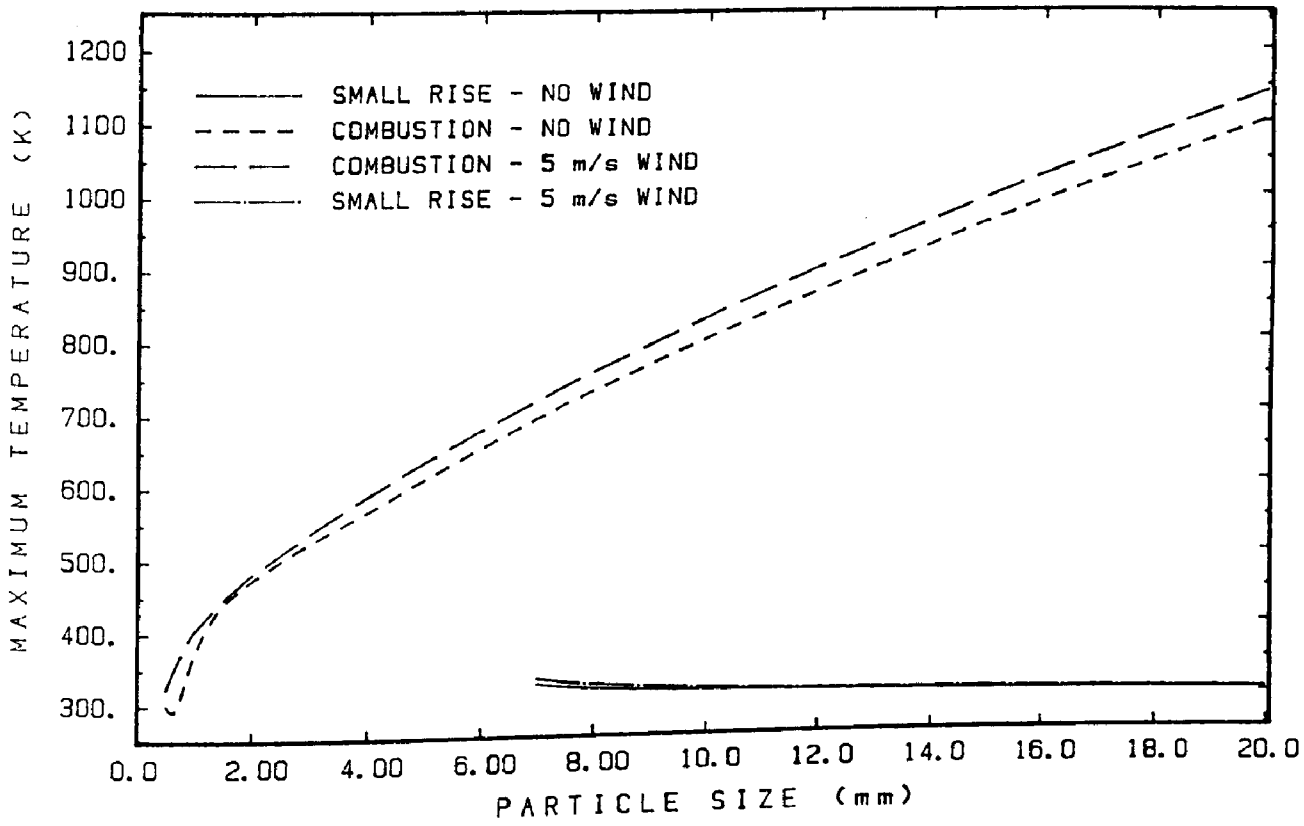


Figure 8.9 Effect of wind on the maximum temperature

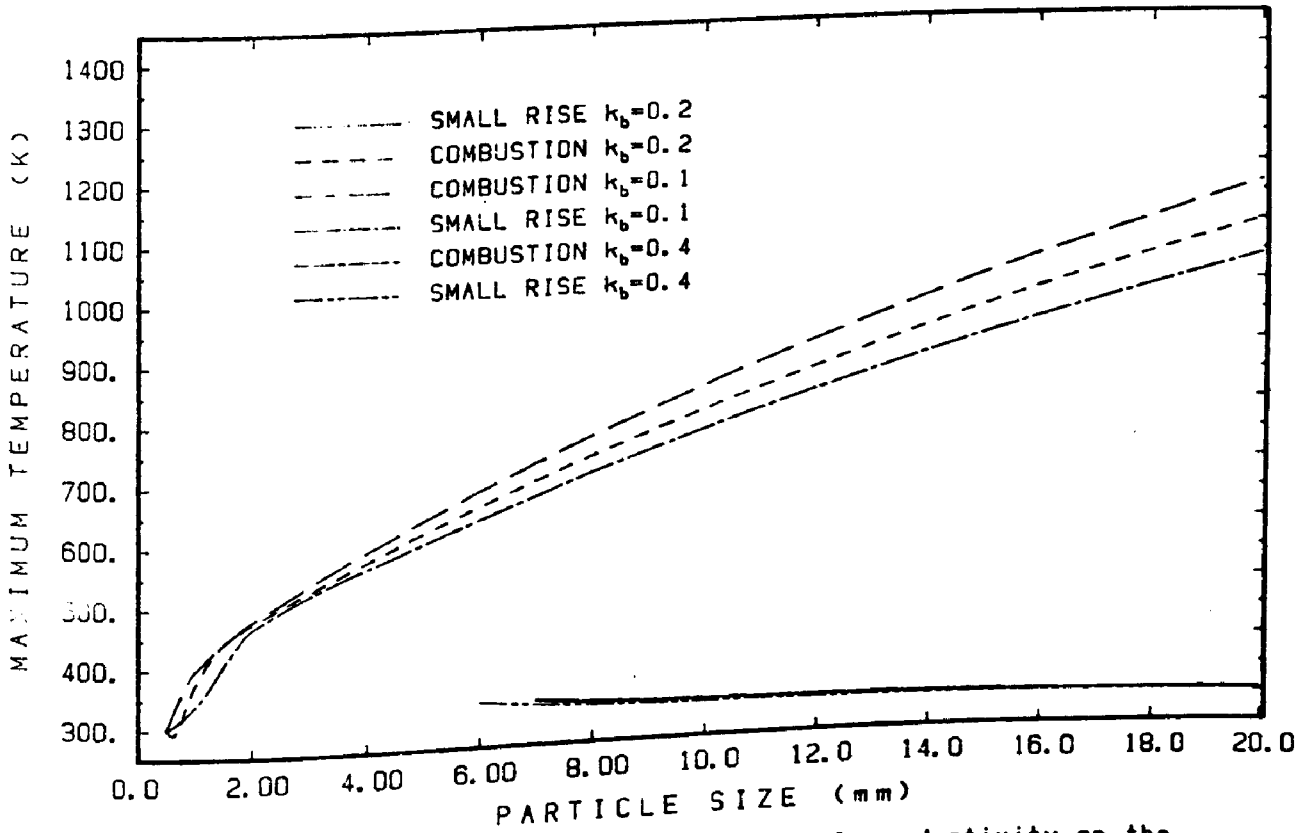


Figure 8.10 Effect of varying bed thermal conductivity on the maximum temperature

nounced on the low temperature solution curves. For the oxygen limited beds, there is little difference between the curves for bed length 5 and 10 m. The curve for bed length 1 m has a somewhat different shape, and for particle sizes less than 1 mm the temperature rise is negligible. In addition the range of particle sizes for which the bed can be considered to be unsafe is between approximately 1.5 and 2 mm.

The fact that the curves for 5 m and 10 m are so similar can be explained as follows: For an oxygen limited bed the oxygen in the flow is used up very close to the inlet to the bed. From that point in the bed where there is to all intents and purposes no oxygen, no more reaction can occur. The temperature profile in the rest of the bed is thus governed by conduction, especially for the beds of finer particles for which the flowrates are low. This implies that making the bed longer will have little effect on the maximum temperature in the bed, since all the temperature rise occurs very close to the inlet.

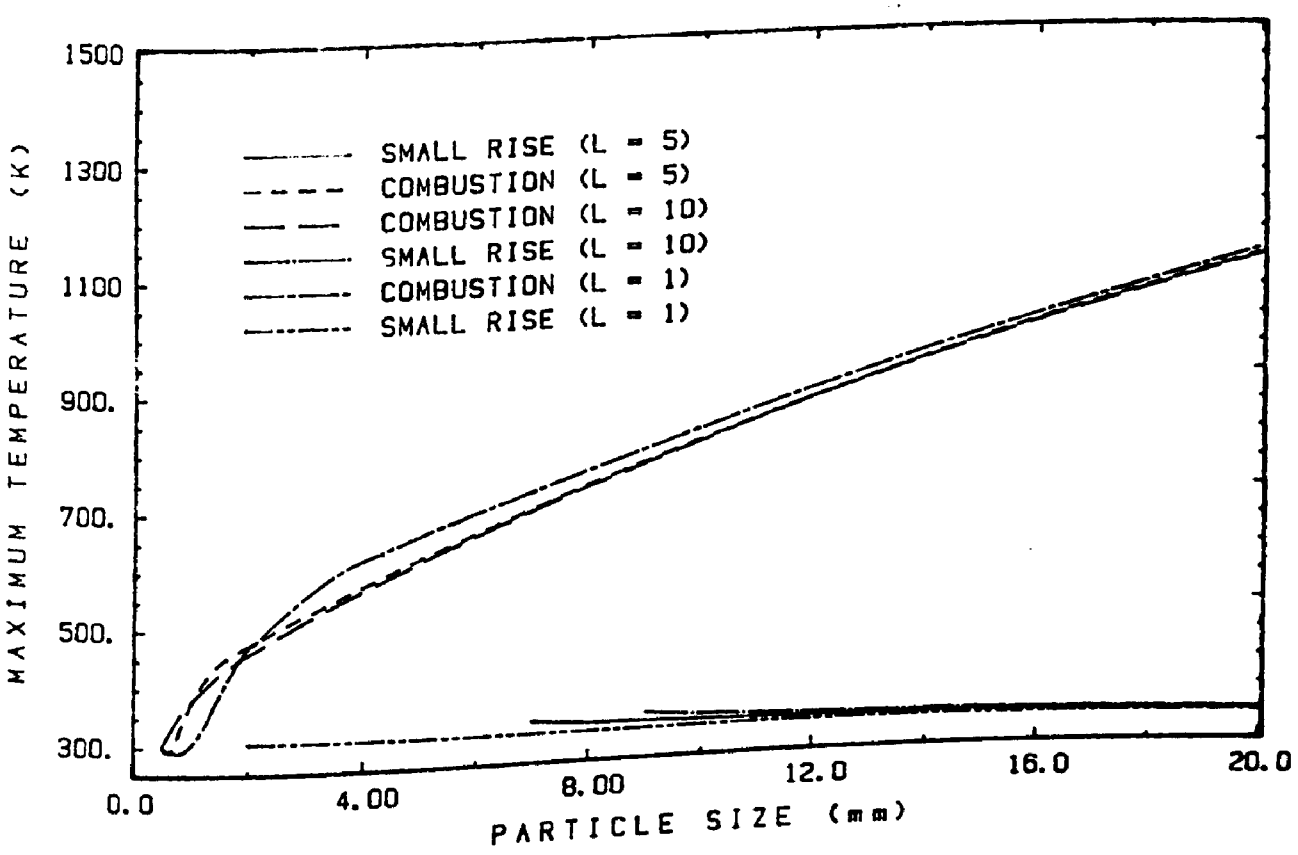


Figure 8.11 Effect of varying bed length on the maximum temperature

8.3 Unsteady-State Solutions for r constant

8.3.1 Introduction

The unsteady-state solution for r constant has been discussed in section 6.3. The resulting solution has been programmed in BASIC on an HP 9835 computer, and a lsiting of the program is given in Appendix 12.

It has been found that obtaining the solution to the analytical equation is in fact slower than obtaining the solution using the numerical method discussed in section 6.4. The aim of what follows is thus to point out the pertinent facts that emerge from solving the equation, without presenting an extensive array of graphs.

8.3.2 The Character of the Solutions

It is already known from calculations in the previous section what the steady-state temperature profiles for a given bed will look like. The advantage of the unsteady-state method thus lies in the fact that should the bed be conditionally safe, the unsteady-state solution will be able to predict from the initial condition what the final steady-state will be.

The temperature time curves in the centre of a coal bed using three different initial conditions are plotted in figure 8.12. The initial condition used is the somewhat artificial one of a coal bed with an initial uniform temperature.

The model parameters used to obtain the curves shown in Figure 8.12 are given in Table 8.2.

TABLE 8.2 MODEL PARAMETERS FOR FIGURE 8.12

Particle Size	5 mm
Voidage	0.4
Bed Length	1 m
K_o	0.7 m/hr
E/R	2889 K

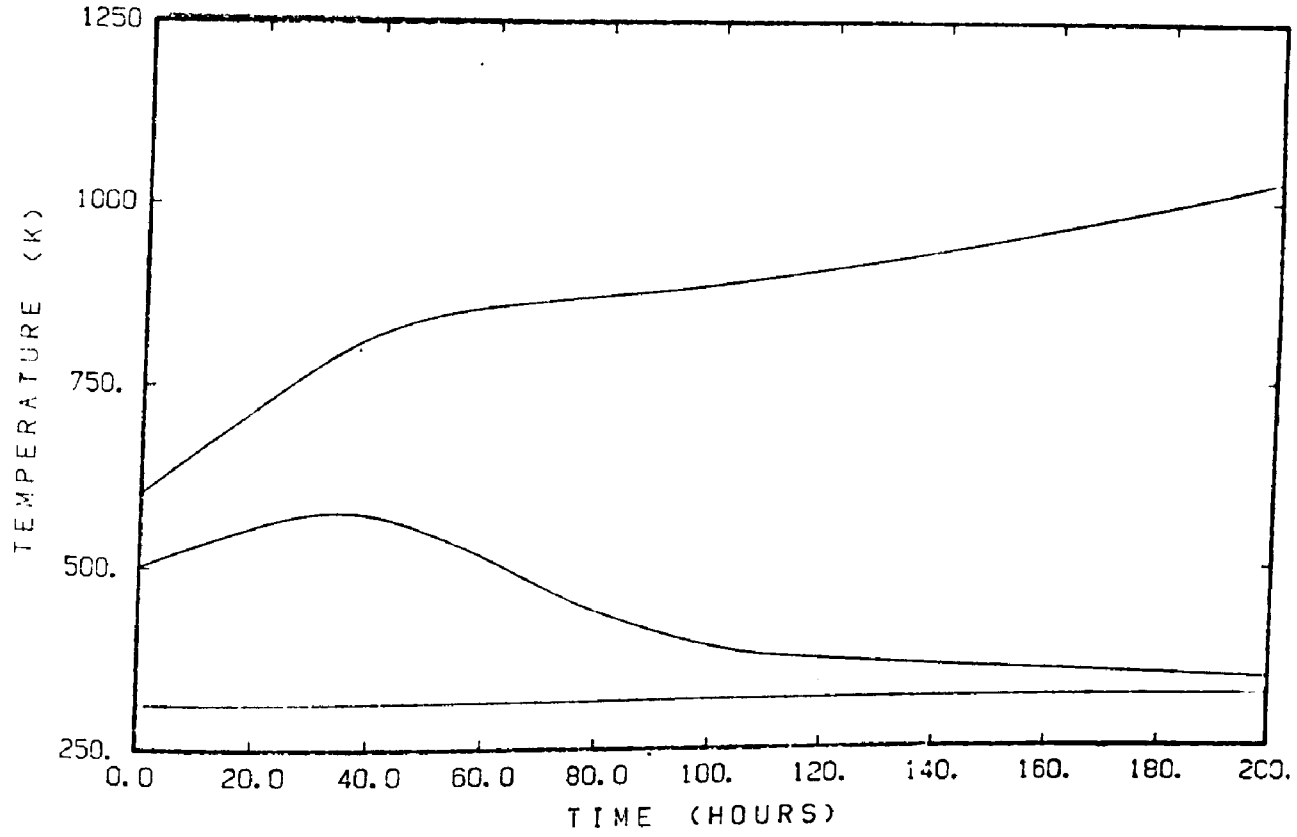


Figure 8.12 Temperature-time curves in the centre of a coal bed for different initial temperatures

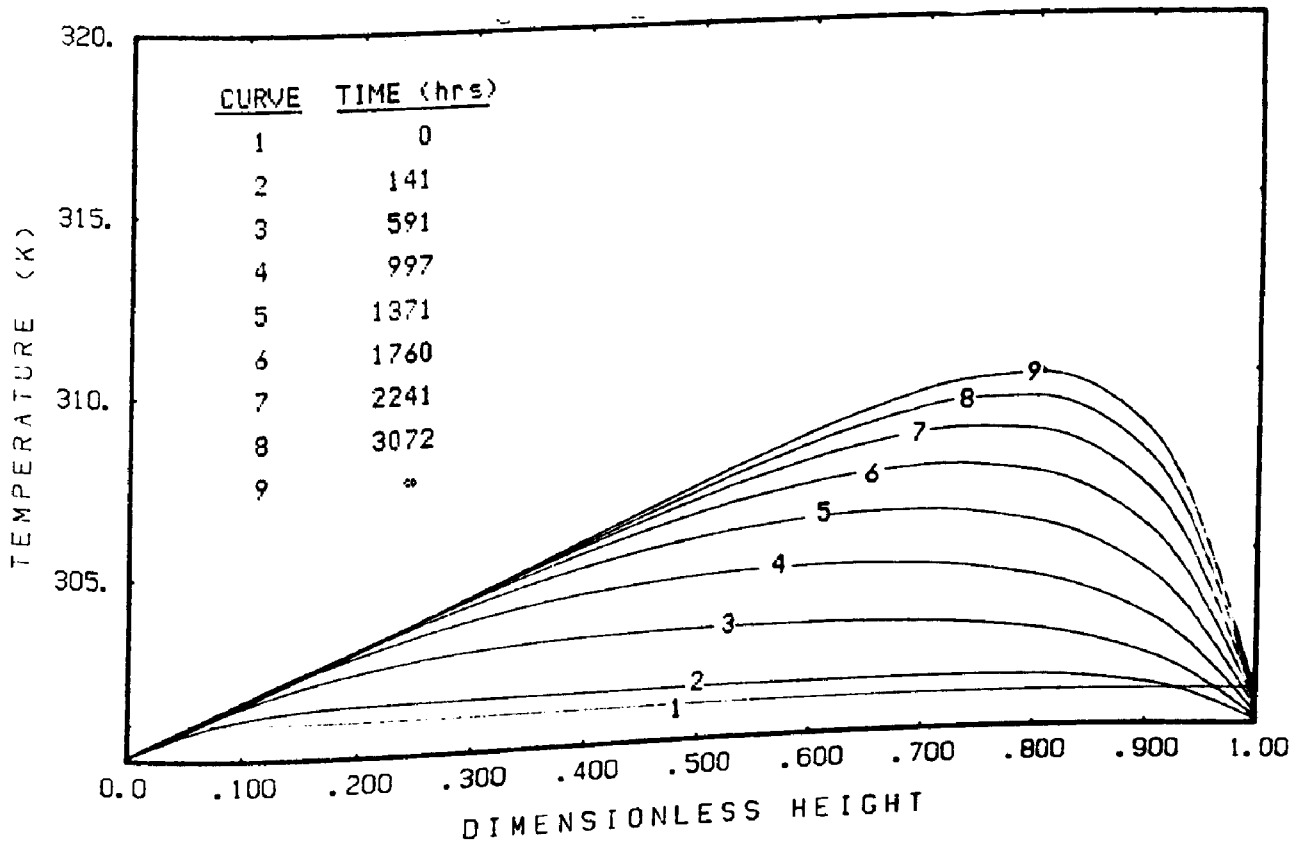


Figure [illegible] Temperature profiles in a coal bed

It can be observed from figure 8.12 that starting with an initial temperature of 301 K the temperature in the bed gradually rises to eventually reach a stable low temperature steady-state. Starting with a bed temperature of 500 K the temperature initially increases but then decreases to eventually again reach the low temperature stable steady-state. However starting at 600 K the temperature increases monotonically, leading to combustion. Thus for this particular bed the critical temperature appears to be between 500 & 600 K. This temperature would in fact correspond to the unstable solution temperature discussed in section 8.2.

Temperature profiles for a coal bed with parameters as given in Appendix 11, for a particle size of 10 mm and length of 5 m are shown in figure 8.13. Referring to figure 8.3 it can be seen that such a bed has a stable steady-state at a maximum temperature of 310 K. In figure 8.13 it can be observed that starting with a temperature of 301 K the bed gradually heats up to its final steady-state temperature. Although in theory the bed reaches steady-state after only an infinite time, it can be seen that after 3568 hrs or nearly 150 days, the bed is to all intents and purposes at steady-state.

It is tempting to try and define a time constant for a coal bed, in order that predictions may be made on safe stockpiling times. In order to do this one would hypothesize that the temperature in a coal bed could be described by an equation of the form

$$\frac{\theta(X,\tau) - \theta_{ss}(X)}{\theta(X,0) - \theta_{ss}(X)} = \exp(-\frac{\tau}{\tau_c}) = \exp(-\frac{t}{t_c}) \qquad 8.3.1$$

where τ_c is a dimensionless time constant, and t_c is a time constant.

In fact using equation 6.3.2, and assuming that only the first term in the series $V(X,\tau)$ need be considered it can be shown that

$$\tau_c = (\beta_1^2 + a^2/4)^{-1} \qquad 8.3.2$$

It is thus immediately obvious that τ_c is not constant, but in fact a function of time, since the quantity, a, which is proportional to the flowrate, is a function of time.

For cases when $\beta_1^2 \gg a^2/4$, the use of a time constant is justified. It can be shown that $\beta_1 \approx \pi$, therefore $a/2 \ll \pi$ is the criterion for using a time constant.

Converting τ_c to time units using the relationship

$$\tau_c = \frac{\kappa t_c}{L^2} \qquad 8.3.3$$

In the case when $a/2 \ll \pi$

$$\tau_c = \frac{1}{\beta_1^2} = \frac{1}{\pi^2}$$

$$t_c = \frac{L^2}{\pi^2 \kappa} \qquad 8.3.4$$

The time constant in this case is governed by the thermal diffusivity of the bed, which implies that the heat transfer in the bed is mainly by conduction.

Then

$$t_c = \frac{L^2}{\pi^2 \times 8 \times 10^{-4}} = 126L^2 \text{ hrs} \approx 5L^2 \text{ days}$$

This implies that for cases where the heat transfer in the bed is governed by conduction, the bed will be 37 % away from its steady-state temperature after $5L^2$ days and 14 % after $10L^2$ days.

A similar calculation for the case $a/2 \gg \pi$ is not justifiable, since a is a function of time. However, using the definition of of the quantity a

$$a = \frac{\hat{G}cL}{k_b}$$

and using the simplified formula for the flowrate G

$$G = \frac{q}{fM_w}\left[\frac{\theta-1}{\bar{\theta}^2}\right]$$

Is is possible to calculate the quantity a, and compare it to 2π to deduce whether the dominant transfer mechanism is conduction or flow.

Using values from Table 2.1 and Appendix 11, and assuming an average dimensionless temperature of 1,1 ie an average temperature of 330 K the values in Table 8.3 have been calculated

TABLE 8.3 THE QUANTITY 'a' FOR VARIOUS PARTICLE SIZES

Particle Size (mm)	a
1	0.1L
2	0.4L
5	2.5L
20	40L

It thus appears that for a 5 m bed of 5 mm particles at an average temperature of 330 K that flow is a more important heat transfer mechanism than conduction. For finer particles in shorter beds conduction will dominate, and then equation 8.3.1 together with 8.3.4 may be used to calculate the time varying behaviour of the coal bed.

Plotted in figure 8.14 is the temperature-time behaviour at the centre of a bed composed of 6 mm particle and 5 m in length. All the other model parameters are base case values. Referring to Figure 8.3 it can be seen that for this coal bed there is no low temperature solution. This conclusion is confirmed by the unsteady-state calculation.

It can be seen that the temperature rise in the centre of this bed is gradual with a value of 0.24 K/day until approximately 80 days. At this time the temperature increases dramatically

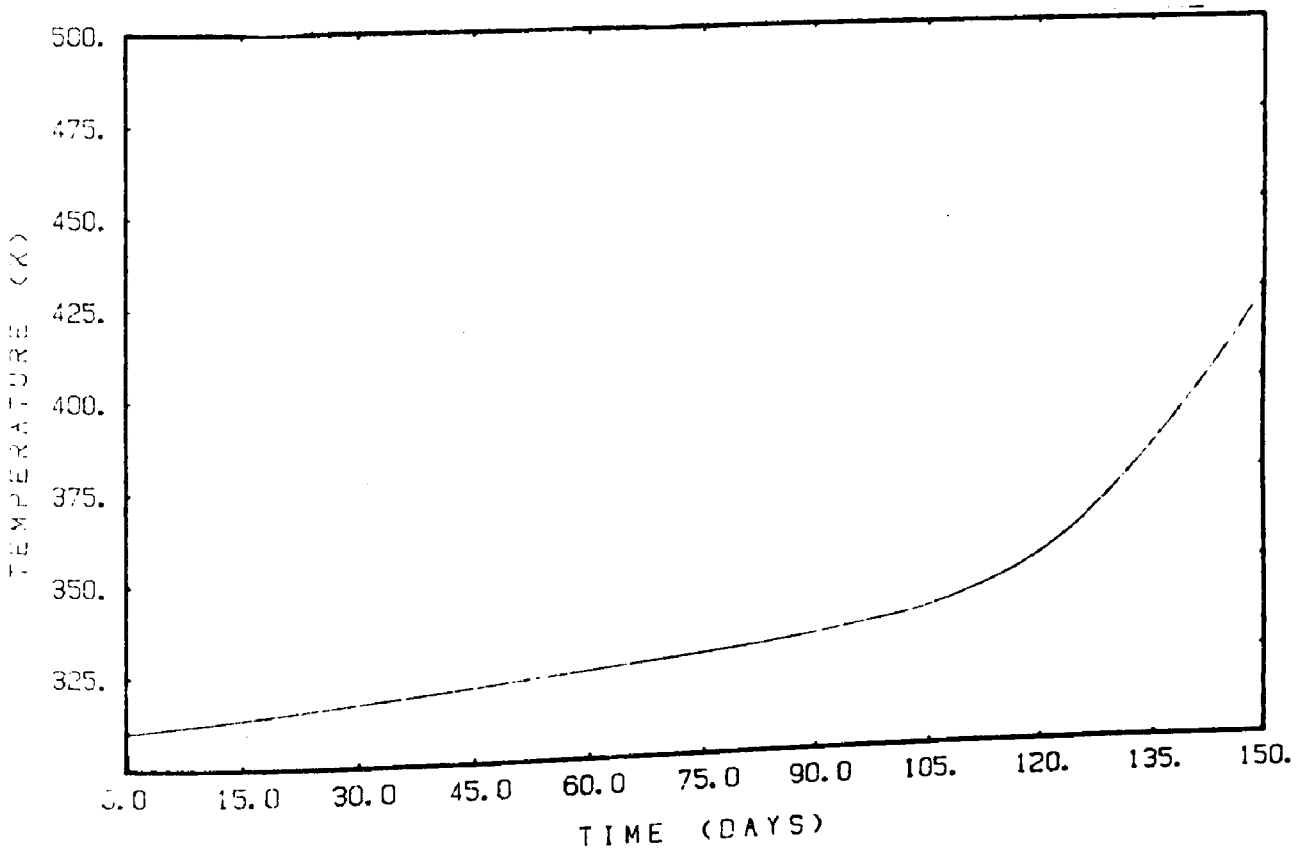


Figure 8.14 Temperature-time behaviour at bed centre
Particle size 6 mm - Analytical solution

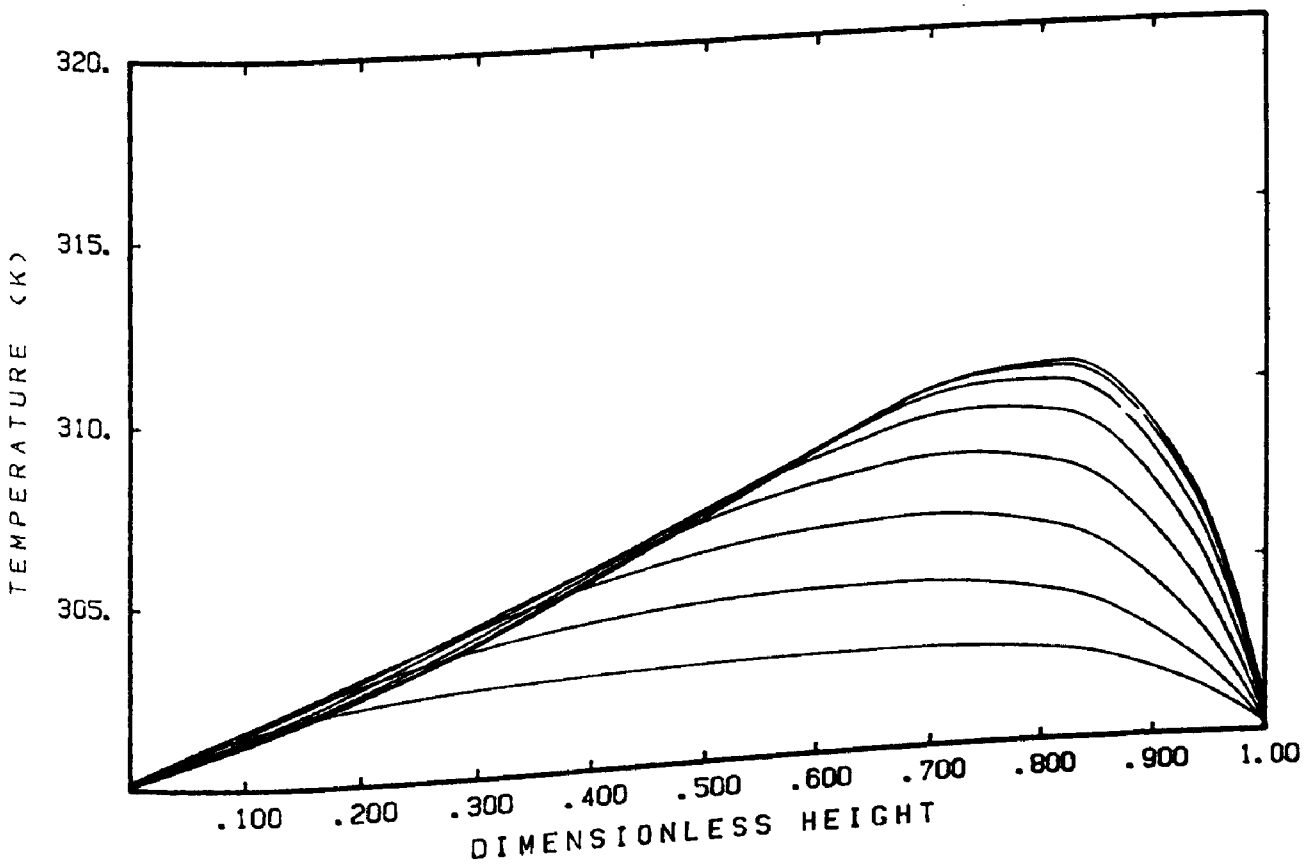


Figure 8.15 Temperature profiles in a coal bed
size 10 mm - Numerical Method

leading to eventual combustion. From this plot 60 ^{o}C appears to be a critical temperature. It is interesting to note that from Table 8.3, at 57 ^{o}C flow is already dominating conduction as the significant heat transfer mechanism, since the value of the quantity 'a' is 3.6L or 18 which is significantly greater than 2π.

8.3.3 Discussion

The results presented in this section confirm the validity of the plots presented in section 8.2. The following are the important conclusions from the section.

a) Depending on the initial condition, a coal bed may either attain a low or high temperature steady state.

b) For coal beds in which conduction is the dominating heat transfer mechanism, a simple formula may be used to calculate the temperature of a coal bed as a function of time.

c) A method has been presented whereby it may be calculated whether conduction or flow is the dominant heat transfer mechanism in a coal bed. In general conduction will only be dominant for short coal beds of fine particles, in which the temperature rise remains small.

d) Results have been presented showing the temperature time behaviour of a coal bed on its way to spontaneous combustion. The bed is characterized by a gradual temperature rise until 60 ^{o}C at which point the temperature rise becomes more dramatic. It has been pointed out that at 60 ^{o}C flow is the dominant heat transfer mechanism in the bed.

8.4 Results of Solving the Equations Numerically

8.4.1 Introduction

As has been discussed, the numerical method for solving the equations involves no assumptions about the reaction rate being constant, and allows for the effect of prior oxidation on the reaction rate. The solutions can be found quickly, even using a fairly unsophisticated microcomputer, and if programmed on a more powerful mainframe computer, the computer time involved would be small.

8.4.2 Comparison Beteewn the Numerical Method and the Analytical Method

The results presented in Figures 8.13 were recalculated using the numerical method. In figure 8.15 the results for the case D_p = 10 mm are presented. It can be seen that for this low temperature case the results obtained are very similar. This is to be expected since the temperature variation in the bed is only of the order of 10 K, and therefore the assumption of a constant rate constant is fairly good.

In figure 8.16 temperature profiles through a reacting bed of coal of size 2 mm with a wind velocity of 5 m/s. A glance at Figure 8.9 will show that for this range of the parameters the bed is unsafe, with a final predicted maximum temperature of 450 K. In fact, as can be seem from figure 8.16 the maximum temperature reached is approximately 1100 K, indicating that the assumption of constant rate constant used to generate the curves in Figure 8.9 is a poor one for this case.

A point of interest in Figure 8.16 is the way in which ignition appears to occur. Between day 40 and day 45 a hump appears in the temperature profile, subsequently the maximim temperature in the bed moves toward the entrance of the bed. This effect is due to the fact that as the temperature increases so does the rate of reaction, leading to the oxygen being depleted near the entrance of the bed. The curves between day 55 and day 80 show some evidence that the numerical method does not cope very well with the ingition, which is in fact a shock phemomenon. In particular the curve for day 55, which exhibits two maxima is unrealistic, Nevertheless the temperature profile after 80 days appears to be in agreement with what one would expect, except for a slightly concave shape.

In Figure 8.17 is shown a cross plot of the results in Figure 8.16 at the bed centre. This curve shows a dramatic increase in temperature between 40 and 45 days of 130 K. The critical temperature from this plot appears to be in the region of 75 ^{o}C.

This bed appears to "take-off" after 40 days whereas the results shown in Figure 8.14 appears to become dangerous after 80 days. The difference between these two cases is the particle sizes of the coal and the fact that that for the results shown in Figure

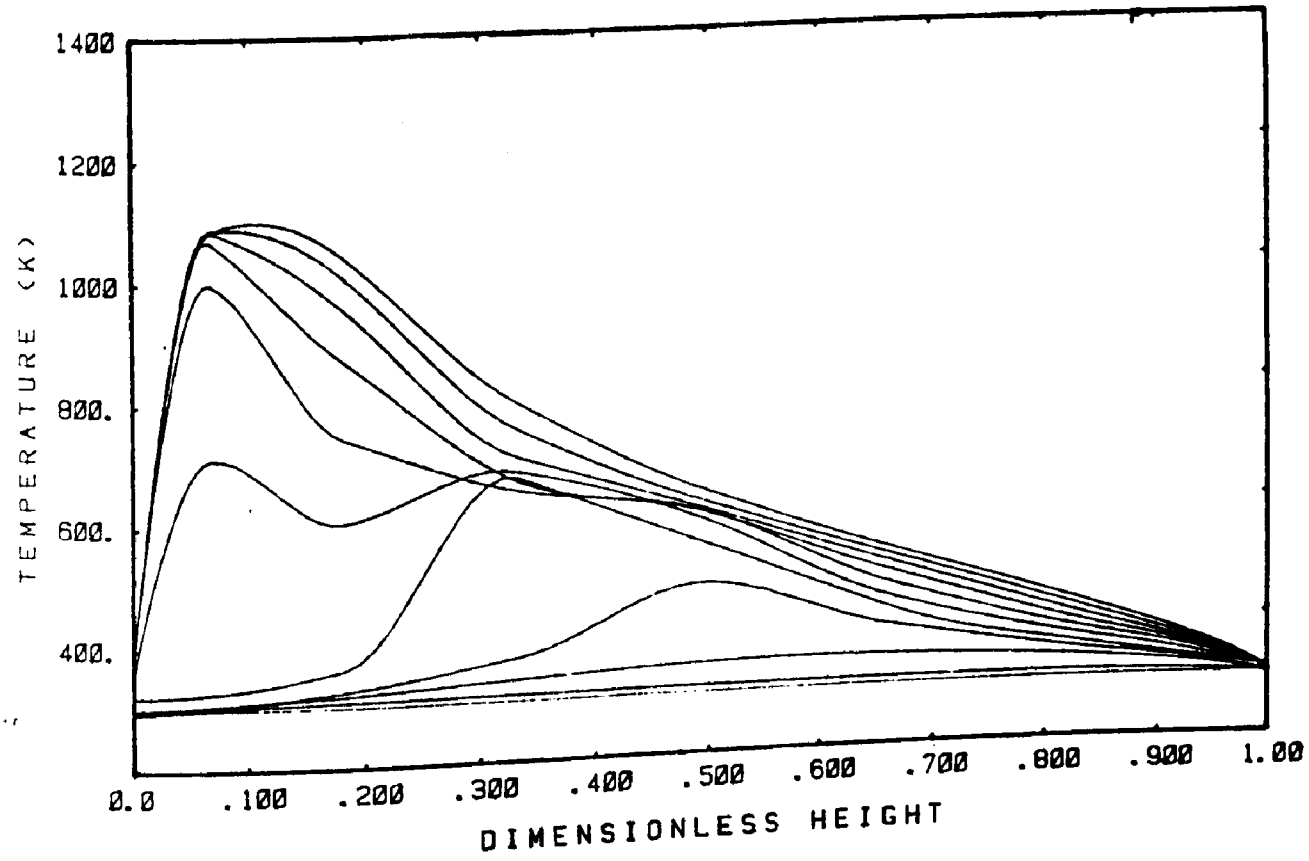
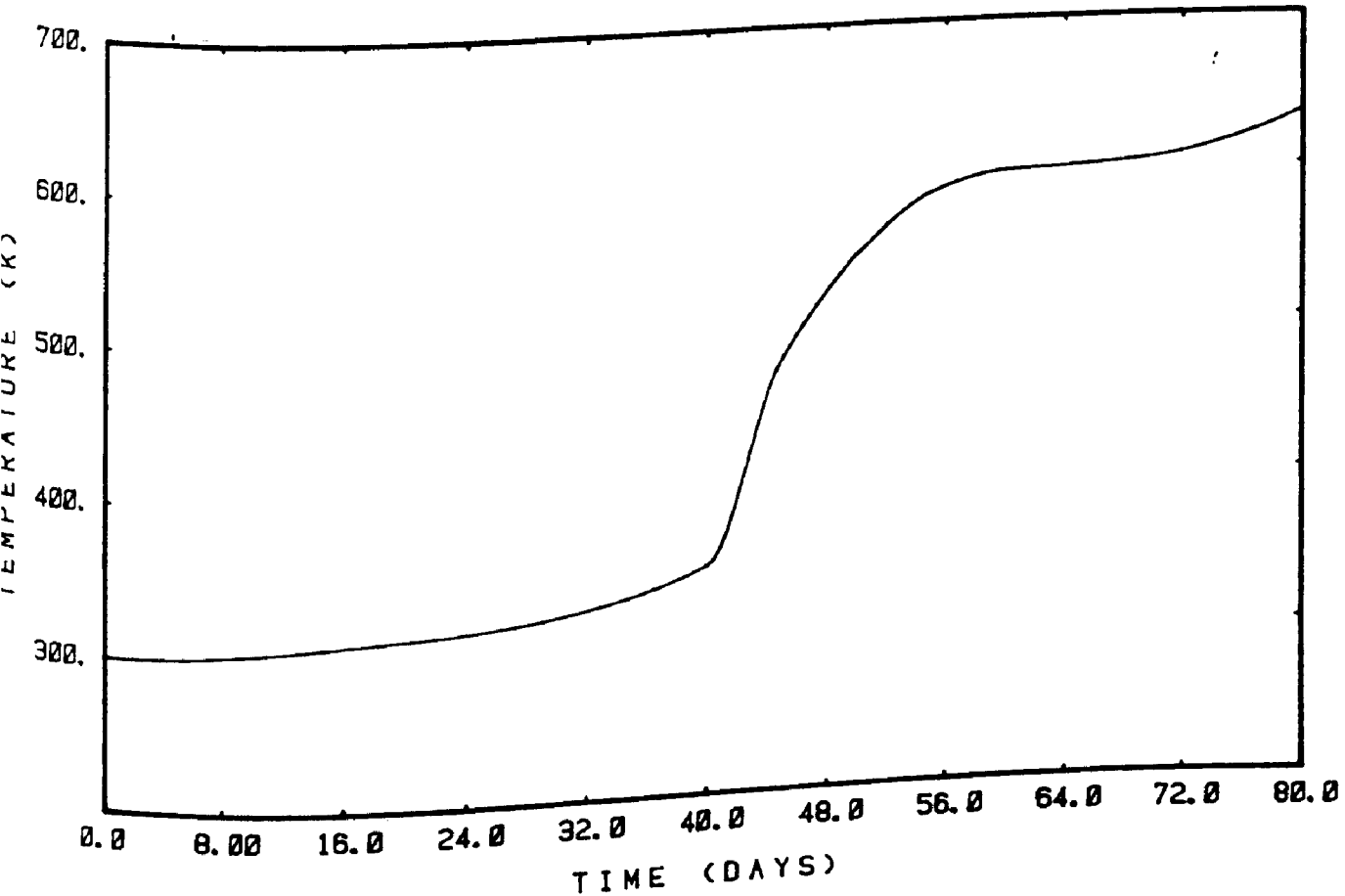


Figure 8.16 Temperature profiles with ignition
Particle size 2 mm - 5 m/s wind - Numerical method
First three curves 20 days apart
Subsequent curves 5 days apart



8.16 a 5 m/s wind has been assumed to blow constantly. It would be expected that the finer, more reactive coal would combust in a shorter time provided is is supplied with enough oxygen, as is the case here with the wind blowing.

8.6 Conclusions

The results presented in this chapter represent the results of solving the model equations for various values of the model parameters. It is felt that the parameters used are realistic, and therefore that the results obtained can be regarded as at the worst semi-quantitative.

The results of solving the equations for both the steady and unsteady-states have been presented. The results are consistent with practical experience. It has been shown that the assumption of a constant rate constant is a good one for beds in which the temperature remains less than approximately 350 K. The results of solving the unsteady-state equations numerically show that the model can predict the onset of spontaneous combustion, although numerical difficulties occur when the temperature gradients become large.

9. CONCLUSIONS

The important physical processes occuring in coal dumps have been identified and modelled. They are:

a. The ingress of reactants into the dump

b. The reaction between these reactants and coal

c. Heat transfer in the coal dump

It has been shown that natural convection and wind pressure are the most imprtant mechanisms whereby reactants are transported into a coal dump, with molecular diffusion only being of importance for fine material.

A shrinking-core model for the oxidation of coal at low temperatures has been proposed. This model explains the well known but little understood fact that the reactivity of the coal falls off with time.

It has been shown that heat transfer in a coal dump may be modelled using an effective thermal conductivity; the effective thermal conductivity of a typical coal bed has been measured.

All these effects have been incorporated into a one-dimensional model, with the aim of studying their combined effect on spontaneous combustion of coal. The model has been shown to have the correct characteristics in the prediction of the onset of spontaneous combustion. The model equations exhibit multiple solutions for certain values of the model parameters; it is concluded that stockpiles may be classified as safe, unsafe or conditionally safe.

Safe coal dumps have been shown to be either oxygen limited or heat transfer limited. In both cases the dump is safe because the sensible heat of reaction can be dissipated at temperatures near ambient. For oxygen limited beds the high reactivity of the coal toward oxygen causes oxygen to be consumed and thus the sensible heat to be produced close to the surface of the dump, where it is easily dissipated. For heat transfer limited beds, oxygen is readily available throughout the bed, but the reactivi-

ty per unit bed volume of the coal is sufficiently low that the sensible heat of reaction may be dissipated even from deep within the dump at near ambient temperatures.

The important parameters that must be known in order to make qualitative predictions about the safety of coal dumps have been shown to be:

a. The particle size distribution of the coal.

b. The voidage of the bed.

c. The pre-exponential factor and activation energy for the oxidation of the coal.

The model presented here may be used to qualitatively determine the effect of changing certain parameters which are under the control of the persons responsible for coal plant operation and particular dumping practise. In particular the effects of particle size distribution and compaction have been clearly pointed out. Compaction makes oxygen limited dumps safer, but appears to be ineffective in improving the safety of heat transfer limited dumps.

The efect of particle size distribution on the safety of dumps may be summarized as follows:

If the dump is oxygen limited adding fines may help make the dump safer, both by reducing the voidage and increasing the rate of oxygen depletion. If the dump is heat transfer limited then removing fine material may help make it safer.

An important practical implication of this work is that there is a dump size for an oxygen limited coal dump, above which the dump is effectively no more liable to spontaneous combustion. For very reactive coals this is a comforting result, since it implies that very reactive coals may be safely stockpiled on very large dumps, with obvious economic advantages. Caution must be exercised to ensure that the dump is oxygen limited, and that the oxygen levels below a certain depth remain negligible. At this stage the quantification of what this depth is, is not possible, but it appears from practical experience that 2 metres is a sensible upper limit on the depth at which the percentage oxygen in a safe

coal dump should be negligible.

Safe stockpiling times are not available from the model, and there is reason to believe that the concept of a safe stockpiling time can be misleading. It has been shown, both in practise and from the model, that a slow rise in temperature may suddenly become a rapid rise in temperature. The critical temperature appears to be in the region of 60 to 100 ^{o}C. The time taken to reach this critical temperature might be a better way of arriving at a safe stockpiling time.

The concepts presented in this thesis may also help to answer questions about stockpiling practise. In particular the following points are of practical importance:

Segregated coal dumps i.e. dumps in which particle size segregation occurs due to stacking methods employed, are potentially dangerous. It can clearly be seen from the results presented in this thesis that such dumps are dangerous because air can penetrate the dump through the coarse material, and react deep in the dump with finer material, that is inherently more reactive, thus leading to a temperature rise deep within the dump where the energy cannot easily be dissipated.

Covering dumps of coal has been suggested as a means of preventing spontaneous combustion. Broadly speaking a dump may be covered with either an inert or reactive material. An inert covering may be permeable or impermeable. In the case of an inert permeable covering such as sand, the fact that there is a balance between oxygen ingress and heat loss must always be borne in mind. Enough sand must be put down to substantially reduce the amount of oxygen ingress, recognising that the dump is being insulated at the same time. If an attempt is made to cover the dump with an impermeable layer of a material such as tar, it must be recognized that cracks in the covering may lead to large localized flows of oxygen into the dump, possibly giving rise to a hot spot.

Schmidt (1945) states that covering a coal dump with a layer of very fine coal and then with a layer of coarser coal provides an efficient coating. The coarse coal is packed on top of the fine coal to prevent wind and water erosion. In the light of the results presented in this chapter, this is an eminently

reasonable suggestion provided all the oxygen can be removed close to the surface.

In the case of dumps that are safe due to the fact that they are oxygen limited, the danger exists that with time the outer layer of coal will become unreactive due to the ageing effect, and that oxygen will penetrate deeper into the dump where any reaction that occurs may lead to a dangerous temperature rise. One of the practical conclusions that arises out of this analysis is that analysing for oxygen at various depths in a coal dump is an excellent way of monitoring the dump. It has been found in practise that in oxygen limited type of dump, the gas in the dump will contain virtually no oxygen at a depth of 2m. It has therefore been suggested that should appreciable oxygen be found at this depth an attempt be made to recompact the dump. Should this fail to rectify the situation the next logical step is the laying down of fresh coal on the dump. This would have the effect of limiting the amount of oxygen that is able to penetrate to appreciable depths. In the light of the model presented here, these suggestions seem sensible as well as practical.

A limitation of the model presented here is the inability at this stage to easily translate the size of a coal dump to the parameter of bed length used in the model. It can be demonstrated that there is a worst depth associated with natural convection, and a worst path length associated with wind driven flows. However at this stage it has not been possible to calculate these distances. A full three- dimensional analysis of the situation could give an idea of the magnitude of these distances; these could then be used in the simpler one-dimensional model for predictive purposes.

The omission of moisture effects in the model is simply rectified as has been demonstrated by Murtagh (1966). It must be borne in mind that in addition to the heat transfer mechanism of condensation and vaporization, moisture appears to exert a catalytic effect on the oxidation reaction. Schmidt (1945) discusses moisture effects in some detail; the ommision of these effects in the model presented here is mainly due to lack of data. There is thus scope for further work in determining the effects of both atmospheric and coal moisture content on the rate of oxidation.

One of the main areas of uncertainty in the field of spontaneous combustion of coal is the functional relationship between rates of oxidation and coal particle size. Much conflicting data has been published in ths regard (Schmidt, 1945, Sondreal & Ellman, 1974). It is felt that there is much need for further study in this regard.

APPENDIX 1 DERIVATION OF A RATE EQUATION FOR THE LOW TEMPERATURE OXIDATION OF COAL

The reaction mechanism considered here is one of diffusion of O_2 through an inert layer of oxycoal followed by reaction between the O_2 and the coal. No reaction products are formed and reaction at the reaction zone is considered to first order with respect to the O_2 concentration

In order to account for the fact that coal has both internal and external surface, the simplification is made that this surface area S′ may be considered to behave as if it was all external i.e. pore diffusion is neglected. This is a good assumption provided the particle size is not too large, as has been mentioned by Gijbels & Bruining (1982).

The coal particle is thus considered to have the geometry shown in Figure A1.1.

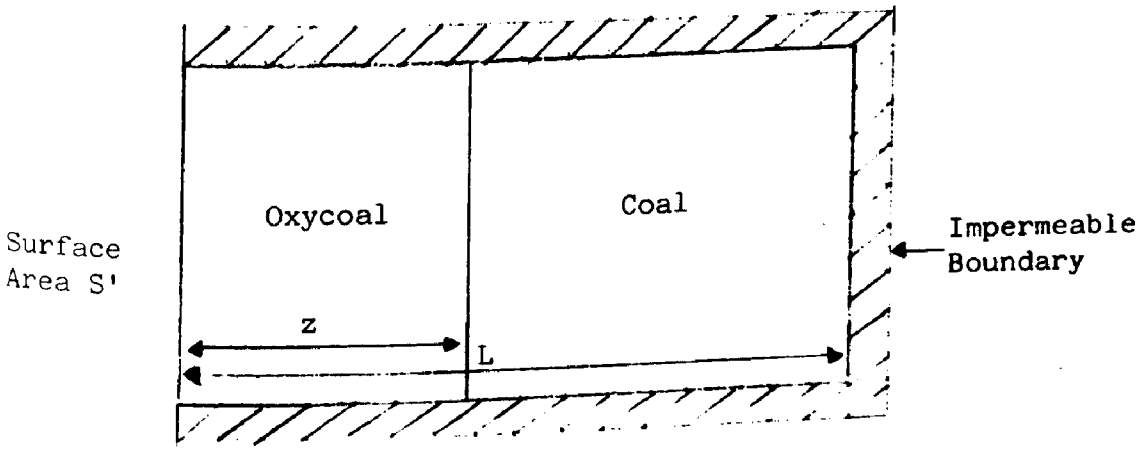


Figure A1.1 Simplified coal particle geometry

A particle length L is defined such that

$$S'L = V_p \qquad \text{A1.1}$$

where V_p = particle volume

At a time when the oxycoal layer has a thickness x the following equations may be written:

$$\text{Rate of diffuson of } O_2 \text{ through oxycoal} = S'D_e\,(C-C_s)/x \qquad \text{A1.2}$$

Rate of reaction of O_2 at reaction front = $S' k_s C_s$ A1.3

where D_e = effective diffusivity of oxycoal layer
C = free stream oxygen concentration
C_s = oxygen concentration at reaction boundary
k_r = surface rate constant

Under the pseudo steady state assumption that there is no accumulation of O_2 in the oxycoal these two rates must be equal i.e.

$$D_e (C - C_s)/x = k_r C_s \qquad \text{A1.4}$$

and solving for C_s gives

$$C_s = \frac{C}{1 + k_r x/D_e} \qquad \text{A1.5}$$

Back substitution in equation A1.2 gives

Rate of adsorption of O_2 by one particle $= \dfrac{S' k_r c}{1 + k_r x/D_e}$ A1.6

Now in a time Δt let the reaction front move a distance Δx.

Volume of coal reacted $= S' \Delta x$ A1.7

Moles of coal reacted $= \rho_m S' \Delta x$ A1.8

where ρ_m = molar density of reactive unit.

However the moles of coal reacted must equal the rate of adsorption times the time interval i.e.

$$\rho_m S' \Delta x = \frac{k_r C S' \Delta t}{1 + k_r x/D_e} \qquad \text{A1.9}$$

letting Δt, Δx tend to zero gives

$$\rho_m \frac{dx}{dt} = \frac{k_r C}{1 + k_r x/D_e} \qquad \text{A1.10}$$

In order to write the equations in terms of fractional

conversion of the coal, rather than the thickness of the oxycoal layer, it is noted that the volume of reacted material is S′x and the total volume is S′L.

Therefore the fractional conversion X is $S'x/(S'L) = x/L$

However L as defined by equation A1.1 is equal to V_p/S'.

Therefore $L = V_p/S' = 1/S_t$ A1.11

where S_t is now the total particle surface area per unit volume of particle.

Therefore, fractional conversion $X = xS_t$ A1.12

and substituting in equation A1.10 gives

Rate of adsorption of O_2 by one particle $= \dfrac{S_t\ V_p\ k_r\ C}{1 + k_r\ X/(S_t\ D_e)}$ A1.13

$$\rho_m\ S'\ \frac{dX}{dt} = \frac{k_r\ C\ S_t}{1 + k_r\ X/(S_t\ D_e)} \qquad \text{A1.14}$$

The rate that is required is however the rate per unit bed volume.

Rate / unit bed volume = Rate per particle x $\dfrac{\text{no of particles}}{\text{unit bed volume}}$

A volume V of the bed contains a volume $V(1-\epsilon)$ of coal where ϵ is the bed voidage.

The number of particles in the volume is therefore

$$V(1 - \epsilon)/V_p$$

and the number of particles per unit volume is

$$(1 - \epsilon)/V_p$$

Therefore the rate per unit bed volume is

$$r = \frac{S_t\, k_r\, C\, (1-\epsilon)}{1 + k_r\, X/(S_t\, D_e)} \qquad \text{A1.15}$$

APPENDIX 2 TABULATION OF MEASURED THERMAL CONDUCTIVITIES

A2.1 Details of Coal Used

Particle size range: -6.32 + 3.4 mm

Mass of coal: 67 Kg

Density of coal (measured): 1.36 g/cm^3

Volume of apparatus: .08 m^3

Voidage of bed: 0.38

A2.2 Measured Values

The values measured during 1982 are given in Table A2.1.

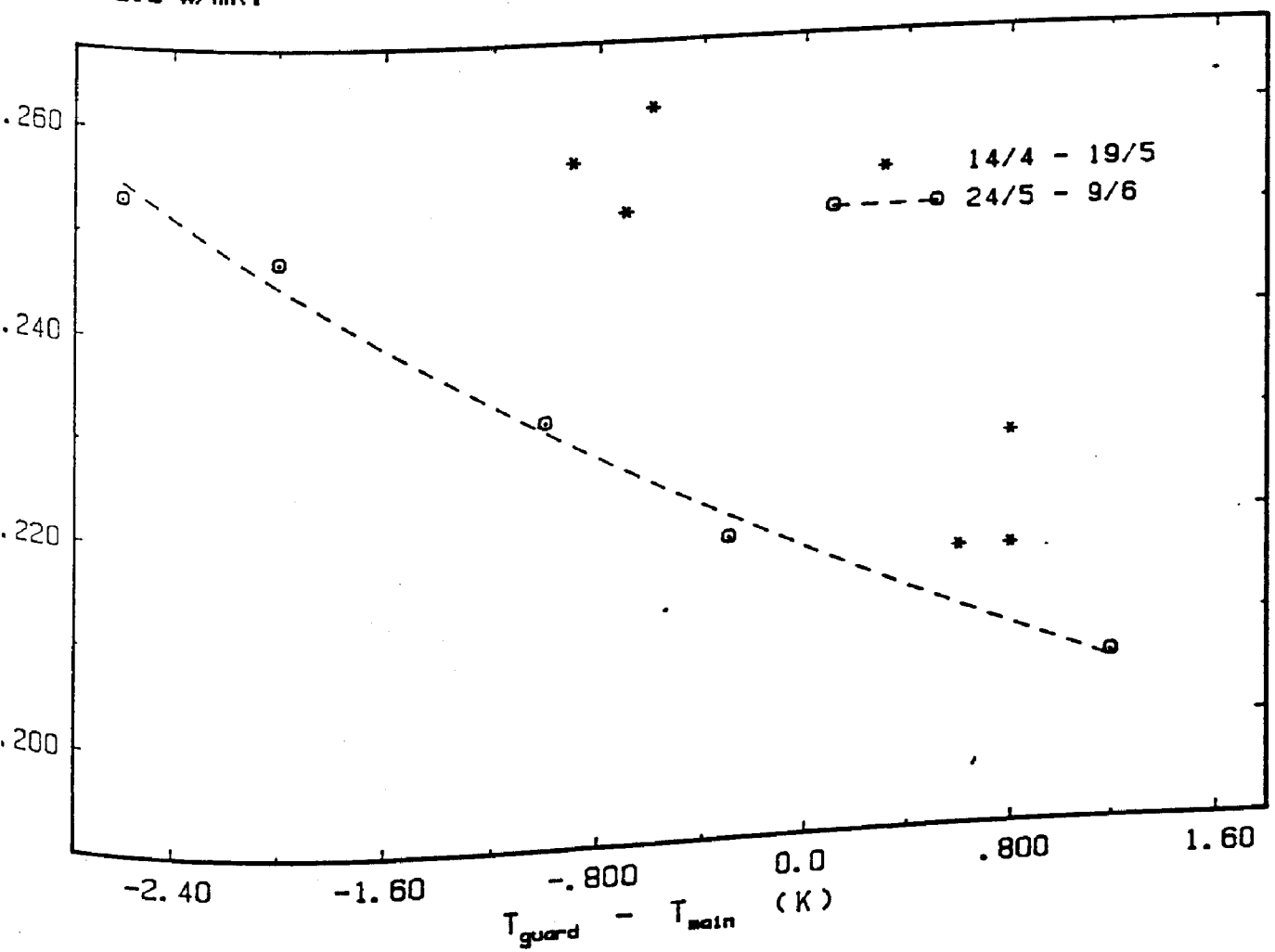
TABLE A2.1 MEASURED THERMAL CONDUCTIVITIES

DATE	MAIN TEMP(^{o}C)	GUARD TEMP(^{o}C)	MAIN VOLTAGE(V)	MAIN CURRENT(mA)	WATER TEMP(^{o}C)	k_b(W/mK)
14/4	67.8	68.6	11.66	139.8	23.0	0.217
16/4	68.7	69.5	11.66	139.8	24.0	0.228
6/5	57.8	58.4	11.64	139.5	24.0	0.286
10/5	62.2	61.6	11.64	139.7	25.0	0.261
18/5	60.2	59.5	11.69	140.2	22.0	0.251
19/5	60.0	59.1	11.69	140.2	22.5	0.256
24/5	98.2	95.6	16.46	196.7	23.0	0.253
27/5	99.7	97.7	16.45	196.7	23.0	0.247
28/5	104.9	103.9	16.46	196.6	23.0	0.231
4/6	109.2	108.9	16.45	196.4	23.0	0.219
9/6	114.8	116.0	16.45	196.5	23.0	0.206
25/6	86.8	88.6	13.94	166.6	23.0	0.213
23/7	91.3	91.1	14.00	167.2	23.0	0.201

The thermal conductivities measured between 14/4 and 9/6 are graphed against the temperature difference between the main and guard heaters on Figure A2.1. The reason for this choice

of plot is that in theory the guarded hot ring apparatus should be operated with the guard ring and main heater temperatures equal. Since this is impossible to achieve in practice, and since the calculated thermal conductivity is sensitive to differences between the main and guard heater temperatures, some form of interpolation must be used in calculating the thermal conductivty for the case of equal guard and main heater temperatures.

In figure A2.1 the data is plotted for the two different power inputs used. As can be seen, the data for the period 14/4 to 19/5, at the lower power input, shows considerable scatter. This could be due to a number of factors including failure to allow the apparatus to come to steady-state, as well as the variations in the cooling water temperature which are evident from Table A2.1. Due to the scatter in the data no attempt has been made to interpolate to $T_{guard} = T_{main}$. The data for the period 24/5 - 9/6 shows far more consistency. A quadratic least squares curve fits this data well, as can be seen from the graph. The interpolated value for $T_{guard} = T_{main}$ is 0.216 W/mK. The value obtained by linear interpolation between the values measured on 25/6 and 23/7 (which are not shown on the graph) is 0.202 W/mK.



APPENDIX 3 DERIVATION OF MODEL EQUATIONS

A3.1 Mass Balances

A3.1.1 Gas Phase Mass Balances

Consider the element of a bed of coal shown in Figure A3.1. The element has cross sectional area A and height Δx. The volume of gas in the element is $A \Delta x \epsilon$. The molar flowrate per unit area of the gas through the voids is G .

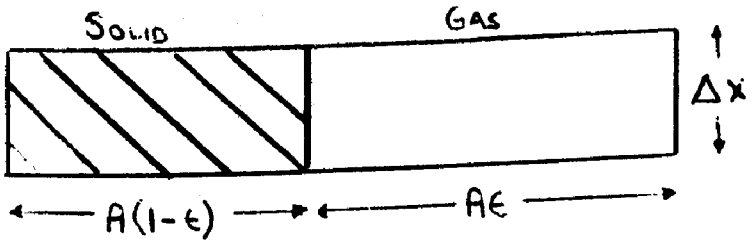


Figure A3.1 Differential element of a coal bed

The mass balance for component i in the gas phase is:

$$(\text{Moles of i in gas})\big|_{t+\Delta t} - (\text{Moles of i in gas})\big|_{t}$$

$$= (\text{Moles in})\big|_{x} - (\text{Moles in})\big|_{x+\Delta x} + \text{Moles produced in time } \Delta t$$

or

$$\left(\frac{P \epsilon}{R T_g} A \Delta x \, y_i\right)\Big|_{t+\Delta t} - \left(\frac{P \epsilon}{R T_g} A \Delta x \, y_i\right)\Big|_{t}$$

$$= (A G y_i \Delta t)\big|_{x} - (A G y_i \Delta t)\big|_{x+\Delta x} + r_i A \Delta x \Delta t$$

where
- G = molar flowrate per unit area
- y_i = mole fraction of i in the gas phase
- x = distance along bed
- P = pressure
- R = gas constant
- ϵ = bed voidage
- T_g = gas temperature
- t = time
- r_i = rate of formation of i per unit bed volume

Dividing by A Δx Δt and letting Δx and Δt tend to zero gives:

$$\frac{\partial}{\partial t}\left(\frac{P \epsilon}{R T_g} y_i\right) + \frac{\partial}{\partial x}(G y_i) = r_i \qquad \text{A3.1.1}$$

Equation A3.1.1 may be summed over all i to give:

$$\frac{\partial G}{\partial x} + \frac{\epsilon}{R} \frac{\partial}{\partial t} \frac{P}{T_g} = \sum_{i=1}^{N} r_i \qquad \text{A3.1.2}$$

where N = number of components in gas phase

Substitution of equation A3.1.1 in A3.1.2 gives:

$$G \frac{\partial y_i}{\partial x} + \frac{P \epsilon}{R T_g} \frac{\partial y_i}{\partial t} = r_i - y_i \sum_{j=1}^{N} r_j \qquad (i = 1 \text{ to } N) \qquad \text{A3.1.3}$$

A3.2 Solid Phase Mass Balances

Let the mass fraction of component j in the solid phase be f_j, and the rate of formation of j per bed volume be p_j.

The mass balance for the solid phase is:

Increase of mass of j in time Δt
= rate of formation of j x bed volume x Δt

or: $(A \Delta x \rho (1-\epsilon) f_j)_{t+\Delta t} - (A \Delta x \rho (1-\epsilon) f_j)_t = p_j \Delta t A \Delta x$

Dividing by A Δx Δt and letting Δt tend to zero gives:

$$(1-\epsilon) \frac{\partial (\rho f_j)}{\partial t} = p_j \qquad (j = 1 \text{ to } M) \qquad \text{A3.1.4}$$

ρ = density of solid
f_j = mass fraction of j in the solid
p_j = rate of formation of j in the solid
M = number of components in solid phase

where it has been assumed that the voidage of the bed does not change with time.

Summing over all j gives:

$$(1-\epsilon)\frac{\partial \rho}{\partial t} = \sum_{j=1}^{M} p_j \qquad \text{A3.1.5}$$

A3.2 Energy Balances

The general energy balance used in this section is:

Rate of change of internal energy of the volume =

Internal energy in - Internal energy out +

energy transferred thermally + energy transferred mechanically

In the derivations that follow changes in kinetic and potential energy have been neglected.

A3.2.1 Gas Phase Energy Balance

Application of the above formula to the gas in the volume shown in Figure A3.1 gives:

$\frac{\partial U_g}{\partial t}$ Rate of change of internal energy

$= (A\ \epsilon\ q_g)_{/x} - (A\ \epsilon\ q_g)_{/x+\Delta x}$ conduction/radiation

$+ (A\ G\ \hat{H})_{/x} - (A\ G\ \hat{H})_{/x+\Delta x}$ flow

$+ A\ \Delta x \sum_{i=1}^{N} r_i\ \hat{H}_i$ Reaction

$+ Q_c\ A\ \Delta x$ Convection from solid to gas

where U_g = Internal energy of gas in volume

q_g = flux due to conduction and radiation in gas

$\hat{H}$ = molar enthalpy of flowing gas

$\hat{H}_i$ = molar enthalpy of gas leaving or entering by reaction

Q_c = rate of convection from gas to solid

It should be noted that the flow and reaction terms involve enthalpies and not internal energies. This is because the process is to all intents and purposes constant pressure and reversible, and therefore the mechanical work term may be combined with the flow and reaction terms which then may be written as enthalpies.

Now:

$$U_g = A\,\Delta x\,\epsilon\,\rho_g\,\hat{U} = A\,\Delta x\,\epsilon\,P\,\hat{U}/(R\,T_g)$$

where the ideal gas law

$$\rho_g = P/(R\,T_g)$$

has been used.

Substituting this in the above energy balance, dividing by $A\,\Delta x$ and letting Δx tend to zero gives:

$$\epsilon\,\frac{\partial}{\partial t}\,\frac{P\,\hat{U}}{R\,T_g} = -\,\epsilon\,\frac{\partial q_g}{\partial x} - \frac{\partial}{\partial x}\,(G\,\hat{H}) + \sum_{i=1}^{N} r_i\,\hat{H}_i + Q_c \qquad \text{A3.2.1}$$

But

$$\hat{U} = \hat{H} - R\,T_g$$

since the ideal gas assumption has been made. Substituting this in Equation A3.2.1 gives:

$$\epsilon\,\frac{\partial}{\partial t}\,\frac{P\,\hat{H}}{R\,T_g} - \epsilon\,\frac{\partial P}{\partial x} = -\,\epsilon\,\frac{\partial q_g}{\partial x} - \frac{\partial}{\partial x}\,(G\,\hat{H}) + \sum_{i=1}^{N} r_i\,\hat{H}_i + Q_c \qquad \text{A3.2.2}$$

For an ideal gas

$$\hat{H} = \sum_{i=1}^{N} y_i\,\hat{H}_i$$

and

$$d\hat{H} = \sum_{i=1}^{N} (y_i\,d\hat{H}_i + \hat{H}_i\,dy_i)$$

Therefore

$$\epsilon \frac{\partial}{\partial t}\frac{P\hat{H}}{R T_g} + \frac{\partial}{\partial x}(G\hat{H}) = \frac{\epsilon P}{R T_g}\frac{\partial \hat{H}}{\partial t} + G\frac{\partial \hat{H}}{\partial x} + \epsilon \hat{H}\frac{\partial}{\partial t}\frac{P}{R T_g} + \hat{H}\frac{\partial G}{\partial x}$$

$$= \frac{P\epsilon}{R T_g}\sum_{i=1}^{N}\left(y_i\frac{\partial \hat{H}_i}{\partial t} + \hat{H}_i\frac{\partial y_i}{\partial t}\right) + G\sum_{i=1}^{N}\left(y_i\frac{\partial \hat{H}_i}{\partial x} + \hat{H}_i\frac{\partial y_i}{\partial x}\right) + \hat{H}\left(\epsilon\frac{\partial}{\partial t}\frac{P}{R T_g} + \frac{\partial G}{\partial x}\right)$$

Combining terms and using the gas phase mass balance (equation A3.1.3) the right hand side of the above equation may be written as

$$\sum_{i=1}^{N}\left(\hat{H}_i\left(r_i - y_i\sum_{j=1}^{N} r_j\right)\right) + \frac{P\epsilon}{R T_g}\sum_{i=1}^{N}\left(y_i\frac{\partial \hat{H}_i}{\partial T}\frac{\partial T}{\partial t}\right)$$

$$+ G\sum_{i=1}^{N}\left(y_i\frac{\partial \hat{H}_i}{\partial T}\frac{\partial T}{\partial t}\right) + \hat{H}\sum_{i=1}^{N} r_i$$

For an ideal gas $\frac{\partial \hat{H}_i}{\partial T} = \hat{c}_i$ by definition

and $$\sum_{i=1}^{N} y_i\,\hat{c}_i = \hat{c}$$

Substituting in the above expression gives:

$$RHS = \sum_{j=1}^{N}\hat{H}_i\,r_i + \frac{P\epsilon}{RT_g}\hat{c}\frac{\partial T_g}{\partial t} + G\,\hat{c}\frac{\partial T_g}{\partial x}$$

Finally, back substitution in A3.2.2 gives the gas phase energy balance:

$$\frac{P\epsilon}{RT_g}\hat{c}\frac{\partial T_g}{\partial t} - \epsilon\frac{\partial P}{\partial t} = -G\,\hat{c}\frac{\partial T_g}{\partial x} + \epsilon k_g\frac{\partial^2 T_g}{\partial x^2} + Q_c$$

where use has been made of Fourier's law in writing

$$\frac{\partial q_g}{\partial x} = -k_g\frac{\partial^2 T_g}{\partial x^2}$$

A3.2.2 Solid Phase Energy Balance

The approach taken is to write an energy balance for the whole system, and then to subtract the gas phase energy balance to leave the solid phase energy balance.

Thus, using equation A3.2.1

$$(U_s + U_g)/_{t+\Delta t} - (U_s + U_g)/_t$$

$$= [A\epsilon q^g_{cr}/_x - A\epsilon q^g_{cr}/_{x+\Delta x}]\Delta t \qquad \text{(Conduction and radiation in gas)}$$

$$+ [A(1-\epsilon)q^s_c/_x - A(1-\epsilon)q^s_c/_{x+\Delta x}]\Delta t \qquad \text{(Conduction in solid)}$$

$$+ [A\hat{G}\hat{H}/_x - A\hat{G}\hat{H}/_{x+\Delta x}]\Delta t \qquad \text{(Bulk Flow)} \quad \text{A3.2.6}$$

Note that there are no reaction or convection terms since these terms are associated with transport between the phases.

Subtracting the appropriate gas-phase energy balance leaves:

$$U_s/_{t+\Delta t} - U_s/_t$$

$$= [A(1-\epsilon)q^s_c/_x - A(1-\epsilon)q^s_c/_{x+\Delta x}]\Delta t$$

$$- Q_c A\Delta x\Delta t \qquad \text{A3.2.7}$$

Now $U_s = \rho A\Delta x(1-\epsilon)\bar{U}_s$ since $A\Delta x(1-\epsilon)$ is the volume of the solid phase and $\bar{U}_s$ is the specific mass internal energy of the solid.

Substituting this in equation A3.2.7, dividing by $A\Delta x\Delta t$ and letting Δx and Δt tend to zero gives:

$$\frac{\partial}{\partial t}(\rho\bar{U}_s) = -(1-\epsilon)\frac{\partial q^s_c}{\partial x} - Q_c \qquad \text{A3.2.8}$$

Now

$$\bar{U}_s = \bar{H}_s - \frac{P}{\rho} \qquad \text{A3.2.9}$$

Therefore

$$\frac{\partial}{\partial t}(\rho\bar{U_s}) = \frac{\partial}{\partial t}(\rho\bar{H_s}) - \frac{\partial P}{\partial t} \qquad \text{A3.2.10}$$

$$= \bar{H}_s\frac{\partial\rho}{\partial t} + \rho\frac{\partial\bar{H}}{\partial t}s - \frac{\partial P}{\partial t} \qquad \text{A3.2.11}$$

Assuming $\bar{H}_s$ may be written as the sum of pure component enthalpies ie:

$$\bar{H}_s = \sum_{j=1}^{N} f_j\bar{H}_j \qquad \text{A3.2.12}$$

Therefore

$$\frac{\partial\bar{H}}{\partial t}s = \sum_{j=1}^{N}\frac{\partial}{\partial t}(f_j\bar{H}_j) = \sum_{j=1}^{N}(\bar{H}_j\frac{\partial f}{\partial t}j + f_j\frac{\partial\bar{H}}{\partial t}j) \qquad \text{A3.2.13}$$

Now, using equation A3.2.13 and the solid phase mass balance A3.1.5 it may be shown that:

$$(1-\epsilon)\frac{\partial}{\partial t}(\rho\bar{H}_s) = \sum_{j=1}^{N}\bar{H}_j\rho_j + (1-\epsilon)\rho\sum_{j=1}^{N}f_j\frac{\partial\bar{H}}{\partial t}j \qquad \text{A3.2.14}$$

Now

$$\frac{\partial\bar{H}}{\partial t}j = \left(\frac{\partial\bar{H}}{\partial T}j\right)_p\frac{\partial T}{\partial t}s + \left(\frac{\partial\bar{H}}{\partial P}j\right)_{T_s}\frac{\partial P}{\partial t} \qquad \text{A3.2.15}$$

$$= \bar{c}_j\frac{\partial T}{\partial t}s + \left(\frac{\partial H}{\partial P}j\right)_{T_s}\frac{\partial P}{\partial t} \qquad \text{A3.2.16}$$

Therefore

$$\sum_{j=1}^{N}f_j\frac{\partial\bar{H}}{\partial t}j = \sum_{j=1}^{N}\left(f_j\bar{c}_j\frac{\partial T}{\partial t}s + f_j\left(\frac{\partial\bar{H}}{\partial t}j\right)_{T_s}\frac{\partial P}{\partial t}\right) \qquad \text{A3.2.17}$$

$$= \bar{c}_s\frac{\partial T}{\partial t}s + \frac{\partial P}{\partial t}\sum_{j=1}^{N}f_j\left(\frac{\partial\bar{H}}{\partial P}j\right)_{T_s} \qquad \text{A3.2.18}$$

At this point the assumption is made that the solid enthalpy is not a function of pressure. Thus the last term of equation

A3.2.18 can be dropped. Substitution of the above results in equation A3.2.18 yields:

$$(1-\epsilon)\rho_s \bar{c}_s \frac{\partial T_s}{\partial t} - (1-\epsilon)\frac{\partial P}{\partial t} = (1-\epsilon)\frac{\partial q^s_c}{\partial x} - Q_c - \sum_{j=1}^{N} p_j H_j$$

Finally, use is made of Fourier's Law in writing

$$\frac{\partial q^s_c}{\partial x} = \eta k_s \frac{\partial^2 T_s}{\partial x^2}$$

where η is a tortuosity factor allowing for the fact that the conduction in the solid does not occur in a straight line.

A3.3 Momentum Balance

The equation of motion for the one-dimensional flow of a Newtonian fluid is given by Bird, Stewart & Lightfoot (1960) to be:

$$\rho \frac{\partial U}{\partial t} = -\rho U \frac{\partial U}{\partial x} + \mu \frac{\partial^2 U}{\partial x^2} - \rho g - \frac{\partial P}{\partial x} \qquad \text{A3.3.1}$$

Bird et al (1960) state that for flow through packed beds the steady-state equation of motion may be simplified to:

$$0 = -fU - \rho g - \frac{\partial P}{\partial x} \qquad \text{A3.3.2}$$

This implies that the unsteady-state equation of motion in the case of a packed bed is:

$$\rho \frac{\partial U}{\partial t} = -fU - \rho g - \frac{\partial P}{\partial x} \qquad \text{A3.3.3}$$

The equation of motion for the air far from the bed is:

$$0 = -\rho_\infty g - \frac{\partial P_\infty}{\partial x} \qquad \text{A3.3.4}$$

Subtracting A3.3.4 from A3.3.3 gives:

$$\rho \frac{\partial U}{\partial t} = -fU + g(\rho_\infty - \rho) - \frac{\partial}{\partial x}(P - P_\infty) \qquad \text{A3.3.5}$$

If the gas is assumed to behave ideally, and its molecular weight is constant then

$$\frac{\rho}{\rho_\infty} = \frac{T_\infty}{T}$$

Substituting this in equation A3.3.5 gives, for the steady-state:

$$\frac{\partial}{\partial x}(P-P_\infty) = -fU + g\,\rho_\infty\left(1 - \frac{T}{T_\infty}\right) \qquad 2.2.1$$

APPENDIX 4 THE CONTINUUM AND PSEUDO STEADY-STATE ASSUMPTIONS

The continuum assumption for a packed bed may be made when the solid and gas temperatures are not very different. In this case equations 5.4.5 and 5.6.4 may be added to give equation 6.1.1.

Edwards (1983) has discussed the conditions under which the particle and gas temperatures tend to equilibrate, and has shown that this will occur within a time τ_d given by:

$$\tau_d = \frac{\rho_s \, C_s \, D_p^2}{4 \, k_s} \qquad \text{A4.1}$$

This author's calculations indicate that the particle surface and air temperatures are nearly in equlibrium. This can be understood if τ_d is evaluated for the following values:

$$\rho_s = 1200 \text{ kg/m}^3$$
$$C_s = 1000 \text{ J/kg/K}$$
$$k_s = 0.4 \text{ W/m/K}$$

Then $\tau_d = 750 \times 10^3 \, D_p^2$

For $D_p = 1$ mm $\qquad \tau_d = 750 \times 10^{-3}$ s

For $D_p = 20$ mm $\qquad \tau_d = 300$ s

Both of these times are small in comparison to the residence time of the gas in the bed, and therefore thermal equilibrium between gas and solid should be reached.

The pseudo-steady state assumption may be made when the time constant for one process is very much larger than the time constant for the other process. In the case of a coal bed the time constant for conduction is given by

$$\tau_c = \frac{4L^2 \, \rho_b \, C_b}{\pi^2 \, k_b} = \frac{4 \, L^2}{\pi^2 \, \kappa}$$

Using a typical value for κ of 8×10^{-4} m^2/hr gives

$$\tau_c = \frac{4 \, L^2}{\pi^2 \, 8 \times 10^{-4}} = 500 \, L^2 \text{ hours}$$

The time constant for gas flow and gas composition is the residence time of the gas i.e.

$$\tau_f = \frac{L}{U} = \frac{P\,L}{G\,R\,T}$$

Using values from Table 2.1 for D_p = 5 mm gives

$$\tau_f = \frac{8.3 \times 10^3 \times 320 \times 1.3 \times 10^{-4}\,L}{1 \times 10^5} = 0.08\,L \text{ hours}$$

The time constant associated with the momentum balance is

$$\tau_p = \frac{\rho_g L}{f} = \frac{1.173\,L}{2.2 \times 10^3} = 5.3 \times 10^{-4}\,L \text{ seconds}$$

It can be seen that the time constants for gas flow and composition and for pressure changes are very much smaller than that for conduction. Furthermore the time constant for conduction depends on L^2 while the other time constants depend on L. For these reasons the pseudo-steady state assumption on the gas mass balances and the momentum balance is a good one.

APPENDIX 5 THE INCLUSION OF A RADIAL HEAT LOSS TERM IN EQUATION 6.1.4

In order to include radial heat losses in equation 6.1.4, an alternative derivation of the temperature equation is used.

Consider an element in the form of a ring, as shown in Figure A5.1:

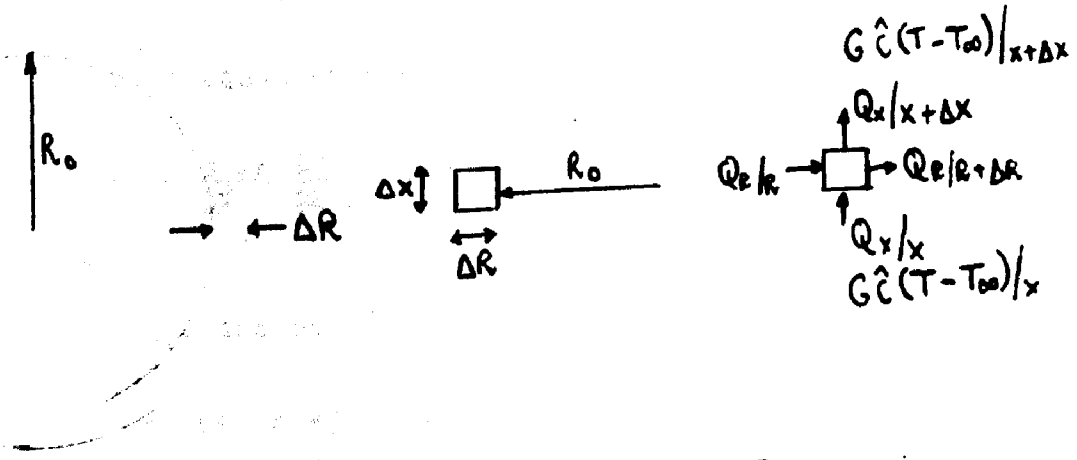


FIGURE A5.1 ELEMENT IN THE FORM OF A RING

The following energy balance may be written:

Rate of accumulation of energy in the volume =

Rate of energy transfer into volume +

Rate of generation in volume -

Rate of energy transfer out of volume

or

$$\rho C_p \frac{\partial}{\partial t}(T\ 2\pi R\ \Delta R\ \Delta x)$$

$$= (Q_R\ 2\pi R\ \Delta x)|_R + (Q_x\ 2\pi R\ \Delta R)|_x + G\hat{c}\ 2\pi R\ \Delta R\ (T-T_\infty)|_x$$

$$+ r_x(-\Delta H_r)\ 2\pi R\ \Delta R\ \Delta x$$

$$- (Q_R\ 2\pi R\ \Delta x)|_{R+\Delta R} - (Q_x\ 2\pi R\ \Delta R)|_{x+\Delta x} - G\hat{c}\ 2\pi R\ \Delta R\ (T-T_\infty)|_{x+\Delta x}$$

Dividing by $\Delta R\ \Delta x$ and letting them tend to zero gives:

$$\rho\ C_p\ 2\pi R\ \frac{\partial T}{\partial t} = -\frac{\partial}{\partial R}(Q_R\ 2\pi R) - \frac{\partial}{\partial x}(Q_x\ 2\pi R) - G\ \hat{c}\ 2\pi R\ \frac{\partial T}{\partial x} + ry(-\Delta H_r)2\pi R$$

Using Fourier's law $\quad Q_R = -k_{b,R}\ \frac{\partial T}{\partial R}$

and $\quad Q_x = -k_{b,x}\ \frac{\partial T}{\partial x}$

Substituting in above equation gives:

$$\rho\ C_p\ 2\pi R\ \frac{\partial T}{\partial t} = 2\pi\ k_{b,R}\ \frac{\partial}{\partial R}(R\ \frac{\partial T}{\partial R}) + 2\pi R\ k_{b,x}\ \frac{\partial^2 T}{\partial^2 x} - G\ \hat{c}\ 2\pi R\ \frac{\partial T}{\partial x} + ry(-\Delta H_r)2\pi R$$

assuming $k_{b,R}$ and $k_{b,x}$ are not functions of R and x respectively.

This equation may now be integrated from 0 to R_o. Assuming that ρ, C_p, G, r and ΔH_r are not functions of R, this gives:

$$\rho\ C_p\ 2\pi\ \frac{\partial}{\partial t}(\int_0^{R_o} T\ R\ dR) = 2\pi\ k_{b,R}\int_0^{R_o}\frac{\partial}{\partial R}(R\ \frac{\partial T}{\partial R})\ dR + 2\pi\ k_{b,x}\ \frac{\partial^2}{\partial x^2}(\int_0^{R_o} T\ R\ dR)$$

$$- G\ \hat{c}\ 2\pi\ \frac{\partial}{\partial x}(\int_0^{R_o} T\ R\ dR) + ry(-\Delta H_r)2\pi(\int_0^{R_o} R\ dR)$$

Defining $T' = \frac{2}{R_o^2}\int_0^{R_o} T\ R\ dR$ and substituting gives

$$\rho\ C_p\ \pi\ R_o^2\ \frac{\partial T'}{\partial t} = 2\pi\ k_{b,R}\ \ R\ \frac{\partial T}{\partial R}\Big]_{R=R_o} + \pi\ R_o^2\ k_{b,x}\ \frac{\partial^2 T'}{\partial x^2}$$

$$- G\ \hat{c}\ \pi\ R_o^2\ \frac{\partial T'}{\partial x} + ry(-\Delta H_r)\ \pi\ R_o^2$$

The radial boundary conditions is:

$$k_{b,R}\ \frac{\partial T}{\partial R} = -h_R\ (T(R=R_o)-T_\infty)$$

Substituting this in the above equation gives:

$$\rho C_p \pi R_o^2 \frac{\partial T'}{\partial t} = -2\pi R_o h_R (T(R=R_o)-T_\infty) + \pi R_o^2 k_{b,x} \frac{\partial^2 T'}{\partial x^2}$$

$$- G \hat{c} \pi R_o^2 \frac{\partial T'}{\partial x} + r y(-\Delta H_r) \pi R_o^2$$

If the radial gradients are not too large, $T(R=R_o)$ will not be very different from T'. Assuming this to be the case the above equation may be written as:

$$\rho C_p \frac{\partial T'}{\partial t} = -2h_R/R_o (T'-T_\infty) + k_{b,x} \frac{\partial^2 T'}{\partial x^2} - G \hat{c} \frac{\partial T'}{\partial x} + r y(-\Delta H_r)$$

This equation is the same as equation 6.1.1 apart from the first term on the right hand side. This is the radial heat loss term.

Finally, the above equation is made dimensionless using the substitutions given in Section 6.1. The result is equation 6.1.5 i.e.

$$\frac{\partial \theta}{\partial \tau} = \frac{\partial^2 \theta}{\partial X^2} - a \frac{\partial \theta}{\partial X} + b y - C (\theta - 1) \qquad 6.1.5$$

where $C = 2 h_R L^2/(k_b R_o)$.

It should be noted that as R_o tends to infinity, C tends to zero.

APPENDIX 6 EXPLANATION FOR THE INSTABILITY OF THE RUNGE-KUTTA ALGORITHM

The equation is

$$0 = \frac{d^2\theta}{dX^2} - a\frac{d\theta}{dX} - b\,y \qquad \text{A6.1}$$

with boundary conditions:

at X=0 $\quad \frac{d\theta}{dX} = (Bi_0+a)(\theta-1)$

at X=1 $\quad \frac{d\theta}{dX} = -Bi_1(\theta-1)$

For the first step along the bed the coefficients of equation A6.1 may be assumed constant. In effect the Runge-Kutta algorithm is stepping along the solution of 6.2.1 but with boundary conditions both at X = 0 i.e.

$$\frac{d\theta}{dX} = (Bi_0+a)(\theta-1)$$

$$\theta(X=0) = \theta_0$$

The solution to A6.1 with these boundary conditions is:

$$\theta = \theta_0 + a(\exp(aX)-1)((Bi_0+a)(\theta_0-1)-b/a) + b\,X/a \qquad \text{A6.2}$$

It can be seen that the value of θ_0 is critical, since if

$(Bi_0+a)(\theta_0-1)-b/a > 0$ then the second term of equation A6.2 increases without bound. If on the other hand:

$(Bi_0+a)(\theta_0-1)-b/a < 0$

then the second term becomes very large negative.

The real problem is that the boundary condition at X = 1 is not included in the method of solution, and thus the method will always become unstable.

APPENDIX 7 SOLUTION OF EQUATION 6.2.1 WITH r CONSTANT

If r is assumed constant then equation 6.1.2 may be integrated

i.e. $$\frac{dy}{dx} = \frac{-r\ y}{G}$$

gives $$y = y_o \exp(-rx/G) = y_o \exp(\gamma_3 X) \qquad A7.1$$

Substituting this in equation 6.2.1 give:

$$0 = \frac{d^2\theta}{dX^2} - a\frac{d\theta}{dX} - b\ y_o \exp(\gamma_3 X) - C\ (\theta - 1) \qquad A7.2$$

The solution of this equation is

$$\theta(X) = 1 + C_1\exp(\gamma_1 X) + C_2\exp(\gamma_2 X) + C_3\exp(\gamma_3 X)$$

$$C_3 = -b/(\gamma_3^2 + a\gamma_3 - C)$$

$$\gamma_1 = (a - (a^2 + 4C))^{1/2})/2$$

$$\gamma_2 = (a + (a^2 + 4C))^{1/2})/2$$

C_1 and C_2 may be determined from the boundary conditions.

Equation 6.1.3 may be integrated to give

$$-\rho_\infty\ v^2/2 = -f\ G\ R\ T_\infty\ L/P(\int_o^1 \theta\ dX + \rho_\infty\ g\ L(\int_o^1 \theta^{-1}\ dX)) \qquad A7.3$$

or $$G = P\ \rho_\infty(v^2/2L + g\ L(1-\int_o^1 \theta^{-1}dX))/(f\ R\ T_\infty\ L\ \int_o^1 \theta dX) \qquad A7.4$$

APPENDIX 8 SOLUTION OF EQUATION 6.1.5 WITH r CONSTANT

The equation to be solved is:

$$\frac{\partial\theta}{\partial\tau} = \frac{\partial^2\theta}{\partial X^2} - a\frac{\partial\theta}{\partial X} + b\,y - C\,(\theta - 1) \qquad \text{A8.1}$$

with boundary conditions

at X=0 $\quad \frac{\partial\theta}{\partial X} = (Bi_0+a)(\theta-1)$

at X=1 $\quad \frac{\partial\theta}{\partial X} = -Bi_1(\theta-1)$

The initial condition is $\theta(X,0) = \theta_0(X)$

The first step in the solution is to write:

$$\theta(X,\tau) = u(X,\tau) + \phi(X) \qquad \text{A8.2}$$

Substituting equation A8.2 in equation A8.1 gives:

$$\frac{\partial u}{\partial\tau} = \frac{\partial^2 u}{\partial X^2} - a\frac{\partial u}{\partial X} - C\,u + \frac{d^2\phi}{dX^2} - a\frac{d\phi}{dX} + b\exp(\gamma_s X) - C(\phi-1) \qquad \text{A8.3}$$

This may be written as two equations:

$$\frac{\partial u}{\partial\tau} = \frac{\partial^2\theta}{\partial X^2} - a\frac{\partial u}{\partial X} - C\,u \qquad \text{A8.4}$$

and

$$0 = \frac{d^2\phi}{dX^2} - a\frac{d\phi}{dX} + b\exp(\gamma_s X) - C(\phi-1) \qquad \text{A8.5}$$

with boundary conditions:

at X=0 $\quad \frac{\partial u}{\partial X} = (Bi_0+a)\,u$ and $\frac{d\phi}{dX} = (Bi_0+a)(\phi-1)$

at X=1 $\quad \frac{\partial u}{\partial X} = -Bi_1\,u$ and $\frac{d\phi}{dX} = -Bi_1(\phi-1)$

and initial condition $u(X,0) = \theta_0(X) - \phi(X)$

Equation A8.5 with its associated boundary conditions is merely the steady-state temperature equation, whose solution has been dealt with in Appendix 7.

The problem has thus been reduced to solving equation A8.4 with its boundary and initial conditions.

Defining a new variable $v(X,\tau)$ as:

$$u(X,\tau) = v(X,\tau) \exp(-\tau(a^2/4-C) + aX/2)$$

and substituting in equation A8.4 gives the diffusion equation i.e

$$\frac{\partial v}{\partial \tau} = \frac{\partial^2 v}{\partial X^2} \qquad \text{A8.6}$$

The boundary conditions on v are:

At X=0 $\quad \frac{\partial v}{\partial \tau} = (Bi_0 + a/2)v$

At X=1 $\quad \frac{\partial v}{\partial \tau} = -(Bi_1 + a/2)v$

and initial condition:

$$v(X,0) = (\theta_0(X) - \phi(X)) \exp(-aX/2)$$

The solution to equation A8.6 may be found in Carslaw & Jaeger (1959), and is:

$$v(X,\tau) = \Sigma \left(Z_n(X) \exp(-\beta_n^2\tau) \int Z_n(X') g(X') dX'\right) \qquad \text{A8.7}$$

$$Z_n(X) = \frac{2(\beta_n^2+Bi_3^2)(\beta_n \cos(\beta_n X)+Bi_2 \sin(\beta_n X))}{((\beta_n^2+Bi_2^2)(\beta_n^2+Bi_3^2+Bi_3)+Bi_2(\beta_n^2+Bi_3^2))}$$

$$g(X) = (\theta_0(X) - \phi(X)) \exp(-aX/2)$$

$$Bi_2 = Bi_0 - a/2$$

$$Bi_3 = Bi_1 + a/2$$

and the β_n are the positive roots of

$$\tan(\beta) = \frac{\beta(Bi_3 + Bi_2)}{(Bi_2\, Bi_3 + \beta^2)}$$

APPENDIX 9 APPLICATION OF THE METHOD OF LINES TO THE SOLUTION OF EQUATION 6.1.5

Equation 6.4.1 is:

$$\frac{\partial\theta(X_i,\tau)}{\partial X} = \Sigma(a_{ij}\ \theta(X_j,\tau) \qquad i=1 \text{ to } N \qquad \text{A9.1}$$

where the X_i are the nodes of the Nth order shifted Legendre polynomial.

Similarly

$$\frac{\partial^2\theta(X_i,\tau)}{\partial X} = \Sigma(b_{ij}\ \theta(X_j,\tau) \qquad i=1 \text{ to } N \qquad \text{A9.2}$$

It may easily be shown that the matrix $\underline{A}$ of coefficients a_{ij} is related to the matrix $\underline{B}$ of coefficients b_{ij} by:

$$\underline{B} = \underline{A}^2$$

Using equations A9.1 and A9.2 equation 6.1.5 may be written as:

$$\frac{d\theta_i}{d\tau} = \Sigma((b_{ij}-a\ a_{ij})\theta_j)+by_i\exp\{-E/(RT_\infty\theta_i)\}-C(\theta_i-1) \qquad \text{A9.3}$$

where $\theta_i = \theta(X_i,\tau)$

$y_i = y(X_i)$

The bondary conditions are also discretized:

$$\Sigma\ a_{1j}\theta_j = (Bio + a)(\theta_1 - 1) \qquad \text{A9.4}$$

$$\Sigma\ a_{Nj}\theta_j = -Bi_1(\theta_N - 1) \qquad \text{A9.5}$$

It can be seen that the partial differential equation has been rteduced to N ordinary differentail equations. The procedure used to solve is to calculate all the derivatives $d\theta_i/d\tau$ for one time and then use a Runge-Kutta algorithm to calculate the value of θ_i at the next time. The boundary values are included explicitly by solving equations A9.4 and A9.5 for θ_1 and θ_N in [illegible] at each time step. In addition a

backward difference formula is used to calculate the oxygen profile at each time. If the effects of ageing are incuded it is neccessary to calculate the fractional conversion of the coal at each time and distance using equation 1.4.4.

APPENDIX 10 TABULATION OF RESULTS OF CHIMNEY EXPERIMENT

A10.1 Introduction

In this Appendix the measured data for the chimney experiment is presented in tabular form. In the printouts it will be noted that 10 channels were used to log data. Channel 1 is the thermocouple at the very bottom of the bed, while channel 9 is the thermocouple at the very top of the bed. Channel 10 is a thermocouple placed in the oven.

The printouts show the time at which the data was logged and the temperature in degrees centigrade (labelled as deg_C). It should be noted that in some instances the data logger was re-started, with a greater interval between scans.

A10.2 Cooling Run

This run was used to obtain the heat transfer coefficients necessary for the model. The bed was heated under nitrogen and then removed from the oven. The model parameters used to obtain figure 7.2 were:

Coal particle size range : -3.4 + 1.19 mm
Bed Length : 0.2 m
Bed Radius : 0.039 m
C : 23
Bi_o : 3.7
Bi_1 : 9.3
Bed voidage : 0.38
D_p : 2.5 mm

EXP 10--SCAN 01---24:01:08:58:03
"COOLING"

ch: 01	190.3	deg_C
ch: 02	194.1	deg_C
ch: 03	196.5	deg_C
ch: 04	198.3	deg_C
ch: 05	197.1	deg_C
ch: 06	192.8	deg_C
ch: 07	189.6	deg_C
ch: 08	185.3	deg_C
ch: 09	181.4	deg_C
ch: 10	55.2	deg_C

EXP 10--SCAN 02---24:01:09:17:1
"COOLING"

ch: 01	179.3	deg_C
ch: 02	189.0	deg_C
ch: 03	191.7	deg_C
ch: 04	194.2	deg_C
ch: 05	193.5	deg_C
ch: 06	188.9	deg_C
ch: 07	187.2	deg_C
ch: 08	179.0	deg_C
ch: 09	157.2	deg_C
ch: 10	32.6	deg_C

EXP 10--SCAN 03---24:01:09:28:
"COOLING"

ch: 01	155.1	deg_C
ch: 02	171.7	deg_C
ch: 03	178.0	deg_C
ch: 04	181.2	deg_C
ch: 05	181.1	deg_C
ch: 06	176.0	deg_C
ch: 07	174.7	deg_C
ch: 08	158.3	deg_C
ch: 09	129.4	deg_C
ch: 10	29.8	deg_C

EXP 10--SCAN 04---24:01:09:47:
"COOLING"

ch: 01	171.9	deg_C
ch: 02	150.2	deg_C
ch: 03	160.1	deg_C
ch: 04	165.5	deg_C
ch: 05	165.6	deg_C
ch: 06	160.4	deg_C
ch: 07	157.7	deg_C
ch: 08	136.6	deg_C
ch: 09	108.7	deg_C
ch: 10	25.5	deg_C

EXP 10--SCAN 05---24:01:09:58:02:
"COOLING"

ch: 01	112.7	deg_C
ch: 02	129.1	deg_C
ch: 03	141.2	deg_C
ch: 04	145.5	deg_C
ch: 05	150.1	deg_C
ch: 06	144.7	deg_C
ch: 07	140.2	deg_C
ch: 08	117.8	deg_C
ch: 09	92.9	deg_C
ch: 10	26.2	deg_C

EXP 10--SCAN ---24:01:10:38:20
"COOLING"

ch: 01	50.6	deg_C
ch: 02	57.3	deg_C
ch: 03	64.3	deg_C
ch: 04	72.8	deg_C
ch: 05	75.3	deg_C
ch: 06	71.0	deg_C
ch: 07	65.2	deg_C
ch: 08	54.0	deg_C
ch: 09	45.3	deg_C
ch: 10	22.8	deg_C

EXP 10--SCAN 03---24:01:10:58:20
"COOLING"

ch: 01	42.9	deg_C
ch: 02	47.6	deg_C
ch: 03	53.1	deg_C
ch: 04	59.9	deg_C
ch: 05	62.0	deg_C
ch: 06	59.6	deg_C
ch: 07	54.0	deg_C
ch: 08	45.6	deg_C
ch: 09	39.1	deg_C
ch: 10	22.1	deg_C

EXP 10--SCAN 07---24:01:11:28:20
"COOLING"

ch: 01	38.4	deg_C
ch: 02	41.0	deg_C
ch: 03	44.9	deg_C
ch: 04	50.1	deg_C
ch: 05	51.9	deg_C
ch: 06	49.2	deg_C
ch: 07	45.6	deg_C
ch: 08	39.4	deg_C
ch: 09	34.6	deg_C
ch: 10	22.4	deg_C

EXP 10--SCAN 04---24:01:13:08:20
"COOLING"

ch: 01	32.4	deg_C
ch: 02	26.0	deg_C
ch: 03	38.3	deg_C
ch: 04	42.6	deg_C
ch: 05	44.1	deg_C
ch: 06	42.2	deg_C
ch: 07	39.5	deg_C
ch: 08	34.9	deg_C
ch: 09	31.7	deg_C
ch: 10	21.9	deg_C

EXP 10--SCAN 08---24:01:15:08:20
"COOLING"

ch: 01	25.7	deg_C
ch: 02	26.4	deg_C
ch: 03	27.2	deg_C
ch: 04	28.3	deg_C
ch: 05	28.6	deg_C
ch: 06	28.1	deg_C
ch: 07	27.2	deg_C
ch: 08	25.9	deg_C
ch: 09	24.8	deg_C
ch: 10	22.3	deg_C

EXP 10--SCAN 05---24:01:13:38:20
"COOLING"

ch: 01	30.6	deg_C
ch: 02	32.4	deg_C
ch: 03	34.5	deg_C
ch: 04	37.4	deg_C
ch: 05	38.6	deg_C
ch: 06	37.9	deg_C
ch: 07	34.9	deg_C
ch: 08	31.5	deg_C
ch: 09	28.9	deg_C
ch: 10	22.3	deg_C

EXP 10--SCAN 09---24:01:15:38:20
"COOLING"

ch: 01	24.8	deg_C
ch: 02	25.3	deg_C
ch: 03	25.9	deg_C
ch: 04	26.6	deg_C
ch: 05	26.9	deg_C
ch: 06	26.5	deg_C
ch: 07	25.9	deg_C
ch: 08	24.9	deg_C
ch: 09	24.1	deg_C
ch: 10	22.2	deg_C

EXP 10--SCAN 06---24:01:14:08:20
"COOLING"

ch: 01	28.4	deg_C
ch: 02	29.8	deg_C
ch: 03	31.3	deg_C
ch: 04	33.4	deg_C
ch: 05	34.1	deg_C
ch: 06	33.1	deg_C
ch: 07	31.6	deg_C
ch: 08	29.1	deg_C
ch: 09	27.1	deg_C
ch: 10	21.9	deg_C

EXP 10--SCAN 10---24:01:16:08:20
"COOLING"

ch: 01	24.2	deg_C
ch: 02	24.5	deg_C
ch: 03	24.9	deg_C
ch: 04	25.5	deg_C
ch: 05	25.7	deg_C
ch: 06	25.3	deg_C
ch: 07	24.9	deg_C
ch: 08	24.2	deg_C
ch: 09	23.6	deg_C
ch: 10	21.9	deg_C

EXP 10--SCAN 07---24:01:14:38:20
"COOLING"

ch: 01	26.8	deg_C
ch: 02	27.8	deg_C
ch: 03	28.9	deg_C
ch: 04	30.4	deg_C
ch: 05	31.0	deg_C
ch: 06	30.2	deg_C
ch: 07	29.1	deg_C
ch: 08	27.2	deg_C
ch: 09	25.8	deg_C
ch: 10	22.0	deg_C

EXP 10--SCAN 11---24:01:16:38:20
"COOLING"

ch: 01	23.7	deg_C
ch: 02	24.0	deg_C
ch: 03	24.3	deg_C
ch: 04	24.6	deg_C
ch: 05	24.7	deg_C
ch: 06	24.5	deg_C
ch: 07	24.2	deg_C
ch: 08	23.6	deg_C
ch: 09	23.2	deg_C
ch: 10	21.9	deg_C

A10.3 Ageing Run 1

The results of this run were used to obtain the plot shown in figure 7.2. The experimental conditions and model parameters were:

Coal particle size range: -3.4 + 1.19 mm

C : 23

Bi_o : 3.7

Bi_1 : 9.3

Bed voidage: 0.38

K_o : 3.33 m/s

E/R : 7000 K

$D_e\rho_m$: 1.42×10^{-13}

D_p : 2.5 mm

O_2 flowrate: 1.14×10^{-4} kmol/m^2/s

Oven temperature : 135°C

EXP 10---------- 19:01:14:35:54

ch: 01	131.8	deg_C
ch: 02	130.8	deg_C
ch: 03	129.2	deg_C
ch: 04	126.9	deg_C
ch: 05	125.6	deg_C
ch: 06	125.6	deg_C
ch: 07	127.1	deg_C
ch: 08	128.9	deg_C
ch: 09	130.1	deg_C
ch: 10	129.5	deg_C

EXP 10--SCAN 01---19:01:14:43:05

ch: 01	132.0	deg_C
ch: 02	131.1	deg_C
ch: 03	129.5	deg_C
ch: 04	127.2	deg_C
ch: 05	126.0	deg_C
ch: 06	125.9	deg_C
ch: 07	127.4	deg_C
ch: 08	129.1	deg_C
ch: 09	130.2	deg_C
ch: 10	125.3	deg_C

EXP 10--SCAN 02---19:01:14:43:29

ch: 01	132.0	deg_C
ch: 02	131.1	deg_C
ch: 03	129.5	deg_C
ch: 04	127.3	deg_C
ch: 05	126.0	deg_C
ch: 06	125.9	deg_C
ch: 07	127.4	deg_C
ch: 08	129.1	deg_C
ch: 09	130.2	deg_C
ch: 10	127.2	deg_C

EXP 10--SCAN 03---19:01:15:43:05

ch: 01	139.1	deg_C
ch: 02	139.9	deg_C
ch: 03	138.4	deg_C
ch: 04	135.0	deg_C
ch: 05	132.5	deg_C
ch: 06	131.1	deg_C
ch: 07	131.7	deg_C
ch: 08	132.0	deg_C
ch: 09	132.0	deg_C
ch: 10	128.3	deg_C

EXP 10--SCAN 04---19:01:16:43:05

ch: 01	145.2	deg_C
ch: 02	147.9	deg_C
ch: 03	147.8	deg_C
ch: 04	144.1	deg_C
ch: 05	140.1	deg_C
ch: 06	137.1	deg_C
ch: 07	136.6	deg_C
ch: 08	135.3	deg_C
ch: 09	134.3	deg_C
ch: 10	128.2	deg_C

EXP 10--SCAN 05---19:01:17:43:05

ch: 01	147.7	deg_C
ch: 02	151.3	deg_C
ch: 03	152.3	deg_C
ch: 04	149.5	deg_C
ch: 05	145.1	deg_C
ch: 06	141.3	deg_C
ch: 07	140.0	deg_C
ch: 08	137.7	deg_C
ch: 09	136.0	deg_C
ch: 10	126.6	deg_C

EXP 10--SCAN 06---19:01:18:43:05

ch: 01	148.6	deg_C
ch: 02	152.5	deg_C
ch: 03	154.1	deg_C
ch: 04	152.3	deg_C
ch: 05	148.1	deg_C
ch: 06	143.9	deg_C
ch: 07	142.1	deg_C
ch: 08	139.1	deg_C
ch: 09	137.1	deg_C
ch: 10	127.4	deg_C

EXP 10--SCAN 07---19:01:19:43:05

ch: 01	148.8	deg_C
ch: 02	152.7	deg_C
ch: 03	154.8	deg_C
ch: 04	153.7	deg_C
ch: 05	149.8	deg_C
ch: 06	145.4	deg_C
ch: 07	143.3	deg_C
ch: 08	139.8	deg_C
ch: 09	137.6	deg_C
ch: 10	126.9	deg_C

EXP 10--SCAN 08---19:01:20:43:05

ch: 01	148.5	deg_C
ch: 02	152.5	deg_C
ch: 03	154.0	deg_C
ch: 04	154.3	deg_C
ch: 05	150.7	deg_C
ch: 06	146.3	deg_C
ch: 07	143.9	deg_C
ch: 08	140.2	deg_C
ch: 09	137.9	deg_C
ch: 10	126.2	deg_C

EXP 10--SCAN 09---19:01:21:43:05

ch: 01	148.3	deg_C
ch: 02	152.2	deg_C
ch: 03	154.4	deg_C
ch: 04	154.4	deg_C
ch: 05	151.1	deg_C
ch: 06	146.8	deg_C
ch: 07	144.2	deg_C
ch: 08	140.4	deg_C
ch: 09	138.0	deg_C
ch: 10	126.2	deg_C

EXP 10--SCAN 10---19:01:22:43:05

ch: 01	147.9	deg_C
ch: 02	151.7	deg_C
ch: 03	154.0	deg_C
ch: 04	154.3	deg_C
ch: 05	151.3	deg_C
ch: 06	147.0	deg_C
ch: 07	144.4	deg_C
ch: 08	140.5	deg_C
ch: 09	138.1	deg_C
ch: 10	127.0	deg_C

EXP 10--SCAN 11---19:01:23:43:05

ch: 01	147.5	deg_C
ch: 02	151.3	deg_C
ch: 03	153.6	deg_C
ch: 04	154.1	deg_C
ch: 05	151.3	deg_C
ch: 06	147.1	deg_C
ch: 07	144.5	deg_C
ch: 08	140.6	deg_C
ch: 09	138.2	deg_C
ch: 10	126.9	deg_C

EXP 10--SCAN 12---20:01:00:43:05

ch: 01	147.2	deg_C
ch: 02	150.8	deg_C
ch: 03	153.1	deg_C
ch: 04	153.7	deg_C
ch: 05	151.2	deg_C
ch: 06	147.2	deg_C
ch: 07	144.6	deg_C
ch: 08	140.6	deg_C
ch: 09	138.2	deg_C
ch: 10	127.8	deg_C

EXP 10--SCAN 13---20:01:01:43:05

ch: 01	146.8	deg_C
ch: 02	150.3	deg_C
ch: 03	152.6	deg_C
ch: 04	153.3	deg_C
ch: 05	151.0	deg_C
ch: 06	147.1	deg_C
ch: 07	144.6	deg_C
ch: 08	140.6	deg_C
ch: 09	138.1	deg_C
ch: 10	128.2	deg_C

EXP 10--SCAN 14---20:01:02:43:05

ch: 01	146.4	deg_C
ch: 02	149.9	deg_C
ch: 03	152.1	deg_C
ch: 04	152.9	deg_C
ch: 05	150.8	deg_C
ch: 06	147.0	deg_C
ch: 07	144.5	deg_C
ch: 08	140.5	deg_C
ch: 09	138.1	deg_C
ch: 10	129.0	deg_C

EXP 10--SCAN 15---20:01:03:43:05

ch: 01	146.1	deg_C
ch: 02	149.4	deg_C
ch: 03	151.6	deg_C
ch: 04	152.5	deg_C
ch: 05	150.6	deg_C
ch: 06	146.9	deg_C
ch: 07	144.4	deg_C
ch: 08	140.5	deg_C
ch: 09	138.1	deg_C
ch: 10	127.4	deg_C

EXP 10--SCAN 16---20:01:04:43:05

ch: 01	145.8	deg_C
ch: 02	149.0	deg_C
ch: 03	151.1	deg_C
ch: 04	152.2	deg_C
ch: 05	150.3	deg_C
ch: 06	146.8	deg_C
ch: 07	144.4	deg_C
ch: 08	140.4	deg_C
ch: 09	138.0	deg_C
ch: 10	125.4	deg_C

EXP 10--SCAN 17---20:01:05:43:05

ch: 01	145.5	deg_C
ch: 02	149.7	deg_C
ch: 03	150.8	deg_C
ch: 04	151.9	deg_C
ch: 05	150.1	deg_C
ch: 06	146.6	deg_C
ch: 07	144.3	deg_C
ch: 08	140.4	deg_C
ch: 09	138.0	deg_C
ch: 10	127.1	deg_C

EXP 10--SCAN 18---20:01:06:43:05

ch: 01	145.3	deg_C
ch: 02	148.4	deg_C
ch: 03	150.4	deg_C
ch: 04	151.5	deg_C
ch: 05	149.9	deg_C
ch: 06	146.5	deg_C
ch: 07	144.2	deg_C
ch: 08	140.3	deg_C
ch: 09	138.0	deg_C
ch: 10	125.9	deg_C

EXP 10--SCAN 19---20:01:07:43:05

ch: 01	145.1	deg_C
ch: 02	148.1	deg_C
ch: 03	150.1	deg_C
ch: 04	151.1	deg_C
ch: 05	149.7	deg_C
ch: 06	146.4	deg_C
ch: 07	144.2	deg_C
ch: 08	140.3	deg_C
ch: 09	137.9	deg_C
ch: 10	125.1	deg_C

A10.4 Ageing Run 2

The results of this run were used to obtain the plot shown in figure 7.3. The experimental conditions and model parameters used to obtain figure 7.3 were:

Coal particle size range : -3.4 + 1.19 mm
C : 23
Bi_0 : 3.7
Bi_1 : 9.3
Bed voidage: 0.38
K_o : 3.33 m/s
E/R : 7000 K
$D_e\rho_m$: 1.42×10^{-13}
D_p : 2.5 mm
O_2 flowrate: 1.14×10^{-4} kmol/m^2/s
Oven temperature : 88°C

ch: 01	83.7	deg_C
ch: 02	83.9	deg_C
ch: 03	83.2	deg_C
ch: 04	83.2	deg_C
ch: 05	82.5	deg_C
ch: 06	82.0	deg_C
ch: 07	82.0	deg_C
ch: 08	82.4	deg_C
ch: 09	82.3	deg_C
ch: 10	88.7	deg_C

EXP 10--SCAN 01---09:02:09:06 19

ch: 01	83.7	deg_C
ch: 02	83.9	deg_C
ch: 03	83.2	deg_C
ch: 04	83.2	deg_C
ch: 05	82.5	deg_C
ch: 06	82.0	deg_C
ch: 07	82.0	deg_C
ch: 08	82.4	deg_C
ch: 09	82.3	deg_C
ch: 10	90.2	deg_C

EXP 10--SCAN 02---09:02:08:21 19

ch: 01	86.7	deg_C
ch: 02	87.7	deg_C
ch: 03	86.9	deg_C
ch: 04	85.3	deg_C
ch: 05	85.9	deg_C
ch: 06	85.0	deg_C
ch: 07	84.3	deg_C
ch: 08	85.2	deg_C
ch: 09	84.5	deg_C
ch: 10	89.2	deg_C

EXP 10--SCAN 03---09:02:08:36 19

ch: 01	87.9	deg_C
ch: 02	89.9	deg_C
ch: 03	89.4	deg_C
ch: 04	89.3	deg_C
ch: 05	88.4	deg_C
ch: 06	87.2	deg_C
ch: 07	86.8	deg_C
ch: 08	87.1	deg_C
ch: 09	85.8	deg_C
ch: 10	89.1	deg_C

EXP 10--SCAN 04---09:02:09:51 19

ch: 01	88.7	deg_C
ch: 02	91.3	deg_C
ch: 03	91.2	deg_C
ch: 04	91.3	deg_C
ch: 05	90.3	deg_C
ch: 06	89.0	deg_C
ch: 07	88.4	deg_C
ch: 08	88.4	deg_C
ch: 09	86.8	deg_C
ch: 10	86.4	deg_C

EXP 10--SCAN 05---09:02:09:06 19

ch: 01	89.3	deg_C
ch: 02	92.3	deg_C
ch: 03	92.6	deg_C
ch: 04	93.0	deg_C
ch: 05	92.0	deg_C
ch: 06	90.5	deg_C
ch: 07	89.6	deg_C
ch: 08	89.5	deg_C
ch: 09	87.6	deg_C
ch: 10	87.9	deg_C

EXP 10--SCAN 06---09:02:09:21 19

ch: 01	89.7	deg_C
ch: 02	93.1	deg_C
ch: 03	93.7	deg_C
ch: 04	94.4	deg_C
ch: 05	93.5	deg_C
ch: 06	91.9	deg_C
ch: 07	90.7	deg_C
ch: 08	90.4	deg_C
ch: 09	88.2	deg_C
ch: 10	88.6	deg_C

EXP 10--SCAN 07---09:02:09:36 19

ch: 01	90.1	deg_C
ch: 02	93.6	deg_C
ch: 03	94.5	deg_C
ch: 04	96.6	deg_C
ch: 05	94.7	deg_C
ch: 06	93.0	deg_C
ch: 07	91.5	deg_C
ch: 08	90.2	deg_C
ch: 09	88.1	deg_C
ch: 10	89.2	deg_C

EXP 10--SCAN 09---09:02:09:51:19

ch: 01	90.4	deg_C
ch: 02	94.1	deg_C
ch: 03	95.2	deg_C
ch: 04	96.6	deg_C
ch: 05	95.0	deg_C
ch: 06	94.0	deg_C
ch: 07	92.3	deg_C
ch: 08	91.0	deg_C
ch: 09	89.3	deg_C
ch: 10	90.4	deg_C

EXP 10--SCAN 09---09:02:10:06:19

ch: 01	90.6	deg_C
ch: 02	94.4	deg_C
ch: 03	95.7	deg_C
ch: 04	97.4	deg_C
ch: 05	96.9	deg_C
ch: 06	94.9	deg_C
ch: 07	93.0	deg_C
ch: 08	92.4	deg_C
ch: 09	89.7	deg_C
ch: 10	90.0	deg_C

EXP 10--SCAN 10---09:02:10:21:19

ch: 01	90.7	deg_C
ch: 02	94.6	deg_C
ch: 03	96.1	deg_C
ch: 04	98.1	deg_C
ch: 05	97.7	deg_C
ch: 06	95.7	deg_C
ch: 07	93.6	deg_C
ch: 08	92.9	deg_C
ch: 09	90.1	deg_C
ch 10	88.8	deg_C

EXP 10--SCAN 11---09:02:10:36:19

ch: 01	90.9	deg_C
ch: 02	94.8	deg_C
ch: 03	96.4	deg_C
ch: 04	99.6	deg_C
ch: 05	98.4	deg_C
ch: 06	96.4	deg_C
ch: 07	94.1	deg_C
ch: 08	93.3	deg_C
ch: 09	90.3	deg_C
ch: 10	88.6	deg_C

EXP 10--SCAN 12---09:02:10:51:19

ch: 01	91.0	deg_C
ch: 02	94.9	deg_C
ch: 03	96.6	deg_C
ch: 04	99.0	deg_C
ch: 05	98.9	deg_C
ch: 06	96.9	deg_C
ch: 07	94.5	deg_C
ch: 08	93.6	deg_C
ch: 09	90.6	deg_C
ch: 10	89.4	deg_C

EXP 10--SCAN 13---09:02:11:06:19

ch: 01	91.0	deg_C
ch: 02	94.9	deg_C
ch: 03	96.8	deg_C
ch: 04	99.2	deg_C
ch: 05	99.3	deg_C
ch: 06	97.4	deg_C
ch: 07	94.8	deg_C
ch 08	93.9	deg_C

EXP 10--SCAN 14---09:02:11:21:19

ch: 01	91.0	deg_C
ch: 02	94.9	deg_C
ch: 03	96.8	deg_C
ch: 04	99.4	deg_C
ch: 05	99.5	deg_C
ch: 06	97.7	deg_C
ch: 07	95.1	deg_C
ch: 08	94.1	deg_C
ch: 09	90.9	deg_C
ch: 10	90.1	deg_C

EXP 10--SCAN 15---09:02:11:36:19

ch: 01	91.0	deg_C
ch: 02	94.9	deg_C
ch: 03	96.8	deg_C
ch: 04	99.5	deg_C
ch: 05	99.7	deg_C
ch: 06	97.9	deg_C
ch: 07	95.3	deg_C
ch: 08	94.3	deg_C
ch: 09	91.0	deg_C
ch 10	90.1	deg_C

EXP 10--SCAN 16---09:02:11:51:19

ch: 01	91.0	deg_C
ch: 02	94.8	deg_C
ch: 03	96.8	deg_C
ch: 04	99.5	deg_C
ch: 05	99.8	deg_C
ch: 06	98.0	deg_C
ch: 07	95.4	deg_C
ch: 08	94.2	deg_C
ch: 09	91.1	deg_C
ch 10	90.6	deg_C

EXP 10--SCAN 17---09:02:12:06:19

ch: 01	90.9	deg_C
ch: 02	94.7	deg_C
ch: 03	96.7	deg_C
ch: 04	99.4	deg_C
ch: 05	99.9	deg_C
ch: 06	98.1	deg_C
ch: 07	95.4	deg_C
ch 08	94.4	deg_C
ch: 09	91.1	deg_C
ch: 10	87.3	deg_C

EXP 10--SCAN 18---09:02:12:21:19

ch: 01	90.8	deg_C
ch: 02	94.6	deg_C
ch: 03	96.5	deg_C
ch: 04	99.3	deg_C
ch: 05	99.7	deg_C
ch: 06	98.1	deg_C
ch: 07	95.4	deg_C
ch: 08	94.4	deg_C
ch: 09	91.1	deg_C
ch: 10	89.0	deg_C

EXP 10--SCAN 19---09:02:12:36:19

ch: 01	90.8	deg_C
ch: 02	94.5	deg_C
ch: 03	96.4	deg_C
ch: 04	99.1	deg_C
ch: 05	99.5	deg_C
ch: 06	98.0	deg_C
ch: 07	95.3	deg_C
ch: 08	94.3	deg_C
ch: 09	91.0	deg_C
ch: 10	89.5	deg_C

EXP 10--SCAN 20---09:02:12:51:19

ch: 01	90.7	deg_C
ch: 02	94.3	deg_C
ch: 03	96.2	deg_C
ch: 04	98.9	deg_C
ch: 05	99.3	deg_C
ch: 06	97.8	deg_C
ch: 07	95.2	deg_C
ch: 08	94.2	deg_C
ch: 09	91.0	deg_C
ch: 10	90.6	deg_C

EXP 10--SCAN 21---09:02:13:06:19

ch: 01	90.6	deg_C
ch: 02	94.2	deg_C
ch: 03	96.0	deg_C
ch: 04	98.7	deg_C
ch: 05	99.1	deg_C
ch: 06	97.6	deg_C
ch: 07	95.0	deg_C
ch: 08	94.1	deg_C
ch: 09	90.9	deg_C
ch: 10	88.2	deg_C

EXP 10--SCAN 22---09:02:13:21:19

ch: 01	90.5	deg_C
ch: 02	94.0	deg_C
ch: 03	95.8	deg_C
ch: 04	98.4	deg_C
ch: 05	98.8	deg_C
ch: 06	97.4	deg_C
ch: 07	94.9	deg_C
ch: 08	93.9	deg_C
ch: 09	90.7	deg_C
ch: 10	87.4	deg_C

EXP 10--SCAN 23---09:02:13:36:19

ch: 01	90.4	deg_C
ch: 02	93.8	deg_C
ch: 03	95.5	deg_C
ch: 04	98.1	deg_C
ch: 05	98.5	deg_C
ch: 06	97.1	deg_C
ch: 07	94.6	deg_C
ch: 08	93.7	deg_C
ch: 09	90.6	deg_C
ch: 10	89.1	deg_C

EXP 10--SCAN 24---09:02:13:51:19

ch: 01	90.3	deg_C
ch: 02	93.6	deg_C
ch: 03	95.3	deg_C
ch: 04	97.8	deg_C
ch: 05	98.2	deg_C
ch: 06	96.9	deg_C
ch: 07	94.4	deg_C
ch: 08	93.5	deg_C
ch: 09	90.4	deg_C
ch: 10	89.8	deg_C

EXP 10--SCAN 01---09:02:14:07:24

ch: 01	90.2	deg_C
ch: 02	93.4	deg_C
ch: 03	95.0	deg_C
ch: 04	97.5	deg_C
ch: 05	98.0	deg_C
ch: 06	96.6	deg_C
ch: 07	94.1	deg_C
ch: 08	93.2	deg_C
ch: 09	90.2	deg_C
ch: 10	90.3	deg_C

EXP 10--SCAN 02---09:02:14:07:46

ch: 01	90.2	deg_C
ch: 02	93.4	deg_C
ch: 03	95.0	deg_C
ch: 04	97.5	deg_C
ch: 05	97.8	deg_C
ch: 06	96.5	deg_C
ch: 07	94.1	deg_C
ch: 08	93.2	deg_C
ch: 09	90.3	deg_C
ch: 10	88.5	deg_C

EXP 10--SCAN 03---09:02:15:07:24

ch: 01	89.7	deg_C
ch: 02	92.7	deg_C
ch: 03	94.0	deg_C
ch: 04	96.2	deg_C
ch: 05	96.5	deg_C
ch: 06	95.2	deg_C
ch: 07	93.1	deg_C
ch: 08	92.3	deg_C
ch: 09	89.6	deg_C
ch: 10	88.0	deg_C

EXP 10--SCAN 04---09:02:16:07:24

ch: 01	89.2	deg_C
ch: 02	92.0	deg_C
ch: 03	93.1	deg_C
ch: 04	95.0	deg_C
ch: 05	95.1	deg_C
ch: 06	93.9	deg_C
ch: 07	92.0	deg_C
ch: 08	91.4	deg_C
ch: 09	88.9	deg_C
ch: 10	87.7	deg_C

EXP 10--SCAN 05---09:02:17:07:24

ch: 01	88.8	deg_C
ch: 02	91.3	deg_C
ch: 03	92.2	deg_C
ch: 04	93.9	deg_C
ch: 05	93.9	deg_C
ch: 06	92.8	deg_C
ch: 07	91.1	deg_C
ch: 08	90.6	deg_C
ch: 09	88.4	deg_C
ch: 10	89.9	deg_C

EXP 10--SCAN 06---09:02:18:07:24

ch: 01	88.4	deg_C
ch: 02	90.9	deg_C
ch: 03	91.5	deg_C
ch: 04	93.0	deg_C
ch: 05	92.9	deg_C
ch: 06	91.9	deg_C
ch: 07	90.4	deg_C
ch: 08	90.0	deg_C
ch: 09	87.9	deg_C
ch: 10	90.4	deg_C

EXP 10--SCAN 07---09:02:19:07:24

ch: 01	88.1	deg_C
ch: 02	90.2	deg_C
ch: 03	90.9	deg_C
ch: 04	92.2	deg_C
ch: 05	92.1	deg_C
ch: 06	91.1	deg_C
ch: 07	89.8	deg_C
ch: 08	89.4	deg_C
ch: 09	87.5	deg_C
ch: 10	89.1	deg_C

EXP 10--SCAN 08---09:02:20:07:24

ch: 01	87.2	deg_C
ch: 02	89.9	deg_C
ch: 03	90.4	deg_C
ch: 04	91.5	deg_C
ch: 05	91.4	deg_C
ch: 06	90.5	deg_C
ch: 07	89.2	deg_C
ch: 08	88.9	deg_C
ch: 09	87.2	deg_C
ch: 10	87.5	deg_C

EXP 10--SCAN 09---09:02:21:07:24

ch: 01	87.6	deg_C
ch: 02	89.5	deg_C
ch: 03	89.9	deg_C
ch: 04	91.1	deg_C
ch: 05	89.9	deg_C
ch: 06	89.9	deg_C
ch: 07	88.8	deg_C
ch: 08	88.6	deg_C
ch: 09	85.9	deg_C
ch: 10	86.6	deg_C

EXP 10--SCAN 10---09:02:22:07:24

ch: 01	87.4	deg_C
ch: 02	89.2	deg_C
ch: 03	89.5	deg_C
ch: 04	90.6	deg_C
ch: 05	90.4	deg_C
ch: 06	89.5	deg_C
ch: 07	88.5	deg_C
ch: 08	88.3	deg_C
ch: 09	86.7	deg_C
ch: 10	90.0	deg_C

EXP 10--SCAN 11---09:02:27:07:24

ch: 01	87.2	deg_C
ch: 02	89.0	deg_C
ch: 03	89.2	deg_C
ch: 04	90.3	deg_C
ch: 05	90.0	deg_C
ch: 06	89.2	deg_C
ch: 07	88.2	deg_C
ch: 08	88.1	deg_C
ch: 09	86.5	deg_C
ch: 10	88.2	deg_C

EXP 10--SCAN 12---10:02:00:07:24

ch: 01	87.1	deg_C
ch: 02	88.8	deg_C
ch: 03	89.0	deg_C
ch: 04	90.0	deg_C
ch: 05	89.7	deg_C
ch: 06	88.9	deg_C
ch: 07	88.0	deg_C
ch: 08	87.9	deg_C
ch: 09	86.4	deg_C
ch: 10	88.9	deg_C

EXP 10--SCAN 13---10:02:01:07:24

ch: 01	87.0	deg_C
ch: 02	88.6	deg_C
ch: 03	88.9	deg_C
ch: 04	89.8	deg_C
ch: 05	89.5	deg_C
ch: 06	88.7	deg_C
ch: 07	87.9	deg_C
ch: 08	87.7	deg_C
ch: 09	86.3	deg_C
ch: 10	88.9	deg_C

EXP 10--SCAN 14---10:02:02:07:24

ch: 01	86.9	deg_C
ch: 02	88.4	deg_C
ch: 03	89.6	deg_C
ch: 04	89.5	deg_C
ch: 05	89.2	deg_C
ch: 06	88.5	deg_C
ch: 07	87.7	deg_C
ch: 08	87.6	deg_C
ch: 09	86.2	deg_C
ch: 10	90.5	deg_C

EXP 10--SCAN 15---10:02:03:07:24

ch: 01	86.8	deg_C
ch: 02	88.3	deg_C
ch: 03	89.5	deg_C
ch: 04	89.4	deg_C
ch: 05	89.1	deg_C
ch: 06	88.3	deg_C
ch: 07	87.5	deg_C
ch: 08	87.4	deg_C
ch: 09	86.1	deg_C
ch: 10	87.1	deg_C

EXP 10--SCAN 16---10:02:04:07:24

ch: 01	86.7	deg_C
ch: 02	88.2	deg_C
ch: 03	88.3	deg_C
ch: 04	89.2	deg_C
ch: 05	88.9	deg_C
ch: 06	88.1	deg_C
ch: 07	87.4	deg_C
ch: 08	87.3	deg_C
ch: 09	86.9	deg_C
ch: 10	89.7	deg_C

EXP 10--SCAN 17---10:02:05:07:24

ch: 01	86.6	deg_C
ch: 02	88.1	deg_C
ch: 03	88.2	deg_C
ch: 04	88.1	deg_C
ch: 05	88.0	deg_C
ch: 06	87.3	deg_C
ch: 07	87.2	deg_C
ch: 08	86.9	deg_C
ch: 09	86.4	deg_C
ch: 10		

EXP 10--SCAN 18---10:02:06:07:24

ch: 01	86.6	deg_C
ch: 02	88.0	deg_C
ch: 03	88.1	deg_C
ch: 04	89.0	deg_C
ch: 05	88.6	deg_C
ch: 06	87.9	deg_C
ch: 07	87.2	deg_C
ch: 08	87.2	deg_C
ch: 09	85.9	deg_C
ch: 10	88.3	deg_C

EXP 10--SCAN 19---10:02:07:07:24

ch: 01	86.5	deg_C
ch: 02	87.9	deg_C
ch: 03	89.0	deg_C
ch: 04	88.8	deg_C
ch: 05	88.5	deg_C
ch: 06	87.8	deg_C
ch: 07	87.1	deg_C
ch: 08	87.1	deg_C
ch: 09	85.8	deg_C
ch: 10	90.9	deg_C

EXP 10--SCAN 20---10:02:08:07:24

ch: 01	86.5	deg_C
ch: 02	87.9	deg_C
ch: 03	87.9	deg_C
ch: 04	88.7	deg_C
ch: 05	88.4	deg_C
ch: 06	87.7	deg_C
ch: 07	87.0	deg_C
ch: 08	87.0	deg_C
ch: 09	85.7	deg_C
ch: 10	88.7	deg_C

EXP 10--SCAN 21---10:02:09:07:24

ch: 01	86.4	deg_C
ch: 02	87.8	deg_C
ch: 03	87.9	deg_C
ch: 04	88.7	deg_C
ch: 05	88.3	deg_C
ch: 06	87.5	deg_C
ch: 07	87.0	deg_C
ch: 08	87.0	deg_C
ch: 09	85.7	deg_C
ch: 10	90.3	deg_C

EXP 10--SCAN 22---10:02:10:07:24

ch: 01	86.4	deg_C
ch: 02	87.8	deg_C
ch: 03	87.8	deg_C
ch: 04	88.6	deg_C
ch: 05	88.7	deg_C
ch: 06	87.5	deg_C
ch: 07	86.9	deg_C
ch: 08	86.9	deg_C
ch: 09	85.7	deg_C
ch: 10	87.7	deg_C

EXP 10--SCAN 23---10:02:11:07:24

ch: 01	86.4	deg_C
ch: 02	87.9	deg_C
ch: 03	87.9	deg_C
ch: 04	88.6	deg_C
ch: 05	88.7	deg_C
ch: 06	87.6	deg_C
ch: 07	86.9	deg_C
ch: 08	86.9	deg_C
ch: 09	85.7	deg_C
ch: 10	90.5	deg_C

EXP 10--SCAN 24---10:02:12:07:24

ch: 01	86.4	deg_C
ch: 02	87.8	deg_C
ch: 03	87.8	deg_C
ch: 04	88.6	deg_C
ch: 05	88.2	deg_C
ch: 06	87.6	deg_C
ch: 07	87.0	deg_C
ch: 08	87.0	deg_C
ch: 09	85.9	deg_C
ch: 10	87.6	deg_C

EXP 10--SCAN 25---10:02:13:07:24

ch: 01	86.5	deg_C
ch: 02	87.9	deg_C
ch: 03	87.8	deg_C
ch: 04	88.6	deg_C
ch: 05	88.2	deg_C
ch: 06	87.6	deg_C
ch: 07	86.9	deg_C
ch: 08	87.0	deg_C
ch: 09	85.8	deg_C
ch: 10	90.4	deg_C

A10.5 Ageing run 3

The results of this run have not been analyzed. The run conditions were as follows:

Coal particle size range	: - 3.4 + 1.19 mm
Oven temperature	: 180°C
Oxygen flowrate	: 1.42 x 10^{-5} kmol/m^2/s

EXP 10----------20:01 13:53:45

ch: 01	178.4	deg_C
ch: 02	178.2	deg_C
ch: 03	177.1	deg_C
ch: 04	175.5	deg_C
ch: 05	174.2	deg_C
ch: 06	173.5	deg_C
ch: 07	174.7	deg_C
ch: 08	175.2	deg_C
ch: 09	175.2	deg_C
ch: 10	174.8	deg_C

EXP 10--SCAN 01---20:01 13:55:24

ch: 01	178.5	deg_C
ch: 02	178.2	deg_C
ch: 03	177.2	deg_C
ch: 04	175.5	deg_C
ch: 05	174.3	deg_C
ch: 06	173.5	deg_C
ch: 07	174.8	deg_C
ch: 08	175.2	deg_C
ch: 09	175.2	deg_C
ch: 10	175.3	deg_C

EXP 10--SCAN 02---20:01 13:55:58

ch: 01	178.5	deg_C
ch: 02	178.2	deg_C
ch: 03	177.2	deg_C
ch: 04	175.5	deg_C
ch: 05	174.3	deg_C
ch: 06	173.5	deg_C
ch: 07	174.8	deg_C
ch: 08	175.2	deg_C
ch: 09	175.2	deg_C
ch: 10	174.6	deg_C

EXP 10--SCAN 03---20:01 14:10:34

ch: 01	179.3	deg_C
ch: 02	179.1	deg_C
ch: 03	178.0	deg_C
ch: 04	176.1	deg_C
ch: 05	174.9	deg_C
ch: 06	174.0	deg_C
ch: 07	175.3	deg_C
ch: 08	175.7	deg_C
ch: 09	175.4	deg_C
ch: 10	174.2	deg_C

EXP 10--SCAN 04---20:01 14:25:34

ch: 01	185.1	deg_C
ch: 02	185.6	deg_C
ch: 03	183.5	deg_C
ch: 04	179.8	deg_C
ch: 05	177.2	deg_C
ch: 06	175.6	deg_C
ch: 07	176.4	deg_C
ch: 08	176.4	deg_C
ch: 09	175.8	deg_C
ch: 10	174.5	deg_C

EXP 10--SCAN 05---20:01 14:40 34

ch: 01	190.9	deg_C
ch: 02	193.0	deg_C
ch: 03	190.4	deg_C
ch: 04	184.5	deg_C
ch: 05	180.3	deg_C
ch: 06	177.6	deg_C
ch: 07	178.0	deg_C
ch: 08	177.4	deg_C
ch: 09	176.4	deg_C
ch: 10	174.7	deg_C

EXP 10--SCAN 06---20:01 14 55 34

ch: 01	195.8	deg_C
ch: 02	198.4	deg_C
ch: 03	196.7	deg_C
ch: 04	188.8	deg_C
ch: 05	183.2	deg_C
ch: 06	179.6	deg_C
ch: 07	179.5	deg_C
ch: 08	178.4	deg_C
ch: 09	176.9	deg_C
ch: 10	173.1	deg_C

EXP 10--SCAN 07---20:01 15:10 34

ch: 01	199.6	deg_C
ch: 02	204.5	deg_C
ch: 03	202.0	deg_C
ch: 04	192.5	deg_C
ch: 05	185.6	deg_C
ch: 06	181.2	deg_C
ch: 07	180.7	deg_C
ch: 08	179.1	deg_C
ch: 09	177.4	deg_C
ch: 10	174.1	deg_C

EXP 10--SCAN 00---20:01:15:25:34

ch: 01	202.7	deg_C
ch: 02	208.7	deg_C
ch: 03	206.5	deg_C
ch: 04	195.6	deg_C
ch: 05	187.5	deg_C
ch: 06	182.6	deg_C
ch: 07	181.7	deg_C
ch: 08	179.7	deg_C
ch: 09	177.8	deg_C
ch: 10	173.8	deg_C

EXP 10--SCAN 09---20:01:15:40:3

ch: 01	205.2	deg_C
ch: 02	212.1	deg_C
ch: 03	210.1	deg_C
ch: 04	198.2	deg_C
ch: 05	189.1	deg_C
ch: 06	183.7	deg_C
ch: 07	182.5	deg_C
ch: 08	180.2	deg_C
ch: 09	178.2	deg_C
ch: 10	173.5	deg_C

EXP 10--SCAN 10---20:01:15:55:3

ch: 01	207.2	deg_C
ch: 02	214.7	deg_C
ch: 03	213.0	deg_C
ch: 04	200.4	deg_C
ch: 05	190.4	deg_C
ch: 06	184.5	deg_C
ch: 07	183.1	deg_C
ch: 08	180.6	deg_C
ch: 09	178.5	deg_C
ch: 10	172.9	deg_C

EXP 10--SCAN 01---20:01:16:10:0

ch: 01	208.7	deg_C
ch: 02	216.8	deg_C
ch: 03	215.4	deg_C
ch: 04	202.2	deg_C
ch: 05	191.4	deg_C
ch: 06	185.1	deg_C
ch: 07	183.5	deg_C
ch: 08	180.8	deg_C
ch: 09	178.6	deg_C
ch: 10	173.6	deg_C

EXP 10--SCAN 02---20:01:17:10:02

ch: 01	212.1	deg_C
ch: 02	221.5	deg_C
ch: 03	221.3	deg_C
ch: 04	207.2	deg_C
ch: 05	194.3	deg_C
ch: 06	186.5	deg_C
ch: 07	184.0	deg_C
ch: 08	180.9	deg_C
ch: 09	178.8	deg_C
ch: 10	173.9	deg_C

EXP 10--SCAN 03---20:01:18:10:02

ch: 01	212.9	deg_C
ch: 02	222.8	deg_C
ch: 03	223.6	deg_C
ch: 04	210.0	deg_C
ch: 05	196.0	deg_C
ch: 06	187.2	deg_C
ch: 07	184.0	deg_C
ch: 08	180.8	deg_C
ch: 09	178.7	deg_C
ch: 10	174.8	deg_C

EXP 10--SCAN 04---20:01:19:10:02

ch: 01	212.5	deg_C
ch: 02	222.6	deg_C
ch: 03	224.3	deg_C
ch: 04	211.7	deg_C
ch: 05	197.3	deg_C
ch: 06	187.8	deg_C
ch: 07	184.3	deg_C
ch: 08	180.8	deg_C
ch: 09	178.7	deg_C
ch: 10	175.2	deg_C

EXP 10--SCAN 05---20:01:20:10:02

ch: 01	211.7	deg_C
ch: 02	221.7	deg_C
ch: 03	224.2	deg_C
ch: 04	212.9	deg_C
ch: 05	198.4	deg_C
ch: 06	188.5	deg_C
ch: 07	184.6	deg_C
ch: 08	181.0	deg_C
ch: 09	178.8	deg_C
ch: 10	173.8	deg_C

EXP 10--SCAN 06---20:01:21:10:02

ch: 01	210.7	deg_C
ch: 02	220.6	deg_C
ch: 03	223.6	deg_C
ch: 04	213.5	deg_C
ch: 05	199.3	deg_C
ch: 06	189.2	deg_C
ch: 07	185.1	deg_C
ch: 08	181.2	deg_C
ch: 09	179.0	deg_C
ch: 10	173.4	deg_C

EXP 10--SCAN 07---20:01:22:10:02

ch: 01	209.7	deg_C
ch: 02	219.4	deg_C
ch: 03	222.9	deg_C
ch: 04	214.0	deg_C
ch: 05	200.3	deg_C
ch: 06	189.9	deg_C
ch: 07	185.6	deg_C
ch: 08	181.5	deg_C
ch: 09	179.2	deg_C
ch: 10	173.7	deg_C

EXP 10--SCAN 08---20:01:23:10:02

ch: 01	208.7	deg_C
ch: 02	218.2	deg_C
ch: 03	222.2	deg_C
ch: 04	214.4	deg_C
ch: 05	201.1	deg_C
ch: 06	190.6	deg_C
ch: 07	186.1	deg_C
ch: 08	181.8	deg_C
ch: 09	179.4	deg_C
ch: 10	175.6	deg_C

EXP 10--SCAN 09---21:01:00:10:02

ch: 01	207.9	deg_C
ch: 02	217.1	deg_C
ch: 03	221.3	deg_C
ch: 04	214.7	deg_C
ch: 05	201.9	deg_C
ch: 06	191.3	deg_C
ch: 07	186.6	deg_C
ch: 08	182.1	deg_C
ch: 09	179.6	deg_C
ch: 10	174.5	deg_C

EXP 10--SCAN 10---21:01:01:10:02

ch: 01	206.9	deg_C
ch: 02	216.9	deg_C
ch: 03	220.4	deg_C
ch: 04	214.8	deg_C
ch: 05	202.6	deg_C
ch: 06	191.9	deg_C
ch: 07	187.1	deg_C
ch: 08	182.4	deg_C
ch: 09	179.7	deg_C
ch: 10	174.8	deg_C

EXP 10--SCAN 11---21:01:02:10:02

ch: 01	206.1	deg_C
ch: 02	215.0	deg_C
ch: 03	219.6	deg_C
ch: 04	214.9	deg_C
ch: 05	203.2	deg_C
ch: 06	192.5	deg_C
ch: 07	187.5	deg_C
ch: 08	182.7	deg_C
ch: 09	179.9	deg_C
ch: 10	174.8	deg_C

EXP 10--SCAN 12---21:01:03:10:02

ch: 01	205.2	deg_C
ch: 02	214.0	deg_C
ch: 03	218.?	deg_C
ch: 04	214.8	deg_C
ch: 05	203.7	deg_C
ch: 06	193.1	deg_C
ch: 07	188.0	deg_C
ch: 08	182.9	deg_C
ch: 09	180.0	deg_C
ch: 10	174.2	deg_C

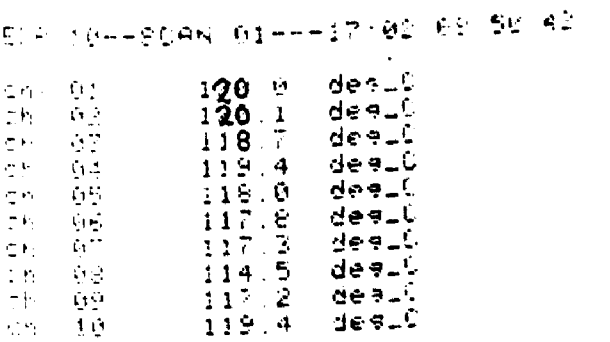
EXP 10--SCAN 13---21:01:04:10:02

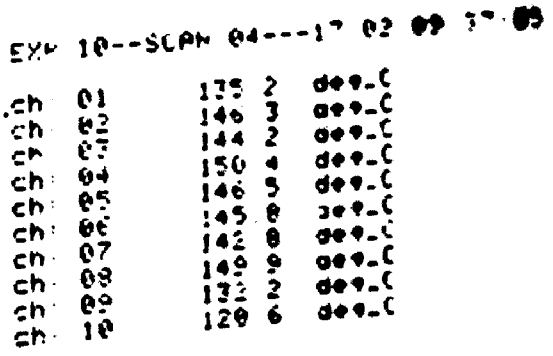
ch: 01	204.4	deg_C
ch: 02	213.0	deg_C
ch: 03	217.8	deg_C
ch: 04	214.?	deg_C
ch: 05	204.2	deg_C
ch: 06	193.5	deg_C
ch: 07	188.4	deg_C
ch: 08	183.1	deg_C
ch: 09	180.1	deg_C
ch: 10	173.6	deg_C

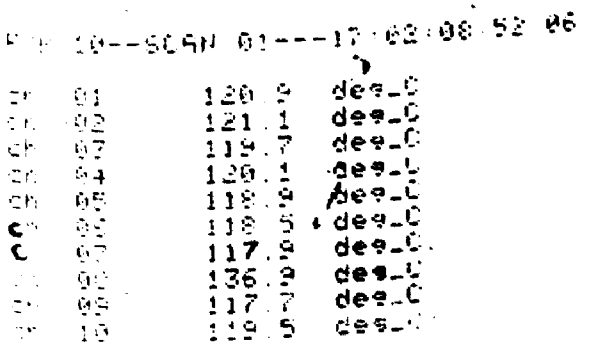
A10.6 Ignition run 1

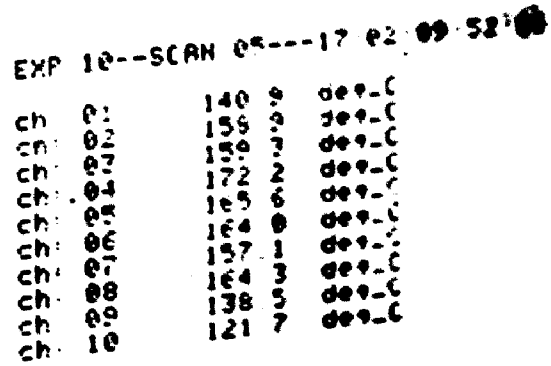
The results from this run were used in figure 7.4. The experimental conditions and model parameters used were as follows:

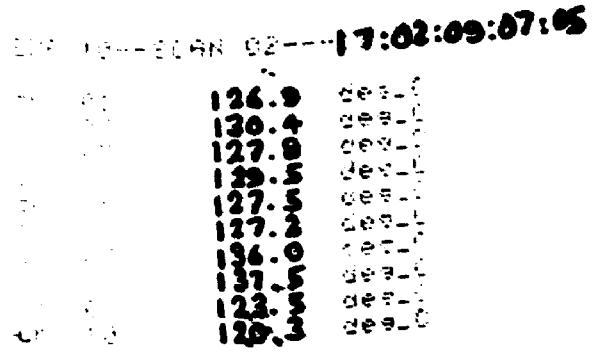
Coal particle size range	: -1.19 mm
Oven temperature	: 120 ^{o}C
Oxygen flowrate	: 4.33 x 10^{-5} kmol/m^2/s
C	: 23
Bi_o	: 3.7
Bi_1	: 9.3
Bed voidage	: 0.38
K_o	: 4.84 m/s
E/R	: 7000 K
$D_e \rho_m$	: 1.42 x 10^{-13}
D_p	: 0.5 mm

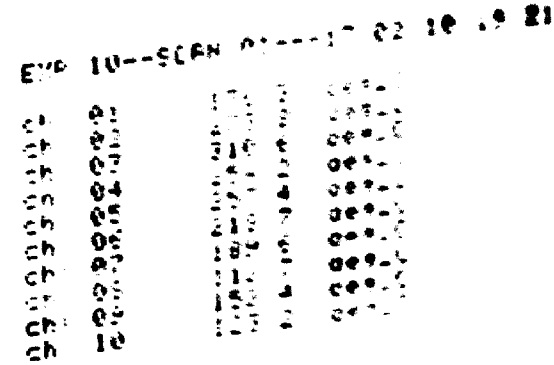

EXP 10--SCAN 01---17 02 09 52 42
CH 01 120.9 deg_C
CH 02 120.1 deg_C
CH 03 118.7 deg_C
CH 04 119.4 deg_C
CH 05 118.0 deg_C
CH 06 117.8 deg_C
CH 07 117.3 deg_C
CH 08 114.5 deg_C
CH 09 117.2 deg_C
CH 10 119.4 deg_C

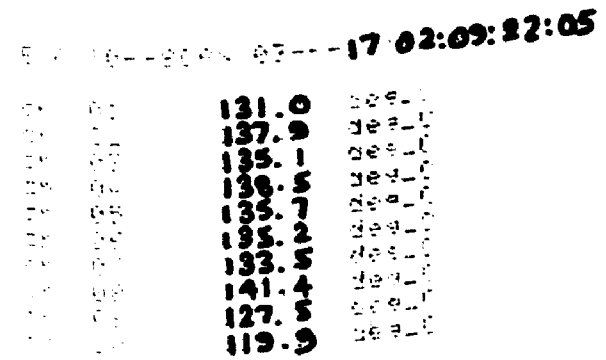

EXP 10--SCAN 04---17 02 09 1? 05
CH 01 175.2 deg_C
CH 02 146.3 deg_C
CH 03 144.2 deg_C
CH 04 150.4 deg_C
CH 05 146.5 deg_C
CH 06 145.8 deg_C
CH 07 142.8 deg_C
CH 08 140.9 deg_C
CH 09 132.2 deg_C
CH 10 120.6 deg_C

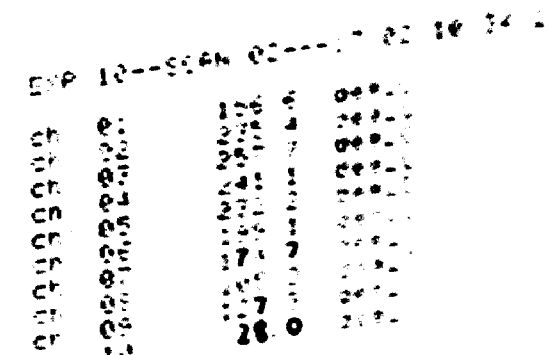

EXP 10--SCAN 01---17 02 09 52 06
CH 01 120.9 deg_C
CH 02 121.1 deg_C
CH 03 119.7 deg_C
CH 04 120.1 deg_C
CH 05 119.9 deg_C
CH 06 118.5 deg_C
CH 07 117.9 deg_C
CH 08 136.9 deg_C
CH 09 117.7 deg_C
CH 10 119.5 deg_C


EXP 10--SCAN 05---17 02 09 52 08
CH 01 140.9 deg_C
CH 02 155.9 deg_C
CH 03 159.7 deg_C
CH 04 172.2 deg_C
CH 05 165.6 deg_C
CH 06 164.0 deg_C
CH 07 157.1 deg_C
CH 08 164.3 deg_C
CH 09 138.5 deg_C
CH 10 121.7 deg_C


EXP 10--SCAN 02---17:02:09:07:05
126.9 deg_C
130.4 deg_C
127.8 deg_C
129.5 deg_C
127.5 deg_C
127.4 deg_C
136.0 deg_C
137.5 deg_C
122.3 deg_C
120.3 deg_C


EXP 10--SCAN 01---17 02 10 09 21


EXP 10--SCAN 07---17:02:09:22:05
131.0 deg_C
137.9 deg_C
135.1 deg_C
136.5 deg_C
135.7 deg_C
135.2 deg_C
133.5 deg_C
141.4 deg_C
127.5 deg_C
119.9 deg_C


EXP 10--SCAN 01---17 02 10 14 ??
26.0

A10.7 Ignition run 2

The results from this run were used in figure 7.4. The experimental conditions and model parameters used were as follows:

Coal particle size range	: -1.19 mm
Oven temeprature	: 100 ^{o}C
Oxygen flowrate	: 4.33 x 10^{-5} kmol/m^2/s
C	: 23
Bi_o	: 3.7
Bi_1	: 9.3
Bed voidage	: 0.38
k_o	: 4.9 m/s
E/R	: 7000 K
$D_e\rho_m$	: 1.42 x 10^{-13}
D_p	: 0.5 mm

25 02 10:15:50

ch:	01	deg_C
ch:	02	deg_C
ch:	03	deg_C
ch:	04	deg_C
ch:	05	deg_C
ch:	06	deg_C
ch:	07	deg_C
ch:	08	deg_C
ch:	09	deg_C
ch:	10	deg_C

EXP 05--SCAN 06---25 02 10 45 50

ch:	01	deg_C
ch:	02	deg_C
ch:	03	deg_C
ch:	04	deg_C
ch:	05	deg_C
ch:	06	deg_C
ch:	07	deg_C
ch:	08	deg_C
ch:	09	deg_C
ch:	10	

EXP 05--SCAN 07---25 02 11 15 50

ch:	01	deg_C
ch:	02	deg_C
ch:	03	deg_C
ch:	04	deg_C
ch:	05	deg_C
ch:	06	deg_C
ch:	07	deg_C
ch:	08	deg_C
ch:	09	deg_C
ch:	10	

EXP 05--SCAN 08---25 02 11 45 50

ch:	01	deg_C
ch:	02	deg_C
ch:	03	deg_C
ch:	04	deg_C
ch:	05	deg_C
ch:	06	deg_C
ch:	07	deg_C
ch:	08	deg_C
ch:	09	deg_C
ch:	10	

EXP 05--SCAN 09---25 02 12 15 50

ch:	01	deg_C
ch:	02	deg_C
ch:	03	deg_C
ch:	04	deg_C
ch:	05	deg_C
ch:	06	deg_C
ch:	07	deg_C
ch:	08	deg_C
ch:	09	deg_C
ch:	10	

APPENDIX 11 **MODEL PARAMETERS USED AS 'BASE CASE'**

The following model parameters have been used as the base-case:

k_o = 10 m/s

E_a/R = 7000 K

ϵ = .3

ΔH_r = 3 x 10^8 J/kmol

k_b = 0.2 W/m/K

$\hat{c}$ = 3 x 10^4 J/kmol/K

ρ_b = 900 kg/m^3

C_b = 1000 J/kg/K

P = 1.013 x 10^5 Pa

y_o = .21

L = 5 m

$h_1 = \sigma\,(T_\infty+T_o)(T_\infty^2+T_o^2)$

$h_2 = \sigma\,(T_\infty+T_e)(T_\infty^2+T_e^2)$

C = 0

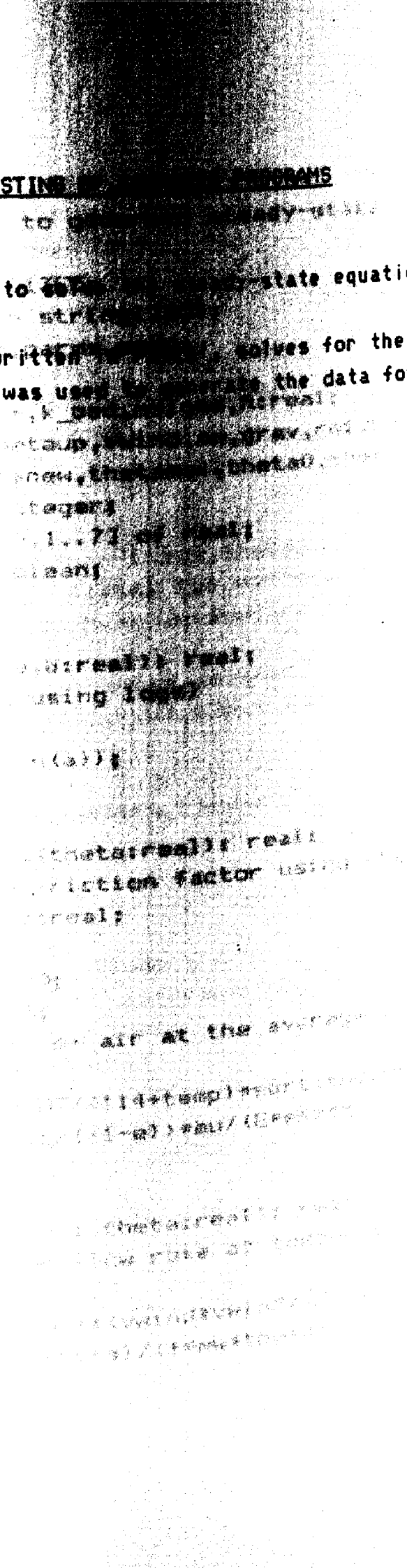
V = 0

APPENDIX 12 **LISTING**

A12.1 Program to

This program, written

solutions. It was used



```
program coal;
{Pascal program to generate steady-state stable solutions}

const pres = 1.013E5;
type string255 = string[255];
label startloop,parms,endp;
var
g,DelH,L,YO,Tinf,k_bed,msigma,R:real;
tad,thetalow,thetaup,vwind,mw,grav,roi,Eor,E,k0,S,dp,cp:real;
diff,theta,thetanew,thetamax,theta0,theta1,lhs,rhs:real;
imax,imin,i,j:integer;
tem:array[-1..10,1..7] of real;
ok,increased:boolean;
ch:char;

function power(a,b:real): real;
{calculates a^b using logs}
begin
  power:=exp(b*ln(a));
end;

function fricfac(theta:real): real;
{calculates the friction factor using the Ergun equation}
var mu,thet,temp:real;
begin
  temp:=theta*300;
  thet:=temp/273;
  {the viscosity of air at the average temperature}
  {Perry 3rd ed}
  mu:=1.709e-5*387/(114+temp)*sqrt(thet*thet*thet);
  FricFac:=180*sqr((1-e))*mu/(E*e*e*sqr(dp));
end;

function flowrate(f,theta:real): real;
{calculates molar flow rate at temperature theta}
begin
 flowrate:=sqr(roi)*(vwind*vwind/(2*1)+
 grav*(theta-1)/theta)/(f*mw*theta);
end;
```

```
procedure printparms;
{Prints the parameters with a heading}
var heading:string255;
begin
write('Heading for this run ? ');readln(heading);
writeln(lst,heading);
writeln(lst,'Voidage: ',e:4:1,' k0: ',k0:6:1,' E/R: ',eor*tinf:6:0);
writeln(lst,'Wind speed: ',vwind:4:1,' k_bed: ',k_bed*1000:4:1,
' Bed length: ',l:2:0);
writeln(lst);
end;

procedure calcall(var theta,thetabar,difference:real;flag:boolean);
{This routine calculates the difference between the LHS and}
{RHS of the equation at an average temperature theta}
label 330;
var expc,w,heat,deltheta0,deltheta1,Bi0,Bi1,f,p,
theta0n,theta1n,a2,a,c,a1,c2p,t,expma2,expa,c2a,c2,c1overam:real;
begin

  {Set up the parameters required}

  theta0:=theta;
  theta1:=theta;
  f:=fricfac(theta);
  p:=sqr(roi)*grav/(f*mw);
  w:=k0*6*(1-e)*l*f/(dp*grav*roi);
  heat:=msigma/(p*cp*mw);
  g:=flowrate(f,theta);
  a2:=w*theta*exp(-eor/theta)/(theta-1);
  a:=g*cp*l*mw/(k_bed);
  c:=delh*g*l/(tinf*k_bed);
  a1:=c*y0/(a2+a);
  if a2>80 then expma2:=0 else expma2:=exp(-a2);
  if abs(a)>80 then expa:=0 else expa:=exp(a);

  {Jump back here if the end temperatures don't converge}

330:  bi0:=msigma*((theta0)+1)*(sqr(theta0)+1)*l/k_bed;
  bi1:=msigma*((theta1)+1)*(sqr(theta1)+1)*l/k_bed;
```

```
c2a:=-a1*a2*exp                    (bi0+a)+a1*(1-expma2));
if a>80 then c2
c2:=c2a/(a*expa-                   +expa*bi1);
cloveram:=a1*a2/                   )*a1-c2+1;
if a>80 then c2p                   else c2p:=c2*expa;
theta0n:=clover
theta1n:=clover
t:=sqr(theta-1);
deltheta0:=abs(t
deltheta1:=abs(

{Check for conver                  temperatures}

if (1.e5/t*(sqr(                   sqr(deltheta1)))>1 then begin
  theta0:=(theta0n
  theta1:=(theta1n
  goto 330;
end;

{Calculate the LHS                 the energy balance}

lhs:=bi0*(theta0n-                 theta1n-1)/a+theta1n-1;
if a2>80 then rhs
rhs:=tad*(1-exp(-                  theta-1)*exp(-eor/theta)));

{Write answers on screen as a check for the operator}

writeln('Mean temperature guessed: ',theta*tinf:6:2);
thetabar:=cloveram*a2/a2*(expma2-1)+c2p/a-c2/a;
writeln('Mean temperature calculated ',thetabar*tinf:6:2);
difference:=lhs-rhs;
if ((a*a2/(a+a2))>80) then expc:=0 else expc:=exp(-a*a2/(a2+a));
thetamax:=cloveram*power((c*y0/a),(a/(a+a2)))*
          power((-c2p*(1+a/a2)),(a2/(a2+a)))*expc;
writeln('Flowrate ',g);
writeln('Inlet & outlet temps ',theta0n*tinf:6:2,' ',theta1n*tinf:6:

writeln('LHS ',lhs,' RHS  ',rhs);
writeln('Difference ',difference);
writeln('Maximum temperature  ',thetamax*tinf:6:2);
writeln;
end;
```

```
procedure PrintAnswers;
begin
  writeln(lst,'Mean temperature ',thetanew*tinf:6:2,
  '  Flowrate ',g);
  writeln(lst,'Inlet & outlet temps ',theta0*tinf:6:2,
  ' ',theta1*tinf:6:2);
  writeln(lst,'LHS ',lhs,' RHS ',rhs);
  writeln(lst,'Difference ',lhs-rhs);
  writeln(lst,'Maximum temperature ',thetamax*tinf:6:2);
  writeln(lst);
end;

{**** MAIN PROGRAM *****}
begin
  parms:
  {Parameters for the model}
  Tinf:=300;          {Ambient temperature}
  delh:=3.e5;         {Delta H reaction in kJ/kmol}
  mw:=30.;            {Molecular weight}
  l:=5;               {Bed length in metres}
  y0:=0.21;           {Mole fraction of oxygen in air}
  k_bed:=0.2e-3;      {Thermal conductivity in kW/m/K}
  Eor:=7000./tinf;    {Activation energy divided by (R T_ambient)}
  E:=0.3;             {Bed voidage}
  k0:=10.0;           {Surface rate constant in m/s}
  cp:=1.;             {Gas specific heat in kJ/kgK}
  roi:=1.2;           {density of ambient air in kg/m^3}
  {modified Stefan-Boltzmann constant}
  msigma:=5.67e-11*tinf*tinf*tinf;
  grav:=9.81;         {acceleration due to gravity}
  vwind:=0.1;         {wind velocity in m/s}
  R:=8.314e3;         {gas constant in kJ/kmol/K}
  gotoxy(1,1);
  writeLN('Do you want to print a heading ? ');read(kbd,ch);
  if upcase(ch)='Y'then printparms;      {Print the parameters}
  {Adiabatic dimensionless temperature rise}
  tad:=delh*y0/(cp*tinf*mw);
  write('Minimum loop counter ? ');readln(imin);
  write('Maximum loop counter ? ');readln(imax);
  if imin=imax then begin
     write('Particle size in mm ? ');readln(dp);
     dp:=dp/1000;
  end;

                                    answers are stored}
                                    i,j]:=0;
```

```
for j:=1 to 2 do begin

{if j=1 then calculations done on the upper branch
 if j=2 then calculations done on the lower branch}

theta:=3.0;if j=2 then theta:=1.01;  {initial guesses}
increased:=false;
for i:=imax downto imin do begin;
 if imin<>imax then begin
    dp:=i*2;
    if i=0 then dp:=0.4;
    if i=-1 then dp:=0.5;
    dp:=dp/1000;
 end;
 startloop:
 ClrScr;
 tem[i,4]:=dp;
 writeln('Particle size ',dp*1000:4:2);writeln;
 thetanew:=0;
 while (sqr(abs(theta-thetanew))>1.e-6) do begin
  calcall(theta,thetanew,diff,true);
  if (((thetanew*tin(j)>360) and (j=2)) then begin

  {The program was moving along the lower branch and then}
  {jumped onto the upper branch.}
  {Increase dp by 1mm and try again}

    if not(increased) then
    begin
      dp:=dp+1.e-3;
      increased:=true;
      theta:=1.05;          {initial guess}
      goto startloop;
    end else goto endp;   {if dp was already increased, exit}
  end;
  {Repeat calculation with new theta}
  theta:=0.4*thetanew+0.6*theta;
 end;
 tem[i,j]:=thetanew;
 tem[i,j+4]:=thetamax;
end;
end;
```

```
p:
teln(lst,'SUMMARY OF SOLUTIONS');
teln(lst);
teln(lst,'DP':5,'LOWER':9,'LOWER MAX':9,'UPPER':9,'UPPE
teln(lst);
 i:=imax downto imin do begin
riteln(lst,tem[i,4]*1000:5:1,tem[i,2]*tinf:9:2,tem[i,3]
ea[i,1]*tinf:9:2,tem[i,5]*tinf:9:2);
;
.
```

A12.2 Program to solve the unsteady-state equations for constant r

This program, written in BASIC, uses the analytical solution to solve for the time varying behaviour of the bed.

```
10    ! PROGRAM "                    YTIC SOLUTION
20    ! WITH A
30    OPTION BASE
40    DIM Beta(50)                   (50)
50    COM C(3),Dat                   (11),B(4),Phi(4)
60    PRINTER IS
70 Values:    ! THI                  all the constants and data used
80    MAT READ Cp                    ! N2
90    DATA 6.524,                    ! O2
100   DATA 6.148,
110   DATA 6.214,1                   ! CO2
120   DATA 4.18,                     ! C  NB:Cp=a + bT + c/T^2
130   ! THIS DATA I
140   MAT Cp=Cp*(4.                  J/kmol K
150   P=1.013E5 ! N/
160   ! Initial mole
170   C(1)=.79
180   C(2)=.21
190   C(3)=0
200   ! INITIAL
210    INPUT "Enter                  ,Te,Tavss
220   ! Convert                      atures
230   Ti=300                         nt temperature
240   T0=T0/Ti
250   Te=Te/Ti
260   Tavss=Tavss/
270   ! T0 is the
280   ! Tavss is
290   ! Te is the                    is the density of the ambient air in kg/m^3
300   CALL Density(Ti,               constant in J/kmol/K
310   R=8.314E3
320   E=.4                           particle size in mm
330   Dp=2                           !Surface per volume in m^-1
340   S=6000/Dp                      !Effective thermal conductivity in W/mK
350   Ke=.2                          !Path length in m
360   L=1                            !Modified Stefan-Boltzmann constant
370   Msig=5.67E-8                   !Density of bed in kg/m^3
380   Rho=900                        !Specific heat of bed in J/kg/K
390   Cps=1000                       !Viscosity in m^2/hr
400   ! Effective
410   Kappa=Ke*3600/(Rho*Cps)        !+.448*((.35/.25)^2-1)*500*Cps)
420   K0=0/3600                      !Pre-exponential factor in m/s
430   Eor=0                          !Activation energy/R in K
440   G=9.81                         !Acceleration due to gravity in m/s^2
450   Hc=.76                         !Heat transfer coefficient in W/m^2/K
460   Radius=.25                     !Radius of bed
470   C=0                            !Heat loss coefficient
480   Power=0                        !Power input to heater in W
490   Df=Power*L/(PI*Radius^2*Msig*Ti) !Dimensionless flux
```

```
500  ! Write data into array Dat for passing to subroutines
510  Dat(1)=Roi
520  Dat(2)=R
530  Dat(3)=E
540  Dat(4)=Dp
550  Dat(5)=S
560  Dat(6)=P
570  Dat(7)=Ke
580  Dat(8)=Msig
590  Dat(9)=K0
600  Dat(10)=Eor
610  Dat(11)=L
620  Dat(12)=G
630  Dat(13)=C
640  Dat(14)=Ti
650  Dat(15)=Df!
660  ! Input name of file into which values are written
670  INPUT "Name of data file",Name$
680  ! Print initial values and constants
690  PRINTER IS 7,1,WIDTH(80)
700  PRINT CHR$(27);"&dD";"METHOD OF SOLUTION:";CHR$(27);"&dE";" ANALYTIC SOLU
ON WITH RATE CONSTANT AT I ev"
710  PRINT LIN(2);"Rav set to a constant to check methods"
720  PRINT LIN(2);CHR$(27);"&dD";"BED CONSTANTS";CHR$(27);"&dE"
730  PRINT LIN(1);"Particle size=";Dp;"mm",,"Voidage=";E
740  PRINT LIN(1);"Bed radius=";Radius;"m",,"Bed length=";L;"m"
750  PRINT LIN(1);"Power input=";Power;"W",,"Loss coefficient=";C
760  PRINT USING "/4A,X,4D,X,A,29X,4A,X,D.DDDE,X,4A";"E/R=";Eor;"K",,"K0=";K0
0;"m/hr"
770  PRINT LIN(1);"Bed density=";Rho;"kg/m^3","Cp of bed=";Cps;"J/kg/K"
780  PRINT USING "/12A,X,D.DDDE,X,6A";"Diffusivity=";Kappa;"m^2/hr"
790  ! PRINT LIN(1);"Name of data file is ";Name$
800  ! PRINT PAGE
810  PRINTER IS 16
820  ! Calculate  predicted steady state profile
830  CALL Tsteady(Tavss,T0,Te,Tmax)
850  ! Tmax is used to give upper limit for "PLOT"
860  Tup=100*INT(Tmax*Ti/100+.5)
870  ! Write steady state profile into matrix T as first element
880  FOR I=1 TO 11
890     T(I,1)=Z(1)
900  NEXT I
910  ! Input Tin which is the initial bed temperature
920  INPUT "Initial temperature?",Tin
930  Tin=Tin/Ti
940  T0=Tin
950  Te=Tin
960   PRINTER IS 7,1,WIDTH(80)
970  PRINT CHR$(27);"&dD";"UNSTEADY STATE SOLUTION";CHR$(27);"&dE"   Initial tem
erature=";INT(Tin*Ti+.5);"K"
980  PRINTER IS 16
990  Ta=Tin          !For the first time slice
1010 ! Decide on time scaling
1020 Dtmax=Ti*ABS(Tavss-Tin)
1030 PRINT "The difference in average temperatures is ";Dtmax
1040 Reinput:  INPUT "Maximum temperature rise per time slice?",Delt
1050    Lastj=INT(Dtmax/Delt)+1  !Lastj is the number of curves
1060    PRINT "This gives ";Lastj;" curves (including steady state). Is this O K
?"
1070    A$=""
1080    INPUT A$
1090 IF A$="N" THEN Reinput !
```

```
1100 ! Initialize the array Beta to (N-1)*PI except for the first value
1110 Beta(1)=PI/2
1120 FOR N=2 TO 50
1130    Beta(N)=(N-1)*PI
1140 NEXT N
1150 Time=2              !First time at which calculation is done
1160 Lastj=50
1170 FOR J=2 TO Lastj    !Outer loop for time increments
1180    ! Put time into matrix
1190    Tim(J)=Time
1200    ! Calculate flowrate and reaction rate based on average temperature
1210    Tai=Ta*Ti
1220    CALL Darcy(Tai,Fr)
1230    CALL Cp(Tai,Cpav)
1240    CALL H_react(Tai,Delh)
1250    ! Calculate dimensionless flow number
1260    Dfn=L*Roi*G*P*Cpav/(Fr*R*Ti*Ke)
1270    A=Dfn*((Ta-1)/Ta/Ta)
1280    Gg=A*Ke/(Cpav*L)
1290    ! Calculate dimensionless reaction number
1300    Rav=K0*EXP(-Eor/Tai)*P*(1-E)*S/(R*Tai)
1310  ! Rav=5E-7
1320    B=Rav*Delh*L*L*C(2)/(Ke*Ti)
1330    M=Rav*L/Gg
1340    ! Calculate values for 'steady state' coefficients
1350    IF Df=0 THEN CALL Coe(A,B,C,R1,R2,M,T0,Te,C1,C2,C3,Bi0,Bi1,0)
1360    IF Df<>0 THEN CALL Coe2(A,B,C,R1,R2,M,T0,Te,C1,C2,C3,Bi0,Bi1,Df)
1370    Hi=Bi0+A/2
1380    H2=Bi1+A/2
1390    ! Calculte constants needed for unsteady state profile
1400    Kt=Kappa*Time
1410    Inter=EXP(-Kt*A*A/4-C*Kt)
1420    V=0
1430    FOR N=1 TO 20
1440            CALL Integral(Beta(N),N,H1,H2,A,B,C,R1,R2,M,C1,C2,C3,Tin,In(N))
1450            ! Calculate and print 'V' at 1 as a check for convergence
1460            Zn=Beta(N)*COS(Beta(N))+H1*SIN(Beta(N))
1470            V=V+In(N)*Zn*EXP(-Kt*Beta(N)^2)
1480            PRINT N,V
1490    NEXT N
1500    V1=V
1510    ! Calculate unsteady state profile
1520    FOR I=0 TO 9
1530       X=I/10
1540       V=0
1550       FOR N=1 TO 20
1560             Betax=Beta(N)*X
1570             Zn=Beta(N)*COS(Betax)+H1*SIN(Betax)
1580             V=V+In(N)*Zn*EXP(-Kt*Beta(N)^2)
1590       NEXT N
1600       CALL Temp(X,Tss,R1,R2,M,C1,C2,C3)!Tss is the steady state temperature
1610       Z(I+1)=Tss
1620       T(I+1,J)=Tss+V*Inter*EXP(A*X/2)
1630    NEXT I
1640    ! The value of 'V' at the exit is V1
1650    CALL Temp(1,Tss,R1,R2,M,C1,C2,C3)
1660    Z(11)=Tss
1670    T(11,J)=Tss+V1*Inter*EXP(A/2)
1680    T0=T(1,J)
1690    Te=T(11,J)!
```

```
1700     ! Print heading on printer
1710      PRINTER IS 7,1,WIDTH(80)
1720     PRINT LIN(2);CHR$(27);"&dD";"TIME=";Time;"hrs";CHR$(27);"&d@"
1730     ! Call subroutine to print 'constants'
1740     CALL Print(Ta*Ti,Rav,Delh,Cpav,Fr,Gg,Bi0,Bi1,A,B)
1750     ! Calculate average bed temperature & print profile
1760     PRINT LIN(1);"X (m)","TEMPERATURE (K)","   T ss(K)","    Y02"
1770     FOR I=1 TO 11
1780        Y(I)=T(I,J)
1790        Xx=I/10-.1
1800        PRINT Xx,Y(I)*Ti,Z(I)*Ti,.21*EXP(-M*Xx)
1810     NEXT I
1820     ! Throw a page if J is odd
1830     IF FRACT(J/2)<>0 THEN PRINT PAGE
1840     PRINTER IS 16
1850     CALL Simpson(Ta)
1860     ! Calculate time step using exponential scaling
1870    Del_time=LOG((Lastj+2-J)/(Lastj+1-J))/(Kappa*Beta(1)^2)
1880    Time=Time+PROUND(Del_time,0)
1900    PRINT "NEXT TIME IS";Time;"hrs","TAV=";Ta*Ti
1910 NEXT J
1920 STOP
1930 ! Write temperature profiles onto tape for plotting
1940 Record: Recl=INT((11+23*Lastj)/32)+1   !This number is the record length
1950 GOTO 2150
1960 CREATE Name$,Recl
1970 ASSIGN #1 TO Name$
1980 PRINT #1;Lastj+2
1990 ! Set upper and lower limits
2000 PRINT #1;2
2010 PRINT #1;0,Ti
2020 PRINT #1;1,Tup
2030 ! Put initial temperature on tape
2040     PRINT #1;2
2050     PRINT #1;0,Tin*Ti
2060     PRINT #1;1,Tin*Ti
2070 ! Put array T onto tape                !Lastj is the number of curves
2080 FOR J=1 TO Lastj                      !Number of points
2090     PRINT #1;11
2100     FOR I=1 TO 11                     !Point
2110        PRINT #1;I/10-.1,T(I,J)*Ti
2120     NEXT I
2130 NEXT J
2140 ASSIGN #1 TO *
2150 ! Put temperature vs. time plot on tape
2160 CREATE Name$&"T",Recl
2170 ASSIGN #2 TO Name$&"T"
2180 PRINT #2;12
2190 PRINT #2;2
2200 PRINT #2;0,300
2210 PRINT #2;Tim(Lastj),Tup
2220 FOR I=1 TO 11
2230 PRINT #2;Lastj
2240 PRINT #2;0,Tin*Ti
2250 FOR J=2 TO Lastj
2260 PRINT #2;Tim(J),T(I,J)*Ti
2270 NEXT J
2280 NEXT I
2290 ASSIGN #2 TO *
2300 STOP !
```

```
2310 Tsteady:  SUB Tsteady(Ta,T0,Te,Tmax)
2320 OPTION BASE 1
2330 ! This subroutine calculates the steady state temperature profile
2340 ! It is quite separate to the calculation of the unsteady state profiles
2350 COM C(3),Data(20),Cp(4,3),Y(11),T(11)
2360 ! Give variables in array 'Data' desriptive names
2370 Roi=Data(1)
2380 R=Data(2)
2390 E=Data(3)
2400 Dp=Data(4)
2410 S=Data(5)
2420 P=Data(6)
2430 Ke=Data(7)
2440 Msig=Data(8)
2450 K0=Data(9)
2460 Eor=Data(10)
2470 L=Data(11)
2480 G=Data(12)
2490 C=Data(13)
2500 Ti=Data(14)
2510 Df=Data(15)
2520 ! Make estimates of flowrate & reaction rate constant
2530 Tai=Ta*Ti
2540 Rav=K0*EXP(-Eor/Tai)*P*(1-E)*S/(R*Tai)
2550 Rav=1E-5
2560 CALL Darcy(Tai,Fr)
2570 Gg=P*Roi*G/(Fr*R*Tai)*(1-1/Ta)
2580 ! Outer loop which iterates for reaction rate constant
2590 Calc_rate: Tai=Ta*Ti
2600   CALL Darcy(Tai,Fr)
2610   CALL Cp(Tai,Cpav)
2620   CALL H_react(Tai,Delh)
2630   B=Rav*Delh*C(2)*L*L/(Ke*Ti)
2640   ! Inner loop to calculate flowrate
2650 Calc_flow:     A=Gg*Cpav*L/Ke
2660     M=Rav*L/Gg
2670     IF Df=0 THEN CALL Coe(A,B,C,R1,R2,M,T0,Te,C1,C2,C3,Bi0,Bi1,1)
2680     IF Df<>0 THEN CALL Coe2(A,B,C,R1,R2,M,T0,Te,C1,C2,C3,Bi0,Bi1,Df)
2690     PRINT "T0=";T0*Ti,"G=";Gg
2700     ! Calculate temperature at 11 points
2710     FOR I=0 TO 10
2720       X=I/10
2730       CALL Temp(X,T,R1,R2,M,C1,C2,C3)
2740       T(I+1)=T
2750       Y(I+1)=1/T
2760     NEXT I
2770     ! Calculate integral of T^-1 using Simpson's Rule
2780     CALL Simpson(Di1)
2790     ! Calculate integral of T analytically
2800     CALL Intt(It,R1,R2,M,C1,C2,C3,C)
2810     ! Calclulate new flowrate
2820     Gg1=P*G*Roi*(1-Di1)/(Fr*R*It*Ti)
2830     Dif=ABS(Gg1-Gg)
2840     Gg=.8*Gg1+.2*Gg
2850     ! Check for convergence of flowrate
2860     IF Dif>Gg/500 THEN GOTO Calc_flow
2870   ! Calculate new end temperature and rate expression
2880   Dif1=ABS(Te-T(11))
2890   Te=T(11)!
```

```
2900   GOTO 3000
2910   ! Evaluate exp(-E/(RT))/T numerically
2920    FOR I=1 TO 11
2930       Temp=T(I)*Ti
2940       Y(I)=EXP(-Eor/Temp)/Temp
2950    NEXT I
2960    CALL Simpson(Di2)
2970    Rav1=K0*P*Di2*S*(1-E)/R
2980    Dif=ABS(Rav-Rav1)
2990    Rav=.8*Rav1+.2*Rav
3000    Ta=It
3010    PRINT "T av=";Ta*Ti,,"RAV=";Rav
3020 ! Check for convergence
3030 IF (Dif)Rav/500) OR (Dif1).001) THEN GOTO Calc_rate
3040 ! The iteration is finished
3050 Tmax=T(1)
3060 ! Calculate maximum temperature if Flux=0
3070 IF Df=0 THEN CALL Tmax(Xmax,Tmax,R1,R2,M,C1,C2,C3)
3080 ! Print steady state profile & constants
3090  PRINTER IS 7,1,WIDTH(80)
3100 PRINT LIN(2);CHR$(27);"&dD";"STEADY STATE SOLUTION";CHR$(27);"&d@"
3110 CALL Print(Ta*Ti,Rav,Delh,Cpav,Fr,Gg,Bi0,Bi1,A,B)
3120 PRINT LIN(1);"X    ","TEMPERATURE (K)"
3130 FOR I=0 TO 10
3140 PRINT I/10,T(I+1)*Ti
3150 NEXT I
3160 PRINT LIN(1);"T max=";Tmax*Ti;"K @ X=";Xmax;
3170 ! Check on overall energy balance
3180 Hr=Bi0*(T0-1)+Bi1*(Te-1)+A*(Te-1)+C*(It-1)
3190 Hg=B/M*(1-EXP(-M))+Df
3200 PRINT LIN(1);"HR=";Hr,,"HG=";Hg
3210  PRINT PAGE
3220  PRINTER IS 16
3230 SUBEND !
```

```
3240 SUB Cp(T,Cpav)
3250 OPTION BASE 1
3260 COM C(3),Data(20),Cp0(4,3)
3270 DIM Cp(3)
3280 ! Cp's in J/kmol K FOR T IN K:
3290 MAT Cp=(0)
3300 FOR I=1 TO 3
3310 FOR J=1 TO 3
3320 Cp(I)=Cp(I)+Cp0(I,J)*T^(J-1)
3330 NEXT J
3340 NEXT I
3350 ! C(*) IS VECTOR OF MOL FRACTIONS, SO
3360 Cpav=DOT(C,Cp)
3370 SUBEND !


3380 SUB Density(T,P,Ro,Mass)
3390 OPTION BASE 1
3400 COM C(3)
3410 DIM Mwt(3)
3420 Mwt(1)=28   ! N2
3430 Mwt(2)=32   ! O2
3440 Mwt(3)=44   ! CO2
3450 ! C(*) IS VECTOR OF MOL FRACTIONS, SO FOR 1 MOL:
3460 Mass=DOT(C,Mwt)
3470 R=8.3E3    ! J/kmol K
3480 Vol=R*T/P
3490 Ro=Mass/Vol    ! kg/m3
3500 SUBEND !


3510 SUB Darcy(T,Darcy)
3520 OPTION BASE 1
3530 COM C(3),Data(20)
3540 E=Data(3)
3550 D=Data(4)
3560 S=Data(5)
3570 ! T = TEMP K
3580 ! D = PARTICLE DIAM m
3590 ! E = VOIDAGE
3600 ! S = PARTICLE AREA/VOLUME
3610 CALL Viscosity(T,Mu)
3620 K=5
3630 Darcy=K*(1-E)^2*Mu*S^2/E^3
3640 SUBEND !


3650 SUB Viscosity(T,Mu)
3660 ! VISCOSITY OF AIR
3670 ! PERRY THIRD ED P 370
3680 C=114
3690 Mu0=.01709                                    ! IN cp FOR T IN K
3700 Mu=Mu0*(273.1+C)/(T+C)*(T/273.1)^1.5
3710 Mu=Mu/1000    ! IN kg/m s
3720 SUBEND !
```

```
3730 SUB H_react(T,Delh)
3740 ! Subroutine to calculate Delta H reaction
3750 OPTION BASE 1
3760 COM X(3),Data(20),Cp(4,3)
3770 Delta_h_0=-9.4E7*4.18  !J/kmol !Enthalpy of formation of CO2
3780 Ho2=0
3790 Hco2=0
3800 T0=298
3810 I=2  !2 refers to CO2
3820 FOR J=1 TO 3     ! CP = CP(I,1)+CP(I,2)*T+CP(1,3)*T^2
3830 Ho2=Ho2+Cp(I,J)*(T^J-T0^J)/J
3840 NEXT J
3850 I=3 !3 refers to O2
3860 FOR J=1 TO 3     ! CP = CP(I,1)+CP(I,2)*T+CP(I,3)*T^2
3870 Hco2=Hco2+Cp(I,J)*(T^J-T0^J)/J
3880 NEXT J
3890 ! Enthalpy of Carbon with Cp=Cp(4,1)+Cp(4,2)*T+Cp(4,3)*T^-2
3900 Hc=Cp(4,1)*(T-T0)+Cp(4,2)/2*(T^2-T0^2)-Cp(4,3)*(1/T-1/T0)
3910 Delh=Ho2-Hco2+Hc-Delta_h_0
3920 ! This is actually -Delta H reaction
3930 SUBEND !


3940 Temp: SUB Temp(X,T,R1,R2,M,C1,C2,C3)
3950 ! Steady state temperature expression
3960 T=1+C1*EXP(R1*X)+C2*EXP(R2*X)+C3*EXP(-M*X)
3970 SUBEND !


3980 SUB Intt(It,R1,R2,M,C1,C2,C3,C)
3990 ! Calculates the integral of T
4000 It=1+C1+C2/R2*(EXP(R2)-1)-C3/M*(EXP(-M)-1)
4010 IF C<>0 THEN It=It-C1*(1-(EXP(R1)-1)/R1)
4020 SUBEND!


4030 Simp: SUB Simpson(Di)
4040    ! Simpson's Rule for 11 evenly spaced points on interval length 1
4050    OPTION BASE 1
4060    COM C(3),Dat(20),Cp(4,3),Y(11),T(11)
4070    LET Di=Y(1)+Y(11)
4080    FOR J=2 TO 10
4090       Di=Di+2*Y(J)
4100       IF J/2-INT(J/2)=0 THEN Di=Di+2*Y(J)
4110    NEXT J
4120    Di=Di/30
4130 SUBEND !
```

```
4140 In: SUB Integral(Beta,N,H1,H2,A,B,C,R1,R2,M,C1,C2,C3,Tin,In)
4150 ! Calculates the coefficient of the series
4160 OPTION BASE 1
4170 COM C(3),Dat(20),Cp(4,3),Y(11),Z(11),B(4),Phi(4)
4180 ! Calculate value of Beta  using succesive substitution
4190 ! Best estimate for Beta  is the one from the previous time slice
4200 Mult=H1*H2
4210 Add=H1+H2
4220 Pre=N*PI-PI/2
4230 Again: X1=Pre-ATN((Beta*Beta-Mult)/(Add*Beta))
4240    Dif=ABS(X1-Beta)
4250    Beta=X1
4260    ! Note strict convergence criterion for acceptable accuracy
4270 IF Dif)1E-8 THEN Again
4280 B(1)=-C1
4290 B(2)=-C2
4300 B(3)=-C3
4310 B(4)=Tin-1
4320 Phi(1)=R1-A/2
4330 Phi(2)=R2-A/2
4340 Phi(3)=-M-A/2
4350 Phi(4)=-A/2
4360 An=2*(Beta^2+H2^2)/((Beta^2+H1^2)*(Beta^2+H2^2+H2)+H1*(Beta^2+H2^2))
4370 In=0
4380 FOR I=1 TO 4
4390    Im=Beta*(EXP(Phi(I))*(Phi(I)*COS(Beta)+Beta*SIN(Beta))-Phi(I))
4400    Im=Im+H1*(EXP(Phi(I))*(Phi(I)*SIN(Beta)-Beta*COS(Beta))+Beta)
4410    Im=Im*B(I)/(Phi(I)^2+Beta^2)
4420    In=In+Im
4430 NEXT I
4440 In=In*An
4450 SUBEND !


4460 Coe: SUB Coe(A,B,C,R1,R2,M,T0,Te,C1,C2,C3,Bi0,Bi1,Flag)
4470 ! Calculates the coefficients in the steady state temperature equation
4480 OPTION BASE 1
4490 COM C(3),Data(20)
4500 Ke=Data(7)
4510 Msig=Data(8)
4520 Bi1=Msig*(Te*Te+1)*(Te+1)
4530 R1=(A-SQR(A*A+4*C))/2
4540 R2=(A+SQR(A*A+4*C))/2
4550 Again: Bi0=(T0+1)*(T0*T0+1)*Msig
4560    C3=-B/(M*M+A*M-C)
4570    C2=1/((R1+Bi1)*(A+Bi0-R2)*EXP(R1)+(R2+Bi1)*(R1-A-Bi0)*EXP(R2))
4580    C2=C2*C3*((M-Bi1)*(R1-A-Bi0)*EXP(-M)-(R1+Bi1)*(M+Bi0+A)*EXP(R1))
4590    C1=(C2*(A+Bi0-R2)+C3*(A+Bi0+M))/(R1-A-Bi0)
4600    CALL Temp(0,T,R1,R2,M,C1,C2,C3)
4610    Dif=ABS(T-T0)
4620    T0=T
4630    ! Check for convergence but  only iterate if doing 'proper'
4640    ! steady state calculation
4650 IF (Dif).001) AND (Flag=1) THEN Again
4660 SUBEND !
```

```
4670 Tmax: SUB Tmax(X,Tmax,R1,R2,M,C1,C2,C3)
4680 ! Subprogram to find maximum temperature and where it occurs
4690 ! Method used is Newton-Raphson
4700 X=.5
4710 Recalc: D2tdx2=C1*R1*R1*EXP(R1*X)+C2*R2*R2*EXP(R2*X)+C3*M*M*EXP(-M*X)
4720         Dtdx=C1*R1*EXP(R1*X)+C2*R2*EXP(R2*X)-C3*M*EXP(-M*X)
4730         X1=X-Dtdx/D2tdx2
4740         Dif=ABS(X1-X)
4750         X=X1
4760 IF Dif).01 THEN Recalc
4770 CALL Temp(X,Tmax,R1,R2,M,C1,C2,C3)
4780 SUBEND !


4790 Prnt: SUB Print(Ta,Rav,Delh,Cp,Fr,Gg,Bi0,Bi1,A,B)
4800 ! Subroutine to print 'constants'
4810 PRINT LIN(1);"T average=";PROUND(Ta,-2);"K",,"RAV=";Rav;"kmol/m^3/s"
4820 PRINT LIN(1);"DELTA H REACTION=";INT(Delh+.5);"J/kmol","CP=";INT(Cp+.5);"J/
kmol/K"
4830 PRINT LIN(1);"DARCY'S CONSTANT=";INT(Fr+.5);"kg/m^2/s"  !?
4840 PRINT LIN(1);"FLOWRATE=";Gg;"kmol/m^2/s"
4850 PRINT LIN(1);"BI0=";Bi0,"BIi=";Bi1
4860 PRINT LIN(1);"A=";A,,"B=";B
4870 SUBEND !


4880 Coe2: SUB Coe2(A,B,C,R1,R2,M,T0,Te,C1,C2,C3,Bi0,Bi1,Df)
4890 ! Calculates the coefficients in the steady state temperature equation
4900 ! for the case of heating on the bottom
4910 OPTION BASE 1
4920 COM C(3),Data(20)
4930 Ke=Data(7)
4940 Msig=Data(8)
4950 ! Bi0 is due to the glass wool insulation
4960 Bi0=120
4970 Bi1=Msig*(Te*Te+1)*(Te+1)
4980 R1=(A-SQR(A*A+4*C))/2
4990 R2=(A+SQR(A*A+4*C))/2
5000 C3=-B/(M*M+A*M-C)
5010 C2=C3*((M-Bi1)*(R1-A-Bi0)*EXP(-M)-(R1+Bi1)*(A+Bi0+M)*EXP(R1))+Df*(R1+Bi1)*E
XP(R1)
5020 C2=C2/((R1+Bi1)*(A+Bi0-R2)*EXP(R1)+(R2+Bi1)*(R1-A-Bi0)*EXP(R2))
5030 C1=(C2*(A+Bi0-R2)+C3*(A+Bi0+M)-Df)/(R1-A-Bi0)
5040 CALL Temp(0,T0,R1,R2,M,C1,C2,C3)
5050 SUBEND !
```

A12.3 Program to solve the equations numerically

This program, written in BASIC, uses the method of lines to solve the equations without the assumption of constant r.

```
10   ! PROGRAM "LIN" WHICH DOES CALCULATIONS AT THE ROOTS OF THE NITH
20   ! ORDER LEGENDRE POLYNOMIAL
30    OPTION BASE 1
40    DIM Th(15),Yo2(15),Z(15),Temp(15,25),Tim(25)
60    N1=15                          !Number of lines
70    REDIM Th(N1),Yo2(N1),Z(N1),Temp(N1,20),X(N1),Aw(N1,N1),A2w(N1,N1)
75    COM Cc(3),Dat(25),Cp(4,3),Aw(15,15),A2w(15,15),X(15),U(15),Ks(15),Rate(15)
80   ! Read the matrix of the nodes of the polynomial from tape
81    OFF ERROR
90    ASSIGN @F1 TO "X"&VAL$(N1)
100   ENTER @F1;X(*)
101   ASSIGN @F1 TO *
110  ! Read the matrix of coefficients from tape
120   ASSIGN @F1 TO "MAT"&VAL$(N1)
130   ENTER @F1;Aw(*)
131   ASSIGN @F1 TO *
140  ! Calculate the matrix AW*AW for 2nd derivatives
150   MAT A2w= Aw*Aw
160   Dif=X(N1)-X(1)          !Scaling factor since nodes are not at 0 and 1
170  ! Calculate the matrix Z which contains rescaled x values
180   FOR I=1 TO N1
190     Z(I)=(X(I)-X(1))/Dif
200   NEXT I
210 Values:  ! This section contains all the constants and data used
290   P=1.013E+5                      ! N/m2 = 1 ATM
300  ! Initial mole fractions
310   Cc(1)=.79                       !N2
320   Cc(2)=.21                       !O2
330   Cc(3)=0                         !CO2
340 Restart:PRINTER IS 1
350   MAT U= (0)
360   Ti=300                          !Ambient temperature
370   CALL Density(Ti,P,Roi,W)        !Roi is the density of the ambient air in kg/m^3
380   R=8.314E+3                      !Gas Constant in J/kmol/K
390   E=.3                            !Voidage
400   Dp=6                            !Particle size in mm
410   S=6000/Dp                       !Surface per volume in m^-1
420   Ke=.2                           !Effective thermal conductivity in W/mK
430   L=5                             !Bed length in m
440   Msig=5.67E-8*Ti^3*L/Ke          !Modified Stefan-Boltzmann constant
450   Rho=900                         !Density of bed in kg/m^3
460   Cps=1000                        !Specific heat of bed in J/kg/K
470   Kappa=Ke*3600/(Rho*Cps)         !Effective thermal diffusivity in m^2/hr
480   Drho=1.E+99                     !Constant for shrinking core (1E99 = no ageing)
490   K0=10                           !Pre-exponential factor in m/s
500   Eor=7000                        !Activation energy/R in K
510   Vwind=0                         !Wind velocity in m/s
520   G=9.81                          !Acceleration due to gravity in m/s^2
530   Radius=0                        !Radius of bed
540   C=0                             !Heat loss coefficient
550 Time:Delt=60                      !Size of time step in hours
560    Deltau=Delt*Kappa/L/L          !Dimensionless time step
```

```
561   Time0=0
570   Time=Time0                    !First time at which calculation is done
580   Lastj=50                      !Number of times calculation is performed
590   Skip=10                       !Not every point is stored and recorded
600   Lastr=Lastj/Skip              !Number of profiles to be recorded
610   REDIM Tim(Lastr+1)
611   REDIM Temp(N1,Lastr+1)
620 ! Write data into array Dat for passing to subroutines
630   Dat(1)=Roi
640   Dat(2)=R
650   Dat(3)=E
660   Dat(4)=Dp
670   Dat(5)=S
680   Dat(6)=P
690   Dat(7)=Ke
700   Dat(8)=Msig
710   Dat(9)=K0
720   Dat(10)=Eor
730   Dat(11)=L
740   Dat(12)=G
750   Dat(13)=C
760   Dat(14)=Ti
770   Dat(15)=Df
780   Dat(16)=N1
790   Dat(19)=Kappa
800   Dat(20)=Dif
810   Dat(21)=Vwind
820   Dat(25)=Drho
830 ! Input name of file into which values are written
840   INPUT "Name of data file",Name$
850 ! Print initial values and constants
860 Prntc:  PRINTER IS 9;WIDTH (2000)
870   PRINT RPT$("
                 ",2);N1;"TH ORDER LEGENDRE POLYNOMIAL-MARCHING BY RUNGE-KUTTA"
880   PRINT RPT$("
                 ",2);"BED CONSTANTS"
890   PRINT RPT$("
                 ",1);"Particle size=";Dp;"mm","Voidage=";E
900   PRINT RPT$("
                 ",1);"Bed length=";L;"m"
910   IF Drho()1.E+99 THEN PRINT USING "/16A,D.DDE";"Ageing factor=";Drho
920   PRINT USING "/,4A,X,4D,X,A,29X,3A,X,DDDD.DD,X,4A";"E/R=";Eor;"K","K0=";K0 "
930   PRINT RPT$("
                 ",1);"Bed density=";Rho;"kg/m^3","Cp of bed=";Cps;"J/kg/K"
940   PRINT USING "/,21A,D.DDDE,X,6A";"Thermal Diffusivity=";Kappa;"m^2/hr"
950 ! PRINT RPT$("
                 ",1);"Wind velocity=";Vwind;"m/s"
960   PRINT RPT$("
                 ",1);"Name of data file:";Name$
970   PRINT RPT$("
                 ",1);"Size of time step:";Delt;"hrs","Number of lines:";N1
971   PRINT RPT$("
                 ",1);"Number of time steps=";Lastj,"Every";Skip;"th recorded"
980   PRINT CHR$(12)
990   PRINTER IS 1
991   A$=""
992   Time0=0
1000  INPUT "DO YOU WANT TO INPUT A TEMPERATURE PROFILE?",A$
1010  IF A$()"Y" THEN GOTO 1100
1020  FOR I=1 TO N1
1030    PRINT "T(";I;") IN K?"
1040    INPUT Th(I)
```

```
1060  MAT Th= Th/(Ti)
1070  INPUT "TIME0 IN HOURS?",Time0
1071  Time=Time0
1080  CALL Tav(Th(*),Ta)
1090  GOTO 1150
1100 ! Input Tin which is the initial bed temperature
1110  INPUT "Initial temperature?",Tin
1120  Tin=Tin/Ti  !Made dimensionless
1130  Ta=Tin!For the first time slice the average temperature is the initial
1140  MAT Th= (Tin)!Th is the matrix that contains the dimensionless temperature
1150  MAT Yo2= (Cc(2))  !Yo2 is the matrix that contains the oxygen profile
1160 ! Store initial temperature profile
1170  FOR I=1 TO N1
1180    Temp(I,1)=Th(I)*Ti
1190  NEXT I
1200  Tim(1)=Time0        !First time
1210  Pflag=1             !Flag to control printing
1220  Nprint=0            !Counter to control output
1250 !
1260 Startloop:FOR J=1 TO Lastj    !Outer loop for time increments
1270    PRINTER IS 9;WIDTH (2000)
1280    ! Calculate flowrate based on average temperature
1290    Tai=Ta*Ti
1300    CALL Darcy(Tai,Fr)
1310    Gg=P*Roi/(Fr*R*Tai)*(G*(1-Ti/Tai)+Vwind^2/L/2)
1320    Dat(18)=Gg
1330    ! Call program to march forward
1340    ! March2 marches forward using forward differences
1350    ! March uses a 4th order Runge Kutta algorithm
1360    CALL March2(Th(*),Yo2(*),Deltau)
1370    ! Call subroutine to calculate O2 profile
1380    CALL Newo2(Yo2(*),Th(*))!
```

```
1381    IF (Th(1))1) AND (Th(N1))1) THEN GOTO 1390!CHECK TO SE IF UNSTABLE
1382    PRINTER IS 1
1383    BEEP
1385    PRINT "WARNING: TIME=";Time;"T0=";Th(1)*Ti;"TE=";Th(N1)*Ti
1386    Th(1)=1
1387    Th(N1)=1
1389    PRINTER IS 9;WIDTH (2000)
1390    IF J MOD Skip()0 THEN GOTO 1560
1400    FOR I=1 TO N1
1410      Temp(I,J/Skip+1)=Th(I)*Ti
1420    NEXT I
1430    IF Pflag=0 THEN GOTO 1560
1440    PRINT RPT$("
                   ",2);"TIME=";Time+Delt;"hrs"
1450    ! The Biot numbers are now in the matrix Dat
1460    Bi0=Dat(21)
1470    Bi1=Dat(22)
1480    ! Call subroutine to print 'constants'
1490    CALL Print(Ta*Ti,Fr,Gg,Bi0,Bi1)
1500    ! Calculate average bed temperature & print profile
1510    PRINT RPT$("
                   ",1);"  X","TEMPERATURE (K)","  Y02"
1520    FOR I=1 TO N1
1530      PRINT USING "Z.DDD,17X,DDDD.DDD,11X,.DDDD,4D,5X,4D";Z(1),Temp(I,J/Skip+
1540    NEXT I
1550    ! Calculate the average dimensionless temperature
1560    CALL Tav(Th(*),Ta)
1570    ! Rescale Ta
1580    Ta=Ta/Dif
1590    ! Throw a page if J is a multiple of 2
1600    IF (J/Skip MOD 3=0) AND (Pflag=1) THEN PRINT CHR$(12)
1610    IF Pflag=0 THEN PRINT USING "#,X,5A,DD.D,X,2A,DDD.DDD";"DAY=",Time/24,"!=
1620    Nprint=Nprint+1
1630    IF (Nprint MOD 4=0) AND (Pflag=0) THEN PRINT
1640 !  DISP J,Ta*Ti,Th(1)*Ti,Th(N1)*Ti
1641    IF Time<1800 THEN GOTO 1650
1642    Delt=5
1643    Deltau=Delt*Kappa/L/L
1650    Time=Time+Delt
1660    IF J MOD Skip=0 THEN Tim(J/Skip+1)=Time
1670 Endloop:NEXT J
1680 ! Print stored temperatures
1681  GOTO 1800
1690  PRINTER IS 9;WIDTH (2000)
1700  PRINT CHR$(12)
1710  FOR J=1 TO Lastr+1
1720    PRINT RPT$("
                   ",2);"TIME=";Tim(J);"days"
1730    PRINT RPT$("
                   ",1);"  X","TEMPERATURE (K)"
1740    FOR I=1 TO N1
1750      PRINT USING "Z.DDD,17X,DDDD.DDD,";Z(I),Temp(I,J)
1760    NEXT I
1770    IF J MOD 3=0 THEN PRINT CHR$(12)
1780  NEXT J
1790  PRINT CHR$(12)
1800  PRINTER IS 1
1810 Qrec:A$=""
1820  INPUT "DO YOU WANT TO RECORD RESULTS?",A$
1830  IF A$="Y" THEN CALL Record(Name$,Temp(*),Z(*),Tim(*),Lastr,N1)
1840  STOP!
1841  END
```

```
1850 Cp:SUB Cp(T,Cpav)
1860    OPTION BASE 1
1890    Cpav=28930
2000  SUBEND!
2010 Dens:SUB Density(T,P,Ro,Mass)
2020    OPTION BASE 1
2030    COM Cc(3),Dat(25),Cp(4,3),Aw(15,15),A2w(15,15),X(15),U(15),Ks(15),Rate(15
2040    DIM Mwt(3)
2050    Mwt(1)=28! N2
2060    Mwt(2)=32! O2
2070    Mwt(3)=44! CO2
2080 ! CC(*) IS VECTOR OF MOL FRACTIONS, SO FOR 1 MOL:
2090    Mass=DOT(Cc,Mwt)
2100    R=8.3E+3! J/kmol K
2110    Vol=R*T/P
2120    Ro=Mass/Vol! kg/m3
2130  SUBEND!


2140 Darcy:SUB Darcy(T,Darcy)
2150    OPTION BASE 1
2160    COM Cc(3),Data(25),Cp(4,3),Aw(15,15),A2w(15,15),X(15),U(15),Ks(15),Rate(
2170    E=Data(3)
2180    D=Data(4)
2190    S=Data(5)
2200 ! T = TEMP K
2210 ! D = PARTICLE DIAM m
2220 ! E = VOIDAGE
2230 ! S = PARTICLE AREA/VOLUME
2240    CALL Viscosity(T,Mu)
2250    K=5
2260    Darcy=K*(1-E)^2*Mu*S^2/E^3
2270  SUBEND!
2280 Visc:SUB Viscosity(T,Mu)
2290 ! VISCOSITY OF AIR
2300 ! PERRY THIRD ED P 370
2310    C=114
2320    Mu0=.01709
2330    Mu=Mu0*(273.1+C)/(T+C)*(T/273.1)^1.5 ! IN cp FOR T IN K
2340    Mu=Mu/1000! IN kg/m s
2350  SUBEND!
2360 Delh:SUB H_react(T,Delh)
2370 ! Subroutine to calculate Delta H reaction
2380    OPTION BASE 1
2400    Delh=3.E+8
2580  SUBEND!
2590 Prnt:SUB Print(Ta,Fr,Gg,Bi0,Bi1)
2600 ! Subroutine to print 'constants'
2610    PRINT RPT$("
                  ",1);"T average=";PROUND(Ta,-2);"K"
2620    PRINT "DARCY'S CONSTANT=";INT(Fr+.5);"kg/m^2/s" !?
2630    PRINT "FLOWRATE=";Gg;"kmol/m^2/s"
2640    PRINT "BI0=";Bi0,"BI1=";Bi1
2650  SUBEND!
```

```
2660 02:SUB Newo2(Y(*),Th(*))
2670 ! Calculates oxygen profile using backward differences
2680    OPTION BASE 1
2690    COM Cc(3),Data(25),Cp(4,3),Aw(15,15),A2w(15,15),X(15),U(15),Ks(15),Rat
2700    L=Data(11)
2710    Delx=Data(17)
2720    N1=Data(16)
2730    Dif=Data(20)
2740    G=Data(18)!Flowrate
2750    Ti=Data(14)
2760    Drho=Data(25)
2770    S=Data(5)
2780    E=Data(3)
2790    FOR I=1 TO N1
2800       T=Th(I)*Ti
2810       CALL React(T,Ratei,Ks(I),U(I))
2820       IF I=1 THEN 2850
2830       Delx=(X(I)-X(I-1))/Dif
2840       Y(I)=Y(I-1)/(1+Delx*Ratei*L/G)
2850       U(I)=U(I)+Ratei*Y(I)/(S*(1-E)*Drho)
2860    NEXT I
2870  SUBEND!
2880 Func:SUB Func(Dydt,Y(*),Ix,Yo2(*))
2890 ! Subroutine to calculate dY/dt
2900    OPTION BASE 1
2910    COM Cc(3),Data(25),Cp(4,3),Aw(15,15),A2w(15,15),X(15),U(15),Ks(15),Rat
2920    Ti=Data(14)
2930    L=Data(11)
2940    C=Data(13)
2950    Ke=Data(7)
2960    G=Data(18)
2970    N1=Data(16)
2980    Dif=Data(20)
2990    T=Y(Ix)*Ti
3000    CALL Cp(T,Cpav)
3010    CALL H_react(T,Delh)
3020    CALL React(T,Ratei,Ks(Ix),U(Ix))
3030    Rate(Ix)=Ratei
3040    A=G*Cpav*L/Ke
3050    B=Delh*Ratei*L*L*Yo2(Ix)/(Ti*Ke)
3060    CALL Deriv(Y(*),Ix,Dydx,D2ydx2)
3070    Dydt=Dif*Dif*D2ydx2-A*Dif*Dydx+B-C*(Y(Ix)-1)
3080  SUBEND!
3090 Deriv:SUB Deriv(Y(*),Ix,Dydx,D2ydx2)
3100 ! Derivatives of Y by calculation at the roots of the
3110 ! shifted Legendre polynomial of order N1
3120    OPTION BASE 1
3130    COM Cc(3),Data(25),Cp(4,3),Aw(15,15),A2w(15,15),X(15),U(15),Ks(15),Rate(1
3140    N1=Data(16)
3150    Dydx=0
3160    D2ydx2=0
3170    FOR J=1 TO N1
3180       Dydx=Dydx+Aw(Ix,J)*Y(J)
3190       D2ydx2=D2ydx2+A2w(Ix,J)*Y(J)
3200    NEXT J
3210  SUBEND!
```

```
3220 Bvals:SUB Bvals(Y(*))
3230 ! Subroutine to calculate the end temperatures
3240    OPTION BASE 1
3250    COM Cc(3),Data(25),Cp(4,3),Aw(15,15),A2w(15,15),X(15),U(15),K<(15),Rat<(
3260    Ke=Data(7)
3270    Msig=Data(8)
3280    L=Data(11)
3290    Ti=Data(14)
3300    Df=Data(15)
3310    N1=Data(16)
3320    Diff=Data(20)
3330    Gg=Data(18)
3340    T0=Y(1)
3350    Te=Y(N1)
3360 Again:CALL Cp(T0*Ti,Cpav)
3370    Af=Gg*Cpav*L/Ke
3380    Bi0=Msig*(T0+1)*(T0*T0+1)
3390    Bi1=Msig*(Te+1)*(Te*Te+1)
3400    S1=0
3410    S2=0
3420    FOR J=2 TO N1-1
3430      S1=S1+Aw(1,J)*Y(J)
3440      S2=S2+Aw(N1,J)*Y(J)
3450    NEXT J
3460    A1=(Bi0+Af)/Diff
3470    A2=Aw(N1,N1)+Bi1/Diff
3480    Numer=A1+Df/Diff+S1+Aw(1,N1)*(Bi1/Diff-S2)/A2
3490    Den=A1+Aw(1,N1)*Aw(N1,1)/A2-Aw(1,1)
3500    T01=Numer/Den
3501    IF T01<1 THEN T01=1
3510    Te1=(Bi1/Diff-S2-Aw(N1,1)*T01)/A2
3511    IF Te1<1 THEN Te1=1
3520    Dif1=ABS(T01-T0)
3530    Dif2=ABS(Te1-Te)
3540    T0=.5*(T01+T0)
3550    Te=.5*(Te1+Te)
3560 ! Check for convergence of the two end temperatures
3570    IF (Dif1>1.E-3) OR (Dif2>1.E-3) THEN Again
3580    Y(1)=T0
3590    Y(N1)=Te
3600 ! Write the Biot numbers into the matrix Data for passing back
3610    Data(21)=Bi0
3620    Data(22)=Bi1
3630  SUBEND!
```

```
3220 Bvals:SUB Bvals(Y(*))
3230 ! Subroutine to calculate the end temperatures
3240    OPTION BASE 1
3250    COM Cc(3),Data(25),Cp(4,3),Aw(15,15),A2w(15,15),X(15),U(15),K<(15),Rate((
3260    Ke=Data(7)
3270    Msig=Data(8)
3280    L=Data(11)
3290    Ti=Data(14)
3300    Df=Data(15)
3310    N1=Data(16)
3320    Diff=Data(20)
3330    Gg=Data(18)
3340    T0=Y(1)
3350    Te=Y(N1)
3360 Again:CALL Cp(T0*Ti,Cpav)
3370    Af=Gg*Cpav*L/Ke
3380    Bi0=Msig*(T0+1)*(T0*T0+1)
3390    Bi1=Msig*(Te+1)*(Te*Te+1)
3400    S1=0
3410    S2=0
3420    FOR J=2 TO N1-1
3430      S1=S1+Aw(1,J)*Y(J)
3440      S2=S2+Aw(N1,J)*Y(J)
3450    NEXT J
3460    A1=(Bi0+Af)/Diff
3470    A2=Aw(N1,N1)+Bi1/Diff
3480    Numer=A1+Df/Diff+S1+Aw(1,N1)*(Bi1/Diff-S2)/A2
3490    Den=A1+Aw(1,N1)*Aw(N1,1)/A2-Aw(1,1)
3500    T01=Numer/Den
3501    IF T01<1 THEN T01=1
3510    Te1=(Bi1/Diff-S2-Aw(N1,1)*T01)/A2
3511    IF Te1<1 THEN Te1=1
3520    Dif1=ABS(T01-T0)
3530    Dif2=ABS(Te1-Te)
3540    T0=.5*(T01+T0)
3550    Te=.5*(Te1+Te)
3560 ! Check for convergence of the two end temperatures
3570    IF (Dif1)1.E-3) OR (Dif2)1.E-3) THEN Again
3580    Y(1)=T0
3590    Y(N1)=Te
3600 ! Write the Biot numbers into the matrix Data for passing back
3610    Data(21)=Bi0
3620    Data(22)=Bi1
3630  SUBEND!
```

```
3640 March:SUB March(Y(*),Yo2(*),Deltau)
3650 ! Marching forward using 4th order Runge Kutta
3660    OPTION BASE 1
3670    COM Cc(3),Data(25),Cp(4,3),Aw(15,15),A2w(15,15),X(15),U(15),Ks(15),Rate
3680    DIM Z(15),Dy(15)
3690    N1=Data(16)
3700    REDIM Z(N1),Dy(N1)
3710    CALL Bvals(Y(*))
3720    FOR I=2 TO N1-1
3730      CALL Func(Dt,Y(*),I,Yo2(*))
3740      Yk=Deltau*Dt
3750      Dy(I)=Yk
3760      Z(I)=Y(I)+Yk/2
3770    NEXT I
3780    Z(1)=Y(1)
3790    Z(N1)=Y(N1)
3800    FOR I=2 TO N1-1
3810      CALL Func(Dt,Z(*),I,Yo2(*))
3820      Yk=Deltau*Dt
3830      Dy(I)=Dy(I)+2*Yk
3840      Z(I)=Y(I)+Yk/2
3850    NEXT I
3860    FOR I=2 TO N1-1
3870      CALL Func(Dt,Z(*),I,Yo2(*))
3880      Yk=Deltau*Dt
3890      Dy(I)=Dy(I)+2*Yk
3900      Z(I)=Y(I)+Yk
3910    NEXT I
3920    FOR I=2 TO N1-1
3930      CALL Func(Dt,Z(*),I,Yo2(*))
3940      Yk=Deltau*Dt
3950      Dy(I)=(Dy(I)+Yk)/6
3960      Y(I)=Y(I)+Dy(I)
3970    NEXT I
3980    Y(1)=Z(1)
3990    Y(N1)=Z(N1)
4000  SUBEND!
4010 React:SUB React(T,Rate,Ks,U)
4020    OPTION BASE 1
4030 ! Rate of oxidation for unity O2 mole fraction
4040    COM Cc(3),Data(25),Cp(4,3),Aw(15,15),A2w(15,15),X(15),Ui(15),Ksi(15),Rate
4050    R=Data(2)
4060    S=Data(5)
4070    P=Data(6)
4080    E=Data(3)
4090    K0=Data(9)
4100    Eor=Data(10)
4110    Ks=K0*EXP(-Eor/T)
4120    Rate=P*(1-E)*S/(R*T)/(1/Ks+U)
4130  SUBEND!
```

```
4140 March2:SUB March2(Y(*),Yo2(*),Deltau)
4150 ! Marching using forward differences
4160    OPTION BASE 1
4170    COM Cc(3),Data(25),Cp(4,3),Aw(15,15),A2w(15,15),X(15),Ui(15),Ks(15),Rat
4180    DIM Z(15)
4190    N1=Data(16)
4200    REDIM Z(N1)
4210    CALL Bvals(Y(*))
4220    Z(1)=Y(1)
4230    Z(N1)=Y(N1)
4240    FOR I=2 TO N1-1
4250      CALL Func(Dt,Y(*),I,Yo2(*))
4260      Z(I)=Y(I)+Dt*Deltau
4270    NEXT I
4280    MAT Y= Z
4290  SUBEND!
4300 Tav:SUB Tav(Y(*),Ta)
4310 ! Average temperature using trapezium rule
4320    OPTION BASE 1
4330    COM Cc(3),Data(25),Cp(4,3),Aw(15,15),A2w(15,15),X(15),U(15),Ks(15),Rate
4340    N=Data(16)
4350    Ta=0
4360    FOR I=1 TO N-1
4370      Ta=Ta+(Y(I)+Y(I+1))*(X(I+1)-X(I))/2
4380    NEXT I
4390  SUBEND!
4400 Record:SUB Record(N$,T(*),Z(*),Tim(*),Lj,N1)
4410 ! Subroutine to record profile on tape for plotting
4420    OPTION BASE 1
4430    GOTO 4480
4440    INPUT "T,X OR B?",A$
4450    INPUT "TMIN IN KELVIN?",Tmin
4460    INPUT "TMAX IN KELVIN?",Tmax
4470    IF A$="T" THEN GOTO Time
4480    A$="X"
4490    Tmin=300
4500    Tmax=320
4510    Nrec=INT((12+2*(1+N1)*(Lj+1))/32)+1!Number of records
4520    CREATE BDAT N$,Nrec
4530    ASSIGN @F1 TO N$
4540    OUTPUT @F1;INT(Lj+1)          !Number of curves
4580    FOR J=1 TO Lj+1       !Now the temperature profiles are stored
4590      OUTPUT @F1;INT(N1)
4600      FOR I=1 TO N1
4610        OUTPUT @F1;Z(I),T(I,J)
4620      NEXT I
4630    NEXT J
4640    ASSIGN @F1 TO *
4650    IF A$="X" THEN SUBEXIT
4660 !Time: CREATE N$&"T",Nrec
4670    ASSIGN @F2 TO N$&"T"
4680    OUTPUT @F2;N1+1
4690    OUTPUT @F2;2
4700    OUTPUT @F2;0,Tmin
4710    OUTPUT @F2;Tim(Lj+1),Tmax
4720    FOR I=1 TO N1
4730      OUTPUT @F2;Lj+1
4740      FOR J=1 TO Lj+1
4750        OUTPUT @F2;Tim(J),T(I,J)
4760      NEXT J
4770    NEXT I
4780    ASSIGN @F2 TO *
4790  SUBEND!
```

REFERENCES

ARGO, W.B., & Smith, J.M., Heat transfer in packed beds - Prediction of radial rates in gas-solid beds. Chem. Eng. Prog., 49, 443 (1953)

ASTM C177, ASTM Stand. (1963)

BADZIOCH, S., Gregory, D.R., & Field, M.A., Investigation of the thermal conductivity and thermal diffusivity of coal. Fuel, 43(4), 267 (1964)

BALAKOTAIAH, V., & Luss, D., Global Analysis of the Multiplicity Features of Multi-Reaction Lumped-Parameter Systems. Chem. Eng. Sci. 39(5), 865 (1984)

BELLMAN, R., Kashef, B.G., & Casti, J., Differential quadrature: A technique for the rapid solution of non-linear partial differential equatins. Journal of Computational Physics 10, 40 (1972)

BEJAN, A., Natural convection in an infinite porous medium with a concentrated heat source. J. Fluid Mech. 89(1) 97 (1978)

BEVERIDGE, G.S.G & Haughey, D.P., Axial Heat Transfer In Packed Beds. Stagnant Beds Between 20 And 750 °C.
Int. J. Mass Heat Transfer, 14, 1093 (1971)

BEVERIDGE, G.S.G & Haughey, D.P., Axial Heat Transfer In Packed Beds. Gas Flow Through Beds Between 20 and 650 °C.
Int. J. Mass Heat Transfer, 15, 953 (1972)

BHATTACHARRYA, K.K., Effect of humidity on oxidation of coal and its spontaneous heatng. J. Mines Metal Fuel, 18(1), 5 (1970)

BIRD, R.B., Stewart, W.E. & Lightfoot, E.N., Transport Phenomena, Wiley, New York (1960)

BOSWORTH, R.C.L., Heat Transfer Phenomena, Wiley, New York (1952)

BROOKS, K.S. & Woods, E.G.K., Thermal Conductivity of a Coal Bed Laboratory Report, Department of Chemical Engineering, University of the Witwatersrand (1980)

BS 874, British Standards Institution , London (1956)

CARSLAW, H.S., & Jager, J.C., Conduction of Heat in Solids. 3rd Ed., Clarendon Press, Oxford (1959)

CHEN, J.C. & Churchill, S.W., Radiant heat transfer in packed beds. AIChE J. 9, 35 (1963)

DEISSLER, R.G. & Eian, C.S., Investigation of effective thermal conductivities of powders. N.A.C.A., Washington, RME52C05 (1952)

ECKERT, E.R.G., & Drake, R.M., Analysis of Heat & Mass Transfer, Mcgraw-Hill, New York (1972)

EDWARDS, J.C., Mathematical modelling of spontaneous combustion of coal. Presented at the 112th Annual meeting of A.I.M>E., (1983)

GIJBELS M.R., & Bruining J., Spontaneous ignition time of underground coal - Estimation from oxidation rates determined in the laboratory. Erdoel und Kohle, 8, 376, (1982)

GUNEY, M. & Hodges, D.J., Adiabatic apparatus designed to study self-heating rates of coal. Chem & Industry, 42, 1429 (1968)

GUNEY, M., Oxidation and spontaneous heating of coal. J. of Pure And Applied Sciences, 5, 1, (1972)

GUNN, D.J. & Khalid, M., Thermal dispersion and wall heat transfer in packed beds. Chem. Eng. Sci., 30, 261 (1975)

KIBRIA, J., Effect of properties and enviromental variables on self heating tendencies of lignite. M.Sc. Thesis, University of North Dakota (1972)

KRAMERS, H. & Westerterp, K., Elements of Chemical Reactor Design & Operation, Academic Press, New York (1963)

KUNII, D. & Smith, J.M., Heat Transfer characteristics of porous rocks. AIChE J., 6(1), 71, (1960)

LAPWOOD, E.R., Convection of a fluid in a porous medium. Proc. Cam. Phil. Soc., 44, 508, (1948)

LEVENSPIEL, O., Chemical Reaction Engineering, Wiley, New York (1962)

LUSS, D., Sufficient Conditions for Uniqueness of the Steady State Solutions in Distributed Parameter Systems. Chem. Eng. Sci., 23, 1249, (1968)

LUSS, D. & Amundson, N.R., Uniqueness of the Steady State Solutions For Chemical Reaction Occcurring in a Catalyst Particle or in a Tubular Reactor with Axial Diffusion. Chem. Eng. Sci. 22, 253, (1967)

MURTAGH, B.A., The spontaneous heating of coal. M.Eng Thesis, Department of Chemical Engineering, University of Canterbury (1966)

NORDON, P., Model for the self-heating reaction of coal and char. Fuel, 58, 456 (1979)

NORDON, P., Young, B.C. & Bainbridge, N.W., The rate of oxidation of char and coal in relation to their tendency to self-heat. Fuel, 58, 443 (1979)

PERRY, R.H., & Chilton, C.H., editors of Chemical Engineer's Handbook, 5th edition, Mcgraw Hill, Tokyo (1973)

SCHMIDT, L.D., in Chemistry of Coal Utilization, Wiley, New York (1945)

SCHOTTE, W., Thermal conductivity of packed beds. AIChE J. 3, 373 (1960)

SONDREAL, E.A. & Ellman, R.C., Laboratory Determination of factors affecting storage of North Dakota Lignite. Bureau of Mines Report. R.I. 7887, (1974)

A SIMPLIFIED MODEL FOR SPONTANEOUS COMBUSTION IN COAL STOCKPILES

Kevin Seth Brooks

A thesis submitted to the Faculty of Engineering, University of the Witwatersrand, Johannesburg, in fulfilment of the requirements for the degree of Doctor of Philosophy.

July 1985

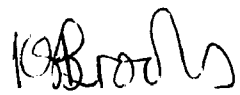
Johannesburg

NK 6717/1

DECLARATION

The work described in this thesis was carried out in the Department of Chemical Engineering of the University of the Witwatersrand, Johannesburg, and is the original and independent work of the author except where specifically acknowledged in the text.

No part of the thesis has previously been submitted for a degree in the University of the Witwatersrand, or is being submitted to any other University.



K S BROOKS

July 1985

ABSTRACT

Based on a study of the fundamental processes of heat,mass and momentum transfer, a one-dimensional model to predict the behaviour of coal dumps with respect to spontaneous combustion is presented.

Heat transfer within the dump is modelled using an effective thermal conductivity. This quantity has been measured for a typical coal sample using a guarded hot ring apparatus. Mass transfer is considered to occur by natural convection and wind pressure. Diffusion is shown to be unimportant except for very fine material.

A shrinking-core model for the low temperature oxidation of coal is proposed; the model explains the fact that the coal reactivity decreases with time. The effects of moisture on the coal reactivity are neglected due to lack of data.

Estimates of the parameters required for the model have been obtained experimentally. The equations are solved analytically in both the steady and unsteady-state under the assumption of unchanging rate constant. A numerical method has been used to solve the equations without this assumption.

It has been shown that coal dumps may be classified as either safe, unsafe or conditionally safe. Safe coal dumps are either oxygen limited or heat transfer limited. The former is the case for fine reactive coal; the high reactivity of the coal means that all the oxygen reacts close to the surface where the heat produced can easily be dissipated. The latter is the case for for coarse, unreactive material; although the oxygen is freely available throughout the dump, the reactivity per unit volume of the coal is sufficiently low such that heat produced can be dissipated without the temperature rising significantly.

It is shown that the important parameters in predicting the behaviour of a coal bed are the particle size distribution of the coal, the bed voidage and the reaction rate parameters. The effect on the temperature in a coal bed of changing each of parameter is presented graphically. The unsteady-state behaviour of the model shows that the time taken to reach a certain critical temperature may be the best way of arriving at a safe stockpiling time.

For my wife, Ilana:

A good typist and an even better cook

ACKNOWLEDGEMENTS

I should like to express my gratitude to my supervisor, Professor David Glasser, for his help, interest and encouragement during the course of this work.

As well as being a good friend, Mr (now Dr) Michael Itay performed the experimental work described in Chapter 2.

Mr L Schwartz and Mr A C Harris were of great assistance in the building of experimental apparatus.

The work described in this thesis was made possible by the financial assistance of the Iron and Steel Corporation of South Africa.

CONTENTS

	Page
DECLARATION	ii
ABSTRACT	iii
DEDICATION	iv
ACKNOWLEDGEMENTS	v
CONTENTS	vi
LIST OF FIGURES	x
LIST OF TABLES	xii
LIST OF SYMBOLS	xiii
1. AN OVERVIEW OF SPONTANEOUS COMBUSTION	1
1.1 Introduction	1
1.2 Previous Investigations into Spontaneous Combustion	3
1.3 Transport in a Coal Dump	6
1.4 The Chemical Reactivity of Coal	6
1.4.1 Reaction between Coal and Water	7
1.4.2 Low Temperature Oxidation of Coal	8
1.5 Heat Transfer within a Coal Dump	12
1.6 A Mathematical Model for Spontaneous Combustion	12
1.7 Experimental Investigation	13
1.8 Results and Conclusions	13
2. ANALYSIS OF SUGGESTED MECHANISMS FOR INGRESS OF REACTANTS	14
2.1 Introduction	14
2.2 Natural Convection and Wind Pressure	14
2.3 Analysis of Molecular Diffusion	18
2.4 Barometric Breathing	21
2.5 Thermal Breathing	22
2.6 Conclusions	23
3. THEORETICAL MODELS FOR HEAT TRANSFER IN PACKED BEDS	25
3.1 Introduction	25
3.2 Mechanisms of Energy Transfer in Packed Beds	25
3.3 Describing the Overall Energy Transfer in a Packed Bed	26

3.4 Models for Energy Transfer in which only conduction is considered 26

3.5 Models for Energy Transfer in which conduction and radiation are considered 31

3.5.1 Conditions under which radiation in a packed bed is likely to be significant 33

3.6 Theoretical Studies of Natural Convection 34

3.7 The Effect of flow on Energy Transfer in a Packed Bed 37

3.8 Conclusions 37

4. MEASUREMENT OF THE EFFECTIVE THERMAL CONDUCTIVITY OF A PACKED BED OF COAL 39

4.1 Introduction 39

4.2 Theory of the Measurement of Thermal Conductivity 39

4.3 Steady-state Methods for Measuring Thermal Conductivity 40

4.3.1 Measurements in the rectangular system 41

4.3.2 Measurements in the cylindrical system 43

4.3.3 Measurements in the spherical system 44

4.4 Unsteady-state or Dynamic Methods 44

4.5 Choice of Measurement Method for Packed Bed of Coal 45

4.6 Design and Construction of Guarded Hot Ring Apparatus 46

4.6.1 General Design Considerations 46

4.6.2 Heat Sinks 46

4.6.3 Heating Elements 48

4.6.4 Outer Containing Vessel 48

4.6.5 Water supply to heat sinks 50

4.6.6 Measurement Techniques 50

4.7 Experimental Procedure 51

4.8 Results and Discussion 52

5. MATHEMATICAL MODELLING OF A ONE-DIMENSIONAL ANALOGUE OF A COAL DUMP 54

5.1 Introduction 54

5.2 Literature survey of mathematical models 54

5.3 A One-dimensional Analogue of a Coal Dump 61

5.4 Model Equations 63

5.5 Discussion of the Model Equations 65

5.6 Boundary and Initial Conditions 66

6. SIMPLIFICATION OF THE MODEL EQUATIONS AND THEIR SOLUTION 67

6.1 Introduction 67
6.2 The Steady-State form of the Equations 69
6.3 The Solution of the Unsteady-State Equations with a constant rate 71
6.4 A Numerical Method for Solving the Unsteady-State Equations 72

7. EXPERIMENTAL INVESTIGATION OF THE BEHAVIOUR OF A ONE-DIMENSIONAL ANALOGUE OF A COAL DUMP 75

7.1 Introduction 75
7.2 Experimental 75
7.3 Results 78
7.4 Discussion 81

8. RESULTS OF SOLVING THE MODEL EQUATIONS 82

8.1 Introduction 82
8.2 Steady-State Solution for constant r 82
8.2.1 The Character of the Solutions 83
8.2.2 Effect of varying the voidage 90
8.2.3 Effect of varying the pre-exponential Factor 92
8.2.4 Effect of varying the activation energy 94
8.2.5 Effect of different assumptions about the reactive surface area of coal 94
8.2.6 The Meaning of Particle Size 95
8.2.7 Effect of wind on maximum Temperature 98
8.2.8 Effect of Thermal Conductivity on maximum Temperature 98
8.2.9 Effect of Changing the Bed Length 98
8.3 Unsteady-State solutions for r constant 101
8.3.1 Introduction 101
8.3.2 The Character of the Solutions 101
8.3.3 Discussion 107
8.4 Results of solving the equations numerically 107
8.4.1 Introduction 107
8.4.2 Comparison Between the Numerical Method and the Analytical Method 108
8.5 Conclusions 110

9. CONCLUSIONS 111

Appendix 1 Derivation of a rate equation for the low temperature oxidation of coal 116

Appendix 2 Tabulation of measured thermal conductivities 120

Appendix 3 Derivation of model equations 122

Appendix 4 The continuum and pseudo steady-state assumptions 130

Appendix 5 The inclusion of a radial heat loss term in equation 6.1.4 132

Appendix 6 Explanation for the Instability of the Runge-Kutta algorithm 135

Appendix 7 Solution of equation 6.2.2 with r constant 136

Appendix 8 Solution of equation 6.1.5 with r constant 137

Appendix 9 Application of the method of lines to the solution of equation 6.1.5 140

Appendix 10 Results of chimney experiment 142

Appendix 11 Model Parameters used as base case 165

Appendix 12 Listing of computer programs 166

REFERENCES 194

LIST OF FIGURES

Figure		Page
1.1	Temperature, Oxygen and Carbon Dioxide Versus Time	9
3.1	Geometrical Conduction Models (Beveridge & Haughey, 1971)	28
4.1	Guarded hot ring apparatus - Heat sink	47
4.2	Guarded hot ring apparatus - Assembled apparatus	49
5.1	Streamlines in a packed bed containing a line source	62
7.1	Chimney experiment - Apparatus	76
7.2	Chimney experiment - Fitting heat transfer coefficients	79
7.3	Chimney experiment - Fitting ageing run 1	79
7.4	Chimney experiment - Fitting ageing run 2	80
7.5	Chimney experiment - Fitting ignition runs	80
8.1	LHS and RHS of equation 8.2 as a function of θ	86
8.2	Locus of solutions to equation 8.2	86
8.3	Stable and unstable solutions for the base-case	91
8.4	Effect of varying voidage on the maximum temperature	91
8.5	Effect of varying the pre-exponential factor on the maximum temperature	93
8.6	Effect of varying the activation energy on the maximum temperature	93
8.7	Pre-exponential factor versus particle size for the two cases considered	96
8.8	Effect of different assumptions about surface area on the maximum temperature	96
8.9	Effect of wind on the maximum temperature	99
8.10	Effect of varying bed thermal conductivity on the maximum temperature	99
8.11	Effect of varying bed length on the maximum temperature	100
8.12	Temperature-time curves in the centre of a coal bed for different initial temperatures	102
8.13	Temperature profiles in a coal bed Particle size 10 mm - Analytical solution	102
8.14	Temperature-time behaviour at bed centre Particle size 6 mm - Analytical solution	106
8.15	Temperature profiles in a coal bed Particle size 10 mm - Numerical Method	106

Figure		Page
8.16	Temperature profiles with ignition Particle size 2 mm - 5 m/s wind - Numerical method	109
8.17	Cross plot of Figure 8.16 at bed centre	109
A1.1	Simplified coal particle geometry	116
A2.1	Measured thermal conductivities versus difference between guard and main heater temperatures	121
A3.1	Differential element of a coal bed	122
A5.1	Differential element in the form of a ring	132

LIST OF TABLES

Table		Page
2.1	Molar Flowrates for Various Particle Sizes	17
2.2	Comparison of Molecular Diffusion and Convection	21
5.1	Values of ΔT L Required for Ra = 4 π^2	59
5.2	Unknowns in the model equations	65
8.1	Particle Size Distribution for a typical sample	97
8.2	Model Parameters for Figure 8.12	101
8.3	The Quantity 'a' For Various Particle Sizes	105
A2.1	Measured Thermal Conductivities	120

LIST OF SYMBOLS

a: Dimensionless quantity in equation 6.1.4

a': Fitting constant in equation 5.2.1

a_{ij}: Weighting coefficients for first derivatives

A: Area

A': Fitting constant in equation 5.2.1

A^*: Arrhenius pre-exponential factor

$\underline{A}$: Matrix of coefficeints a_{ij}

A_o: Pre-exponential factor in equation 5.2.8

b: Dimensionless quantity in equation 6.1.4

b_{ij}: Weighting coefficients for second derivatives

B: Elovich constant

$\underline{B}$: Matrix of coefficients b_{ij}

Bi_o: Biot number at $X = 0$

Bi_1: Biot number at $X = 1$

Bi_2: $Bi_o + a/2$

Bi_3: $Bi_1 + a/2$

c: Heat loss coefficient

$\bar{c}$: Heat capacity per unit mass

$\bar{c}_s$: Heat capacity per unit mass of solid

$\bar{c}_w$: Heat capacity per unit mass of liquid water

$\bar{c}_j$: Heat capacity per unit mass of component j in the solid

$\bar{c}_b$: Heat capacity per unit mass of bed

$\hat{c}$: Molar heat capacity of the gas

$\hat{c}_i$: Molar heat capacity of component i in the gas

C_p: Specific heat capacity

C: Oxygen concentration

C_s: Oxygen concentration at reaction surface

C_1: Integration constant

C_2: Integration constant

C_3: Integration constant

D: Molecular diffusion coefficient

D_e: Effective diffusivity of oxycoal

D_p: Particle diameter

E: Activation energy

f: d'Arcy's law constant

f_j: Mass fraction of component j in the solid

g: Acceleration due to gravity

$g(X)$: Auxilary temperature function

G: Molar flowrate per unit area

h_o, h_1: Heat transfer coefficients

h_R: Heat transfer coefficient on radial surface

$\hat{H}$: molar enthalpy of gas

$\hat{H}_i$: molar enthalpy of component i in the gas

$\bar{H}$: Solid enthalpy per unit mass

$\bar{H}_j$: Enthalpy per unit mass of component j in solid

I_m: Main heater current

J_i: ith order Bessel function of the first kind

k: Thermal Conductivity

k_g: Gas thermal conductivity

k_s: Solid thermal conductivity

k_b: Bed thermal conductivity

$k_{b,x}$: Bed thermal conductivity in axial direction

$k_{b,R}$: Bed thermal conductivity in radial direction

k_o: Pre-exponential factor

k_r: $k_o \exp(-E/(RT))$

l: sample thickness

l_1, l_2: Distances between heater and sinks (equation 4.6.2)

L: Bed length or height

L_e: Effective particle length

m: Moles of oxygen per moles of nitrogen in the gas

m: Water flowrate

M: number of components in the solid phase

M_c: Mass of coal

M_w: Mass of absorbed water in the coal

M_p: Percent moisture in the coal

M_n: n th root of the equation $J_o(M_n)=0$

M': Dimensionless quantity defined by equation 5.2.3

n: Order of the Legendre polynomial P_n

N: Number of components in the gas phase

N': Dimensionless quantity defined by equation 5.2.4

p_j: Rate of Formation per unit bed volume of component j in the solid

P: Pressure

P_∞: ambient pressure

$\hat{P}$: $P - P_\infty$

$P_n(X)$: n th order Legendre polynomial

$P_n^*(X)$: n th order shifted Legendre polynomial

q: Amount of O_2 taken up per unit mass of coal

q_g: Flux in gas

q_s: Flux in solid

q': Source term in Diffusion Equation

Q': Rate of energy transfer by Conduction

Q_c: Rate of Convection from Solid to Gas

Q: Rate of energy input

Q_q: Rate of Energy absorption

Q_R: Radial Flux

Q_x: Axial Flux

r_i: Rate of formation per unit bed volume of i in the gas phase

r_o: Rate of oxidation at T_∞ for fresh coal

r: Rate of oxygen adsorption per unit bed volume for unity mole fraction oxygen

R: Gas constant

r: Radial co-ordinate (Chapter 4)

R: Spherical co-ordinate (Chapter 4)

R: Radial Distance (Appendix 5)

R_o: Bed Radius (Appendix 5)

S_t: Total reactive surface per particle volume

S: Total external surface per particle volume

S_m: External surface area per unit mass

S': Total surface area for reaction

t: Time

T: Temperature

T_∞: Ambient Temperature

T_g: Gas Temperature

T_s: Solid temperature

T': Temperature averaged radially

T_∞: Ambient Temperature

T_{av}: Average temperature = $L/\int_0^L T^{-1}dx$

$T_o(X)$: Initial temperature profile

U: Flow velocity

U_g: Gas internal energy

U_s: Solid internal energy

$\hat{U}$: Molar internal energy of the gas

$\bar{U}_s$: Internal energy of the solid per unit mass

$u(X,\tau)$: Auxilary temperature function (equation A8.2)

V: Wind velocity

v: Temperature above ambient

$v(X,\tau)$: Auxilary temperature function (equation 6.3.2)

V_b: Bed volume

V_p: Particle volume

V_m: Main heater voltage
x: Distance along bed
X: Dimensionless distance = x/L
y: Rectangular co-ordinate (Chapter 4)
y_i: Mole fraction of i in the gas phase
y_o: Mole fraction of oxygen at X=0
y: Mole fraction oxygen in the gas phase
z: Rectangular co-ordinate (Chapter 4)
z: Thickness of oxycoal layer
Z: Fractional conversion of coal
$Z_n(X)$: See equaiton 6.3.3

Greek Symbols

α: Fitting constant in equation 5.2.1
β: Roots of equation 6.3.4
γ_1,γ_2: $((a\pm(a^2+4C))^{1/2})/2$
γ_3: $-rL/G$
ΔH_w: Latent heat + heat of wetting
ΔH_r^i: Enthalpy of reaction
ΔH_r: Enthalpy of reaction for oxygen adsorption
ΔT: Temperature rise or temperature difference
ϵ: Voidage
η: Tortuosity factor
θ: Dimensionless temperature
$\theta_o(X)$: Initial dimensionless temperature profile
$\theta_{ss}(X)$: Steady-state dimensionless temperature profile
κ: Thermal diffusivity
μ: Gas viscosity
ν: D P/(R T)
ξ: $1/\tau'$
ρ: Density
ρ_s: Solid density
ρ_b: Bed density
ρ_g: Molar density of gas
ρ_∞: Density of gas at T_∞,P_∞
ρ_m: Molar density of oxycoal
σ: Stefan-Boltzmann constant
τ: Dimensionless time
τ_o: Period of oscillation
τ': Time constant for heat loss (Equation 5.2.5)
$\phi(X)$: Auxilary temperature function (equation A8.2)
ϕ_1,ϕ_2: Fitting constants in equation 8.1
τ_d: Time constant for equilibration of gas and solid

temperatures

τ_c: Time constant for conduction

τ_f: Time constant for flow

τ_p: Time constant for pressure change

1. AN OVERVIEW OF SPONTANEOUS COMBUSTION OF COAL

1.1 Introduction

The need to stockpile coal arises in many situations, most importantly in the following fields:

a) The generation of electricity

b) The coal mining industry

c) Coal transport

d) Steel making

It is well known that certain types of coal, when stockpiled, are liable to spontaneous combustion. Coal may undergo spontaneos combustion in many storage situations, among them:

a) In coal dumps

b) Underground

c) In the holds of ships

d) In storage silos or bunkers

The work described in this thesis concerns mainly spontaneous combustion as it relates to coal dumps. However, many of the conclusions reached are of significance, to a greater or lesser extent, in all of the storage situations mentioned above.

Spontaneous combustion of coal may lead to some or all of the following problems:

a) Loss of all or part of the coal dump. If the coal dump is a large one, as is the case at many mines and power stations, the economic effects of spontaneous combustion may well be disastrous.

b) Pollution. A burning coal dump presents a very real environmental problem, with noxious gases and particulate matter

being introduced into the atmosphere. This can present serious problems to communities in the vicinity of the burning dump.

c) Danger to human lives. Burning coal dumps can give rise to a dangerously high level of carbon monoxide, which may affect people working in the vicinity. Similarly, fires in ship's holds or underground can be extremely dangerous as well as costly.

Methods have been suggested, and are in use, for making coal dumps less liable to spontaneous combustion. These methods include compacting the dump, covering the dump with tar or sand, or spraying a cement-like substance on the surface of the dump. In addition much discussion has revolved around the monitoring of coal dumps, in order to obtain early warning of potential problems. Temperature monitoring by means of thermocouples, the taking of infra-red photographs and gas sampling have all been suggested and used as means of monitoring coal dumps.

One of the problems with the methods discussed above is that they tend to be costly, and the economic justification for their use is often not immediately obvious. The reason for this is that the knowledge that has been obtained in the field of spontaneous combustion is largely empirical, being based on experience gained by people working in the field. Although this knowledge is exteremely valuable, it is not always of great use when new stockpiling situations arise, or when a new mine is opened and the newly mined coal's liability to spontaneous combustion is an unknown quantity.

It seems clear that what is required is a sound scientific analysis of spontaneous combustion, on which decisions as to stockpiling practice can be based. The aim of this thesis is to provide this analysis, by analyzing the fundamental processes occuring in a coal dump, and synthesizing their effects in a mathematical model. The model can then be used as a basis on which predicitions about the behaviour of a certain coal in a certain stockpiling situation can be made. Hopefully this will lead to the construction of stockpiles in which the chances of spontaneous combustion occuring are minimized.

1.2 Previous Investigations into Spontaneous Combustion

A comprehensive reviews of spontaneous combustion of coal has been presented by Itay (1984). The aim of this section is to provide a critical review in which the important facts that have emerged are summarised. These facts will then be further discussed.

Many workers have concerned themselves with oxidation of coal (Van Krevelen,1981) and the literature on the subject has been reviewed by Guney (1968). The main conclusions reached are

a) The oxidation of coal appears to be a chemisorption reaction at temperatures under 70 ^{o}C; oxygen is taken up without water or carbon dioxide being formed.

b) The enthalpy of reaction is of the order of 300 kJ per mole of oxygen adsorbed (Edwards, 1983 and Sondreal & Ellman, 1974). This may be compared with an enthalpy of reaction of 390 kJ/mole for the reaction

$$C(graphite) + O_2(g) = CO_2(g).$$

c) The rate of oxidation decreases with time i.e. the coal ages.

d) The reaction rate appears to be of order ½ to 1 with respect to the oxygen concentration.

A series of investigators have reported different activation energies for the oxidation; these discrepancies appear to be due to the various ranges of temperature covered.

Van Krevelen (1981) believed that the primary reaction of chemisorption of oxygen has a relatively low activation energy of approximately 3 - 4 Kcal/mole.

Above a temperature of 70 ^{o}C decomposition of the adsorption complex may occur, with an activation energy of approximatley 6.5 Kcal/mole. However, chemisoption of oxygen occurs up to a temperature of 350 ^{o}C.

Many other investigators, notably Guney (1972) and Bhattacharyya

(1970) have investigated the effect ot moisture in the coal and reacting gas. The absorption of water is, not surprisingly, associated with a large enthalpy of reaction. In addition it appears that the absorbed moisture in the coal plays a part in the oxidation reaction, for dry coal oxidises at a far lower rate than moist coal. However, the effect of moisture on self heating of coal is still a subject of intense debate, mainly because different investigators have reported different results. This appears to be due to different apparatus and analysis methods being used, as well as different sample preparation techniques (e.g. vacuum drying, oil drying and air drying all at room temperature or elevated temperatures).

One important point has emerged from the studies performed by Murtagh (1966) who used a computer simulation technique. His main conclusion is that at low temperature moisture transfer is the dominant heat transfer mechanism in a dump, but that spontaneous ignition does not occur when only moisture is considered. His explanation for this is that at about 100 ^{o}C inherent moisture is driven from the coal, causing a cooling. Since there can be no further absorption of water, the maximum temperature that can occur is approximately 100 ^{o}C. It should be pointed out that should a coal dump reach a temperature of 100 ^{o}C, then it might be well on the way to combustion, since the rate of oxidation could be very high at this temperature.

It thus appears from the literature that moisture effects, especially the absorption of water by dry coal, can lead to an increase in the temperature of a coal dump to the point where the rate of oxidation becomes appreciable. In this situation the coal dump could be at risk.

This conclusion has a important consequence when one considers spontaneous combustion underground as opposed to spontaneous combustion above ground. In the underground situation the coal is likely to be dry, especially if it is newly mined. In addition the humidity of the air in the mine is high. Thus underground spontaneous combustion could be largely triggered by moisture absorption. However, when considering coal stockpiles, it should be remembered that these are normally laid down with water to facilitate compaction. In addition the coal that is stockpiled has generally come from a washing plant, and is thus wet. Thus the effect of moisture on a newly laid down coal dump is likely

(1970) have investigated the effect ot moisture in the coal and reacting gas. The absorption of water is, not surprisingly, associated with a large enthalpy of reaction. In addition it appears that the absorbed moisture in the coal plays a part in the oxidation reaction, for dry coal oxidises at a far lower rate than moist coal. However, the effect of moisture on self heating of coal is still a subject of intense debate, mainly because different investigators have reported different results. This appears to be due to different apparatus and analysis methods being used, as well as different sample preparation techniques (e.g. vacuum drying, oil drying and air drying all at room temperature or elevated temperatures).

One important point has emerged from the studies performed by Murtagh (1966) who used a computer simulation technique. His main conclusion is that at low temperature moisture transfer is the dominant heat transfer mechanism in a dump, but that spontaneous ignition does not occur when only moisture is considered. His explanation for this is that at about 100 ^{o}C inherent moisture is driven from the coal, causing a cooling. Since there can be no further absorption of water, the maximum temperature that can occur is approximately 100 ^{o}C. It should be pointed out that should a coal dump reach a temperature of 100 ^{o}C, then it might be well on the way to combustion, since the rate of oxidation could be very high at this temperature.

It thus appears from the literature that moisture effects, especially the absorption of water by dry coal, can lead to an increase in the temperature of a coal dump to the point where the rate of oxidation becomes appreciable. In this situation the coal dump could be at risk.

This conclusion has a important consequence when one considers spontaneous combustion underground as opposed to spontaneous combustion above ground. In the underground situation the coal is likely to be dry, especially if it is newly mined. In addition the humidity of the air in the mine is high. Thus underground spontaneous combustion could be largely triggered by moisture absorption. However, when considering coal stockpiles, it should be remembered that these are normally laid down with water to facilitate compaction. In addition the coal that is stockpiled has generally come from a washing plant, and is thus wet. Thus the effect of moisture on a newly laid down coal dump is likely

to be a beneficial one i.e. the evaporation of water will cause cooling. However, should there be very dry conditions causing drying out of the coal, followed by humid conditions, moisture absorption may well occur.

It is neccessary to look at the other factors involved in spontaneous combustion. These have been shown by many investigators (Sondreal & Ellman, 1974, Nordon, 1979) to be:

a) Transport into the dump and
b) Heat transfer within the dump.

As many investigators have pointed out, the importance of these two effects should not be underestimated. No matter how reactive a given coal is it will not undergo spontaneous combustion if

a) The reactants cannot get to it or
b) The heat generated by reaction can be readily transferred out of the dump.

Investigators have previously used mathematical models, based on energy balances for a reacting bed of coal, to try and predict the onset of spontaneous combustion. Notable among these investigators are Van Doornum (1954), Murtagh (1966), Sondreal & Ellman (1974) and Nordon (1979). The work of Murtagh (1966) has been discussed, and the work of the other three investigators will be further discussed in section 5.2. It is shown that the models used by these investigators suffer from the shortcoming that the effect of natural convection is ignored. The justification for ignoring this effect has been based on conclusions drawn by these researchers from the work of Lapwood (1948). The validity of these conclusions will be discussed in section 5.2.

Having reviewed the literature on the subject of spontaneous combustion of coal, it is felt that three main areas of importance in predicting the behaviour of a coal dump have been identified.

They are:

a) Mechanisms whereby reactants such as oxygen and water are transported into a dump.

b) The chemical reactions that occur betwen coal and these reactants, in particular the thermal effects of these reactions.

c) Heat transfer within the dump.

These three areas will now be discussed separately.

1.3 Transport in a Coal Dump

Five mechanisms whereby reactants may be transported into a coal dump have been identified. They are:

a) Natural convection caused by self heating of the dump.

b) Wind pressure on the inclined surfaces of the dump which causes flow.

c) Molecular diffusion caused by concentration gradients.

d) Barometric breathing caused by changes in barometric pressure.

e) Thermal breathing caused by the daily variation in temperature.

In order to decide which, if any, of these mechanisms is the most important source of reactants to a coal dump it was felt necessary to derive simple models to describe each mechanism. These models give an idea of the order of magnitude of each of the effects and lead to important conclusions regarding which mechanisms may be neglected and which may not. A full discussion of these models is given in Chapter 2.

1.4 The Chemical Reactivity of Coal

Spontaneous combustion of coal occurs due to reaction between atmospheric gases and coal. The gases that are of importance are water vapour and oxygen. A discussion of the reactivity of coal towards these reactants follows.

1.4.1 Reaction between Coal and Water

Much experimental effort has been devoted to the elucidation of the effect of moisture on spontaneous combustion of coal. Nordon, Young & Bainbridge (1979) have pointed out that the effect of moisture on the self heating of coal is two-fold. Firstly absorbed water exerts a catalytic effect on the oxidation rate, and secondly there is a transient effect which occurs as moisture is absorbed or desorbed. This partly explains why so many apparently contradictory results in connection with the effect of gas and coal moisture on self heating of coal have been obtained, since confusion arises due to the different ways in which the coal is dried, and the coal and atmospheric moisture contents are reported.

The catalytic effect of coal moisture content on the oxidation rate is well documented in the literature. Sondreal & Ellman (1974) report oxidation rates of lignite as being proportional to

$$1 + 0.674\ M_p - 0.01634\ M_p^2$$

where M_p is the moisture content expressed in percent. This expression implies that the rate of oxidation is a maximum when M_p is equal to twenty percent. This value is close to the equilibrium moisture content of coal.

The second effect mentioned is the transient absorption and desorption of moisture. The heat effect associated with the absorption of moisture is the latent heat of vaporization plus the heat of wetting. The former has a value of 500 cal/g at 25 °C and the latter has been reported by Sondreal & Ellman (1974) to be of the order of 24 cal/g. A simple energy balance may be written to calculate the temperature rise due to absorption of moisture by dry coal.

1.4.1

$$M_c\ \bar{c}_b\ \Delta T = M_w\ \Delta H_w$$

where M_c = mass of coal
$\bar{c}_b$ = specific heat capacity of coal
ΔT = temperature rise
M_w = mass of water absorbed
ΔH_w = latent heat + heat of wetting

Therefore $\Delta T = \frac{M_w \Delta H_w}{M_c \bar{c}_b}$ 1.4.2

Assume $M_w/M_c = 0,05$ i.e the coal absorbs five percent of its mass of moisture. The specific heat of a typical coal is 0,25 cal/g/K. By equation 1.4.2

$$\Delta T = \frac{0,05 \times 524}{0,25} = 104,8 \text{ K}$$

This is a substantial temperature rise, which will never be achieved in practise since as the coal absorbs moisture and the temperature increases the vapour pressure of the water above the coal increases and the reaction rapidly comes to equilibrium.

As has been pointed out by Kibria (1972) heating due to moisture absorption may bring coal to a temperature where oxidation occurs at a dangerous rate. This point is extremely important; water absorption may well be a starting mechanism whereby the tempe- rature inside a coal pile which is at risk starts rising leading to the onset of a large amount of oxidation and eventual com- bustion. The opposite is also true; if a coal dump is inherently safe no amount of water absorption will start it burning; com- bustion occurs due to oxidation, and not due to moisture effects.

1.4.2 Low Temperature Oxidation of Coal

The amount of literature on the chemical reactivity of coal, and in particular its low temperature oxidation, is vast. However, for the reason that every coal is likely to have a different reactivity, it was felt that a new study had to be undertaken. This work was performed by M. Itay, at the department of Chemical Engineering at the University of the Witwatersrand. A summary of the conclusions reached by Itay (1984) is presented in this section.

The experimental apparatus used to conduct these studies was a nearly adiabatic reaction vessel into which coal is packed and oxygen introduced. The temperature-time history of the reaction is recorded, and gas samples are taken periodically and analyzed for O_2, N_2, CO, CO_2, and H_2O. The measured temperature time

curve is used to back calculate the adiabatic temperature time curve, and this curve is used to obtain information on the rate of reaction and on the thermal effects associated with the reaction.

The data obtained thus far points very strongly to the conclusion that the chemical reactivity of the coal falls off with the degree of oxidation of the sample. This effect is well known and has been much reported in the literature (see for example Van Krevelen, 1981). However few plausible explanations for the effect have been given.

Another important conclusion is that the disappearance of oxygen is not neccessarily accompanied by the appearance of reaction products e.g. CO_2. It appears that at a low temperature coal adsorbs O_2 strongly and desorbs CO_2 at a far lower rate. This has also been noted in the literature, and the increase in density of reacting coal samples strongly supports this fact (Van Krevelen, 1981). In addition the desorption of the CO_2 appears to have a small enthalpy of reaction. This behaviour is shown graphically in Figure 1.1.

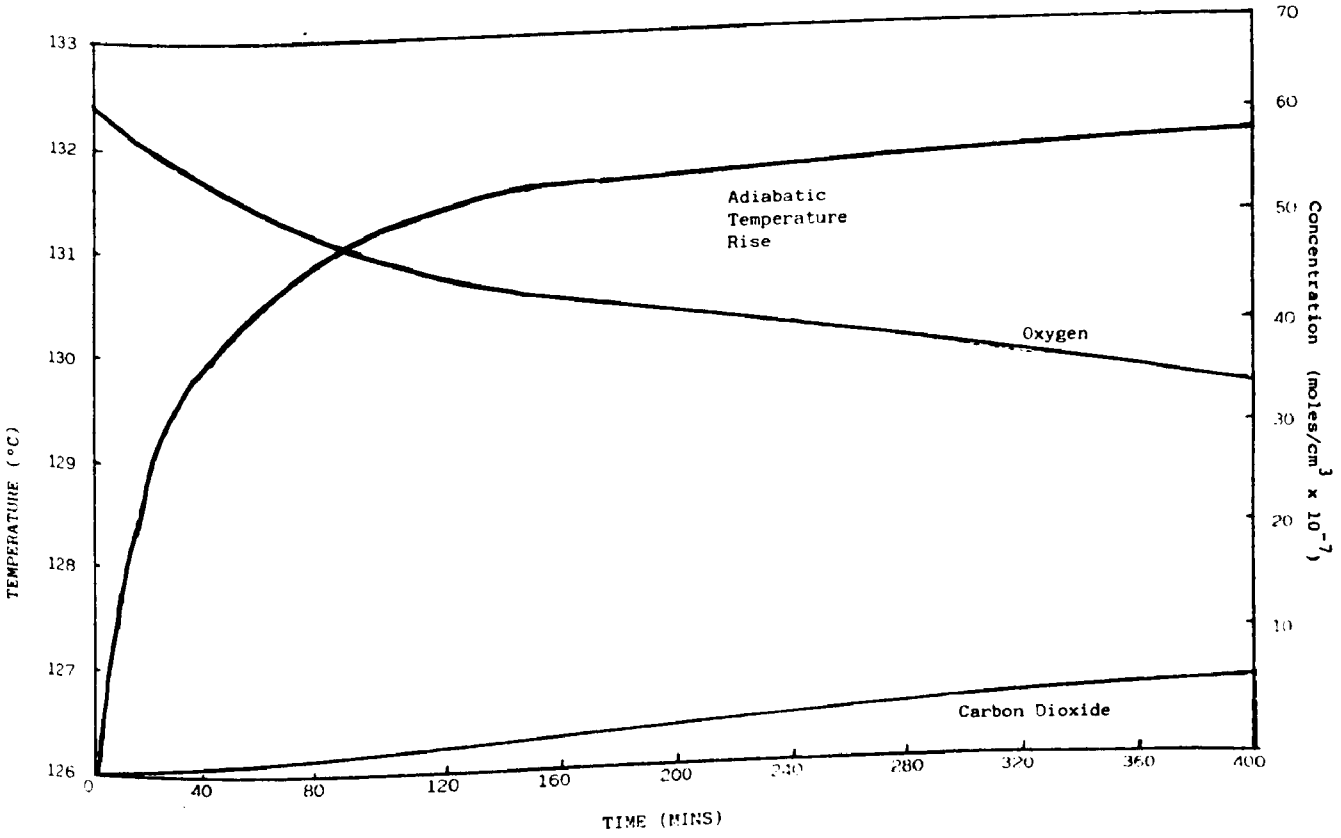


Figure 1.1 Temperature, Oxygen and Carbon Dioxide Versus Time

(After Itay, 1984)

In order to explain these effects a model for the reaction of coal with oxygen has been jointly derived by this researcher and Itay . The model is based on the hypothesis that coal absorbs oxygen to form a complex, which may be called oxycoal, without the formation of any gaseous products. The formation of an oxycoal layer on the surface of the coal has been demonstrated in the literature, and photographs showing this effect have been published by Van Krevelen (1981). As the oxycoal layer builds up the reaction rate slows down due to the fact that oxygen now has to diffuse through the oxycoal to react with the coal. This reaction model is an example of the so called shrinking core model, which is thoroughly discussed by Levenspiel (1962).

The derivation of the rate equation that follows from these assumptions is given in Appendix 1. The equations take the form:

Rate of adsorption of oxygen / unit volume of bed =

$$r = \frac{S_t\ (1-\epsilon)\ C}{1/k_r + Z/(S_t\ D_e)} \qquad 1.4.3$$

$$\frac{dZ}{dt} = \frac{S_t\ C}{\rho_m\ (1/k_r + Z/(S_t\ D_e))} \qquad 1.4.4$$

Where $S_t = \dfrac{\text{total surface area of particle}}{\text{volume of particle}}$

ϵ = bed voidage

C = O_2 concentration

k_r = surface rate constant

Z = fractional conversion of coal

D_e = effective diffusivity of oxycoal layer

ρ_m = molar density of coal

The temperature dependence of the reaction is given by the usual Arrhenius relationship i.e.

$$k_r = k_o \exp(-E/(R\,T)) \qquad 1.4.5$$

k_o = pre-exponential factor
E = activation energy
R = gas constant
T = temperature

In order to better understand the behaviour of this reaction model, the equations were solved under the assumptions of constant O_2 concentration and a constant value of k_r, the surface rate constant.

Under this assumption equation 1.4.4 gives

$$Z/(S_t\,D_e) = -1/k_r^2 + (1/k_r^2 + 2Ct/(\rho_m\,D_e))^{1/2} \qquad 1.4.6$$

Back substitution in equation 1.4.5 gives

$$r = S_t\,(1-\epsilon)\,C\,/(1/k_r^2 + 2Ct/(\rho_m\,D_e))^{1/2} \qquad 1.4.7$$

Two limiting cases were considered. In the early stages of reaction the oxycoal layer has not built up and the rate of the chemical reaction is limiting. In this case

$$1/k_r^2 \gg 2Ct/(\rho_m\,D_e)$$

$$\text{and } r = k_r S_t (1-\epsilon) C \qquad 1.4.8$$

i.e. in the early stages of reaction the rate is first order with respect to the O_2 concentration and is time independent.

However when more reaction has taken place it is reasonable to assume that the diffusion through the oxycoal layer is limiting. In this case

$$1/k_r^2 \ll 2Ct/(\rho_m\,D_e)$$

$$\text{and} \qquad r = ((\rho_m\,D_e\,C/(2t))^{1/2}\,S_t\,(1-\epsilon) \qquad 1.4.9$$

In the later stages of the reaction the rate is half order with respect to the O_2 concentration and exhibits a $1/t^{1/2}$ dependence on time.

This model therefore is in agreement with the observed behaviour of coal reactivity i.e. that the reactivity shows a definite falling off with time, which is in fact a falling off with degree of oxidation, and that the reaction order with respect to oxygen varies between one and a half . Fractional reaction orders have been reported by Sondreal & Ellman (1974).

It is therefore felt that a reaction model has been derived which is consistent with the available evidence. The problem that remains is to use the available experimental data to derive the model constants, in order that the model may be checked and used with confidence.

1.5 Heat Transfer within a coal dump

The safety or otherwise of a coal dump is likely to depend upon the balance between the rate of temperature rise due to reaction and the rate at which this energy is transferred away from the hot zone. It is known that coal is a fairly good insulator, but little data is available on the physical characteristics of heat transfer in coal beds. In addition these characteristics are likely to be dependent on both the voidage and particle size of the coal bed. For these reasons a literature survey was performed on the subject of heat transfer in packed beds; the results of this survey are presented in Chapter 3.

Following from this work, it was felt worth while to design and construct an apparatus to measure the so called effective thermal conductivity of a packed bed of coal. This aspect of the work is also discussed in Chapter 4 together with the results obtained.

1.6 A Mathematical Model For Spontaneous Combustion

In Chapter 5 a literature survey of existing mathematical models for spontaneous combustion of coal is presented. It is shown that all of these models suffer from one or more shortcomings. A set of equations, describing the behaviour of a so-called one-dimensional analogue of a coal dump is thus derived and discussed. In Chapter 6 certain simplifications to the model are discussed and justified. The methods used to solve this simplified set of equations are discussed.

1.7 Experimental Investigation

In Chapter 7 an experiment used to test the model as well as to obtain parameters for the model is discussed. The conclusion is reached that the model accurately describes the behaviour of a one-dimensional analogue of a coal dump.

1.8 Results and Conclusions

The large majority of Chapter 8 is devoted to a parameter study on the effect of on the model of changing certain parameters. The results obtained are discussed and the implications for the practising engineer pointed out. A simplified analysis is performed in order to deduce the temperature-time behaviour of the model, and the practical implications discussed. Shortcomings of the model are also discussed, together with suggestions for further research. Finally, in Chapter 9, the important conclusions reached in the thesis are summarised.

2. ANALYSIS OF SUGGESTED MECHANISMS FOR INGRESS OF REACTANTS

2.1 Introduction

The various mechanisms suggested for transport into a coal dump have been mentioned in section 1.2. They are repeated here for convenience.

a) Natural convection caused by self heating of the dump.

b) Flow caused by differential pressure between inclined and flat surfaces of the dump.

c) Molecular diffusion caused by concentration gradients.

d) Barometric breathing caused by changes in barometric pressure.

e) Thermal breathing caused by the daily variation in temperature.

In order to decide which of these mechanisms are important simple models were used to obtain order of magnitude estimates of their effect. It proves convenient to analyze mechanisms a) and b) together.

2.2 Natural Convection and Wind Pressure

In Chapter 5 a so-called one-dimensional model of the processes occuring in a coal dump is discussed. In Appendix 3 it is shown that the following momentum balance, for a vertically aligned bed open at both ends, may be written:

$$\frac{d\hat{P}}{dx} = -f\,U + \rho_\infty\, g\,(1 - T_\infty/T) \qquad 2.2.1$$

$\hat{P}$ = Pressure - ambient pressure
f = D'Arcy's law constant for the packed bed.
U = Superficial flow velocity
ρ_∞ = density of ambient air
g = acceleration due to gravity
T_∞ = ambient air temperature
T = bed temperature

Bird, Stuart & Lightfoot (1960) have discussed equations that attempt to correlate the factor f. One such equation is the Ergun equation which is

$$f = \frac{150\ (1-\epsilon)^2\ \mu\ S^2}{36\ \epsilon^3} + \frac{10.5\ (1-\epsilon)\ \rho\ U\ S}{\epsilon^3} \qquad 2.2.2$$

ϵ = bed voidage
μ = gas viscosity
ρ = gas density
$S = \frac{\text{total particle external surface area}}{\text{volume of particle}}$

It has been shown that for small flowrates the second term on the R.H.S. is negligible giving:

$$f = \frac{150\ (1-\epsilon)^2\ \mu\ S^2}{36\ \epsilon^3} \qquad 2.2.3$$

Note that no assumption need be made on the geometry of the particles or the bed packing. A mean particle diameter may be defined to be

$$D_p = 6/S \qquad 2.2.4$$

Under still air conditions the following boundary conditions are used for equation 2.2.1:

$$\hat{P}\ (x=0) = 0 \qquad 2.2.5$$

$$\hat{P}\ (x=L) = 0 \qquad 2.2.6$$

These boundary conditions merely reflect the fact that the ends of the bed are at atmospheric pressure.

In an attempt to compare the magnitude of natural convection induced flows with those of flows due to pressure differences, it is assumed that the stagnation pressure of a wind flow of velocity U may be use as an upper bound on the pressure difference that can arise between any two points on the surface of a coal dump. It is thus assumed that an estimate of the flows due to wind pressure may be obtained by assuming that the pressure at the bottom of the bed is increased by the stagnation pressure of the wind of velocity U.

Therefore

$$P(x=0) = P_\infty + \rho_\infty U^2/2 \qquad 2.2.7$$

and

$$\hat{P}(x=0) = \rho_\infty U^2/2 \qquad 2.2.8$$

Therefore the effect of wind is to change the boundary condition at $x = 0$ to

$$\hat{P} = \rho_\infty U^2/2 \qquad 2.2.9$$

Assuming U constant for small variations in temperature, equation 2.2.1 may be integrated to give:

$$\hat{P}(x=L)-\hat{P}(x=0) = -f\ U\ L + \rho_\infty\ g\ (L - \int_0^L (T_\infty/T\ dx)) \qquad 2.2.10$$

or

$$-\rho_\infty U^2/2 = -f\ U\ L + \rho_\infty\ g\ L\ (1 - (T_\infty/T_{aU})) \qquad 2.2.11$$

where

$$1/T_{aU} = 1/L \int_0^L T^{-1}\ dx \qquad 2.2.12$$

Therefore

$$U = \frac{\rho_\infty U^2}{2\ f\ L} + \frac{\rho_\infty g}{f}\ (1-T_\infty/T_{aU}) \qquad 2.2.13$$

or $$U = U(\text{Wind pressure}) + U(\text{Natural convection}) \quad 2.2.14$$

therefore

$$\frac{U(\text{Wind})}{U(\text{convection})} = \frac{v^2}{2\,L\,g\,(1-T_\infty/T_{av})} \quad 2.2.15$$

To illustrate the use of this equation, it will be used to calculate the wind velocity required to cause the same flow through a 10 m bed as a temperature rise of 20 ^{o}C.

i.e. $$1 = \frac{v^2}{2 \times 10 \times 9.8 \times (1-300/320)} \quad 2.2.16$$

or $$v = 3.5 \text{ m/s} = 12.6 \text{ km/hr}$$

This implies that for a windspeed of 12.6 km/hr natural convection will supply as much oxygen to the dump as will the differential wind pressure effect.

In order to compare these effects with the effects of molecular diffusion it is neccesary to calculate the molar flow rate per unit area for various average particle sizes. The relationships used are

$$G = \frac{P\,U}{R\,T} \quad 2.2.17$$

together with equations 2.2.2 and 2.2.15.

This calculation has been performed for L = 10 m, T_{av} = 320 K and ϵ = 0.3. The results are presented in Table 2.1.

TABLE 2.1 MOLAR FLOWRATES FOR VARIOUS PARTICLE SIZES

D_p (mm)	f (kg/m^2/s)	G (kmol/m^2/s)
1	5.6×10^{4}	5.1×10^{-7}
2	1.4×10^{4}	2.0×10^{-6}
5	2.2×10^{3}	1.3×10^{-4}

2.3 Analysis of Molecular Diffusion

In order to analyze the importance of diffusion as a mechanism for oxygen ingress a simplified analysis was performed. Considering diffusion as the only transport mechanism for oxygen into the dump the following energy and mass balances may be written:

Energy balance: $$K_b \frac{\partial^2 T}{\partial x^2} - r \Delta H = 0 \qquad 2.3.1$$

Mass balance: $$D\epsilon \frac{\partial^2 C}{\partial x^2} - r = 0 \qquad 2.3.2$$

The boundary conditions are:

$$\text{At } x=0 \quad T = T_\infty \quad C = C_\infty$$

$$\text{At } x=L \quad \frac{\partial T}{\partial x} = 0 \quad \frac{\partial C}{\partial x} = 0$$

These correspond to ambient conditions on the top surface of the dump, and a bottom surface that is perfectly insulating and impervious. These conditions will lead to a maximum temperature rise. Although this geometry is somewhat different to the geometry used in section 2.2, and thus the results obtained will not be directly comparable, it should be stressed that all that is required is an upper bound for comparison purposes; the geometry is unlikely to make a large difference on the bound.

Multiplying 2.3.2 by ΔH and subtracting the result from 2.3.1 gives:

$$K_b \frac{\partial^2 T}{\partial x^2} - D\epsilon\Delta H \frac{\partial^2 C}{\partial x^2} = 0 \qquad 2.3.3$$

or $$\frac{\partial^2}{\partial x^2}\left(T - \frac{D\epsilon\Delta H}{K_b} C\right) = 0 \qquad 2.3.4$$

This equation may be integrated to give:

$$T - \frac{D\epsilon\Delta H}{K_b} C = Ax + B \qquad 2.3.5$$

A and B may be determined from the boundary conditions as

follows:

At $x=0$ $T=T_\infty$ $C=C_\infty$

Therefore $$T_\infty - \frac{D\epsilon\Delta H}{k_b} C_\infty = B$$

and $$T - T_\infty - \frac{D\epsilon\Delta H}{k_b} (C - C_\infty) = Ax \qquad 2.3.6$$

Differentiating 2.3.5 wrt x gives:

$$\frac{\partial T}{\partial x} - \frac{D\epsilon\Delta H}{k_b} \frac{\partial C}{\partial x} = A \qquad 2.3.7$$

but at $x=L$ both derivatives in 2.3.7 are 0, therefore $A=0$.

Therefore $$T - T_\infty = \frac{D\epsilon\Delta H}{k_b} (C_\infty - C) \qquad 2.3.8$$

From 2.3.8 the maximum temperature rise with diffusion as the only transport mechanism may be calculated. This maximum temperature rise will occur at a point where $C=0$. Then:

$$T - T_\infty = \frac{D\epsilon\Delta H C_\infty}{k_b} \qquad 2.3.9$$

Typical values for the quantites in this equation are:

$$D = 2 \times 10^{-5} \text{ m}^2/\text{s}$$
$$\epsilon = 0.3$$
$$\Delta H = 3 \times 10^{8} \text{ J/kmol}$$
$$C_\infty = 8 \times 10^{-3} \text{ kmol/m}^3$$
$$k_b = 0.2 \text{ W/m/K}$$

Therefore

$$T - T_\infty = \frac{2\times10^{-5}\times0.3\times3\times10^{8}\times8\times10^{-3}}{0.2}$$

$$= 72 \text{ K}$$

This temperature rise, though appreciable, is not sufficient to explain the high temperatures observed in burning coal dumps. It is thus suggested that, in the same way that moisture absorption can act as a trigger for the oxidation reaction, diffusion can act as a trigger whereby the temperature in a coal dump starts rising, eventually giving rise to stable natural convection flows. These flows supply more oxygen to the dump than diffusion can, and eventually lead to spontaneous combustion.

Having concluded that diffusion can not explain spontaneous combustion, it is felt important to attempt to calculate the flowrates that diffusion causes. This facilitates the comparison of the magnitude of the flowrate caused by diffusion with the flowrates already calculated for wind and natural convection. To model molecular diffusion the coal is considered to adsorb oxygen, as discussed in section 1.3, and the isothermal steady state material balance for oxygen is

$$0 = \frac{D\ P}{R\ T}\frac{d^2y}{dx^2} - G\frac{dy}{dx} - r\ y \qquad 2.3.10$$

D = molecular diffusion coefficient
y = mole fraction oxygen
r = reaction rate per unit bed volume

The boundary conditions for equation 2.3.1 are:

$$y(x = 0) = .21 \qquad 2.3.11$$

and $$y(x \to \infty) = 0 \qquad 2.3.12$$

The solution is:

$$y = .21\ \exp((G - (G^2 + 4\ r\ \nu)^{1/2})\ x/\nu) \qquad 2.3.13$$

where $$\nu = D\ P/(R\ T)$$

The oxygen flux at x = 0 is

$$\frac{D\ P}{R\ T}\frac{dy}{dx} = .21\ ((G^2/4 + r\ \nu)^{1/2} - G/2) \qquad 2.3.14$$

Using the simplified equation

$$r = k_o\ S_t\ (1-\epsilon)\ \exp(-E/(R\ T))\ P/(R\ T) \qquad 2.3.15$$

with the values

k_o = 10 m/s
E/R = 7000 K
$S_t = 6/D_p$
ϵ = 0.3

$$D = 1.8 \times 10^{-8} \ m^2/s$$

and the data from Table 2.1 the entries in Table 2.2 have been calculated.

TABLE 2.2 COMPARISON OF MOLECULAR DIFFUSION AND CONVECTION

D_D (mm)	r (kmol/m^3/s)	Diffusional O_2 Flux (kmol/m^2/s)	Convective O_2 Flux (kmol/m^2/s)
1	1.2×10^{-7}	2.8×10^{-8}	1.0×10^{-7}
2	6.2×10^{-8}	4.4×10^{-9}	4.0×10^{-6}
5	2.5×10^{-8}	2.8×10^{-10}	2.6×10^{-5}

It can be seen from Table 2.2 that the effect of molecular diffusion is very much less pronounced for larger particles. For a particle size of 1 mm molecular diffusion supplies approximately 1/4 as much O_2 as a natural convection flow driven by a 20 ^oC temperature rise. In addition the molecular diffusion flux decreases with increasing particle size, while the convective flux increases. Although the analysis presented above may be criticized on the grounds that the transport equations have been decoupled, it can be seen that, except for the smallest particle sizes, the convective flux is orders of magnitude larger than the diffusional flux. This result justifies the use of the decoupled analysis to obtain order of magnitude estimates.

In the absence of wind or any temperature rise molecular diffusion may well be the only mechanism for O_2 transport into the dump. However it can be seen that as soon as there is any temperature rise in the dump natural convection will take over as the mechanism of O_2 transport.

2.4 Barometric Breathing

Barometric breathing occurs when the barometric pressure changes, causing a change in the volume of air that was in the dump. If the barometric pressure increases, this will cause a flow of air into the dump.

Consider a dump of 100 m x 50 m x 20 m high. Assume the barometric pressure increases from 620 mm Hg to 630 mm Hg in a time period of 24 hrs.

The air in the dump has a volume

$$100 \times 20 \times 50 \times 0.3 = 3 \times 10^4 \text{ m}^3$$

assuming $\epsilon = 0.3$.

This amount of air would shrink to a volume of

$3 \times 10^4 \times 620/630 \text{ m}^3 = 2.95 \times 10^4 \text{ m}^3$

and thus $4{,}76 \times 10^2 \text{ m}^3$ of air will flow in.

This flow will occur through the sides and the top of the dump i.e. a surface area of

$100 \times 50 + 2 \times 20 \times 50 + 2 \times 100 \times 20 = 11\,000 \text{ m}^2$

Thus the flowrate of air into the dump will be

$$\frac{4.76 \times 10^2}{11\,000 \times 24 \times 3600} = 5 \times 10^{-7} \text{ m/s}$$

This corresponds to a flux of 2×10^{-8} kmol/m^2/s which is an extremely small flux, and can safely be ignored.

Under certain weather conditions the barometric pressure may change far more rapidly than 10 mm Hg over a 24 hr period. This is the case for instance after a thunderstorm. These rapid changes may supply the dump with an appreciable amount of gas over a short period of time. The effect of this may well be to increase local temperatures in the dump and lead to the onset of natural convection flows. Thus rapid changes in barometric pressure may be a starting mechanism for the onset of spontaneous combustion in a dump that is in an unsafe condition.

2.5 Thermal Breathing

It has been hypothesized that the daily variation in temperature may lead to breathing of the dump i.e. hot air may leave the dump at night and be replaced by cold air thus supplying the dump with fresh reactants.

Measurements made at Grootegeluk coal mine indicate that surface temperature variations extend into the dump only a short distance; typically 325 mm.

A theoretical analysis of a problem of a semi-infinite solid with the surface temperature varying sinusoidally with time is discussed by Eckert & Drake (1972) who draw the conclusion that the oscillations are unimportant when

$$\frac{x}{2\,(\pi K \tau_o)^{1/2}} > 0.8 \qquad 2.5.1$$

Where K = thermal diffusivity of medium
τ_o = period of oscillation
x = distance into medium

For the case of daily fluctuations τ_o = 24 hrs. A typical value for the diffusivity of a coal bed is 8×10^{-4} m^2 / hr.

Therefore equation 2.5.1 gives

$$x > 2 \times 0.8 \times (\pi \times 8 \times 10^{-4} \times 24)^{1/2}$$

or $$x = 0.37 \text{ m}$$

This value agrees well with the measurements made on coal dumps discussed above.

It can be seen that thermal breathing will only supply reactants to the surface of the dump. Since any temperature rise near the surface of the dump is likely to be dissipated to the surface, it is unlikely that thermal breathing need be considered as an important reactant transport mechanism.

2.6 Conclusions

It may be concluded from the admittedly simplified analyses presented above that both wind pressure and natural convection must be considered as important mechanisms of O_2 transport into a coal dump. Molecular diffusion and barometric breathing may well be starting mechanisms, whereby the temperature begins rising in a coal dump. Natural convection soon becomes the dominant mech-

anism supplying O_2. This process may lead to eventual spontaneous combustion of a coal dump that is in an unsafe situation.

3. THEORETICAL MODELS FOR HEAT TRANSFER IN PACKED BEDS

3.1 Introduction

Thermal transfer of energy in packed beds is a field in which much work has been performed. The main reason for this is the importance of heat transfer in the design of packed bed catalytic chemical reactors. Other fields in which this knowledge is required include drying, nuclear reaction engineering and powder technology.

The literature survey that follows is very general, with no specific reference to coal beds. This is because the processes occuring in a packed bed of coal are no different to those occuring in packed beds of other materials.

3.2 Mechanisms of Energy Transfer in Packed Beds

In general energy transfer in a packed bed containing stagnant or moving fluid occurs by conduction, convection and radiation. The following potential mechanisms can be identified in the general case (Beveridge & Haughey, 1971).

Conductions Mechanisms

1. Conduction through the solid particles
2. Conduction across the gas in the voids
3. Conduction across the stagnant gas surrounding the points of contact between particles.
4. Conduction through the points of contact between particles

Radiation Mechanisms

5. Radiation between adjacent particle surfaces
6. Radiation between particle surfaces seen through more than one void space
7. Radiation absorption by the gas

Convection Mechanisms

8. Natural convection in the gas
9. Forced convection solid-gas transfer
10. Forced convection due to bulk flow, turbulent diffusion or mixing of the gas.

Of these mechanisms, mechanisms 1,2,4,5,6 and 7 are independent of fluid flow, while the other mechanisms depend to a greater or lesser extent on fluid flow, especially at low Reynolds numbers (Yagi & Kunii, 1957).

In general, thermal transfer of energy will take place by various combinations of series and parallel paths of these mechanisms.

3.3 Describing the overall energy transfer in a packed bed

The most common way of describing the overall transfer in a packed bed is by means of the so called effective thermal conductivity of the bed (Beveridge & Haughey, 1971). This quantity has also been called the thermal dispersion coefficient in the literature (Gunn & Khaled, 1975).

This formulation treats the system as homogeneous allowing the Fourier equation for the flux per unit area Q to be written

$$Q' = -k_b \frac{\partial T}{\partial X}$$

where $\partial T/\partial X$ is the temperature gradient in the required direction (axial or radial).

It can be seen from the discussion in 3.2 that k_b, the effective thermal conductivity, is in fact a function of many parameters including gas velocity, gas and solid temperatures, relative directions of gas and energy flow, fluid and solid properties as well as bed voidage and structural characteristics. It is the elucidation of this functional relationship that has been the goal of much of the work, both theoretical and experimental, that has been done in this field.

3.4 Models for energy transfer in which only conduction is considered

Many researchers have used as their starting point a model of a packed bed in which only conduction is considered. Models so derived should give good results provided the following conditions are met:

1. There is no gas flow
2. The particles are sufficiently small, and the temperature

sufficiently low, so that natural convection and radiation may be ignored.

Exactly what is meant by sufficiently small and sufficiently low will be discussed in greater detail later. Suffice it to say that if these conditions are met then the effective thermal conductivity, k_b, will be primarily a function of the thermal conductivities of the solid particle and stagnant gas. k_s and k_g respectively, and the structure of the bed.

Many models have been published to account for the four conduction mechanisms discussed in section 2, most of which describe the system in terms of its fluid and solid phase elements arranged in some regular array.

These models have been summarized by Beveridge & Haughey (1971), and their geometric significance is shown in figure 3.1

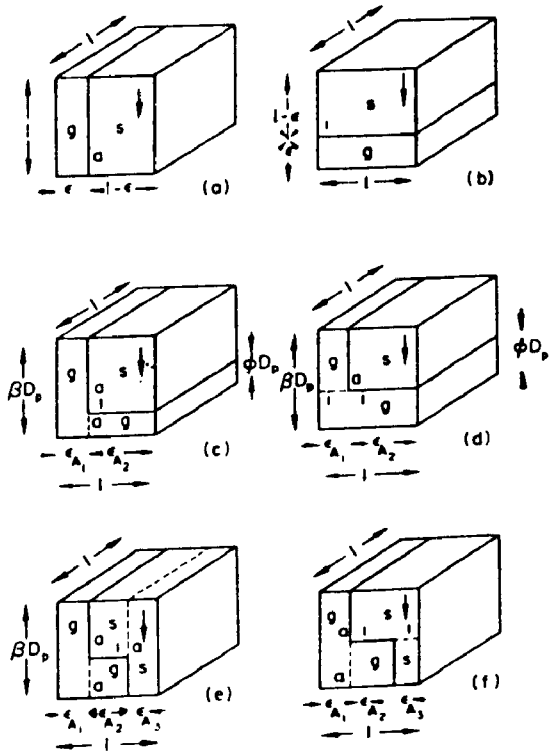


FIGURE 3.1 GEOMETRICAL CONDUCTION MODELS

a. adiabatic plane

i. isothermal plane

g. gas phase

s. solid phase

→ direction of energy transfer

(Beveridge & Haughey, 1971)

The simplest model is that represented by Fig 3.1a which postulates that conduction through the solid (mechanism 1) acts over a solid volume $1-\epsilon$, and the conduction across the gas in the voids and the stagnant gas round the points of contact (mechanisms 2 and 3) act over a gas volume ϵ. An arithmetic mean corresponding to a parallel arrangement of the two phases gives

$$\frac{k_b}{k_g} = \epsilon + (1 - \epsilon) \frac{k_s}{k_g} \qquad 3.4.1$$

The harmonic mean which corresponds to a series arrangement of the phases (Fig 3.1b) yields

$$\frac{k_b}{k_g} = \frac{k_s}{\epsilon\, k_s + (1 - \epsilon)\, k_g} \qquad 3.4.2$$

In attempting the formulation of more realistic models the concept of the unit cell is introduced, i.e. a representative element which is repeated throughout the packing. The basic geometric cell is that of Fig 3.1c with a cell of unit area perpendicular to the energy flow and height equal to the particle layer thickness $\beta' D_p$ where D_p = average diameter of particles.

Energy flow is one dimensional in parallel paths which are insulated from each other, and the distribution on the two phases is handled only by a two dimensional variation. This system then gives (see Fig 3.1c)

$$k_b = k_g\, \epsilon_{a1} + \frac{(1 - \epsilon_{a1})\, k_s}{\alpha' X + 1 - \alpha'} \qquad 3.4.3$$

where $\alpha' = \frac{\phi}{\beta'}$

and $\epsilon_{a1} = \frac{\epsilon - \alpha'}{1 - \alpha'}$

Modifications include that shown in Fig 3.1d which gives

$$k_b = \left[\alpha' k_g + \frac{1 - \alpha'}{k_g\, \epsilon_{a1} + k_s\, (1 - \epsilon_{a1})} \right]^{-1} \qquad 3.4.4$$

However, none of these models take into account the point to point

contact resistance (mechanism 4). One approach to this problem is that one used by Kunii & Smith (1960) who define a "heat" transfer coefficient h_p, accounting for an energy transfer contact resistance in parallel with the gas phase portion of the gas-solid series mechanism yielding:

$$\frac{k_b}{k_g} = \epsilon_{a1} + \frac{(1 - \epsilon_{a1})\, k_s/k_g}{(1 - \alpha) + \dfrac{\alpha\, k_s/k_g}{1 + \dfrac{h_p\, D_p}{k_g}}} \qquad 3.4.5$$

The quantity h_p has not been well correlated in the literature.

A more logical approach is the inclusion of the contact resistance in the idealized cell model as a solid energy flux path (represented by an area fraction ϵ_{a3}) arranged parallel to the gas path (Fig 3.1e) giving:

$$k_b = \epsilon_{a1}\, k_g + \frac{\epsilon_{a2}\, k_s}{\alpha' \dfrac{k_s}{k_g} + 1 - \alpha'} + \epsilon_{a3}\, k_s \qquad 3.4.6$$

A further extension to this approach is the one presented by Beveridge & Haughey (1971) in which the adiabatic boundary between the two parallel paths is replaced by an isothermal boundary (Fig 3.1f). This yields

$$\frac{k_b}{k_g} = \epsilon_{a1} + \left[\frac{1 - \alpha'}{\dfrac{k_s}{k_g}(1 - \epsilon_{a1})} + \frac{\alpha'}{\epsilon_{a2} + \epsilon_{a3}}\right]^{-1} \qquad 3.4.7$$

This approach has the advantage of allowing flux line bending in the solid phase.

It is shown by Beveridge & Haughey (1971) that k_b is a function of k_s/k_g, ϵ and ϵ_{a3} only. While k_s/k_g and ϵ are definable physical properties the parameter ϵ_{a3} must be determined experimentally for a given set of particles, since it will be affected by the particle loading and deformation as well as the surface

characteristics of the solid. It is also important to note that the effect of pressure on the thermal conductivity of the gas, k_g, must be properly taken into account.

3.5 Models for energy transfer in which conduction and radiation are considered.

Although radiant energy transfer will occur only through the voids of a packed bed of opaque solid pseudo-homogenous models have beem proposed which consider the solid and the gas as a single homogenous medium. The solution of the resultant integro-differential equations for conduction and radiation in absorbing and scattering models has been examined, most notably by Chan & Churchill (1963). They found that in an optically thick bed that the so called radiant conductivity $k_{b,r}$ could be written as

$$k_{b,r} = \frac{8 \sigma T^3}{a' + 2b'} \qquad 3.5.1$$

where σ = Stephan - Boltzmann constant
T = average bed temperature
a' = absorption cross section per unit volume of packing
b' = back scattering cross seciton per unit volume of packing

Note that the radiant conductivity is defined as the radiant energy flux density divided by the temperature gradient.

The radiant contribution has also been calculated by Bosworth (1952) from a random walk model giving

$$k_{b,r} = \frac{4 D_p T^3}{3}$$

The simplest radiation geometric model is that with two radiating plane surfaces at temperature T_1 and T_2, the radiant energy flux Q_r' being given by

$$Q'_r = \chi \sigma (T_1^4 - T_2^4) \qquad 3.5.3$$

where χ = view factor and emmisivity function

The elucidation of the function χ is difficult both theoretically and experimentally.

The energy flux Q'_r can be related to a radiation thermal conductivity $k_{b,r}$, and to a radiation coefficient $h_{b,r}$, by

$$Q'_r = -k_{b,r} \frac{\partial T}{\partial x} = h_{b,r} (T_1 - T_2) \qquad 3.5.4$$

When $T_1 - T_2$ is small compared to the absolute value of $T = T_1$ then:

$$\frac{k_{b,r}}{\beta D_p} = h_{b,r} = 4 \chi \sigma T^3 \qquad 3.5.5$$

The parameters in these models have a highly complex interaction with the structural and physical properties of the bed, and for this reason Beveridge & Haughey (1971) feel that there is little justification in representing the radiation mechanism other than by adding suitable terms to the simplest model such as the geometrical conduction models of Fig 1. Schotte (1960) used an analysis similar to that of Argo & Smith (1953) accounting for both the radiation between adjacent particle surfaces (mechanism 5) and the radiation between particle surfaces seen through more than one void space (mechanism 6) giving

$$Y_r = \epsilon X_{r,g} + \frac{1 - \epsilon}{\frac{k_g}{k_s} + \frac{1}{X_{r,s}}} \qquad 3.5.6$$

where $Y_r = \frac{k_{b,r}}{k_g}$

$$X_{r,g} = X_{r,s} = \frac{h_r D_p}{k_g} = \frac{4 D_p \chi \sigma T^3}{k_g} \qquad 3.5.7$$

The thermal conductivity of the bed is then given by

$$Y_t = Y_c + Y_r$$

In fact there is an interaction between the radiation and other energy transfer mechanisms and the contribution Yr cannot be added simply to the conduction terms. It is more satisfactory to utilize h_r within the conduction type model (Fig 3.1e). This was done by Yagi & Kunii (1957) who obtained

$$y_t = \epsilon_{a1}\,(1+ X_{r,g}) + \frac{\epsilon_{a2}}{\frac{\alpha'}{1 + \alpha' X_{r,s}} + \frac{1-\alpha'}{X}} + \epsilon_{a3} X \qquad 3.5.9$$

Normally no distinction is made between the Nusselt Numbers $X_{r,s}$ and $X_{r,g}$, although Yagi and Kunii (1957) used

$$X_{r,s} = \frac{4D_p}{k_g}\left[\frac{e}{2-\epsilon}\right] T^3 \qquad 3.5.10$$

$$X_{r,g} = \frac{4D_p}{k_g}\left[1 + \frac{\epsilon(1-e)}{2(1-\epsilon)e}\right]^{-1} \qquad 3.5.11$$

The model used by Beveridge and Haughey (1971) results in the expression

$$Y = \epsilon_{a1}(1+H_r) + \left[\frac{1-\alpha'}{X(1-\epsilon_{a1})} + \frac{\alpha'}{\epsilon_{a2}(1+H_r) + X\epsilon_{a3}}\right]^{-1}$$

$$H_r = \frac{\beta h_r D_p}{k_g} = \frac{4\beta D_p X \sigma T^3}{k_g} \qquad 3.5.12$$

Beveridge & Haughey (1971) treated X as an unknown function of temperature, and deduced the functional form experimentally.

3.5.1 Conditions under which radiation in a packed bed is likely to be significant

Young (1975) has performed calculations of the radiation contribution to the effective thermal conductivity of packed beds. The calculations were based on the radiation model of Schotte (1960) in conjunction with the correlation of Deissler and Eian (1952). The calculations show that radiation will become important for 1 mm particles about 400 °C and for 0,1 mm particles above 1500 °C. For

5 mm particles at an average bed temperature of 400 ^{o}C radiation will account for approximately 20 % of the total energy transfer.

3.6 A Theoretical Study of Natural Convection.

The first theoretical study of natural convection in packed beds is that of Lapwood (1948). This author formulated the equations describing natural convection in a porous medium with an imposed vertical temperature gradient as follows:

Equation of motion:

$$\rho \frac{D}{Dt}(U,V,W) = -\left[\frac{\partial}{\partial x},\frac{\partial}{\partial y},\frac{\partial}{\partial z}\right] P - \frac{\rho g}{K'}(U,V,W) - (0,0,\rho g) \qquad 3.6.1$$

Equation of continuity:

$$\frac{1}{\rho}\frac{D\rho}{Dt} = \frac{\partial U}{\partial x} + \frac{\partial V}{\partial y} + \frac{\partial W}{\partial z} \qquad 3.6.2$$

Conservation of energy:

$$\frac{DT}{Dt} = \kappa \nabla^2 T \qquad 3.6.3$$

Equation of state:

$$\rho = \rho_{\infty}[1 - \alpha(T-T_{\infty})] \qquad 3.6.4$$

(U,V,W) = the macroscopic velocity components of an element of fluid at (x,y,z)

P = pressure at (x,y,z).

T = temperature at (x,y,z)

ρ = gas density at (x,y,z)

g = acceleration due to gravity

κ = thermal diffusivity = $k_b/(\rho\, c_g)$

k_b = effective thermal conductivity of medium

c_g = specific heat capacity of gas

α = coefficient of thermal expansion of fluid

K' = coefficient of permeability of medium for fluid concerned
= Kg/ν

ρ_{∞} = density at ambient temperature

ν = kinematic viscosity of fluid

K = permeability of medium

Note that Darcy's law has been used in the equation of motion in place of the usual viscosity term.

In order to reduce these equations to a more manageable form Lapwood (1948) makes the following assumptions:

1) All velocities, and departures of temperature, density, and pressure from the equilibrium state, are small enough to neglect second order terms and to formulate a useful first order theory.

2) Variations of density can be neglected, except in so far as they modify the action of gravity (the Boussinesq assumption).

These assumptions mean that D/Dt can be replaced everywhere except in the energy equation to give

Equation of motion:

$$\rho \frac{\partial}{\partial t}(U,V,W) = -\left(\frac{\partial}{\partial x},\frac{\partial}{\partial y},\frac{\partial}{\partial z}\right) P - \frac{\rho g}{K'}(U,V,W) - (0,0,\rho g)$$

Equation of continuity:

$$\frac{\partial U}{\partial x} + \frac{\partial V}{\partial y} + \frac{\partial W}{\partial z} = 0$$

Conservation of energy:

$$\frac{DT}{Dt} = \kappa \nabla^2 T$$

Equation of state:

$$\rho = \rho_\infty [1 - \alpha(T-T_\infty)] = \rho_\infty \frac{T}{T_\infty} \quad \text{for an ideal gas}$$

Lapwood (1948) reworks this set of equations for small disturbances from equilibrium, and obtains the 4th order differential equation

$$\left(\frac{\partial}{\partial t} + \frac{Q}{K}\right)\left(\frac{\partial}{\partial t} - K'^2\right)\nabla^2\theta = g\frac{\Delta T}{L}\nabla^2\theta$$

where $\theta = T-T_0$, $T_0 = -\Delta T(z/L)$

The equation is solved for the following boundary conditions:

$$T, \quad \frac{\partial^2 T}{\partial z^2} = 0 \qquad \text{at } z=0 \text{ and } z=L$$

It is shown that the solution obtained leads to exponential decay for

$$Ra = \frac{\Delta T \ \rho_0 K \ L \ g}{\kappa \ \mu \ T_\infty} < 4\pi^2 \qquad 3.6.5$$

where Ra = Rayleigh Number

Lapwood (1948) thus states that $Ra = 4\pi^2$ is the criterion for convective flow; if Ra is less than this value the disturbance dies away, but if it reaches this value steady convection becomes possible.

These results also show that the temperature depth relationship is, except in the vicinity of the boundaries,

$$T = T_0 - \frac{\Delta T}{L} z + A \sin\left(\frac{\pi z}{L}\right) \sin(lx) \sin(my) \qquad 3.6.6$$

Where A,l,m are constants.

This equation shows that in the presence of convection the temperature is no longer a linear function of z.

3.7 The Effect of Flow on Energy Transfer in Packed Beds

When there is bulk flow of gas through a packed bed, the thermal transfer of energy becomes many times more complicated. It has been mentioned in section 2 that of the 10 proposed mechanisms of energy transfer, only 6 are completely independent of fluid flow. Briefly the mechanisms which are believed to be dependent on the fluid flow are:

1) Conduction across the stagnant gas surrounding the contact points. (This is likely to be a weak function of fluid flow).
2) Natural convection in the gas.
3) Forced convection in the gas.
4) Forced convection due to bulk flow, turbulent diffusion or mixing of the gas.

Mechanisms 3 and 4 are unlikely to be of importance for a coal bed, since forced convection is not being considered except for the case of wind. The flowrates through packed beds of coal are in any case very small. The flow velocity may be calculated from the entries in Table 2.1. For a particle size of 5 mm the velocity is of the order of 10 m/hr.

It may thus be concluded that the effects of flow on heat transfer in packed beds of coal is likely to be negligible.

3.8 Conclusions

A variety of theoretical models have been presented in this chapter. In order to apply the results of this literature survey to reacting coal beds, the following should be borm in mind:

a) The temperature range considered to be important is 100 ^{o}C and below. From practical experience as well as from considerations of the oxidation rate once a coal bed reaches 100 ^{o}C it is well on its way to combustion, and the model developed in this work no longer describes the situation accurately.

b) The flowrate through a bed of coal is sufficiently small (as shown above) that the effect of flow on the effective thermal conductivity is likely to be negligible.

The first point means that radiation can for all practical purposes be ignored as a significant mechanism for heat transfer in coal beds. The second point suggests that the effects of flow on the effective thermal conductivity can be ignored.

The conclusion is that only conduction type models need be considered for describing the effective thermal conductivity. Thus an equation like 3.4.5 could be rewritten

$$k_b = \epsilon k_g + (1-\epsilon)\ \eta k_s \qquad 3.8.1$$

where η = tortuosity factor

and η can be determined experimentally, with the expectation that η will not be a strong function of temperature.

Having reached this conclusion it was decided to measure k_b for a packed bed of coal. This is the subject of the next chapter.

4. MEASUREMENT OF THE EFFECTIVE THERMAL CONDUCTIVITY OF A PACKED BED OF COAL

4.1 Introduction

Very broadly speaking, methods for measuring thermal conductivities fall into one of two categories, i.e. steady-state or unsteady-state methods. The vast majority of unsteady-state methods do not measure the thermal conductivity directly, but instead measure the thermal diffusivity, κ, where:

$$\kappa = \frac{k}{\rho C_p} \qquad 4.1.1$$

k = thermal conductivity
ρ = density
C_p = specific heat capacity

One exception to this is the hot wire method which measures both the thermal conductivity and the thermal diffusivity. Steady state methods, on the other hand, measure the thermal conductivity directly.

4.2 Theory of the Measurement of Thermal Conductivity

Thermal conductivity is defined by Fourier's law:

$$Q' = -kA \frac{dT}{dx} \qquad 4.2.1$$

Q' is the rate of energy transfer by conduction

A is the area at right angles to the direction of transfer

$\frac{dT}{dx}$ is the temperature gradient in the direction of transfer

This equation may be combined with an energy balance for a solid or static fluid to give:

$$\rho C_p \frac{\partial T}{\partial t} = \frac{\partial}{\partial x}\left[k \frac{\partial T}{\partial x}\right] + \frac{\partial}{\partial y}\left[k \frac{\partial T}{\partial y}\right] + \frac{\partial}{\partial z}\left[k \frac{\partial T}{\partial z}\right] + q' \qquad 4.2.2$$

T is the temperature
q' is a source term, which may be due to chemical or nuclear reaction or the passage of a current.

In general in the measurment of thermal conductivities an attempt is made to ensure that only one dimensional conduction takes place. In this case equation 4.2.2 becomes:

$$\rho C_p \frac{\partial T}{\partial t} = k \frac{\partial^2 T}{\partial x^2} + q' \qquad 4.2.3$$

This equation may be written for cylindrical or spherical coordinate systems giving:

Cylindrical co-ordinates: $$\rho C_p \frac{\partial T}{\partial t} = \frac{k}{r} \frac{\partial}{\partial r}\left[r \frac{\partial T}{\partial r}\right] + q' \qquad 4.2.4$$

Spherical co-ordinates: $$\rho C_p \frac{\partial T}{\partial t} = \frac{k}{R^2} \frac{\partial}{\partial R}\left[R^2 \frac{\partial T}{\partial R}\right] + q' \qquad 4.2.5$$

4.3 Steady-State Methods for Measuring Thermal Conductivity

The second order differential equations 4.2.3 - 4.2.5 may be solved in the steady-state to give:

Rectangular co-ordinates: $$T = \frac{-q'x^2}{2k} + C_1 x + C_2 \qquad 4.3.1$$

Cylindrical co-ordinates: $$T = \frac{-q'r^2}{4k} + C_1 \ln(r) + C_2 \qquad 4.3.2$$

Spherical co-ordinates: $$T = \frac{-q'R^2}{6k} - \frac{C_1}{R} + C_2 \qquad 4.3.3$$

The constants of integration are found from known boundary conditions. In writing the above equations k has been assumed to be independent of temperature. In general in attempting to

measure thermal conductivity one would avoid introducing sources into the sample i.e. q′ would be zero in the above equations.

4.3.1 Measurements in the Rectangular System

The temperature-position equation in the rectangular system with q′=0 is:

$$T = C_1 x + C_2 \qquad 4.3.4$$

This equation implies a linear temperature profile.

In order to use equation 4.3.4 to measure thermal conductivity a heater is used to provide a known energy input Q. The boundary condition at x=0 is therefore:

$$Q = -kA \left.\frac{dT}{dx}\right]_{x=0} \qquad 4.3.5$$

The sample is cooled at the end. The boundary condition at x = L is therefore:

$$T = T_o \qquad 4.3.6$$

Solving for the integration constants C_1 and C_2:

$$C_1 = \frac{Q}{-kA} \qquad 4.3.7$$

$$C_2 = T_o + \frac{QL}{kA} \qquad 4.3.8$$

Therefore $$T = T_o + \frac{Q}{kA}(L - x) \qquad 4.3.9$$

Suppose that the measured temperature at x = 0 is T_1. Then:

$$T_1 = T_o + \frac{QL}{kA} \qquad 4.3.10$$

$$K = \frac{QL}{A(T_1 - T_0)} \qquad 4.3.11$$

This formula is the basis for measurements of the thermal conductivity of a material in rod or slab form. It requires measurement of five quantities i.e

The power input	Q
The sample length	L
The sample area	A
The temperature	T_0
The temperature	T_1

An improved version of the apparatus is one in which two identical samples, heated in the middle are used. The apparatus has the advantage that no energy loss can occur through the ends provided $T_0 = T_\infty$.

The equation used to calculate the thermal conductivity is now:

$$K = \frac{QL}{2A\ (T_1 - T_0)} \qquad 4.3.12$$

Despite the advantages of this apparatus energy loss may still occur along the sides. For this reason the so called guarded hot ring method has been developed. In this apparatus a circular electrical heating element is used and it is surrounded by a heating element in the form of a ring. During the experiment the power input to this guard ring is adjusted so that the temperature measured on the ring is the same as that measured on the main heater. This implies that any energy losses are supplied by the guard heater, and that all the energy supplied by the main heater passes through the sample.

The design of guarded hot plate apparatus has been the subject of much study, and is covered in ASTM C177 (1963) and BS 874 (1956). This method has been used by many investigators in the field of thermal conductivity of packed beds; notably Beveridge & Haughey (1971).

4.3.2 Measurements in the Cylindrical System.

In radial flow methods use is made of equation 4.3.2 with $q' = 0$:

$$T = C_1 \ln (r) + C_2 \qquad 4.3.13$$

With boundary conditions:

$$Q = -2\pi r_1 l \, k \left.\frac{dT}{dr}\right]_{r_1} \quad \text{at } r = r_1 \qquad 4.3.14$$

$$T = T_2 \quad \text{at } r = r_2 \qquad 4.3.15$$

Solving equation 4.3.14 for the constants and rewriting in terms of k gives:

$$k = \frac{Q}{2\pi l \, (T_1 - T_2)} \ln \left[\frac{r_1}{r_2}\right] \qquad 4.3.16$$

Two different experimental apparatus may be designed in order to make use of equation 4.3.16. In the first type of apparatus the specimen is placed between an outer shell which is kept at temperature T_2, and is heated centrally. In the second type of apparatus the sample is heated on the outside surface, and the energy is removed at the centre of the sample.

In order to ensure that energy transfer is occuring only in the radial direction it is neccesary either to use a large sample length to thickness ratio, or to make use of end guard heaters. If guard heaters are used a fairly complicated experimental apparatus is neccesary, involving movable thermocouples in order to measure axial temperature gradients. This aspect of the design of such equipment is covered by Tye (1969).

Examples of the use of such methods for measurements of thermal conductivity of packed beds are Yagi & Kunii (1957) who used a centrally heated specimen, and Young (1975) who used a centrally cooled specimen.

4.3.3 Measurements in the Spherical System

Equation 4.3.3 may be solved to give:

$$k = \frac{Q\ (1/r_1 - 1/r_2)}{4\pi(T_2 - T_1)} \qquad 4.3.17$$

The spherical system has the advantage that all the energy supplied by a central heater passes through the specimen. The disadvantages of the method include the difficulty of fabricating a uniform heater and specimen, and the fact that the thermo-couples used for temperature measurement cannot lie along isotherms.These disadvantages mean that the spherical system has not been used for the measurement of thermal conductivity of packed beds.

4.4 Unsteady-State or Dynamic Methods

In general dynamic methods involve the measurement of the thermal diffusivity. The experiment consists of measuring the temperature history of a heated sample of known geometry, and then using this data and the appropriate integrated form of equation 4.2.2 to solve for the thermal diffusivity.

These methods have the advantage that no measurement of power input need be made. The disadvantages include the fact that many temperature measurements must be made, and that solving for the diffusivity may require complex numerical techniques.

An example of the use of a dynamic method to measure the thermal conductivity of a coal bed is the investigation by Brooks & Woods (1980). These investigators used a cylindrical vessel of diameter 500 mm and height 1600 mm. The vessel was heated on the outside surface by steam and radial temperature profiles were measured as a function of time. These measurements were made every 15 minutes for periods of up to 8 hrs.

It can be shown that under the above experimental conditions equation 4.2.4 may be solved to give

$$\frac{T - T_s}{T_o - T_s} = 2 \sum_{n=1}^{\infty} \frac{\exp \frac{-M_n^2 K t}{R^2} \; J_o \frac{M_n r}{R}}{M_n \; J_1(M_n)} \qquad 4.4.1$$

where T = temperature at radial position r

T_s = surface temperature

T_o = initial bed temperature

R = radius of cylinder

r = radius measured from axis of cylinder

t = time

J_i = i th order Bessel function of the first kind

M_n = n th root of the equation $Jo(M_n) = 0$

A computer program was used to minimize the sum of squared errors between the measured and predicted temperatures by choice of K. It can be appreciated that this process is far more complicated than the direct application of an equation such as 4.3.12.

Although only one dynamic method has been discussed it should be appreciated that all such methods involve the same sort of experiment and analysis, and differ only in the sample geometry chosen. One of the problems with applying these methods to coal beds is the small value of K of such beds which leads to long experiments.

4.5 Choice of Measurement Method for a Packed Bed of Coal

From experience gained by Brooks & Woods (1980) in trying to measure this quantity by use of an unsteady-state method, it was felt that a steady-state method would be better. The reason for this is that it is far easier to analyze the effect of a temperature dependent thermal conductivity in the case of a simple equation such as 4.3.12, whereas this task may be extremely difficult in the case of an equation such as 4.4.1. Put another way, it was felt that a thermal conductivity calculated by equation 4.3.12 is far better defined than one calculated from equation 4.4.1.

Having decided on a steady-state method the choice had to be made between axial or radial energy transfer. Again experience gained

in a previous study led to the choice of axial energy transfer. The reason for this was that the previous study indicated that convection may be a significant mechanism of energy transfer. If this is the case the axial method would lead to the determination of the "correct" thermal conductivity i.e the one in which the energy transfer by conduction and convection are in the same direction (This of course assumes that the apparatus has the heater horizontal).

It was also felt that, by designing the equipment in such a way that the energy absorbed at the two sinks could be measured, the presence or absence of convection could be detected, and its effect measured. To do this would be much more difficult in a radial type of apparatus.

4.6 Design and Construction of Guarded Hot Ring Apparatus

4.6.1 General Design Considerations

Although standards exist for the design of guarded hot ring apparatus, it was felt in the present case that accuracy of measurement could be sacrificed for ease of experimental design and construction, and for versatility of the apparatus. It was felt that due to the inhomogeneous nature of coal and variations in packing geometry, accurate and repeatable values for the thermal conductivity would not in any case be achieved.

In order to make measurements on coal up to 20 mm in size it was decided to make the test section of the apparatus of diameter 200 mm and length 200 mm. These dimensions should be sufficient to make end and edge effects negligible. However it was noted that the recommended D/L ratio is three or more, and that using a smaller ratio would lead to a loss in accuracy (Tye ,1969).

4.6.2 Heat Sinks

As mentioned before the sinks are designed in such a way that the energy absorbed by the sinks can be measured. This is achieved by placing thermistors in the inlet and outlet streams from the sinks, in order to measure the temperature difference in the water flowing through the sinks. The rate of energy absorption

is calculated as

$$Q = m\ \bar{c}\ \Delta T_w \qquad 4.6.1$$

Q = rate of energy absorption
m = water flowrate
$\bar{c}$ = specific heat capacity of water
ΔT_w = temperature difference of water

The sinks are provided with spiral baffles in order to ensure good mixing of the cooling fluid, which was in all cases water. The sinks are surrounded by guard sinks in order to prevent radial energy losses.

A sketch of one heat sink is shown in Figure 4.1.

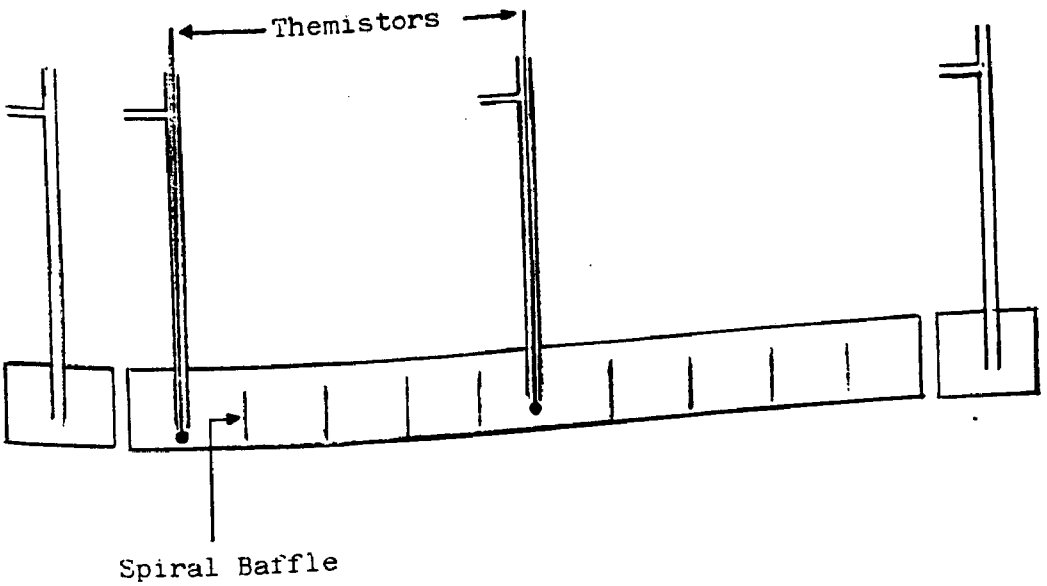


Figure 4.1 Guarded hot ring apparatus - Heat sink

4.6.3 Heating Elements

The heating elements were fabricated commercially, and consist of Nichrome wire ribbon wrapped around mica formers, which assembly is then sandwiched between more mica. The heaters are clad in light aluminium, and the whole assembly then sandwiched between 2 mm steel plates which are bolted together. The steel plates are used to prevent buckling.

The central heater has a diameter of 145 mm and the guard ring has an internal diameter of 150 mm and an external diameter of 200 mm. There is thus a 2.5 mm gap between the main and guard heaters.

4.6.4 Outer containing Vessel

The vessel has a diameter of 600 mm and a length of 600 mm. It is constructed from 6 mm mild steel. The ends of the vessel have 10 mm mild steel flanges in order to support the 10 mm MS end plates. The flanges are fitted with 5 mm rubber ring gaskets, and the endplates are held on with 18 bolts.

In order to facilitate electrical connections to the heaters as well as the placement of the thermocouples, six bushes have been placed on the midline of the apparatus. The bushes are shown in figure 4.2 and have proved satisfactory in sealing.

The end plates are provided with four similar bushes in order that the cooling sink pipes may pass through them. In addition the bottom end plate has an additional bush for connection of a vacuum pump or gas cylinder.

A sketch of the assembled apparatus is shown in Figure 4.2.

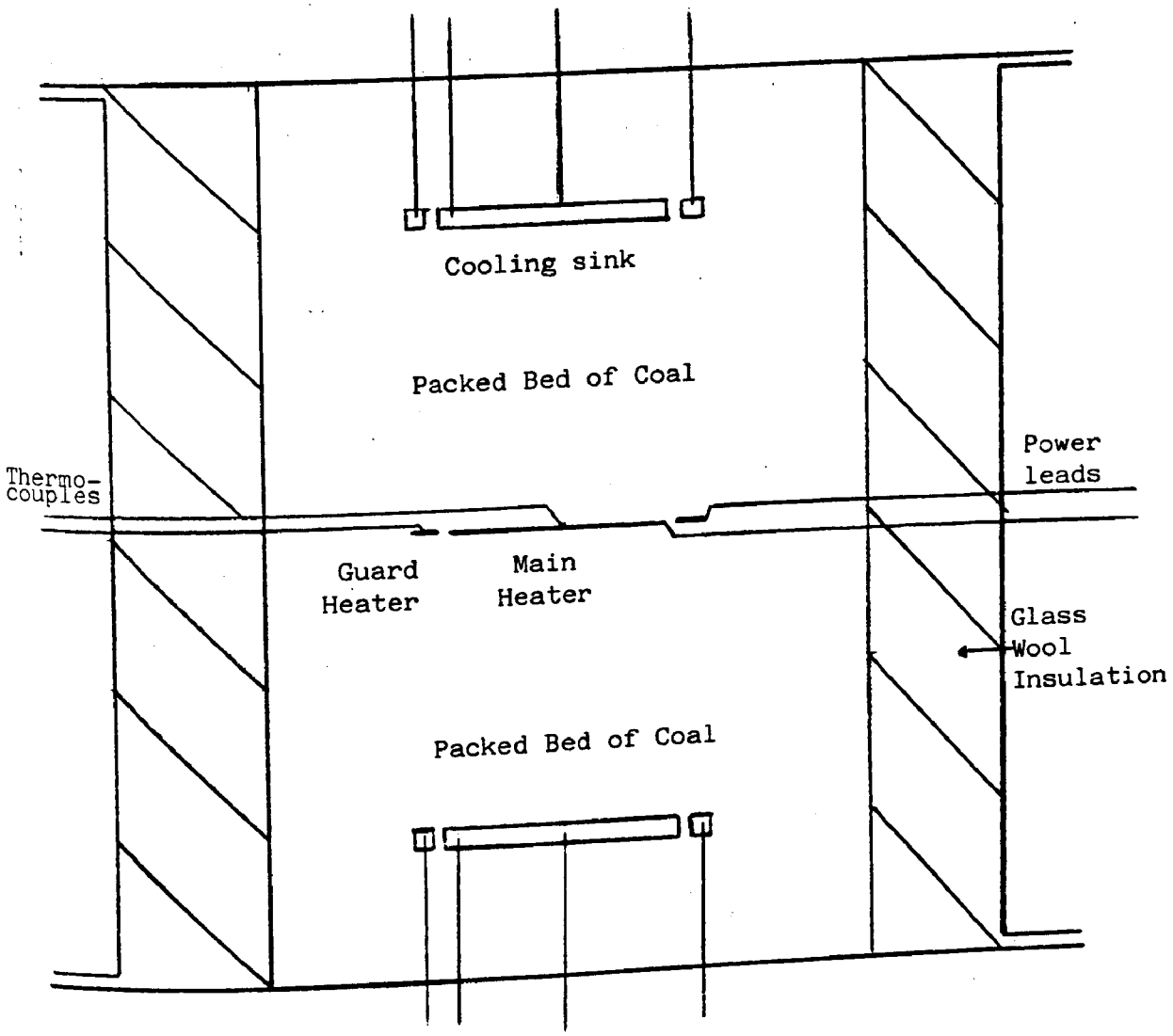


Figure 4.2 Guarded hot ring apparatus - Assembled apparatus

4.6.5 Water Supply to Heat Sinks

The apparatus is designed so that the temperature rise of the water flowing through the sinks is approximately 1 ^{o}C. A larger temperature rise is not used as this would upset the accuracy of the measurement of the temperature difference between the hot and cold faces. In order to measure this 1 ^{o}C temperature rise accurately it is neccessary to control the temperature of the water entering the sinks to at least 0.05 ^{o}C and preferably to 0.01 ^{o}C. To achieve this the following system is used:

Water flows from a constant head tank through a coil which is immersed in a constant termperature bath. The bath is controlled with a proportional controller. After leaving the bath the water flows through a jacketed copper pipe and hence to the heat sink. The jacketed pipe has water flowing in the jacket countercurrent to the flow to the sink. The water in the jacket is pumped from the constant temperature bath.

4.6.6 Measurement Techniques

The temperature of the main heater and guard heater are measured with chromel-alumel thermocouples. The cold junctions of the thermocouples are placed in glass tubes filled with glycerine, which are then placed in a "Thermos" flask filled with ice. The thermocouple voltage is measured using a Cambridge Slide Wire Potentiometer, i.e the voltage is measured at zero current.

The current supplied to the main heater is measured by a Fluke digital multimeter which is continuously in the circuit. This prevents the neccessity of correcting for the internal resistance of the meter. The voltage across the heaters is measured when required by another Fluke multimeter.

The resistances of the thermistors in the cooling sinks are measured in a Wheatstone bridge circuit, using a Kipp and Zonen recorder to measure the off balance voltage from the bridge.

The other values required to solve equation 4.3.12 for K are the heater area A and the length l. A is measured by measuring the diameter of the heater, and l is measured at the time of packing

the equipment with coal.

In fact the heater is not exactly betwen the two sinks, and thus l must be averaged. The correct average is

$$l = \frac{2\, l_1\, l_2}{l_1 + l_2} \qquad 4.6.2$$

where l_1, l_2 are the distances from the bottom and top sinks to the heater respectively.

4.7 Experimental Procedure

The experimental procedure is to switch on the main and guard heaters, setting the voltages so that there is no temperature difference between the guard and main heaters. The equipment takes approximately one week to reach steady-state, and each subsequent adjustment of the guard heater voltage requires further time for steady-state to be reached.

At the time of taking measurements the following are measured:

1) The voltage across the main heater and the guard heater.
2) The current through the main heater.
3) The thermocouple voltages on the main and guard heaters.
4) The resistance of the thermistors in the cooling sinks.

Once the thermocouple voltages and thermistor resistances have been converted to temperatures using calibration tables, the thermal conductivity is calculated from

$$k = \frac{V_m\, I_m\, l}{2\, A\, \Delta T} \qquad 4.6.3$$

V_m = main heater voltage
I_m = main heater current
ΔT = temperature difference between heater and sink

4.8 Results and Discussion

The results of the series of runs performed over the period March 1982 to August 1982 are tabulated in Appendix 2.

Although the resistances of the thermistors in the heat sinks were measured, it was not possible to calculate the energy absorbed at one heat sink. This was due to the fact that the thermistors are not identical i.e. they have slightly different resistances at the same temperature. An attempt was made to calibrate the thermistor pairs, but this was not succesful due to the fact that the calibration drifts with time. In addition problems were experienced with thermistors leaking and giving erratic readings. This facet of the experiment was consequently abandoned.

As can be seen from these results the thermal conductivity of the coal does not vary significantly in the temperature range considered. The mean value is 0.22 W/m/K.

It should be noted that for the largest tempeature difference used in the apparatus, the Rayleigh number as calculatedfrom equation 3.6.5 is 1.9. Therefore it may be safely assumed that only heat transfer by conduction was measured in this series of experiments, since this Rayleigh number is below the value required for the onset of natural convection.

The original intention of this experiment was to obtain experimental values for the so-called effective thermal conductivity of a coal bed, and deduce its functional relationship with particle size and voidage. However during the early stages of the mathematical modelling performed as part of this investigation, it was found that the thermal conductivity did not play as crucial a role in the equations as first believed. For this reason the experimental work was considered complete once a value of the thermal conductivity had been obtained for a typical sample of coal.

It is felt that a simple relationship for relating the thermal conductivity of the bed to that of the coal and the gas is all that is required. The relationship

$$k_b = \epsilon\, k_g + (1-\epsilon)\, \eta\, k_s \qquad 3.8.1$$

k_g = gas thermal conductivity
k_s = solid thermal conductivity
ϵ = voidage
η = tortuosity factor

which was presented and discussed in chapter 3 is probably satisfactory for a study of this type.

Using the values

k_g = 0.026 W/m/K (Perry & Chilton, 1973)
k_s = 0.28 W/m/K (Badzioch, Gregory & Field, 1964)
k_b = 0.22 W/m/K
ϵ = 0.38 (Appendix 2)

gives a value for η of 1.2.

5. MATHEMATICAL MODELLING OF A ONE-DIMENSIONAL ANALOGUE OF A COAL DUMP

5.1 Introduction

In any attempt to understand a natural phenomenon a model for the phenomenon is invaluable. In the case of a coal dump a mathematical model is required which has the ability to show the behaviour of a real coal dump, while still being simple enough to be solved. The full three dimensional equations for the transport processes occuring in a coal dump would be extremely complicated, and may indeed be impossible to solve without a tremendous amount of computation. A simpler model is required which may be solved without the excessive use of computation, but which nevertheless within its limits of applicability has the ability to predict whether a given coal dump may be considered to be safe or unsafe, and if unsafe what measures may be taken to render it safe. A model which is fundamentally based may be used to extrapolate measured data, which is not the case with models that are mainly empirical in nature. In addition the mathematical model points to the best experiments to measure the parameters required. It is believed that the mathematical model presented here has many of these desirable characteristics.

Mathematical models for coal dumps have been presented before, and in order to understand the reason for deriving a new one, a brief survey of these models and their shortcomings follows.

5.2 Literature survey of mathematical models for coal dumps

Much experimental effort has been devoted to measurement of physiochemical properties of coal over the last century. Less attention has been given to the development of a method to predict self heating.

An early model that attempts to predict safe conditions of storage of coal is that of Van Doornum (1954). The essential assumption of this model is that the coal may be considered to be a source of energy given by:

$$q' = A' \exp (a'v - \alpha t) \qquad 5.2.1$$

where q' = rate of generation
A' = fitting constant
a' = fitting constant
v = temperature above ambient
α = fitting constant
t = time

It should be noted that the form of equation 5.2.1 is in disagreement with the usual Arrhenius type temperature dependence of chemical reactions.

Van Doornum (1954) solves the conduction equation:

$$\rho_b \bar{c}_b \frac{\partial v}{\partial t} = \nabla^2(kv) + q' \qquad 5.2.2$$

where ρ_b = density of pile
$\bar{c}_b$ = specific heat capacity of coal
k = thermal conductivity
q' = source given by 5.2.1

for various geometries. From an analysis of the stability of the solutions the following is made that the safety or otherwise of a coal pile may be characterized by two dimensionless numbers M' and N' given by:

$$M' = \frac{A'a'}{\alpha \rho_b \bar{c}_b} \qquad 5.2.3$$

$$N' = \alpha \tau' \qquad 5.2.4$$

τ' = time constant for heat loss

τ' depends on the storage situation. For heat loss by conduction

$$\tau' = \frac{k \pi^2}{4 L^2 \rho_b \bar{c}_b} \qquad 5.2.5$$

L = height of pile

The criterion derived is as follows:

For $M' < 0.63$: a coal is unconditionally safe
$M' > 1.2$: the occurence of spontaneous combustion is very likely.

For the region $0.63 < M' < 1.2$ the situation, depending on the value of N', is normally manageable if care is taken.

This work has been adopted by the National Institute for Coal Research of South Africa as a test on the exportability of coal. The numbers M' and N' are found experimentally from a non-linear regression of the temperature-time curve at the centre of a 15 ton sample of coal which is aerated in a test bunker.

The chief disadvantage of this model is that no specific account is taken of the effect of oxygen depletion on the safety of a dump. In addition the constants in equation 5.2.1 have to be measured experimentally for every different coal; for instance, it is not possible to extrapolate measured data for one size grading of coal to a different size grading of the same coal.

Sondreal & Ellman (1974) performed exhaustive tests on North Dakota lignite, which data was used to perform computer simulations of spontaneous heating. The quantities measured by these investigators were the following:

a) The rate of oxidation of lignite, and the heat of reaction.
b) The specific heat of lignite.
c) The heat of wetting.
d) Airflow through a bed of compacted lignite.
e) The thermal conductivity of solid lignite.

In all case the quantities were measured at various moisture contents and bulk densities. The authors have used least squares techniques to fit the data to equations which are largely empirical in nature. These empirical equations have been used in computer simulations of spontaneous heating, using finite difference forms of the differential equation 5.2.2 together with a material balance equation for oxygen.

The authors present a large number of graphs showing the temperature rise in lignite under various assumptions. The cases

considered include the effects of prior oxidation, pressure gradients due to wind, porosity and moisutre content of the coal.

Although these investigators were most thorough in their approach, the chief disadvantage of this study is that it is highly specific to the particular lignite used. The authors state that the range of validity of their empirical correlations is limited to the range studied, and that extrapolations should only be made with caution. In addition Sondreal & Ellman (1974) take no account of airflow due to natural convection.

Nordon (1979) has presented a model for the self heating reactions of coal or char. The reactants considered are oxygen and water vapour, which are transported into the pile by molecular diffusion and forced convection due to differential wind pressure. A one-dimensional model is used in which the differential equations describing heat and mass transfer are:

$$(1-\epsilon)\,\rho_b\,\bar{c}_b\,\frac{\partial T}{\partial t} = \frac{(1-\epsilon)}{K}\,\frac{\partial^2 T}{\partial x^2} - \epsilon\,U\,\rho_g\,\hat{c}\,\frac{\partial T}{\partial x} - r\,\Delta H_r \qquad 5.2.6$$

where
K = thermal diffusivity
x = length along bed
U = flow velocity
ρ_g = density of gas
$\hat{c}$ = specific heat capacity of gas
r = reaction rate per volume of coal
ΔH_r = enthalpy of reaction

$$0 = \epsilon\,\frac{\partial m}{\partial t} + U\,\frac{\partial m}{\partial x} - D\,\frac{\partial^2 m}{\partial x^2} + \rho_g\,r \qquad 5.2.7$$

m = moles of oxygen per moles of nitrogen in gas
D = diffusion coefficient

These equations are solved using a finite difference method. No account is taken of natural convection flow. The reaction rate of the oxidation reaction is modelled using the so-called Elovich equation:

considered include the effects of prior oxidation, pressure gradients due to wind, porosity and moisutre content of the coal.

Although these investigators were most thorough in their approach, the chief disadvantage of this study is that it is highly specific to the particular lignite used. The authors state that the range of validity of their empirical correlations is limited to the range studied, and that extrapolations should only be made with caution. In addition Sondreal & Ellman (1974) take no account of airflow due to natural convection.

Nordon (1979) has presented a model for the self heating reactions of coal or char. The reactants considered are oxygen and water vapour, which are transported into the pile by molecular diffusion and forced convection due to differential wind pressure. A one-dimensional model is used in which the differential equations describing heat and mass transfer are:

$$(1-\epsilon)\,\rho_b\,\bar{c}_b\,\frac{\partial T}{\partial t} = \frac{(1-\epsilon)}{\kappa}\,\frac{\partial^2 T}{\partial x^2} - \epsilon\,U\,\rho_g\,\hat{c}\,\frac{\partial T}{\partial x} - r\,\Delta H_r \qquad 5.2.6$$

where
κ = thermal diffusivity
x = length along bed
U = flow velocity
ρ_g = density of gas
$\hat{c}$ = specific heat capacity of gas
r = reaction rate per volume of coal
ΔH_r = enthalpy of reaction

$$0 = \epsilon\,\frac{\partial m}{\partial t} + U\,\frac{\partial m}{\partial x} - D\,\frac{\partial^2 m}{\partial x^2} + \rho_g\,r \qquad 5.2.7$$

m = moles of oxygen per moles of nitrogen in gas
D = diffusion coefficient

These equations are solved using a finite difference method. No account is taken of natural convection flow. The reaction rate of the oxidation reaction is modelled using the so-called Elovich equation:

$$\frac{dq}{dt} = r_o A' \exp(-(E + Bq)/RT) \qquad 5.2.8$$

where q = amount of O_2 taken up per unit weight of char.
r_o = rate of oxidation at $T_\infty = 20^oC$ when q = 0.
A' = Arrhenius pre-exponential factor = $\exp(E/RT_\infty)$.
E = activation energy.
B = Elovich constant.

In the results by Nordon (1979) no account has been taken of the presence of moisture. As in the case of Sondreal & Ellman (1974) this author presents graphs showing the effect of various parameters on the temperature rise in char beds. The cases considered are:

a) Self heating for various bed lengths where diffusion is the only transport process.

b) Dependence of steady state temperature on critical bed size for various activation energies.

c) Self heating where diffusion and convection processes are present.

d) The moderating influence of Elovich kinetics.

The author concludes that there is a critical bed length above which spontaneous combustion will occur. He states that for bed lengths smaller that this critical value the steady state temperature rise is small and is limited by heat transfer. The high temperature steady state is caused by the reaction being limited by the rate of oxygen diffusion. With forced convection present this oxygen limitation may be removed; however when the forced convection becomes large loss of heat through flow will limit the reaction, leading to a low temperature steady state. Note however that the air flow required for this to occur is of the order of 10^{-4} m/s which is a fairly large flowrate for the fine (-3,35 mm) material considered in this study.

This study then is theoretically sound, and the author presents a

good discussion of the nature of self-heating. The main drawback of the model is the failure to take account of natural convection flows.

The omission by these researchers of natural convection deserves some explanation. It has been suggested by some researchers that the work of Lapwood (1948), as discussed in section 3.6, shows that natural convection is unimportant in coal dumps. The argument used is that Lapwood (1948) states that a Rayleigh number of $4\pi^2$ is a criterion for the onset of stable convection flows. This would seem to imply that the temperature rise required for natural convection flows to take place in a coal dump can be calculated using equation 3.6.5. The equation is

$$Ra = \frac{\Delta T \; \rho_g^2 \; L \; g \; c_g}{k_b \; f \; T_\infty}$$

where the identities $f = \mu/K$ and $\alpha = 1/T_\infty$ for an ideal gas have been used.

Setting the Rayleigh number equal to $4\pi^2$ in the above equation, the quantity $\Delta T \; L$ may be solved for. The results of doing this calculation are summarised in Table 5.1 below.

TABLE 5.1 VALUES OF $\Delta T \; L$ REQUIRED FOR $Ra = 4\pi^2$

D_p (mm)	f ($kg/m^3/s$)	$\Delta T \; L$ (K m)
1	5.6×10^4	9500
2	1.4×10^4	2375
5	2.2×10^3	380
20	1.4×10^2	24

These results have been taken by other researchers to indicate that for a 2 metre bed of 20 mm particles a 12 K temperature rise is necessary for the onset of natural convection flows, and that for 1 mm particles natural convection flows are very unlikely to occur.

There is however a fallacy in this argument. Lapwood investigated natural convection flows for the case of an imposed temperature gradient in the vertical direction, and with impermeable

horizontal faces. The problem is thus constrained to a one-dimensional temperature gradient. The boundary conditions that are implied are not appropriate for the case of a coal dump. A coal dump has no impermeable sides and has each of its surfaces at nearly ambient temperature, and experiences a three-dimensional temperature field.

Young (1985) has reworked this problem for the case of a coal bed open on the top surface, with impermeable sides and a two-dimensional temperature field. For this case it can be shown that the equation governing the stream function of the flow in the bed is:

$$\frac{\partial^2 \psi}{\partial X^2} + \frac{\partial^2 \psi}{\partial Y^2} = \frac{\partial \theta}{\partial X}$$

The right hand side of this equation represents the horizontal temperature gradient. If this quantity is 0 and the boundary conditions are such that ψ is zero everywhere, then this equation can be satisfied by the case of no flow. However, when the temperature gradient in the horizontal direction is non-zero, convection can be expected under all conditions.

Young (1985) has also shown experimentally that for his case as soon as there is any temperature rise in such a bed, natural convection will occur. There is thus no obvious critical Rayleigh number for this case.

Weber (1974) has studied theoretically a similar situation to Lapwood, but with a small horizontal temperature gradient. It appears from this work that there exists no critical Rayleigh number below which there is no flow, but rather that there is a critical Rayleigh number above which there is a fairly rapid increase in flow. The application of this work to coal beds is not completely obvious, because the infinite region considered requires infinite temperatures at the ends; hence only horizontal flows occcur at Rayleigh numbers below a certain critical value.

Bejan (1978) has studied convection in an infinite porous medium with a concentrated heat source; for this case there is no critical Rayleigh nmuber for the onset of convection. The steady-state flow pattern shows an upward flow that becomes very intense near the source. The upward flow extends throughout the medium, and as the Rayleigh number increases, the warmer region

moves upwards. It is felt that this case is likely to be more similar to the situation in a coal dump, than the situation modelled by Lapwood (1948) and Weber (1974).

In conclusion, having reviewed the available models for self-heating it is felt that a model similar to that used by Nordon (1979), but taking into account natural convection flows and neglecting diffusion, (as discussed in Chapter 2), should be developed in order to make predictions about the behaviour of stockpiled coal.

5.3 A one-dimensional analogue of a coal dump

In order to derive a mathematical model of a coal dump which will yield results fairly simply, certain simplifying assumptions have to be made. The main assumption in the model presented here is that the processes of heat, mass and momentum transfer occur in one direction only. Although this is known not to be true in a real coal dump, it does represent a limiting case which in many respects is the worst case. It can be seen that considering heat transfer in one direction only is likely to be the worst case, since the heat loss is limited to one direction only. Similarly considering flow in only one direction is the worst case, since reactant depletion is likely to be less in a one dimensional model than in one in which reactant flows from many directions.

In many important respects the one-dimensional model is accurate. A one-dimensional model is likely to be accurate for the case of coal stored in a silo, if proper allowance is made for radial heat losses that can occur. In the middle of a very large dump of coal heat transfer to the sides is unlikely to be significant because of the large distances involved; significant heat transfer will occur only to the surface of the dump. In addition should a "hot-spot" occur in a dump the flow due to natural convection will be in the same direction as the heat transfer. The existence of hot spots in coal dumps is well known; spontaneous combustion in its early stages is localized, as has been shown by infra-red photography. The reasons for the existence of hot-spots in coal dumps may include inhomogeneity of the bed in respect of degree of compaction, coal reactivity or moisture content. Experimental work by Young (1985), on natural convection in a porous bed containing a line source, shows

clearly that there is a region close to the source through which most of the flow passes. This is shown diagramatically in Figure 5.1, in which model streamlines are plotted for one half of a symmetrical bed, of infinite length in the Z direction, containing a line source located at X=0, Y=0.6. Note that the reason that no flow occurs through the side X=1 is that in solving the model equations Young assumed that this surface was impermeable. This assumption should not drastically effect the behaviour of the streamlines near the source. Although the situation modelled by Young (1985) is not identical to that in a coal bed, it is felt that the flow patterns near a hot-spot are unlikely to be very different to the flow patterns found near a line source.

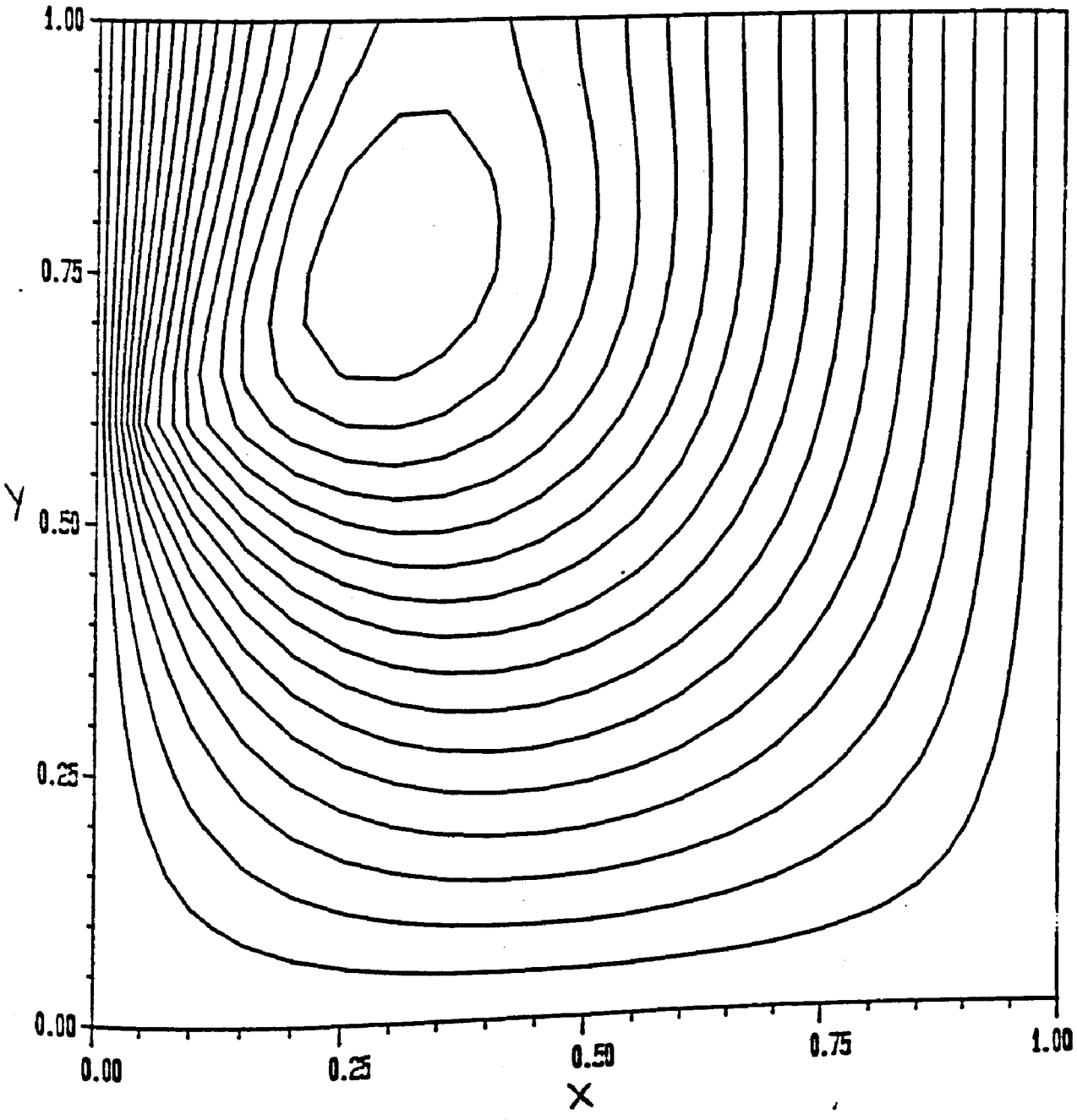


Figure 5.1 Streamlines in a Packed Bed Containing a Line Source (From Young, 1985)

Assuming that a hot spot arises in a coal dump for some reason, it can be reasoned that a chimney effect will take place. Air will flow up the chimney, and be replaced by air flowing in from the sides and top of the dump. If the behaviour of this chimney inside the coal dump can be modelled, then valuable insight into the nature of spontaneous combustion can be obtained. This is the physical basis for the model presented here.

To model the chimney inside the coal bed would be difficult. To make the model simpler the chimney is considered to be perfectly insulating radially. All the flow is considered to occur through the bottom of the bed, with no flow occurring through the sides. The bottom of the bed is considered to be open to atmosphere. These assumptions mean that the chimney can be modelled separately from the rest of the coal dump.

The disadvantages of this model are the following:

a) No simple relationship has been found relating the length of the chimney in the model to the size of the coal dump. Since the bed length is an important model parameter, this limits the applicability of the results obtained. This point will be further discussed in chapter 8.

b) It is assumed that the bottom of the chimney is open and thus loses heat to the atmosphere. In a real dump the bottom of the chimney loses heat to the surrounding coal. It is difficult to gauge how dissimilar these heat loss mechanisms are, and in what way this assumption will affect the results.

Despite these disadvantages the chimney or one-dimensional model may be considered to be a model that has a sound physical basis. The behaviour of the chimney should be similar to the behaviour of a coal dump in many important respects. The shortcomings of the the model are appreciated, but are not expected to invalidate the results obtained, provided these results are not taken to be directly applicable in a quantitative sense.

The great advantage of the model is that the equations derived may be solved fairly easily. A study of the parameters that are important in the prediction of spontaneous combustion may thus be performed without excessive computation.

The main assumptions in the mathematical model used in this study are therefore:

a) Flow and heat transfer occur in the same direction, and since the gas is assumed to flow in plug flow there are no radial gradients in the bed.

b) The reactions considered are

$$n\,C(s) + O_2(g) \rightarrow C_nO_2(s)$$
$$C_nO_2 \rightarrow CO_2 + (n-1)\,C(s)$$
$$\tfrac{1}{2}\,C_nO_2 \rightarrow CO(g) + (\tfrac{1}{2}n-1)\,C(s)$$
$$H_2O(g) \rightleftarrows H_2O(abs)$$

This reaction scheme is in agreement with the observed behaviour of the low temperature reactions of coal, as discussed in Chapter 1. C_nO_2 is oxycoal but note that no specific hypothesis about its structure needs to be made. The fourth reaction is water absorption, which has been reported to be of importance in spontaneous combustion of coal dumps, as has been discussed in chapter 2.

c) Flow is considered to be caused by natural convection and by differential pressure. Molecular diffusion is neglected as discussed in Chapter 2. Natural convection flows occur as soon as there is any temperature rise in the bed, since the bed is considered to be vertically aligned and open top and bottom.

Under these assumptions and some other minor assumptions which arise in the derivation of the equations a mathematical model has been derived. The full derivation is given in Appendix 3.

5.4 Model Equations

The model equations are:

5.4.1 Component mass balances (Gas phase)

$$G\frac{\partial y_i}{\partial x} + \frac{P\,\epsilon}{R\,T_g}\frac{\partial y_i}{\partial t} = r_i - y_i \sum r_j \qquad (i = 1 \text{ to } N)$$

G = molar flowrate per unit area

y_i = mole fraction of i in the gas phase

x = distance along bed

P = pressure

R = gas constant

ϵ = bed voidage

T_g = gas temperature

t = time

r_j = rate of formation of j in the gas phase per unit bed volume

N = number of components in gas phase

5.4.2 Overall gas mass balance

$$\frac{\partial G}{\partial x} + \frac{\epsilon}{R}\frac{\partial (P/T)}{\partial t} = \sum_{j=1}^{N} r_j$$

5.4.3 Component mass balances (Solid phase)

$$(1-\epsilon)\frac{\partial (\rho_s f_j)}{\partial t} = p_j \qquad (j = 1 \text{ to } M)$$

ρ_s = density of solid

f_j = mass fraction of j in the solid

p_j = rate of formation of j in the solid

M = number of components in solid phase

5.4.4 Overall solid mass balance

$$(1-\epsilon)\frac{\partial \rho_s}{\partial t} = \sum_{j=1}^{M} p_j$$

5.4.5 Gas phase energy balance

$$\frac{P\epsilon}{RT_g}\hat{c}\frac{\partial T_g}{\partial t} - \epsilon\frac{\partial P}{\partial t} = -G\hat{c}\frac{\partial T_g}{\partial x} + \epsilon K_g\frac{\partial^2 T_g}{\partial x^2} + Q_c$$

$\hat{c}$ = molar specific heat capacity of gas

K_g = thermal conductivity of gas

Q_c = rate of convection from solid to gas

5.4.6 Solid phase energy balance

$$(1-\epsilon)\,\rho_s\,\bar{c}_s\,\frac{\partial T_s}{\partial t} - (1-\epsilon)\,\frac{\partial P}{\partial t} = (1-\epsilon)\,\eta\,k_s\,\frac{\partial^2 T_s}{\partial x^2} - Q_c - \Sigma\,(r_i \Delta H_r^i)$$

T_s = solid temperature
η = tortuosity factor
k_s = thermal conductivity of solid
ΔH_r^i = enthalpy of reaction for formation of i

5.4.7 Momentum balance

$$\rho\,\frac{\partial U}{\partial t} = -f\,U + g\,\rho_\infty(1-T_\infty/T) - \frac{\partial(P-P_\infty)}{\partial x}$$

U = flow velocity
f = D'Arcy's law constant
ρ_∞ = density of ambient air
P_∞ = ambient air pressure

5.5 Discussion of the model equations

This is a set of M + N + 5 differential equations. The unknowns are tabulated in Table 5.2.

TABLE 5.2 UNKNOWNS IN THE MODEL EQUATIONS

UNKNOWN	DESCRIPTION	NUMBER
y_i	Gas mole fractions	N
G	Molar flowrate/area	1
f_i	Solid mass fractions	M
ρ_s	Solid density	1
T_g	Gas temperature	1
T_s	Solid temperature	1
P	Gas pressure	1

Although the equations have been derived for any number of gas and solid components, in the discussions that follow the gases considered are O_2, N_2, CO_2, CO and H_2O. The solid is considered to be composed of four fractions i.e. carbon, oxycoal, absorbed water and inert material.

5.6 Boundary and Initial Conditions

The following are the boundary conditions used: (x=0 refers to the bottom of the bed and x=L refers to the top).

$$y_i(0,t) = \text{Mole fraction of i in ambient air}$$

The pressure boundary conditions have been discussed in section 2.2 and are:

$$P(0,t) = P_\infty + \rho_\infty V^2/2$$

$$P(L,t) = P_\infty$$

$$V = \text{wind velocity}$$

For the gas phase energy balance

$$\epsilon k_g \frac{\partial T_g(0,t)}{\partial x} = G \hat{c} (T(0,t) - T_\infty)$$

$$\frac{\partial T_g(L,t)}{\partial x} = 0$$

The first boundary condition reflect the fact that the gas entering the bed is heated to the gas temperature. At the end of the bed it is assumed that there is no heat loss due to flow; the gas is assumed to leave the bed in plug-flow, implying that the temperature just outside the bed is equal to the temperature just inside the bed.

For the solid phase energy balance

$$(1-\epsilon) \eta k_s \frac{\partial T_s(0,t)}{\partial x} = h_1 (T_s(0,t) - T_\infty)$$

$$(1-\epsilon) \eta k_s \frac{\partial T_s(L,t)}{\partial x} = -h_2 (T_s(L,t) - T_\infty)$$

These are convective boundary conditions, but h_1 and h_2 may be interpreted as radiation heat transfer coefficients. Initial conditions for the equations involve assigning values to each of the variables at time zero for all x. In most cases ambient values would be used.

6. SIMPLIFICATON OF THE MODEL EQUATIONS AND THEIR SOLUTION

6.1 Introduction

Although a one-dimensional formulation has been used to simplify the equations and reduce their number, the equations remain complicated. In order to simplify them further to perform computation the following assumptions (which are discussed more fully in Appendix 4) were made:

a) The gas and solid temperatures are unlikely to be very different; therefore equations 5.4.5 and 5.4.6 may be combined to give one equation in temperature, ie a continuum assumption is made. The reason for deriving the gas and solid phase energy balances separately is that the boundary conditions for use in the continuum model are not clear; deriving the balances separately and then combining them allows the correct boundary conditions to be deduced mathematically.

b) Since the heat transfer is by far the slowest transfer process occuring in the bed, the other transfer processes may be considered to be at steady state i.e. a pseudo steady state formulation is used.

In order to simplify still further it is convenient to define a rate (ry) which is the rate at which oxygen disappears. Similarly an enthalpy of reaction ΔH_r is defined; this may be considered to be the enthalpy of reaction associated with the disappearance of oxygen. The reaction involving water is ignored for the following reasons:

a) It is likely to be only a starting mechanism whereby the temperature in a coal bed is raised to the point where natural convection flows and oxidation become the mechanisms whereby the dump combusts.

b) As yet no reliable data for this reaction is available, and it is in any case believed that the reaction is likely to be close to equilibrium in most cases.

It would appear from equation 5.4.2 that the change in flowrate due to reaction has to be considered. However, if air is the reactant then even if all the oxygen in the flow is removed the flowrate will only change by twenty percent. It is therefore

6. SIMPLIFICATON OF THE MODEL EQUATIONS AND THEIR SOLUTION

6.1 Introduction

Although a one-dimensional formulation has been used to simplify the equations and reduce their number, the equations remain complicated. In order to simplify them further to perform computation the following assumptions (which are discussed more fully in Appendix 4) were made:

a) The gas and solid temperatures are unlikely to be very different; therefore equations 5.4.5 and 5.4.6 may be combined to give one equation in temperature, ie a continuum assumption is made. The reason for deriving the gas and solid phase energy balances separately is that the boundary conditions for use in the continuum model are not clear; deriving the balances separately and then combining them allows the correct boundary conditions to be deduced mathematically.

b) Since the heat transfer is by far the slowest transfer process occuring in the bed, the other transfer processes may be considered to be at steady state i.e. a pseudo steady state formulation is used.

In order to simplify still further it is convenient to define a rate (ry) which is the rate at which oxygen disappears. Similarly an enthalpy of reaction ΔH_r is defined; this may be considered to be the enthalpy of reaction associated with the disappearance of oxygen. The reaction involving water is ignored for the following reasons:

a) It is likely to be only a starting mechanism whereby the temperature in a coal bed is raised to the point where natural convection flows and oxidation become the mechanisms whereby the dump combusts.

b) As yet no reliable data for this reaction is available, and it is in any case believed that the reaction is likely to be close to equilibrium in most cases.

It would appear from equation 5.4.2 that the change in flowrate due to reaction has to be considered. However, if air is the reactant then even if all the oxygen in the flow is removed the

6. SIMPLIFICATON OF THE MODEL EQUATIONS AND THEIR SOLUTION

6.1 Introduction

Although a one-dimensional formulation has been used to simplify the equations and reduce their number, the equations remain complicated. In order to simplify them further to perform computation the following assumptions (which are discussed more fully in Appendix 4) were made:

a) The gas and solid temperatures are unlikely to be very different; therefore equations 5.4.5 and 5.4.6 may be combined to give one equation in temperature, ie a continuum assumption is made. The reason for deriving the gas and solid phase energy balances separately is that the boundary conditions for use in the continuum model are not clear; deriving the balances separately and then combining them allows the correct boundary conditions to be deduced mathematically.

b) Since the heat transfer is by far the slowest transfer process occuring in the bed, the other transfer processes may be considered to be at steady state i.e. a pseudo steady state formulation is used.

In order to simplify still further it is convenient to define a rate (ry) which is the rate at which oxygen disappears. Similarly an enthalpy of reaction ΔH_r is defined; this may be considered to be the enthalpy of reaction associated with the disappearance of oxygen. The reaction involving water is ignored for the following reasons:

a) It is likely to be only a starting mechanism whereby the temperature in a coal bed is raised to the point where natural convection flows and oxidation become the mechanisms whereby the dump combusts.

b) As yet no reliable data for this reaction is available, and it is in any case believed that the reaction is likely to be close to equilibrium in most cases.

It would appear from equation 5.4.2 that the change in flowrate due to reaction has to be considered. However, if air is the reactant then even if all the oxygen in the flow is removed the flowrate will only change by twenty percent. It is therefore considered adequate to regard the flowrate as a constant to be considered adequate to regard the flowrate as a constant to be calculated from equation 5.4.7.

Under these assumptions the number of equations to be solved is reduced to three i.e. a temperature equation, an oxygen equation and a flowrate equation. These equations are given below.

Temperature: $$\rho C_b \frac{\partial T}{\partial t} = k_b \frac{\partial^2 T}{\partial x^2} - G \hat{c} \frac{\partial T}{\partial x} + r\, y\, \Delta H_r \qquad 6.1.1$$

ρ_b = density of bed
C_b = specific heat capacity of bed
k_b = thermal conductivity of bed
y = mole fraction oxygen
ΔH_r = enthalpy of reaction for oxygen disappearance

Oxygen: $$G \frac{dy}{dx} = -r\, y \qquad 6.1.2$$

Flowrate: $$\frac{d(P-P_\infty)}{dx} = -f\, G\, R\, T/P + g(\rho_\infty - \rho) \qquad 6.1.3$$

One possible functional form for the rate of reaction r has been discussed in Section 1.3, but should a superior rate expression for the oxidation be proposed it would be a simple matter to use this expression in the model.

The boundary conditions on the equations are:

$$k_b \frac{\partial T(0,t)}{\partial x} = (h_0 + G \hat{c})\,(T(0,t)-T_\infty)$$

$$k_b \frac{\partial T(L,t)}{\partial x} = -h_1\,(T(L,t)-T_\infty)$$

$y(x=0)$ = mole fraction of oxygen in air

$P(x=0) = P_\infty + \rho_\infty V^2/2$

$P(x=L) = P_\infty$

The initial condition for equation 6.1.1 is a given temperature profile e.g. $T(x,0) = T_0(x)$.

It is convenient in what follows to make equation 6.1.1 dimen-

sionless. To do this the following substitutions are made:

$$\theta = T/T_\infty$$
$$X = x/L$$
$$\tau = \kappa t/L^2$$
$$a = G\,\hat{c}\,L/k_b$$
$$b = L^2\,r\,(-\Delta H_r)/(T_\infty\,k_b)$$
$$\gamma_s = -r/G$$
$$Bi_0 = h_0\,L/k_b$$
$$Bi_1 = h_1\,L/k_b$$

Equation 6.1.1 becomes:

$$\frac{\partial\theta}{\partial\tau} = \frac{\partial^2\theta}{\partial X^2} - a\,\frac{\partial\theta}{\partial X} - b\,\gamma \qquad 6.1.4$$

with boundary conditions

at X=0 $$\frac{\partial\theta}{\partial X} = (Bi_0+a)(\theta-1)$$

at X=1 $$\frac{\partial\theta}{\partial X} = -Bi_1(\theta-1)$$

The initial condition is $\theta(X,0) = \theta_0(X)$

This equation may be improved by including a heat loss term. This heat loss term takes into account radial heat losses that are not taken into account in the original model. The term, as is shown in Appendix 5, may be written as $C(\theta - 1)$. In a sense C is a free parameter. It does however have real meaning in simulating a coal dump as will be seen in Chapter 7. Equation 6.1.4 becomes:

$$\frac{\partial\theta}{\partial\tau} = \frac{\partial^2\theta}{\partial X^2} - a\,\frac{\partial\theta}{\partial X} - b\,\gamma - C\,(\theta - 1) \qquad 6.1.5$$

with boundary and initial conditions as above.

6.2 The Steady-State form of the Equations

It may be argued that the set of equations does not have a steady-state solution since the reaction rate r is a function of the amount of oxidation and therefore of time. If the reaction rate is constantly falling off with time, i.e. the coal is

ageing, then there is no steady state. However it is convenient to study the behaviour of the equations in the limit of steady state, and for this purpose the ageing of the coal is ignored, and the so-called reaction rate of fresh coal is used. This is in a sense the worst case since the fresh coal has the highest reaction rate.

The temperature equation then becomes

$$0 = \frac{d^2\theta}{dX^2} - a\frac{d\theta}{dX} - b\,y - C\,(\theta - 1) \qquad 6.2.1$$

First attempts to solve equation 6.2.1 with equation 6.1.2 and 6.1.3 involved the use of a Runge - Kutta algorithm. The method used was a shooting one i.e. a temperature at X = 0 and flowrate were guessed, and the equations integrated forward to try and meet the boundary conditions at X = 1. This method met with no success at all, since the calculated temperature was very sensitive to the assumed value of the inlet temperature. Changing the value of this temperature led either to the temperature increasing without bound or becoming negative. An explanation for this behaviour is given in Appendix 6.

An alternative method of solving equation 6.2.1 involves making the assumption that the reaction rate r may be considered constant throughout the bed. This is a very large assumption since the form of r involves an exponential of the temperature, and thus r cannot in fact be constant unless the bed temperature is constant. However over a fairly small range of temperature the assumption of an average rate in the bed is acceptable, even though the answers it gives will not be quite correct. A further justification for making this assumption is that an analytic form for the temperature profile in the coal bed may be obtained, and thus the characteristics of the solution may be quickly investigated.

The details of the solution are given in Appendix 7, and the temperature equation has the form:

$$\theta_{ss}(X) = 1 + C_1\exp(\gamma_1 X) + C_2\exp(\gamma_2 X) + C_3\exp(\gamma_3 X) \qquad 6.2.2$$

The coefficients γ_1, γ_2, C_1, C_2, and C_3 are given functions of the known parameters.

The solution of the equation set is in fact iterative, since some average temperature is assumed and the flowrate and average reaction rate calculated. This in turn leads to a new temperature profile, flowrate, and average reaction rate and so on till the process converges. The computer code to perform this calculation is given in Appendix 12.

The character of the solutions so obtained and their significance is discussed in Chapter 8.

6.3 The Solution of the Unsteady-State Equations with a Constant Rate

The unsteady state behaviour of the equation set is of great practical importance. If a coal dump is going to be reclaimed in a relatively short time, then its long time or steady-state behaviour is of little importance in predicting the safety or otherwise of the dump. In addition it is only possible to decide whether a given dump will achieve a safe or unsafe steady-state by considering the behaviour of the temperature with time.

As a continuation of the work in which the equation set is solved using a constant rate, a solution was sought for the unsteady state behaviour under the same assumption.

The equation to be solved is equation 6.1.5 and the details of the solution are given in Appendix 8. The solution is:

$$\theta(X,\tau) = \theta_{ss}(X) + v(X,\tau)\exp(-\tau(a^2/4-C) + aX/2) \qquad 6.3.1$$

where $$v(X,\tau) = \Sigma \{Z_n(X)\exp(-\beta_n^2\tau)\ Z_n(X')\ g(X')\ dX'\} \qquad 6.3.2$$

$$Z_n(X) = \frac{2(\beta_n^2+Bi_3^2)(\beta_n\cos(\beta_n X)+Bi_2\sin(\beta_n X))}{((\beta_n^2+Bi_2^2)(\beta_n^2+Bi_3^2+Bi_3)+Bi_2(\beta_n^2+Bi_3^2))}$$

$$g(X) = (\theta_o(X) - \phi_{ss}(X))\exp(-aX/2) \qquad 6.3.3$$

$$Bi_2 = Bi_0 + a/2$$

$$Bi_3 = Bi_1 + a/2$$

and the β_n are the positive roots of

$$\tan(\beta) = \frac{\beta(Bi_3 + Bi_2)}{(Bi_2\, Bi_3 + \beta^2)} \qquad 6.3.4$$

Obtaining the final solution (equation 6.3.1) at a given X and τ is a stepwise process, since starting with the initial condition $\theta_0(X)$ the coefficients a, b, and γ_3 are calculated. A time step is then taken and the temperature profile calculated. This in turn gives new values of a, b, and γ_3 and the process continued.

The solution has been programmed in BASIC on a HP 9835 computer, and the code is given in Appendix 12. In practice it has been found that only twenty terms of the series need be taken. Nevertheless obtaining the solution is a fairly lengthy process, since for each time step $Z_n(X)$ and the integral in equation 6.3.2 must be calculated for a number of X values.

The character of the solutions obtained by this method is discussed in Chapter 8.

6.4 A Numerical Method for Solving the Unsteady State Equations

A numerical method for solving the equation set has the following advantages:

a) The variation of the reaction rate with temperature and amount of oxidation of coal can be taken into account.

b) The model can be used to fit data obtained from experiments such as the one described in Chapter 7. This data can then be used to make predictions about the behaviour of a given coal in a given stockpiling situation.

The disadvantage of a numerical method is that no general observations can be made about the form of the solution, as is possible with an analytic solution. Also the amount of computation may become prohibitive.

The method chosen for solving the equations in this case is one first presented by Bellman, Kashef & Casti (1972), which has been

termed the method of lines. The technique involves the use of a Legendre polynomial to fit the temperature profile at any given time t. This has the effect of reducing the partial differential equation to a set of ordinary differential equations, which may then be solved by one of many available methods e.g. Runge-Kutta or Adams-Moulton.

The advantage of this method over the more normally used finite difference approach is that the finite difference methods require calcualtion at a large number of points in order to obtain accurate results at the points of interest. Consequently both the computing time and storage required are large. In contrast, the approach of doing the calculation at the nodes of the shifted Legendre polynomial offers a moderately accurate solution at a few points, and the solution may be calculated rapidly.

The essence of the method rests in writing

$$\frac{\partial\theta(X_j,\tau)}{\partial X} = \Sigma(a_{ij}\ \theta(X_j,\tau)) \qquad \text{for } i=1 \text{ to } n \qquad 6.4.1$$

The X_j are chosen to be the nodes of the shifted Legendre polynomial

$$P_n^*(X) = P_n(1-2X) \qquad 6.4.2$$

and the matrix a_{ij} of weighting factors may be calculated once and for all.

The details of the application of the technique to the particular set of equations under consideration are given in Appendix 9. In many respects the solution procedure is similar to that discussd in Section 6.3, since the coefficients a, b, and γ_3 are recalculated at each time step.

This solution method has also been programmed in BASIC on an HP 9816 computer, and the code is given in Appendix 12. The choice of the length of the time step chosen is critical to the stability of the method, but apart from this the method is very effective. Calculational time is in fact shorter than that required to obtain the solution 6.3.1 and it has been found that using a ninth order Legendre Polynomial is entirely adequate.

Further discussion of the method and the results obtained is given in Chapter 8.

7. EXPERIMENTAL INVESTIGATION OF THE BEHAVIOUR OF A ONE DIMENSIONAL ANALOGUE OF A COAL DUMP

7.1 Introduction

In order to attempt to validate the equations derived in the previous sections, as well as to obtain data to use in a parameter study, it was decided to build a coal chimney. The apparatus used and results obtained are discussed in this chapter.

7.2 Experimental

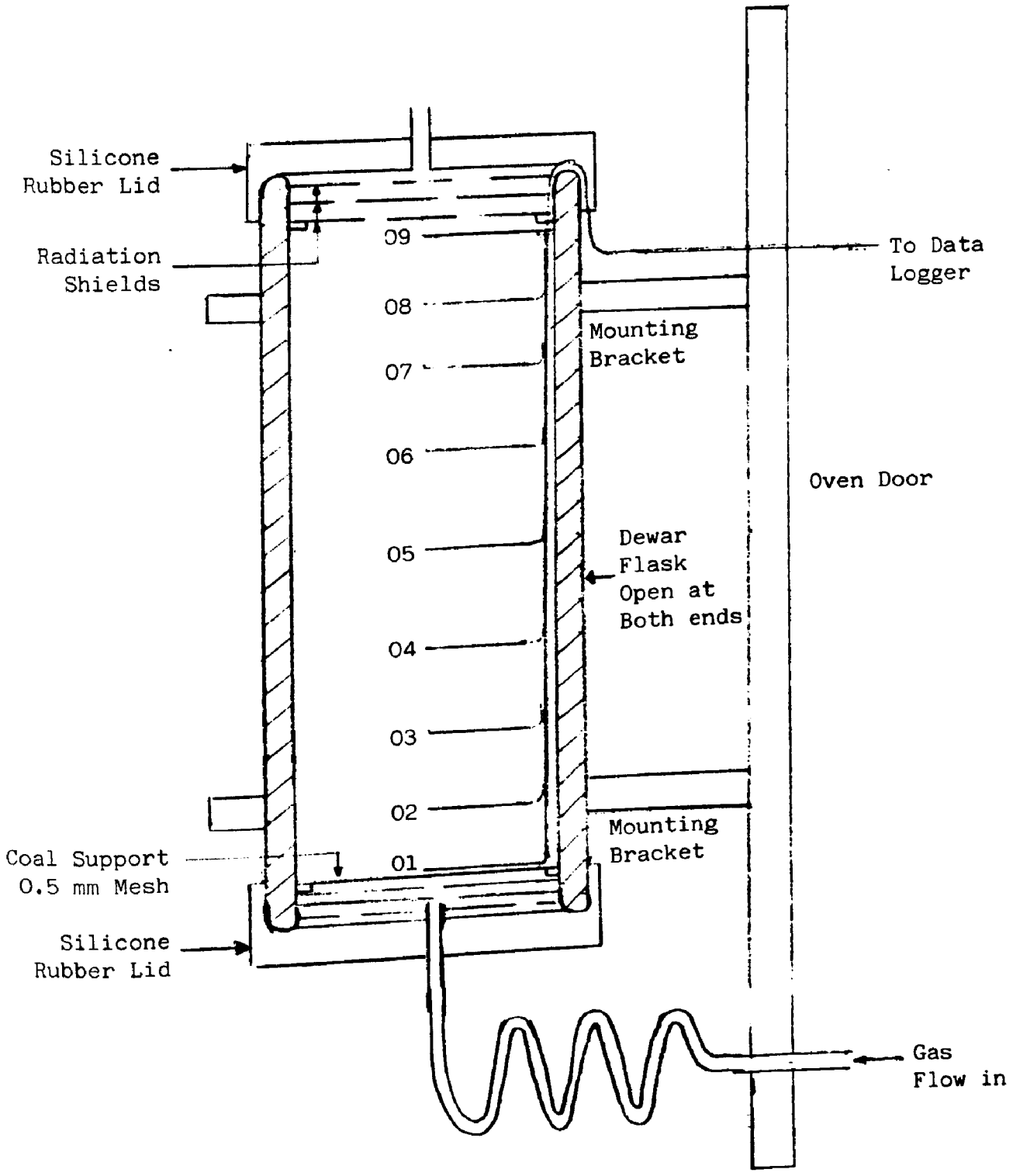
A skethch of the apparatus used is shown in figure 7.1. The coal chimney is constructed from an open ended Dewar Flask of 78 mm internal diameter and 240 mm height. Dimples of glass 20 mm from the bottom of the apparatus provide support for a piece of thin mesh, which in turn supports the coal. The chimney is provided with removable silicone rubber lids above and below. Both lids have 6 mm copper tubing moulded in, to provide for flow of gas in and out.

To minimize heat losses radiation shields manufactured from aluminium foil covered balsa wood discs are used. 10 mm Holes are punched in these discs in such a way that if three discs are assembled 5 mm apart, no direct rays of radiation can escape.

Thermocouples are manufactured by sparking together 20 SWG fabric coverd copper and constantan. The thermocouples are tested at 0°C and at the boiling point of water.

At the time of packing the bed with coal, the thermocouples are placed with their exposed ends on the centre line of the apparatus. Nine thermocouples are placed in the apparatus at positions corresponding to the nodes of the ninth order Legendre polynomial used in the solution method discussed in section 6.4.

In order to record the temperature-time behaviour of the chimney, these nine thermocouples, together with a tenth thermocouple placed in the oven containing the apparatus, are connected to a HP 3054 Data Aquisition Unit controlled by an HP 85 computer. A program



01 - 09: Copper Constantan Theromcouples

Figure 7.1 Chimney Experiment - Apparatus

supplied by Hewlett Packard is used to record the temperatures at a suitable time interval, as well as to print the temperatures and record them on tape. The program converts thermocouple voltages to temperatures using a fourth order polynomial; a silicon device built in to the data logger provides the cold junction reference temperature.

The apparatus is contained within a thermostatically controlled oven. Considerable care is taken to ensure that the temperature variations within the oven are small. The temperature in the oven is continually recorded using an eleventh thermocouple and a recorder. The temperature control of the oven is better than one degree centigrade.

The bed is supplied with gas (either nitrogen and oxygen) from cylinders. A series of valves are used to drop the pressure from the cylinder to the inlet of the bed, and to provide control over the flowrate of gas into the bed. This flowrate is measured usng a Tri Flat Variable Area Floe Meter. The manufacturer's curves are used to convert a reading on the meter to a volumetric flowrate. The barometric pressure is recorded in order that the volumetric flowrate can be converted to a molar flowrate. In order to ensure that the gas entering the bed is at oven temperature, a coil of length 0.5 m of 6 mm copper pipe is provided within the oven. enables the temperature time and temperature distance profiles to be automatically logged at any suitable time interval.

Experimental procedure consists of setting the oven temperature to the desired level, and placing the apparatus in the oven with a flow of nitrogen through the bed. Temperatures are recorded until they are considered to be steady. The flow is then switched to oxygen, and the temperature-time data recorded. For each run fresh coal that has been stored under water is used, in order to minimize the amount of prior oxidation of the coal. The coal is allowed to dry in a thin layer overnight at ambient temperature.

The experimental data obtained is tabulated in Appendix 10.

7.3 Experimental Results

The accuracy of results obtained from this experiment is limited by the accuracy to which the heat transfer characteristics of the apparatus are known. In order to calculate the numbers Bi_o, Bi_1, and C required for the model the bed was heated under nitrogen and then removed from the oven while continuing the nitrogen flow. The temperature time curve was then recorded, and a trial and error method used to calculate the values of the coefficients which best fit the data. The results of this fitting procedure are shown in Figure 7.2.

It can be seen that the experimental data is fitted very well at the centre of the bed but rather poorly at the ends of the bed. This indicates that the heat transfer mechanism at the ends of the bed is not well modelled by a heat transfer coefficient. However it was felt that if the rest of the fitting was done with temperature time curves at the centre of the bed the results would at least yield suitable values to use in a parameter study.

Two different sorts of behaviour have been observed during the experiments in which oxygen is flowed through a preheated coal bed. The different sorts of behaviour depend on the particle size of the coal used and the oven temperature.

The first type of behaviour which is observed is a fairly gentle rise of the temperature in the bed, with some maximum temperature being reached, after which the temperature begins to fall off again. This behaviour can only occur if the reactivity of the coal is falling off with time; this implies that the coal is ageing. This behaviour, observed for the larger particle sizes at oven temperatures of approximately 90 ^{o}C, has been used to calculate the various constants in the shrinking core model discussed in Section 1.3; these fits are shown in Figures 7.3 and 7.4.

The second type of behaviour observed is a fairly rapid temperature increase in the coal bed with the rate of temperature rise increasing with time. This behaviour may be considered to be combustion. When this occurs the coal bed has to be cooled down by taking the apparatus out of the oven and restoring the

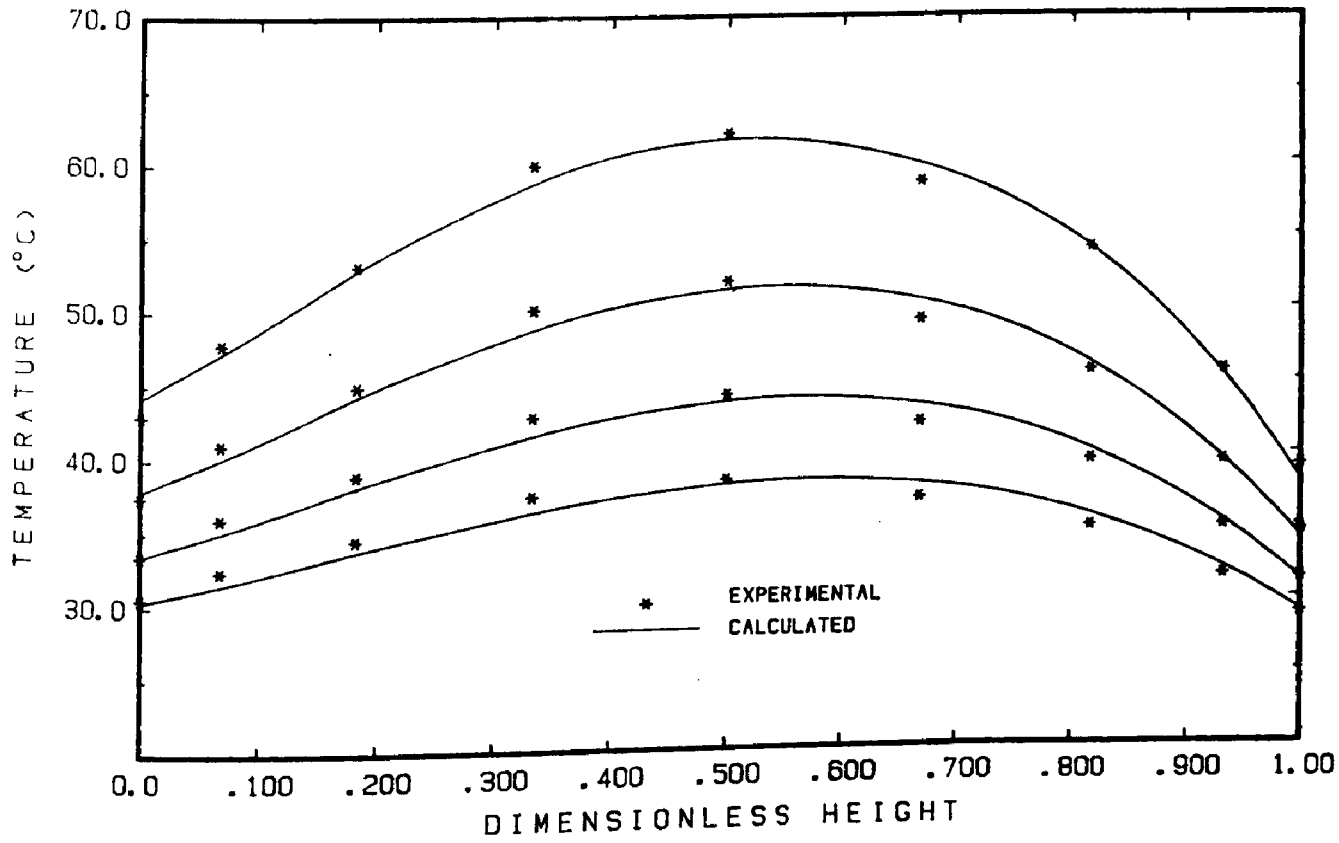


Figure 7.2 Chimney experiment - Fitting heat transfer coefficients

Profiles plotted every 30 minutes

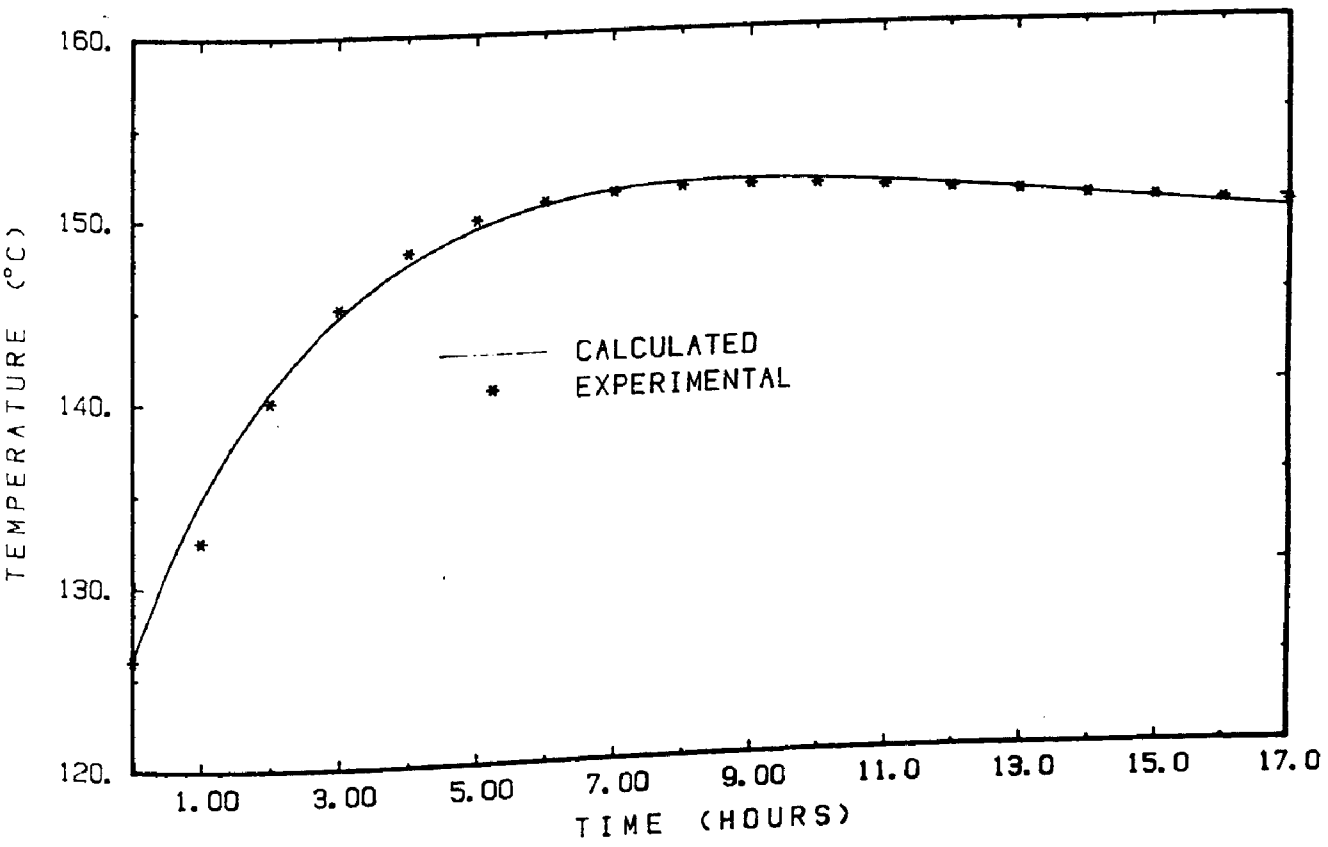


Figure 7.3 Chimney experiment - Fitting ageing run 1

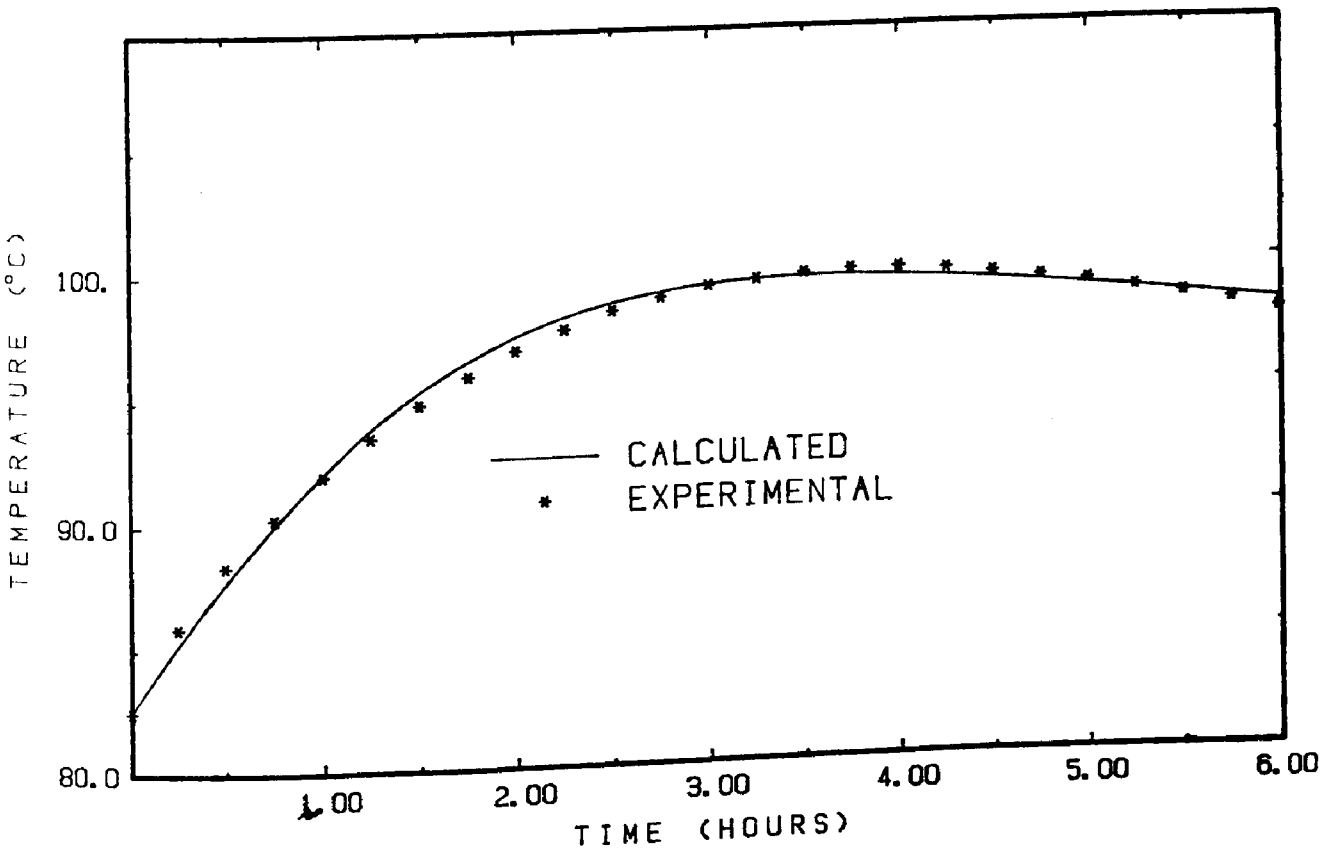


Figure 7.4 Chimney experiment - Fitting ageing run 2

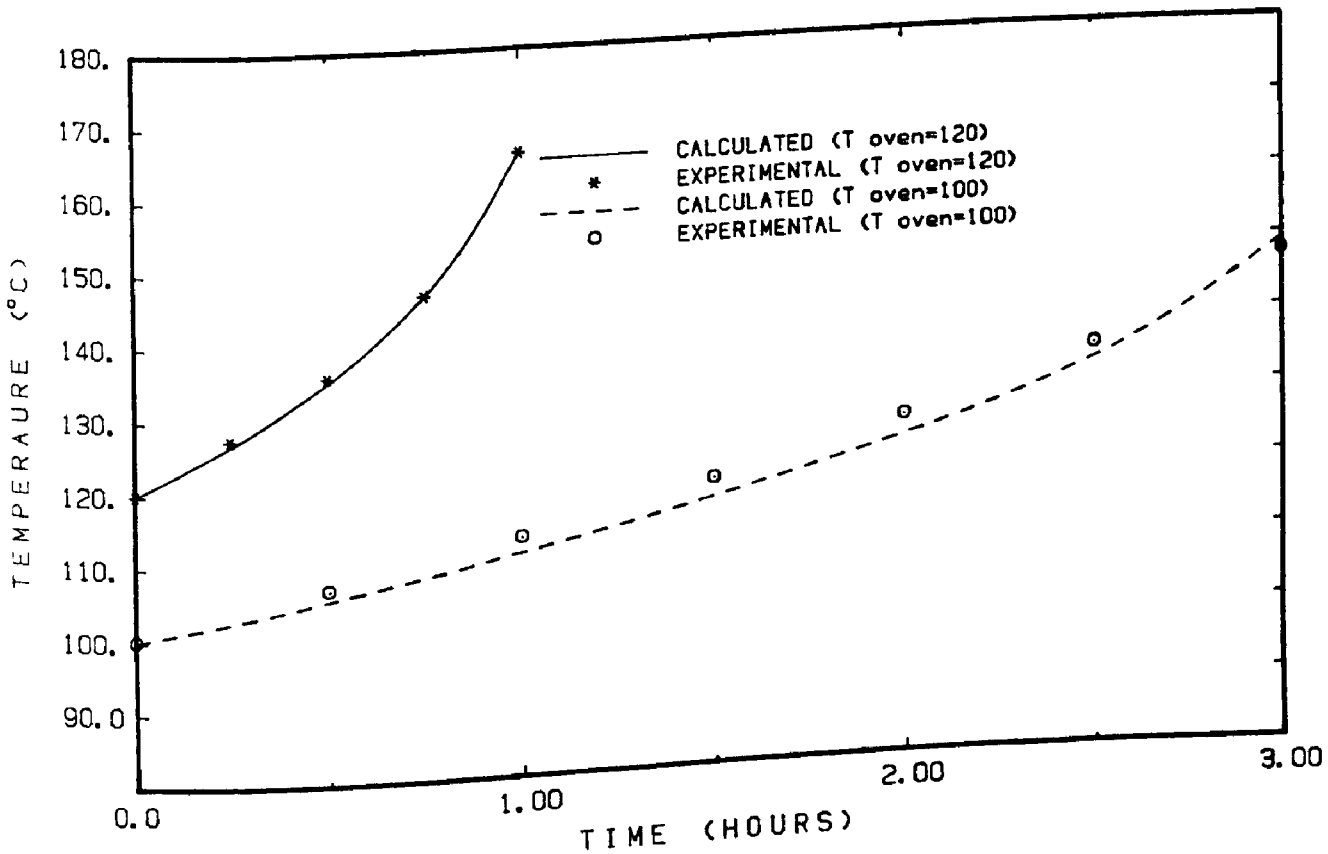


Figure 7.5 Chimney experiment - Fitting ignition runs

nitrogen flow.

These ignition runs yield very valuable information since it proves simpler to deduce the kinetic data from these runs then from the runs in which there is a gentle temperature rise. The reasons for this are that the temperature rises are much larger, meaning that ageing is a smaller effect. An example of the fitting of this data is shown in Figure 7.5 where two different experimental runs are fitted with the same data. The fit is fair but tends to be poorer as the temperature increases more rapidly. The reason for this is that at these higher temperature some of the model assumptions breakdown.

The values of the parameters used to obtain the fits shown in figures 7.2 to 7.5 are tabulated in Appendix 10. It must be stressed that these parameters, in particular the reaction rate values, are likely to be very different for different coals.

7.4 Discussion

The experiment used to derive the results in this section is not a good experiment from the point of view of analyzing the results to obtain the parameters required. This is partly because many of the parameters required in the model need to be estimated, and there may be a high cross correlation between the estimated parameters, and those found by curve fitting. However it is felt that the parameters calculated are accurate enough to give starting values for the parameter analysis discussed in the next chapter.

The analysis of the experiment may be improved in many respects e.g. by the use of a minimization routine to calculate the parameters. This was not felt neccessary in the present study.

8. RESULTS OF SOLVING THE MODEL EQUATIONS

8.1 Introduction

In this chapter the results of solving the model equations are presented. The three cases considered are:

a) Solving the steady-state equations with constant r.
b) Solving the unsteady-state equations with constant r.
c) Solving the equations with no assumptions, using a numerical method.

8.2 Steady-State Solution for constant r

Since an analytic solution exists for the temperature profile in this case, it has been used to perform a parameter study of the effect that changing the model parameters has on the calculated temperature profiles. In order to perform this parameter study a base set of parameter values had to be chosen, and certain assumptions made. The values of the parameters for this base case are given in Appendix 11. The assumptions made were the following:

a) The coal may be characterized by a single particle diameter, D_p, where

$$D_p = 6/S$$

S = external surface area per particle volume

b) The surface area for reaction, S_t, is set equal to the external surface area, S. However, the effect of changing this assumption has been investigated.

c) The wind velocity is set to zero, as is the heat loss coefficient, C.

d) Radiation heat transfer coefficients are used for h_1 and h_2; these could easily be replaced by natural convection heat transfer coefficients, if these were found to be more appropriate.

8.2.1 The Character of the Solutions

In order to investigate the character of the solutions, the following analysis was used:

Equaton 6.1.5 with C set equal to zero (i.e. no radial heat loss) is :

$$\frac{\partial\theta}{\partial\tau} = \frac{\partial^2\theta}{\partial X^2} - a\frac{\partial\theta}{\partial X} - by$$

Integrating from X = 0 to X = 1 gives

$$\int_0^1 \frac{\partial\theta}{\partial\tau}\,dX = \int_0^1 \frac{\partial^2\theta}{\partial X^2}\,dX - \int_0^1 a\frac{\partial\theta}{\partial X} - \int_0^1 by\,dX \qquad 8.1$$

Now, as shown in Appendix 4, $y = y_o \exp(\gamma_3 X)$. In addition a and b are not functions of X since they are calculated at an average temperature.

Thus equation 8.1 becomes

$$\frac{\partial\bar{\theta}}{\partial\tau} = \frac{\partial\theta}{\partial X}\Big]_1 - \frac{\partial\theta}{\partial X}\Big]_0 - a\,[\theta_1 - \theta_0] - \frac{by_o}{\gamma_3}[\exp(\gamma_3) - 1]$$

$$\frac{\partial\bar{\theta}}{\partial\tau} = -Bi_1(\theta_1 - 1) - (Bi_o + a)(\theta_0 - 1) - \frac{by_o}{\gamma_3}[\exp(\gamma_3) - 1]$$

$$\frac{1}{a}\frac{\partial\bar{\theta}}{\partial\tau} = -\frac{Bi_1}{a}(\theta_1 - 1) - \left(\frac{Bi_o}{a} + 1\right)(\theta_0 - 1) + \frac{by_o}{a\gamma_3}[1-\exp(\gamma_3)]$$

This equation may be written as

$$\frac{1}{a}\frac{\partial\bar{\theta}}{\partial\tau} = RHS - LHS \qquad 8.2$$

where

$$LHS = \frac{Bi_1}{a}(\theta_1 - 1) + \left(\frac{Bi_o}{a} + 1\right)(\theta_0 - 1)$$

$$RHS = \frac{by_o}{a\gamma_3}[1-\exp(\gamma_3)]$$

Equation 8.2 is the overall energy balance for the bed.

The quantity $by_o/(a\gamma_3)$ may be evaluated by substituting for a,b and γ_3 to give $(-\Delta H_r y_0) / (\hat{c}T_\infty)$. This quantity is the dimensionless adiabatic temperature rise i.e. the temperature rise that would occur if there was total conversion and no heat loss.

The steady-state solutions to equation 8.2 may be found by plotting LHS and RHS against θ , and observing where the two curves cross, since where the two curves cross

$$\frac{\partial\theta}{\partial\tau} = 0$$

The advantage of this procedure over solving the equation directly is that both stable and unstable steady-state solutions may be easily found.

A problem that occurs in using equation 8.2 is that , in the absence of wind, $T = T_\infty$ is always a solution of the equation. This is not a realistic solution, and arises from the assumpton in the model that natural convection is the only flow mechanism. In reality some diffusion will occur, and in this case this solution will vanish. In order to avoid numerical difficulties that arise, and also to make the solutions more realistic, in what follows it is assumed that the flowrate G may be written as

$$G = G_0 + G_{convection} \qquad 8.3$$

where G_0 is small but non-zero.

In the programs used to generate the figures in this section G_0 is assumed to caused by a 0.1 m/s wind. Equation 2.2.13 can be used to show that for a 5m long bed, this wind velocity causes the same flow as a temperature rise of 10^{-4} K, which is of course entirely negligible.

Several general points may be deduced from the definitions of RHS and LHS. In particular it is instructive to take limits of both the RHS and LHS as θ tends to 1 and to infinity.

When θ tends to 1, r tends to a finite quantity and G tends

to G_o by equation 8.3. (When $\theta = 1$ $G_{convection} = 0$). However since G_o can be chosen arbitrarily small the quantity exp(-rL/G) tends to 0. No other quantities in equation 8.2 are functions of θ , therefore

$$\lim_{\theta \to 0} (RHS) = - \frac{\Delta H_r y_o}{\hat{c}\, T_\infty}$$

For the values tabulated in Appendix 11 this quantity, which is the dimensionless adiabatic temperature rise, evaluates to 7.

When θ tends to 1 the LHS tends to zero by equation 8.2 , since both θ_o and θ_1 and tend to 1 as θ tends to 1.

When θ tends to infinity, the RHS tends to 0. This may be seen by considering the behaviour of rL/G for this case.

When θ tends to inifinity the LHS is not bounded, since both θ_o and θ_1 tend to infinity.

This suggests that the behaviour of the graph of RHS and LHS versus θ is as sketched in Figure 8.1.

From figure 8.1 it is clear that there must be an odd number of solutions to equation 8.2, and that the curves intersect at least once.

A further analysis of equation 8.2 leads to the ability to predict whether a cetain solution is an unstable or stable solution. Referring to equation 8.2 it may be seen that if LHS < RHS then $\partial\theta/\partial\tau > 0$ i.e. the bed tempeature is increasing. Referring to figure 8.1, and in particular to point B, it can be seen that at a temperature just above the temperature at which LHS and RHS intesect RHS is greater then LHS i.e. the derivative is positive. This implies that should the bed be at point B and the temperature rise, it will carry on rising since the derivative remains positive. Only at point C when this derivative is again 0 will the temperature stop rising. This implies that point B represents an unstable steady-state. A similar analysis can be performed to show that points A and C are stable steady-states.

The general conclusion from this analysis is:

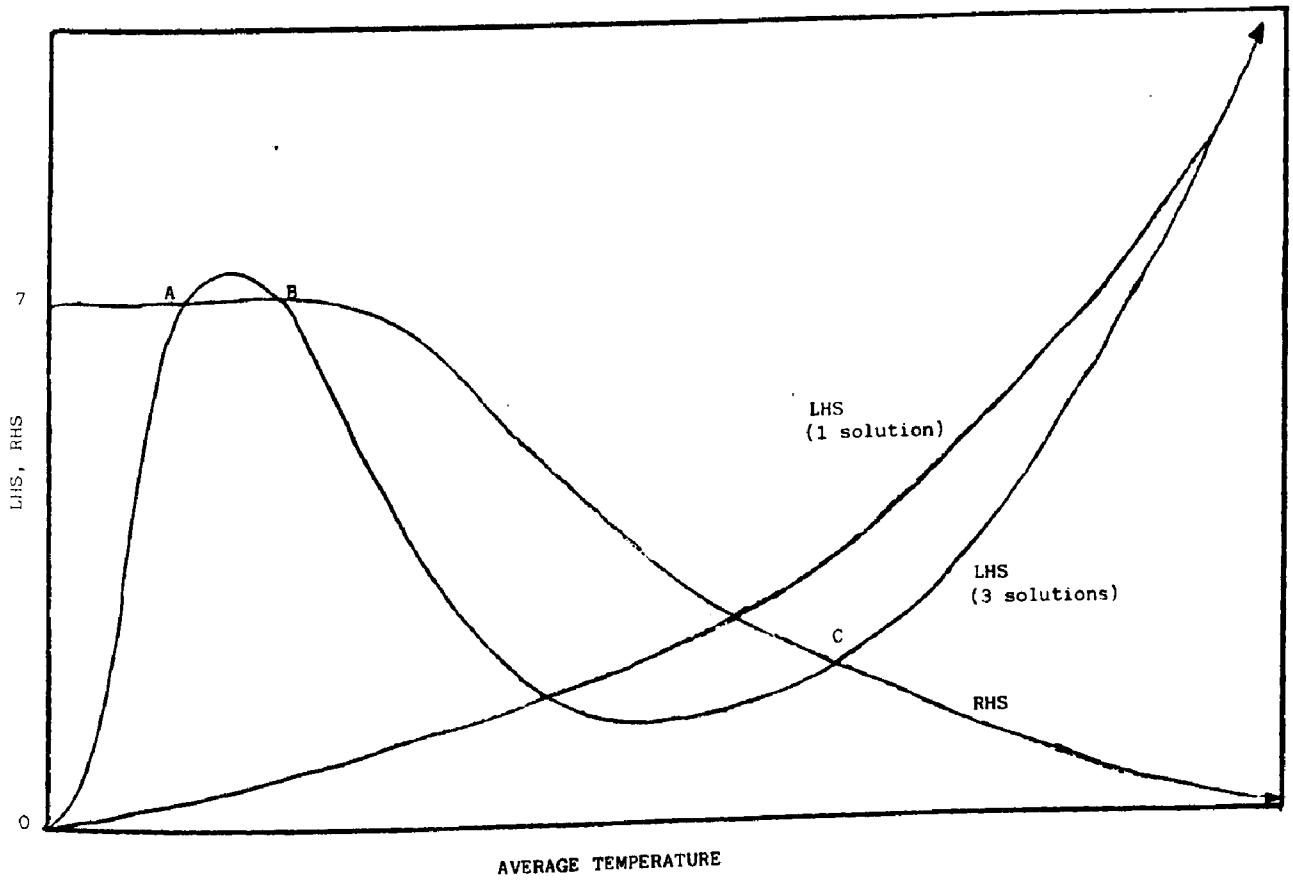


Figure 8.1 LHS and RHS of equation 8.2 as a function of θ

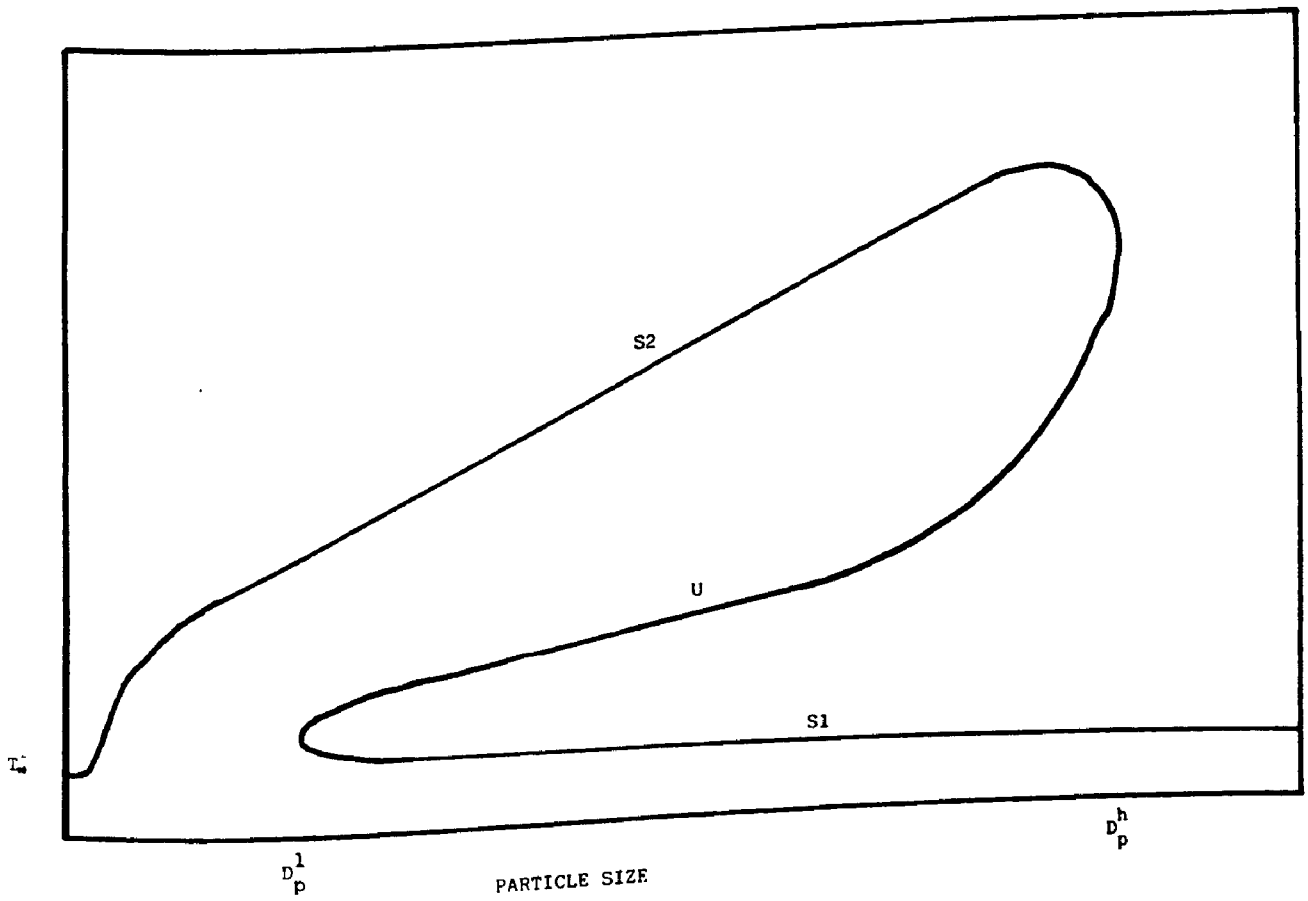


Figure 8.2 Locus of solutions to equation 8.2

For a stable solution at crossing θ_c the following condition must be true:

$$\left.\frac{d\ RHS}{d\bar{\theta}}\right]_{\theta_c} < \left.\frac{d\ LHS}{d\bar{\theta}}\right]_{\theta_c}$$

and conversely for an unstable solution:

Referring to figure 8.1 it is clear that the solutions A and C are stable solutions, while B is an unstable solution. In general the first and last solutions must be stable, and in between the solutions occur as unstable-stable-unstable etc. If there is only one solution it is stable.

This discussion serves to relate the behaviour of coal beds, as deduced in this study, to the behaviour of autothermal chemical reactors, and is extremaly valuable in understanding the nature of the solutions. A further discussion of the behaviour of autothermal reactors is given by Kramers & Westerterp (1963). In the beds investigated in this study, only beds with 1 or 3 solutions have been found. This does not mean that it is not possible that a certain coal bed may have more solutions; indeed this may be possible depending on the parameters in the model.

The procedure of plotting LHS and RHS versus θ has been performed for the base case, for different particle sizes. The graphs obtained are summarized in figure 8.2, in which is sketched the locus of solutions to equation 8.2, with particle size along the x-axis and average temperature on the y-axis.

The following conclusions may be drawn from figure 8.2:

a) Below a certain particle size, which may be called D_p^l, there exists only only 1 solution to equation 8.2.

b) Above D_p^l, but below a certain particle size D_p^h, there exist 3 solutions to equation 8.2.

c) Above D_p^h there exists only one solution to the equation.

Referring to figure 8.2 it can be seen that two different types of stable solution exist, labelled S1 and S2 respectively. The branch labelled S1 is characterized by a temperature rise of less than 30 ^{o}C. This implies that the assumption of a constant rate is a good one in this region. This solution is associated with little use up of oxygen. Beds in this region may be considered to be heat-transfer limited, i.e. they do not experience a large temperature rise because the heat transfer is high enough to remove most of the sensible heat of reaction. This solution ceases to exist below D_p^l since the heat transfer is no longer high enough to remove the sensible heat.

The branch labelled S2 is characterized by total consumption of oxygen. It should be noted that the values of the temperature on this branch are likely to be quite wrong, since the assumption of a constant rate used to calculate these values is a poor one. This is not of great practical importance since these beds may be considered to be burning, and the temperature at which the burning occurs is not of great importance. What is of importance is that for small temperature rises, ie safe beds, the model is accurate, and it is safe beds that are of interest. This high temperature solution ceases to exist above D_p^h since the surface area available for reaction becomes too small to support combustion. It should be pointed out that the values of D_p^h obtained in this study are in the region of 100 mm, which is above the particle size at which coal is normally stockpiled. A further point to note is that the details of the kinetics on branch S2 are also not of great importance. The reason for this is that when there is total consumption of oxygen the energy balance no longer contains any kinetic parameters ie the RHS of the energy balances reduces to the dimensionless adiabatic temperature rise.

Of great practical importance is the behaviour of branch S2 for small particle sizes. Below a certain particle size, which for the base-case parameters is of the order of 1 mm, the average temperature rise falls to less than 70 ^{o}C. Practical experience has shown that these beds, although experiencing a substantial temperature rise, are safe. In many practical cases, the effective particle size of a sample of coal will be below this value, and the bed will be safe. The meaning of particle size, as used in this study, is further discussed in section 8.2.6.,

It should be pointed out that neglecting molecular diffusion as a transport mechanism for oxygen is not a good assumption for particles in the sub 1mm range. Thus the temperatures the model predicts for these particle sizes in likely to be in error. However as has been shown in Chapter 2, the maximum temperature rise due to diffusion is of the order of 70 K. This temperature rise will not occur in practice due to the fact that that heat losses will occur. It is important to realise that even if there is a 70 K rise, the natural convection flows will be extremely small for these fine particles, implying that the beds will remain safe.

It can be seen from figure 8.2 that between D_p^1 and some small particle size the only solution to equation 8.2 is one in which the average temperature in the bed is dangerously high. Thus the model agrees with the often noted fact that certain coals cannot be safely stockpiled, and will, given enough time, spontaneously combust.

Also of practical importance is the branch labelled u in Figure 8.2. This is the locus of the unstable solutions, and serves to separate the stable solutions. The implication of this curve is that should a bed reach an average temperature above the average temperature given by the curve u, then the bed will combust. On the other hand, should the average temperature stay below u, then the temperature of the bed cannot reach the value given by the branch S2.

The possibility of multiple steady-states occurring in fixed bed chemical reactors has been noted in the literature. Luss (1968) and Luss & Amundson (1967) have used bifurcation theory to derive sufficient conditions for the existence of a unique steady-state in a fixed bed chemical reactor. This knowledge would be very valuable in the present study. The problem solved by Luss (1968) is similar, but not identical, to the problem studied in the present work. Unfortunately, the results obtained are not directly applicable to the model presented here, due to the differing mechanisms for reactant transport. This factor makes the application of the method presented by Luss (1968) to the present problem somewhat less than straightforward.

It would indeed be very useful to predict parameter values for which there are a given number of solutions to equation 8.2.

Balakotaiah & Luss (1984) have presented methods for determining the regions of parameters for which a given number of steady-state solutions exist in reacting systems. This work hhas been applied to the problem of predicting multiple steady-states in continuous stirred tank chemical reactors. In these cases the systems are described by algebraic rather than differential equations. The extension of the methods presented by Balakotaiah & Luss (1984) to differential equations is in principle simple; in practice the mathematics soon become intractable.

For the purposes of this study a less mathematically involved, albeit simple minded, approach has been used to determine how many steady-states exist for a given set of parameter values. The approach taken is to calculate the low temperature solution for particle size 20 mm. The particle size is then reduced by 1 mm and the calculation repeated. Eventually no low temperature solution to the equation can be found; thus the particle size at which the low temperature solution ceases to exist is found to an accuracy of 1 mm. The high temperature solution to the equation is then calculated. Although it is known that the model is poor for high temperatures, it is nevertheless important to calculate along this branch since, for sufficiently small particle sizes, the calculated temperatures are below 340 K. These beds may be considered to be safe. It should be noted that if a calculational scheme had been adopted whereby only the number of solutions to equation 8.2 was calculated, then these safe oxygen limited dumps would not have been identified.

The computational effort in performing the calculation described above is minor, even for a large range of parameter values. A computer program to perform the calculation is listed in Appendix 12. In figure 8.3 the results of calculating the locus of solutions to equation 8.2 for the parameter values given in Appendix 11, is presented. The results have been calculated in steps of 1 mm up to particle size 20 mm. Figure 8.3 is the base case, and is used in what follows as a means of comparing the effects of changing the parameters in the model.

The results presented in this section are critical to understanding the behaviour of coal dumps, and will therefore now be summarised:

a) Coal dumps may be classified as either safe, unsafe or con-

ditionally safe.

b) Dumps that are safe are composed of either fine reactive material in which case they are oxygen limited, or coarse unreactive material, in which case they are heat transfer limited.

c) Dumps which are conditionally safe may burn if the temperature of the dump rises above a certain critical temperature. If the temperature of the dump stays below this critical value, the dump remains safe.

d) There are cases in which the dump will, given enough time, undergo spontaneous combustion.

In this study particle size has been chosen as the independent variable for the purposes of presenting in a graphical form the results of solving the model equations. The reason for this is that by varying the particle size, the behaviour of different coal dumps may be observed. However, the other physical parameters of the bed are of extreme importance. For this reason the effect of changing one parameter in the model at a time was investigated. The results are presented graphically in figures 8.3 - 8.11 , and discussed in depth below.

It will be noted that the different branches on the curves are labelled 'small temperature rise' and 'combustion'. It may seem contradictory that for fine material the temperatures on the combustion curve are relatively low. However, combustion may be regarded as a situation in which the large majority of available oxygen is reacting, and in this sense the label combustion is accurate for these curves.

In the discussions below 340 K is used as a dividing value between safe and unsafe coal beds. This value must not be taken too literally, since it has been arbitarily chosen. Its use merley proves convenient in comparing the results obtained for different parameter values.

8.2.2 Effect of varying the voidage

Voidage is a parameter which may be varied in practice by means of compaction. The effect of this is shown in Figure 8.4, from which the following conclusions may be drawn:

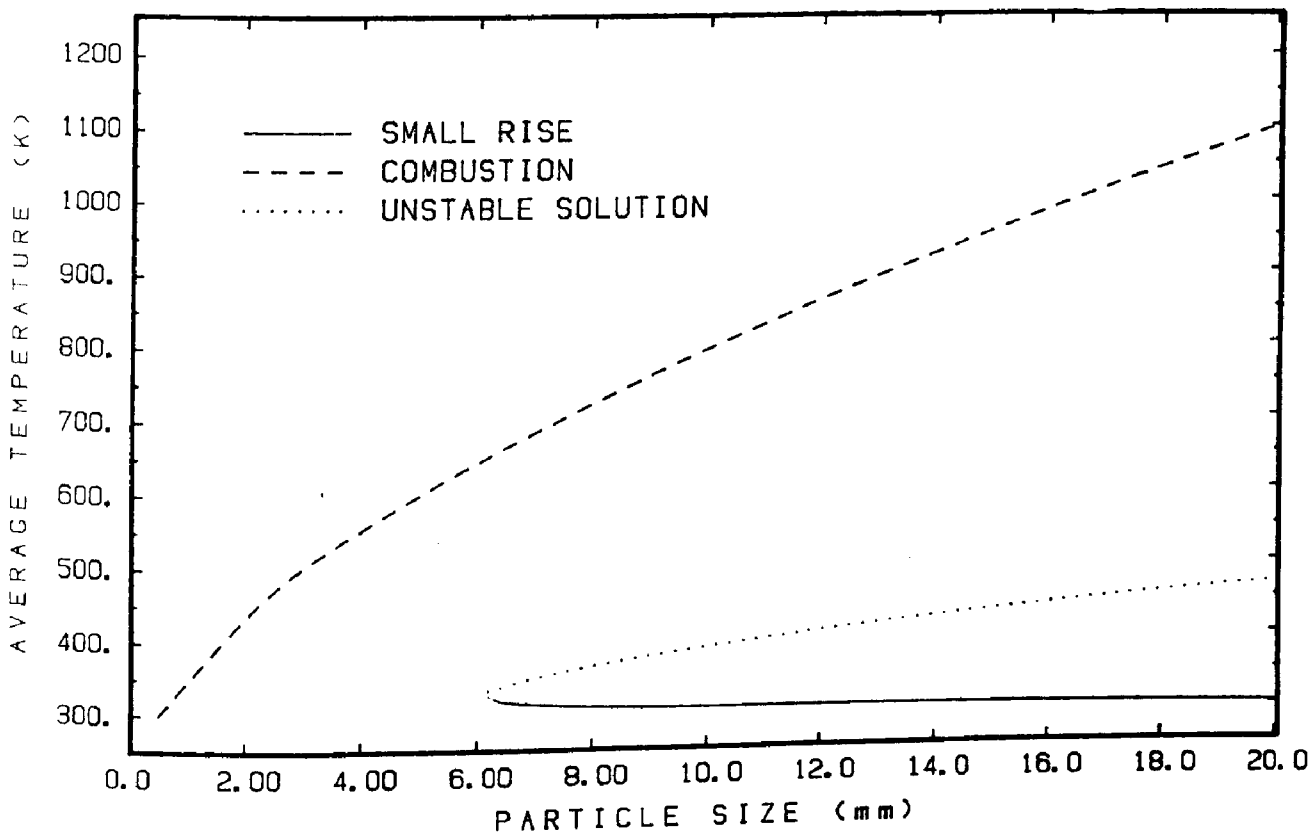


Figure 8.3 Stable and unstable solutions for the base-case

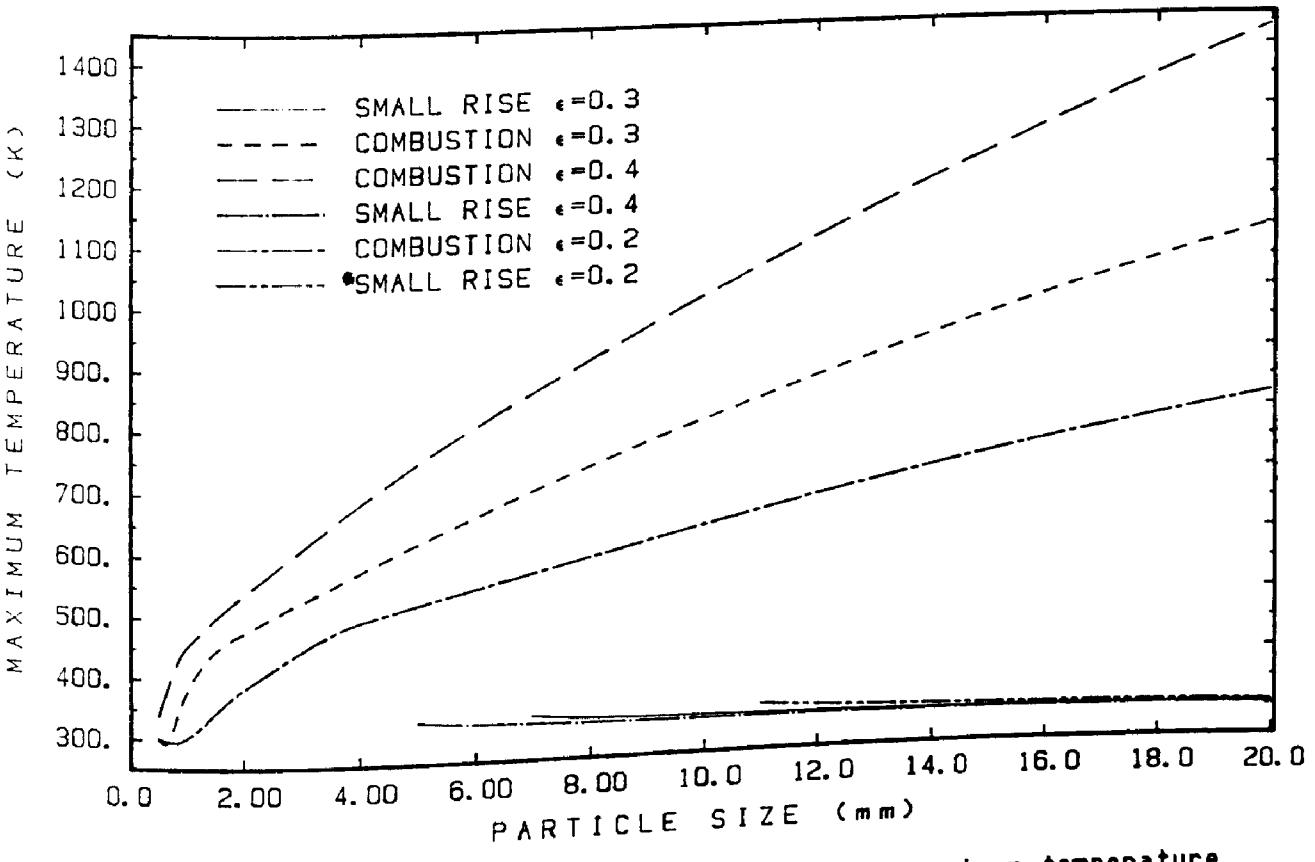


Figure 8.4 Effect of varying voidage on the maximum temperature

a) For fine material, compacting the bed will help make it safer. This can be seen from the fact that the combustion or oxygen limited curve is lower in temperature for lower voidages. Put another way, a fine coal may be safely stockpiled uncompacted, whereas a slightly coarser coal may have to be compacted when stockpiled in order for it to be safe. Using the rough criterion of 340 K then for this particular case material of voidage 0.2 is safe up to particle size 1.8 mm, while for voidage 0.3 the material is safe only up to particle size 0.8 mm.

b) Compacting coarse material may be detrimental. This is shown by the fact that the small temperature rise solution ceases to exist at $D_p = 11$ for $\epsilon = 0.2$, $D_p = 8$ for $\epsilon = 0.3$ and at $D_p = 5$ for $\epsilon = 0.4$.

The last conclusion may seen odd, and deserves some explanation. By compacting the bed the surface area per unit volume of the bed is increased. This in turn has two effects:

a) The resistance to flow is greater and
b) The mass of reactive material per unit bed volume is greater.

For the heat-transfer limited beds, i.e. the ones that experience a small temperature rise, the second result of more reactive material per bed volume more than outweighs the first of reducing oxygen ingress, since the bed was not in any case oxygen limited. (In fact, the reduction in flow also causes a rise in temperature since the heat loss due to flow is decreased). However for the case of oxygen limited beds compaction makes them safer by increasing the rate at which oxygen is scavenged from the air by reaction, as well as increasing the resistance to flow and therefore reducing the flowrate.

8.2.3 Effect of varying the pre-exponential factor

The purpose of varying the pre-exponential factor K_o is to try and simulate the fact that different coals will have different reactivities. Figure 8.5 indicates very clearly that for heat transfer limited beds, the larger K_o, the less safe the bed is. However, the opposite is true for oxygen limited beds. This surprising result can be understood in terms of the fact that

a) For fine material, compacting the bed will help make it safer. This can be seen from the fact that the combustion or oxygen limited curve is lower in temperature for lower voidages. Put another way, a fine coal may be safely stockpiled uncompacted, whereas a slightly coarser coal may have to be compacted when stockpiled in order for it to be safe. Using the rough criterion of 340 K then for this particular case material of voidage 0.2 is safe up to particle size 1.8 mm, while for voidage 0.3 the material is safe only up to particle size 0.8 mm.

b) Compacting coarse material may be detrimental. This is shown by the fact that the small temperature rise solution ceases to exist at $D_p = 11$ for $\epsilon = 0.2$, $D_p = 8$ for $\epsilon = 0.3$ and at $D_p = 5$ for $\epsilon = 0.4$.

The last conclusion may seen odd, and deserves some explanation. By compacting the bed the surface area per unit volume of the bed is increased. This in turn has two effects:

a) The resistance to flow is greater and
b) The mass of reactive material per unit bed volume is greater.

For the heat-transfer limited beds, i.e. the ones that experience a small temperature rise, the second result of more reactive material per bed volume more than outweighs the first of reducing oxygen ingress, since the bed was not in any case oxygen limited. (In fact, the reduction in flow also causes a rise in temperature since the heat loss due to flow is decreased). However for the case of oxygen limited beds compaction makes them safer by increasing the rate at which oxygen is scavenged from the air by reaction, as well as increasing the resistance to flow and therefore reducing the flowrate.

8.2.3 Effect of varying the pre-exponential factor

The purpose of varying the pre-exponential factor k_o is to try and simulate the fact that different coals will have different reactivities. Figure 8.5 indicates very clearly that for heat transfer limited beds, the larger k_o, the less safe the bed is. However, the opposite is true for oxygen limited beds. This surprising result can be understood in terms of the fact that

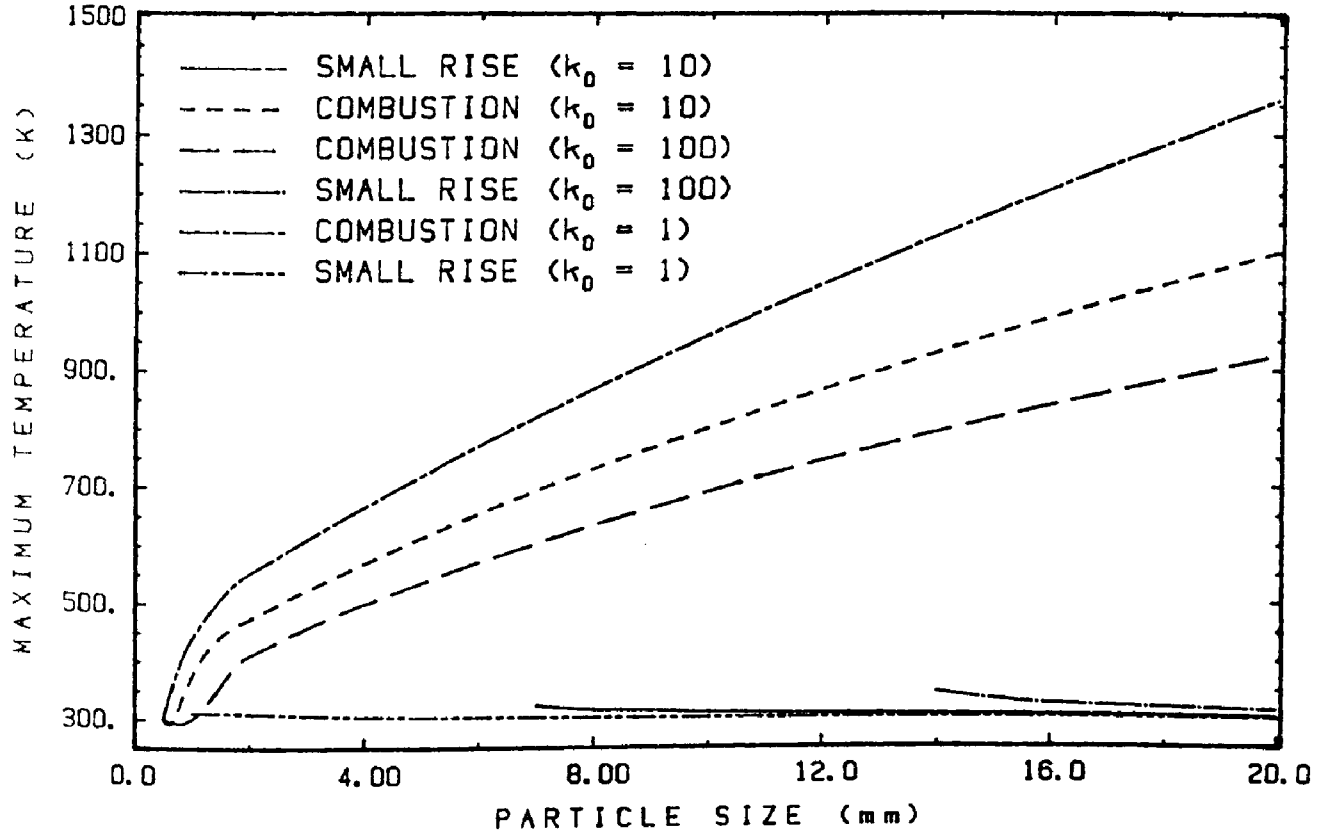


Figure 8.5 Effect of varying the pre-exponential factor on the maximum temperature

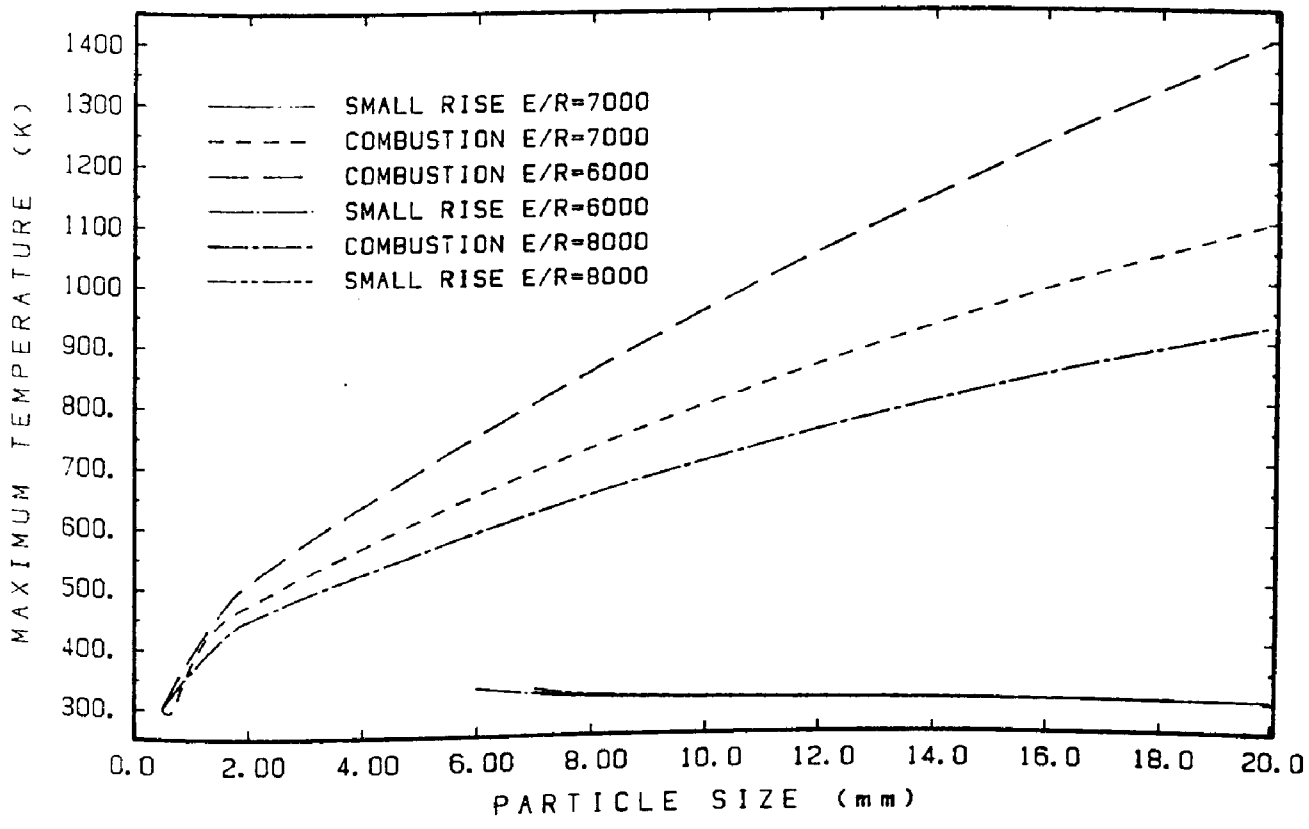


Figure 8.6 Effect of varying the activation energy on the maximum temperature

the oxygen depletion is less when k_o is lower, implying that the oxygen in the bed can penetrate further, leading to a larger temperature rise. When k_o is very large, all the oxygen is consumed close to the surface, where the sensible heat of reaction is easily conducted away.

Using the criterion of 340 K then for k_o = 1 m/s beds are safe below approximately 0.5 mm particle size, whhile for k_o = 100 m/s beds are safe below 1.5 mm particle size. This shows that for these small particle sizes, the more reactive the coal, the safer it is to stockpile.

Also of interest in Figure 8.5 is the fact that that for k_o=1 there is only a small range of particle sizes for which the bed is unsafe. This is a logical conclusion since it is to be expected that very unreactive material will not combust spontaneously.

Figure 8.5 indicates very clearly that k_o is a critical model parameter, and as such needs to be accurately measured.

8.2.4 Effect of varying the activation energy

To study the effect of changing the activation energy, it is necessary at the same time to vary k_o, so that the reactivity is the same at some base temperature. In this case a base temperature of 300 K was chosen. Figure 8.6 thus shows the behaviour of three different coals with the same room temperature reactivity but different activation energies. It can be seen from Figure 8.5 that there is little effect on both the curves. This then indicates that the activation energy is not a critical parameter for coals which have the same room temperature reactivity. However, two coals which have both different activation energies and different room temperature reactivities will have different liabilities toward self heating. The activation energy must thus be measured, and used in conjuction with k_o as a measure of the reactivity of the coal.

8.2.5 Effect of different assumptions about the reactive surface area of coal

The relationship between the particle size of coal and its reactive surface area has been discussed by Sondreal & Ellman (1974). They state that low-temperature oxidation rates have reported to

the oxygen depletion is less when k_o is lower, implying that the oxygen in the bed can penetrate further, leading to a larger temperature rise. When k_o is very large, all the oxygen is consumed close to the surface, where the sensible heat of reaction is easily conducted away.

Using the criterion of 340 K then for k_o = 1 m/s beds are safe below approximately 0.5 mm particle size, whhile for k_o = 100 m/s beds are safe below 1.5 mm particle size. This shows that for these small particle sizes, the more reactive the coal, the safer it is to stockpile.

Also of interest in Figure 8.5 is the fact that that for k_o=1 there is only a small range of particle sizes for which the bed is unsafe. This is a logical conclusion since it is to be expected that very unreactive material will not combust spontaneously.

Figure 8.5 indicates very clearly that k_o is a critical model parameter, and as such needs to be accurately measured.

8.2.4 Effect of varying the activation energy

To study the effect of changing the activation energy, it is necessary at the same time to vary k_o, so that the reactivity is the same at some base temperature. In this case a base temperature of 300 K was chosen. Figure 8.6 thus shows the behaviour of three different coals with the same room temperature reactivity but different activation energies. It can be seen from Figure 8.5 that there is little effect on both the curves. This then indicates that the activation energy is not a critical parameter for coals which have the same room temperature reactivity. However, two coals which have both different activation energies and different room temperature reactivities will have different liabilities toward self heating. The activation energy must thus be measured, and used in conjuction with k_o as a measure of the reactivity of the coal.

8.2.5 Effect of different assumptions about the reactive surface area of coal

The relationship between the particle size of coal and its reactive surface area has been discussed by Sondreal & Ellman (1974). They state that low-temperature oxidation rates have reported to

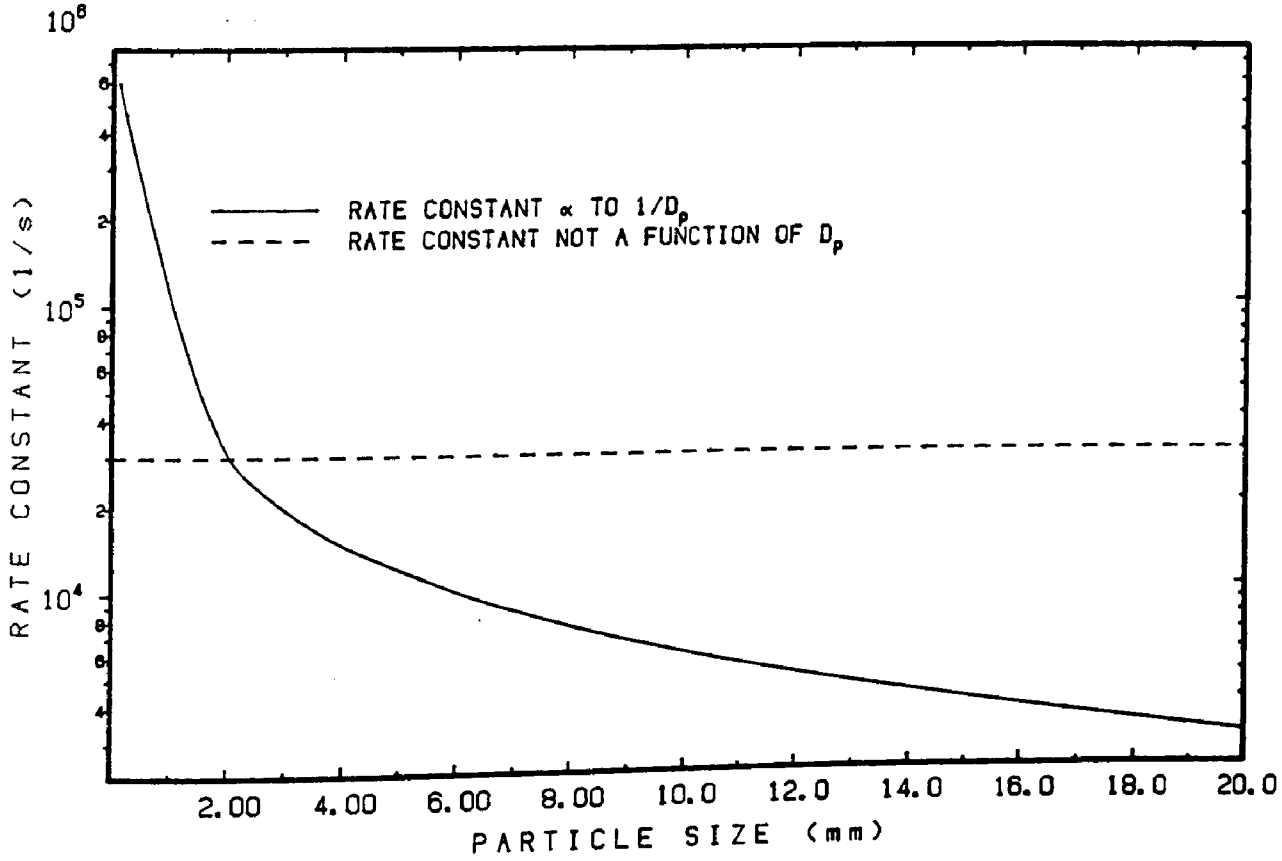


Figure 8.7 Pre-exponential factor versus particle size for the two cases considerd

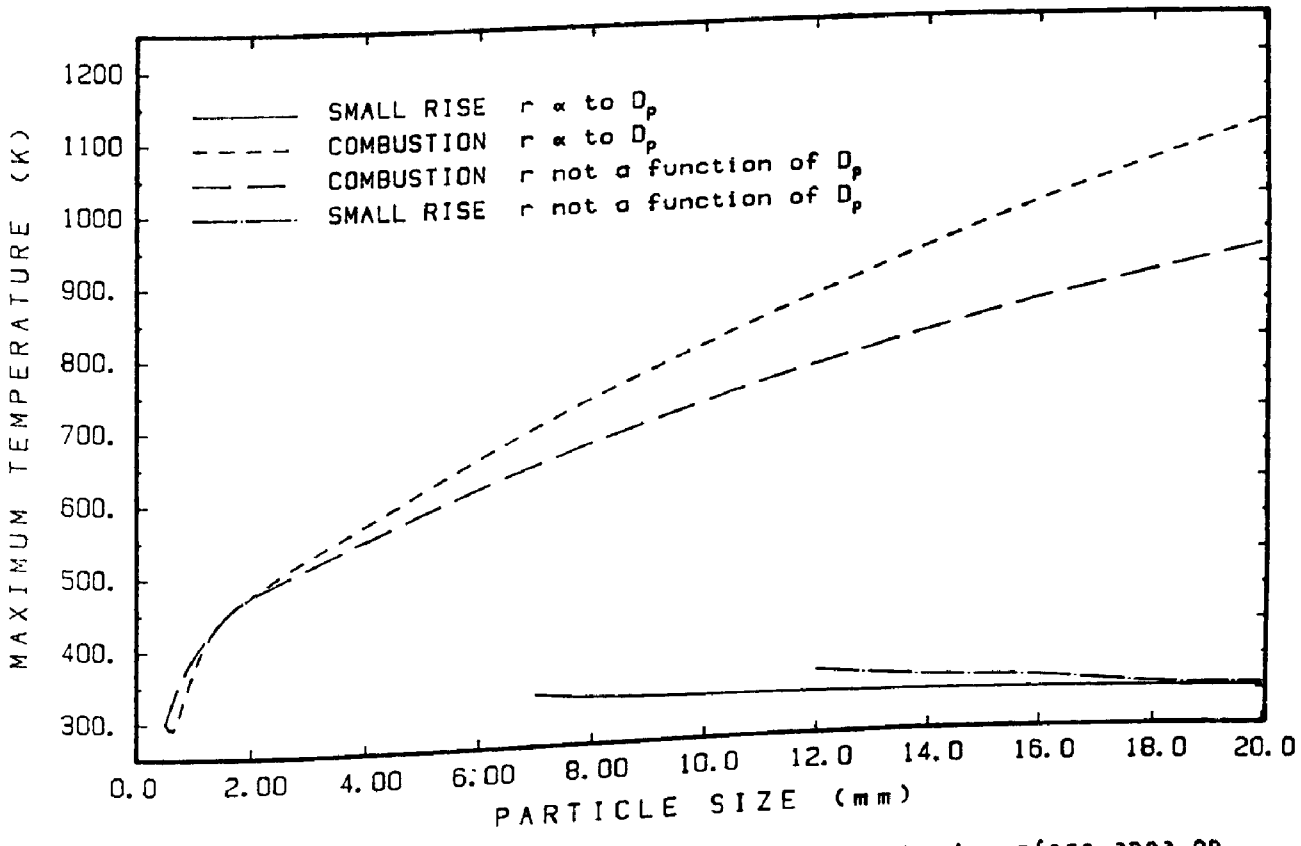


Figure 8.8 Effect of different assumptions about surface area on the maximum temperature

8.2.6 The Meaning of Particle Size

It should be noted that the particle size as used in the graphs presented in this section is defined by:

$$D_p = 6/S_t \qquad 8.5$$

and that this is of great importance when calculating the particle size of a coal sample with a particle size distribution. The correct particle size to use is the one defined by

$$S_t = 6 \sum_{i=1}^{N} \frac{m_i}{D_{p_i}} \qquad 8.6$$

together with equation 8.5

where D_{p_i} = average particle size of class i

m_i = mass fraction of coal in class i

N = number of classes

$$D_p = \sum_{i=1}^{N} D_{p_i} m_i \qquad 8.7$$

is not the correct average for this case.

Should a full particle size distribution be available, the summation in the above equations may be replaced by integrals.

To demonstrate the importance of the above discussion consider a coal with the size distribution given in Table 8.1.

TABLE 8.1 PARTICLE SIZE DISTRIBUTION FOR A TYPICAL SAMPLE

PARTICLE SIZE IN mm		MASS %
	+6.68	26,9
-6.68	+4.70	12.3
-4.70	+2.36	20.2
-2.36	+1.20	12.9
-1.20	+0.59	10.1
-0.59	+0.10	15.7
-.10		1.9

Calculating Dp by equation 8.7 gives a value of 4.5 mm while using equations 8.5 and 8.6 gives 0.9 mm. It can be seen that even a relatively small amount of fine material has the effect of drastically changing the effective particle size of the coal. This is of great importance when considering the liability towards spontaneous combustion of so-called segregated coal

8.2.7 Effect of Wind on Maximum Temperature

The effect of wind on the maximum temperature in the coal bed is shown in Figure 8.9. It appears from this figure that the presence or absence of wind has little effect on the calculated temperatures. However the curve plotted in Figure 8.9 assumes the wind blows constantly until steady-state is reached. This is highly unlikely to occur in practice. The more likely case is a wind which blows for a while, and then dies away. This is obviously on unsteady-state phenomenon, and as such will be discussed in section 8.3.

8.2.8 Effect of Thermal Conductivity on Maximum Temperature

Although the effective thermal conductivity of a packed bed of coal has been measured, it was felt worthwhile to investigate the effect of changing this parameter. It can be seen from Figure 8.10 that both halving and doubling this parameter have little effect on the calculated curves. It thus appears satisfactory to use the measured value of the effective thermal conductivity in all calculations.

8.2.9 Effect of Changing the Bed Length

The bed length is the most difficult model parameter to relate to a real coal dump. It is incorrect to assume that this bed length bears a fixed relationship to the physical size of a coal dump, e.g. its height or width. The bed length in the one-dimensional model in fact corresponds to the path length for flow in the real situation. This path length in general will not be known, although the physical size of the dump sets an upper bound on this quantity.

For the purposes of this study three bed lengths were chosen, in order to see the effect of changing this quantity. From Figure 8.11 it can be seen that the effect of bed length is very pro-

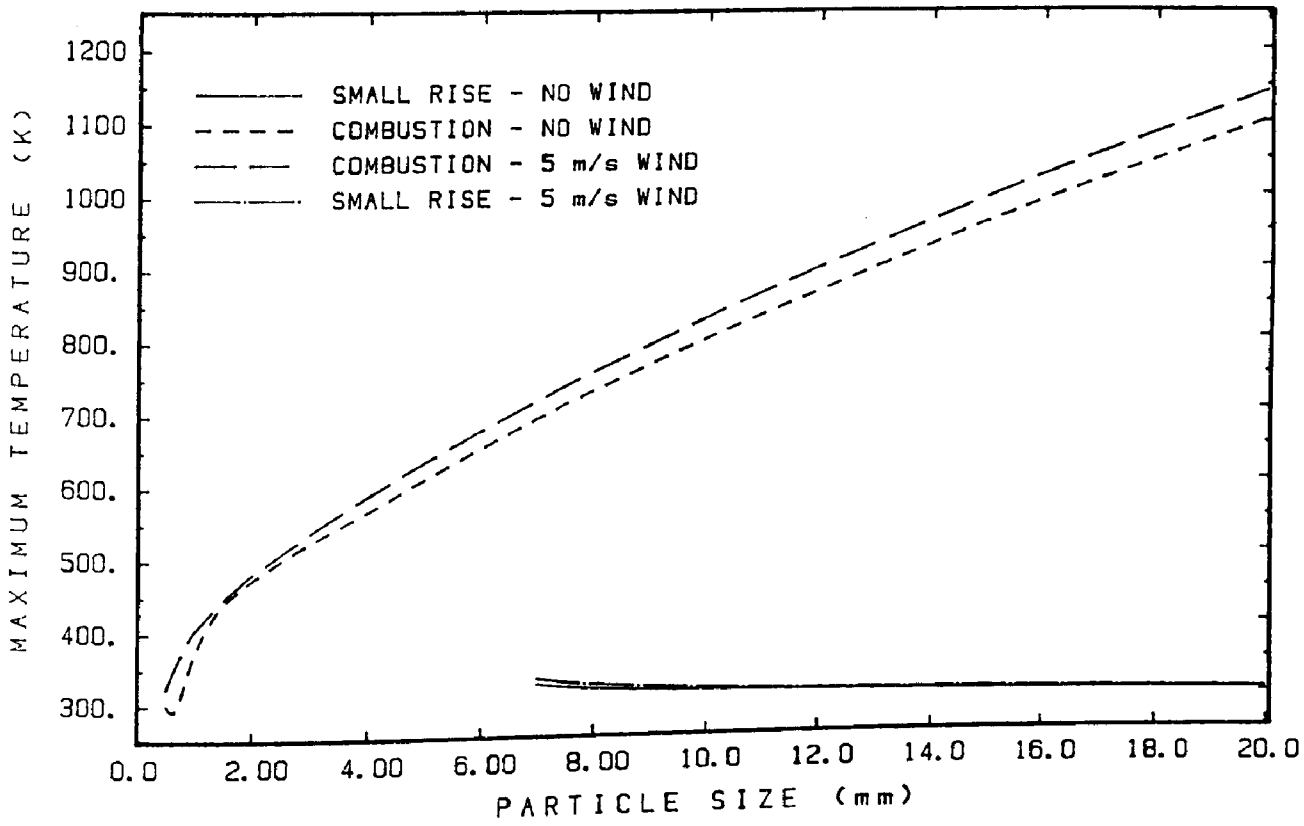


Figure 8.9 Effect of wind on the maximum temperature

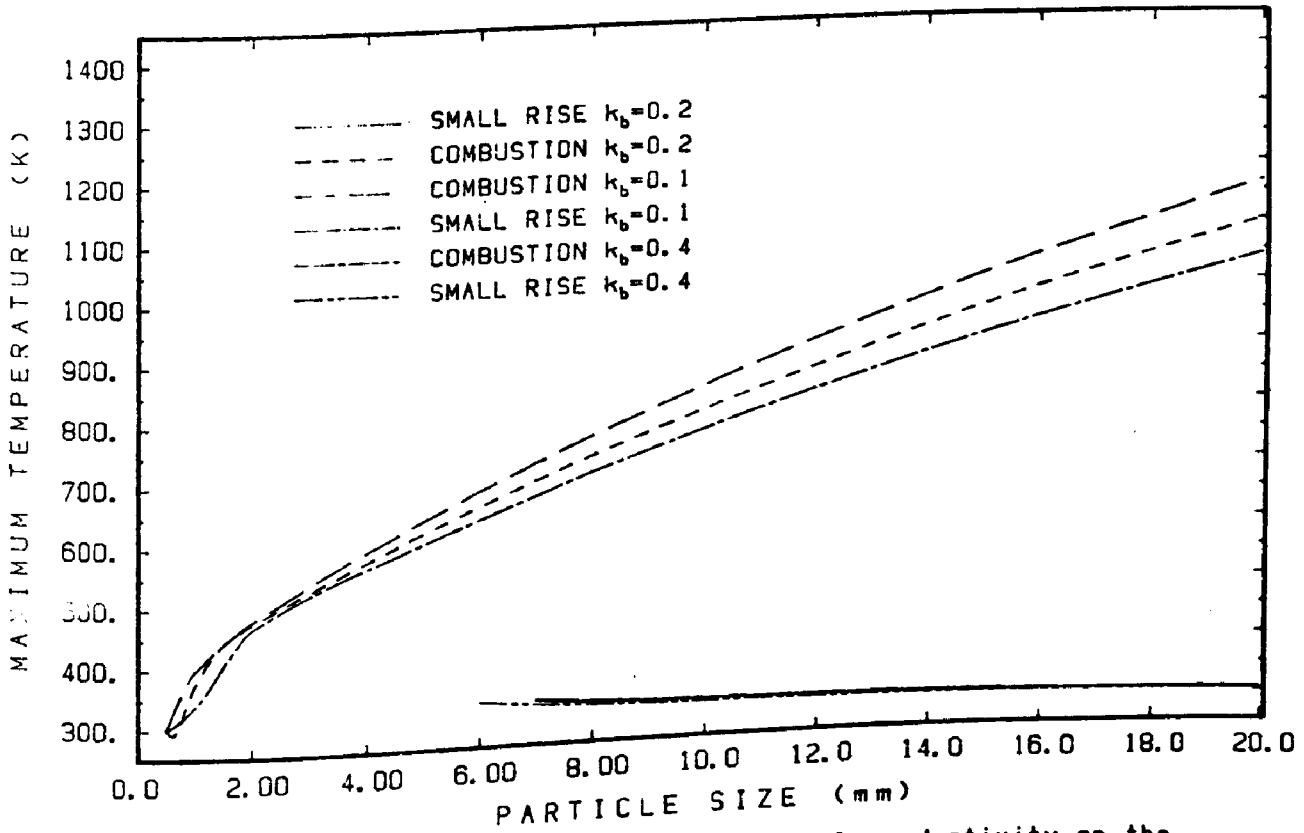


Figure 8.10 Effect of varying bed thermal conductivity on the maximum temperature

nounced on the low temperature solution curves. For the oxygen limited beds, there is little difference between the curves for bed length 5 and 10 m. The curve for bed length 1 m has a somewhat different shape, and for particle sizes less than 1 mm the temperature rise is negligible. In addition the range of particle sizes for which the bed can be considered to be unsafe is between approximately 1.5 and 2 mm.

The fact that the curves for 5 m and 10 m are so similar can be explained as follows: For an oxygen limited bed the oxygen in the flow is used up very close to the inlet to the bed. From that point in the bed where there is to all intents and purposes no oxygen, no more reaction can occur. The temperature profile in the rest of the bed is thus governed by conduction, especially for the beds of finer particles for which the flowrates are low. This implies that making the bed longer will have little effect on the maximum temperature in the bed, since all the temperature rise occurs very close to the inlet.

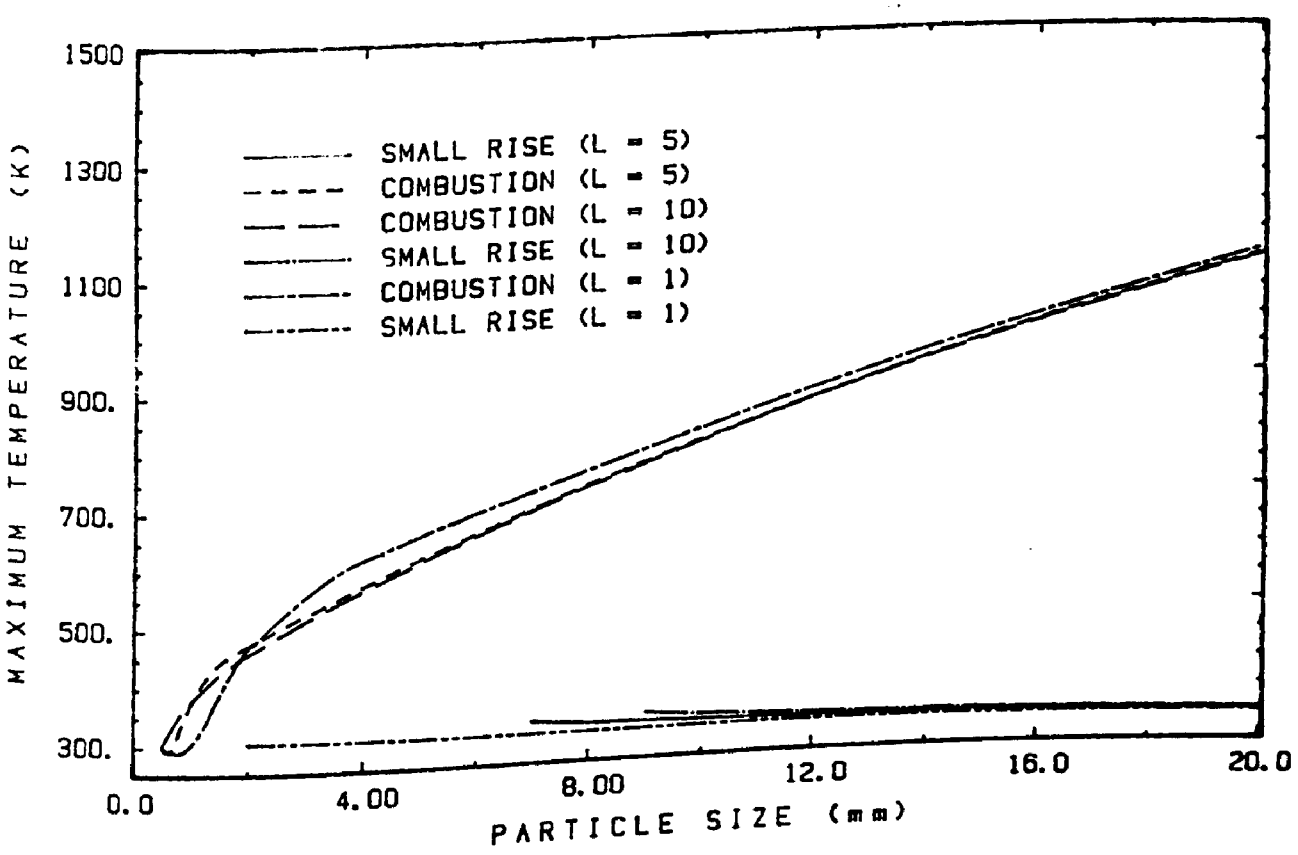


Figure 8.11 Effect of varying bed length on the maximum temperature

8.3 Unsteady-State Solutions for r constant

8.3.1 Introduction

The unsteady-state solution for r constant has been discussed in section 6.3. The resulting solution has been programmed in BASIC on an HP 9835 computer, and a lsiting of the program is given in Appendix 12.

It has been found that obtaining the solution to the analytical equation is in fact slower than obtaining the solution using the numerical method discussed in section 6.4. The aim of what follows is thus to point out the pertinent facts that emerge from solving the equation, without presenting an extensive array of graphs.

8.3.2 The Character of the Solutions

It is already known from calculations in the previous section what the steady-state temperature profiles for a given bed will look like. The advantage of the unsteady-state method thus lies in the fact that should the bed be conditionally safe, the unsteady-state solution will be able to predict from the initial condition what the final steady-state will be.

The temperature time curves in the centre of a coal bed using three different initial conditions are plotted in figure 8.12. The initial condition used is the somewhat artificial one of a coal bed with an initial uniform temperature.

The model parameters used to obtain the curves shown in Figure 8.12 are given in Table 8.2.

TABLE 8.2 MODEL PARAMETERS FOR FIGURE 8.12

Particle Size	5 mm
Voidage	0.4
Bed Length	1 m
K_o	0.7 m/hr
E/R	2889 K

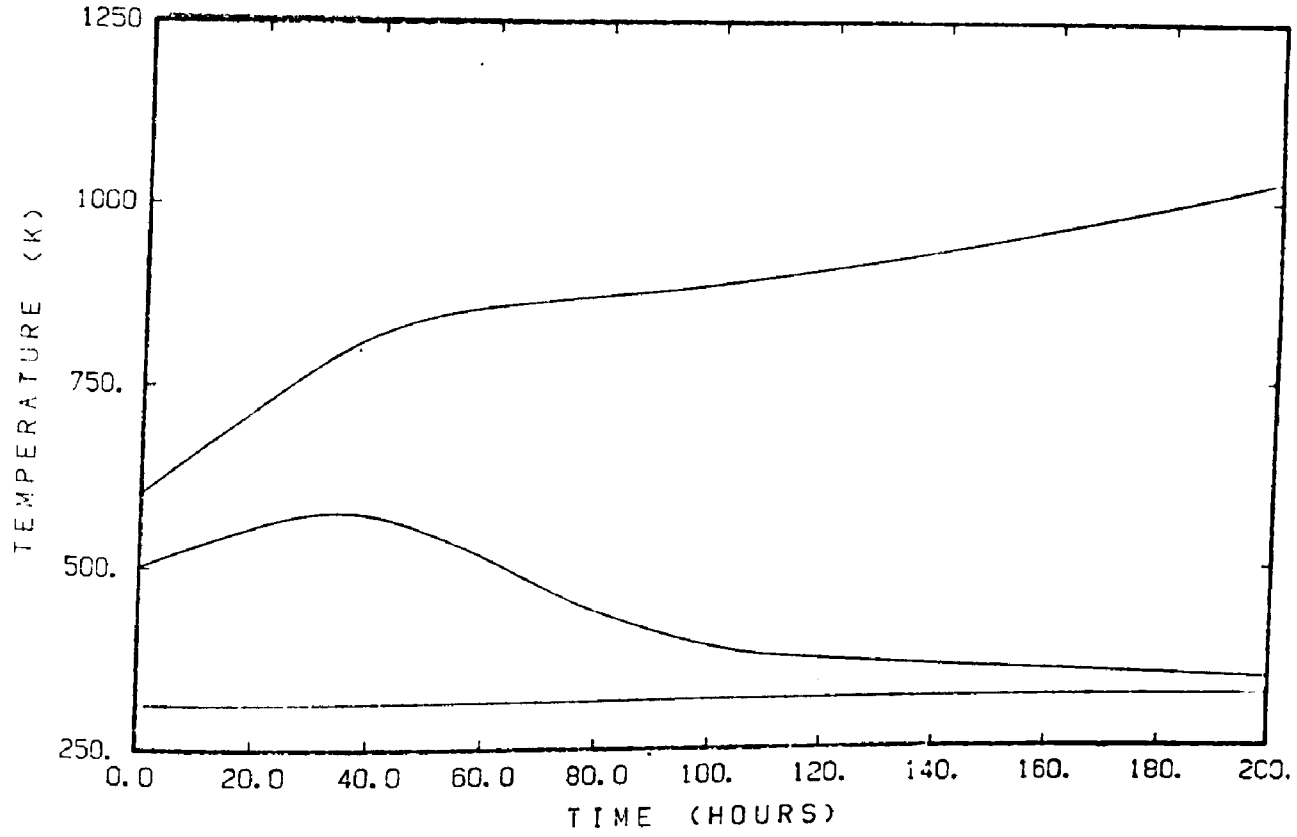


Figure 8.12 Temperature-time curves in the centre of a coal bed for different initial temperatures

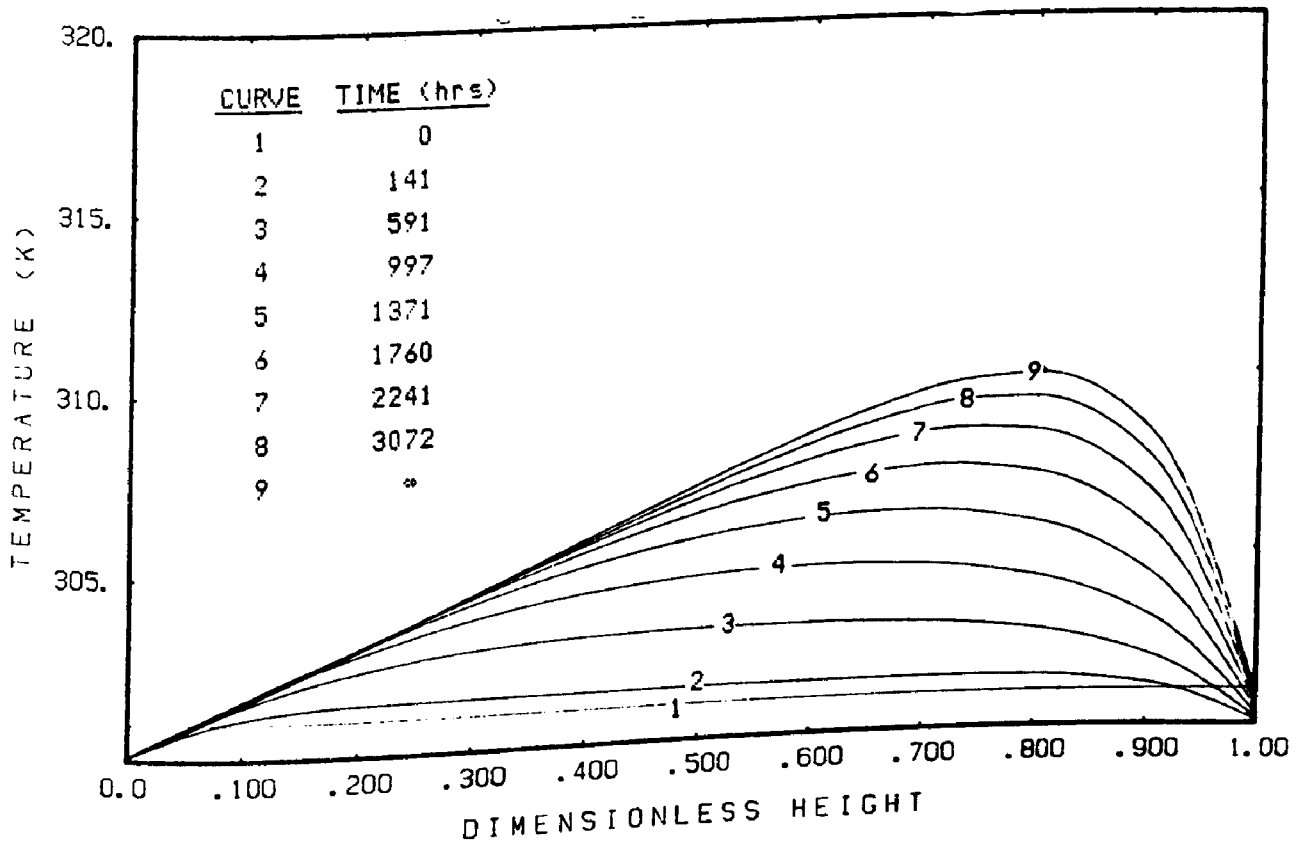


Figure [illegible] Temperature profiles in a coal bed

It can be observed from figure 8.12 that starting with an initial temperature of 301 K the temperature in the bed gradually rises to eventually reach a stable low temperature steady-state. Starting with a bed temperature of 500 K the temperature initially increases but then decreases to eventually again reach the low temperature stable steady-state. However starting at 600 K the temperature increases monotonically, leading to combustion. Thus for this particular bed the critical temperature appears to be between 500 & 600 K. This temperature would in fact correspond to the unstable solution temperature discussed in section 8.2.

Temperature profiles for a coal bed with parameters as given in Appendix 11, for a particle size of 10 mm and length of 5 m are shown in figure 8.13. Referring to figure 8.3 it can be seen that such a bed has a stable steady-state at a maximum temperature of 310 K. In figure 8.13 it can be observed that starting with a temperature of 301 K the bed gradually heats up to its final steady-state temperature. Although in theory the bed reaches steady-state after only an infinite time, it can be seen that after 3568 hrs or nearly 150 days, the bed is to all intents and purposes at steady-state.

It is tempting to try and define a time constant for a coal bed, in order that predictions may be made on safe stockpiling times. In order to do this one would hypothesize that the temperature in a coal bed could be described by an equation of the form

$$\frac{\theta(X,\tau) - \theta_{ss}(X)}{\theta(X,0) - \theta_{ss}(X)} = \exp(-\frac{\tau}{\tau_c}) = \exp(-\frac{t}{t_c}) \qquad 8.3.1$$

where τ_c is a dimensionless time constant, and t_c is a time constant.

In fact using equation 6.3.2, and assuming that only the first term in the series $V(X,\tau)$ need be considered it can be shown that

$$\tau_c = (\beta_1^2 + a^2/4)^{-1} \qquad 8.3.2$$

It is thus immediately obvious that τ_c is not constant, but in fact a function of time, since the quantity, a, which is proportional to the flowrate, is a function of time.

For cases when $\beta_1^2 \gg a^2/4$, the use of a time constant is justified. It can be shown that $\beta_1 \approx \pi$, therefore $a/2 \ll \pi$ is the criterion for using a time constant.

Converting τ_c to time units using the relationship

$$\tau_c = \frac{\kappa t_c}{L^2} \qquad 8.3.3$$

In the case when $a/2 \ll \pi$

$$\tau_c = \frac{1}{\beta_1^2} = \frac{1}{\pi^2}$$

$$t_c = \frac{L^2}{\pi^2 \kappa} \qquad 8.3.4$$

The time constant in this case is governed by the thermal diffusivity of the bed, which implies that the heat transfer in the bed is mainly by conduction.

Then

$$t_c = \frac{L^2}{\pi^2 \times 8 \times 10^{-4}} = 126L^2 \text{ hrs} \approx 5L^2 \text{ days}$$

This implies that for cases where the heat transfer in the bed is governed by conduction, the bed will be 37 % away from its steady-state temperature after $5L^2$ days and 14 % after $10L^2$ days.

A similar calculation for the case $a/2 \gg \pi$ is not justifiable, since a is a function of time. However, using the definition of of the quantity a

$$a = \frac{\hat{G}cL}{k_b}$$

and using the simplified formula for the flowrate G

$$G = \frac{q}{fM_w}\left[\frac{\theta-1}{\bar{\theta}^2}\right]$$

Is is possible to calculate the quantity a, and compare it to 2π to deduce whether the dominant transfer mechanism is conduction or flow.

Using values from Table 2.1 and Appendix 11, and assuming an average dimensionless temperature of 1,1 ie an average temperature of 330 K the values in Table 8.3 have been calculated

TABLE 8.3 THE QUANTITY 'a' FOR VARIOUS PARTICLE SIZES

Particle Size (mm)	a
1	0.1L
2	0.4L
5	2.5L
20	40L

It thus appears that for a 5 m bed of 5 mm particles at an average temperature of 330 K that flow is a more important heat transfer mechanism than conduction. For finer particles in shorter beds conduction will dominate, and then equation 8.3.1 together with 8.3.4 may be used to calculate the time varying behaviour of the coal bed.

Plotted in figure 8.14 is the temperature-time behaviour at the centre of a bed composed of 6 mm particle and 5 m in length. All the other model parameters are base case values. Referring to Figure 8.3 it can be seen that for this coal bed there is no low temperature solution. This conclusion is confirmed by the unsteady-state calculation.

It can be seen that the temperature rise in the centre of this bed is gradual with a value of 0.24 K/day until approximately 80 days. At this time the temperature increases dramatically

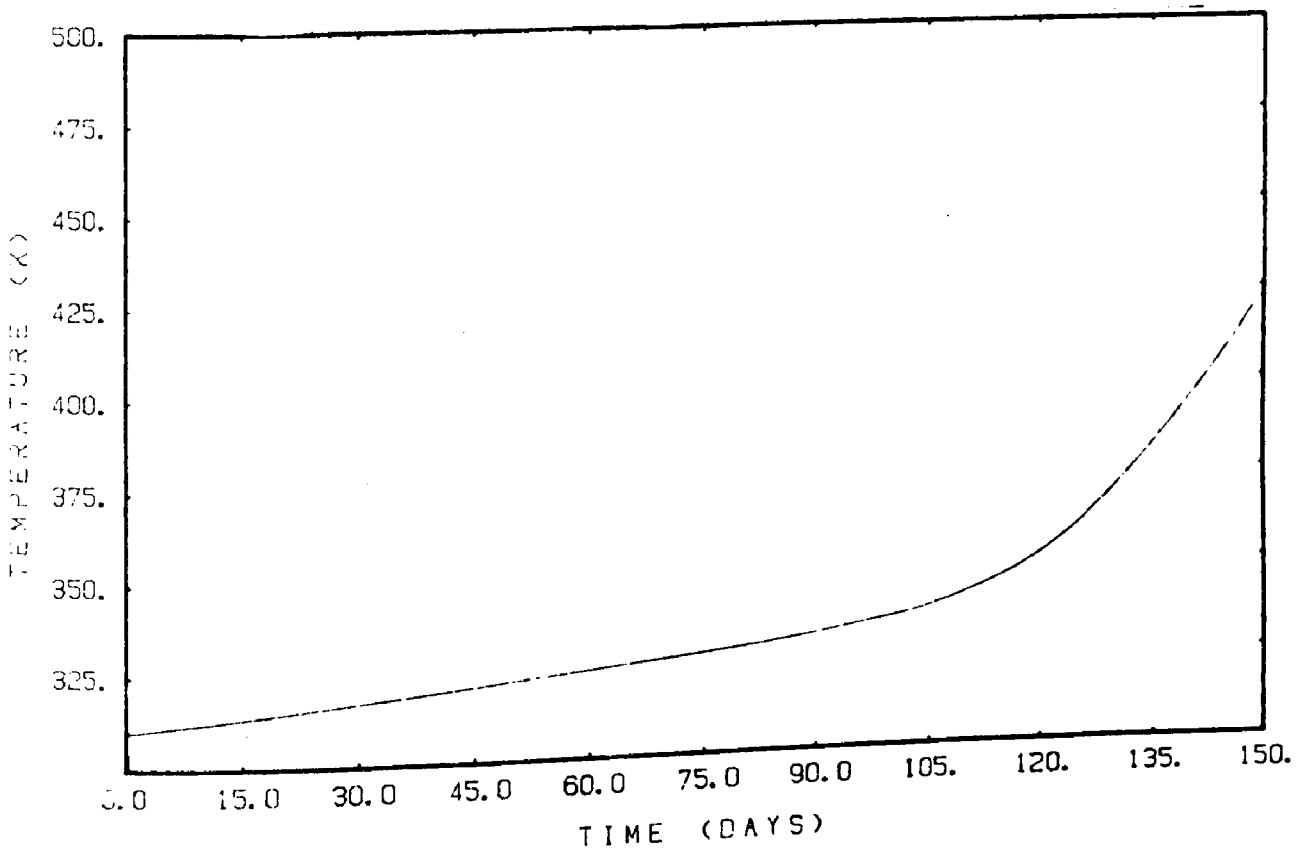


Figure 8.14 Temperature-time behaviour at bed centre
Particle size 6 mm - Analytical solution

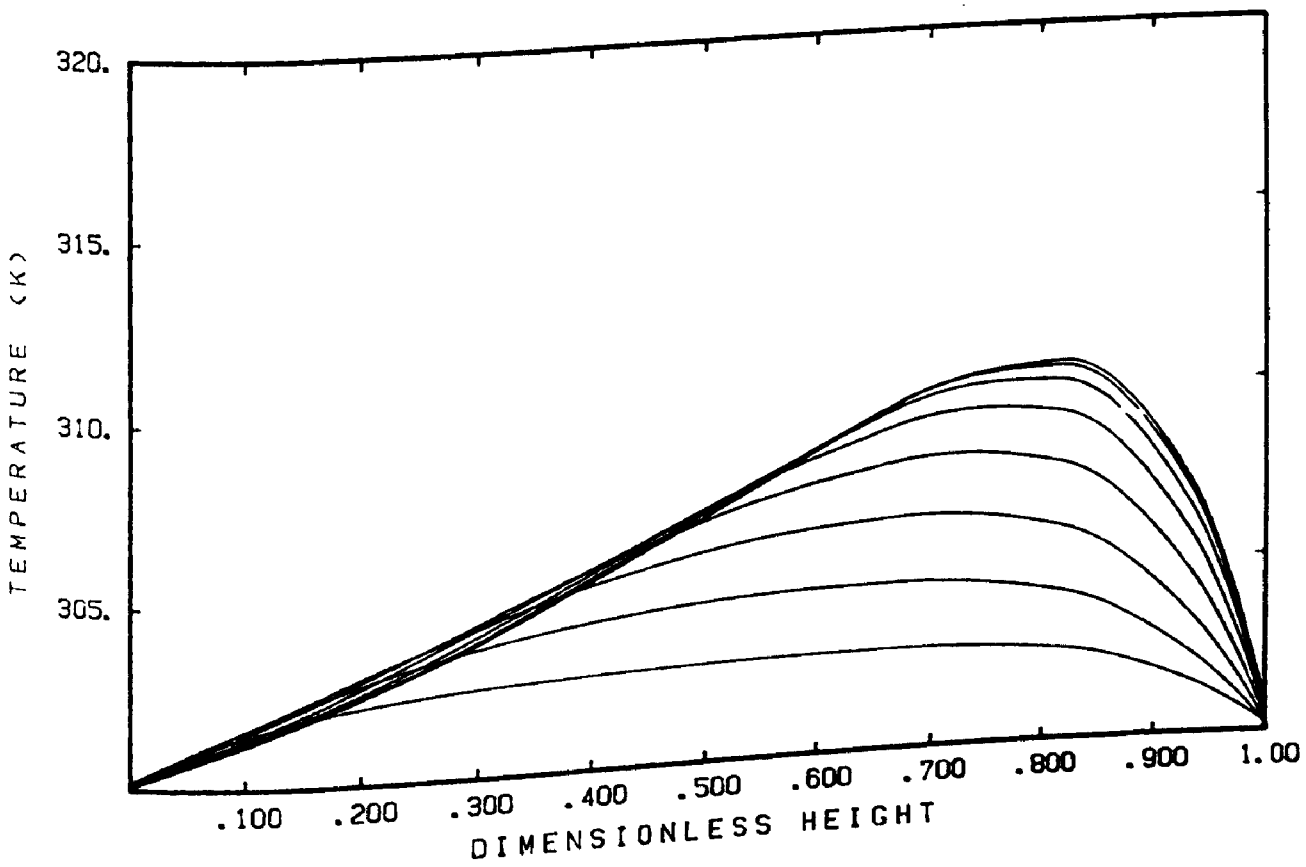


Figure 8.15 Temperature profiles in a coal bed
size 10 mm - Numerical Method

leading to eventual combustion. From this plot 60 ^{o}C appears to be a critical temperature. It is interesting to note that from Table 8.3, at 57 ^{o}C flow is already dominating conduction as the significant heat transfer mechanism, since the value of the quantity 'a' is 3.6L or 18 which is significantly greater than 2π.

8.3.3 Discussion

The results presented in this section confirm the validity of the plots presented in section 8.2. The following are the important conclusions from the section.

a) Depending on the initial condition, a coal bed may either attain a low or high temperature steady state.

b) For coal beds in which conduction is the dominating heat transfer mechanism, a simple formula may be used to calculate the temperature of a coal bed as a function of time.

c) A method has been presented whereby it may be calculated whether conduction or flow is the dominant heat transfer mechanism in a coal bed. In general conduction will only be dominant for short coal beds of fine particles, in which the temperature rise remains small.

d) Results have been presented showing the temperature time behaviour of a coal bed on its way to spontaneous combustion. The bed is characterized by a gradual temperature rise until 60 ^{o}C at which point the temperature rise becomes more dramatic. It has been pointed out that at 60 ^{o}C flow is the dominant heat transfer mechanism in the bed.

8.4 Results of Solving the Equations Numerically

8.4.1 Introduction

As has been discussed, the numerical method for solving the equations involves no assumptions about the reaction rate being constant, and allows for the effect of prior oxidation on the reaction rate. The solutions can be found quickly, even using a fairly unsophisticated microcomputer, and if programmed on a more powerful mainframe computer, the computer time involved would be small.

8.4.2 Comparison Beteewn the Numerical Method and the Analytical Method

The results presented in Figures 8.13 were recalculated using the numerical method. In figure 8.15 the results for the case D_p = 10 mm are presented. It can be seen that for this low temperature case the results obtained are very similar. This is to be expected since the temperature variation in the bed is only of the order of 10 K, and therefore the assumption of a constant rate constant is fairly good.

In figure 8.16 temperature profiles through a reacting bed of coal of size 2 mm with a wind velocity of 5 m/s. A glance at Figure 8.9 will show that for this range of the parameters the bed is unsafe, with a final predicted maximum temperature of 450 K. In fact, as can be seem from figure 8.16 the maximum temperature reached is approximately 1100 K, indicating that the assumption of constant rate constant used to generate the curves in Figure 8.9 is a poor one for this case.

A point of interest in Figure 8.16 is the way in which ignition appears to occur. Between day 40 and day 45 a hump appears in the temperature profile, subsequently the maximim temperature in the bed moves toward the entrance of the bed. This effect is due to the fact that as the temperature increases so does the rate of reaction, leading to the oxygen being depleted near the entrance of the bed. The curves between day 55 and day 80 show some evidence that the numerical method does not cope very well with the ingition, which is in fact a shock phemomenon. In particular the curve for day 55, which exhibits two maxima is unrealistic, Nevertheless the temperature profile after 80 days appears to be in agreement with what one would expect, except for a slightly concave shape.

In Figure 8.17 is shown a cross plot of the results in Figure 8.16 at the bed centre. This curve shows a dramatic increase in temperature between 40 and 45 days of 130 K. The critical temperature from this plot appears to be in the region of 75 ^{o}C.

This bed appears to "take-off" after 40 days whereas the results shown in Figure 8.14 appears to become dangerous after 80 days. The difference between these two cases is the particle sizes of the coal and the fact that that for the results shown in Figure

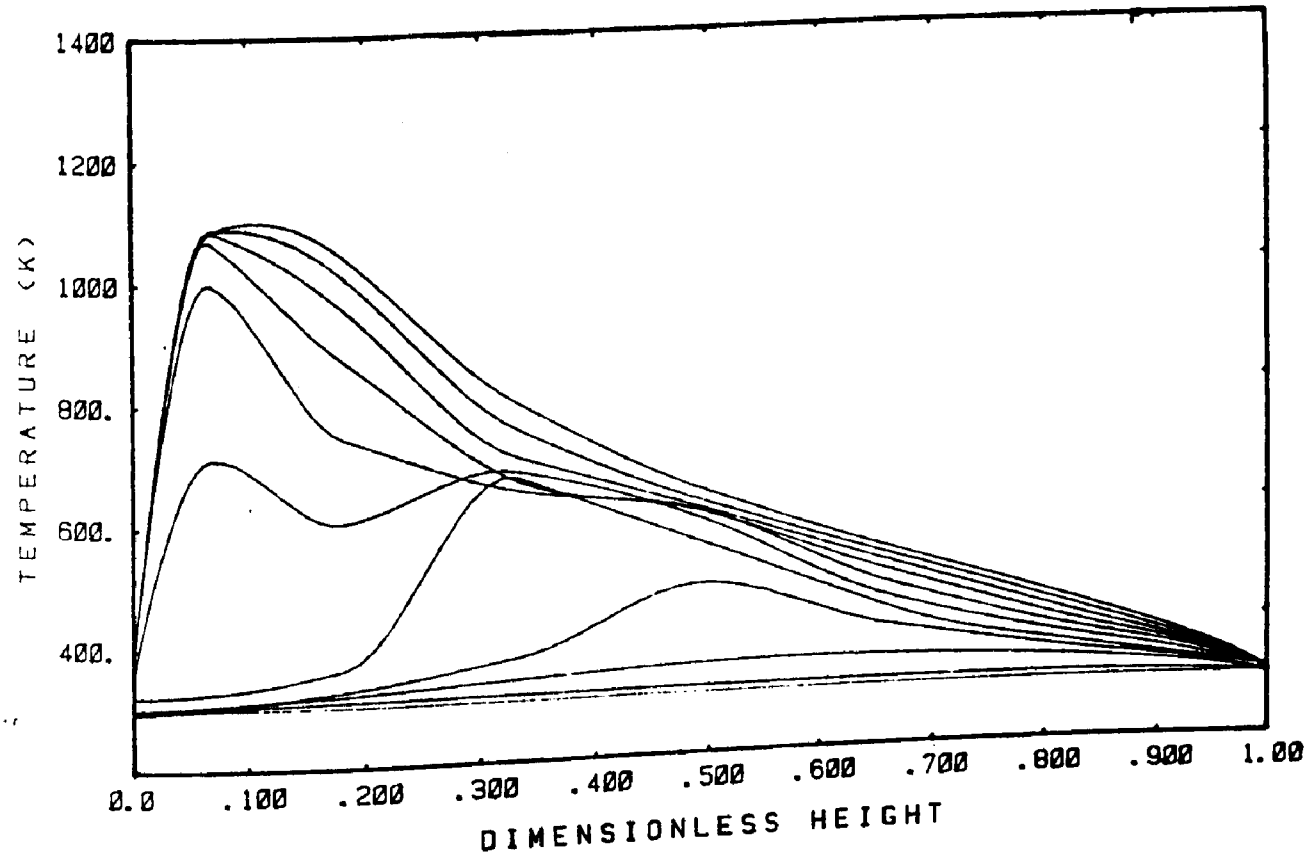
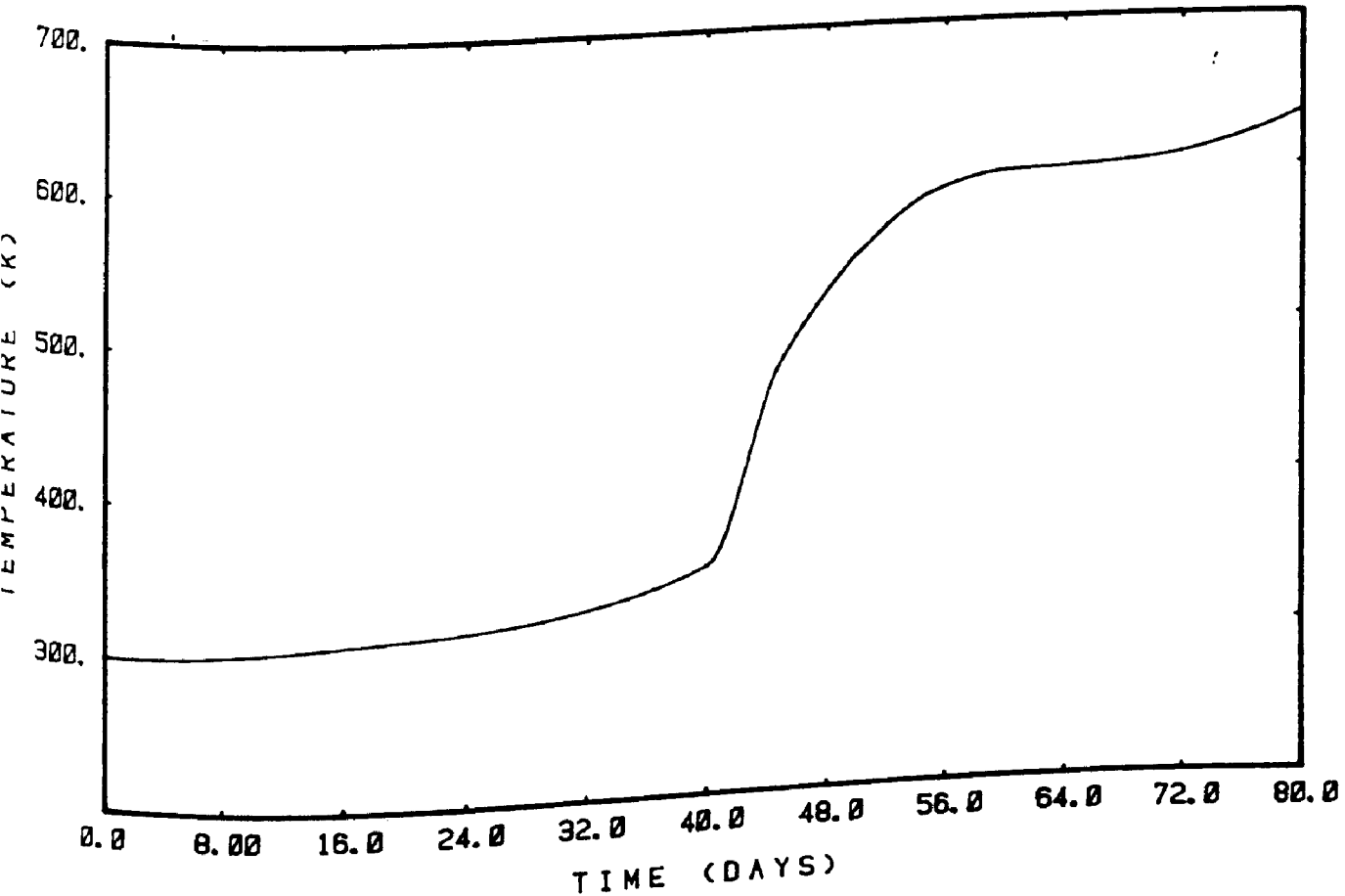


Figure 8.16 Temperature profiles with ignition
Particle size 2 mm - 5 m/s wind - Numerical method
First three curves 20 days apart
Subsequent curves 5 days apart



8.16 a 5 m/s wind has been assumed to blow constantly. It would be expected that the finer, more reactive coal would combust in a shorter time provided is is supplied with enough oxygen, as is the case here with the wind blowing.

8.6 Conclusions

The results presented in this chapter represent the results of solving the model equations for various values of the model parameters. It is felt that the parameters used are realistic, and therefore that the results obtained can be regarded as at the worst semi-quantitative.

The results of solving the equations for both the steady and unsteady-states have been presented. The results are consistent with practical experience. It has been shown that the assumption of a constant rate constant is a good one for beds in which the temperature remains less than approximately 350 K. The results of solving the unsteady-state equations numerically show that the model can predict the onset of spontaneous combustion, although numerical difficulties occur when the temperature gradients become large.

9. CONCLUSIONS

The important physical processes occuring in coal dumps have been identified and modelled. They are:

a. The ingress of reactants into the dump

b. The reaction between these reactants and coal

c. Heat transfer in the coal dump

It has been shown that natural convection and wind pressure are the most imprtant mechanisms whereby reactants are transported into a coal dump, with molecular diffusion only being of importance for fine material.

A shrinking-core model for the oxidation of coal at low temperatures has been proposed. This model explains the well known but little understood fact that the reactivity of the coal falls off with time.

It has been shown that heat transfer in a coal dump may be modelled using an effective thermal conductivity; the effective thermal conductivity of a typical coal bed has been measured.

All these effects have been incorporated into a one-dimensional model, with the aim of studying their combined effect on spontaneous combustion of coal. The model has been shown to have the correct characteristics in the prediction of the onset of spontaneous combustion. The model equations exhibit multiple solutions for certain values of the model parameters; it is concluded that stockpiles may be classified as safe, unsafe or conditionally safe.

Safe coal dumps have been shown to be either oxygen limited or heat transfer limited. In both cases the dump is safe because the sensible heat of reaction can be dissipated at temperatures near ambient. For oxygen limited beds the high reactivity of the coal toward oxygen causes oxygen to be consumed and thus the sensible heat to be produced close to the surface of the dump, where it is easily dissipated. For heat transfer limited beds, oxygen is readily available throughout the bed, but the reactivi-

ty per unit bed volume of the coal is sufficiently low that the sensible heat of reaction may be dissipated even from deep within the dump at near ambient temperatures.

The important parameters that must be known in order to make qualitative predictions about the safety of coal dumps have been shown to be:

a. The particle size distribution of the coal.

b. The voidage of the bed.

c. The pre-exponential factor and activation energy for the oxidation of the coal.

The model presented here may be used to qualitatively determine the effect of changing certain parameters which are under the control of the persons responsible for coal plant operation and particular dumping practise. In particular the effects of particle size distribution and compaction have been clearly pointed out. Compaction makes oxygen limited dumps safer, but appears to be ineffective in improving the safety of heat transfer limited dumps.

The efect of particle size distribution on the safety of dumps may be summarized as follows:

If the dump is oxygen limited adding fines may help make the dump safer, both by reducing the voidage and increasing the rate of oxygen depletion. If the dump is heat transfer limited then removing fine material may help make it safer.

An important practical implication of this work is that there is a dump size for an oxygen limited coal dump, above which the dump is effectively no more liable to spontaneous combustion. For very reactive coals this is a comforting result, since it implies that very reactive coals may be safely stockpiled on very large dumps, with obvious economic advantages. Caution must be exercised to ensure that the dump is oxygen limited, and that the oxygen levels below a certain depth remain negligible. At this stage the quantification of what this depth is, is not possible, but it appears from practical experience that 2 metres is a sensible upper limit on the depth at which the percentage oxygen in a safe

coal dump should be negligible.

Safe stockpiling times are not available from the model, and there is reason to believe that the concept of a safe stockpiling time can be misleading. It has been shown, both in practise and from the model, that a slow rise in temperature may suddenly become a rapid rise in temperature. The critical temperature appears to be in the region of 60 to 100 ^{o}C. The time taken to reach this critical temperature might be a better way of arriving at a safe stockpiling time.

The concepts presented in this thesis may also help to answer questions about stockpiling practise. In particular the following points are of practical importance:

Segregated coal dumps i.e. dumps in which particle size segregation occurs due to stacking methods employed, are potentially dangerous. It can clearly be seen from the results presented in this thesis that such dumps are dangerous because air can penetrate the dump through the coarse material, and react deep in the dump with finer material, that is inherently more reactive, thus leading to a temperature rise deep within the dump where the energy cannot easily be dissipated.

Covering dumps of coal has been suggested as a means of preventing spontaneous combustion. Broadly speaking a dump may be covered with either an inert or reactive material. An inert covering may be permeable or impermeable. In the case of an inert permeable covering such as sand, the fact that there is a balance between oxygen ingress and heat loss must always be borne in mind. Enough sand must be put down to substantially reduce the amount of oxygen ingress, recognising that the dump is being insulated at the same time. If an attempt is made to cover the dump with an impermeable layer of a material such as tar, it must be recognized that cracks in the covering may lead to large localized flows of oxygen into the dump, possibly giving rise to a hot spot.

Schmidt (1945) states that covering a coal dump with a layer of very fine coal and then with a layer of coarser coal provides an efficient coating. The coarse coal is packed on top of the fine coal to prevent wind and water erosion. In the light of the results presented in this chapter, this is an eminently

reasonable suggestion provided all the oxygen can be removed close to the surface.

In the case of dumps that are safe due to the fact that they are oxygen limited, the danger exists that with time the outer layer of coal will become unreactive due to the ageing effect, and that oxygen will penetrate deeper into the dump where any reaction that occurs may lead to a dangerous temperature rise. One of the practical conclusions that arises out of this analysis is that analysing for oxygen at various depths in a coal dump is an excellent way of monitoring the dump. It has been found in practise that in oxygen limited type of dump, the gas in the dump will contain virtually no oxygen at a depth of 2m. It has therefore been suggested that should appreciable oxygen be found at this depth an attempt be made to recompact the dump. Should this fail to rectify the situation the next logical step is the laying down of fresh coal on the dump. This would have the effect of limiting the amount of oxygen that is able to penetrate to appreciable depths. In the light of the model presented here, these suggestions seem sensible as well as practical.

A limitation of the model presented here is the inability at this stage to easily translate the size of a coal dump to the parameter of bed length used in the model. It can be demonstrated that there is a worst depth associated with natural convection, and a worst path length associated with wind driven flows. However at this stage it has not been possible to calculate these distances. A full three- dimensional analysis of the situation could give an idea of the magnitude of these distances; these could then be used in the simpler one-dimensional model for predictive purposes.

The omission of moisture effects in the model is simply rectified as has been demonstrated by Murtagh (1966). It must be borne in mind that in addition to the heat transfer mechanism of condensation and vaporization, moisture appears to exert a catalytic effect on the oxidation reaction. Schmidt (1945) discusses moisture effects in some detail; the ommision of these effects in the model presented here is mainly due to lack of data. There is thus scope for further work in determining the effects of both atmospheric and coal moisture content on the rate of oxidation.

One of the main areas of uncertainty in the field of spontaneous combustion of coal is the functional relationship between rates of oxidation and coal particle size. Much conflicting data has been published in ths regard (Schmidt, 1945, Sondreal & Ellman, 1974). It is felt that there is much need for further study in this regard.

APPENDIX 1 DERIVATION OF A RATE EQUATION FOR THE LOW TEMPERATURE OXIDATION OF COAL

The reaction mechanism considered here is one of diffusion of O_2 through an inert layer of oxycoal followed by reaction between the O_2 and the coal. No reaction products are formed and reaction at the reaction zone is considered to first order with respect to the O_2 concentration

In order to account for the fact that coal has both internal and external surface, the simplification is made that this surface area S′ may be considered to behave as if it was all external i.e. pore diffusion is neglected. This is a good assumption provided the particle size is not too large, as has been mentioned by Gijbels & Bruining (1982).

The coal particle is thus considered to have the geometry shown in Figure A1.1.

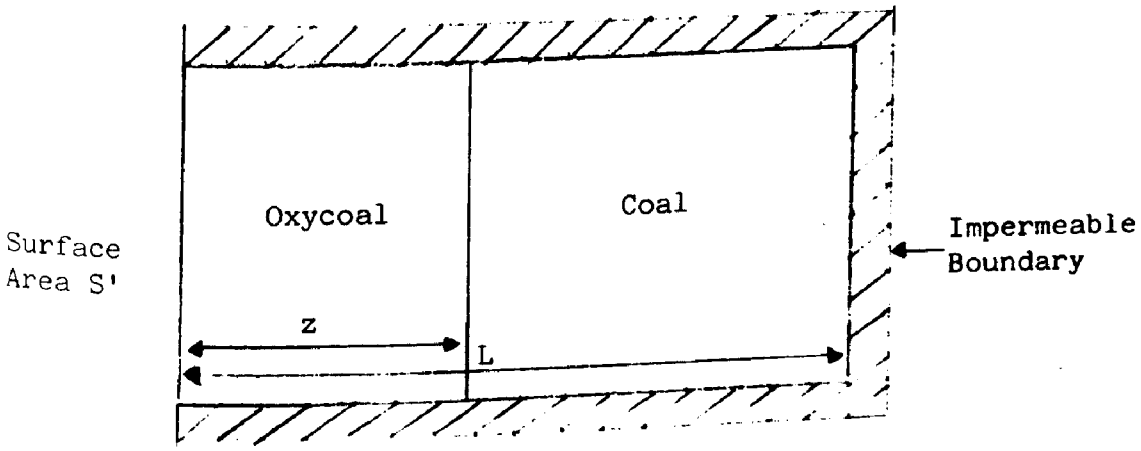


Figure A1.1 Simplified coal particle geometry

A particle length L is defined such that

$$S'L = V_p \qquad \text{A1.1}$$

where V_p = particle volume

At a time when the oxycoal layer has a thickness x the following equations may be written:

$$\text{Rate of diffuson of } O_2 \text{ through oxycoal} = S'D_e\,(C-C_s)/x \qquad \text{A1.2}$$

Rate of reaction of O_2 at reaction front = $S' k_s C_s$ A1.3

where D_e = effective diffusivity of oxycoal layer
C = free stream oxygen concentration
C_s = oxygen concentration at reaction boundary
k_r = surface rate constant

Under the pseudo steady state assumption that there is no accumulation of O_2 in the oxycoal these two rates must be equal i.e.

$$D_e (C - C_s)/x = k_r C_s \qquad \text{A1.4}$$

and solving for C_s gives

$$C_s = \frac{C}{1 + k_r x/D_e} \qquad \text{A1.5}$$

Back substitution in equation A1.2 gives

Rate of adsorption of O_2 by one particle $= \dfrac{S' k_r c}{1 + k_r x/D_e}$ A1.6

Now in a time Δt let the reaction front move a distance Δx.

Volume of coal reacted $= S' \Delta x$ A1.7

Moles of coal reacted $= \rho_m S' \Delta x$ A1.8

where ρ_m = molar density of reactive unit.

However the moles of coal reacted must equal the rate of adsorption times the time interval i.e.

$$\rho_m S' \Delta x = \frac{k_r C S' \Delta t}{1 + k_r x/D_e} \qquad \text{A1.9}$$

letting Δt, Δx tend to zero gives

$$\rho_m \frac{dx}{dt} = \frac{k_r C}{1 + k_r x/D_e} \qquad \text{A1.10}$$

In order to write the equations in terms of fractional

conversion of the coal, rather than the thickness of the oxycoal layer, it is noted that the volume of reacted material is S′x and the total volume is S′L.

Therefore the fractional conversion X is $S'x/(S'L) = x/L$

However L as defined by equation A1.1 is equal to V_p/S'.

Therefore $L = V_p/S' = 1/S_t$ A1.11

where S_t is now the total particle surface area per unit volume of particle.

Therefore, fractional conversion $X = xS_t$ A1.12

and substituting in equation A1.10 gives

Rate of adsorption of O_2 by one particle $= \dfrac{S_t\ V_p\ k_r\ C}{1 + k_r\ X/(S_t\ D_e)}$ A1.13

$$\rho_m\ S'\ \frac{dX}{dt} = \frac{k_r\ C\ S_t}{1 + k_r\ X/(S_t\ D_e)} \qquad \text{A1.14}$$

The rate that is required is however the rate per unit bed volume.

Rate / unit bed volume = Rate per particle x $\dfrac{\text{no of particles}}{\text{unit bed volume}}$

A volume V of the bed contains a volume $V(1-\epsilon)$ of coal where ϵ is the bed voidage.

The number of particles in the volume is therefore

$$V(1 - \epsilon)/V_p$$

and the number of particles per unit volume is

$$(1 - \epsilon)/V_p$$

Therefore the rate per unit bed volume is

$$r = \frac{S_t\, k_r\, C\, (1-\epsilon)}{1 + k_r\, X/(S_t\, D_e)} \qquad \text{A1.15}$$

APPENDIX 2 TABULATION OF MEASURED THERMAL CONDUCTIVITIES

A2.1 Details of Coal Used

Particle size range: -6.32 + 3.4 mm

Mass of coal: 67 Kg

Density of coal (measured): 1.36 g/cm^3

Volume of apparatus: .08 m^3

Voidage of bed: 0.38

A2.2 Measured Values

The values measured during 1982 are given in Table A2.1.

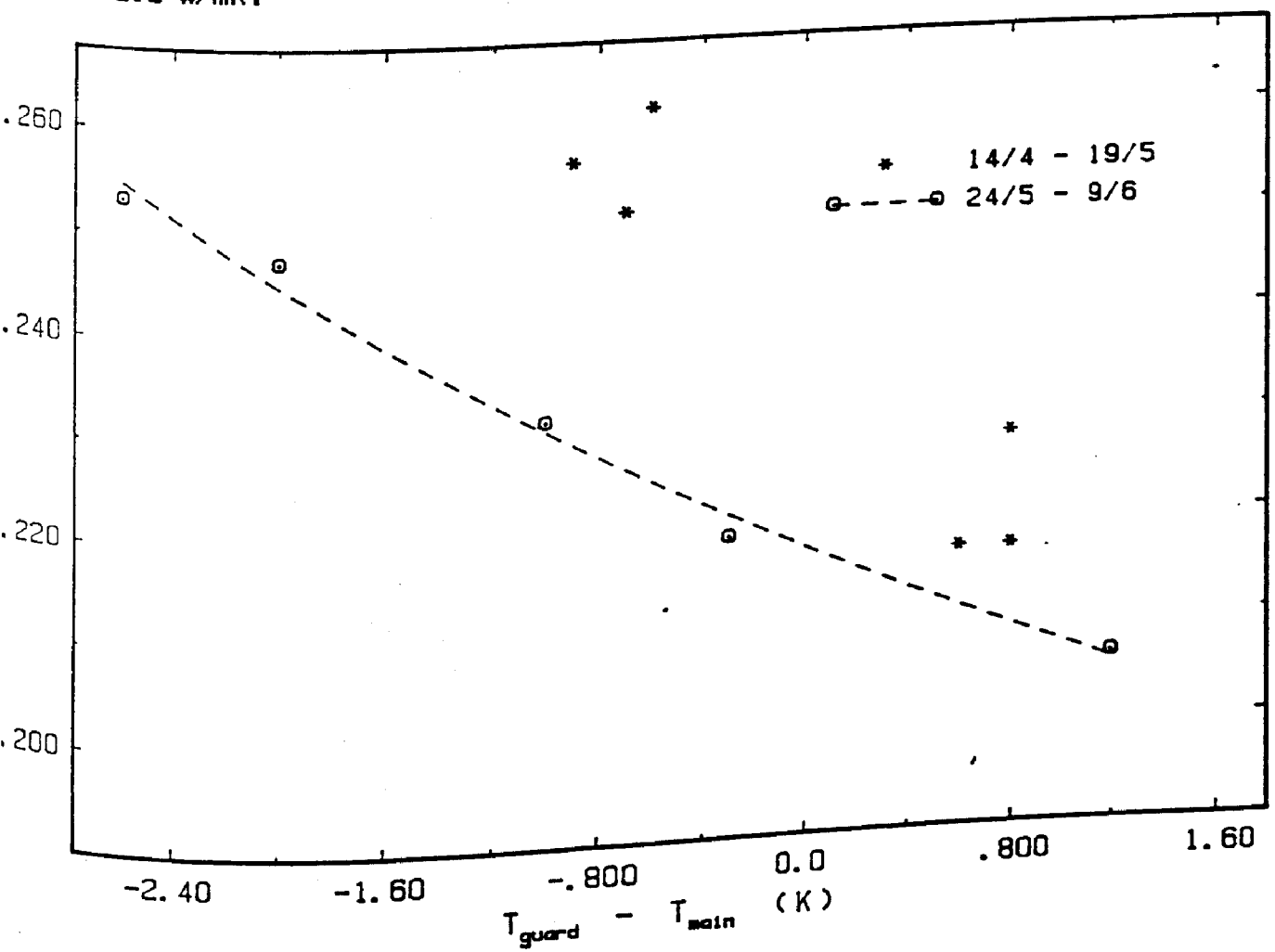
TABLE A2.1 MEASURED THERMAL CONDUCTIVITIES

DATE	MAIN TEMP(^{o}C)	GUARD TEMP(^{o}C)	MAIN VOLTAGE(V)	MAIN CURRENT(mA)	WATER TEMP(^{o}C)	k_b(W/mK)
14/4	67.8	68.6	11.66	139.8	23.0	0.217
16/4	68.7	69.5	11.66	139.8	24.0	0.228
6/5	57.8	58.4	11.64	139.5	24.0	0.286
10/5	62.2	61.6	11.64	139.7	25.0	0.261
18/5	60.2	59.5	11.69	140.2	22.0	0.251
19/5	60.0	59.1	11.69	140.2	22.5	0.256
24/5	98.2	95.6	16.46	196.7	23.0	0.253
27/5	99.7	97.7	16.45	196.7	23.0	0.247
28/5	104.9	103.9	16.46	196.6	23.0	0.231
4/6	109.2	108.9	16.45	196.4	23.0	0.219
9/6	114.8	116.0	16.45	196.5	23.0	0.206
25/6	86.8	88.6	13.94	166.6	23.0	0.213
23/7	91.3	91.1	14.00	167.2	23.0	0.201

The thermal conductivities measured between 14/4 and 9/6 are graphed against the temperature difference between the main and guard heaters on Figure A2.1. The reason for this choice

of plot is that in theory the guarded hot ring apparatus should be operated with the guard ring and main heater temperatures equal. Since this is impossible to achieve in practice, and since the calculated thermal conductivity is sensitive to differences between the main and guard heater temperatures, some form of interpolation must be used in calculating the thermal conductivty for the case of equal guard and main heater temperatures.

In figure A2.1 the data is plotted for the two different power inputs used. As can be seen, the data for the period 14/4 to 19/5, at the lower power input, shows considerable scatter. This could be due to a number of factors including failure to allow the apparatus to come to steady-state, as well as the variations in the cooling water temperature which are evident from Table A2.1. Due to the scatter in the data no attempt has been made to interpolate to $T_{guard} = T_{main}$. The data for the period 24/5 - 9/6 shows far more consistency. A quadratic least squares curve fits this data well, as can be seen from the graph. The interpolated value for $T_{guard} = T_{main}$ is 0.216 W/mK. The value obtained by linear interpolation between the values measured on 25/6 and 23/7 (which are not shown on the graph) is 0.202 W/mK.



APPENDIX 3 DERIVATION OF MODEL EQUATIONS

A3.1 Mass Balances

A3.1.1 Gas Phase Mass Balances

Consider the element of a bed of coal shown in Figure A3.1. The element has cross sectional area A and height Δx. The volume of gas in the element is $A \Delta x \epsilon$. The molar flowrate per unit area of the gas through the voids is G .

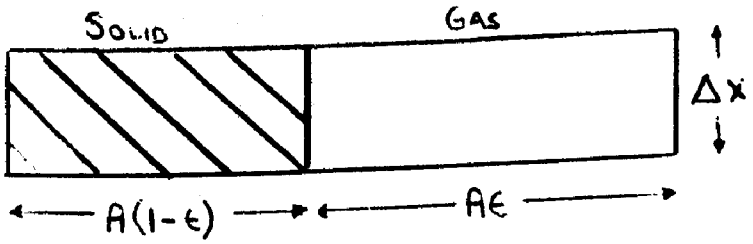


Figure A3.1 Differential element of a coal bed

The mass balance for component i in the gas phase is:

$$(\text{Moles of i in gas})\big|_{t+\Delta t} - (\text{Moles of i in gas})\big|_{t}$$

$$= (\text{Moles in})\big|_{x} - (\text{Moles in})\big|_{x+\Delta x} + \text{Moles produced in time } \Delta t$$

or

$$\left(\frac{P \epsilon}{R T_g} A \Delta x \, y_i\right)\Big|_{t+\Delta t} - \left(\frac{P \epsilon}{R T_g} A \Delta x \, y_i\right)\Big|_{t}$$

$$= (A G y_i \Delta t)\big|_{x} - (A G y_i \Delta t)\big|_{x+\Delta x} + r_i A \Delta x \Delta t$$

where
- G = molar flowrate per unit area
- y_i = mole fraction of i in the gas phase
- x = distance along bed
- P = pressure
- R = gas constant
- ϵ = bed voidage
- T_g = gas temperature
- t = time
- r_i = rate of formation of i per unit bed volume